The Synthesis of Oligothiophene Functionalized Dimethyldihydropyrenes and their Electrical and Photochromic Properties

by

Stephen Garfield Robinson

B.Sc. McMaster University, 2002

A Thesis Submitted in Partial Fulfillment
of the Requirements for the Degree of

DOCTOR OF PHILOSOPY

in the Department of Chemistry

The Synthesis of Oligothiophene Functionalized Dimethyldihydropyrenes and their Electrical and Photochromic Properties

by

Stephen Garfield Robinson

B.Sc. McMaster University, 2002

Supervisory Committee

Dr. Reginald H. Mitchell, Supervisor

(Department of Chemistry)

Dr. David J. Berg, Departmental Member

(Department of Chemistry)

Dr. Robin Hicks, Departmental Member

(Department of Chemistry)

Dr. Paul J. Romaniuk, Outside Member

(Department of Biochemistry and Microbiology)

Dr. Neil R. Branda, External Examiner

(Department of Chemistry, Simon Fraser University)

Supervisory Committee

Dr. Reginald H. Mitchell, Supervisor

(Department of Chemistry)

Dr. David J. Berg, Departmental Member

(Department of Chemistry)

Dr. Robin Hicks, Departmental Member

(Department of Chemistry)

Dr. Paul J. Romaniuk, Outside Member

(Department of Biochemistry and Microbiology)

Dr. Neil R. Branda, External Examiner

(Department of Chemistry, Simon Fraser University)

Abstract

The synthesis of benzo[e]dimethyldihydropyrene (BDHP) photoswitches with ter-**27**, quarter-**36**, and quinque-**28** thiophene oligomers attached on the same side of the switch was achieved using Stille coupling reactions. BDHP photoswitches with bi-**75**, ter-**76** and quinque-**77** thiophene oligomers attached directly to the switch on one side, and via a carbonyl spacer on the opposite side of the switch were also synthesized. Dimethyldihydropyrene (DHP) photoswitches with a naphthoyl functional group in the 2 position were synthesized using a Friedel Crafts reaction, and ter-**96**, quinque-**97** and

septi-**98** thiophene oligomers were attached on opposite sides of the switch using Stille coupling reactions. All compounds were characterized by NMR, IR UV-vis spectroscopy and mass spectrometry.

The relative rates of the photo-opening reactions under excess light conditions and the UV closing reactions versus BDHP were measured. Improvements in the photo-opening properties of the oligothiophene functionalized switches compared to BDHP were observed. The most dramatic photo-opening improvement was found for the quinquethienyl substituted DHP switch **97** which photo-opened when irradiated with visible light over 100 times faster than BDHP. UV closing rates were virtually the same as that of BDHP. However the addition of oligothiophenes led to an increase in the thermal closing reaction rates. Compounds with the naphthoyl functional group in the 2 position of DHP were found to have dramatically increased thermal closing rates.

The electrochemical properties of oligothiophene functionalized BDHP and naphthoyl functionalized DHP switches in the closed form were studied by cyclic voltammetry and spectroelectrochemistry. During the oxidation cycle, a closing reaction from the cyclophanediene (CPD) form to the DHP form of the switches occurred which prevented the study of the electrochemical properties of the switches in the open form.

Conductivity testing was performed on the quinquethienyl substituted DHP switch **97** using a gold interdigitated micro electrode array. The conductivity of undoped **97** was greater in the closed DHP isomer than in the open CPD isomer. Irradiation with red or blue light allowed for repetitive switching between the more highly conducting closed form and the less conducting open form. When electrochemically doped, **97**

showed improved conductivity over the undoped form but only the conductivity of the closed doped form could be measured due to electrochemically induced closing.

Table of Contents

List of Tables

List of Figures

List of Schemes

List of Numbered Compounds

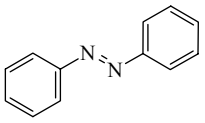

1

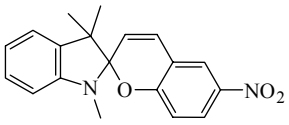

2

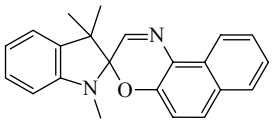

3

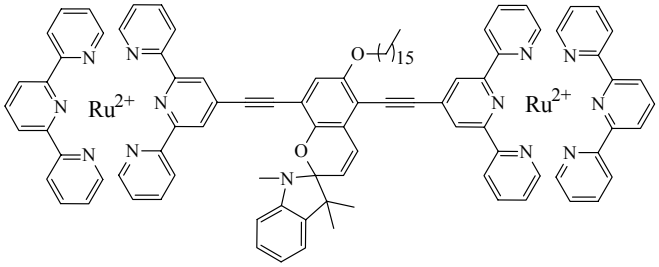

4

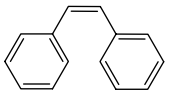

5

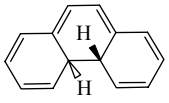

6

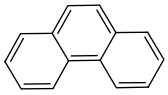

7

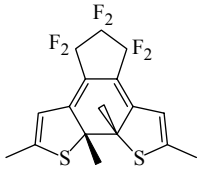

8

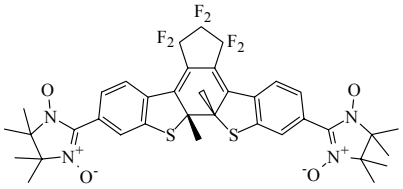

9

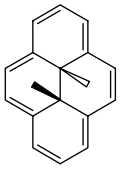

10

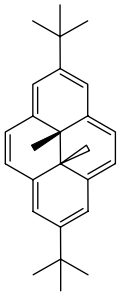

11

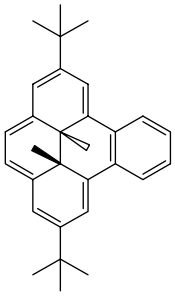

12

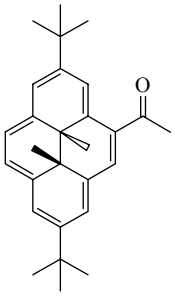

13

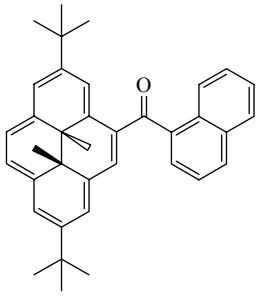

14

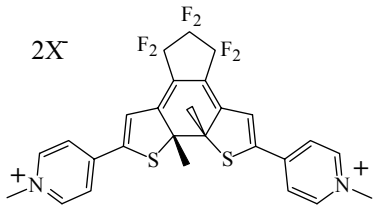

15

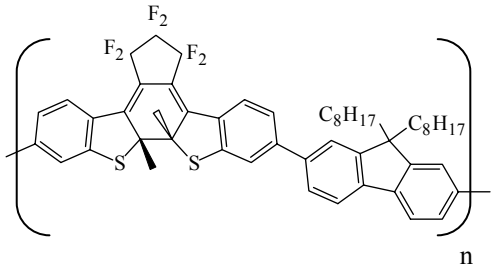

16

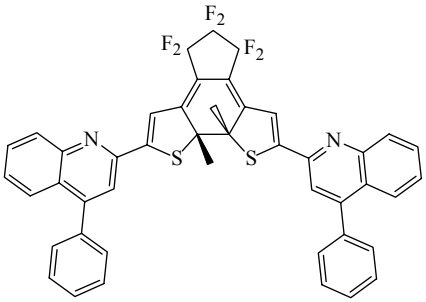

17

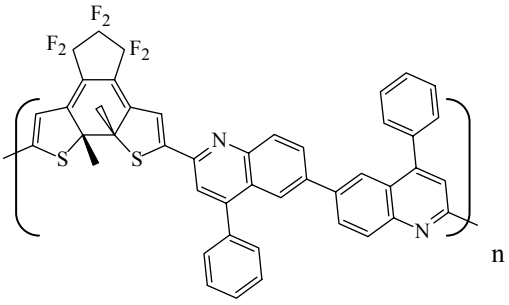

18

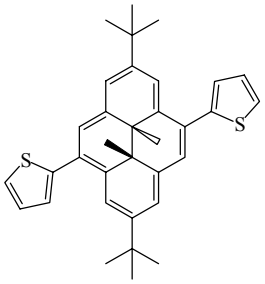

19

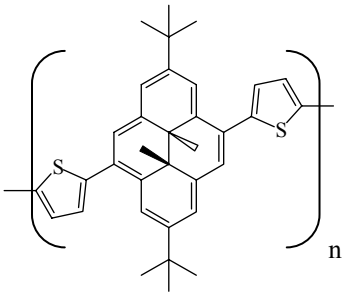

20

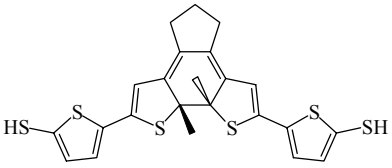

21

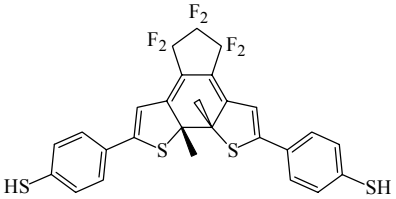

22

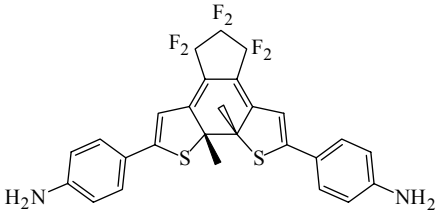

23

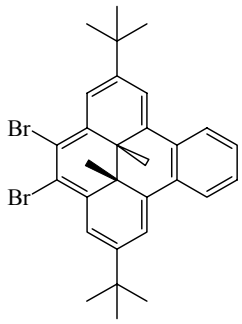

24

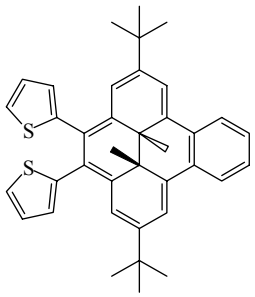

25

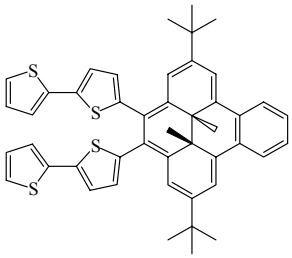

26

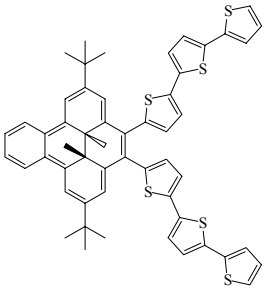

27

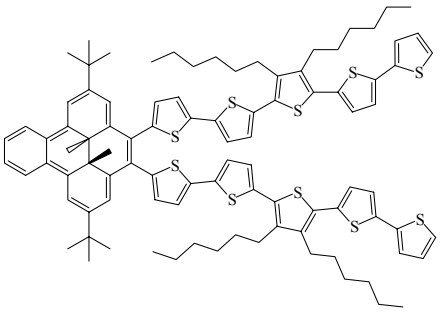

28

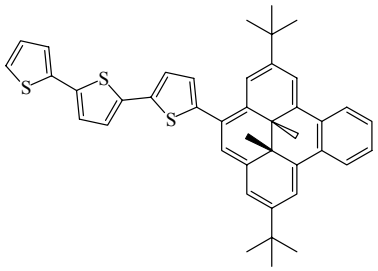

29

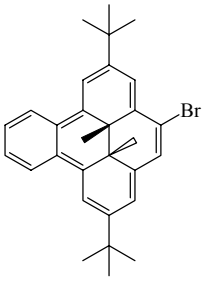

30

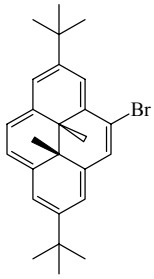

31

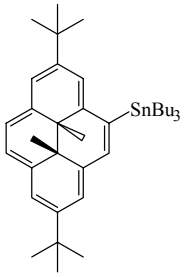

32

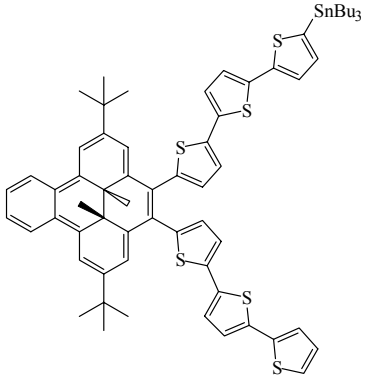

33

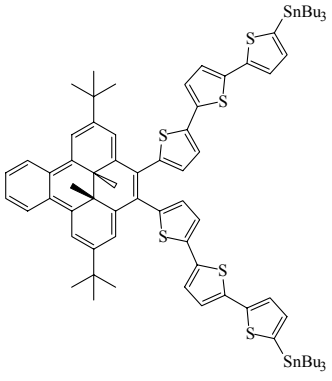

34

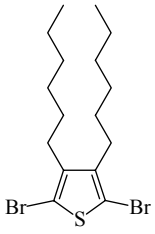

35

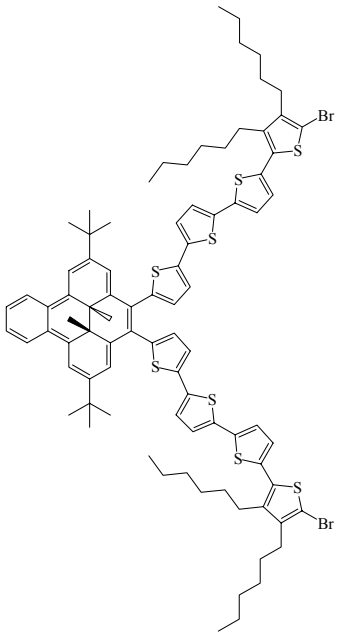

36

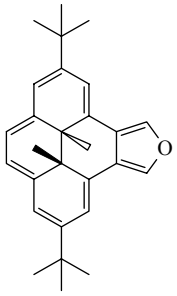

37

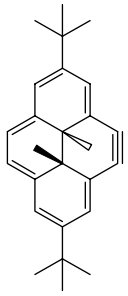

38

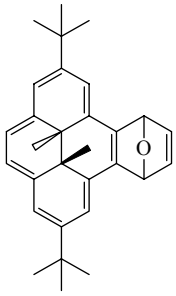

39

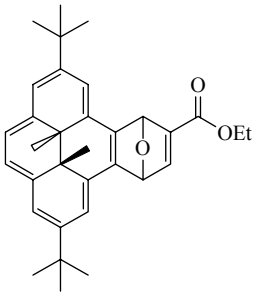

40

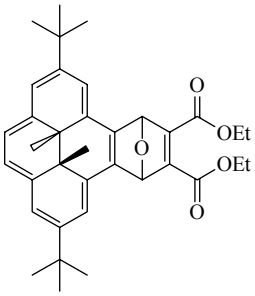

41

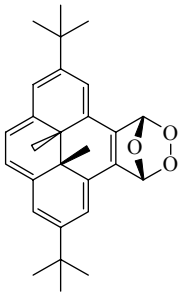

42

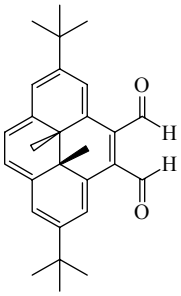

43

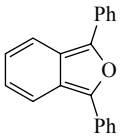

44

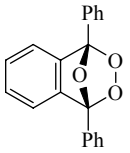

45

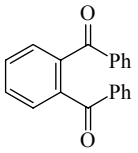

46

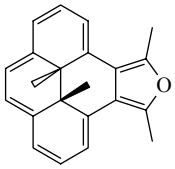

47

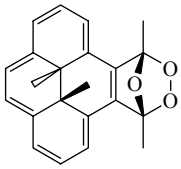

48

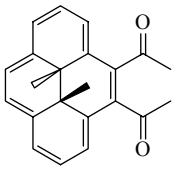

49

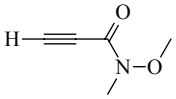

50

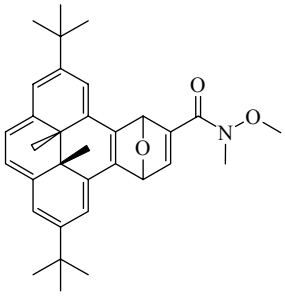

51

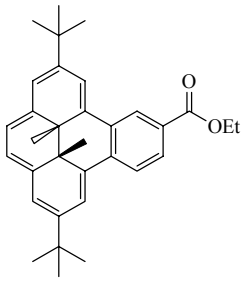

52

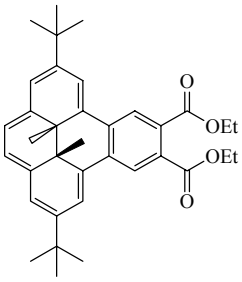

53

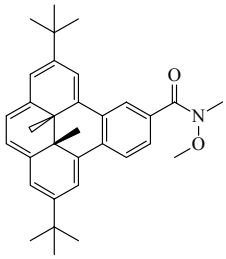

54

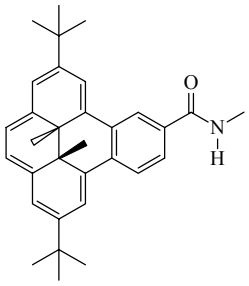

55

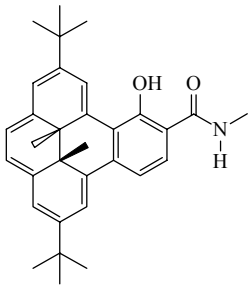

56

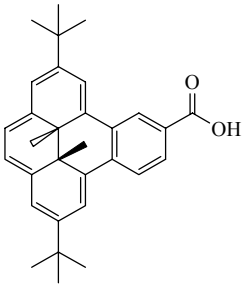

57

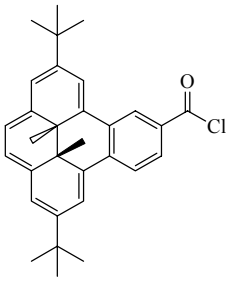

58

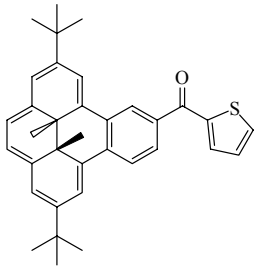

59

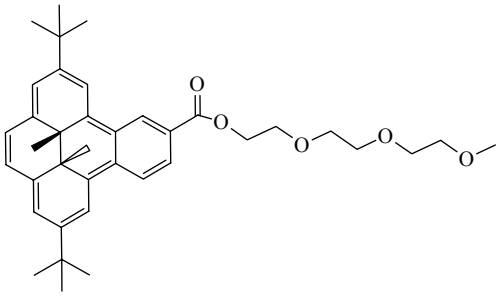

60

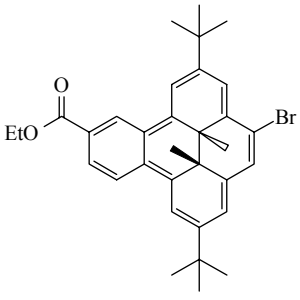

61

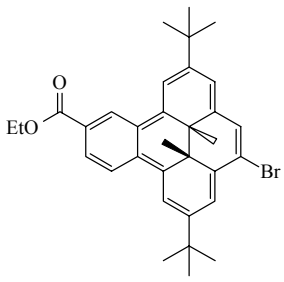

62

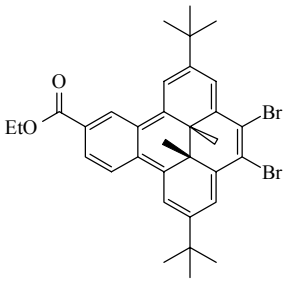

63

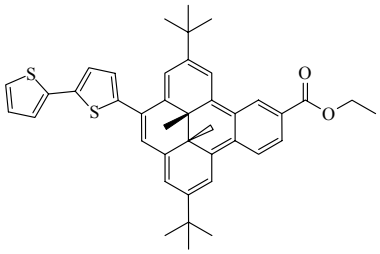

64

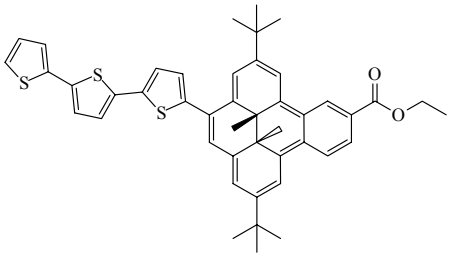

65

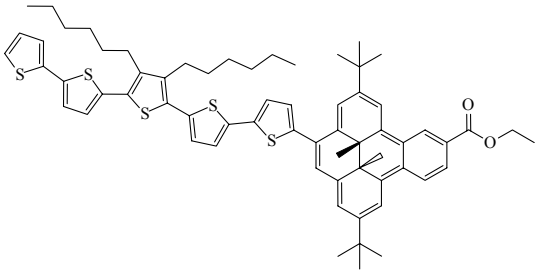

66

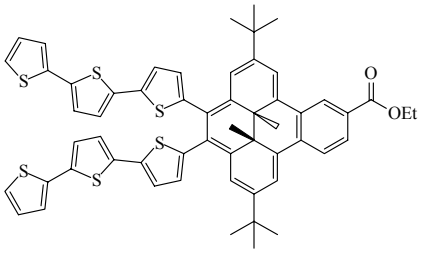

67

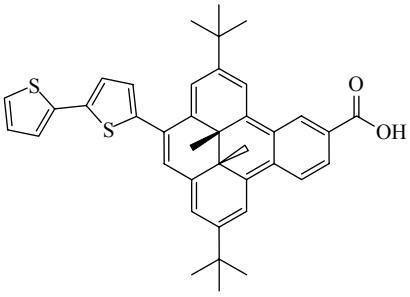

68

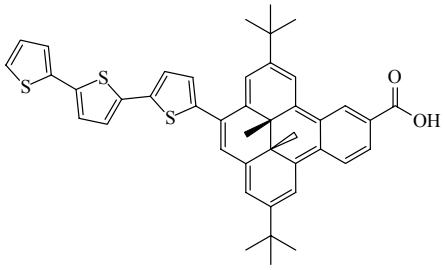

69

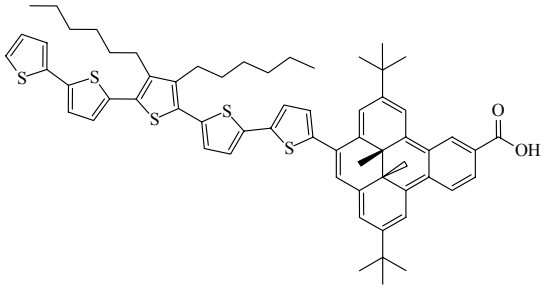

70

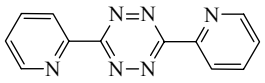

71

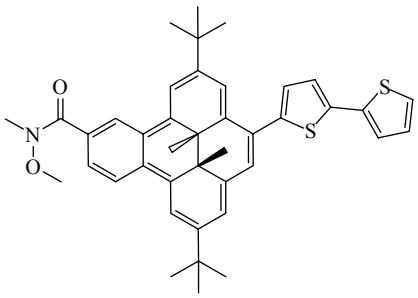

72

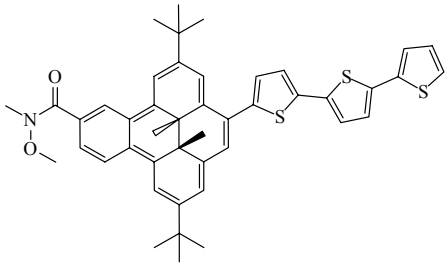

73

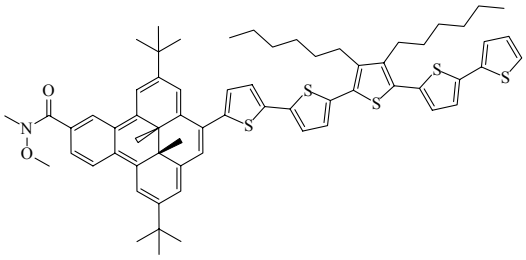

74

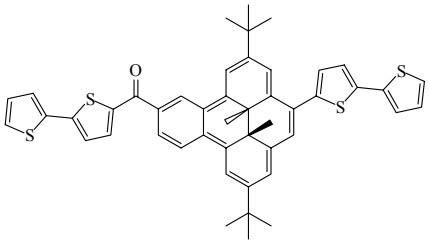

75

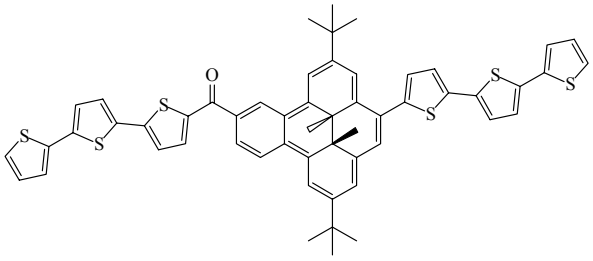

76

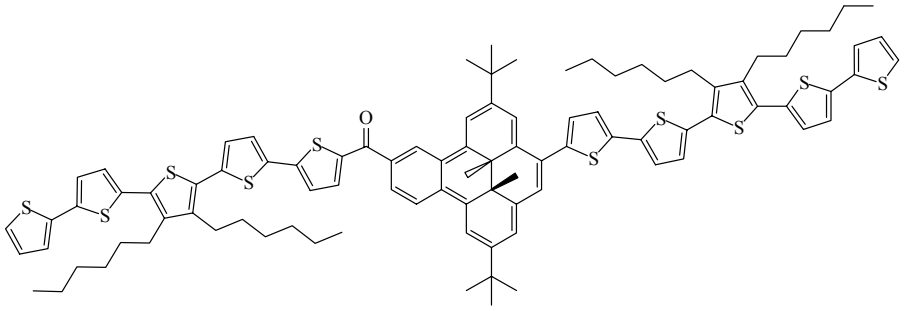

77

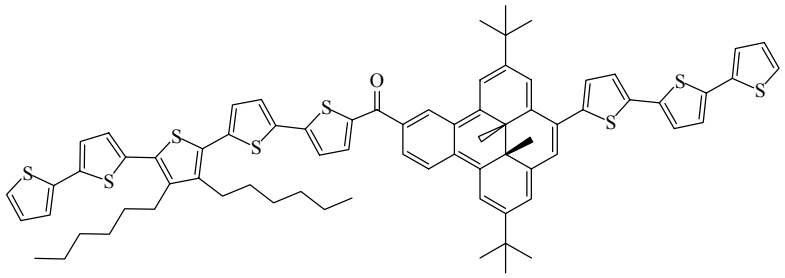

78

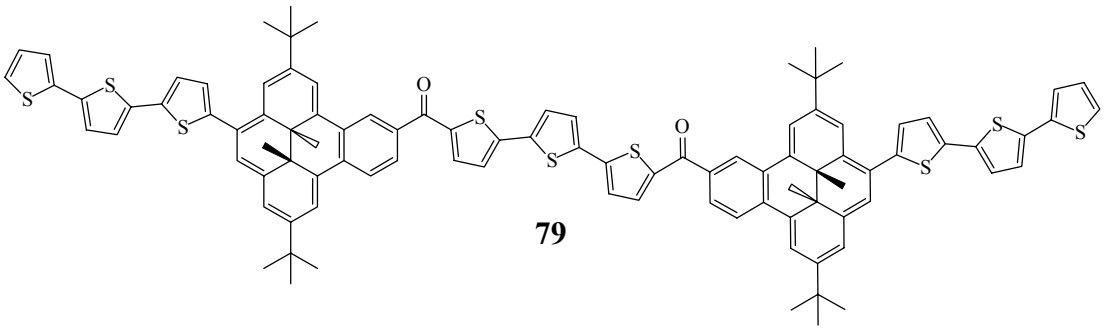

79

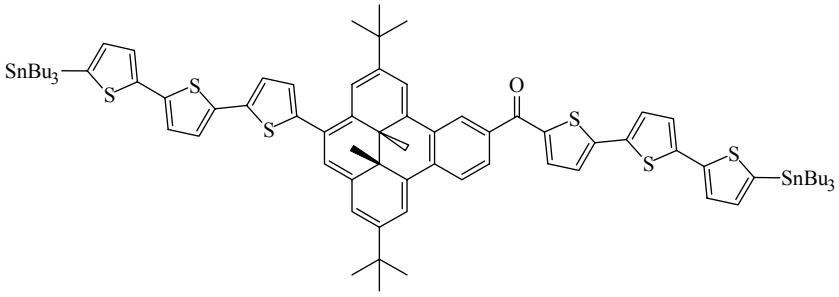

80

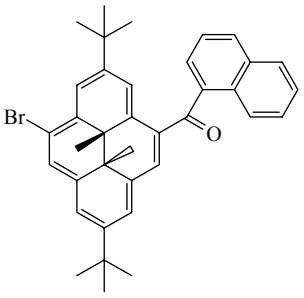

81

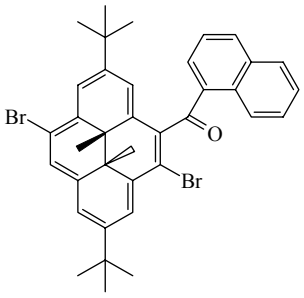

82

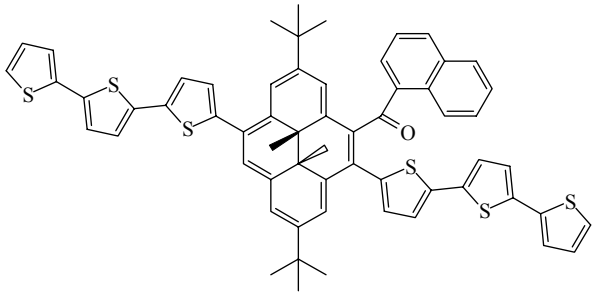

83

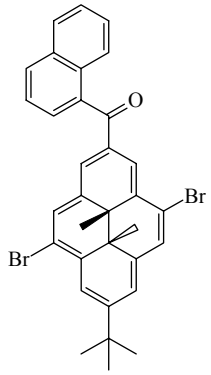

84

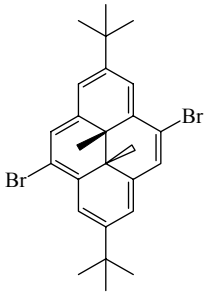

85

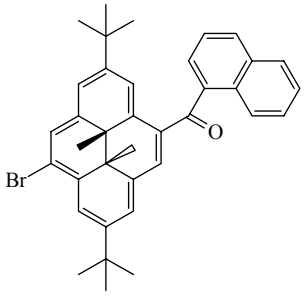

86

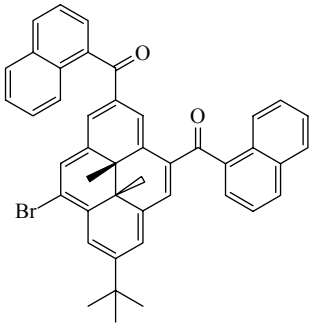

87

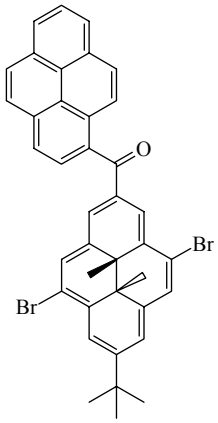

88

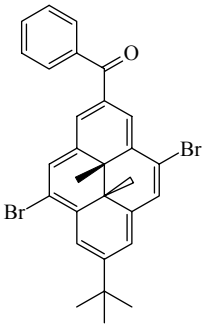

89

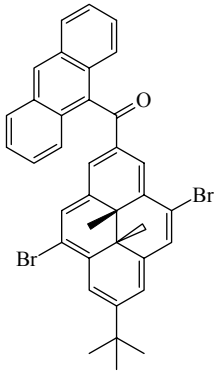

90

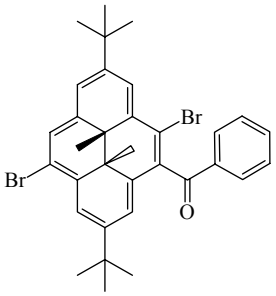

91

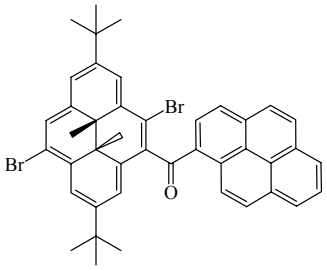

92

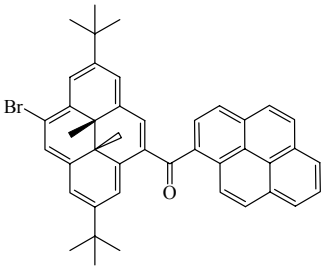

93

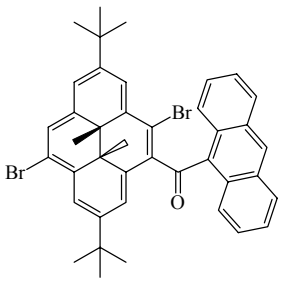

94

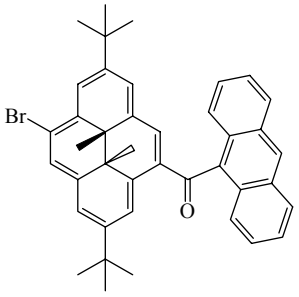

95

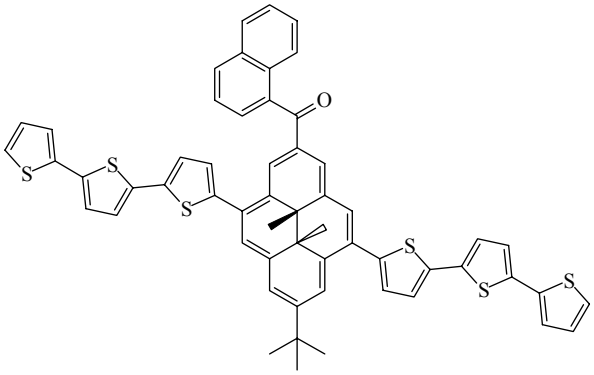

96

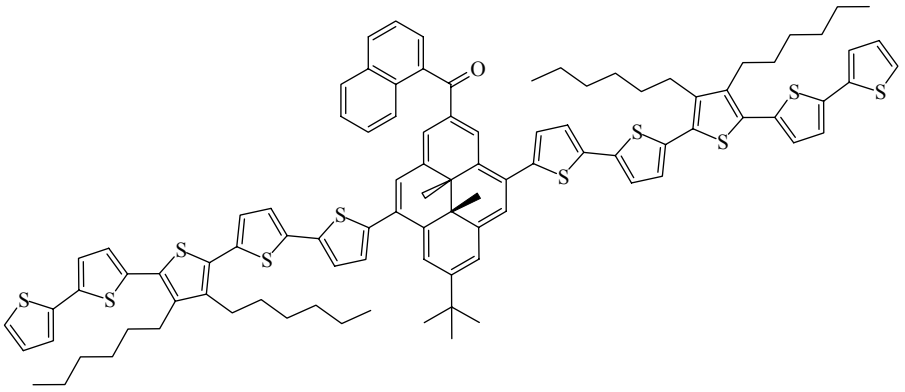

97

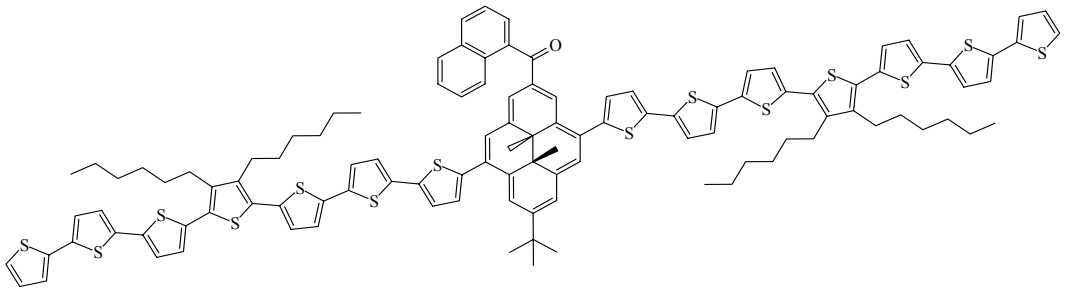

98

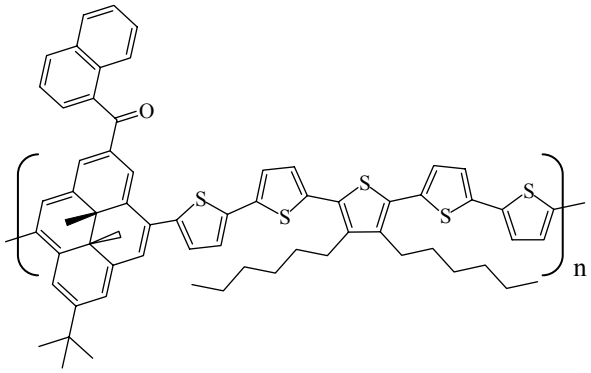

99

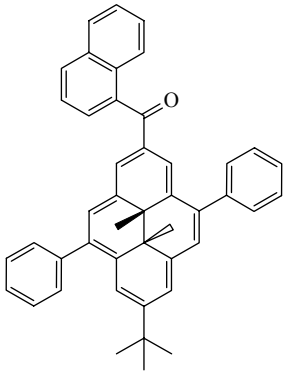

100

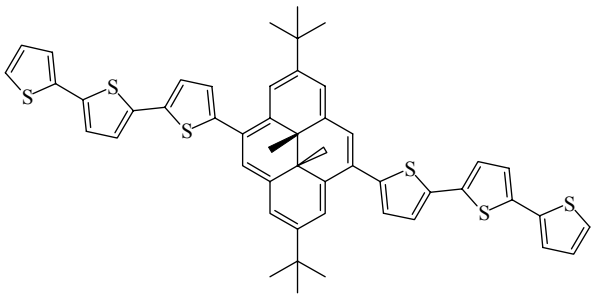

101

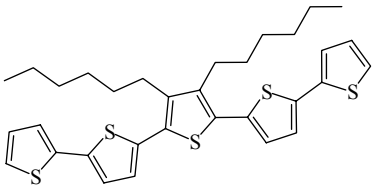

102

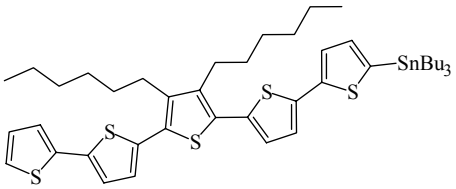

103

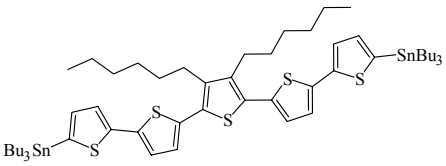

104

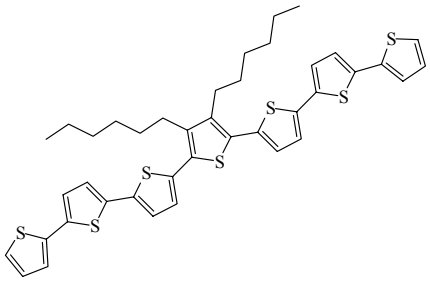

105

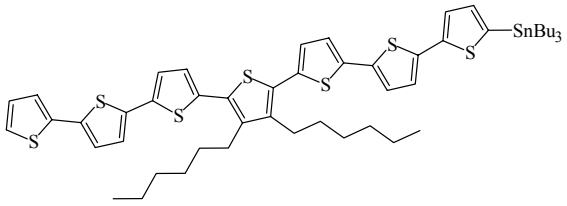

106

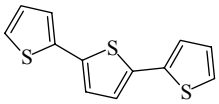

107

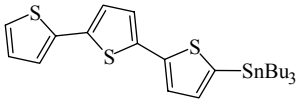

108

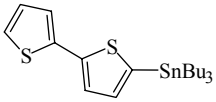

109

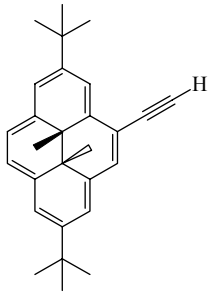

110

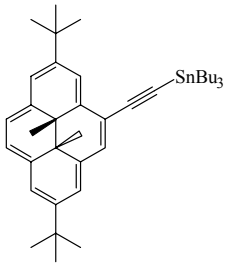

111

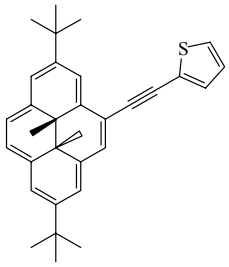

112

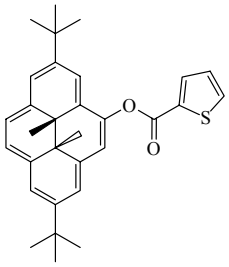

113

List of Symbols, Abbreviations and Nomenclature

Symbol	Definition
^{13}C NMR	carbon-13 nuclear magnetic resonance
^{1}H NMR	proton nuclear magnetic resonance
ACN	acetonitrile
BDHP	benzo[e]dimethyldihydropyrene
bs	broad singlet
COSY	correlated spectroscopy
CPD	cyclophanediene
CV	cyclic voltammetry
d	doublet (NMR)
dba	dibenzylidineacetone
DCM	dichloromethane
dd	doublet of doublets (NMR)
ddd	doublet of doublets of doublets (NMR)
dec	decomposition
DEPT	distortionless enhancement of polarisation transfer (NMR)
DHP	dimethyldihydropyrene
DIC	N,N'-diisopropylcarbodiimide
DMAP	4-(dimethylamino)pyridine
DMF	dimethylformamide
dppf	bis(diphenylphosphino)ferrocene
dqd	doublet of quartets of doublets (NMR)
EI	electron impact
E_g	band gap energy
E^o	formal potential
E_{pa}	peak anodic potential
E_{pc}	peak cathodic potential

EPR	electron paramagnetic resonance
EtOAc	ethyl acetate
EtOH	ethanol
eV	electron volts
Fe	ferrocene
g	grams
HMBC	heteronuclear multiple bond correlation
HOMO	highest occupied molecular orbital
HRMS	high resolution mass spectrometry
h	hours
HSQC	heteronuclear single quantum coherence
Hz	Hertz
IV	current voltage
IR	infrared spectrum
i_{pa}	peak anodic current
i_{pc}	peak cathodic current
IR	infrared
ITO	indium tin oxide
J	coupling constant
K	Kelvin
kcal	kilocalorie
L	litre
LDA	lithium diisopropylamide
LSIMS	liquid secondary ion mass spectrometry
LUMO	lowest unoccupied molecular orbital
m	multiplet (NMR)
MALDI TOF	matrix assisted laser desorption/ionization time of flight
Me	methyl
MeOH	methanol

mg	milligram
min	minute(s)
mL	millilitres
mp	melting point
MS	mass spectrometry
mV	millivolt
m/z	mass per charge
NBS	N-bromosuccinimide
n-BuLi	*normal*-butyl lithium
nm	nanometer
NMR	nuclear magnetic resonance
NOSY	nuclear Overhauser enhancement spectroscopy
Ph	phenyl
ppm	parts per million
q	quartet (NMR)
s	singlet (NMR) or seconds
sh	shoulder
SCE	saturated calomel electrode
t	triplet (NMR)
$TBAPF_6$	tetrabutylammoniumhexafluorophosphate
t-BuLi	*tert*-butyl lithium
THF	tetrahydrofuran
TLC	thin layer chromatography
$TMABF_4$	tetramethylammoniumtetrafluoroborate
UV	ultra-violet
V	volt
vis	visible
ε	extinction coefficient
λ_{max}	maxiumum wavelength absorption

Δ	heat
δ	chemical shift in ppm from standard

Acknowledgments

I would first like to acknowledge and thank my supervisor Professor Reg Mitchell for his guidance and support during my Ph.D studies. His constant enthusiasm for organic chemistry, science, and life in general made this project very enjoyable. I would like to thank Professor Mark Lonergan (University of Oregon) for his help and direction with the electrochemistry experiments and Professors Dave Berg, Cornelia Bohne and Robin Hicks for their advice and helpful discussions during the course of this project. I wish to thank Dave McGillivray for mass spectral analysis and Chris Greenwood for all of her help in training me and helping me to run the NMR experiments. I also wish to thank all the members of the Mitchell group with whom I've shared a lab over the last few years.

Financial support from the Department of Chemistry, the University of Victoria and NSERC is also gratefully acknowledged.

Dedication

To Kristy and Natalie

"Seek and you will find, knock and the door will be opened to you"

Chapter One: Introduction

1.1 Introduction

One of the major thrusts in chemical research over the last few years has been the development of molecular scale devices. However, in order for these molecular scale devices to be made, there is a requirement for a tool box of molecular scale components, an understanding of how these various components interact with each other, and an ability for the macroscopic world to interact with these molecular components.

1.2 Molecular switches

Switches are an integral part of almost all macroscopic devices and they will also be important components of molecular scale devices. As a result, a variety of different molecules and molecular systems that can act as switches have been investigated.

1.2.1 Molecular photoswitches

Molecules which reversibly switch between two different forms when irradiated with light have been the subject of much interest because of the ease in which they can be addressed from the macroscopic world. This property of certain molecules has been known since the late 1800's,[1,2] but it was Hirschberg[3] in 1950 who first used the term photochromism to describe this property (Figure 1-1).

Figure 1-1 Photochromism

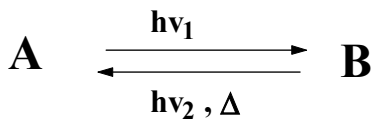

There are several different classes of photochromic molecules. Molecules that exhibit t-type photochromism have a thermal back reaction while molecules which only have a

photochemical back reaction exhibit p-type photochromism.[4] A unimolecular system where the λ_{max} (A) is less than the λ_{max} (B) is termed positive photochromism and when the λ_{max} (A) is greater than the λ_{max} (B) it is termed negative photochromism.[4]

1.2.1.1 Azobenzene

Azobenzene **1** is an example of a t-type positive photochromic molecule. When the more thermally stable *trans* form **1** is irradiated with UV light it undergoes a *trans-cis* isomerization to **1'** (Scheme 1-1). This leads to a decrease in the intensity of the 320 nm π-π* transition of the *trans* form, and an increase in intensity of the 430 nm n-π* transition due to the formation of the *cis* product.[5] When **1'** is irradiated with visible light or if it is heated it reverts back to the *trans* form **1**.

Scheme 1-1 Azobenzene *trans-cis* isomerization

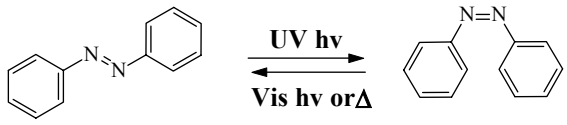

1 **1'**

The *trans-cis* isomerization in azobenzene causes a dramatic change in the stereochemistry as well as the dipole moment. In the *trans* form the distance between the para carbon atoms is 9.0 Å, this distance decreases to 5.5 Å upon conversion to the *cis* form.[5,6] Also the non-planar *cis* form has a dipole moment of 3.0 D while the *trans* form does not have a dipole moment.[5,6] The changes in the stereochemistry and the corresponding change in the 3-D structure of azobenzene have been exploited in a number of molecular systems. Gaub *et al.*[7] showed that the structural changes that occur in azobenzene as a result of *trans-cis* isomerization could be exploited to do mechanical

work. They used polymers containing azobenzene functional groups, and showed that these polymers would expand or contract against an external force when irradiated with light. Kramer[8] exploited this ability of azobenzene to do mechanical work to create a light activated ion channel in an attempt to control neuronal activity. In this work, a quaternary ammonium ion was tethered to the para carbon of an azobenzene molecule which had been attached to the outside of a modified ion channel. The change in the distance between the para carbon atoms in the *trans* and *cis* form was used to reversibly block and unblock an ion channel with the ammonium ion.

1.2.1.2 Spiropyrans and spirooxazines

Spiropyrans **2** and the related spirooxazines **3** (Scheme 1-2) are another type of photochromic molecule. The main difference between the spiropyrans and the spirooxazines is that the spirooxazines have a nitrogen in place of a methine group. Both systems are generally positive t-type photochromic molecules and are usually colorless in the spiropyran or spirooxazine form due to the orthogonality of the two ring systems centered at the spyro carbon. When irradiated with UV light they undergo photodissociation of the spirobond followed by *cis-trans* isomerization to give the highly colored planer merocyanines **2'** and **3'**. Conversion back to the spiropyran or spirooxazine form occurs thermally or upon irradiation with visible light.

Scheme 1-2 Open and closed forms of spyropyrans 2 and spirooxazines 3

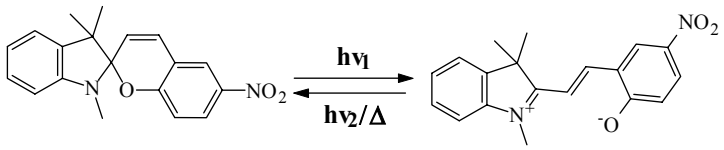

Spiropyran **Merocyanine**

2 **2'**

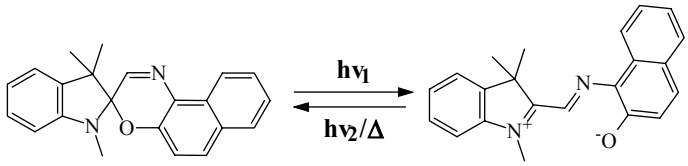

Spirooxazine **Merocyanine**

3 **3'**

There have been a number of applications for these photoswitches. The dramatic color change that occurs when the spiropyran and spirooxazine switches are opened and closed has found use in ophthalmic lenses and sunglasses.[9] There has also been an interest in using these molecular switches to act as a light activated T-junction (Figure 1-2) to control the direction of electron flow in a molecular wire.[10,11]

Figure 1-2 Molecular T-junction using a spiropyran switch. The arrow indicates the direction of electron flow

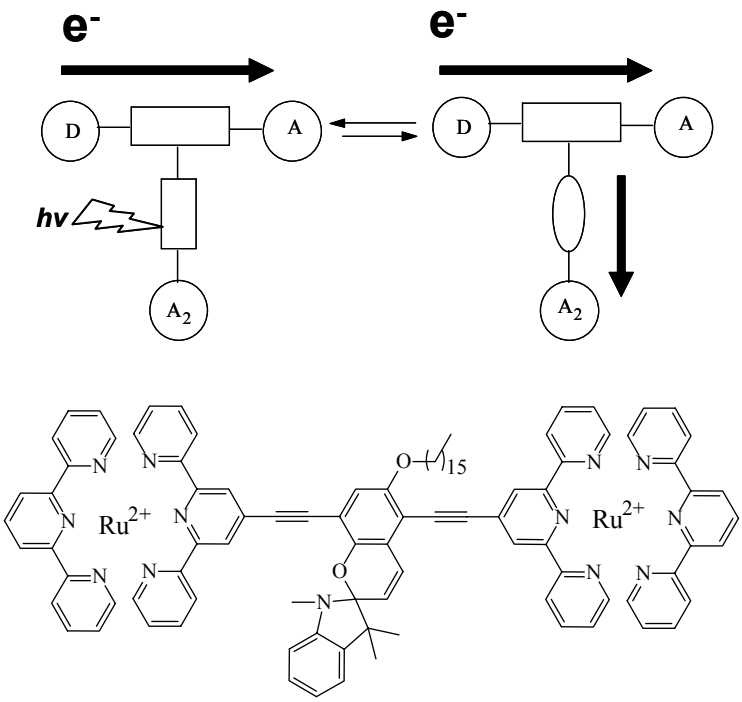

4

In this preliminary work a spiropyran photoswitch was attached between terminal ruthenium(II)bis(2,2':6,2"-terpyridine) complexes with the goal of using the difference between the open and the closed form of the spyropyran to control the direction of electron flow.

1.2.1.3 Diarylethenes

Another class of photoswitches that has received much attention is the diarylethene switches. The simplest form of this class of switches is Z-stilbene **5**, which when irradiated with UV light undergoes an electrocyclic reaction to give dihydrophenanthrene **6** (Scheme 1-3). The Z-stilbene form **5** can be recovered thermally or by irradiating with visible light.

Scheme 1-3 Z-Stilbene irradiation

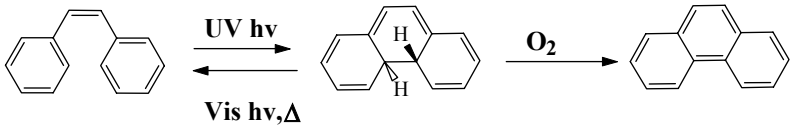

5 **6** **7**

Dihydrophenanthrene **6** is readily oxidized irreversibly in the presence of oxygen to give phenanthrene **7**. If the hydrogens at the 4a and 4b positions are replaced by methyl groups then this oxidation to phenanthrene can be avoided.[12] The diarylethenes have received much attention because if the benzene rings are replaced by heterocyclic aryl groups such as thiophenes, the resulting photoswitches can become thermally irreversible p-type photoswitches.[12] A large number of dithienylethene photoswitches have been made (Scheme 1-4), many of which can undergo more then 10000 cycles with minimal decomposition.[13,14] The backbone of the closed form **8** is planar which allows delocalisation of the π-electrons across the molecule leading to a highly colored compound. In the open form **8'** there is free rotation between the ethene moiety and the aryl rings. This leads to a non-planar structure where the π-electrons are localized in the aryl rings and leads in most cases to a colorless or at least less colored compound.

Scheme 1-4 The dithienylethene photoswitch

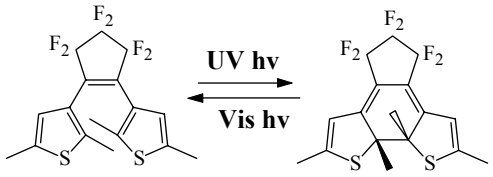

8' **8**

The thermal stability and high fatigue resistance of these switches has led to much effort to explore and exploit the photoswitching ability of the dithienylethene switch in molecular systems and devices. One example is the use of the dithenylethene to switch magnetic interactions.[15-17] Two nitronyl nitroxide functional groups, which act as spin sources, were attached on either side of the dithienylethene switch **9**, which acts as a spin coupler (Scheme 1-5).

Scheme 1-5 Photoswitching magnetism

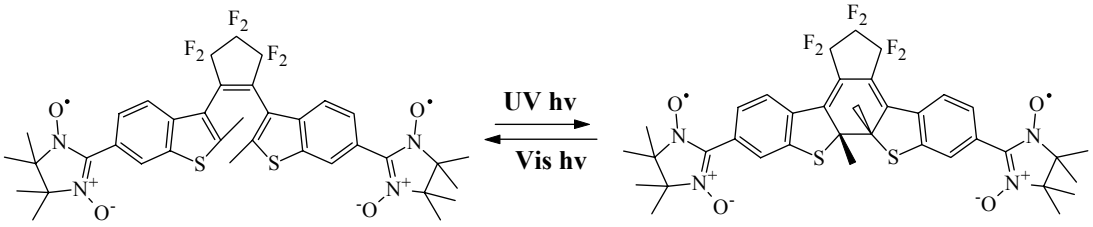

9' **9**

Magnetic susceptibilities were then measured in the open and the closed form of the photoswitch and a change in the magnetic interactions was observed.[17]

1.2.1.4 The dimethyldihydropyrene photoswitches

Dimethyldihydropyrene photoswitches **10** are examples of negative photochromes (Scheme 1-6). The photoisomerization reactions of these compounds was first reported by Boekelheide *et al*.[18] They showed that **10** opened to the colorless cyclophanediene

form **10'** when irradiated with visible light and closed back to the colored closed dimethydihydropyrene form **10** when irradiated with UV light or thermally.

Scheme 1-6 Photoisomerization of dimethyldihydropyrene

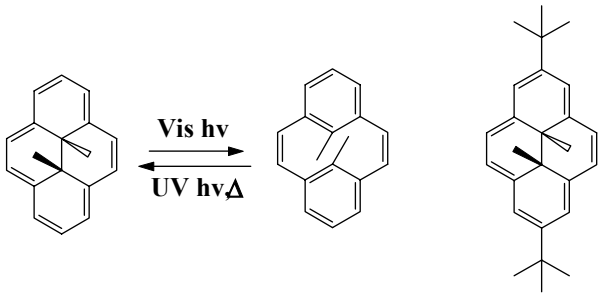

10 **10'** **11**

Structurally these molecules are very similar to stilbene, the difference being an extra double bond which makes for a more rigid molecule. This extra double bond also prevents Z-E isomerization and constrains the molecule to the right orientation in order to undergo the photochemical reaction. Unfortunately the synthesis of dimethyldihydropyrene is synthetically challenging. The initial synthesis by Boekelheide involved 14 steps and gave only a 3% overall yield from *p*-cresol.[19] This synthetic difficulty limited the ability of researchers to make derivatives and study the properties of these compounds. In order to study these compounds and their derivatives more efficient synthetic routes were needed. The development of the thiacyclophane route, allowed for the synthesis of dimethyldihydropyrene in 9 steps with an overall yield of 36% from 2,6-dichlorotoluene.[20] Using this route to synthesize the *t*-butyl substituted DHP version was even more efficient allowing the di-*t*-butyldimethyldihydropyrene **11** to be obtained in 6 steps and an overall yield of 35-45% from 4-*t*-butyltoluene.[21,22] These more efficient syntheses have allowed for a more extensive investigation into the photoswitching ability

of dihydropyrene and its derivatives. The visible light opening of the parent DHP **10** has a low quantum yield (0.006)[23] and the di-*t*-butyl version **11** an even lower quantum yield of opening (0.0015).[23] Recently dihydropyrene based molecules with greatly improved photo-opening reactions have been developed. Annulation of a benzene ring to the side of the dihydropyrene switch to give [e]-benzannelated dihydropyrene **12** (Figure 1-3) was found to improve the opening quantum yield to 0.042[23]. This benzannelated DHP also had a much slower thermal return, with a half life of 7.3 days at 20°C relative to the parent half life **10** of 42 hours at 20°C.[22,24] Adding an electron withdrawing group such as an acetyl group to the side of DHP was also found to improve the photo-opening reaction. With an acetyl group attached **13,** the ring opening quantum yield is 0.0038, and with a napthoyl group **14** it is 0.0092.[25]

Figure 1-3 Dihydropyrenes with improved photoswitching properties

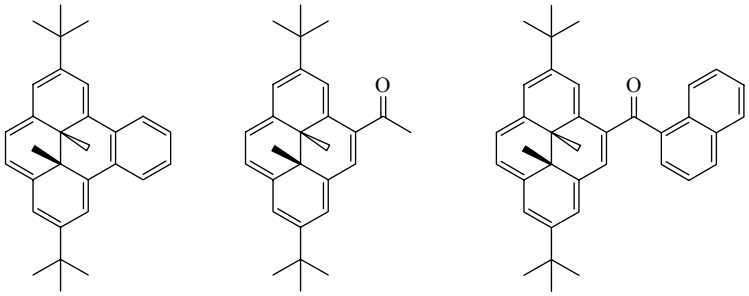

12 **13** **14**

These improved photoswitching properties along with more efficient ways to synthesize them have made the exploitation of the dihydropyrene photoswitch much more attractive. Because of the alternate arrangement of the internal methyl substituents, **12**, **13** and **14** along with many other DHP compounds are chiral. Throughout this thesis, solid and open wedges are used to indicate that the internal methyls are trans to each other, while

not specifying which enantiomer is present. Typically both enantiomers are present, but are indistinguishable and inseparable from each other.

1.3 Molecular wires

Electrically conducting wires are a vital part of many macroscopic devices and will be important in molecular based devices as well. The discovery by MacDiarmid, Heeger and Shirakawa[26] that carbon based polymers could conduct electricity changed the understanding of conductivity and led to their receiving a Nobel prize in 2000. Conducting organic polymers opened up the possibility of controlling electrical conductivity on the molecular scale. This discovery also opened up the tremendous ability developed in organic chemistry to modify structure and function and to use it to modify the properties of these polymers.

1.3.1 Principles of conductivity in conducting polymers

Conductivity is the measurement of a material's ability to allow electrons to flow, and is measured in units of current per voltage applied, or the reciprocal of resistance ($1/\Omega$ or Siemen (S)). Much research has gone into understanding how electrons flow through organic conducting polymers. One theory that has been influential in explaining the conductivity in materials is Band Theory. In an isolated atom there are only certain allowed energy levels (orbitals). These energy levels can be probed using spectroscopic techniques where photons of light are absorbed to excite the electrons in these orbitals to higher energy levels, or are emitted as electrons drop down from higher energy levels to lower energy levels. When an atom bonds to another atom there is a mixing of molecular orbitals, where orbitals with the same or similar energy may interact with each other.

When the number (n) of interacting atoms is small then there will be a substantial difference between the energy levels, but when n is large the energy levels become very tightly packed. When the energy levels are so tightly packed that electrons can easily move between them they are referred to as energy bands (Figure 1-4).

Figure 1-4 Valence energy levels to energy level bands

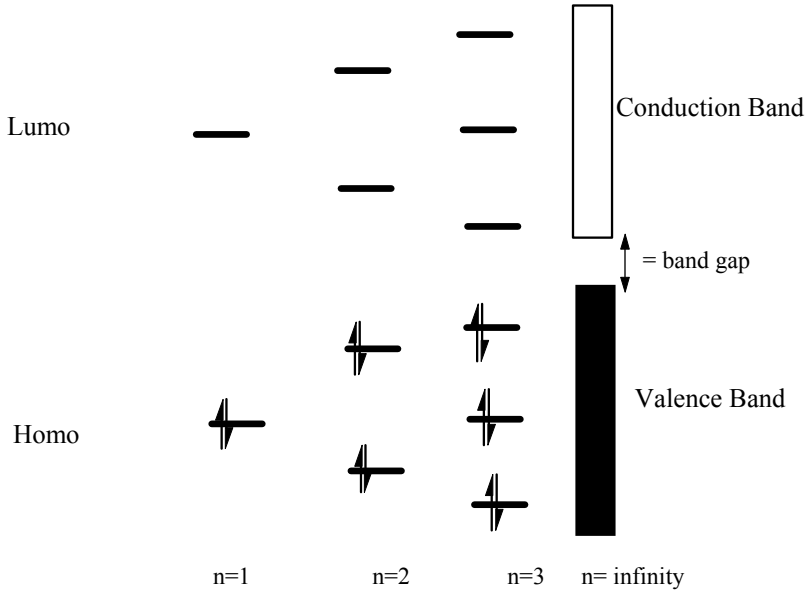

The number of electrons found in these bands and the location (energy) of the highest occupied band (valence band) and the lowest unoccupied band (conduction band) depends on the number of electrons involved and the energy of the various bands. The conductivity of a material is directly related to how the electrons fill the bands and the energy spacing (bandgap) between the bands. If the valence band is partially filled or if there is a very small bandgap, then the electrons can easily move from the valence band to the conduction band. This allows electrons to flow producing a metallic or an intrinsically conducting material. If there is a narrow bandgap, then the electrons, if given enough energy, can bridge the bandgap and reach the conducting band. Materials

with these properties are called semiconductors. If there is a large bandgap it is very difficult for the electrons to bridge the bandgap and materials with these properties are insulators (Figure 1-5).

Figure 1-5 Band gaps in insulators, semi-conductors and metals

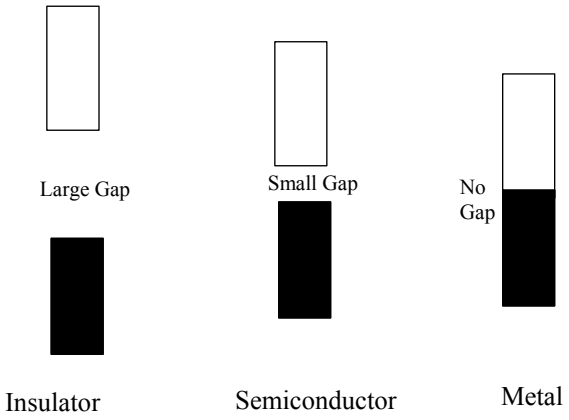

Generally if a material has no bandgap or a bandgap of less than 0.2 eV, it shows metallic conductivity. If the bandgap is between 0.2 and 2.0 eV it is a semiconductor and if it is greater than 2.0 eV, it is an insulator.[27]

It was thought that poly(acetylene), a conjugated organic polymer, might have metallic conductivity (intrinsically conducting). The reasoning was that if each carbon atom of poly(acetylene) only has one π electron and the bond lengths are equal then it can be seen from the graph of electron energy (E) vs the wave vector (k_f) where E_F is the Fermi level (the highest occupied energy level in a solid at absolute zero) and E_G is the bandgap, that a half full valence band results (Figure 1-6).[28]

Figure 1-6 Intrinsically conductive poly(acetylene)[28]

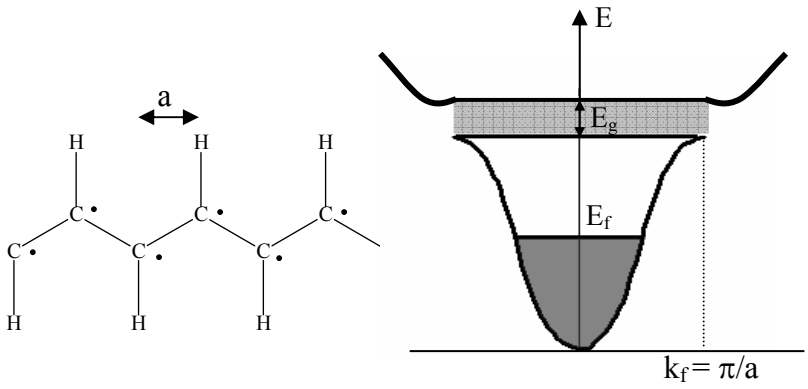

With a half full valence band, poly(acetylene) would show metallic conductivity. When conductivity tests were actually performed on poly(acetylene) it was found to be an insulator. The reason for this is that poly(acetylene) can lower its energy by bond alternation (Peierl's distortion), giving an alternating sequence of single and double bonds (Figure 1-7). This results in a filled valence band as seen in the graph of E vs k_f (Figure 1-7) and an increased bandgap (E_G). Consequently poly(acetylene) is an intrinsically insulating material.[29]

Figure 1-7 Insulating poly(acetylene)[28]

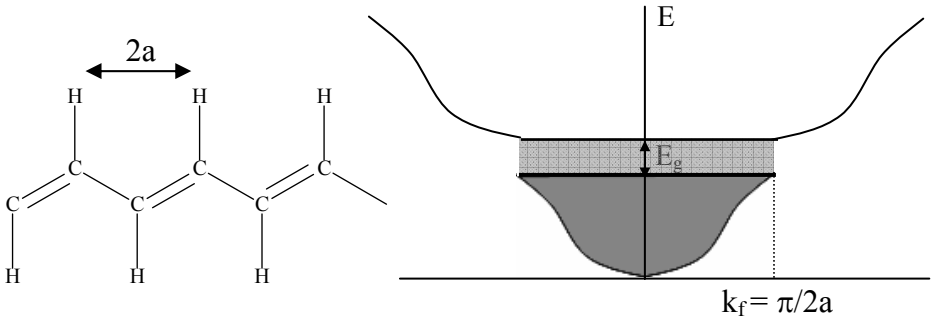

In 1977 MacDiarmid, Heeger and Shirakawa[26] discovered that poly(acetylene), when doped with iodine, became conducting, with a conductivity approaching that of metals

like copper. It was found that doping other conjugated organic polymers could have a huge impact on their conductivity as well, sometimes increasing the conductivity by a factor of twelve. This result required a new look at band theory to explain how doping had such a large impact on the conductivity of organic conjugated polymers.

1.3.2 Doped polymer conductivity

Doping a conjugated polymer either removes electrons (p-type) from the top of the valence band or adds electrons (n-type) to the bottom of the conduction band. It was thought that these unpaired electrons might be the basis of the observed conductivity. However, when doping levels were raised, instead of increasing the number of unpaired electrons, EPR experiments showed that the number of unpaired electrons actually decreased. This pointed to spinless charge carriers being involved in the conductivity rather than unpaired electrons, a result that did not fit with classical band theory. An understanding of this observation was obtained by resorting to theories and terminology used primarily in solid state physics. In a conjugated polymer, when an electron is removed from the top of the valence band, a vacancy (radical cation) is created which causes a bond deformation over a localized area. The energy level associated with this destabilized region has an energy inside of the bandgap. Using the language of solid-state physics this is called a polaron.[29] If another electron is removed from a polymer which already contains a polaron, it can be removed either from a different area of the polymer to make two polarons or the already unpaired electron can be removed. If the polymer is symmetrical, for example relative to the cation in poly(acetylene), if the unpaired electron is removed or if two polarons combine a soliton is formed. If the polymer is unsymmetrical, for example relative to the cation in poly(thiophene) (i.e on

one side of the charge the thiophenes are aromatic, on the other side quinoid), then a bipolaron is formed (Figure 1-8).

Figure 1-8 Formation of polarons, bipolarons and solitons

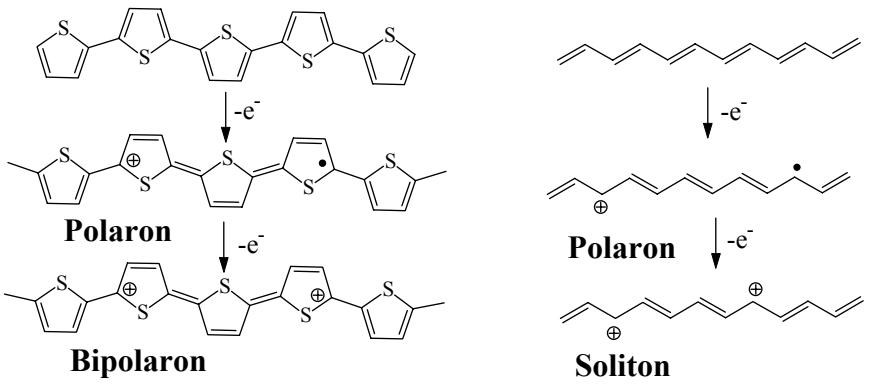

At low doping levels typically polarons are formed, but as the doping levels increase, bipolarons or solitons become predominant. As the number of bipolarons or solitons increases, their energy levels begin to overlap forming bands inside of the bandgap (Figure 1-9).

Figure 1-9 Band structure of compounds with polarons, bipolarons and solitons

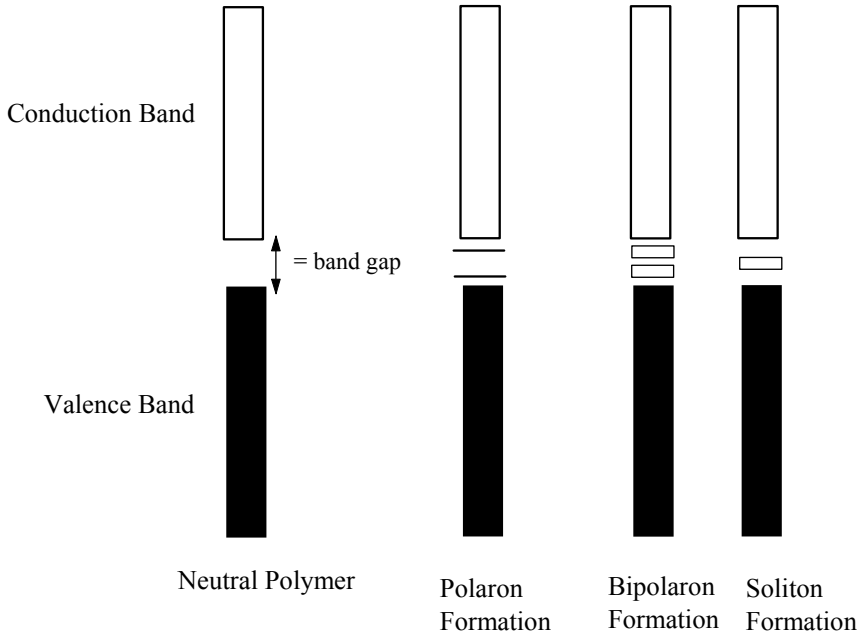

Electrons can easily move from the valence band to the bipolaron and soliton energy bands, allowing electrons to flow through the material, producing a conducting polymer.

1.3.3 Types of conducting polymers

Poly(acetylene), the first highly conducting organic polymer discovered, has a conductivity in the neutral *cis* and neutral *trans* forms of 10^{-10} and 10^{-5} S/cm. However when doped, the conductivity can increase to 10^{3} S/cm.[30] Unfortunately the use of poly(acetylene) is limited by its poor solubility and instability in air. Several new classes of conducting polymers have been developed and studied in order to overcome these problems. The most important and widely studied of these polymers are poly(thiophene), poly(aniline) and poly(pyrrole) (Figure 1-10).[31]

Figure 1-10 Poly(thiophene), poly(aniline) and poly(pyyrole)

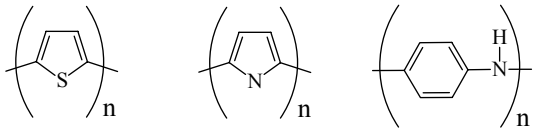

Poly(thiophene) Poly(pyrrole) Poly(aniline)

Poly(thiophene) is one of the most widely studied conducting polymers because of its structural versatility, electrical properties and environmental stability in both its doped and undoped forms. It can also be easily modified in the β-position through standard organic chemistry techniques which facilitates the tailoring of the oligomer and polymer properties. This has proved to be quite important as oligothiophenes with more than seven thiophene units are virtually insoluble in organic solvents.[32] Attaching alkyl groups in the β-position allows longer oligomers and polymers to be dissolved in organic solvents, which greatly facilitates the characterization and processing of these compounds.

1.3.4 Inter and intra chain conductivity

There are two mechanisms for charge to flow through a conducting polymer material. The charge can move along the backbone of a single polymer chain and it can move by hopping between polymer chains. Oligomers have been shown to conduct electricity across gaps much larger than the length of single oligomers, indicating that the interchain hopping of charge is an important component of conductivity. It has also been shown that conductivity occurs due to charge moving along the backbone of a single oligomer,[33] and that like in the macroscopic case, this conductivity scaled with the number of individual "wires" that were connected.[34] Both inter and intra chain conductivity are probably important and play a role in the total conductivity of a polymer.

1.4 Electrochemistry techniques

The focus of electrochemistry is on the movement of charge, the processes and factors which affect the movement of charge, and particularly how electrical quantities like current, potential and charge effect and are affected by chemical parameters. The study of these processes is usually performed using an electrochemical cell. Because it is impossible to measure a potential using only one electrode, at least two electrodes are employed in an electrochemical cell. These electodes are connected by a contacting sample or electrolyte solution. The electrochemical cell can be divided into two half cells and the potential for each half cell is governed by the Nernst equation. For a simple redox reaction (1-1)

$$\mathbf{Ox} + n\,\mathbf{e^-} \rightleftharpoons \mathbf{Re} \qquad \textbf{1-1}$$

where Ox and Re are the oxidized and reduced forms of the redox couple and *n* is the number of electrons transferred, it has the form:

$$\mathbf{E} = \mathbf{E^o} + \frac{\mathbf{RT}}{\mathbf{nF}} \ln \frac{\mathbf{[Ox]}}{\mathbf{[Re]}} \qquad \textbf{1-2}$$

where E is the potential, E^o is the standard potential of the redox couple, R is the gas constant (8.3145 J mol^{-1} K^{-1}), T is the temperature (K), F is the Faraday constant (96500 C mol^{-1}) and [Ox] and [Re] are the concentration of the redox active species at the surface of the electrode. Experimentally the cell potential is measured as the difference between the half cell potential of the working electrode and the half cell potential of the reference electrode. In dynamic electrochemistry, the system is disturbed by controlling either the current or the potential and monitoring the other quantity. Often a three electrode system

is used (Figure 1-11). In this arrangement a potentiostat is used to control the voltage (ΔE) between the working electrode (WE) and the reference electrode (RE) while simultaneously measuring the current (*i)* flowing between the working electrode and the counter electrode (CE).

Figure 1-11 A potentiostat in a three electrode arrangement

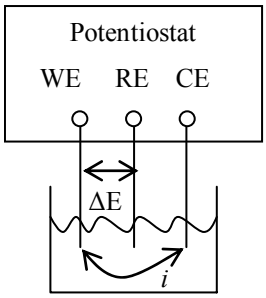

When using a three electrode electrochemical cell, the control over and measurement of the potential is very important, so it is vital to use a reference electrode with an equilibrium half cell that has a constant potential. The normal hydrogen electrode (NHE), although it is by definition the reference for electrode potentials,[35] is not a very practical reference electrode. Usually for practical reasons a metal and a soluble salt of the metal are used. Commonly used reference electrodes of this type include the saturated calomel electrode (SCE) (Hg/Hg_2Cl_2/saturated KCl in H_2O) which has a potential of E = 242 mV vs NHE (25 ^{o}C) and (Ag/AgCl/sat. KCl in H_2O) which has a potential of E = 197 mV vs NHE (25^{o}C).[35] In organic electrochemistry because of the variety of conditions and solvents used, often an internal standard with a known redox potential such as the ferrocene/ferrocenium couple (0.46V vs SCE, CH_2Cl_2, $TBAPF_6$)[36] is used to calibrate the reference electrode. This helps to facilitates the comparison between the system being studied and other electrochemical data.[36]

1.4.1 Cyclic voltammetry

Cyclic voltammetry is one of the most widely used methods to study the redox potentials of a molecule. Cyclic voltammetry is a linear sweep technique where the potential of the working electrode is swept from an initial voltage E_i up to a switching potential E_s at which point the scan direction is reversed (Figure 1-12-A). The current is measured and plotted against the potential (Figure 1-12-B) and the resulting voltammogram can be used to determine the potentials at which redox processes occur. Thus values for the peak anodic potential E_{pa} and the peak cathodic potential E_{pc} can be obtained.

Figure 1-12 Cyclic voltammetry

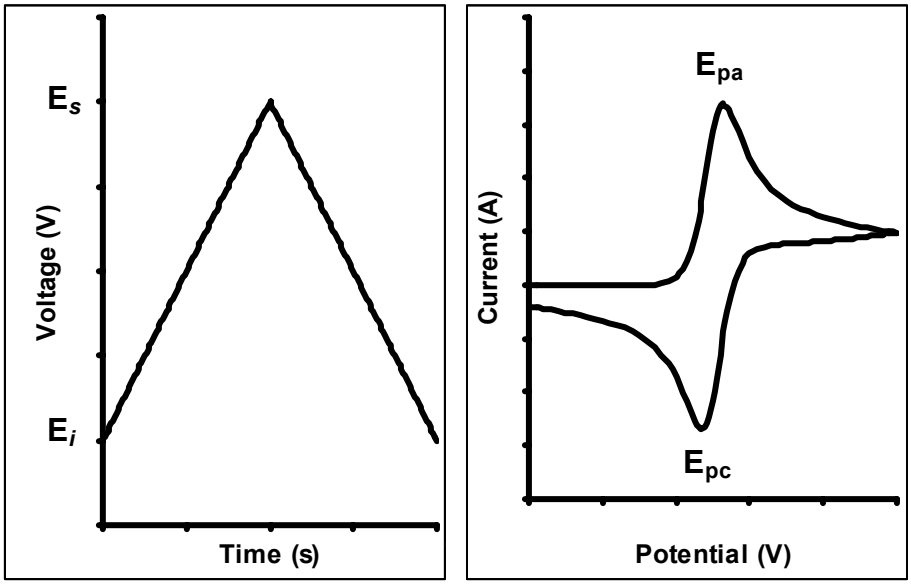

A **B**

Not only can the resulting "electrochemical spectra" be used to determine the potentials at which redox processes occur, it also can be used to monitor (over several cycles) electrodeposition or in the case of conducting polymers electropolymerization. Also by

varying the scan rate and monitoring the response over the different timescales, information can be obtained about the reversibility of the redox processes and chemical reactions that might be coupled to the redox process. For a reversible couple the difference between the peak potentials at 298 K is 0.059 V /*n* where *n* is the number of electrons transferred (1-3) and the peak current ratio of i_{pa}/i_{pc} is equal to one.

$$\Delta E_p = E_{pa} - E_{pc} = \frac{0.059}{n} V \qquad \textbf{1-3}$$

The peak current for a reversible couple is given by the Randles-Sevcik equation (1-4):

$$I_p = (2.69 \times 10^5)\, n^{3/2} A C D^{1/2} \nu^{1/2} \qquad \textbf{1-4}$$

where *n* is the number of electrons, A is the electrode area (cm^2), C is the concentration (mol cm^{-3}), D is the diffusion coefficient ($cm^2\ s^{-1}$) and ν is the scan rate ($V\ s^{-1}$). Irreversible or quasi-reversible systems often occur as a result of chemical reactions which take place during the redox process, adsorption processes or sluggish electron exchange.

1.4.2 Interdigitated microelectrodes

Interdigitated microelectrodes (IDA) are an arrangement of parallel microelectrodes. The electrode fingers are arranged in two sets where each set of fingers is connected to a separate electrode (Figure 1-13).

Figure 1-13 Interdigitated microelectrodes

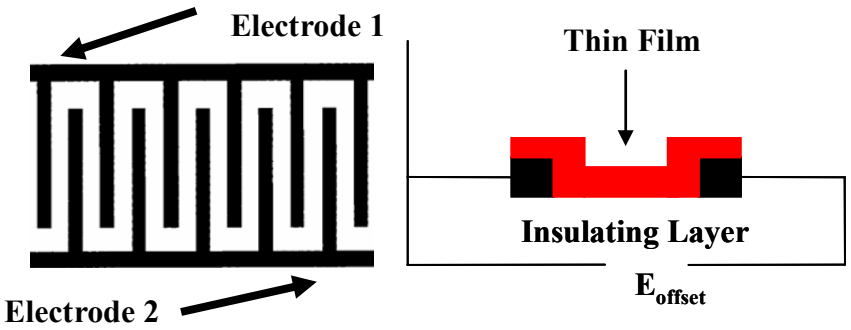

"Top View of microelectrode" "Side view with a thin film "

Microelectrodes have a number of advantages. Because the electrode area is small the film area and thickness applied to the electrode is reduced which allows higher sensitivity and greater potential control, especially in materials with low conductivity and at faster scan rates.[37] Interdigitated microelectrodes have been shown by Wrighton and co-workers to be useful for determining *in-situ* conductivity measurements of conducting polymer films.[37-39]

1.5 Photoswitching electrical properties

The idea of using a photochromic compound to control electrical conductivity in a conducting oligomer or polymer was first proposed by Lehn *et al* .[40] They then went on to attach bispyridinium functional groups on either side of the dithienylethene photoswitch as the first step towards a prototype of a light triggered switchable molecular wire (Scheme 1-7).

Scheme 1-7 Lehn's bispyridinium functionalized photoswitch

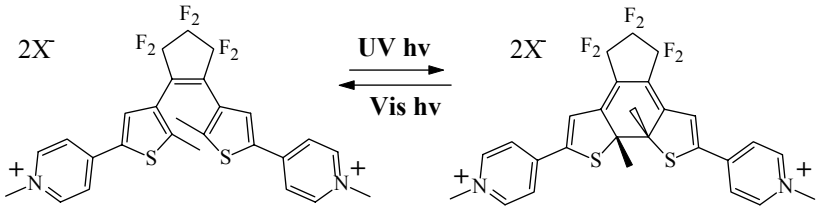

15' **15**

They found that the cyclic voltammogram of the closed ring isomer **15** had a reductive process at -230 mV (versus SCE) while the open form **15'** had a no electrochemical processes in the -600 to +600 mV region.[40] This indicated that the electron delocalisation found in the closed form was interrupted by the use of visible light to open the switch.

1.5.1 Attaching molecular switches to wires

If a photoswitch is to be used to control the electrical conductivity in a wire the way in which the switch is attached to the wire is obviously important. As conductivity in a molecular wire is associated with extended conjugation, the switch should ideally maintain a linear π-conjugated path with the wire.[41] This can be done by either attaching the switch directly to a conducting polymer or using a conjugated spacer in between the switch and the wire.

The functional groups attached to a photoswitch can have dramatic effects on the photoswitching ability. Ideally the attachment of molecular wires to the switch will have little or no negative effects on the functioning of the switch. This was not the case when oligothiophene wires were attached to the dithienylethene switch. Irie[42] found that the ring opening quantum yield of the dithienylethene switch dramatically decreased as the number of thiophene units increased. The addition of oligothiophenes led to extended π-conjugation from the oligothiophenes into the switch. This caused a decrease in the anti-

bonding character of the photogenerated single bond in the excited singlet state which resulted in a drop in the ring opening quantum yield. In order to circumvent this problem Matsuda[43] attached oligothiophenes on only one side of the dithienylethene switch. Unfortunately once again the photoswitching properties of the switch decreased as the length of the thiophene oligomers attached increased. In contrast, attaching thiophenes to the DHP photoswitch **19** was found to cause a small increase in the ring-opening rate.[44]

1.5.2 Electrical conductivity switching using the dithienylethene photoswitch

Irie incorporated the diarylethene photoswitch directly into the main chain of poly(9,9-dialkylfluorene)[45] and found that the electrical conductivity of the polymer containing the photoswitch increased from 5.3×10^{-13} S $\cdot cm^{-1}$ in the open form **16'** to 1.2×10^{-12} S$\cdot cm^{-1}$ in the closed form **16** (Scheme 1-8).

Scheme 1-8 Irie's dialkylfluorene dithienylethene switch

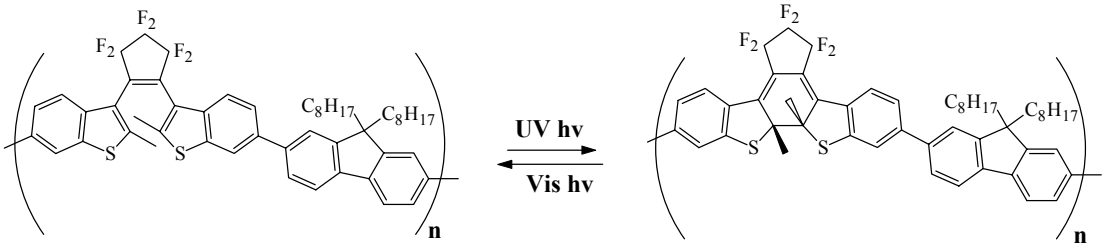

16' **16**

This albeit small change in the electrical conductivity, demonstrated that a change in π-conjugation could affect the conductivity of the material. They also found that the conductivity of the closed form increased from 1.2×10^{-12} S$\cdot cm^{-1}$ to 1.4×10^{-8} S$\cdot cm^{-1}$ when the polymer was doped with iodine. Unfortunately photochromism was not observed in the doped state.[45]

Ko *et al.*[46] synthesized a dyad and a polymer containing dithienylethene and quinoline components (Scheme 1-9).

Scheme 1-9 Dithienylethene quinoline polymer

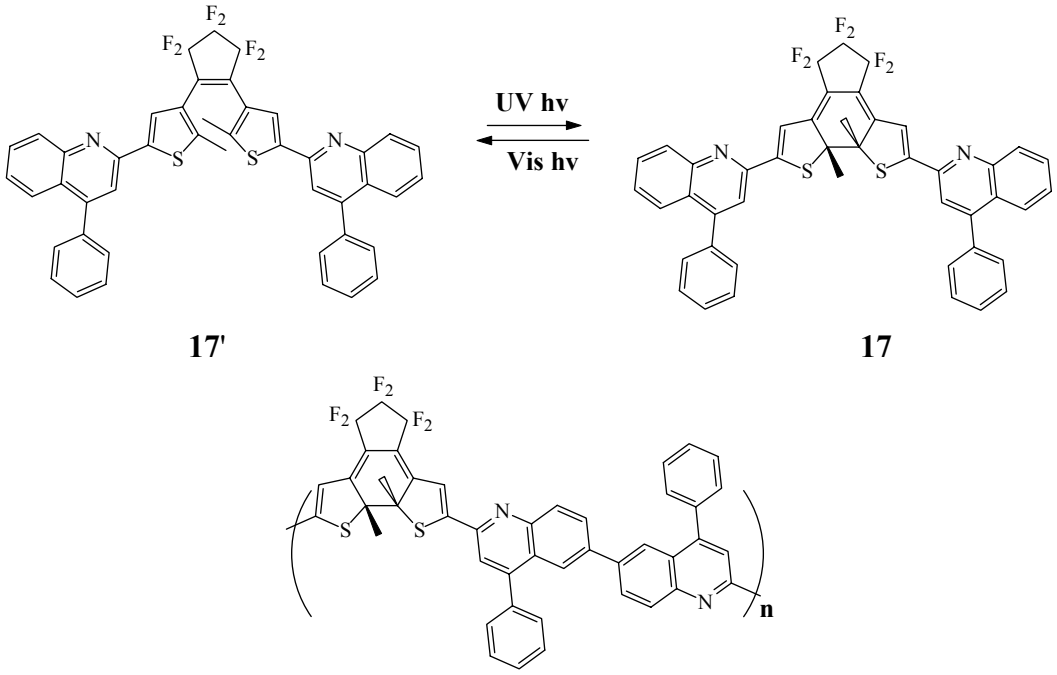

17' **17**

18

They then sandwiched the dyad and the polymer in a polystyrene matrix between ITO coated glass and a vacuum deposited gold electrode and measured the current as a function of voltage. They found that although the current of both the open **18'** and the closed form **18** went up as the voltage increased from 0 to 2V, the slope of the closed form was much steeper than that of the open form. As a result, the closed form of the dyad under an applied voltage of 2V, had a current which was 3.6 times that of the open form, and in the polymer at 2V the current in the closed form was 2 times that of the open form.[46]

1.5.3 Electrical conductivity switching using dihydropyrenes

Dihydropyrenes have also been incorporated into a conducting polymer with the goal of being able to change the conductivity of the polymer by opening and closing the dihydropyrene switch.[44] The dihydropyrene photoswitch is a more rigid photoswitch than the dithienylethene analogues which could be advantageous, especially when used in the solid state. This photoswitch was incorporated directly into a poly(thiophene) polymer (Scheme 1-10) and optoelectronic redox switching was observed by the increase in the current of the oxidation peak upon going from the open to the closed form.

Scheme 1-10 A DHP poly(thiophene) polymer

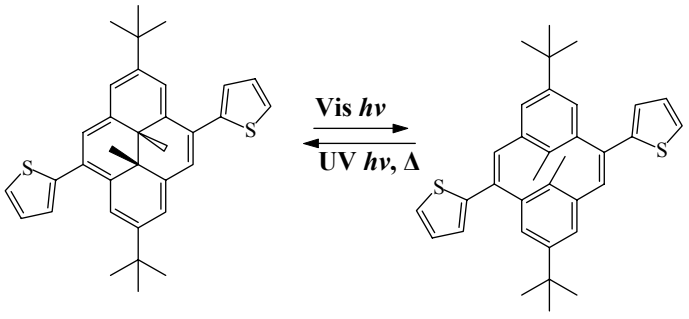

19 **19'**

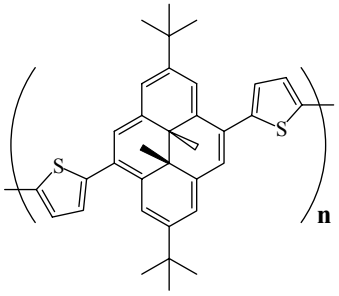

20

Unfortunately because the polymer **20** was soluble in all the organic electrolyte solutions tested, the effect on the electrical conductivity of switching between the open and the closed form in the solid state was not obtained.

1.5.4 Single molecule photoswitchable electrical conductivity

Recently it has been shown that the ability of a photoswitch to change electrical conductivity can be observed at the level of a single molecule. This work is important because not only is electrical switching on the single molecule level the pinnacle of chemical miniaturization, but it also is a first step towards the interfacing of macroscopic wires and switches with the molecular ones being investigated. Dulic[47] used a mechanically controlled break junction technique to control the separation of two gold electrodes and attached across these electrodes a thiol terminated dithienylethene switch with thiophenes on either side (Scheme 1-11).

Scheme 1-11 Dulic's thiophene terminated switch

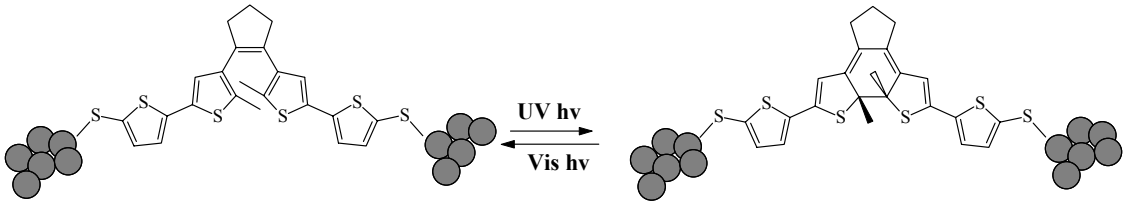

21' **21**

They found that when they measured an IV curve of the closed form of **21** and then opened the switch by irradiation with visible light and re-measured the IV curve that there was an increase in resistance. This indicated that the switch was modulating the conductivity. Unfortunately once the switch was attached to the gold they were unable to close the switch by irradiating it with UV light.[47] This was attributed to the mixing of the molecular electronic excited states of the switch with the gold states. This mixing caused quenching of the excited open state to occur which inhibited ring closure. Interestingly if the thiophene linker was replaced with a phenyl linker then reversible opening and closing was observed.[48] Lindsay used a modified break junction technique[49] where

dithiolated dithienylethene based molecules **22** were absorbed onto a gold surface and then a gold probe was repeatedly pushed onto a gold surface and pulled out while recording the current from the molecules transiently trapped in between (Figure 1-14).[50]

Figure 1-14 Lindsay's single molecule switch

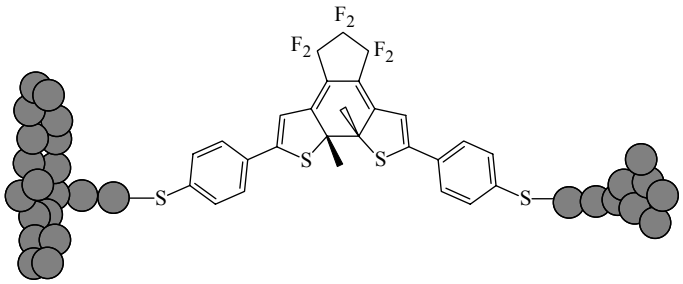

22

The resistance of a single molecule was thus obtained to be 526 +/- 90 MΩ for the open form and 4 +/-1 MΩ in the closed form.[50] They also found that they were able to open and close the photoswitches while attached to gold, although they did observe lower quantum yields of isomerization compared to that observed in solution.

Nuckolls *et al* [51] synthesized amino functionalized dithienylethene switches (Figure 1-15) and attached them to single walled carbon nanotubes via an amide bond.

Figure 1-15 Nuckolls amino functionalized dithienylethene photoswitch

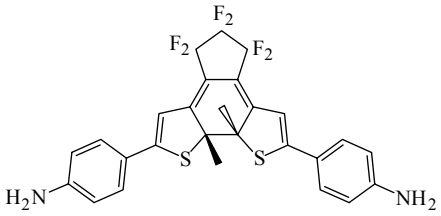

23

They found that the switches could be closed when irradiated with UV light leading to an increase in conductivity. Unfortunately when attached to the nanotubes the switches could not be opened when irradiated with visible light. This inability to photo-open was

hypothesized to be due to the extended conjugation from the carbon nanotube into the switch.[51]

1.6 Research objectives

With the development of more efficient synthetic methodologies and improved photoswitching properties for the dimethyldihydropyrene photoswitches, investigations which explore how to exploit the photoswitching ability of these switches are much more attractive. When the DHP switch is in the planar closed conformation there is extended π conjugation across the backbone of the switch. When the switch is opened to the cyclophanediene (CPD) form, a change in the conformation of the molecule occurs, resulting in the loss of this extended π conjugation (Figure 1-16).

Figure 1-16 Conjugation changes when opening and closing the DHP photoswitch

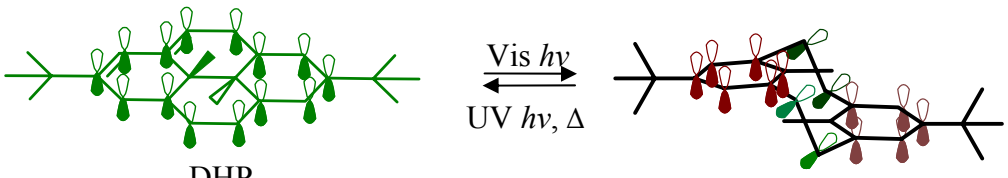

DHP
Extended conjugation

11

CPD
Broken conjugation

11'

If the DHP photoswitch is inserted into the backbone of a highly conjugated electrically conducting oligomer or polymer such as poly(thiophene), the conjugation change that occurs when the switch is opened or closed could be used to control electrical conductivity. When the switch is in the closed form there will be extended π conjugation across the backbone of the switch leading to greater electrical conductivity. When the

switch is opened the extended π conjugation will be broken leading to a drop in the electrical conductivity (Figure 1-17).

Figure 1-17 Change in conjugation along the backbone of a thiophene oligomer when the DHP switch is opened or closed

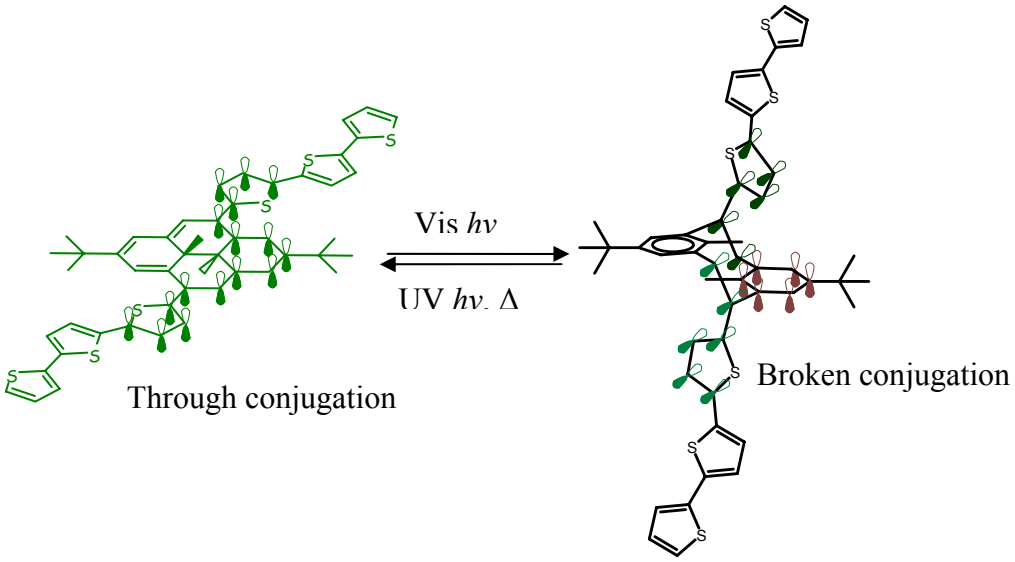

The DHP photoswitch has a number of advantages over other photochromic molecules for this type of application. Typically the DHP photoswitches can be completely opened and closed while other photochromic compounds often have photostationary states which prevent the complete opening and closing of the switch.[52] The DHP photoswitch is a very rigid photoswitch with a small volume change between the open and the closed form,[44] properties which will be advantageous when switching in the solid state, especially when the switch is attached into the backbone of a conjugated oligomer or polymer. Finally, if conjugated oligomers are attached on opposite sides of the switch, photo-opening and closing can occur with very little effect on the position and orientation of these conjugated oligomers which should facilitate switching in the solid state.

Initial studies where the DHP switch was inserted into the backbone of poly(thiophene) showed potential for conductivity changes.[44] Unfortunately the photo-opening properties of the parent DHP photoswitch **11** used are poor, requiring hours of visible light irradiation to open. This made examining the properties of this system difficult. Also the compounds synthesized had poor solubility characteristics which limited the electrochemical studies that could be performed.[44]

The goal of this project was to insert dimethyldihydropyrene photoswitches with improved photoswitching properties directly into, or via conjugated spacers, oligo and polymeric thiophene based molecular wires, and study the photoswitching and conductivity properties of these molecular systems. These systems would incorporate a number of design requirements such as: 1) solubility in organic solvents to allow processability, 2) insolubility in an organic electrolytic solvent to facilitate the study of the compounds in thin films by common electrochemical techniques and 3) environmental stability.

We were particularly interested in using the BDHP photoswitch and DHP photoswitches containing carbonyl functional groups as both switches have been shown to have improved photo-opening properties.[22,25] Ideally the oligothiophenes would be attached on opposite sides of the switch in order to take advantage of the large conjugation change across the backbone of the switch when the switch is opened or closed. In the case of carbonyl functionalized DHP photoswitches, in order to maximize the coplanarity of oligothiophenes attached to the switch, ideally the carbonyl would be attached in a position that would minimize steric interference with the oligothiophenes. (Figure 1-18).

Figure 1-18 Positioning of functional groups on the photoswitches to maximize the change in conjugation between the open and the closed form

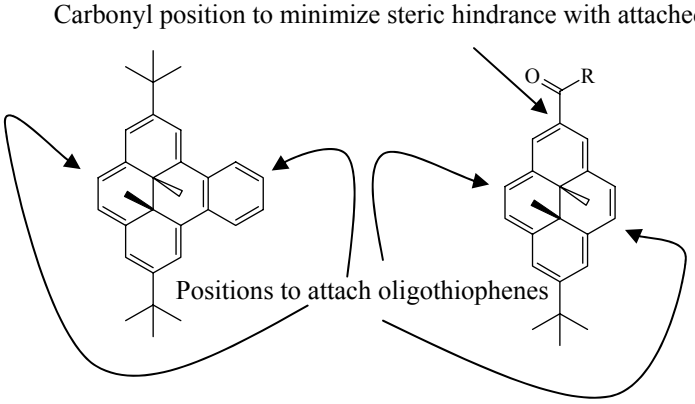

We also wanted to attach oligothiophenes with a variety of different lengths in order to study the effect the increased conjugation had on the photoswitching properties of the switch and the ability of the switch to modify the conjugation in these oligomers. Conductivity testing would then be performed on compounds that could easily be switched and which exhibited large conjugation changes between the open and the closed forms.

Chapter Two: Synthesis

2.1 Attaching oligothiophenes to the benzodihydropyrene photoswitch

The benzodihydropyrene **12** (BDHP) photoswitch has improved photoswitching properties compared to the parent dihydropyrene photoswitch and so was an attractive candidate to insert into an oligothiophene "molecular wire". In order to insert BDHP into a molecular wire, a consideration of the reactivity of BDHP was needed. The reactive positions of BDHP are the 4 and 5 positions, which are both on the same side of the molecule (Scheme 2-1). Attaching oligomeric thiophenes to these positions does not take advantage of the large conjugation changes that occur across the molecule in the open and the closed form.

Scheme 2-1 Reactive positions of BDHP

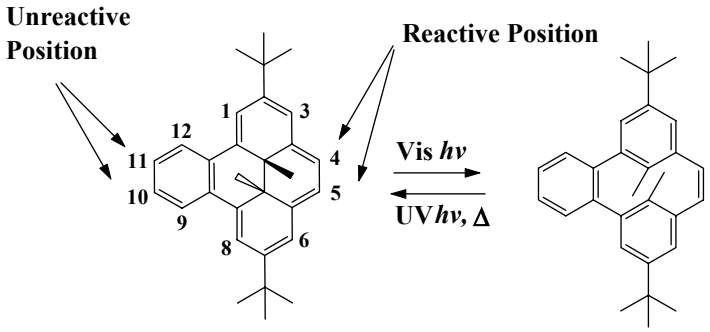

In order to take advantage of the large change in conjugation that results from switching BDHP between the open and the closed forms, the molecular wires needed to be connected to BDHP in the 4/5 and 10/11 positions. Unfortunately the 10/11 positions are not reactive, and so in order to attach the molecular wires to these positions a functional group handle needed to be put in place during an earlier stage of the synthesis.

2.1.1 Justification for putting thiophenes on the same side of BDHP

It was however of interest to attach oligothiophenes on the same side of BDHP in order to see the effect of switching on the oligothiophene conjugation when they were attached through a simple ethylene spacer on the side of the switch. Changes in the conjugation although probably small are expected due to the different orientation of the thiophene oligomers between the open and the closed form. In the closed form it is sterically unfavourable for the π-faces of two thiophenes attached on the same side of BDHP to be planar with the BDHP π-face. In the open form this can be somewhat relaxed and so might allow for increased conjugation (Scheme 2-2).

Scheme 2-2 Thiophenes on the same side of BDHP

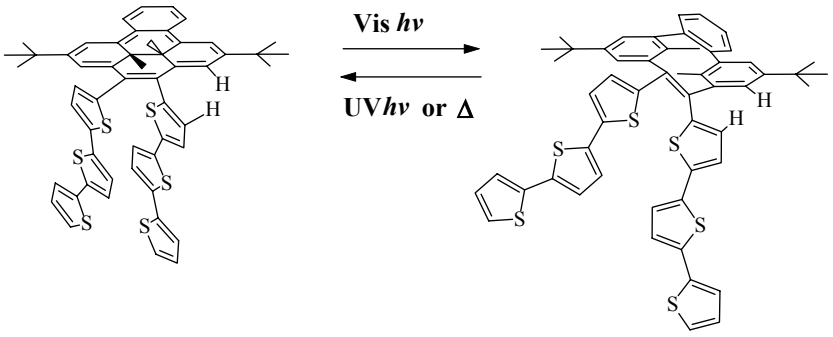

2.2 Synthesis of BDHP with thiophenes on the same side

One way to introduce thiophene oligomers on the same side of BDHP is to dibrominate and then use a palladium catalyzed coupling reaction to add the oligomers.

2.2.1 Bromination of BDHP

Ward[53] reported that when BDHP **12** is dibrominated using NBS at 0°C in dry CH_2Cl_2 and dry DMF, a modest yield (50%) of the desired product **24** was obtained (Scheme 2-3). In order to isolate this product, four chromatography columns were required to remove closely eluting fluorescent biproducts. These fluorescent biproducts

by TLC appeared slightly above and below the desired product which made separation difficult.

Scheme 2-3 Synthesis of the dibromide 24

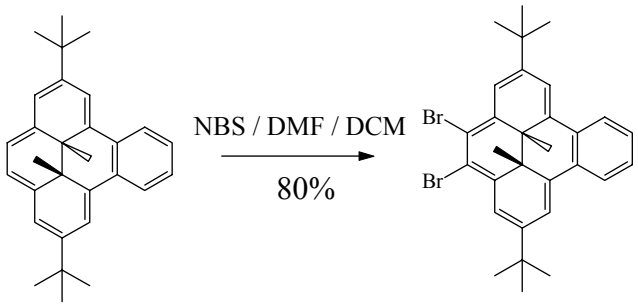

12 **24**

The fact that these products were fluorescent and showed no upfield signal around -1 ppm in the ^{1}H NMR spectrum indicated that the internal methyl groups had migrated. When the reaction was carried out at -78^{o}C, no reaction was observed. Slowly warming the solution from -78^{o}C resulted in the dark red color of the solution rapidly changing to a light red as the solution temperature approached 0^{o}C. This color change indicated methyl migration was occurring, and after work up ^{1}H NMR spectroscopy indicated this to be the case by the loss of the internal methyl signals around -1 ppm. If a reaction temperature of 25^{o}C was used, the amount of fluorescent side products was found to decrease significantly and could be removed by a single chromatography column. Using refluxing dry DCM on a scale of 250 mg or less and adding the NBS in a minimum of dry DMF gave up to 80% of the desired product **24** after one chromatography column with virtually no close running fluorescent biproducts.

2.2.2 Coupling of oligothiophenes

With a more reliable and efficient synthesis of the dibromide **24** in hand, oligomeric thiophenes could then be added using palladium catalyzed coupling reactions. A Suzuki coupling reaction using commercially available 2-thiopheneboronic acid and Na_2CO_3 as the base with the catalyst $Pd(PPh_3)_4$ gave **25** in 60-90% yield (Scheme 2-4).

Scheme 2-4 Coupling thiophene to 24

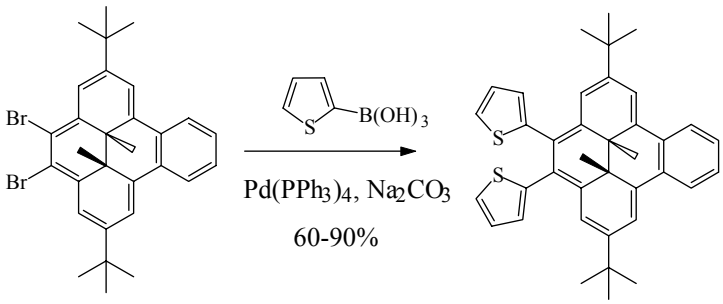

24 **25**

The reaction was quite sluggish, requiring 48 or more hours to go to completion. Palladium catalyzed coupling reactions are well known to proceed more slowly when electron rich aryl halides are used because of a slow oxidative addition step. DHP's are very electron rich, so it is not surprising that the coupling reaction is slow, especially for the addition of the second thiophene molecule which is sterically hindered. When the coupling reaction was tried with bithiophene, very low yields were observed. Kumada coupling, which involved making the Grignard from 2-bromobithiophene and then adding this to a solution containing the dibromide **24** and the catalyst 1,3 bis(diphenylphosphino)propane nickel (II) chloride, was tried, but virtually no product was observed after stirring for 2 days, and a virtually quantitative amount of the dibromide starting material **24** was recovered. A Stille coupling using $Pd(PPh_3)_4$ was tried next and product **26** could be observed to be forming after 12 hours by TLC. But

even after almost 5 days, a significant amount of starting material and the mono-addition product remained. A similar result occurred when the reaction was carried out using the terthienyl-tributylstannane **108** to obtain the terthienyl product **27**. One advantage of the Stille coupling over the Kumada and Suzuki couplings was the ease in which the reaction could be monitored by TLC for the presence of both the bromide and tributyltin containing starting materials. For the Suzuki coupling, the polarity of the boronic acid made monitoring of both components by TLC difficult and with the Kumada coupling, the Grignard decomposed. If the coupling reaction was sluggish as a result of slow oxidative addition due to the electron rich BDHP then it was thought a more active catalyst system might improve the yield. $Pd_2(dba)_3$ along with the dppf ligand was used and after 4 days a 45% yield of the di-addition product was obtained. By using a minimum of solvent this yield could be increased to 60% over 4 days, with the remainder being a mixture of starting material and the mono-adduct, both of which could be recycled in subsequent coupling reactions (Scheme 2-5).

Scheme 2-5 Coupling thiophenes onto the same side of BDHP

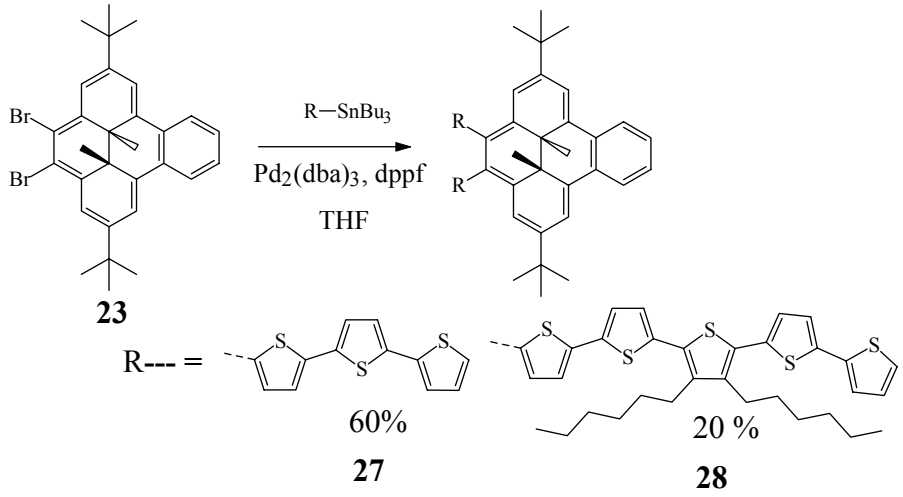

The reaction could also be carried out using a longer thiophene chain **28**. For these compounds, both internal methyl signals in the ^{1}H NMR spectrum appeared at -0.87 ppm and the *t*-butyl peaks were a singlet at 1.36 ppm. All of the aromatic peaks in the ^{1}H NMR spectrum for **27** could be assigned. For **28** all of the BDHP aromatic protons could be assigned, but due to overlap of some of the thiophene peaks, not all the thiophene protons could be fully assigned. Mass spectrometry gave the correct molecular weight of *m/z* 886 for terthienyl **27** and 1536 for quinquethienyl **28**.

Another possible approach to improve the coupling yields is to reverse the molecular functionality. In exploration of this approach, a tributyltin functional group was added to DHP by lithiating the bromide **31** with *n*-BuLi and adding tributyltin chloride. The desired product **32** was obtained in an 80% yield after column chromatography on alumina (Scheme 2-6).

Scheme 2-6 Addition of tributyltin to DHP

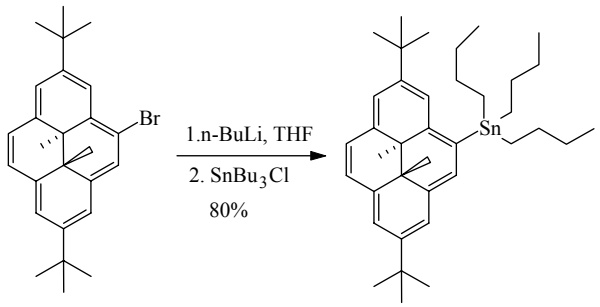

31 **32**

The identity of the product **32** was confirmed by the characteristic internal methyl groups of the dihydropyrene at -3.61 ppm, and the four peaks for the butyl groups on tin in the ^{1}H NMR spectrum at ~1.63, 1.63-1.58, 1.44 and 0.86 ppm. Confirmation of a mono-substituted DHP was obtained from the six aromatic peaks in the ^{1}H NMR spectrum corresponding to seven aromatic protons. Mass spectrometry confirmed these results giving the correct mass at *m/z* 634. The synthesis of **32** demonstrated that tributyltin functional groups could be successfully added to DHP and these molecules have potential to be used in a variety of Stille coupling reactions. With the successful development of Stille coupling reactions using the DHP bromides, the chemistry of these tributyltin functionalized DHP molecules was not investigated further.

2.2.3 Extension of the thiophene chain

In order to extend the thiophene chains attached to the BDHP molecule, it was necessary to add a functional group to the ends of the thiophene oligomers. Bromination of the thiophene modified BDHP **27** was attempted using NBS. This resulted in the decomposition of the starting material as seen by the loss of the internal methyl peaks at -1 ppm. Since bromination was unsuccessful, it was thought lithiation of the terminal thiophenes might be successful. Lithiation could be followed by a reaction with

tributyltin chloride to set up the molecule for a subsequent Stille coupling reaction. To this end, *n*-BuLi was added to a solution of **27** followed by tributyltin chloride (Scheme 2-7). By TLC two new fast moving spots with respect to the starting material were observed. After chromatography these were identified to be the mono-**33** and di-**34** tributyltin adducts.

Scheme 2-7 Addition of tributyltin substituents to terminal thiophenes

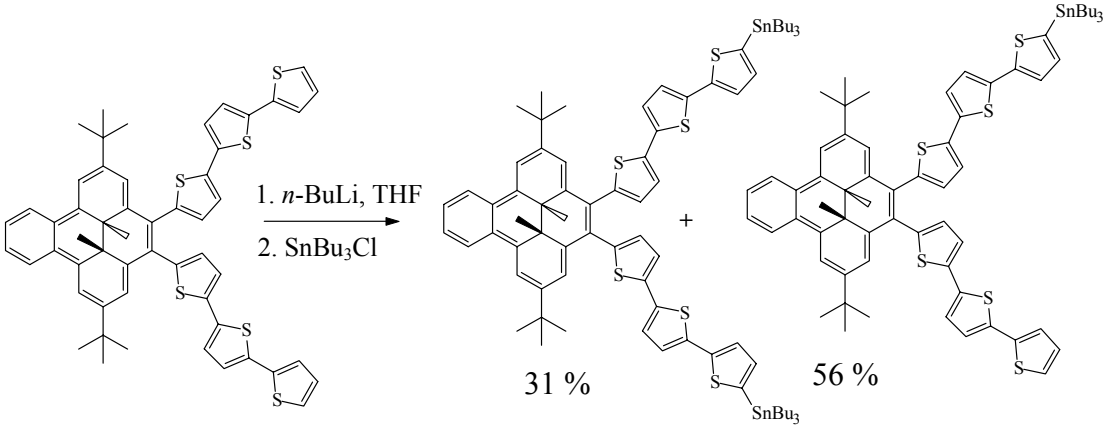

27 **34** **33**

The structures of **33** and **34** were determined by NMR spectroscopy. The ^{1}H NMR spectrum for the BDHP part of the molecule was virtually identical for both **33** and **34**. For **34** because of symmetry there were only 6 thiophene peaks with a total integration of 12. All of these peaks were doublets indicating that the tributyl tin functional groups were located in the desired position at the end of the thiophene chain. For **33** the lack of symmetry gave rise to 13 separate thiophene peaks, which could all be assigned. The butyl peaks on the tin also indicated the presence of mono **33** and di **34** addition products as the butyl peaks for **34** had double the integration of the butyl peaks for **33**. The internal methyl protons for both compounds appeared at δ -0.88. All of the protons could be assigned in the ^{1}H NMR spectrum and virtually all of the carbons in the ^{13}C NMR

spectrum could be assigned. Mass spectrometry confirmed the structure giving the correct molecular weight of *m/z* 1176 for the mono-addition product **33** and 1465 for the di-addition product **34**. Unfortunately, even if less than one equivalent of *n*-BuLi was added, a mixture of the starting material **27**, and the products **33** and **34** was observed, with **33** being the major product**.** If more than two equivalents of *n*-BuLi were added, there remained some starting material along with **33** and **34**, with **34** being the major product. Fortunately these products could be separated by column chromatography, provided the column was deactivated using 1% triethylamine in the eluting solvent. If the column was not deactivated with triethylamine, the tributyltin functional groups were lost and the starting material **27** recovered. The tin functionalized thiophene oligomers could then be reacted with 2,5-dibromo-3,4-dihexylthiophene **35** in a Stille coupling reaction. When an excess of **35** was used the desired product **36** was obtained in a 58% yield along with a small amount of larger oligomer and polymer products (Scheme 2-8).

Scheme 2-8 Addition of bromodihexylthiophene

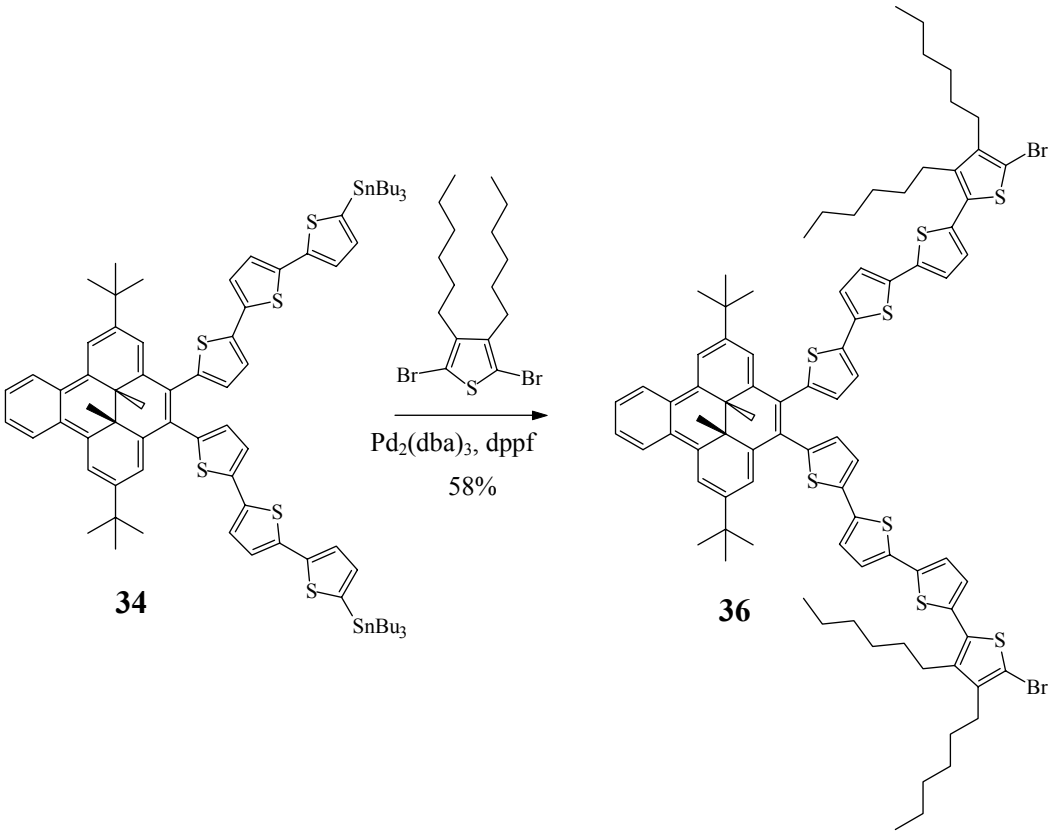

In the ^{1}H NMR spectrum all of the aromatic signals of the BDHP portion of **36** could be assigned, and all of the thiophene peaks were accounted for. There were two different methylene triplets with integrations of 4 protons each from the methylene groups of the hexyl chain closest to the thiophene ring. The most upfield of these two triplets at δ 2.55 was on the bromide side of the terminal thiophene while the more downfield triplet at δ 2.70 was on the BDHP side. The rest of the hexyl peaks were multiplets with no distinction as to which side of the hexyl chain they were on. The *t*-butyl peaks were a singlet at δ 1.37 and the internal methyls were a singlet at δ -0.86. In the ^{13}C NMR spectrum all of the carbons could be accounted for and mass spectrometry gave the correct molecular weight of *m/z* 1546. It was found that the hexyl chains made this

compound completely insoluble in acetonitrile. This was important as it was a requirement for conducting some of the electrochemical studies. With a bromide at each end, this molecule was set up for further palladium catalyzed couplings to make larger oligomers.

2.3 Synthesis of BDHP with oligothiophenes on opposite sides

Simple BDHP does not have reactivity in the 10 or 11 position, so in order to attach oligomeric thiophenes to this position, a functional group handle must be put in place. The nature of this functional group handle is very important. The best option would be for the functional group handle to allow a direct connection between the switch and the wire. However if a spacer is introduced between the switch and the wire it is important that the conjugation between the two components is maintained. In order for conjugation to be maintained, the atoms that form a direct link between the wire and the switch can only have sp or sp_2 hybridization. To minimize the number of synthetic steps required to add the functional group handle it was desirable to modify the existing synthesis of BDHP at a point after the synthesis of DHP. Two ways to accomplish this were investigated, and a retrosynthetic approach to these routes is shown (Scheme 2-9). The first approach involved using a functionalized furan and a Diels Alder reaction with the DHP alkyne **38**. The second approach involved a functionalised alkyne and a Diels Alder reaction with the furan DHP **37**.

Scheme 2-9 Retrosynthesis of BDHP functionalized on the benzo side of the molecule

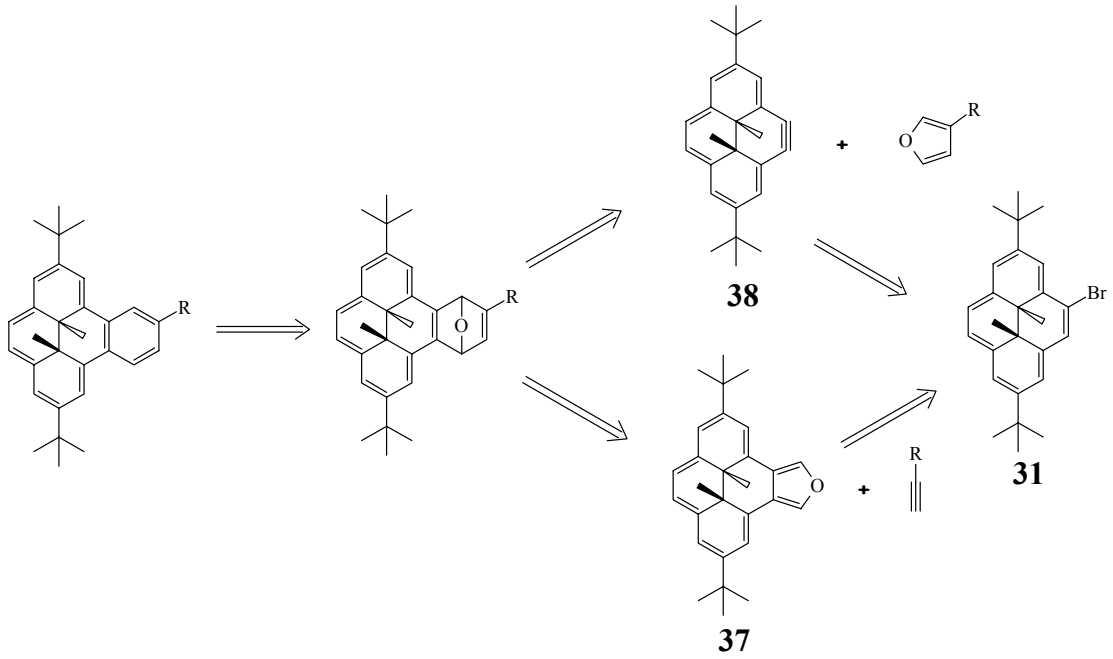

2.3.1 The activated furan approach

The first approach tried, used 3-bromofuran as the functionalised diene in a Diels Alder reaction with the DHP alkyne created *in situ* from the reaction between the bromide **31** and sodium amide. Unfortunately a large number of products were observed by TLC and NMR spectroscopy. Presumably this is because 3-bromofuran could also react with the sodium amide producing an alkyne, leading to decomposition and to the formation of numerous oligomeric products.

2.3.2 The activated acetylene approach

The second approach tried involved a Diels Alder reaction between a functionalised alkyne and the furan DHP **37**. The furan DHP **37** was synthesized previously in our group[53] by a retro Diels Alder reaction between **39** and dipyridyltetrazine[54] (Scheme 2-10).

Scheme 2-10 Synthesis of furan DHP 37

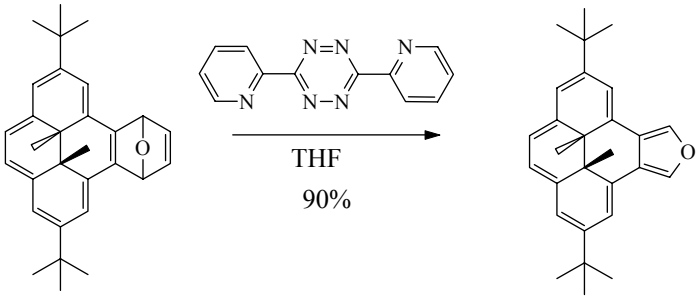

39 **37**

Once **37** had been obtained, it was used in a Diels Alder reaction with ethylpropiolate as the dienophile to give the desired product **40**, as a mixture of two diastereomers ("A" and "B", Figure 2-1), in a 71% yield (Scheme 2-11).

Scheme 2-11 Synthesis of the ester 40

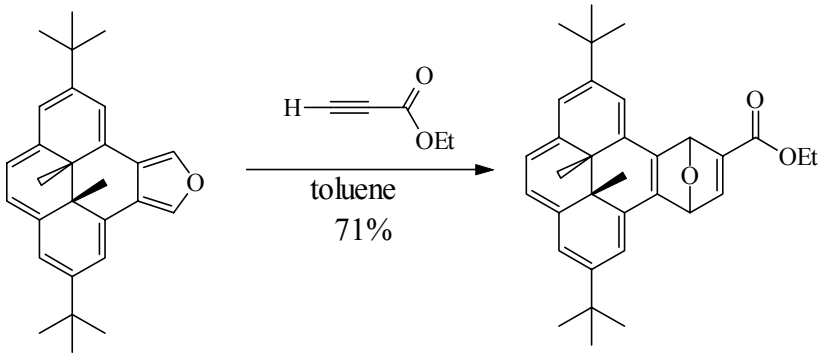

37 **40**

The reaction was very sluggish at room temperature in THF, with virtually no product formation even after 24 hours. At reflux in THF the reaction took over 24 hours to go to completion. In refluxing benzene the reaction was faster, taking about 5 hours for complete disappearance of the staring material. In refluxing toluene the reaction was even faster with complete disappearance of the starting material being observed in 1.5 to

3 hours. The "B" isomer was sparingly soluble in hexanes, while the "A" isomer was quite soluble in hexanes. As a result the virtually pure "B" isomer could be obtained by washing with hexanes and collecting the green powder that remained. The hexane washings could then be purified by column chromatography to isolate a 3:1 mixture of the "A" and "B" isomers. The pure "A" isomer could then be isolated from the "B" isomer by several fractional recrystalizations from hexanes while collecting the mother liquors, which after concentration also gave a green powder. A potential biproduct in this reaction comes from the fact that because an acetylene was used as the dieneophile, two Diels Alder reactions are possible. The desired reaction occurs between the alkyne and the furan DHP, and the second undesired Diels Alder reaction occurs between the alkene from the first reaction **40** and a second molecule of **37**. To minimize the possibility of a second Diels Alder reaction an excess of the functionalized alkyne was used. In the case of ethyl propiolate, the excess alkyne could be recovered after the reaction was complete by distillation. The identity of the product **40** was confirmed by its ^{1}H NMR spectrum. For the "A" isomer the internal methyl protons appear as two singlets at δ -2.72 and -3.04, while for the "B" isomer the internal methyl protons appear as two singlets at δ -2.79 and -3.16. The bridgehead ether protons were found in the "A" isomer at δ 6.95 and 6.33, while in the "B" isomer they were found at δ 7.0 and 6.30. The methylene protons are diastereotopic and so couple to each other, giving two doublets of quartets. In the "B" isomer a long range coupling is also observed for the methylene protons, so two doublets of quartets of doublets is observed. The ^{13}C NMR spectrum showed all of the expected carbons with the carbonyl carbon at δ 163.78 for the A isomer and at 163.76 for the "B" isomer. The internal methyl carbons for the "A" isomer were at δ 17.53 and

14.98, while in the "B" isomer they were at δ 17.56 and 15.52. The difference in the chemical shift of these internal methyls gives a clue as to the structural difference between these two isomers. If the internal methyl group of the "B" isomer is pointing down with respect to the bridging oxygen, this puts it in position to be most affected by the ethyl ester because of its close proximity to the ethyl ester which is also pointed down (Figure 2-1). This would lead to the small downfield shift in the signal observed in the ^{13}C NMR spectrum. The internal methyl group of the "A" isomer which is pointed down is on the other side of the ethyl ester, so because of the larger distance would not feel the same effect.

Figure 2-1 Isomers "A" and "B" of the ester 40

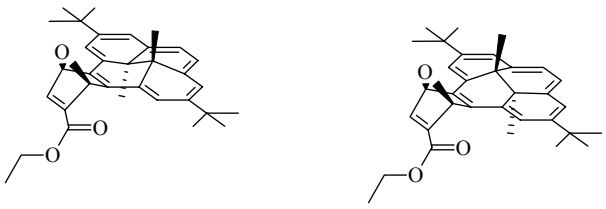

"A" **"B"**

There is very little change in the chemical shift between the "A" and "B" isomers for the internal methyl group which is pointed in the same direction as the bridging oxygen. This is expected because there is very little difference between the two isomers at this portion of the molecule. Additional support can be obtained by examining the ^{13}C spectra for the diester **41** which also has two internal methyl peaks. The internal methyl peak at δ 17.54 has a very similar chemical shift to the internal methyls found in both the "A" and "B" isomers which were assigned to be pointed in the same direction as the bridging oxygen. The second internal methyl at δ 15.29, which would then be pointed

down away from the bridging oxygen and in a similar direction as the ester, is most similar to the chemical shift of the "B" isomer internal methyl. The IR supported the product identification showing an ester carbonyl stretch at 1714 cm^{-1} and mass spectrometry (EI) gave the correct mass at *m/z* 482. Because the products obtained in the following deoxygenation step were indistinguishable regardless of whether the "A" or the "B" isomer was used, the two isomers were usually combined together for subsequent steps.

Diethyl-2-butynedioate could also be used as the dienophile, and gave **41** in a 74% yield as a green powder (Scheme 2-12).

Scheme 2-12 Synthesis of the diester 41

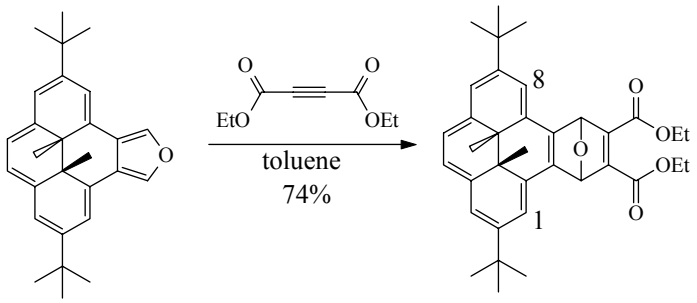

37 **41**

The product was identified by NMR spectroscopy with the ^{1}H NMR spectrum showing two upfield singlets at δ -2.77 and -3.07 which correspond to the internal methyls. The methylene protons are diastereotopic, so this molecule has four doublets of quartets with coupling constants of 10.7 and 7.1 Hz. The bridgehead ether hydrogens were found at δ 6.90 and 6.91 and all of the expected aromatic protons could be assigned. The ^{13}C NMR spectrum had peaks at δ 163.39 and 163.33 indicating that the two ester carbonyls are in slightly different magnetic environments from each other. The IR spectrum had an absorption at

1730 cm^{-1} which confirmed the presence of the ester, and mass spectrometry gave the correct molecular ion at *m/z* 554.

The necessity of using an activated dienophile was apparent as ethynyltrimethylsilane was found to be un-reactive with the furan DHP **37**, giving only a mixture of furan DHP decomposition products. One of these decomposition products was isolated and found to be the dialdehyde **43**. The structure of this product was confirmed by NMR spectroscopy. In the ^{1}H NMR spectrum, due to the high degree of symmetry there were only 7 peaks, all of which were singlets. Interestingly there was a very slight difference in the chemical shift of the protons in the 1 and 8 positions leading to the 7 signals observed. The aldehyde protons were found at δ 11.31 and the internal methyl signals were at δ -3.43. In the ^{13}C NMR spectrum there was a slight difference in the chemical shift of the two aldehyde carbonyl carbons (δ190.83 and 190.80) but other than that perfect symmetry was observed between the top and the bottom halves of the molecule in the ^{13}C NMR spectrum. Mass spectrometry confirmed the structure giving the correct mass of *m/z* 400. The mechanism for the formation of the dialdehyde **43** likely involves the peroxide **42** (Scheme 2-13). Isobenzofurans are well known to be excellent singlet oxygen acceptors.[55] Gollnick *et al*[56] found that a reaction between benz(e)furan **44** with oxygen gave the peroxide **45** which then converted to the diketone **46**. Pu[57] also found evidence (mass spectrometry) for a similar reaction occurring with the furan **47** to form the parent DHP diketone **49** (Scheme 2-13) but was unable to isolate the diketone**.**

Scheme 2-13 Substituted furan reactions with oxygen

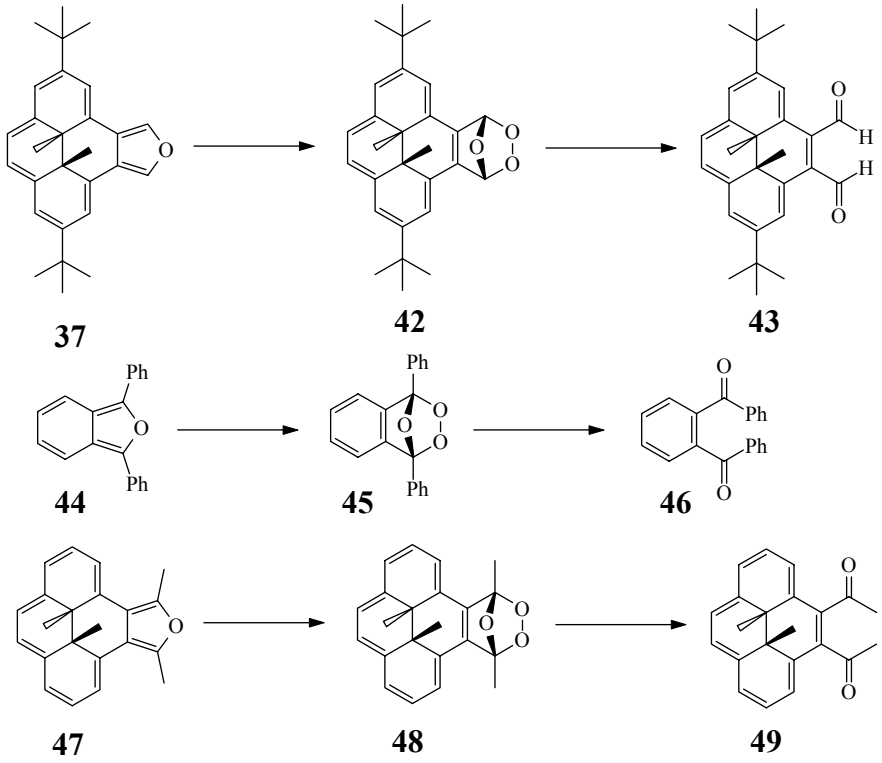

37 **42** **43**

44 **45** **46**

47 **48** **49**

Molecules with extended π systems are known to be singlet oxygen sensitizers[58] and singlet oxygen is known to be produced in the presence of DHP molecules.[59] Consequently it is not surprising to find the dialdehyde **43** as a minor product in this reaction.

In an effort to develop a more convergent synthetic approach, the Weinreb functionalized acetylene **50** [60,61] was used in a Diels Alder reaction with the furan **37** to give **51** in a 66% yield (Scheme 2-14). Two different isomers were present in a ~4:3 ratio, similar to what was observed in the ethyl ester case. The methoxy and the methyl peaks of the Weinreb amide were observed by ^{1}H NMR spectroscopy at δ 2.80 and 2.72. Because of the presence of two isomers there were four different internal methyl peaks,

Scheme 2-14 Synthesis of the Weinreb amide 51

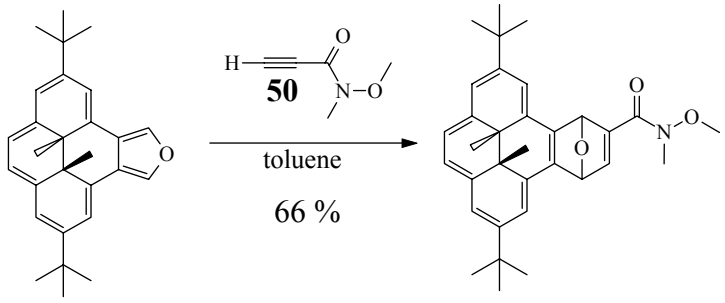

37 **51**

with the peaks at δ -2.69 and -2.98 corresponding to the minor isomer and the peaks at -2.80 and -3.12 to the major isomer. Mass spectrometry gave the correct molecular weight of *m/z* 497.

2.3.3 Deoxygenation of functionalized dihydropyrenes

$Fe_2(CO)_9$ [22,62] in refluxing benzene was used to deoxygenate the green DHP adducts **40**, **41** and **51** to give the functionalized red BDHP's. As the reaction progressed a color change from green to red was observed.

The functionalized dark red BDHP **52** was obtained in a 72% yield (Scheme 2-15).

Scheme 2-15 Deoxygenation of the ester 40

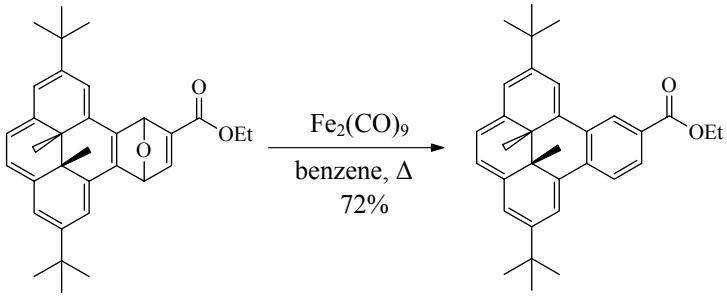

40 **52**

A slight excess of $Fe_2(CO)_9$ was used, however it was important not to use too large of an excess as this led to increased formation of the green iron adduct.[63] On a large scale it was difficult to separate all of the iron adduct from the desired product when using a 20:1 hexane:EtOAc silica gel column. Because the purity of the functionalised BDHP was important in the next (bromination) step, especially when trying to obtain the monobromide, a subsequent short alumina column using hexanes as eluent was often used to further purify the product. The formation of the correct product **52** was confirmed by NMR spectroscopy with the characteristic internal methyl peaks of a BDHP compound appearing in the ^{1}H NMR spectrum as a singlet at δ -1.40. The methylene protons are equivalent and appear as a simple quartet at δ 4.31. The aromatic region showed the expected 9 peaks for a functionalized unsymmetrical BDHP, all of which could be assigned. The ^{13}C NMR spectrum showed a carbonyl at δ 167.16 and the IR spectrum confirmed the presence of a conjugated ester with an absorption at 1719 cm^{-1}. Mass spectrometry gave the correct molecular ion at *m/z* 466.

The diester **41** was also successfully deoxygenated using $Fe_2(CO)_9$ to give **53** with a yield of 80% (Scheme 2-16).

Scheme 2-16 Deoxygenation of the diester 41

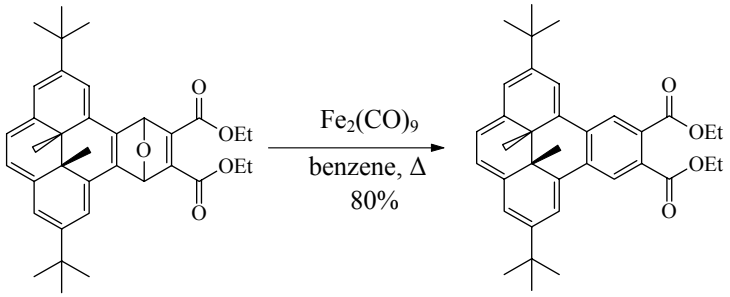

41 **53**

Because of symmetry, both the *t*-butyl groups and the internal methyl groups were equivalent and found at δ 1.34 and δ -1.40 respectively. Also because of symmetry, there were only 4 peaks in the aromatic region in the ^{1}H NMR spectrum and these could be assigned to their respective protons. The ^{13}C NMR spectrum was simplified because of symmetry and both ester carbonyls appeared together at δ 168.51. The IR spectrum confirmed the presence of the carbonyl with a peak at 1722 cm^{-1}. The correct mass of *m/z* 538 from mass spectrometry confirmed the successful synthesis of this compound.

Deoxygenation of the Weinreb amide **51** however, produced only a very small amount of the desired product and a large number of side products. The major side product was isolated and identified as being the amide **55** (Scheme 2-17). A small amount of what appeared to be the phenol **56** was also obtained. This product was identified as the alcohol by its mass of *m/z* 467 and a peak in the ^{1}H NMR spectrum at 14.8 which was assigned as the hydrogen bonded phenol proton.

Scheme 2-17 Deoxygenation of the Weinreb amide 51

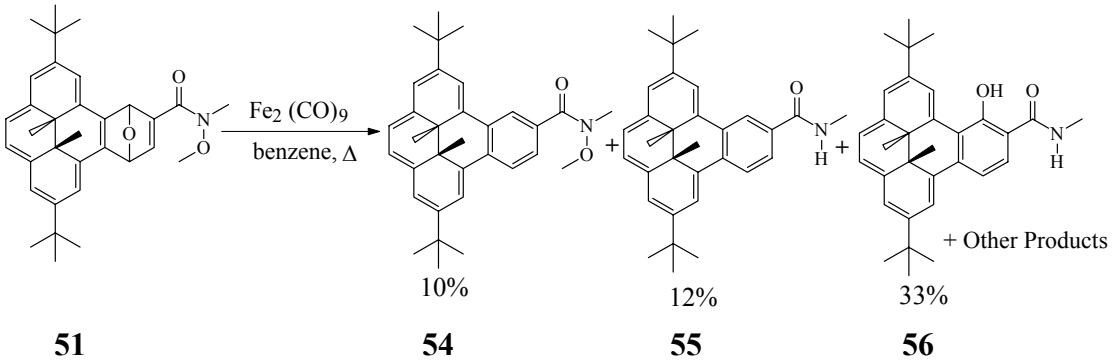

51 **54** **55** **56**

The structure of the amide **55** was confirmed by NMR spectroscopy. In the ^{1}H NMR spectrum the amide proton appeared as a broad singlet at δ 6.48, and the methyl group attached to the nitrogen as a doublet at δ 3.15. The internal methyl peak was at δ -1.59 which is indicative of a BDHP based derivative showing that deoxygenation of the bridging oxygen was successful. The ^{13}C NMR spectrum indicated that a carbonyl was still present as the amide carbonyl was found at δ 169.06. This was confirmed by the IR spectrum which showed a stretch at 1635 cm^{-1}. Mass spectrometry confirmed that the amide had been formed giving the correct mass for the molecular ion of *m/z* 451. Because of the difficulty of deoxygenating in the presence of the Weinreb functional group, this approach was abandoned and a more linear synthetic scheme was used.

2.3.4 Methods to add oligothiophene wires

With the successful synthesis of the BDHP switch with an ethyl ester at the 10 position **52**, the question of how best to functionalize this position and in what order to do the synthetic steps arose. It was necessary as outlined above, to avoid an sp^{3} center between the thiophene wires and the switch. With an ethyl ester in place at this position the most straightforward route to add the thiophene wires would make use of this ester and leave a carbonyl as a spacer between the switch and the wires. Having a carbonyl as

a spacer does incorporate an sp^2 center, but the conjugation between the two components is now cross conjugated. In cross conjugated systems both components are conjugated to the carbonyl but have usually been considered to be un-conjugated with each other.[64] Recently however, it has been shown that there may be some (though diminished) electron delocalisation between the components of a cross conjugated molecule.[65-67] Due to the simpler synthetic accessibility in these molecules of the carbonyl spacer it was decided to use an approach that would leave a carbonyl as a spacer between the BHDP switch and the thiophene wires.

Nucleophilic substitution with a lithiated thiophene or a Grignard on the ester would result in di-substitution and an alcohol. Since the alcohol would be sp^3 hybridized it was important to find an approach which would limit this reaction to just the mono-addition product. An acid chloride would have the same problem as the ester of over addition if a nucleophilic reaction was used. However acid chlorides can be coupled to aryl bromides using a Stille coupling reaction which maintains the carbonyl, especially when the reaction is carried out under a carbon monoxide atmosphere. Another possible approach involves using a Weinreb amide which allows for nucleophilic conditions to be used, but which ensures only mono-addition and so preserves the ketone. The Weinreb amide has, after the first nucleophilic reaction, a stable intermediate that prevents the addition of another nucleophile (Scheme 2-18). After acidic workup the ketone is then isolated.

Scheme 2-18 The Weinreb stable intermediate

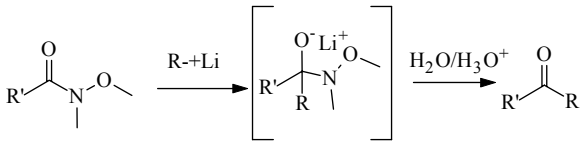

The BDHP ethyl ester **52** can be converted to the acid **57** in virtually quantitative yields by saponification with aq. NaOH. The production of the acid was confirmed by the loss of the ethyl triplet and quartet at 1.16 and 4.31 ppm in the ^{1}H NMR spectrum and the appearance of a broad OH peak at 3450-2500 cm^{-1} in the IR spectrum. This was further confirmed by the correct HRMS mass at *m/z* 438.2559 (calculated at 438.2564). The BDHP acid chloride **58** (Scheme 2-19) could then be synthesized from the acid **57** by a reaction with oxalyl chloride.

Scheme 2-19 The acid chloride approach

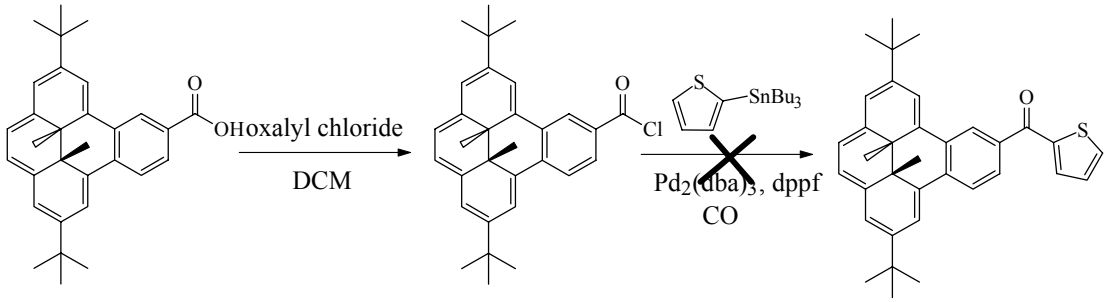

57 **58** **59**

The presence of the desired acid chloride **58** was confirmed by the presence of IR stretches at 1813 and 1750 cm^{-1}. The acid chloride was used immediately in a Stille coupling reaction with a tributyltin functionalized thiophene. Unfortunately none of the desired coupled product was observed after 24 hours, even when a carbon monoxide atmosphere was used.

The Weinreb amide approach was then tried. The acid **57** could be readily converted to the Weinreb amide **54** by reaction with N,O-dimethylhydroxylamine and N,N'-diisopropylcarbodiimide (DIC) as the coupling agent. Treatment of the Weinreb amide **54** with a lithiated thiophene produced after acidic work up, the desired ketone **59,** (Scheme 2-20).

Scheme 2-20 The Weinreb amide approach

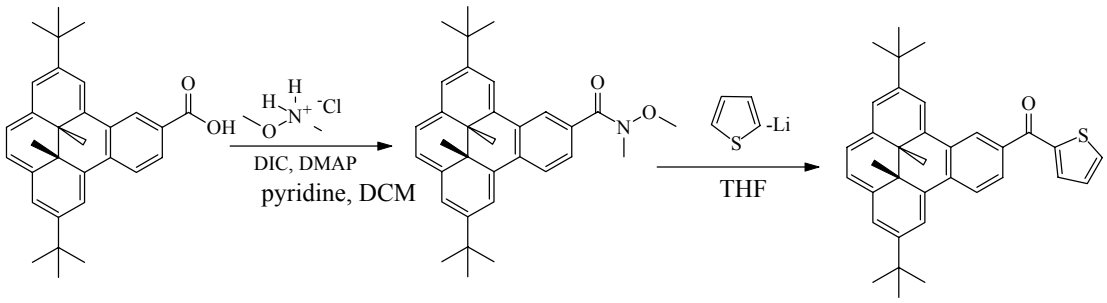

57 **54** **59**

The acid can also be used to attach other functional groups. Using the same conditions as was used to attach the Weinreb amide a polyethyelene glycol (PEG) unit could be added (Scheme 2-21).

Scheme 2-21 Coupling of polyethylene glycol

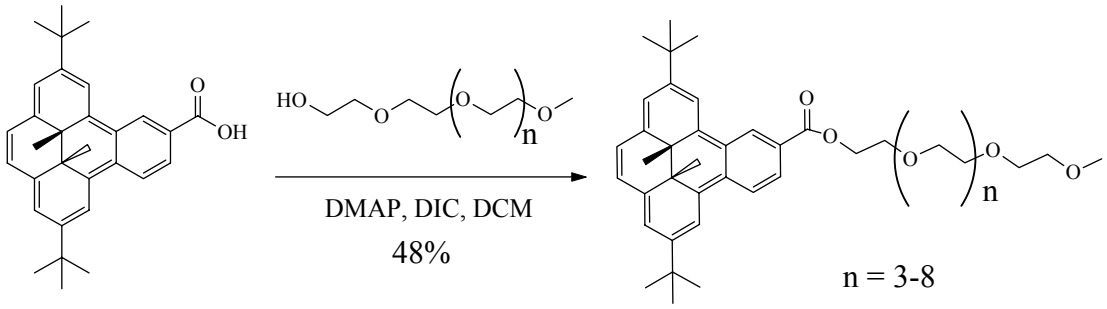

57 **60**

The PEG functionalized product was obtained after stirring for 18 hours and purification by column chromatography in a 48% yield. A commercial sample of PEG was used

which was a mixture of isomers with an average molecular weight of 350. This mixture could be observed in the final product by TLC as a series of close running red spots. Column chromatography did lead to some separation of these isomers, however isolation of individual isomers was not attempted. The mixture of isomers obtained could be seen by mass spectrometry as a distribution of peaks from *m/z* 959 to 709. The product was identified by the characteristic internal methyl peaks in the ^{1}H NMR spectrum at -1.39 ppm as well as a series of PEG multiplets at 4.5, 3.6, 3.5, 3.4, 3.3 and 3.1 ppm. With the PEG tail the compound **60** was soluble in water. This product was used for a successful collaboration with Dr. Sen at SFU to photo-regulate a hammerhead ribozyme.[68]

With the successful development of a method to add the desired thiophenes on opposite sides of the BDHP molecule to take advantage of the large conjugation changes between the open and the closed form, the order in which these synthetic steps are performed needed to be considered. A retrosynthetic analysis gave two different routes to add the oligomeric thiophenes as shown in (Scheme 2-22).

Scheme 2-22 Retrosynthesis scheme for thiophene addition

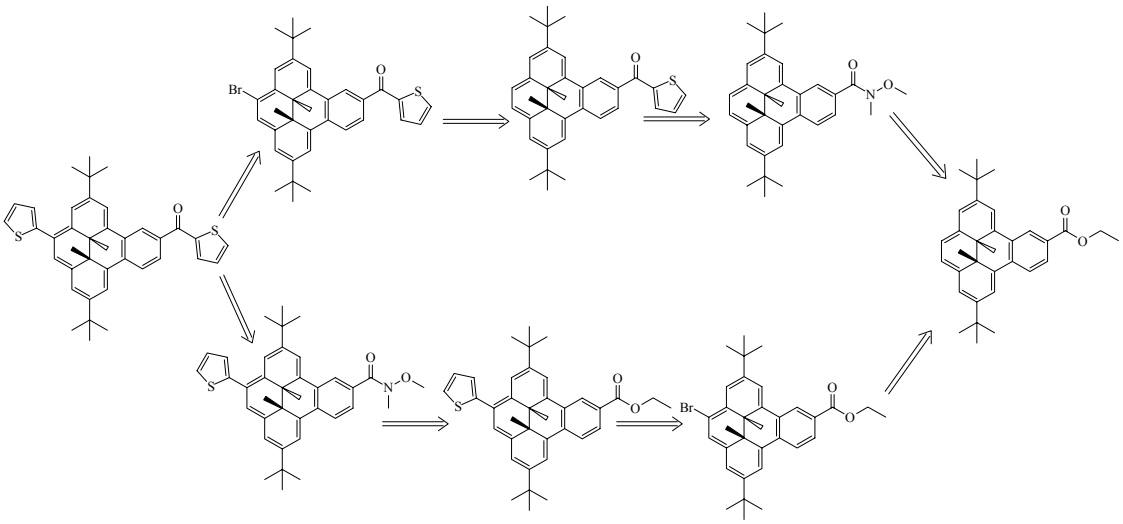

Because of the difficulty of brominating BDHP and the sluggishness of the palladium catalyzed coupling reactions it was decided to do the bromination and coupling steps first, followed by the functionalization of the other side of the molecule.

2.3.5 Bromination of the ester 52

The ester **52** could be mono-brominated by NBS in a 98% yield to give **61** (Scheme 2-23). It was important to have very pure starting material to minimize the amount of dibromination.

Scheme 2-23 Bromination of the ester 52

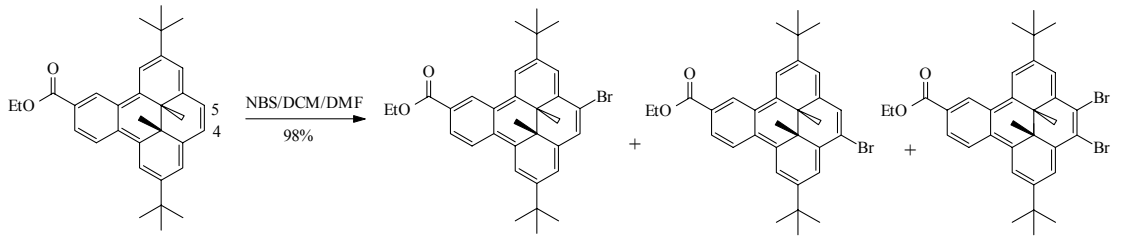

52 **61** **62** **63**

Unfortunately mono-bromination gives little selectivity, and an approximately 1:3 ratio of the bromine in the 4 and the 5 position was obtained (Figure 2-2).

Figure 2-2 500 MHz ^{1}H NMR of 61 and 62 showing the major and minor mono-bromination isomers in C_6D_6

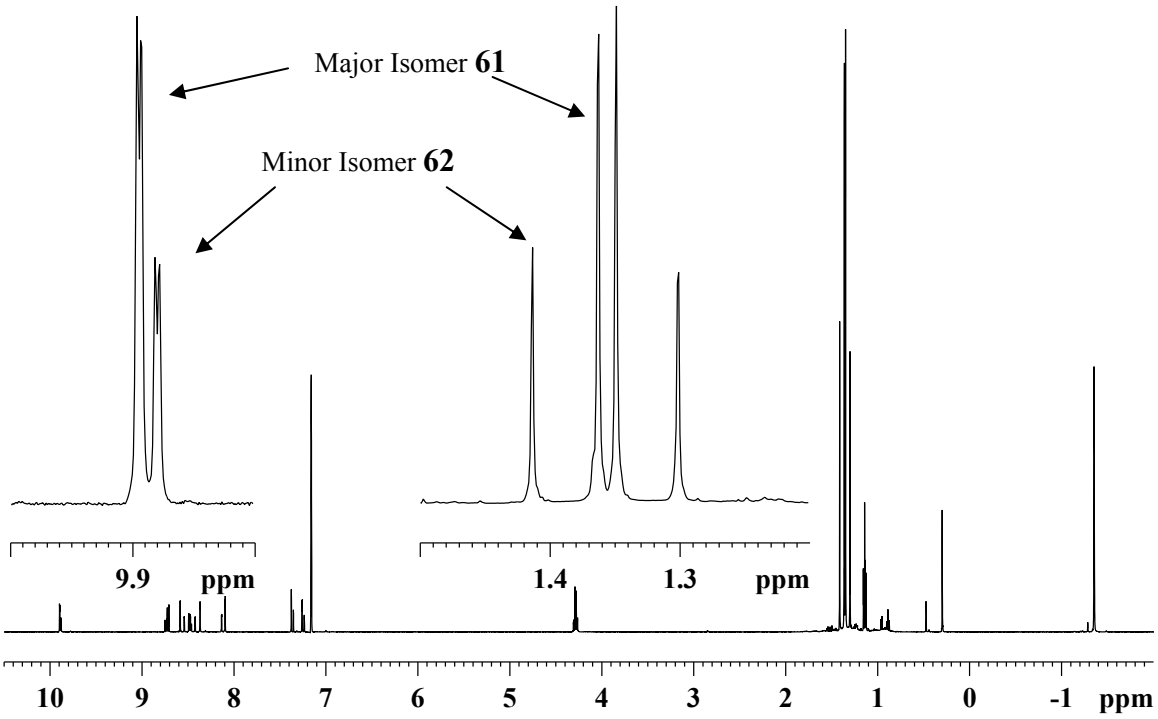

These two bromides could not be separated from each other by column chromatography or crystallization, so this ratio was carried through all subsequent steps. Fortunately functionalization in either position should have little effect on the conjugation changes that occur between the open and the closed forms. All the peaks of the major isomer (bromination in the 5 position) in the ^{1}H NMR spectrum could be assigned distinctly from the minor isomer peaks except for the internal methyl signal which appeared as a broad singlet with the minor isomer internal methyls. Most of the ^{13}C NMR peaks for the major isomer could be assigned as distinct from the minor isomer. There were a few peaks such as the carbonyl peak, where similar chemical shifts (166.97 vs 166.95) made distinction of the major isomer from the minor isomer impossible. NMR assignements were made based on COSY, NOSY, HSQC and HMBC NMR experiments. The IR

spectrum indicated the presence of a conjugated ester at 1711 cm^{-1} and mass spectrometry gave the correct molecular weight of *m/z* 546.

If very pure **52** was used, then only a very small amount of dibromide **63** was detected (<5%), and it could be successfully removed by careful column chromatography. This however was not usually necessary as small amounts of the dibromide **63** were much easier to remove after coupling to oligothiophene. There was then by column chromatography a much larger separation between the mono and di-addition products. Less pure samples of **52** gave much higher amounts of the dibromide **63**. The dibromide could be isolated and was fully characterized. In the ^{1}H NMR spectrum the internal methyl protons appeared as a singlet at δ -1.28. All the ^{1}H and ^{13}C NMR peaks could be assigned. The IR spectrum indicated the presence of the carbonyl at 1717 cm^{-1} and mass spectrometry gave the correct molecular weight of *m/z* 624.

2.3.6 Coupling of oligothiophenes

Various length oligothiophenes (bi, ter, quinque) could be attached using Stille coupling reactions with $Pd_2(dba)_3$ and dppf as the catalysts (Scheme 2-24). These reactions were quite sluggish, taking between 3 and 5 days before the bromide starting material was consumed, with yields varying from 56% to 77%.

Scheme 2-24 Coupling of oligothiophenes to the bromide 61

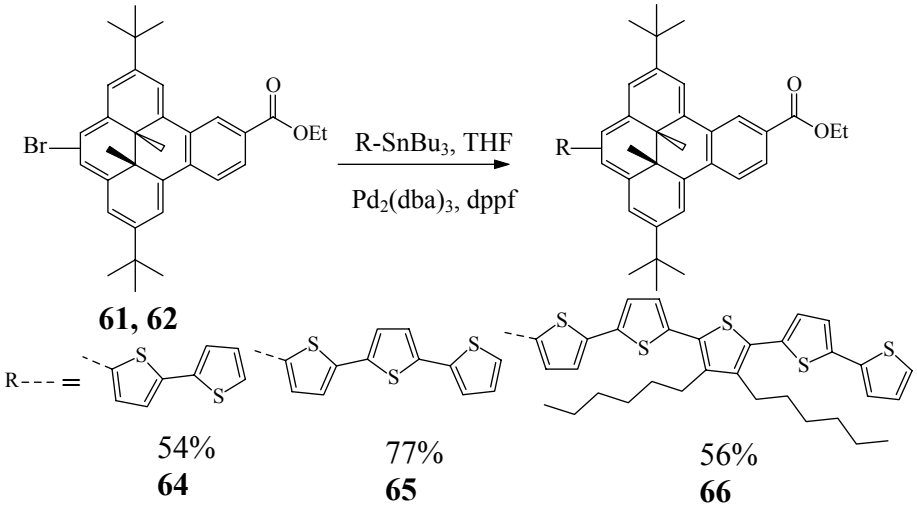

Addition of the oligothiophenes was confirmed by the peaks between 6.60 and 7.24 ppm in the ^{1}H NMR spectrum corresponding to the thiophene protons. The internal methyl protons of the major isomers for these compounds appeared from -1.2 to -1.3 ppm. In the quinquethiophene example **66**, 4 different internal methyl peaks were distinguishable, two each from the major and the minor isomer. In the ^{13}C NMR spectrum the carbonyl peak was at ~167.1 ppm for all compounds and the internal methyl carbons were at ~18.5 and 18.4 ppm. Virtually every proton and carbon of the BDHP portion could be assigned for the major isomer. For the quinquethiophene compound **66**, the hexyl protons appeared as broad multiplets with the methylene closest to the thiophene appearing at ~4.3 ppm, and with the rest of the hexyl protons appearing between 2.9 and 0.8 ppm. In the ^{13}C NMR spectrum there was a difference in the carbon peaks between the two hexyl chains, however it was not possible to distinguish which particular hexyl chain they were from. The IR spectrum indicated the presence of the ester by a stretch at ~1715 cm^{-1} and mass spectrometry gave the correct mass for all products. The di-addition product **67** could be obtained by Stille coupling with the pure dibromide **63**, (Scheme 2-25), or by

isolating the di-addition product that formed due to a small amount of dibromide impurities in the monobromide **61** coupling reactions.

Scheme 2-25 Coupling to the dibromide 63

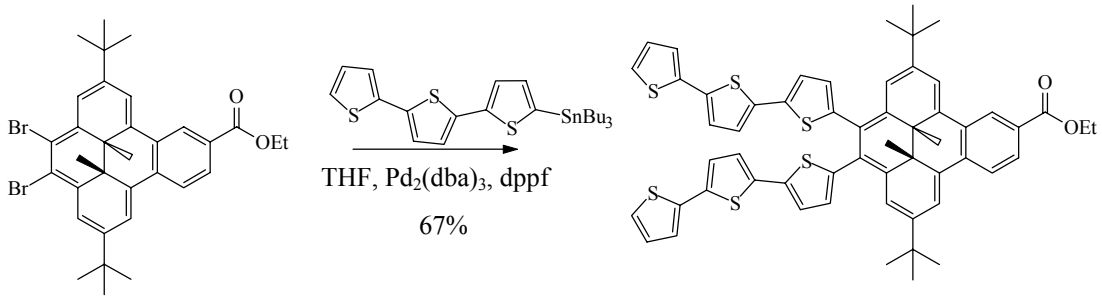

63 **67**

In the NMR of **67** there were no complications due to isomer formation, so all of the ^{1}H and ^{13}C NMR peaks of the BDHP part of the molecule could be assigned and virtually every thiophene peak. Mass spectrometry confirmed the structure of the product with the correct mass of *m/z* 959.

2.3.7 Conversion to the acid

Once oligothiophenes were in place on one side of the switch, functionalization of the other side could begin. The esters **64**, **65** and **66** were converted to the acids **68**, **69** and **70** respectively by saponification using 2M NaOH in EtOH in an almost quantitative yield (Scheme 2-26). The products of these reactions were sparingly soluble in diethyl ether until neutralized with HCl to give the free acids, at which point they became completely soluble in diethyl ether.

Scheme 2-26 Saponification of the ethyl ester

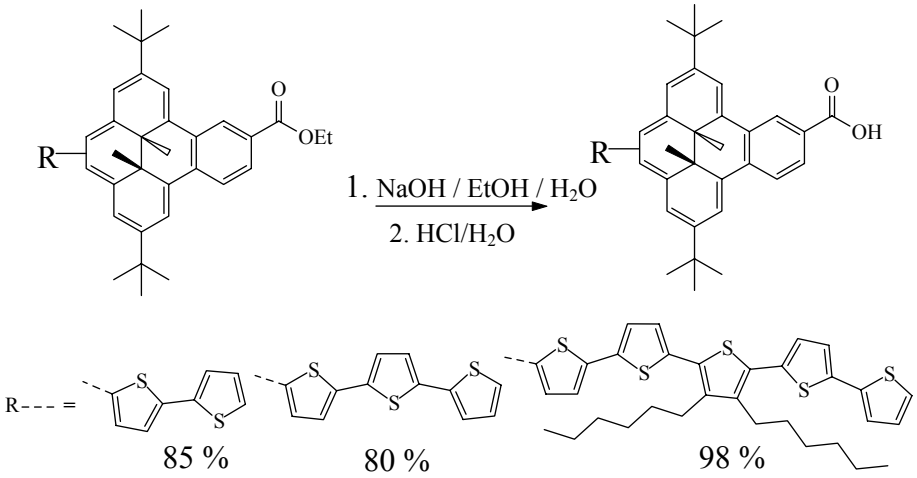

68 **69** **70**

The disappearance of the ethyl peaks in the ^{1}H NMR spectrum from the ethyl ester at ~ δ 4.3 and 1.2 indicated complete conversion to the acid. The presence of the acid carbonyl was observed by ^{13}C NMR spectrum at ~ δ 171.5, and this was corroborated by the IR spectrum which had a carbonyl stretch at ~1685 cm^{-1}. Mass spectrometry gave further support giving the correct molecular ion *m/z* of 684 for **69** and 1017 for **70**. The solubility of the terthiophene compound **69** was low so it was necessary to use a large number of scans to obtain the ^{13}C NMR spectrum. For the quinquethiophene compound **70** the long hexyl chains increased the solubility to a point where this was not a problem.

2.3.8 Conversion to the Weinreb amide

The acids **68**, **69** and **70** were converted to the Weinreb amides **72**, **73** and **74** by a reaction with N,O-dimethylhydroxylamine hydrochloride using DIC as the coupling agent (Scheme 2-27). A few drops of 2M NaOH were added to help dissolve the hydrochloride salt as it was only sparingly soluble under the reaction conditions. Because the amine is a poor nucleophile, the anhydride was a significant biproduct for

this reaction. The formation of the anhydride could however be virtually eliminated by using an excess of DIC and with the addition of a small amount of 4-(dimethylamino)pyridine (DMAP).

Scheme 2-27 Synthesis of the Weinreb amides 72, 73 and 74

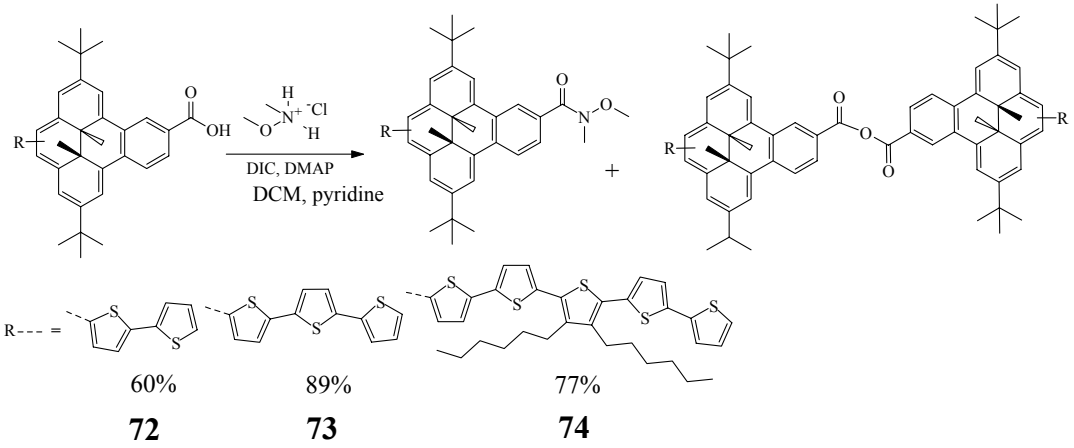

The ^{1}H NMR spectrum showed two new peaks at δ 3.18 and 3.13, corresponding to the methoxy and methyl groups from the amide of the major isomer. The minor isomer (thiophenes in the 4 position) methoxy and methyl peaks were seen as shoulders on the side of the major isomer peaks. The internal methyl peaks in the major isomer were found at -1.18 and -1.21 ppm. The amide carbonyl in the ^{13}C NMR spectrum was at ~δ 170.6, and the presence of the amide carbonyl was confirmed in the IR spectrum by a stretch at 1642 cm^{-1}. Mass spectrometry confirmed the product giving the correct molecular ion of *m/z* 727 for the terthiophene molecule **73** and 1060 for the quinquethiophene molecule **74**.

2.3.9 Addition of oligothiophenes on the opposite side of BDHP

The oligothiophenes were lithiated with *n*-BuLi, and these were subsequently added to the Weinreb amides **72**, **73** and **74** at -78^{o}C (Scheme 2-28).

Scheme 2-28 Synthesis of BDHP with oligothiophenes on opposite sides

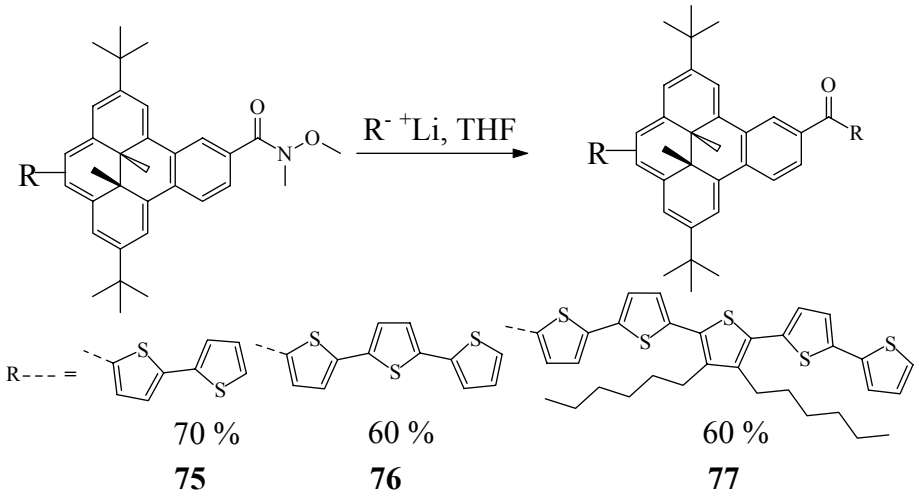

A large excess of the lithiated oligothiophenes were used because of the tendency of the lithiated thiophenes to disproportionate between the starting material, mono lithium and dilithiated products. Even when an excess of the oligothiophene was used a small amount of the di-addition product formed. In the terthiophene case **79**, this product was isolated and identified by mass spectrometry, *m/z* 1581, (Scheme 2-29).

Scheme 2-29 Di-addition product 79

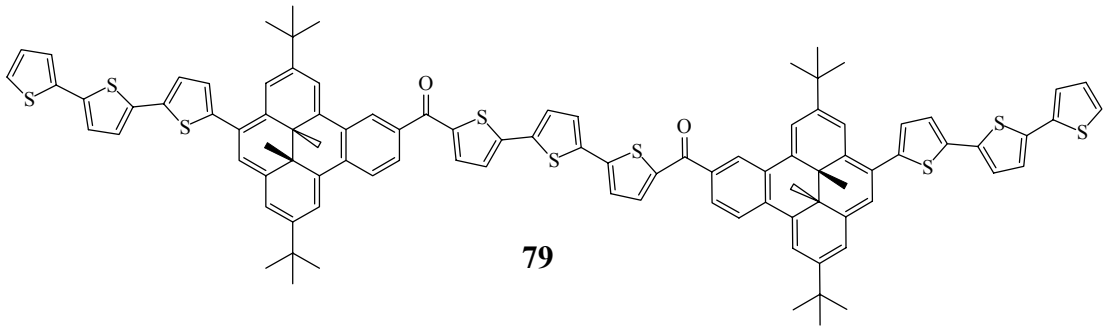

79

After acidic workup the desired products **75**, **76** and **77** were obtained in a 60-70% yield. The ^{1}H NMR spectrum showed the disappearance of the Weinreb amide peaks at ~δ 3.2 and 3.1 and the appearance of additional thiophene peaks from ~δ 6.6 to 7.5. The ketone was observed in the ^{13}C NMR spectrum at ~δ 187 and this was corroborated by an IR stretch at ~1620 cm^{-1}, indicating a highly conjugated ketone. The product was confirmed by mass spectrometry giving the correct molecular ion of *m/z* 751 for the bithienyl **75**, 914 for the terthienyl **76** and 1580 for the quinquethienyl **77**.

2.3.10 Extension of oligothiophene chains

An attempt was made to functionalize the end of the thiophene oligomers. This was done by lithiation, followed by the addition of a tributyltin substituent (Scheme 2-30) so that a Stille coupling reaction could be used to extend or polymerize the molecule.

Scheme 2-30 Attempt to functionalization the oligothiophenes on BDHP

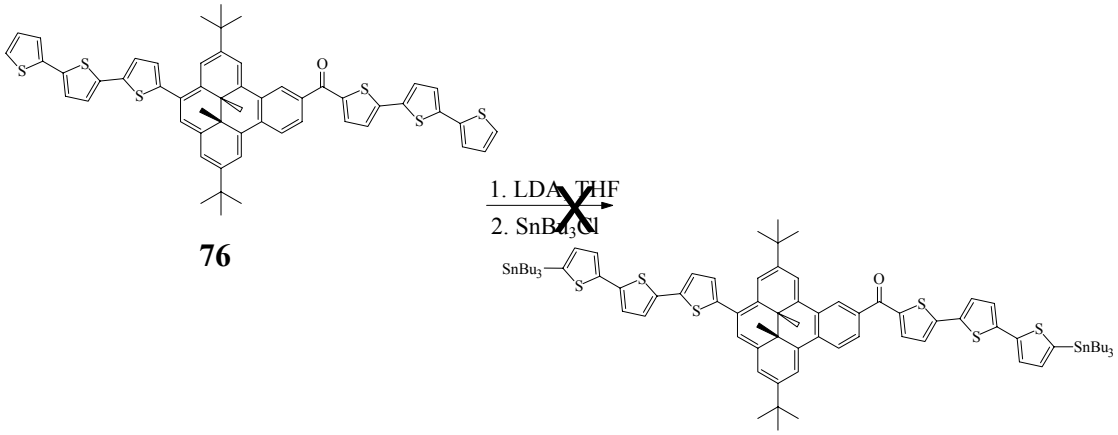

76 **80**

Unfortunately when LDA was used as a base very little reactivity was observed. When *t*-BuLi was used, the desired product could not be isolated from the multiple side products produced.

2.4 Carbonyl substituted dihydropyrenes

Carbonyls have been shown to improve the photoswitching properties of DHP by accelerating the photo-opening reaction.[25] These improved photoswitching properties made them attractive molecules to insert into oligothiophene molecular wires. An added advantage of the carbonyl functionalized DHP photoswitches is that their synthesis involves fewer steps than BDHP and so they are more synthetically accessible. A variety of DHP carbonyls have been synthesized.[25] Of these, the DHP naphthoyls have been shown to be relatively simple to synthesize and quite stable, so they were selected as the carbonyl functionalized DHP switch to which oligothiophenes would be attached.[25]

2.4.1 Bromination of naphthoyl substituted dihydropyrenes

Naphthoyl DHP **14** could be monobrominated using NBS to give the bromide **81** as brown crystals (Scheme 2-31).

Scheme 2-31 Monobromination of naphthoyl DHP 14

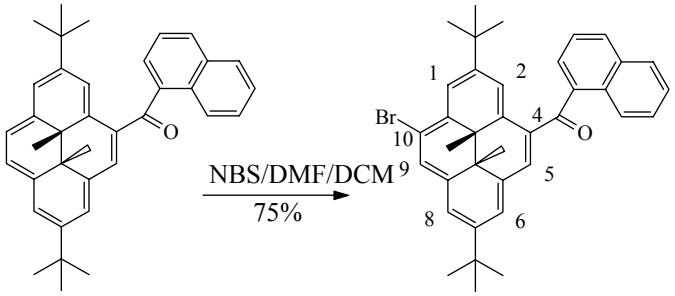

14 **81**

In the ^{1}H NMR, spectrum six aromatic peaks could be assigned corresponding to the DHP protons, and seven aromatic peaks corresponding to the naphthalene protons. The position of the bromine was determined by using HMQC and HMBC NMR techniques to be in the 10 position indicating that the naphthoyl group was causing a significant amount of selectivity on the bromination position. Both internal methyls were observed as a singlet at δ -3.64. The ^{13}C NMR spectrum showed the presence of a carbonyl at δ 200.70. Further confirmation for the carbonyl came from the IR spectrum which had a stretch at 1645 cm^{-1} indicating a conjugated ketone. The product was confirmed by mass spectrometry which gave the correct molecular weight of *m/z* 579. Naphthoyl DHP **14** could be dibrominated if two equivalents of NBS were used (Scheme 2-32), giving, after 3 hours, the product **82** as a green powder along with some of the brown mono-bromide **81**. In this reaction the second bromine adds to the 5 position next to the carbonyl.

Scheme 2-32 Dibromination of naphthoyl DHP 14

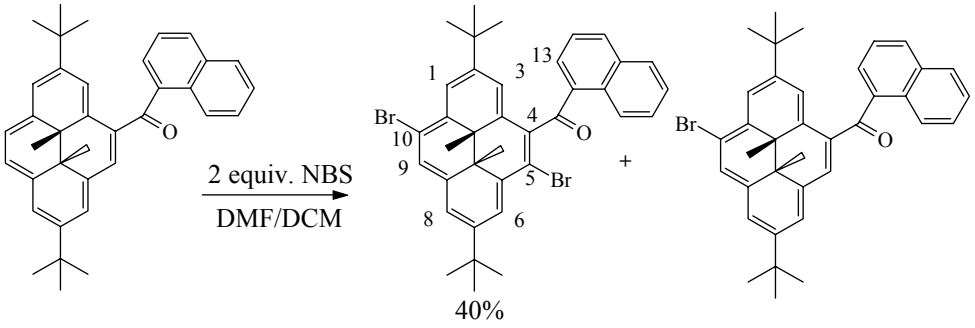

14 **82** **81**

The five aromatic peaks from the DHP and seven peaks from the naphthalene protons could all be assigned. Protons in the 3 position on the DHP and in the 13 position on the naphthalene are broadened due to restricted rotation. The ^{13}C NMR spectrum was fully assigned and indicated that the ketone was present with a peak at δ 199.83. The IR spectrum confirmed the presence of this carbonyl with a stretch at 1662 cm^{-1}. The slightly higher IR stretching frequency when there was a bromine atom in the 5 position, as compared to when there was a hydrogen atom in the 5 position indicates that there was a loss of conjugation between the ketone and the aromatic ring. This loss is due to the large steric bulk of the bromine which dramatically reduces the ability of the carbonyl to be coplanar with the DHP aromatic ring. The product identity was confirmed by mass spectrometry which gave the correct molecular weight of *m/z* 656.

2.4.2 Coupling of oligothiophenes to the dibromide 82

With two bromines on either side of the molecule, the dibromide **82** was suitably functionalized to add thiophene oligomers on either side of the DHP switch via a coupling reaction. This was done using terthienyltributylstannane **108** and a Stille

coupling reaction. The desired product was obtained in a 69% yield and the product was isolated as a red powder (Scheme 2-33).

Scheme 2-33 Synthesis of the di-terthienyl 83

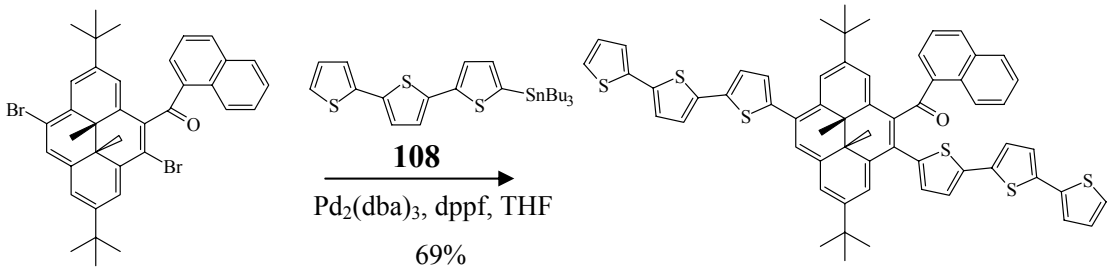

82 **83**

All of the protons and carbons in the NMR spectrum could be assigned and the internal methyl protons for this compound were observed at δ -3.30 and -3.42. The presence of the carbonyl peak was observed at δ 201.56 in the ^{13}C NMR spectrum and this was confirmed by the IR where a stretch at 1654 cm^{-1} was observed. Further proof that the correct product had been synthesized was obtained from mass spectrometry which gave the correct molecular ion mass of *m/z* 991. Unfortunately when attempts were made to isomerize this compound to the open form, no trace of the open form was observed by NMR even after 1 hour of irradiation at 5°C. The lack of photo-opening in **83** demonstrates the importance of having the naphthoyl functional group attached in a positon where the carbonyl can be co-planar with the DHP ring.

2.4.3 Observed *ipso* substitution at the *t*-butyl position

DHP **11** can be readily dibrominated with NBS putting bromines in the 4 and 9 positions (Scheme 2-34).[69]

Scheme 2-34 Di-bromination of DHP

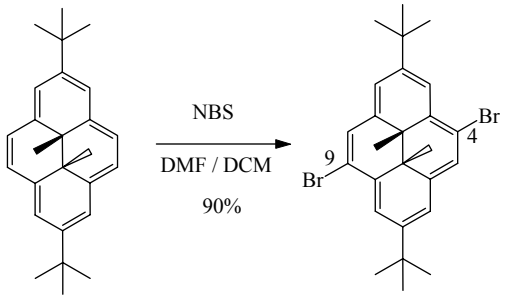

11 **85**

When $AlCl_3$ is added to a solution of the dibromide **85** and naphthoyl chloride, the solution turns an aquamarine color after a few hours. This color is indicative of an aluminum complex. When the solution is quenched with water it instantly turns a dark reddish purple. If only a small amount of water is added the aquamarine color can be regenerated by adding more $AlCl_3$. TLC indicated the presence of four compounds (Scheme 2-35), the green dibromide starting material **85**, close running green mono **86** and di-brominated **82** products, followed by the purple *ipso* substituted dibromide **84**. All of these products could be separated from each other by column chromatography on alumina using hexanes as eluent. Even when long reaction times and an excess of $AlCl_3$ and naphthoyl chloride were used, un-reacted starting material was always recovered. When the reaction was heated to reflux, *ipso*-substitution of the second *t*-butyl was not observed, however a small quantity of the *ipso* substitution of the *t*-butyl of bromide **86** to give **87** was observed to occur as seen by a mass spectometry peak of *m/z* 755. This product was purple and was more polar than the previous compounds and so eluted from the column much later than the other products. Unfortunately **87** eluted as a mixture of products and so was not fully characterized.

Scheme 2-35 Reaction scheme for *ipso* substitution

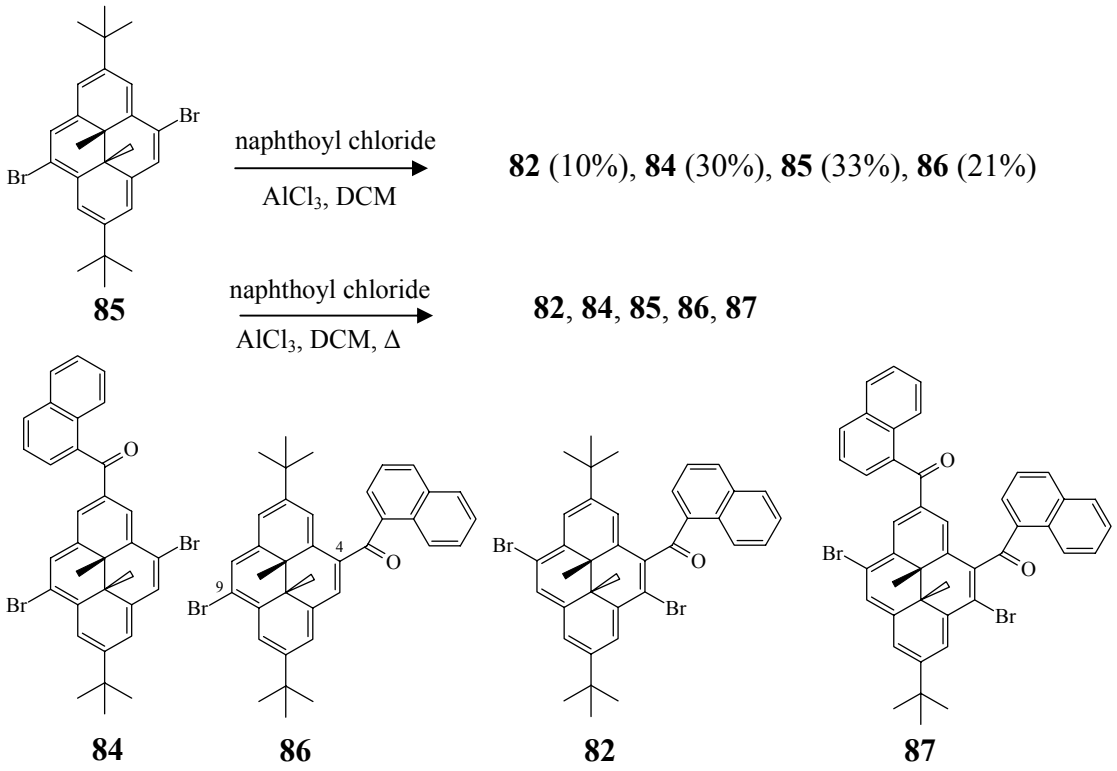

The monobrominated product **86** from this reaction was functionalized with bromine in the 9 position rather than the 10 position as was observed previously when brominating naphthoyl DHP **14**. This change from the 9 position to the 10 position was seen in a slight change in the NMR chemical shifts. The internal methyl peaks were observed as two peaks: one at -3.50 and the other at -3.53 ppm, rather than just one singlet, and all the DHP aromatic peaks were shifted slightly upfield. Mass spectrometry gave the same molecular ion mass of *m/z* 579 as before.

The purple *ipso* substituted product **84** was obtained in 30 – 35% yield. The ^{1}H NMR showed the loss of one of the *t*-butyl peaks and the addition in its place of a naphthoyl group. The internal methyl peaks were observed as two singlets at -3.57 and -3.62 ppm. All of the DHP aromatic protons were singlets and could be assigned along

with the naphthoyl protons in the ^{1}H NMR spectrum. The presence of a carbonyl was observed in the ^{13}C NMR spectrum by a peak at 198.49 ppm and this was confirmed in the IR by a stretch at 1643 cm^{-1}. Mass spectrometry gave the correct molecular weight of *m/z* 600 and the isotopic pattern indicated the presence of two bromines. Having a naphthoyl functional group in the 2 position was found to greatly improve the photo-opening properties of the molecule as the purple color rapidly bleached when irradiated with visible light. Unfortunately, the thermal return was also accelerated.

A variety of different acid chlorides were tried (benzoyl, anthranoyl and pyrenoyl chloride) in order to see if the *ipso* substitution reaction was general and if the yield could be improved. Ipso substitution occurred in all three cases and the *ipso* substituted products were always a red purple color (Scheme 2-36).

Scheme 2-36 Ipso substitution with pyrenoyl, anthranoyl and benzoyl chloride

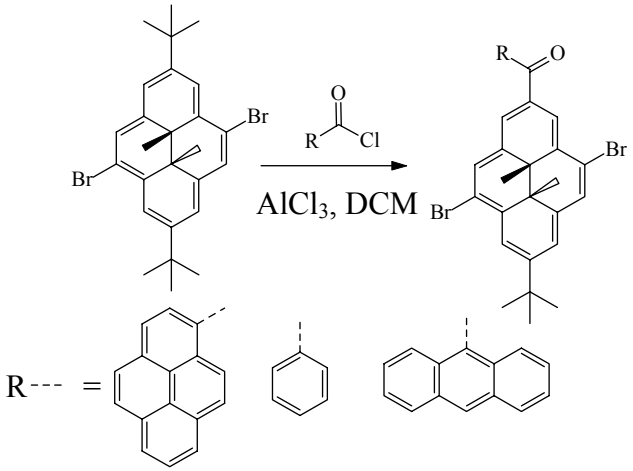

34% 5% 13%

88 **89** **90**

Pyrenoyl chloride was found to give a similar yield (34%) of the *ipso* substituted product **88** as naphthoyl chloride while anthranoyl chloride and benzoyl chloride gave much lower yields for the *ipso* substituted products (13% for **90** and 5% for **89**). This indicates

that the bulk around the acid chloride plays a role in how much *ipso* substitution occurs. Having too much bulk as in the anthranoyl case **90**, or not enough bulk, as in the benzoyl case **89** reduces the amount of *ipso* substitution. This was further supported by the fact that pyrenoyl chloride, which has a similar bulk around the acid chloride as naphthoyl chloride, gave almost identical yields of the *ipso* substituted product **88** as that of naphthoyl chloride. All three *ipso* substituted compounds had internal methyl peaks between -3.55 and -3.65 ppm in the ^{1}H NMR spectrum. For the benzoyl **89** and anthranoyl **90** compounds all of the protons and carbons could be assigned in the ^{1}H NMR and ^{13}C NMR spectra. However for the pyrenoyl compound **88**, due to overlap of some of the pyrene peaks, not all of the peaks could be assigned. Further support that the correct compounds were synthesized was obtained from the mass spectrometry data which gave the correct masses of *m/z* 674 (**88**), 550 (**89**), and 650 (**90**).

2.4.4 Coupling of oligothiophenes to the dibromide 84

With a naphthoyl group in the 2 position causing improved photo-opening and two bromides on either side of the switch, the dibromide **84** was perfectly functionalized to add oligothiophenes via a coupling reaction. A Stille coupling reaction was used to add the terthienyl, quinquethienyl **102**, and septithienyl **105** oligomers (Scheme 2-37).

Scheme 2-37 Coupling of oligothiophenes to the dibromide 84

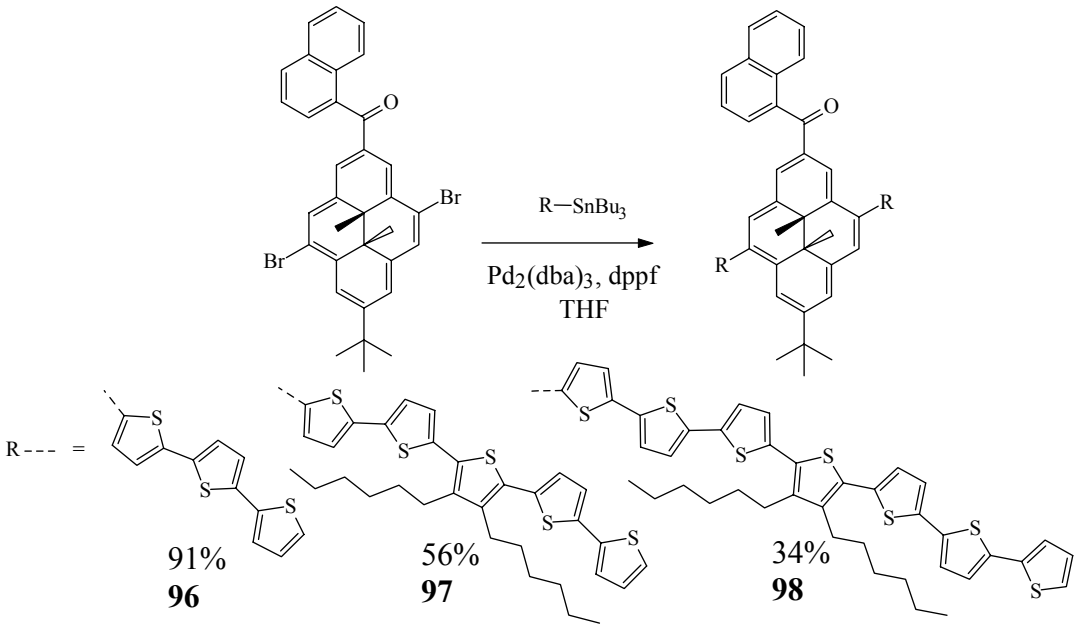

The desired products were obtained with a yield of 91% for the terthienyl **96**, 56% for the quinquethienyl **97** and 34 % for the septithienyl **98** compounds. Virtually all of the protons and carbons could be assigned for the closed ^{1}H and ^{13}C NMR spectra of the terthienyl compound **96**, and most of the protons and the carbons assigned in the closed quinquethienyl **97** and septithienyl **98** compounds. The peaks that could not be assigned were mostly due to the overlap of the oligothiophene peaks. In all three compounds the presence of the carbonyl peaks could be seen in the ^{13}C spectra at 198.7 ppm and in the IR with a stretch at ~1640 cm^{-1}. The internal methyl peaks in the ^{1}H NMR spectra were found in the closed form for these compounds as two singlets at -3.3 and -3.4 ppm. Importantly the compounds could be opened very quickly by irradiation with visible light. The correct mass was obtained for the terthienyl compound **96** at *m/z* 935 and the

quinquethienyl compound **97** at *m/z* 1599, however the mass of the septithienyl compound **98** unfortunately was not obtained.

Polymerization was attempted using the dibromide **84** and the distannyl **104**, using a Stille coupling reaction (Scheme 2-38).

Scheme 2-38 Polymerization of *ipso* substituted DHPs with oligothiophenes

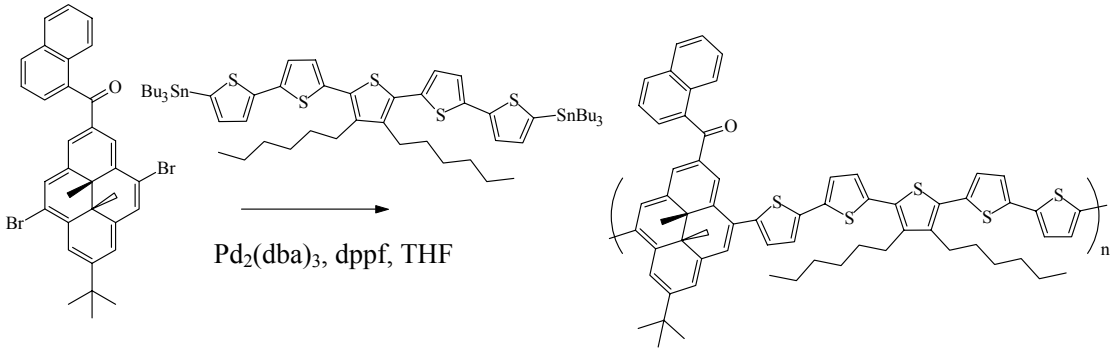

84 **99**

A variety of oligomers were isolated all of which eluted much more slowly than **97** from a silica gel column. The majority of the product, presumably the longest oligomers, were isolated by removing the top of the column and extracting it with pure dichloromethane, giving after evaporation of the solvent a dark black solid. The ^{1}H NMR peaks of this compound **99** were virtually identical to the shorter fully characterized oligomer **97**, though broadened, which is consistent for a polymer. The internal methyl peaks were observed in their usual position as two broadened singlets at -3.29 and -3.35 ppm indicating the polymer contained the DHP functionality. A ^{13}C NMR experiment was performed, but even after ~30000 scans not all the ^{13}C peaks were observed due to the limited solubility of the compound. The carbonyl peak at 198.7 ppm could be observed in the ^{13}C NMR spectrum, which along with the IR stretch at 1640 cm^{-1}, supported the fact that the naphthoyl carbonyl was present. Unfortunately MS and MALDI TOF MS

attempts failed to give the molecular weight of the polymer. The polymer could be opened easily by irradiation with visible light as seen by the disappearance of the two internal methyl signals at -3.29 and -3.35 ppm.

2.4.5 Coupling of phenyls to the dibromide 84

A Suzuki coupling reaction was used to add phenyl groups on either side of the DHP molecule **84** using phenyl boronic acid and $Pd(PPh_3)_4$ as the catalyst to give the product **100** as a purple solid (Scheme 2-39).

Scheme 2-39 Addition of phenyls to the dibromide 84

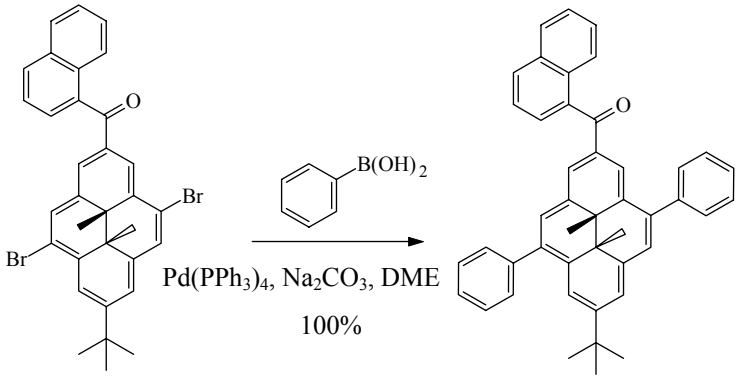

84 **100**

Because the electron withdrawing naphthoyl group reduces the electron density in DHP the coupling reaction was much more efficient, giving virtually a 100% yield after a 24 hour reflux. Uniquely assigning all of the ^{1}H and ^{13}C peaks was not possible due to overlap of the phenyl peaks with the naphthoyl peaks, however the characteristic internal methyl peaks of DHP were distinguishable as two singlets at -3.40 and -3.47 ppm, and all of the other DHP peaks (all singlets) in the ^{1}H NMR spectrum could be uniquely assigned. Confirming the identity of the product mass spectrometry gave the correct

mass HRMS of *m/z* 594.2935 (calculated 594.2922). The compound could be easily opened to the light yellow CPD form when irradiated with visible light.

2.5 Addition of oligothiophenes to the di-*tert*-butyl DHP

The addition of oligothiophenes was found to improve the photo-opening ability of the dihydropyrene switches studied. This was surprising as this effect had not been observed before with DHP. Marsella[44] saw very little effect on the photo-opening properties with the addition of mono and bithiophene functional groups. To probe this effect, a Stille coupling reaction was used to add terthienyl groups to either side of DHP **85** to give **101** (Scheme 2-40).

Scheme 2-40 Adding oligothiophenes to di-*tert*-butyl DHP 85

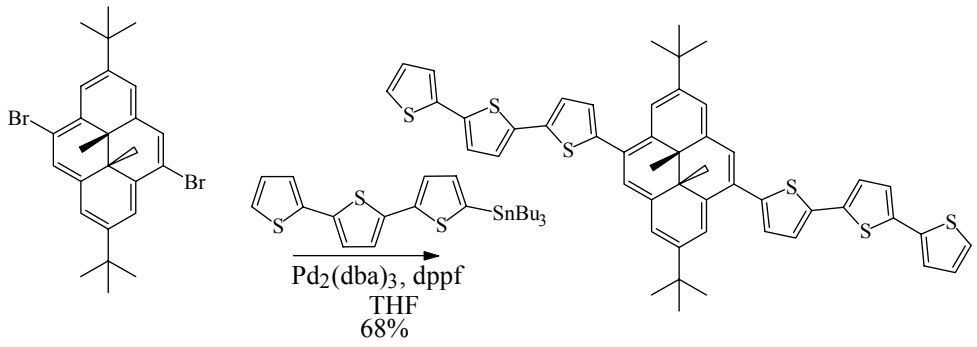

85 **101**

The solution was observed to rapidly change from green to red after a few hours of stirring, but in order to push the reaction to completion it was refluxed for three days. Even with the extended reaction time, a small amount of the mono adduct remained. Separating the desired di-addition product from the mono-addition product proved challenging as they tended to co-elute during purification by silica gel column chromatography. The desired dithienylated product **101** could be obtained after careful

chromatography in 68% yield as a red solid. The product was identified by ^{1}H and ^{13}C NMR spectroscopy and all of the peaks could be assigned. The characteristic internal methyl peaks of the dihydropyrene were found in the ^{1}H NMR spectrum as a singlet at -3.57 ppm. The presence of the two terthienyl functional groups could be seen as a series of 7 doublets or doublet of doublets from 7.53-7.06 ppm. The identity of the product was confirmed by mass spectrometry, which gave the correct mass of *m/z* 837. Because of the low solubility of **101** in hexanes and cyclohexane, UV-vis spectroscopy testing was done in dichloromethane. Irradiation of the compound by visible light showed no detectable amounts of the open form even after 4 hours of visible light irradiation (490 nm cut off filter).

2.6 Synthesis of oligothiophenes

Many different coupling reactions could be used to make thiophene oligomers. Leclerc *et al.*[70] used Kumada coupling to make the dihexyl quinquethiophene **102**, while Barbella *et al.*[71,72] used a Stille coupling to make the S,S dioxide equivalent of both the quinquethiophene **102** and the septithiophene **105** oligomers. A modified version of Barbella's approach using a Stille coupling was used to make both the quinquethiophene **102** and septithiophene **105** oligomers synthesized. For the quinquethiophene oligomers **102**, 2-tributylstannylbithiophene **109**, and for the septithiophene, 2-tributylstannylterthiophene **108** were added to 3,4-dihexyl-2,5-dibromothiophene **35** in THF using $Pd_2(dba)_3$ and dppf as the catalysts and the reaction was generally heated at reflux for 1 day (Scheme 2-41).

Scheme 2-41 Synthesis of quinque 102 and septi 105 oligothiophene

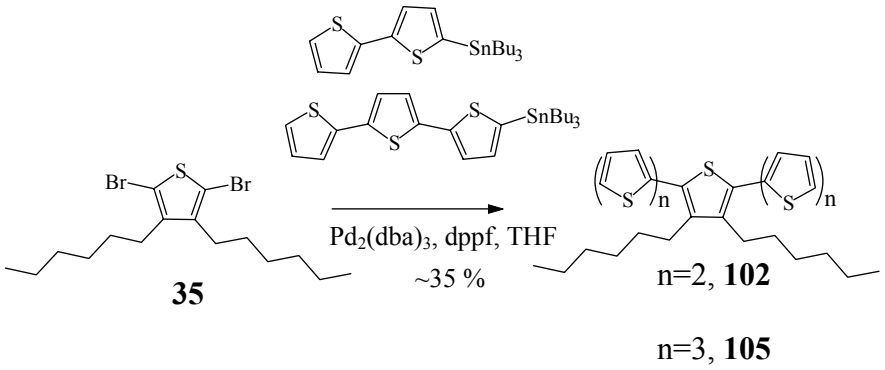

Purification of the quinquethiophene oligomer **102** was accomplished using a long silica gel column to isolate the desired product from a quaterthiophene impurity which tended to co-elute with the product. The yield was generally low (~35%) due to the difficulty in isolating the desired product from this quaterthiophene impurity, and due to the formation of longer thiophene oligomers. The product was identified by the correct molecular weight of *m/z* 580 and by ^{1}H and ^{13}C NMR spectroscopy. For the septithiophene oligomer **105**, purification was accomplished using a silica gel column using 20:1 hexanes:DCM followed by recrystallization from DCM:EtOH to obtain the pure product in a 34% yield. A significant amount of slower running red thiophene oligomers was also recovered from the column. The product was identified by the correct mass spectrometry peak at *m/z* 744 and by ^{1}H and ^{13}C NMR spectroscopy.

2.7 Synthesis of thiophene functionalized dihydropyrenes with an acetylene spacer

In order to explore the possibility of putting a conjugated acetylene spacer between the DHP molecule and thiophene oligomers, the tributyltin functionalized DHP acetylene **110** was synthesized from LDA and tributyl tin chloride. After purification by

a short silica gel chromatography column, a Stille coupling was used to add thiophene to the other end of the acetylene (Scheme 2-42).

Scheme 2-42 DHP with an acetylene spacer

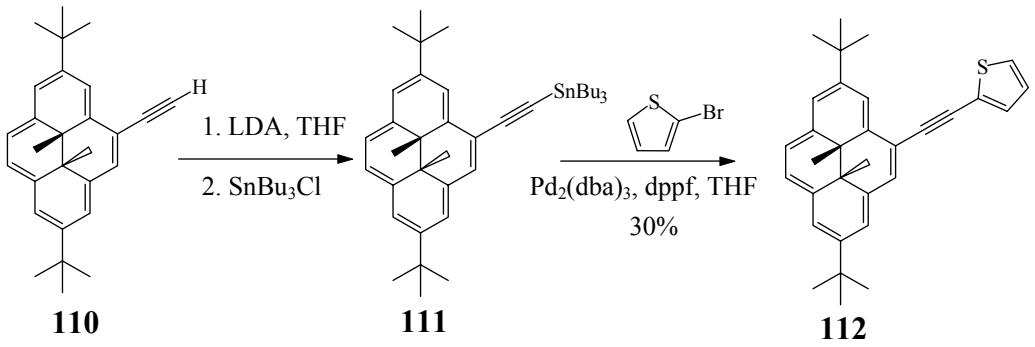

110 **111** **112**

The desired product **112** was obtained but in a low yield (~30%) due to the formation of a large amount of a polymeric biproduct. The ^{1}H and ^{13}C NMR spectra of **112** could be completely assigned. The characteristic internal methyls of the DHP appeared in the ^{1}H NMR as a singlet at -3.78 ppm, the thiophene peaks as doublet of doublets at 7.52, 7.39, and 7.14 ppm, and the acetylene peaks in the ^{13}C appeared at 94.6 and 88.7 ppm. Mass spectrometry gave the correct mass of *m/z* 450.

Chapter Three: Photochemical and Thermochemical Switching Properties

3.1 Introduction

The functional groups attached to the DHP photoswitch have been shown to have a dramatic effect on the DHP switching properties.[23] Because of this functionalization effect we thought it was important to study the switching properties of the key compounds synthesized.

The thermal closing studies were performed using variable temperature NMR spectroscopy. In order to reduce errors due to small integration discrepancies, at each temperature multiple aromatic protons in the closed and the open form were integrated and the results averaged. The activation energy (E_{act}) was obtained using Arrhenius's equation (3-1) and the slope of the plot of ln(k) vs 1/T (3-2). The Eyring equation (3-3) and the slope and intercept from the plot of ln(k/T) vs 1/T (3-4) were used to calculate $\Delta H^{\ddagger}$ and $\Delta S^{\ddagger}$.

$$\mathbf{k = Ae^{\frac{-Eact}{RT}}} \qquad \textbf{3-1}$$

From(3-1) $$\mathbf{\ln(k) = \frac{-E_{act}}{RT} + Constant} \qquad \textbf{3-2}$$

$$\mathbf{k = \frac{kT}{h} e^{\frac{-(\Delta H^{*} - T\Delta S^{*})}{RT}}} \qquad \textbf{3-3}$$

From(3-3) $$\mathbf{\ln\frac{k}{T} = \frac{1}{T}\frac{-\Delta H^{*}}{R} + \frac{\Delta S^{*}}{R} - \ln\frac{k}{h}} \qquad \textbf{3-4}$$

k=1.381x10^{-23} J/K
h= 6.626x10^{-34}Js
R= 8.314 JK^{-1}mol^{-1}

Visible light opening studies were performed using a 500 W tungsten light with a 490 nm cut off filter, and the extent of opening was monitored by UV-vis spectroscopy or by NMR spectroscopy. No special precautions were taken to remove oxygen. During irradiation, the samples were cooled in an ice cooled water bath. The rate of visible light opening was compared to BDHP by performing the irradiations side by side with a BDHP sample of approximately equal concentration.

UV closing studies were performed using quartz cells and a low pressure Hg(Ar) pen light as the UV source (mostly 254 nm UV light) and the samples were cooled during the irradiation by an electric fan. The extent of closing was monitored by UV-vis spectroscopy and was compared to a BDHP sample of approximately equal concentration placed next to the sample being studied during the UV irradiation. A few samples were closed using 350 nm UV light.

When comparing the rates of switching to BDHP using UV-vis spectroscopy the UV-vis absorption data was converted to a concentration. This concentration was then used in the calculation of the kinetic rates. The conversion of the UV-vis data to a concentration was done based on Beers Law (3-5) where **A** is the absorption, **ε** is the molar absorptivity, **b** is the path length and **c** is the concentration. Because for some of the thiophene containing DHP compounds there was a tail in the open form which extended into the closed form at the wavelengths monitored, the absorption measured was a combination of the open and the closed forms (3-6). The total concentration ($\mathbf{c_t}$) however could be obtained from the initial UV-vis spectrum before irradiation, with the assumption that the compound was completely closed. NMR data on the same sample indicated that this was a good assumption as no open peaks were observed in the closed

form and showed that the samples could be fully opened. Knowing $\mathbf{c_t}$ along with the molar absorptivity of the open and the closed form allowed the calculation of the closed concentration (3-8) during the opening and closing studies.

$$\mathbf{A = \varepsilon bc} \qquad \mathbf{3\text{-}5}$$

$$\mathbf{A=\varepsilon_{closed} bc_{closed} + \varepsilon_{open} bc_{open}} \qquad \mathbf{3\text{-}6}$$

$$\mathbf{c_{total} = c_{closed} + c_{open}} \qquad \mathbf{3\text{-}7}$$

$$\mathbf{c_{closed} = \frac{A - \varepsilon_{open} bc_{total}}{(\varepsilon_{closed} - \varepsilon_{open})b}} \qquad \mathbf{3\text{-}8}$$

The reaction rate law of photochemical reactions are typically second order (3-9). This is because, to a simplified approximation, a photochemical reaction is a reaction that occurs as a result of a collision between a molecule [A] and a photon of light [γ]. If a constant light source is used then [γ] becomes a constant and the reaction rate law becomes a pseudo first order reaction (3-10). The differential form of this equation (3-11) can be rearranged (3-12) and after integration (3-13) it can be seen that the apparent rate constant ($k^{'}$) can be obtained from the slope of a graph of ln[A] vs time.

$$\mathbf{Rate = k[A][\gamma]} \qquad \mathbf{3\text{-}9}$$

$$\mathbf{Rate = k^{'}[A]} \qquad \mathbf{3\text{-}10}$$

$$\mathbf{Rate = \frac{-d[A]}{dt} = k^{'}[A]} \qquad \mathbf{3\text{-}11}$$

$$\mathbf{\frac{-d[A]}{[A]} = k^{'}dt} \qquad \mathbf{3\text{-}12}$$

$$\ln[A] = -k't + [A_0] \qquad \textbf{3-13}$$

When UV-vis spectroscopy was used to monitor the rate of the photochemical reaction, the pseudo first order reaction equation was used to obtain the rate constant **k**. When NMR spectroscopy was used to monitor the reaction rate, a zero order equation fitted the data best rather than a first order equation. This can be understood by the fact that an NMR concentration is much higher than a UV-vis concentration, and because the compounds being investigated are highly colored, even though a bright light was used only a small portion of the molecules, those on the outer edge facing the light are actually being irradiated. As the photochemical reaction proceeds and the molecules on the outer edge convert to the open form, molecules further inside the NMR tube become exposed to the light. During this process the number of molecules being irradiated at any one time is virtually a constant and so the rate equation becomes a pseudo zero order reaction (3-14). Converting this equation to a differential equation (3-15) and after rearrangement and integration (3-16), it can be seen that the rate constant k can be obtained from a plot of [A] vs time.

$$\textbf{Rate} = k'' \qquad \textbf{3-14}$$

$$\textbf{Rate} = \frac{-d[A]}{dt} = k'' \qquad \textbf{3-15}$$

$$[A] = -k''t + [A_0] \qquad \textbf{3-16}$$

3.2 Visible light opening

All of the compounds studied (Figure 3-1) opened easily (within a few minutes or less) with visible light irradiation (490 nm cut off filter) and had significant visible light opening rate enhancements over that of BDHP (Table 3-1).

Figure 3-1 Compounds studied

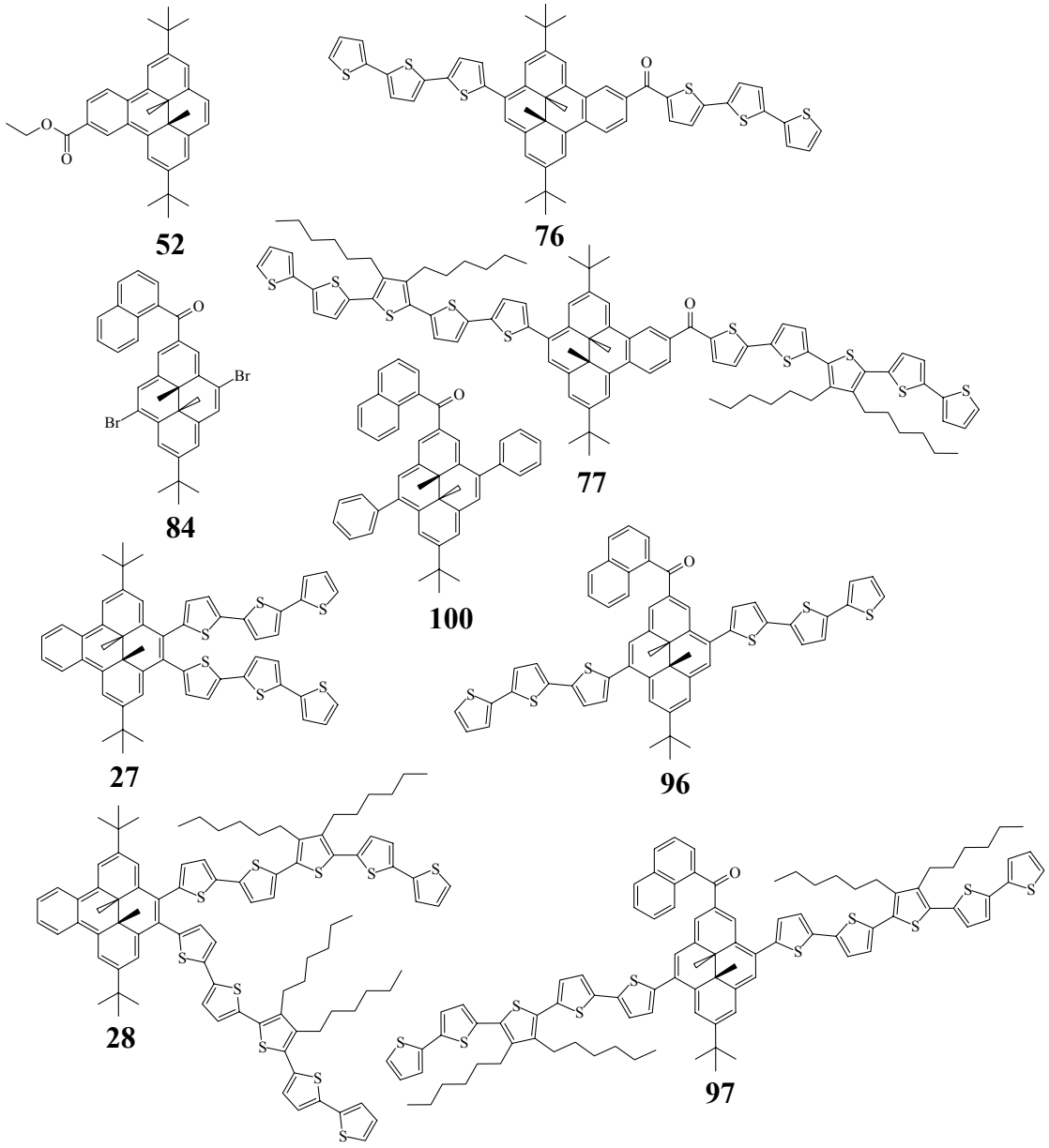

Table 3-1 Photo-opening rate compared to BDHP by UV-vis spectroscopy

Compound (cyclohexane)	**Relative Rate vs BDHP**[#] (cyclohexane)
12 (BDHP)	1
52 (BDHPCOOEt)	2.4 ± 0.2
84[*] (Br_2DHPCONpth)	7.4 ± 0.4
100 (Ph_2DHPCONpth**)**	24 ± 1
27 $(Th_3)_2$BDHP	12 ± 0.5
28 $(Th_5)_2$BDHP	20 ± 1
76 Th_3BDHPCOTh_3	19 ± 1
77 Th_5BDHPCOTh_5	29 ± 1
96 Th_3DHPCONpthTh_3	48 ± 2
97 Th_5DHPCONpthTh_5	130 ± 5

* in $CHCl_3$, # errors calculated based on the standard deviation of the line

The large photo-opening rate enhancement for the oligothiophene functionalized compounds was encouraging as only a slight increase in the rate of visible light opening had been observed for **19** when compared to the parent DHP photo-opening rate.[44] The lack of a significant rate enhancement for **19** was a disappointment as the photo-opening rate of the parent DHP **11** is quite poor (much less than that of BDHP) and it was hoped that the thiophenes would cause a dramatic increase in the photo-opening rate.

Both UV-vis and NMR photo-opening studies were performed for **52** and the irradiation was done side by side with a BDHP **12** sample. When NMR was used, zero

order kinetics fit the data best and when UV-vis spectroscopy was used, first order kinetics fit the data best (Figure 3-2).

Figure 3-2 Photo-opening of the ester 52 vs 12 (BDHP) by UV-vis in cyclohexane and NMR spectroscopy in C_6D_6

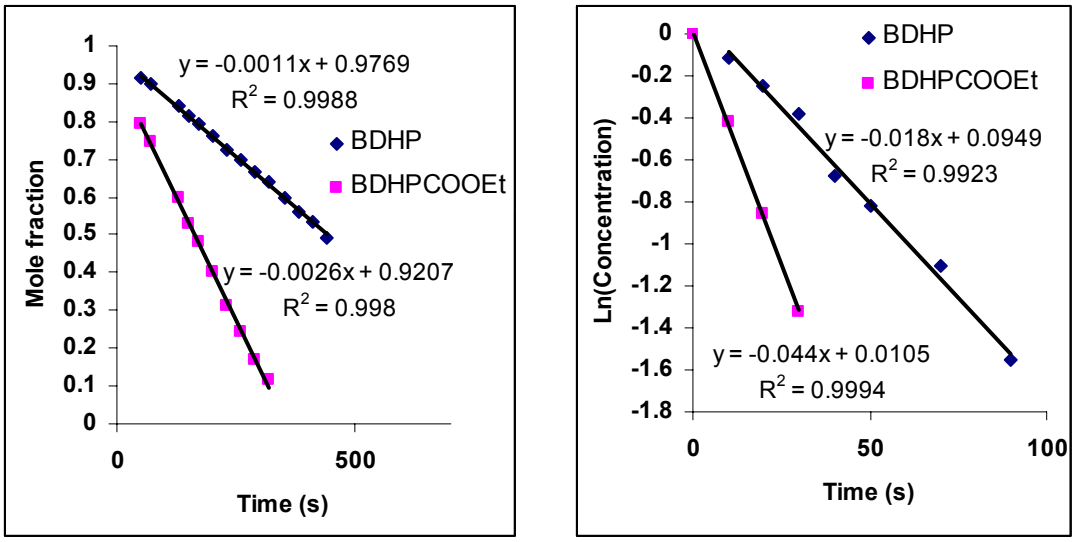

A- By NMR **B- By UV-vis**

Because zero order kinetics were used for the NMR sample and first order kinetics for the UV-vis sample the rate constants were different. However the ratio between the rate constants for **52** and BDHP **12** in the NMR and UV-vis studies were virtually identical (2.4:2.4).

The opening rates for all the thiophene functionalized switches were monitored by UV-vis spectroscopy. Adding terthiophene oligomers (**27)** to the same side of BDHP **12** caused a 12-fold increase in the photo-opening rate as compared to that of BDHP **12**. Increasing the length of the oligomers to a quinquethiophene **28** increased the rate to 20 times that of BDHP **12**. Adding thiophenes on opposite sides of BDHP **12** also caused a large photo-opening rate enhancement. Much of this rate enhancement can be attributed to the addition of the thiophene oligomers, as BDHP **12** with an ethyl ester **52** was only

two times faster than BDHP. With terthiophene oligomers on either side of the switch **76**, the photo-opening was 19 times faster than BDHP **12**, and with the longer quinquethiophene oligomers **77**, it was 29 times faster than BDHP **12**.

Switches based on the DHP switch have typically had a much slower photo-opening rate than BDHP. However the addition of an electron withdrawing group, particularly a carbonyl, has been shown to increase the photo-opening rate.[73] When a naphthoyl group was added in the 2 position **84** the photo-opening rate was found to be 8 times that of BDHP **12**. The photo-opening rate for **84** was measured in chloroform as it was found that when cyclohexane, or hexane was used as the solvent a photostationary state developed (Figure 3-3). This photostationary state did not occur when aromatic or chlorinated solvents were used.

Figure 3-3 Photostationary state of 84 in cyclohexane and fully open in chloroform

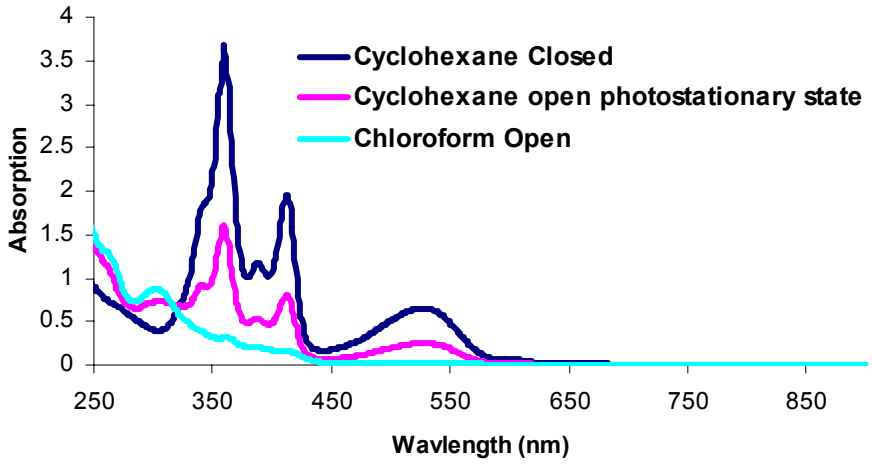

With a phenyl group **100** on either side the photo-opening was 24 times faster than BDHP. The addition of a terthiophene oligomer on either side **96**, led to a dramatic increase in the photo-opening rate of 48 times that of BDHP. And with a longer

quinquethiophene oligomer **97**, there was an even faster photo-opening rate of 130 times that of BDHP. It should be noted that the error in the values given for the fast opening DHP samples will be large due to uncertainty in the light levels for irradiations of just a few seconds. These results however clearly demonstrate that the addition of the thiophene oligomers to the switch does cause a dramatic increase in the photo-opening rate, and that this photo-opening rate is related to the length of the thiophene oligomers. The photo-opening rates of the oligothiophene substituted naphthoyl DHP's are some of the fastest photo-opening rates measured for DHP based photoswitches.

The opening enhancement of the switches by thiophene oligomers does however appear to be confined to switches that already have functional groups which improve photo-opening properties, such as compounds with a naphthoyl group in the 2 position or with a benzene functional group fused to the side of DHP. Adding terthiophene oligomers to either side of DHP **101** does not cause a photo-opening rate enhancement. After 4 hours of visible light irradiation (490 nm cut off filter) at ~5^{o}C, none of the open form was observed by NMR spectroscopy. Visible light opening on a UV-vis sample also did not show any opening of the switch. When terthiophene oligomers were added to DHP molecules functionalized with naphthoyl groups on the side **83**, no opening was observed after irradiation with visible light (490 nm cut off filter) for a few hours by NMR, or for several minutes by UV-vis. This indicates that the position and orientation of the naphthoyl group is important for effective visible light opening.

Robb[74], using high level *ab initio* calculations showed that the photo-opening reaction for the parent DHP **10** occurs through a conical intersection between a biradical excited state and the ground state. They showed that the photo-opening reaction for DHP

is inefficient because the biradical excited state is not the lowest excited state minimum, the biradical state is not highly populated, and there are no pathways from the more highly populated zwiterionic excited state to the biradical excited state.

If the photo-opening reaction only occurs through a biradical intermediate then switches with more effective photo-opening reactions will have a more highly populated biradical excited state. Increased access to the biradical excited state could be achieved by either stabilizing the biradical excited state or destabilizing the other excited states with respect to the biradical excited state.

π-Acceptor functional groups such as the naphthoyl functional group are known to stabilize radicals by delocalizing the radical into their π-system.[75,76] Adding a naphthoyl group to the DHP molecule is known to improve the photo-opening properties of the DHP switch.[25] This improvement might be the result of the naphthoyl functional groups ability to influence the biradical excited state. The 2 position of DHP has been calculated to have the second highest unpaired spin density[77] and so adding the naphthoyl to this position would help to maximize this effect. DHP based switches with this functionality **84**, **100**, **96**, **97**, **98** and **99** were all observed to have a dramatic enhancement in their photo-opening properties compared to that of the parent DHP **10**.

For effective stabilization of a radical by a π-acceptor functional group, co-planarity is important to allow for effective orbital overlap. For **83** where the naphthoyl group was added in the 4 position and which had a terthiophene functional group in the 5 position no improvement was observed in the photo-opening of the switch. With a bulky terthiophene oligomer attached in the 5 position it will be very difficult for the naphthoyl

functional group in the 4 position to be co-planar with the DHP switch. This would reduce the naphthoyl's radical stabilizing ability (Figure 3-4).

Figure 3-4 Steric hindrance between the functional groups in 83

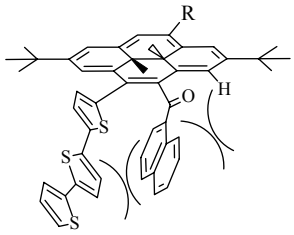

The 4 position of the DHP molecule also has a much lower unpaired spin density compared to the 2 position, so this would also reduce the effectiveness of the added naphthoyl to influence the photo-opening of the switch.

The reason photo-opening properties improve when oligothiophenes are added to activated DHP switches, but not when added to simple DHP switches, is not entirely clear. The activating functional group and the oligothiophenes could be working in combination to modify the position of the excited state energy levels leading to more efficient photo-opening. The oligothiophenes might also be acting as an antenna and channelling the energy they capture into the DHP switch. With an activating functional group making the biradical excited state more accessible, the energy channelled from the oligothiophenes would be available to enhance the photo-opening of the switch. For molecules without an activating functional group, the energy channeled from the oligothiophenes might have no effect on the population of the biradical excited state and result in no improvement in the photo-opening reaction.

3.3 Thermal closing

The rates of thermal closing from the open cyclophanediene form to the closed dihydropyrene form were studied by NMR spectroscopy using C_6D_6 as the solvent for compounds based on BDHP, and $CDCl_3$ for compounds based on DHP. The only exception to this was for the BDHP based **27,** which was studied by NMR in $CDCl_3$ due to the poor solubility of the open CPD form in C_6D_6. At least 3 and up to 6 different temperatures were used for each compound and from the kinetic data obtained, Arrhenius and Eyring equations were applied to determine the activation energy (E_{act}), pre-exponential factor (LnA), enthalpy ($\Delta H^{\ddagger}$) and entropy ($\Delta S^{\ddagger}$) (Table 3-2).

Table 3-2 Thermal closing data determined from variable temperature NMR spectroscopy in $CDCl_3$ or C_6D_6

Compound *$CDCl_3$ # C_6D_6	**$\tau_{1/2}$ (20°C)***	**$\tau_{1/2}$ (50°C)***	**E_{act} (kcal/mol)**	**$\Delta H^{\ddagger}$ kcal/mol**	**$\Delta S^{\ddagger}$ cal/mol**	**lnA**
84 Br_2DHPNpth*	3.4 h	5.7 min	22.5 +/- 0.3	21.9 +/- 0.3	-3.1 +/- 1	28.9 ± 0.5
100 Ph_2DHPNpth*	94 min	2.6 min	21.4 +/- 0.5	20.7 +/- 0.5	-5.2 +/- 2	27.9 ± 0.9
96 $(Th_3)_2$DHPNpth*	41 min	1.1 min	22.6 +/- 0.8	22.0 +/- 0.8	0.5 +/- 3	30.6 ±1.4
97 $(Th_5)_2$DHPNpth*	57 min	2.5 min	19.7 +/- 0.4	19.2 +/- 0.4	-9.9 +/- 1.4	25.4 ± 0.7
52 $BDHPCO_2Et^{\#}$	8.8 days	3.8 h	25.0 +/- 0.5	24.4 +/- 0.5	-2.8 +/- 1.5	29.1 ± 0.8
76 $Th_3BDHPTh_3^{\#}$	6.6 days	3.2 h	24.5 +/- 0.9	24.0 +/- 0.9	-3.9 +/- 3	28.7 ±1.2
77 $Th_5BDHPTh_5^{\#}$	4.5 days	2.5 h	23.5 +/- 0.7	22.9 +/- 0.7	-6.7 +/- 2	27.2 ±1.0
12 BDHP[24]	7.3 days	5.2 h	24.5			
27 $(Th_3)_2$BDHP*	59 h	1.1 h	24.5 +/- 1.5	23.8 +/- 1.5	-2.2 +/- 5	29.5 ± 2
28 $(Th_5)_2BDHP^{\#}$	69 h	1.2 h	25.1 +/- 0.4	24.5 +/- 0.4	-0.3 +/-1	30.4 ±0.6

***** Error estimated as < 5%

Adding an ethyl ester attached to BDHP **52** caused the thermal return to be slower ($\tau_{1/2}$= ~9 days at 20°C) than that of BDHP **12** ($\tau_{1/2}$= ~7 days at 20°C)[22]. The addition of terthiophenes on opposite sides of BDHP **76**, however caused the thermal return to increase ($\tau_{1/2}$= 6.7 days at 20°C) and with quinquethiophenes **77** the thermal return was even faster ($\tau_{1/2}$= 4.5 days at 20°C).

Adding thiophenes to the same side of BDHP also caused an increase in the rate of the thermal return. In this case the shorter terthiophene compound **27** had a faster thermal return ($\tau_{1/2}$= 59 h at 20°C) than the longer quinquethiophene compound **28** ($\tau_{1/2}$= 69 h at 20°C). Although the thermal return of the BDHP based switches with thiophene oligomers attached was faster than BDHP **12**, the thermal returns were still quite slow overall with half lives all over 2 days at 20°C.

The thermal returns of compounds based on DHP with the 2-naphthoyl group, however had significantly faster thermal returns than BDHP **12**. This is not surprising as substitution with a radical stabilizing functional group in the 2 position is known to increase the thermal closing rate.[73] This is because the radical stabilizing functional group lowers the transition state energy, leading to a decreased activation barrier and a faster thermal return.[77] The thermal closing of the dibromide **84** was a few hours ($\tau_{1/2}$= 3.4h) at 20°C, the diphenyl **100** was slightly over 1.5 hours, and when thiophenes were attached the thermal return was even faster. With terthiophene oligomers attached **96** the thermal return half life was 41 minutes and with quinquethiophenes attached **97** the half life was 57 minutes at 20°C.

As expected there is a trend that slower thermal return half lives correspond to higher activation energies, however within this trend there are a number of deviations.

The activation energy of **97** (19.7 kcal/mol) is less than the activation energy for the terthiophene compound **96** (22.6 kcal/mol), but it has a larger half life (57 min vs 41 min at 20^{o}C). The BDHP switch with quinquethiophenes on the same side **28** has the highest activation energy of the compounds studied (25.1 kcal/mol) and yet **52, 76** and **77** all had longer thermal half lives. These discrepancies in the general trend for the activation energy indicate that the pre-exponential factor A and the $\Delta S^{\ddagger}$ play a significant role in the thermal return half-life.

3.4 UV closing

Comparison UV closing experiments were performed for the three compounds **77, 28** and **97**, all of which had the quinquethiophene oligomers attached (Table 3-3).

Table 3-3 UV (254 nm) closing experiments monitored by UV-vis spectroscopy in cyclohexane

Compound	**Relative rate vs BDHP**
28 $(Th_5)_2$BDHP	1.2
77 Th_5BDHPCOTh_5	0.9
97 Th_5DHPCONapthTh_5	2.5

There was very little difference in the UV closing rates from that of BDHP **12**. BDHP with thiophenes on the same side **28** was marginally faster to close than BDHP. With thiophenes on opposite sides **77** it was marginally slower to close than BDHP. Naphthoyl substituted DHP with thiophenes on opposite sides **97** however did have a

faster closing rate than BDHP (2.5 times faster), but this value is certainly partially due to some thermal closing. All three of these compounds did not close completely when irradiated with 254 nm UV light but instead reached a photostationary state.

Cycling with visible and UV light could be achieved with very little change when monitoring the long wavelength absorption (~550nm, Figure 3-5).

Figure 3-5 Cycling visible light (490 nm filter) opening and UV (254 nm) closing in cyclohexane while monitoring the ~550 nm absorption

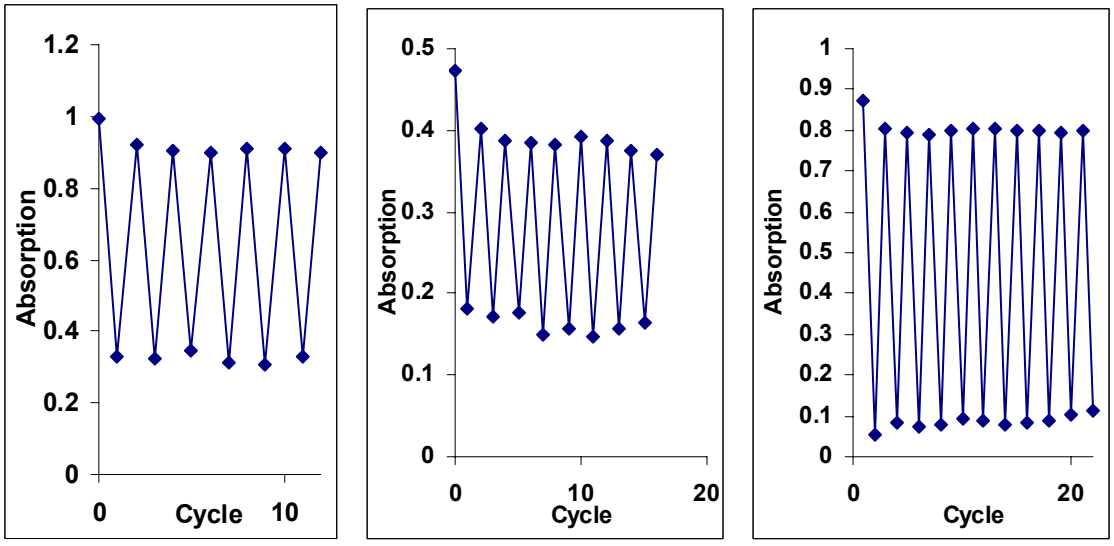

77-(550nm) **28**-(554nm) **97**-(566nm)

The photostationary state produced by UV irradiation can be observed as the original closed absorption is not obtained during any of the subsequent cycles.

3.5 Thin film switching

Opening and closing of **97** was done in the solid state as a thin film prepared by drop coating from dichloromethane onto a quartz or glass cell. The thin film sample could be fully opened by irradiation with visible light (490 nm cut off filter, Figure 3-6).

Figure 3-6 Thin film opening of 97 (drop coated from DCM)

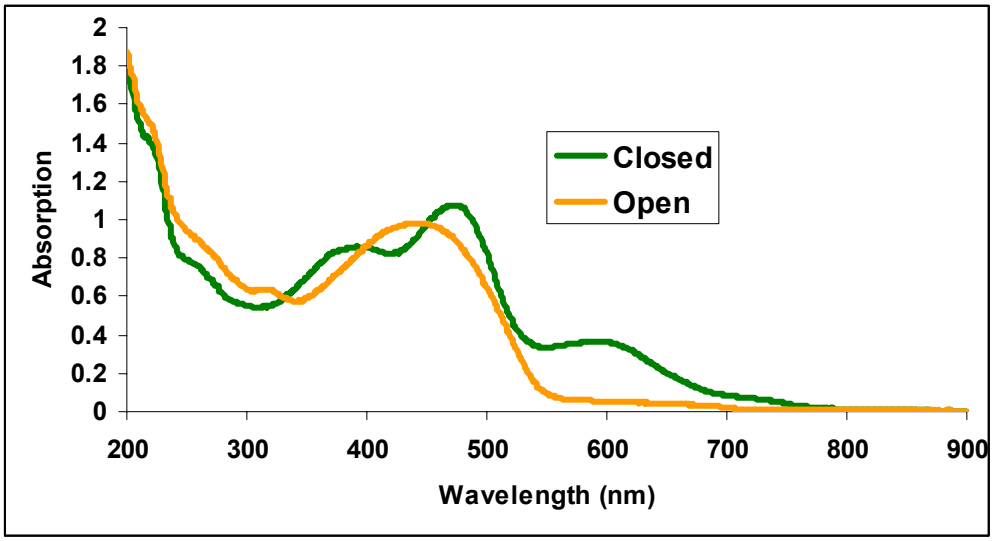

The thin film could also be opened using a hand held laser pointer. When a green laser pointer was used (532 nm, <5mW) a photostationary state was observed. When a red laser pointer (650 nm, <5mW) was used virtually complete opening of the sample could be obtained (Figure 3-7).

Figure 3-7 Green (532 nm) and red laser (650 nm) opening of a thin film of 97 (drop coated from DCM) on glass

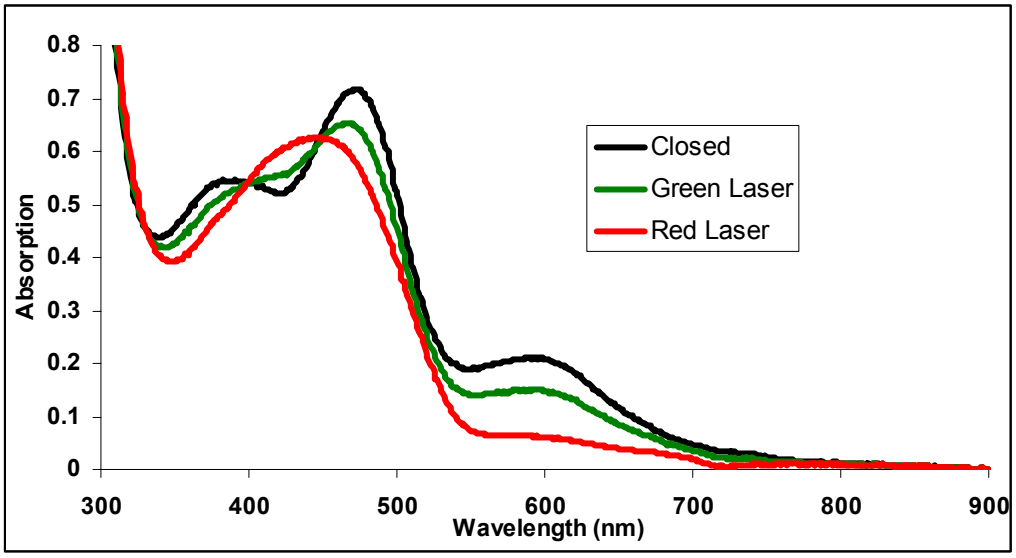

After a sample had been fully opened with the red laser, the green laser could be used to partially close the sample to the photostationary state.

When 254 nm UV light was used to close the sample, a photostationary state resulted. Also after several cycles of opening and closing there were changes in the UV-vis spectrum indicating that some decomposition was occurring (Figure 3-8).

Figure 3-8 Cycling the quinquethienyl photoswitch 97 with 254 nm UV light

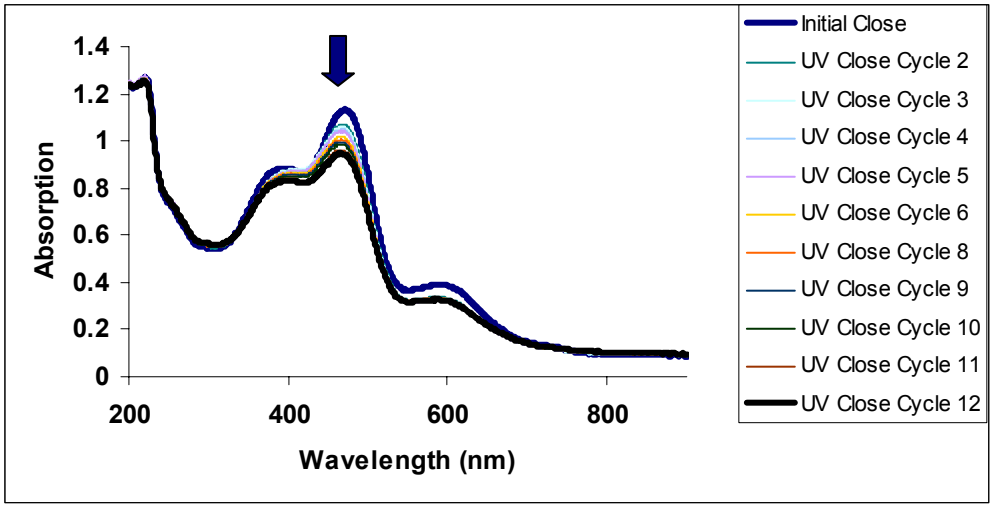

There was very little change in the absorption at ~600 nm except for the initial drop in absorption due to the development of a UV-vis photostationary state. However there was a clear gradual decrease in the 350-550 nm absorption region as the switch was cycled. If 350 nm UV light was used instead of 254 nm UV light then once again a photostationary state was observed but there was no general decrease in the absorption as seen before (Figure 3-9). The sample could also be fully closed thermally, if after reaching a photostationary state it was heated.

Figure 3-9 UV closing of 97 using 350 nm UV light. Visible light opening with a red laser pointer (650 nm)

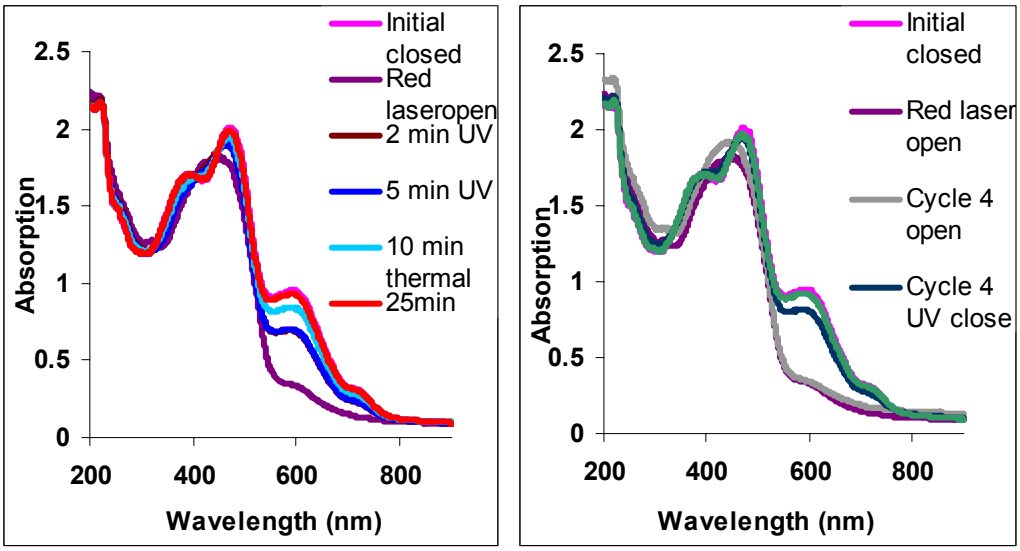

A: First Cycle **B: Fourth Cycle**

In an effort to explore what was happening when 254nm UV light was irradiated on **97**, an NMR solution in d_{12}-cyclohexane was irradiated with 254 nm light. No new peaks were observed in the NMR spectrum. However after extended irradiation (>40 h) it was noticed that a film was forming on the inside of the tube and the concentration of the sample inside the NMR tube was decreasing. This indicated that a polymerization reaction was occurring. UV polymerization of oligothiophenes is known to occur,[78,79] so it is probably not surprising that it occurs for **97** when irradiated for long periods of time with 254nm UV light. This result indicates that longer wavelength (i.e 350nm) UV light is a better choice for UV closing if polymerization is to be avoided. In a further effort to understand what was taking place, a thin film of **97** was irradiated for ~ 3 hours with 254 nm UV light. It was then dissolved in $CDCl_3$ and the ^1H NMR spectrum obtained. The spectrum was virtually the same as the original spectrum except there was clear

broadening in the DHP peaks 5, 8, and 10 as well as the thiophene peaks 27, 47 and 48. If the sample was filtered through alumina then the spectrum returned to the original with no broadening observed (Figure 3-10).

Figure 3-10 NMR spectra of 97 before, after UV irradiation and after filtration

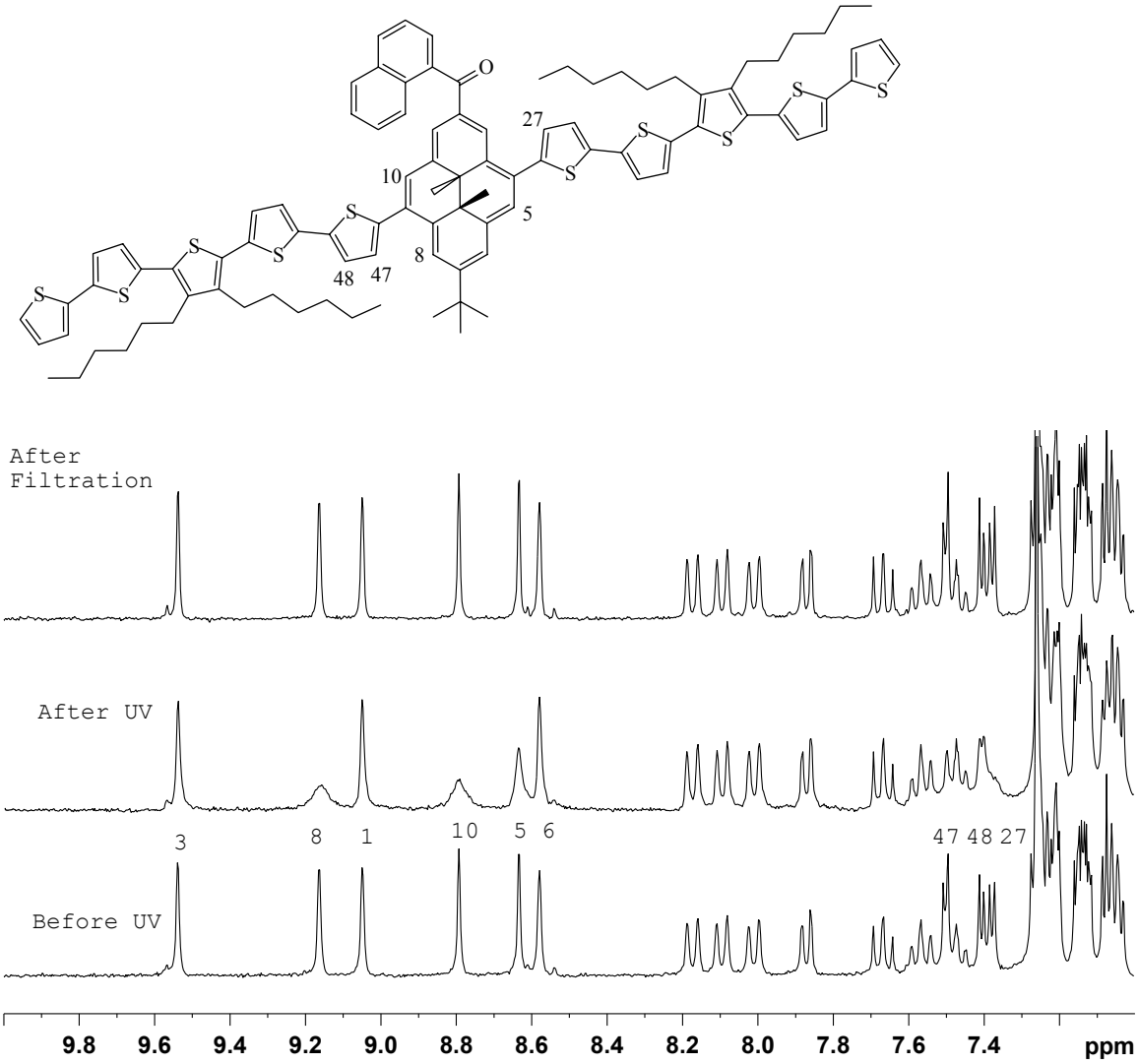

It was found that after extended 254 nm UV irradiation the thermal return was accelerated to a point where an ^{1}H NMR of the open form could not be obtained. UV-vis

spectroscopy showed that complete thermal closing occurred in about 3 minutes at 22°C as compared to the 140 minutes before the UV irradiation (Figure 3-11).

Figure 3-11 Thermal closing, A: before UV irradiation, B: after UV irradiation

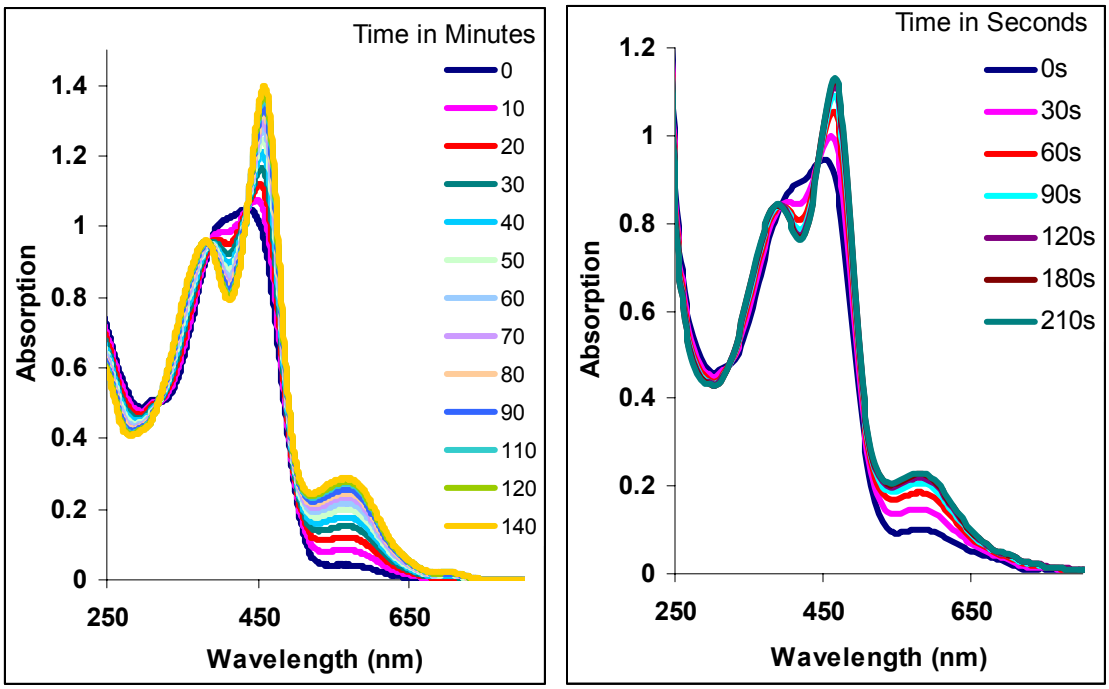

A **B**

DFT calculations by Williams *et al.*[77] showed that the transition state for the thermal closing reaction has biradical character. The addition of radical stabilizing thiophene oligomers would be expected to lower the activation barrier and enhance the thermal closing reaction. Because the oligothiophenes were attached to positions on the DHP molecule which have low spin densities,[77] the effect of the added oligothiophenes on the thermal closing reaction was small. Extended 254 nm UV irradiation, however would cause the formation of some radicals which are then stabilized by the large π system. The presence of these radicals can be seen in the broadening observed in the ^{1}H

NMR (Figure 3-10). The radicals also catalyze the thermal closing reaction, presumably by stabilizing the biradical transition state. Filtration through alumina removes the radicals causing the ^{1}H NMR spectrum to return to its original condition and stopping the radical catalyzed thermal closing.

3.6 Conclusion

Functionalization was found to cause dramatic effects on the switching properties of the switches studied. The addition of a naphthoyl group to the 2 position of DHP was found to increase the rate of visible light photo-opening compared to BDHP and to also increase the rate of thermal closing. The addition of oligothiophenes dramatically increased the rate of photo-opening compared to BDHP **12** as long as they were added to already activated switches, such as the benzo and 2-naphthoyl dihydropyrenes. Longer oligothiophene chain length enhanced this effect. Unfortunately the addition of oligothiophenes increased the rate of thermal closing. The thermal closing of oligothiophene functionalized BDHP based compounds was still quite slow with half lives greater than 2 days at 20^{o}C. However the thermal closing of the oligothiophene functionalized naphthoyl DHPs was much faster with half lives of less than 1 hour at 20^{o}C. Functionalization was found to have little effect on the UV closing when compared to BDHP **12**. Extended exposure to 254 nm UV light was found to accelerate the thermal closing reaction due to the formation of radicals. Consequently 254 nm UV light is probably a poor choice of light to use for closing oligothiophene functionalized switches.

Chapter Four: Conjugation Changes

4.1 Introduction

The extent to which π electrons are conjugated has been shown to have a large impact on the ability of organic oligomers and polymers to conduct electricity.[80,81] Based on this information, if the DHP switch when attached to oligothiophene molecular wires is to have an effect on conductivity it should be observed that: 1) the oligothiophene wires are conjugated with the switch and 2) there is a change in conjugation when the switch is opened and closed. If these effects on conjugation are not observed then the opening or closing of the switch would not be expected to have much of an effect on conductivity.

UV-vis spectroscopy is a useful tool for examining the extent to which the π electrons in a molecule are conjugated. Increasing the amount of conjugation in a molecule leads to a bathochromic shift in the UV-vis absorption spectrum due to a reduction in the HOMO-LUMO gap. Decreasing the extent of conjugation in a molecule leads to a hypsochromic shift due to the increase in the HOMO-LUMO gap. An example of this can be seen in the bathochromic shift in the absorption of oligothiophenes as the number of thiophene units is increased (Table 4-1).[82]

Table 4-1 Absorption of thiophene oligomers in dioxane[82]

n 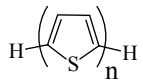	**Abs λ_{max} (nm)**
1	231
2	303
3	354
4	392
5	417
6	436
7	441

Although the magnitude of the red shift decreases as the number of thiophenes increases, Otsubo[83] has shown that an effective conjugation limit is not reached even with a 96 unit thiophene chain,[83] although the difference does become very small (between n=72 and n=96 there was less than a 1 nm difference).

If the thiophene wires attached to the DHP switch are conjugated with the switch then a bathochromic shift in the UV-vis absorption spectrum should be observed when compared to the unconnected switch and wires. If the act of switching the switch has the ability to affect this conjugation then a hypsochromic shift in the UV-vis absorption should be observed when the switch is opened from the closed form.

4.2 DHP based switches

Comparison of the UV-vis spectra of the switch, with terthiophene **96** and without terthiophene wires **84** shows that there is a bathochromic shift in the UV-vis absorption spectra (Figure 4-1).

Figure 4-1 Absorption spectra of 96 and 84

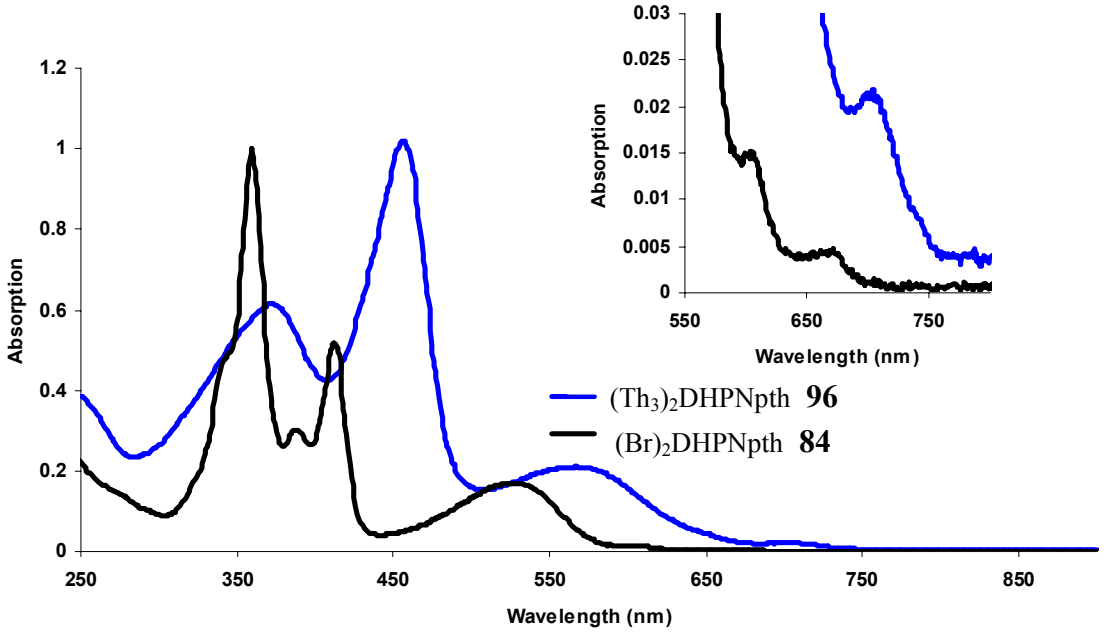

The spectrum of **84** in the closed form has two very small absorptions at 670 nm (ε_{max} =325) and 604 nm (ε_{max} = 1440) followed by a larger absorption characteristic of dihydropyrenes at 527 nm (ε_{max} = 13300). When two terthiophene oligomers were added on either side **96**, a red shift in the absorption spectra of the closed form was observed with a small absorption at 703 nm (ε_{max} = 1600) and a larger one at 568 nm (ε_{max} = 16800). This red shift in the absorption spectra upon addition of the thiophene oligomers indicates that there is extended conjugation from the terthiophene oligomers into the switch. If these results are compared with the diphenyl **100**, then it can be seen that the

spectrum of the diphenyl **100** is red shifted compared to that of the dibromide **84** but blue shifted when compared to the diterthienyl **96** compound. This is expected as there should be extended conjugation from the benzene rings into the DHP switch, but this increased conjugation of the diphenyl **100** is less than the extended conjugation for the terthienyl compound **96** (Figure 4-2) which has a larger π-system.

Figure 4-2 Absorption spectra of 96, 84 and 100

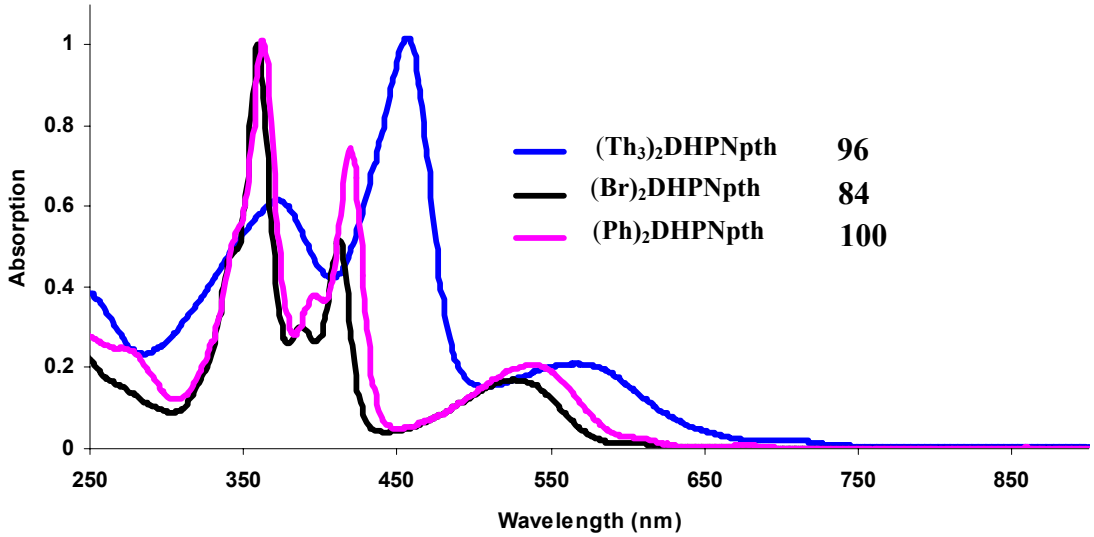

When comparing these results to the UV-vis absorption spectra of compound **97** which has dihexylquinquethiophene **102** oligomers on either side (Figure 4-3), there was virtually no change in the long wavelength absorptions. This indicates that there is essentially no change in the effective conjugation length between compounds with terthiophene **96** or the dihexylquinquethiophene **97** oligomers attached. This is not surprising as the conjugation length in the terthiophene case is already large, therefore only very small changes in the UV-vis absorption are expected with increasing conjugation length. Also the two dihexyl groups on the same thiophene will cause a

slight twist in the thiophene chain which will reduce the conjugation length. Interestingly there is a slight red shift on going to the polymer of the dihexyl compound **99** (Figure 4-3) suggesting that both the terthienyl **96** and quinquethienyl **97** compounds have not yet reached the total effective conjugation length possible.

Figure 4-3 UV-vis spectra of 96, 97, 99

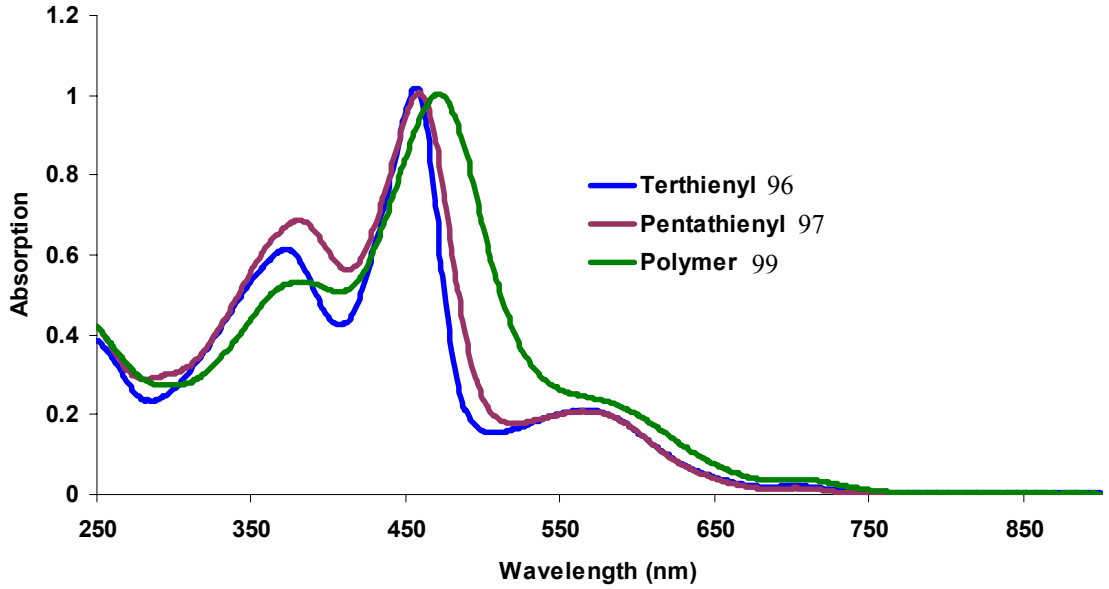

When these compounds were opened by irradiating with visible light, the UV-vis spectra showed the disappearance of the long wavelength absorptions (Figure 4-4), indicating that the switch had "turned off" the extended conjugation observed in the closed form.

Figure 4-4 UV-vis spectra of open and closed form of 96, 97, 99

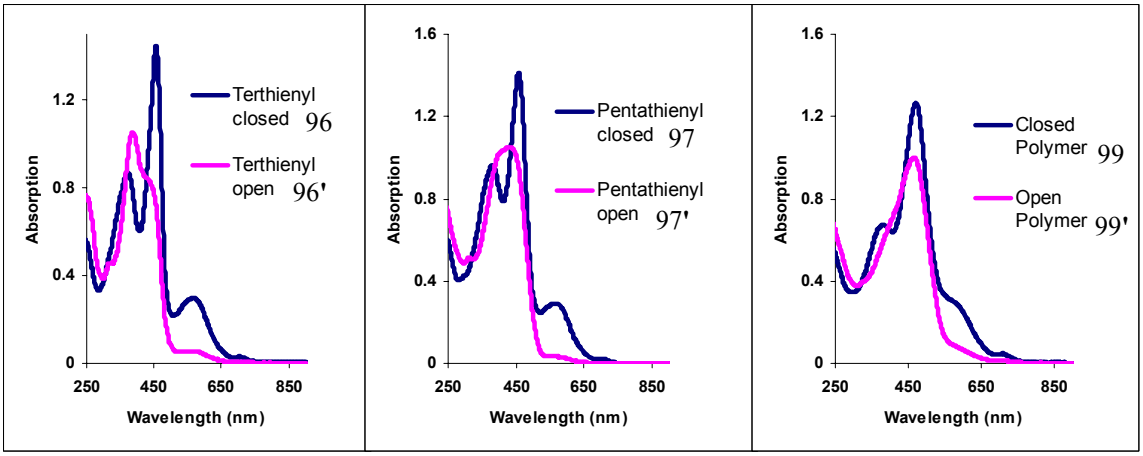

The changes between the open and the closed form became less significant as the thiophene oligomers became longer. This is because the absorption from the thiophene oligomers begins to dominate the UV-vis absorption spectra.

The UV-vis absorption spectra of a film of the closed form of the quinquethienyl **97** had a bathochromic shift in its absorption with respect to a solution sample. This is particularly evident in the two longest wavelength peaks, which in the film are red shifted to 593 and 716 nm from 566 and 703 nm when in solution (Figure 4-5).

Figure 4-5 Comparison of solution and thin film UV-vis absorption for 97

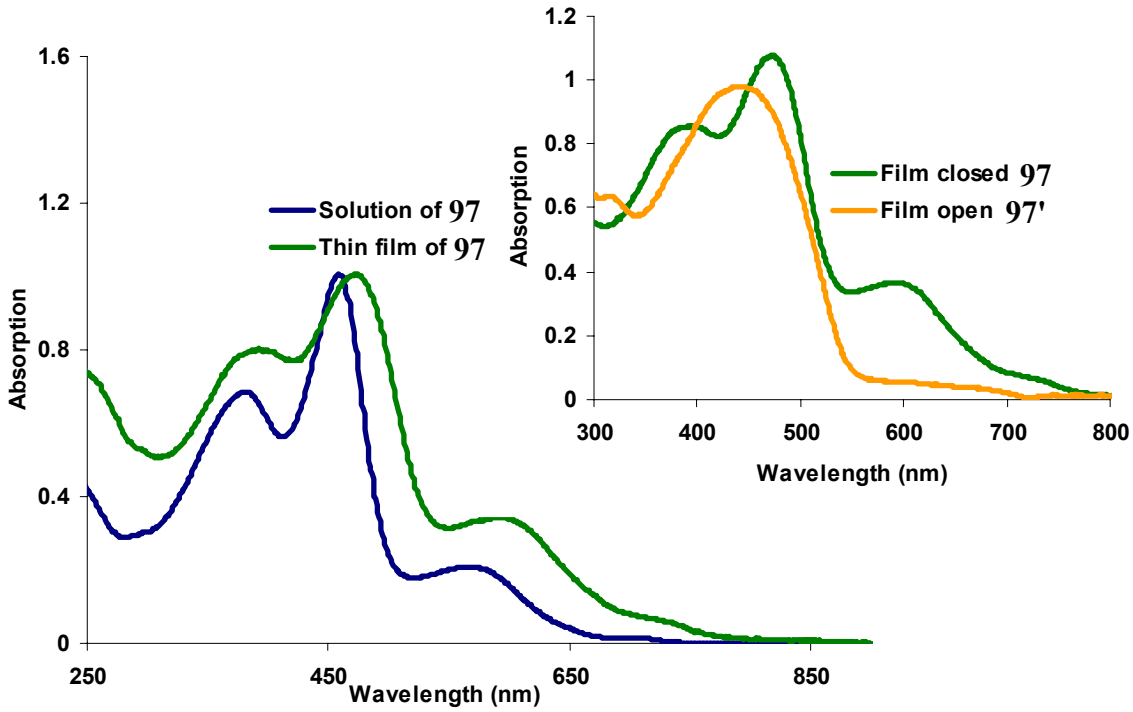

Solid state ordering is well known to cause red shifting in the UV-vis absorption spectrum of thin films of conjugated systems.[84,85] This red shift is due to a reduction in the twisting of the conjugated backbone, which increases the planarity of the oligomers and therefore increases the effective conjugation length.

These results indicate that for systems based on the DHP switch with a naphthoyl in the 2 position the thiophene wires are conjugated with the switch and that the switch can modify the extent of the conjugation in these molecules.

4.3 BDHP based switches with thiophenes on opposite sides

For molecules based on the BDHP switch with thiophenes attached on opposite sides of the switch, a bathochromic shift was observed in the UV-vis absorption spectra

upon addition of the thiophene oligomers (Figure 4-6). Unfortunately the red shift observed was not as large as what was seen in the DHP example, especially for the longest wavelength absorption.

Figure 4-6 UV-vis absorption of BDHP with oligothiophenes on opposites sides

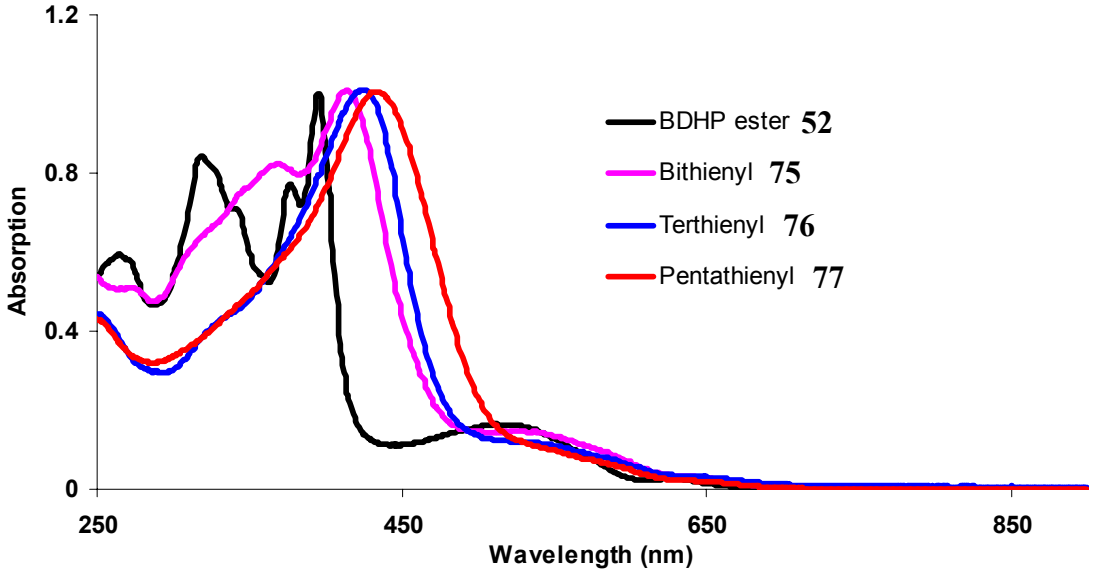

The parent ethyl ester BDHP **52** had long wavelength UV-vis absorptions of 630nm (ε_{max} = 650) and 513nm (ε_{max} = 4060). When bithiophene was added **75**, there was only a slight red shift of the longest wavelength absorptions to 643nm (ε_{max} = 2210) and 532nm (ε_{max} = 10300) peak. When terthiophene was added **76**, the long wavelength absorption was at 647nm (ε_{max} = 1700), a very small red shift from the bithiophene based molecule **75** and identification of the second peak at ~ 526nm (ε_{max} = 8400) was difficult because of the tail of the very large absorption at 426nm (ε_{max} = 69300). When quinquethiophene oligomers were added **77**, the longest wavelength absorption was again only slightly redshifted (655nm (ε_{max} = 1850)) and the tail of the largest peak at 433 nm (ε_{max} = 99500) obscured any peak that might have appeared in between. The most obvious red

shift was seen in the most intense absorptions at 395 (ε_{max} = 24900) for the ester **52**, 414 (ε_{max} = 70200) for the bithienyl compound **75**, 426nm (ε_{max} = 69300) for the terthienyl compound **76**, and 433 (ε_{max} = 99300) for the quinquethienyl compound **77**. These results indicate that although there is extended conjugation between the switch and the wires the effect of this extended conjugation is quite limited.

When examining the changes in the UV-vis spectra between the open and the closed forms it was found that when the thiophene chains were small a large difference between the open and the closed form was observed, particularly for the long wavelength peaks, indicating there was a significant change in the conjugation. However when the length of the thiophene oligomers was increased the changes became smaller so that in the quinquethiophene **77** example there was very little difference between the open and the closed form in the long wavelength region of the spectrum (Figure 4-7).

Figure 4-7 Open and closed UV-vis spectra of 75, 76, 77

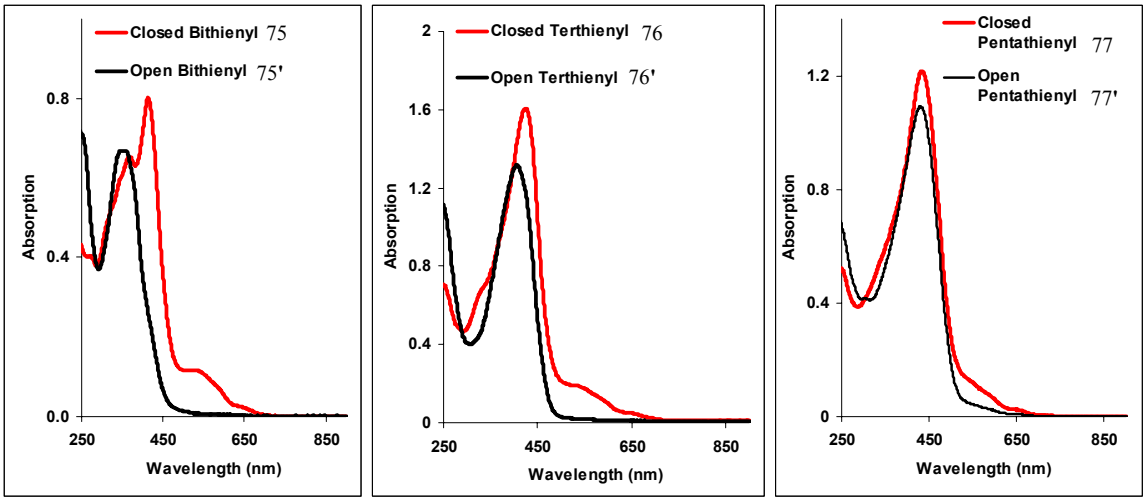

This indicates that although the switch could modify the conjugation length, because there was limited conjugation between the switch and the wires, as conjugation length of

the wires increased the ability of the switch to affect this conjugation length became less significant.

4.4 BDHP based switches with thiophenes on the same side

When comparing the UV-vis spectra of BDHP **12** with those with two terthienyl **27** and quinquethienyl **28** "wires" attached on the same side of the BDHP molecule, a small red shift in the long wavelength absorption was observed (Figure 4-8)**.**

Figure 4-8 Closed form of BDHP with oligo-thiophenes on the same side

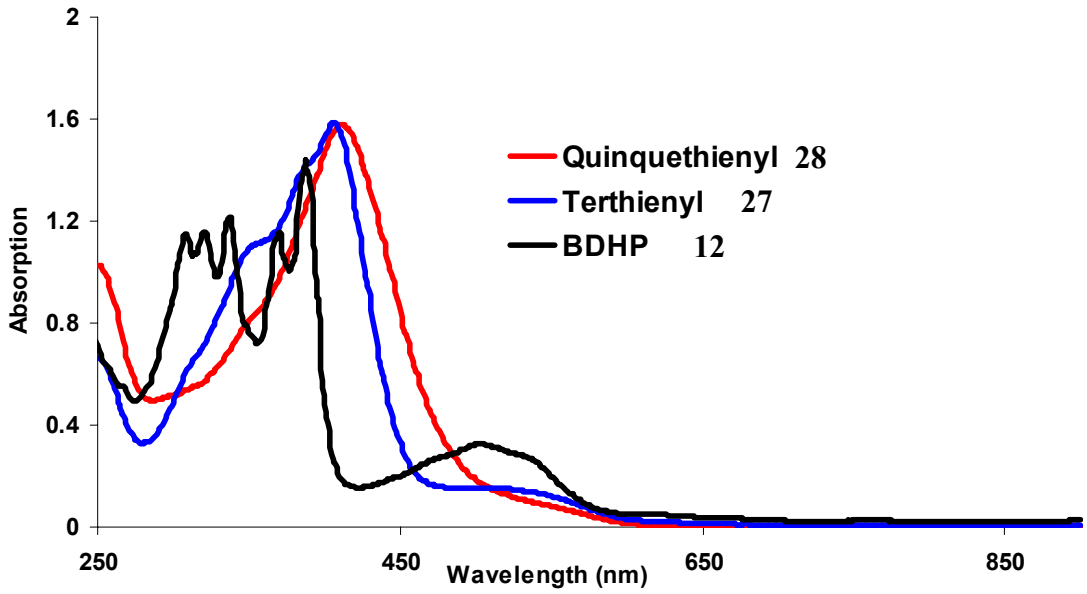

BDHP **12** has an absorption at 504 nm (ε_{max} = 7000),[53] when two terthiophenes are added to the same side **27,** this absorption red shifts slightly to 510 nm (ε_{max} = 6600), and when two quinquethiophene oligomers are added **28,** it red shifts further to ~554 nm (ε_{max} = 5380). In the quinquethiophene example **28**, the tail of the large absorption at 412 nm (103000) partially obscures this peak making it difficult to determine the exact location

of this peak. This indicates that there is some extended conjugation between the thiophene wires and the BDHP switch but it is small.

Opening the switch causes only minor shifts in the λ_{max} absorption between the closed and the open form (Figure 4-9).

Figure 4-9 Open and closed forms of terthienyl 27 and quinquethienyl 28

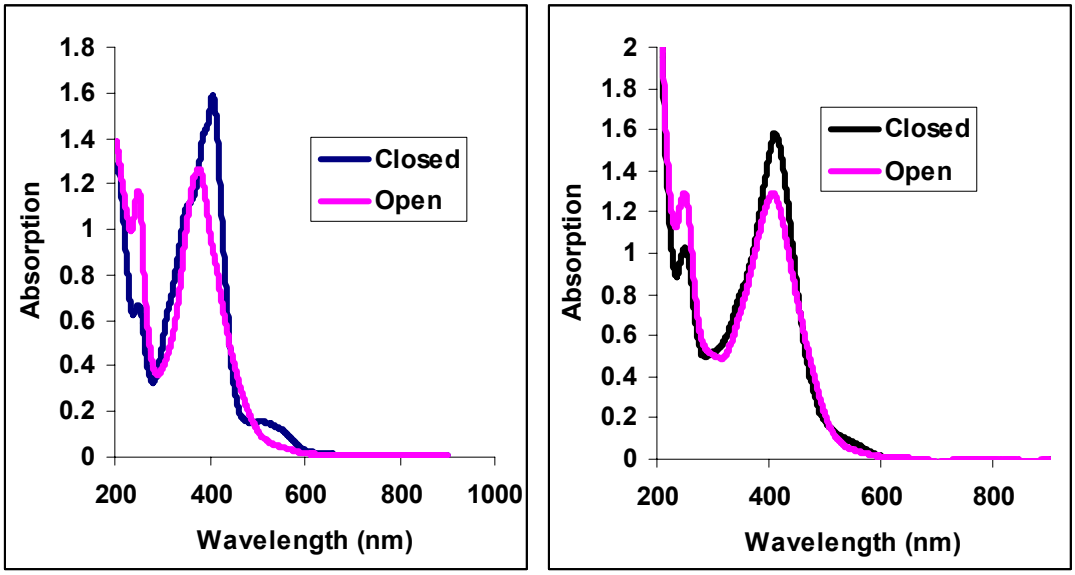

Terthienyl 27 **Quinquethienyl 28**

In the terthienyl closed form **27,** there was a long wavelength peak (510 nm) that was not in the open form **27'**, however the open form did have some absorption in this region due to the tail of the largest peak (λ_{max}=380nm) which extended out to 600 nm. For quinquethienyl **28** there was virtually no difference in the wavelengths of absorption between the closed **28** and the open form **28'**. This indicates that the switch has very little control over the conjugation length particularly with long oligothiophene chains attached.

4.5 Conclusion

These results show that there is extended conjugation from the oligothiophenes into the BDHP and DHP based photoswitches and that opening and closing the switches can modify the effective conjugation length. They also show that the ability of the photoswitch to affect conjugation when opened or closed decreases as the length of the thiophene oligomers attached increases. Thus increasing the length of the oligothiophenes attached beyond quinquethiophene is probably not desirable. The DHP based switches were found to be more effective at influencing the conjugation length than the BDHP switches. This indicates that maximizing the conjugation between the switch and the wire, and placing the wires in a position to take advantage of the large conjugation changes when the switch is opened and closed is important. From these results of the molecules studied the oligothiophene functionalized DHP based molecules are the most promising candidates to photoswitch electrical conductivity.

Chapter Five: Electrochemistry

5.1 Introduction

Solution cyclic voltammetry (CV) experiments were performed in dry DCM under argon using 0.1 M $TBAPF_6$ as the electrolyte. The working electrode was glassy carbon, a platinum wire was used as the counter electrode and a silver wire as the reference electrode. All solution samples were calibrated versus ferrocene and are reported versus the SCE (Fc/Fc^+ = 0.46V vs SCE). Thin film spectroelectrochemistry experiments were performed in dry ACN using $TMABF_4$ as the electrolyte. Films were spin coated onto an ITO coated glass slide. A platinum wire was used as the counter electrode and Ag/Ag^+ as the reference electrode. Full experimental details are provided in the experimental.

5.2 Cyclic voltammetry of switch and wire components

For comparison purposes, the switch and wire components were examined by cyclic voltammetry. The naphthoyl substituted DHP **84** had two redox peaks, an oxidation at $E_{p,a}$=1.15 V and a reduction at $E_{p,c}$=-1.14 V (Figure 5-1).

Figure 5-1 CV of 84 vs SCE at 250 mV/s

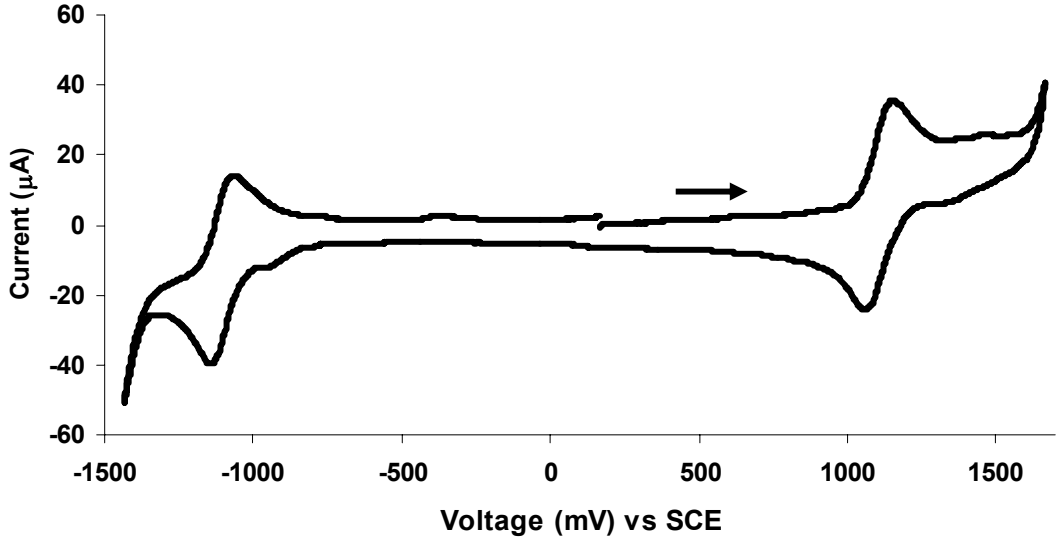

The dihexyl quinquethiophene **102** under the same conditions had two oxidation peaks, the first at $E_{p,a}$ 0.91 V and the second at 1.20 V (Figure 5-2).

Figure 5-2 CV of dihexyl quinquethiophene 102 at 250 mV/s

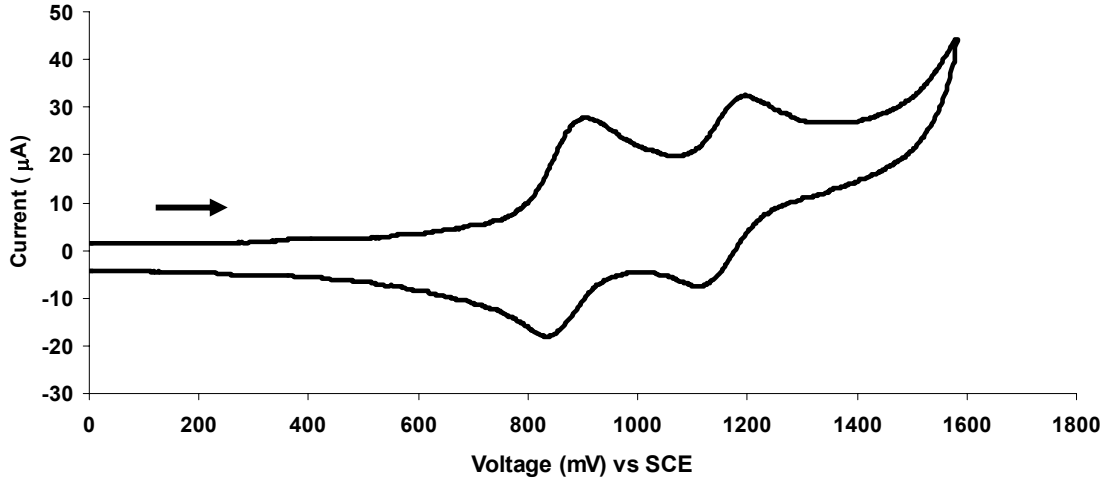

The first oxidation of **102** occurs at a lower oxidation potential when compared to terthiophene (1.07 V vs Ag/AgCl)[86] but higher than quinquethiophene without the hexyl

groups (0.70V vs Ag/AgCl).[87] The increase in the oxidation potential of **102** versus that of quinquethiophene is a result of the addition of the dihexyl groups which cause twisting to occur and so reduces the conjugation. The dihexyl groups are important however as they increase the overall solubility of the oligomer, while also making the compound insoluble in acetonitrile, which is important for the thin film electrochemistry experiments.

5.3 Electrochemistry of quinquethienyl DHP 97

5.3.1 Solution cyclic voltammetry experiments

With dihexyl quinquethiophene oligomers **102** attached to either side of the DHP switch **97,** cyclic voltammetry experiments exhibited a first oxidation peak at $E_{p,a}$ = 0.80 V, a second at $E_{p,a}$=1.01 V and a third at $E_{p,a}$=1.24 (Figure 5-3-A). No polymerization was observed at this point, but if the voltage was scanned to higher potentials then the increase in the current on each subsequent cycle of the CV suggests that polymerization on the electrode is occuring (Figure 5-3-B). Further support for polymerization was obtained from the formation of a black insoluble solid that formed on the electrode.

Figure 5-3 Electrochemical polymerization of 97: scanning to A) 1.25 V, B) 1.6 V at 500 mV/s

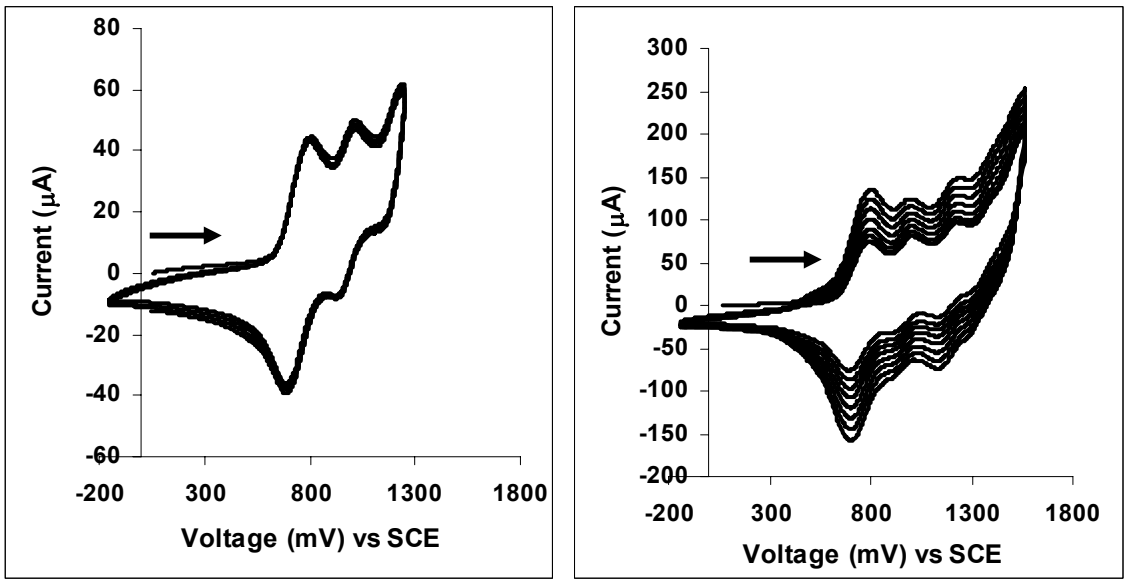

A **B**

The first oxidation potential of **97** is less than both the starting materials **84** and **102** which supports the observation obtained from the UV-vis data that there is extended conjugation from the oligothiopenes into the DHP switch. A reduction peak was observed at $E_{p,c}$= -1.22 V which corresponds quite closely with the reduction potential observed for **84**, the dibromide precursor.

Quinquethienyl **97** was opened by visible light irradiation using a 490 nm cut off filter and the color was observed to change from the dark brown of the closed form to the orange of the open form. Cyclic Voltammetry experiments were then run on the open form (Figure 5-4-A), however, no change was observed in the CV from that of the closed form (Figure 5-4-B), even when the sample was irradiated with visible light as the voltammetry was scanned.

Figure 5-4 CV of closed (A) and open (B) forms of 97 scanned at 250 mV/s

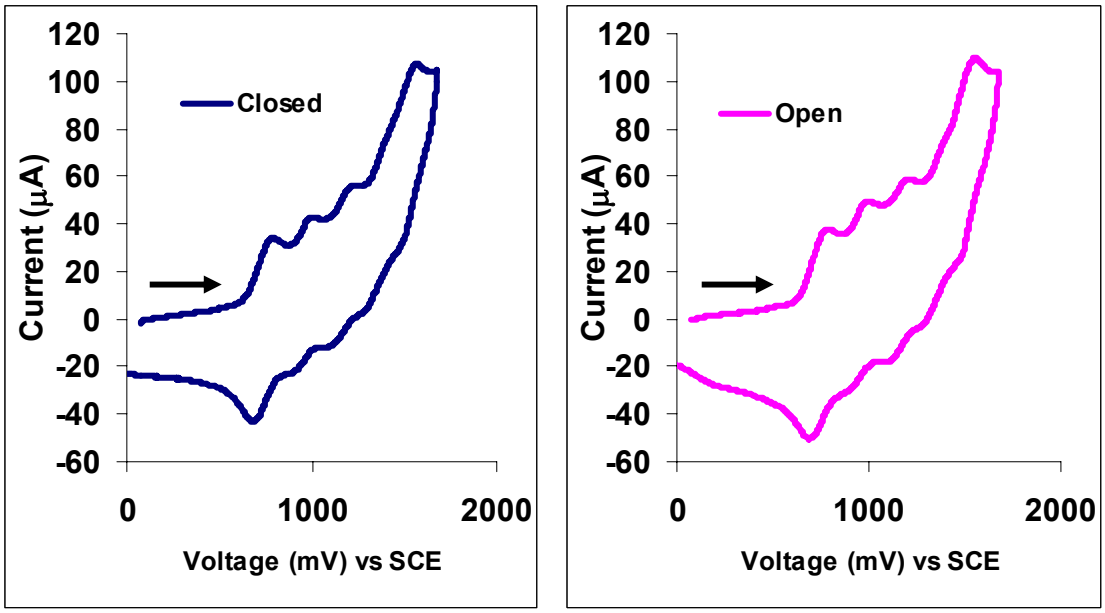

A **B**

This could indicate that either there are no changes in the oxidation and reduction potentials between the open and the close form or that the electrochemistry is causing closing to occur at a rate fast enough to make the open form unobservable under the conditions used.

5.3.2 Spectroelectrochemistry

In order to study what was happening to **97** during the cyclic voltammetry experiments, spectroelectrochemistry experiments were employed on thin film samples spin coated from $CHCl_3$ onto an indium tin oxide coated glass slide. The advantage of using the quinquethiophene wires with dihexyl groups attached **102** was readily apparent as this compound was completely insoluble in ACN whereas using terthiophene wires without the dihexyl groups produced a compound that was sparingly soluble in ACN. In

the first CV cycle the thin film of **97** showed a trace crossing in the oxidation half of the CV (Figure 5-5-A). Later scans (Figure 5-5-B) did not show a trace crossing.

Figure 5-5 CV of a thin film of 97 A) First cycle B) second cycle, 200 mV/s vs Ag/Ag^+

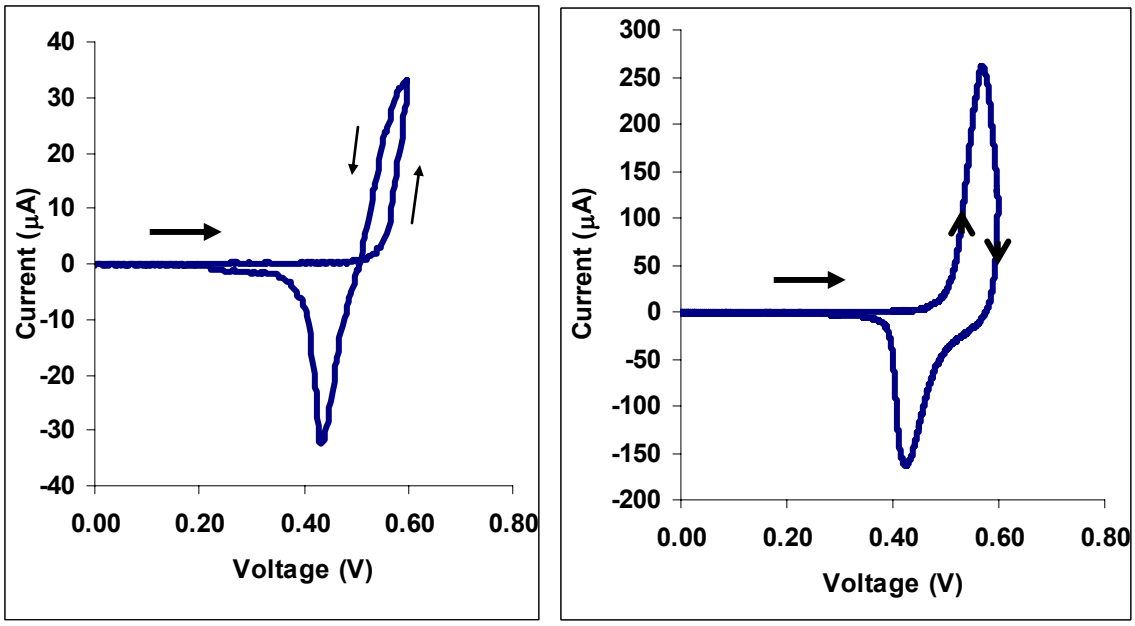

A **B**

Trace crossings are frequently observed in solution cyclic voltammetry and are often called nucleation loops as they have been interpreted to be the start of the nucleation process which requires an overpotential to initiate.[88-90] Another explanation for trace crossings was proposed recently by Heinze *et al.*[91,92] They explain that trace crossings are the result of homogenous follow-up reactions of oligomers in the diffusion layer. They show that in the case of terthiophene, hexathiophene is produced as a product during the CV and that at the terthiophene oxidation potential hexathiophene is oxidized to its dication. If the oxidation of terthiphene at the electrode is slow then the hexathiophene dication can undergo a homogenous comproportionation reaction with

terthiophene to produce the hexathiophene and terthiophene monocations. This produces more hexathiophene and the cycle continues. The net result is that the current is higher in the reverse scan and a trace crossing results. In the case of **97** it is unclear if the trace crossing observed is a surface effect between the electrode and the film necessitating an overpotential on the first cycle or due to reactions from oligomers in the film.

The thin film CV exhibits a fairly large hysteresis (peak separation between cathodic and anodic peaks), a hyseteresis which is scan rate dependant (Figure 5-6). The scan rate dependence indicates that there is a kinetic component to the hysteresis. This could be caused by exchange reactions between neighbouring oligomers and the movement of counter ions to balance the charge.[93-95]

Figure 5-6 CV of a thin film of 97 vs Ag/Ag^+ at various scan rates

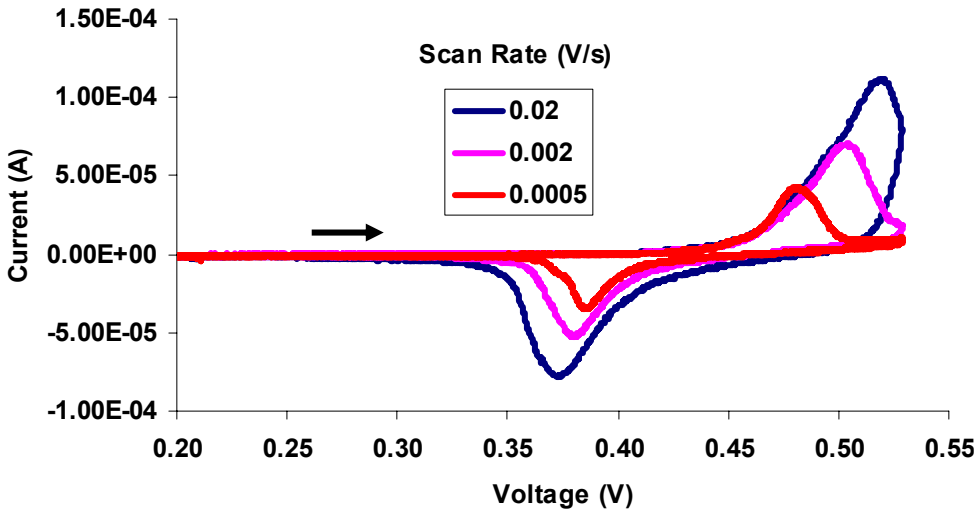

The bipolaron model predicts a flattening of the thiophene oligomers when in the quinoid form. This flattening of the structure and the resulting stabilization of the charge is

another reason that would account for the hysteresis observed.[29] Intermolecular π-interactions[96] and reversible intermolecular σ-dimers[97] have also been proposed as possible reasons for the hysteresis observed in other conducting polymers.

Monitoring the UV-vis of closed **97** as the potential was swept showed no changes in the spectrum until the beginning of the oxidation peak where a hypochromic shift in the absorption occurred below 530nm and a hyperchromic shift above 530nm (Figure 5-7-A).

Figure 5-7 Spectroelectrochemistry of closed 97: CV=0.02 V/s

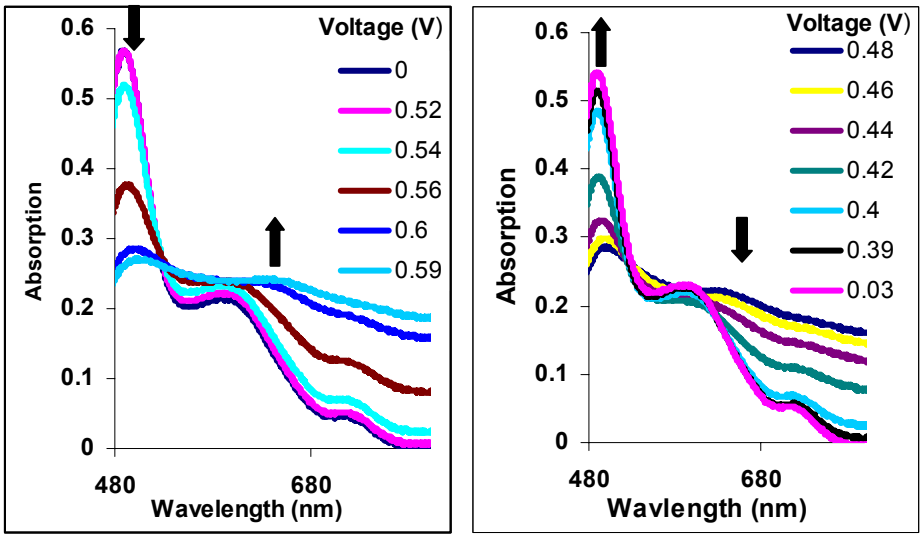

A (increasing potential) **B (decreasing potential)**

The UV-vis spectrum then remained virtually unchanged until the reduction peak at ~0.5V at which point the spectrum returned to that of the original UV-vis spectrum (Figure 5-7-B). There were a few minor differences between the original and the final UV-vis spectra. After the CV scan, the absorption of the peak below 530 nm was slightly less than that of the starting material and the absorption above 530nm was slightly greater than that of the starting material. This could indicate that a polymerization reaction is

occurring, or that there is more planarity in the molecular orientation of the molecules in the film after the electrochemistry.

If the sample is opened with visible light (490 nm cut off filter) and the UV-vis spectrum is monitored while the potential is swept, rapid thermal closing is observed, and this closing accelerates in the beginning stages of the oxidation peak (Figure 5-8-A).

Figure 5-8 Spectroelectrochemistry of the open form 97': CV = 0.02V/s

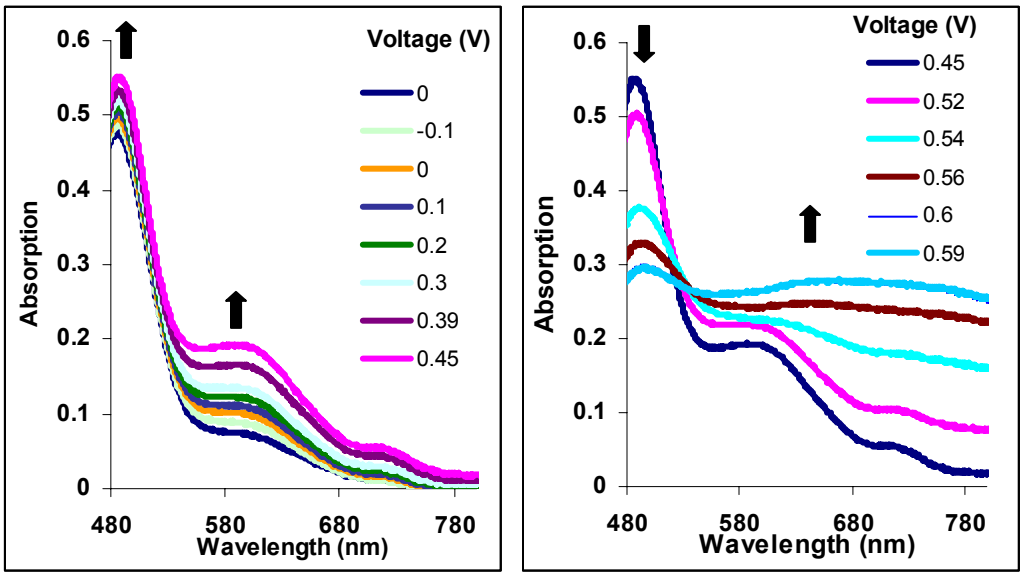

A (increasing potential) **B (decreasing potential)**

Continuing the potential sweep through the oxidation peak causes a hypochromic shift in the absorption below 530 nm and a hyperchromic shift above 530 nm (Figure 5-8-B) as seen before in the closed case. If visible light irradiation is applied continuously throughout the cyclic voltammetry experiment then the thermal closing can be counteracted until the point when the oxidation peak begins (Figure 5-9-A).

Figure 5-9 Constant visible light irradiation during spectroelectrochemistry of 97

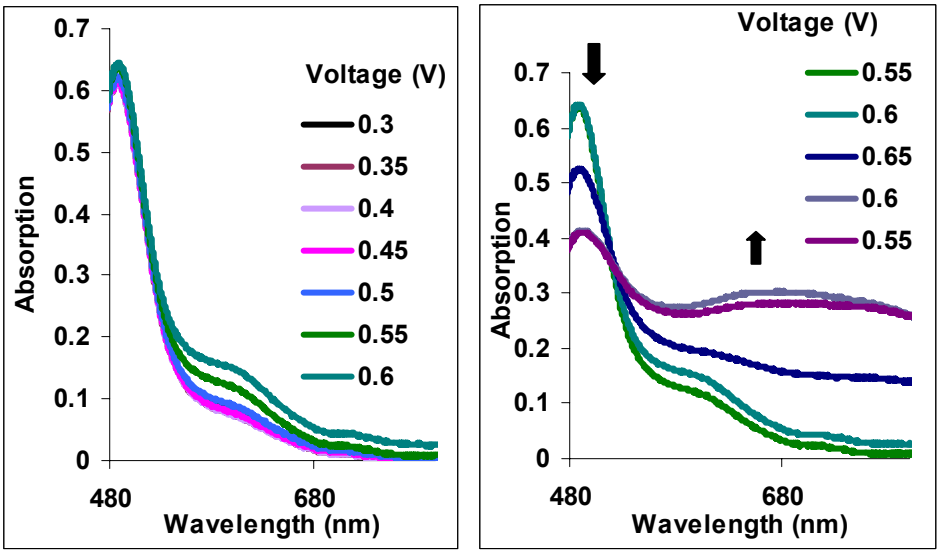

A (increasing potential) **B (potential between 0.55 -0.65)**

At this point, rapid closing is observed in the UV-vis spectra followed by a hyperchromic shift above 530nm (Figure 5-9-B) similar to what was seen before. These results indicate that the electrochemistry is causing rapid closure of the switch to occur which cannot be prevented even with continuous visible light irradiation. It is not altogether surprising to observe switching during the electrochemistry experiments as this has been observed with other functionalized DHP switches[98] and a similar result was observed with the dithienylethene photoswitches.[99]

5.3.3 Conclusion

The solution cyclic voltammetry experiments supported the UV-vis results showing that there was extended conjugation from the thiophenes into the switch. Polymerization was shown to occur on the electrode during solution cyclic voltammetry experiments only if potentials greater than that of the third oxidation peak ($E_{p,a}$ = 1.24 V)

were applied. Unfortunately no difference was observed in the oxidation potentials between the open and the closed forms during the cyclic voltammetry experiments. Spectroelectrochemistry supported that the reason no difference was observed in the oxidation potentials of the open and the closed forms was because rapid electrochemically induced closing of the open form was occurring. Consequently only the oxidation potentials of the closed form were observed

5.4 Electrochemistry of BDHP based compounds with thiophenes on opposite sides of the molecule

5.4.1 Solution cyclic voltammetry of 76

The electrochemical properties of BDHP switches with oligothiophenes attached on opposite sides were studied by cyclic voltammetry. The closed form of the terthienyl **76** exhibited a reversible one electron oxidation at $E_{p,a}$ = 0.58 V. This first oxidation occurs at a much lower potential than simple terthiophene ($E_{p,a}$=1.07 V vs SCE)[86] and slightly lower than BDHP ($E_{p,a}$=0.75, ferrocene $E_{p,a}$=0.55).[22] This lower oxidation potential supports the conclusion obtained from the UV-vis absorption data that there is extended conjugation from the oligothiophenes into the BDHP switch. Although the terminal ends of the oligothiophenes are open, no polymerization is observed when cycling through the first oxidation peak. There are however second ($E_{p,a}$=0.99 V) and third ($E_{p,a}$=1.31 V) oxidation peaks, and cycling out to these potentials does result in polymerization (Figure 5-10).

Figure 5-10 Electrochemical polymerization of 76 at 250 mV/s

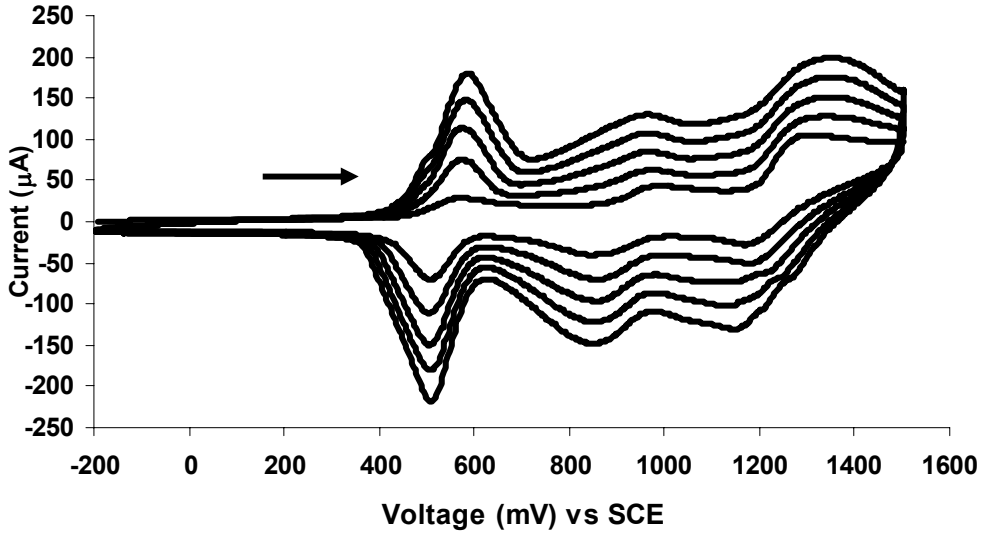

The sample of **76** was opened with visible light irradiation (490 nm cut off filter). On the first cycle there was a change in the oxidation peak to a more negative potential ($E_{p,a}$=0.75 V) (Figure 5-11-A). If the voltage was kept below this first peak then the open sample was redox inactive in this region. If the sample was scanned to more positive potentials than the closed forms oxidation peaks appeared and the solution started to darken around the electrodes indicating the electrochemistry was causing the compound to close (Figure 5-11-B).

Figure 5-11 Cyclic voltammetry of open 76' at 250 mV/s

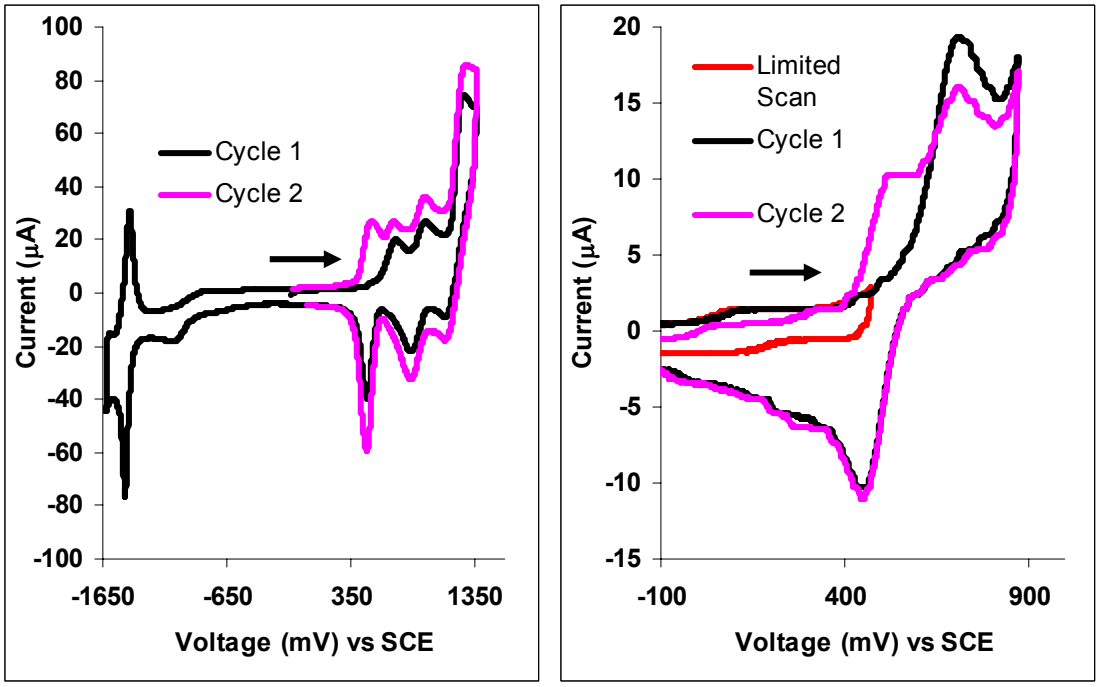

A **B**

As in the DHP, case the cyclic voltammetry experiment appears to be causing the switch to close, although not quite as fast as in the DHP case, as oxidation peaks corresponding to the open form could be identified. It was found that after repeated cycling it was very difficult to get the compound to open by visible light irradiation. This was thought to be a result of accelerated thermal closing due to a small amount of stabilized radicals rather than complete decomposition of the sample as it was found that after addition of the ferrocene standard the sample could be opened as before, as seen by a rapid color change from a dark brown to a light orange when irradiated with visible light. Ferrocene with a very similar, though slightly lower, oxidation potential than **76** would remove any remaining radicals and so eliminate the accelerated thermal closing catalyzed by these radicals.

When cyclic voltammetry was performed on the quinquethienyl functionalized compound **77**, the first oxidative peak ($E_{p,a}$ = 0.59 V) was observed at a very similar potential to the terthiophene compound **76** ($E_{p,a}$ = 0.58 V). A second quasi-reversible peak was observed at $E_{p,a}$ = 0.97 V followed by 3 irreversible peaks at $E_{p,a}$ = 1.21, 1.34 and 1.51 V. A reversible reduction peak at E^o = -1.36 V was also observed (Figure 5-12).

Figure 5-12 Cyclic voltammetry of quinquethienyl 77 at 250 mV/s

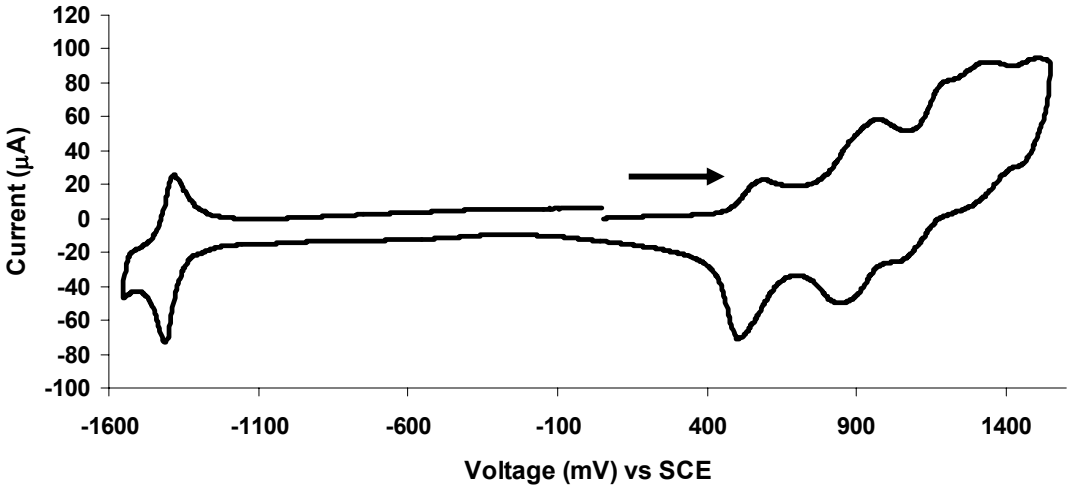

If the peak potential was limited to just the first two oxidation peaks no polymerization was observed (Figure 5-13-A). Continuing the scan to higher potentials did result in polymerization (Figure 5-13-B).

Figure 5-13 Electrochemical polymerization of quinquethienyl 77: Scanning to A) 1.05V (800 mV/s), B) 1.5 V (250 mV/s)

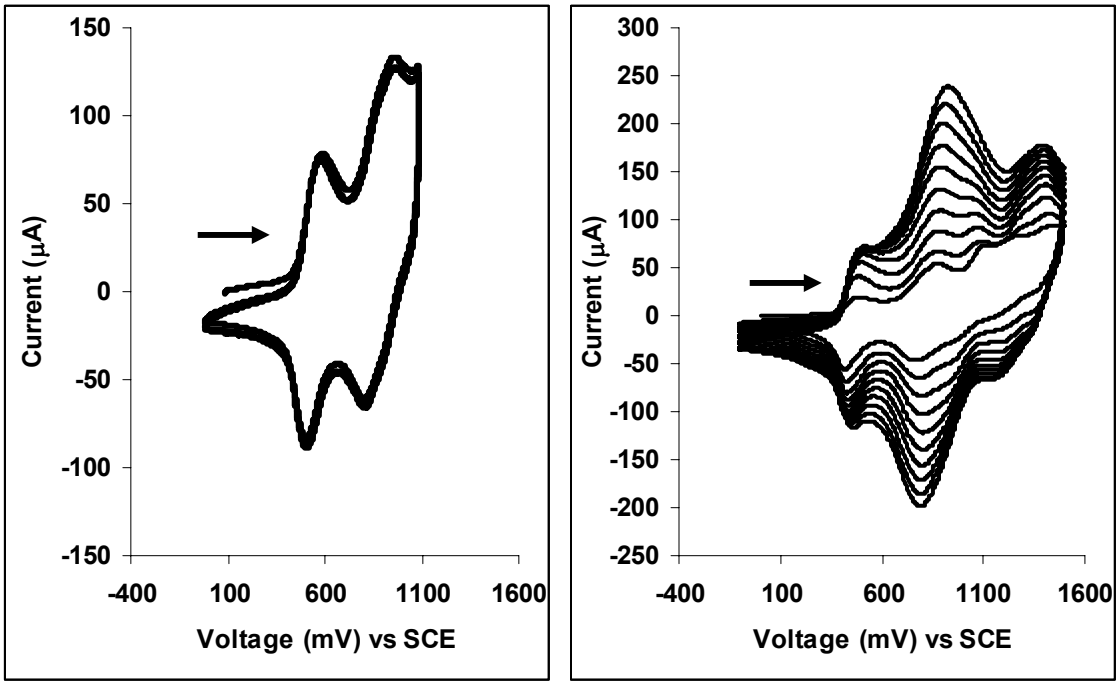

A **B**

The sample was opened by visible light irradiation (490 nm cut off filter) as seen by the color change from dark brown to a light orange brown and a CV was run which proved to be identical to the closed form. This indicates that either the electrochemistry of the open form is the same as the closed form or that more likely rapid electrochemically induced closing is occurring as was seen in the DHP case.

5.4.2 Spectroelectrochemistry of quinquethienyl 77

Spectroelectrochemistry on a thin film of **77** proved to be more difficult to analyze than for the DHP compounds. This was because there was only a small difference in the UV-vis spectra between the open and the closed forms and because CV's of thin film samples of **77** proved to be quite different than the solution CV's. On the first cycle of a CV scan, there was a broad oxidation peak at $E_{p,a} = 0.56$ V, followed

by two reduction peaks at $E_{p,c}$ = 0.47 and 0.37 V. Having cycled through these peaks a new reduction peak at $E_{p,c}$ = -0.11 and oxidation at $E_{p,a}$ = 0.11 (Figure 5-14) were observed. If the potential was limited so as to avoid the main oxidation peaks at 0.56V then the reduction and oxidation peaks at $E_{p,c}$ = -0.11 and $E_{p,a}$ = 0.11 were not observed. Also if after the first cycle the potential was limited so as to not go through the main oxidation peak at ~0.5V then these two peaks slowly disappeared after repeated cycling. These new peaks may be the result of the discharging of protons formed from coupling reactions between oligomers.[100,101]

Figure 5-14 CV of a thin film of 77 on an indium tin oxide coated glass slide vs Ag/Ag^+ at 0.01 V/s

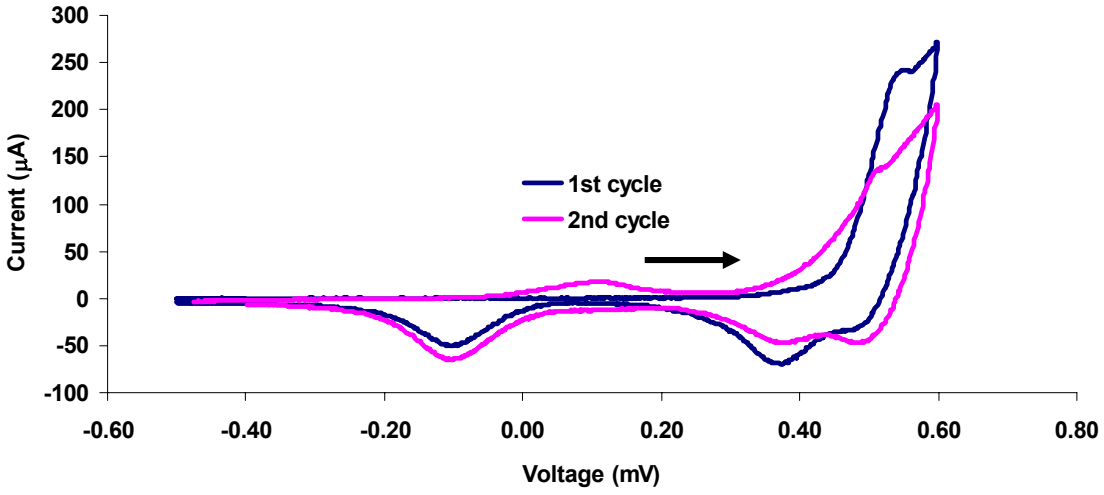

The UV-vis spectra of the thin film of quinquethienyl **77** as the potential was scanned did not change until the beginning of the first oxidation peak which resulted in a broad hyperchromic shift for wavelengths above 510 nm and a slight hypsochromic shift for the peak below 510nm (Figure 5-15-A). As the CV scan reversed and went through the reduction peak there was a general hypochromic shift in absorption (Figure 5-15-B). As the scan cycled through the new reduction peak at $E_{p,c}$= -0.11 there was a

hyperchromic shift from 540-680 nm and a hypochromic shift above 680 nm (Figure 5-15-C). Continuing the CV back to the starting point led to a hypochromic shift in the 540-680 nm window and a hyperchromic shift above 680 nm (Figure 5-15-D).

Figure 5-15 UV-vis absorption of closed 77 during spectroelectrochemistry

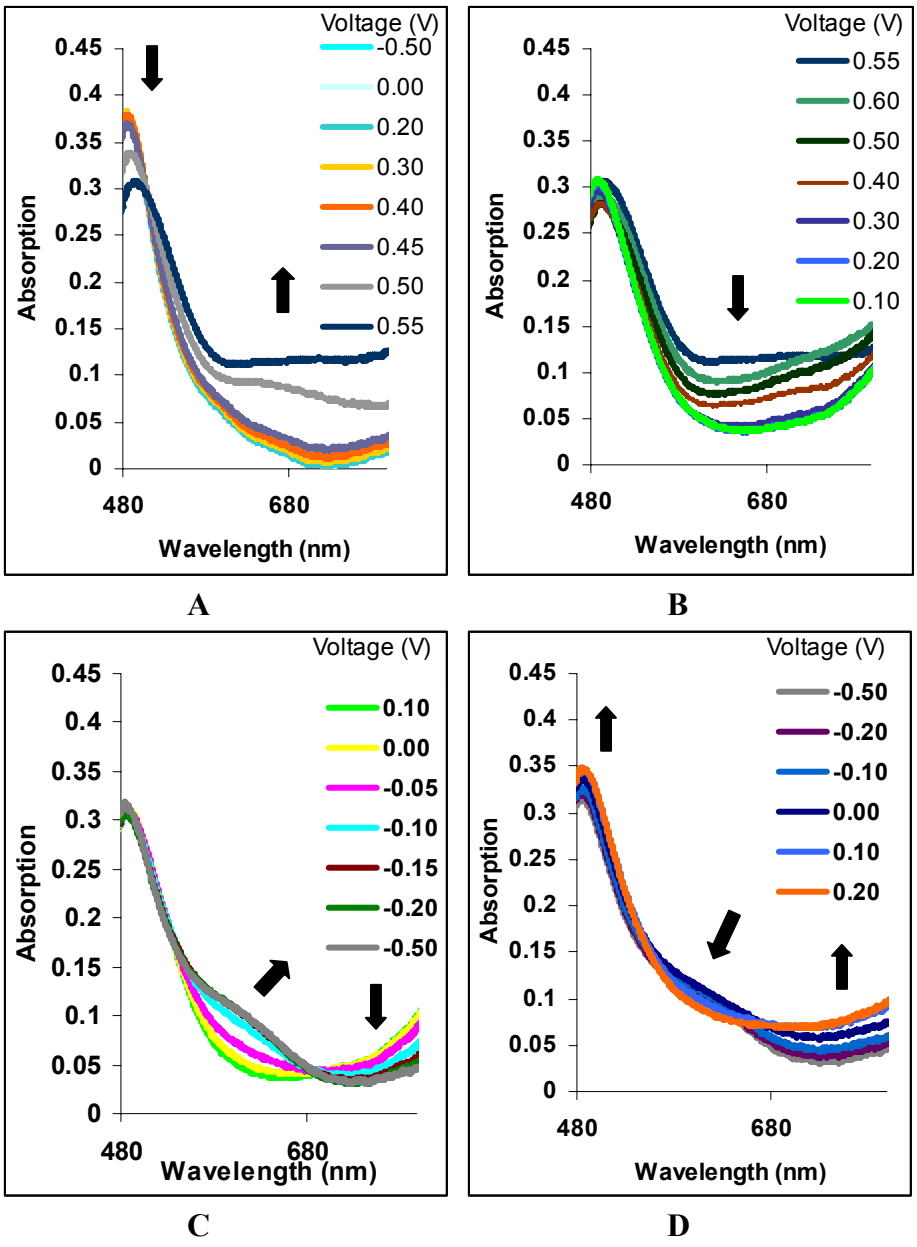

The initial absorption spectrum was not recovered indicating that a reaction had occurred during the electrochemistry experiments. It appears that a polymerization reaction

occurred as the film exposed to the electrochemical cell was found to be a darker red and insoluble in $CHCl_3$ whereas it was quite soluble in $CHCl_3$ before the electrochemistry (Figure 5-16).

Figure 5-16 Appearance of a film of 77 A) Before electrochemistry experiments (see text). B) After electrochemistry experiments. C) After washing with $CHCl_3$

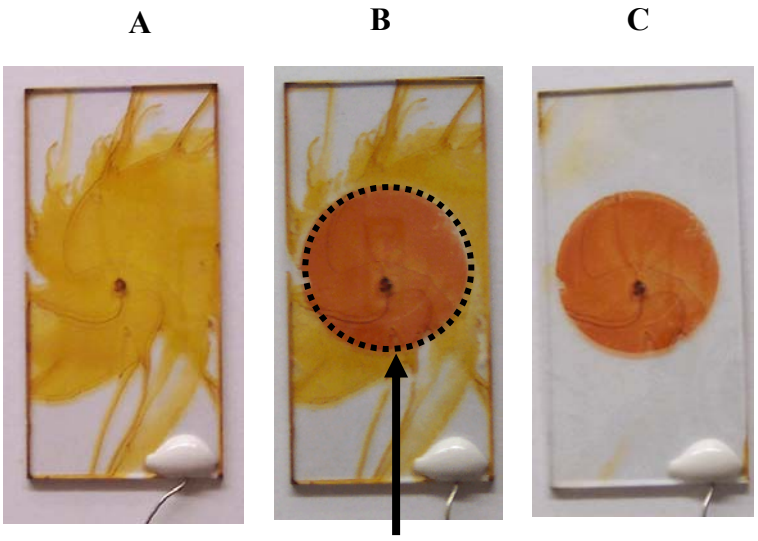

The first cycle of the CV of the open form of **77** was slightly different than the first cycle of the closed CV for **77** as the onset of the oxidation peak was at a slightly higher potential. The second cycle of the scan was however virtually identical to the closed form (Figure 5-17).

Figure 5-17 CV of a thin film of 77 after 4 minutes of visible light irradiation (490 nm cut off filter) on an indium tin coated glass slide at 0.01 V/s vs Ag/Ag^+

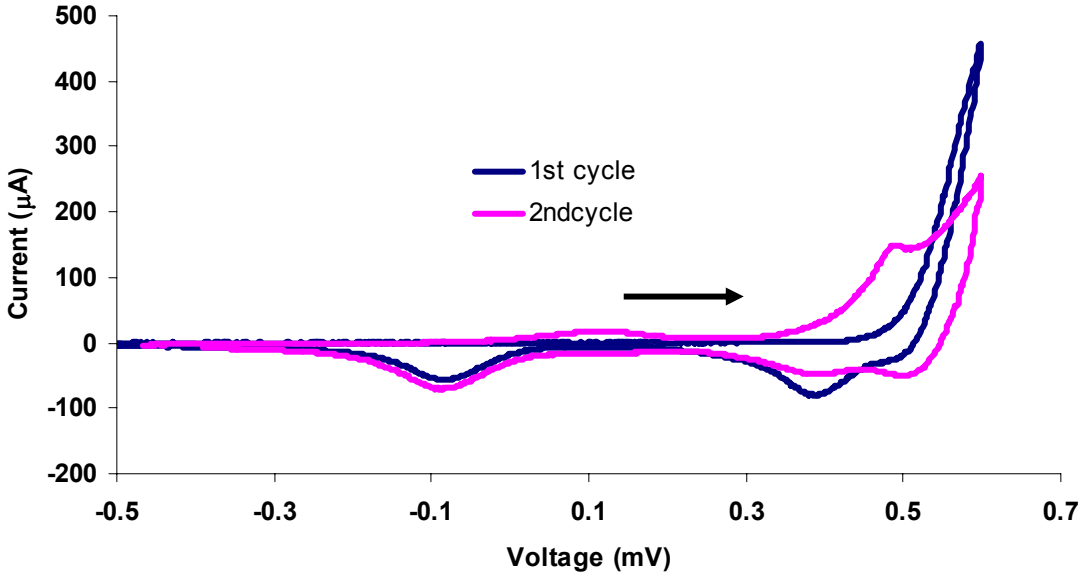

The UV-vis absorption spectrum of the film in the open form was obtained and it had the characteristic hypsochromic shift in the absorption of the tail from 560 to 730 nm indicating that the sample was open (Figure 5-18).

Figure 5-18 Closed and open form of quinquethienyl 77 film

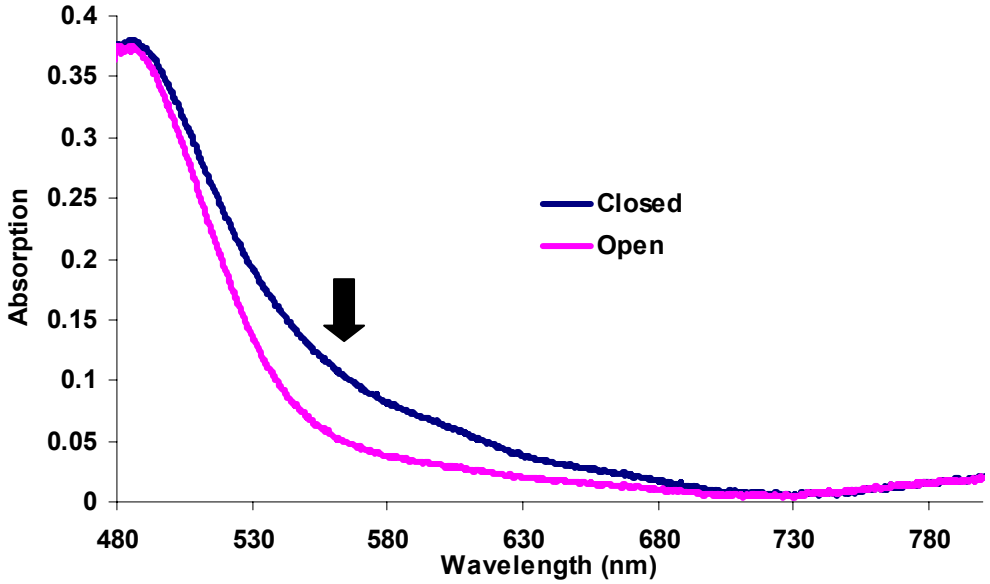

However despite a few minor differences the UV-vis spectra taken as the potential was scanned was the same as the closed form (Figure 5-19).

Figure 5-19 Spectroelectrochemistry of the open form of 77

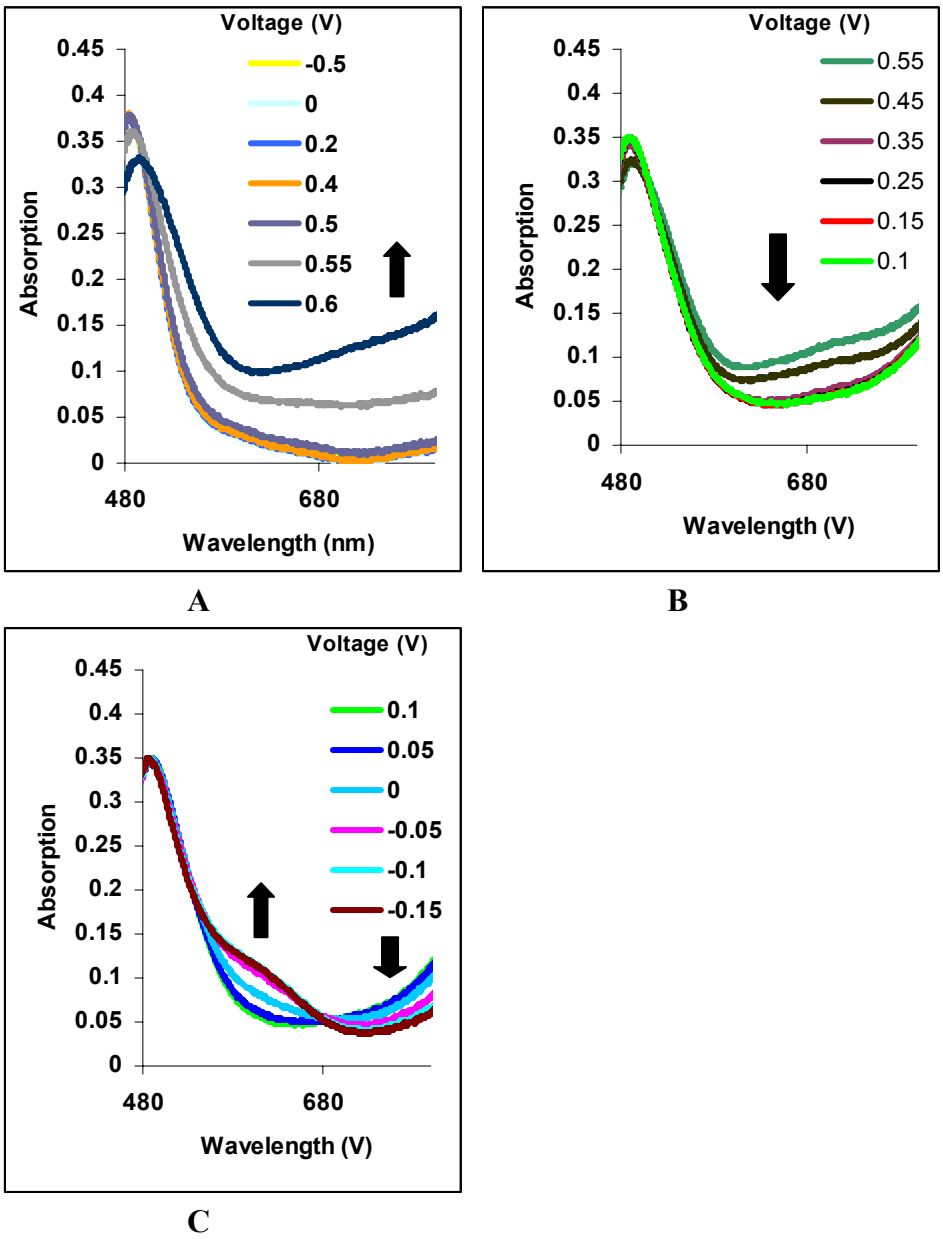

The lack of change in the UV-vis spectra between the close and the open form suggests that the open form is closing during the electrochemistry and undergoing a similar polymerization reaction.

5.5 Electrochemistry of BDHP compounds with thiophenes on the same side

5.5.1 Cyclic voltammetry

Cyclic voltammetry experiments on BDHP with quinquethiophene oligomers attached on the same side **28** had a first oxidation potential at $E_{p,a}$ 0.55 V and a second oxidation at $E_{p,a}$ 0.95V (Figure 5-20).

Figure 5-20 Cyclic voltammetry of 28 in the closed form at 500 mV/s

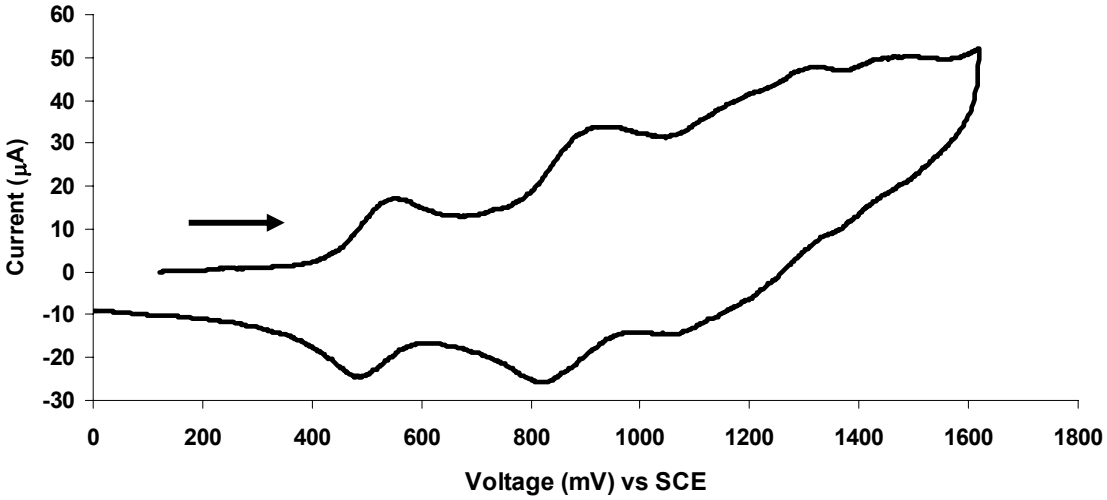

Opening **28** with visible light changed the color from a dark brown to a light orange brown. Cyclic voltammetry on this open compound produced a CV that was virtually identical to the CV of the closed compound. There was however, a small new peak in the open CV at 0.77 V which was present in the first few scans of the open sample but was absent in subsequent scans (Figure 5-21).

Figure 5-21 Cyclic voltammetry of 28' (open form) at 500 mV/s. Arrow indicates a new oxidation peak in the open form

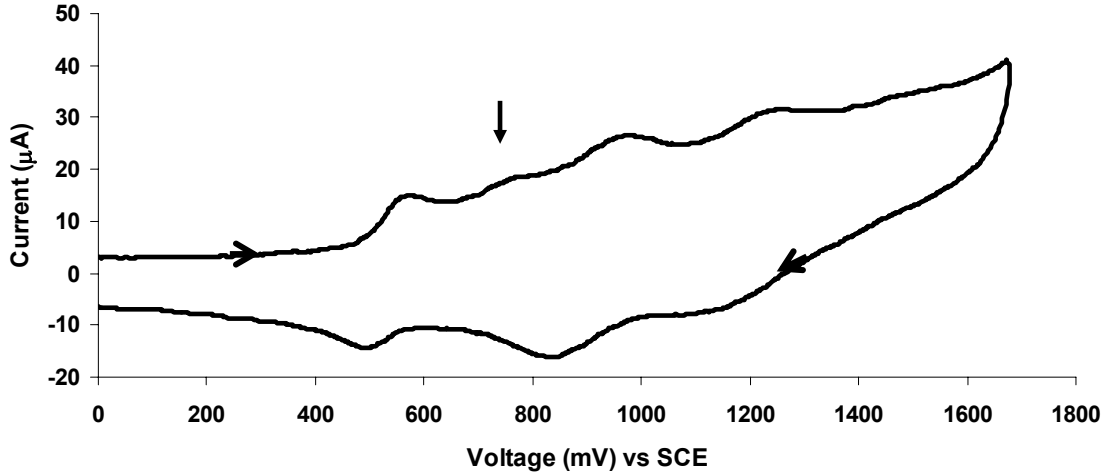

This small peak is most likely due to the open form and its disappearance due to conversion of the open form to the closed form during the electrochemistry experiment as was seen in previous compounds.

5.5.2 Spectroelectrochemistry of 28

Spectroelectrochemistry experiments were performed on a thin film of **28**. The CV of the thin film was quite different than the solution CV. After the first cycle a new peak at a lower oxidation potential was observed (Figure 5-22-A). Scanning out to higher potentials resulted in a new reduction peak at -0.04 V (Figure 5-22-B) and after repeated scans gave a bulbous CV similar to that of a polymer (Figure 5-22-C).

Figure 5-22 CVs of a thin film of 28 at 0.01 V/s vs Ag/Ag^{+}, A) First two cycles of a new film scanning to 0.5 V. B) Third cycle scanning to 0.7 V. C) After repeated cycling, scanning to 0.8 V

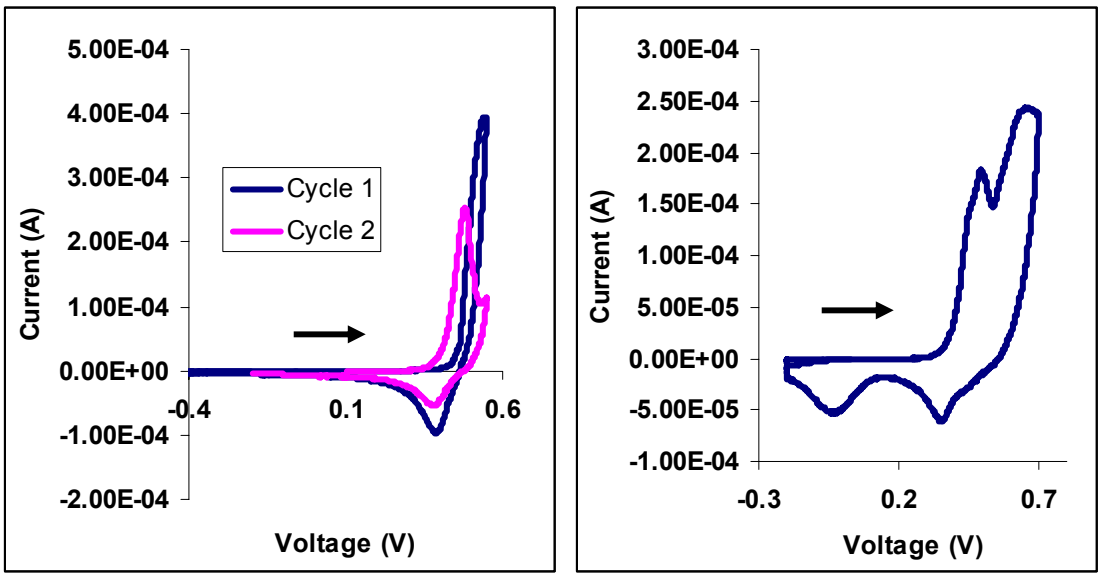

A **B**

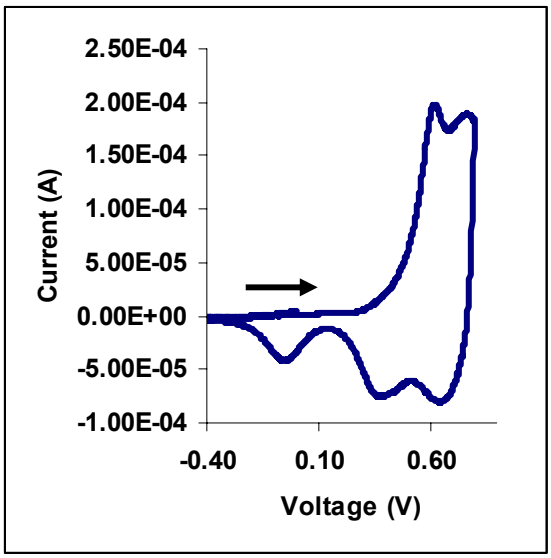

C

In the UV-vis spectrum no changes occurred until the beginning of the oxidation peak at which point there was a general hyperchromic shift centred at 635 nm (Figure 5-23-A).

Figure 5-23 Spectroelectrochemistry of 28

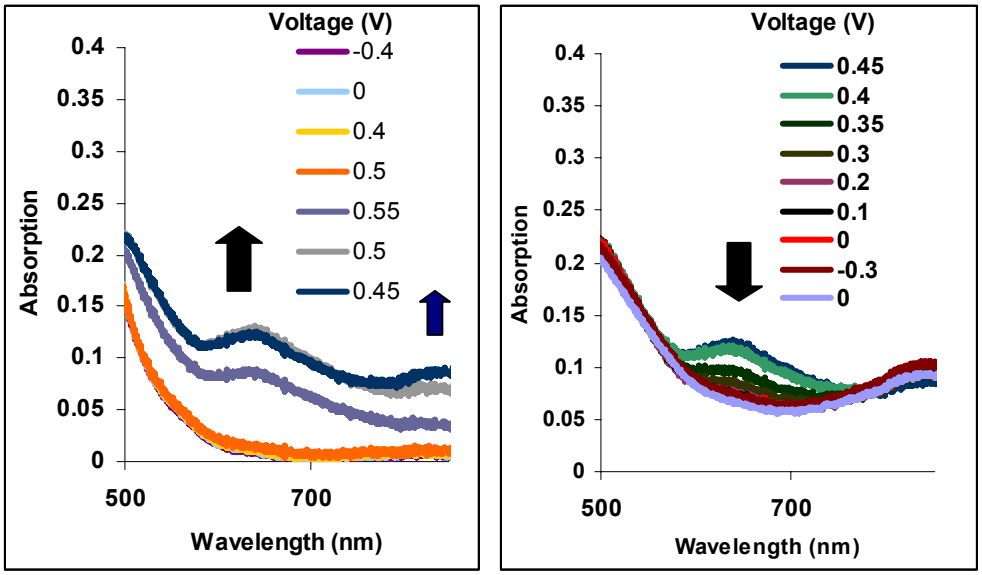

A

B

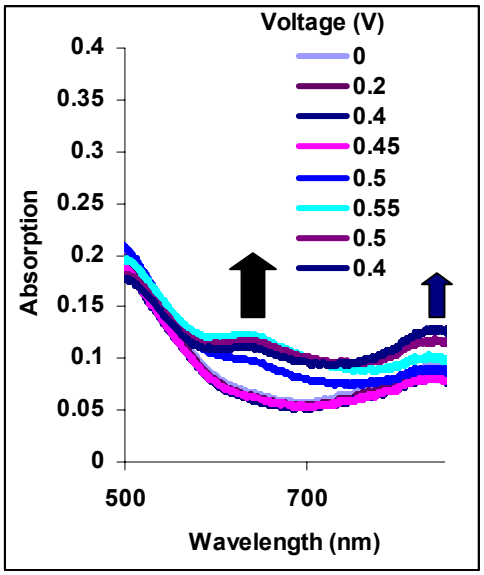

C

At the end of the oxidation peak and as the potential began to reverse there was a small but distinct hyperchromic shift centred at approximately 840 nm. As the CV scan continued through the reduction half reaction a hypochromic shift in the absorption

occurred which was centred at 635 nm (Figure 5-23-B). This hypochromic shift was not as large as the previous hyperchromic shift and so the UV-vis spectrum did not return to that of the starting material. Cycling back through the oxidation peak for the second time gave, once again, a hyperchromic shift centered at 635 nm (Figure 5-23-C) and in the latter half of this oxidation, there was again an increase in the absorption centred at 840 nm. Polymerization of the compound during the cyclic voltammetry cycles and extension of the conjugation length would explain the formation and persistence of this new peak. This was supported by the fact that after completion of the electrochemistry experiments the film exposed to the electrochemical cell had become insoluble in $CHCl_3$ (Figure 5-24).

Figure 5-24 Appearance of a film of 28 A) Before electrochemistry experiments (see text). B) After electrochemistry experiments. C) After washing with $CHCl_3$

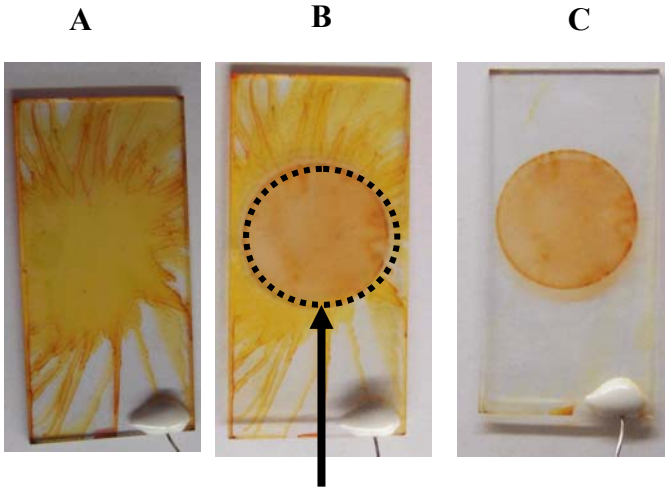

5.6 Conclusion

Cyclic voltammetry and spectroelectrochemistry results confirmed the UV-vis observations that there was extended conjugation between the molecular switch and

wires. This extended conjugation was larger in the DHP based compounds and less for the BDHP based compounds. No difference or very little difference was found in the electrochemistry between the open and the closed forms of the samples studied. To study why this was the case spectroelectrochemistry experiments were performed which indicated that electrochromic switching was occurring converting the open form of the switch to the closed form. The CV of the open form could not be obtained because it was converting to the closed form. This electrochromic switching is a serious problem if the switches are to be used as a means of controlling electrical conductivity. The electrochemistry also led to polymerization of the compounds from solution onto the glassy carbon electrode and in the case of the thin film BDHP samples led to intractable films on the indium tin oxide electrode.

Chapter Six: Conductivity

6.1 Undoped conductivity measurements

Conductivity testing was performed on an undoped thin film of **97** spin coated onto an interdigitated gold electrode and 30V was applied across the fingers of the electrodes. After a preliminary period of 120s in the dark a red light (490 nm cut off filter) followed by a blue light (BG6 bandpass filter, 310-530 nm) was applied at 30s intervals. When the red light was applied, causing the switch to open, a drop in the current was observed. When the blue light was applied, causing the switch to close, an increase in the current was observed (Figure 6-1).

Figure 6-1 Opening and closing of the DHP switch 97 on an interdigitated electrode

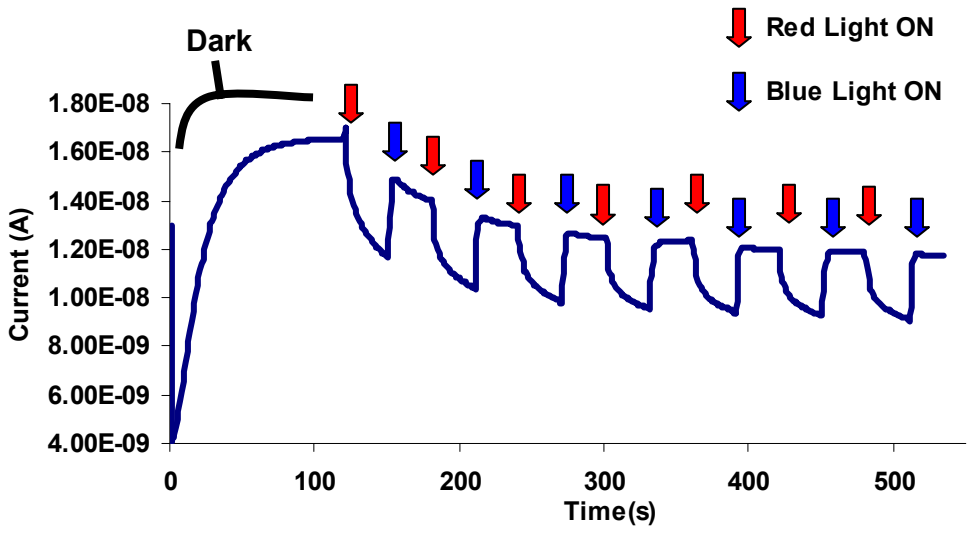

The blue light does not however cause complete closure of the switch but instead leads to a photostationary state. Thus when the blue light is applied to a fully closed sample partial opening occurs. This opening of the switch when blue light is applied to a fully closed sample leads to a decrease in the conductivity and a drop in the current (Figure

6-2). Applying the red light after the blue light then causes the sample to open further causing the current to drop again.

Figure 6-2 Irradiating an undoped film of 97 with blue light followed by red light

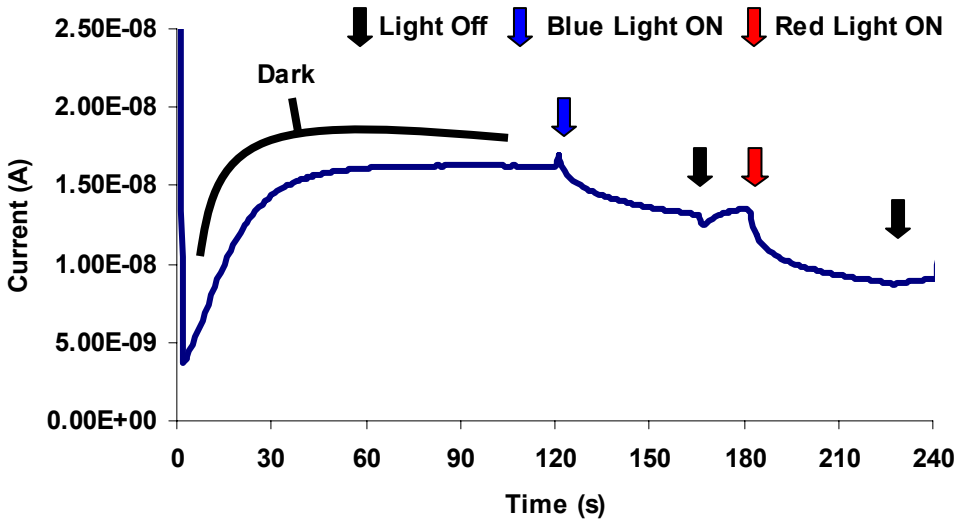

If a 15s period of darkness is applied between the blue and red light irradiation then an increase in the current is observed as a result of the switch beginning to thermally close (Figure 6-3).

Figure 6-3 Applying darkness between red and blue light irradiations

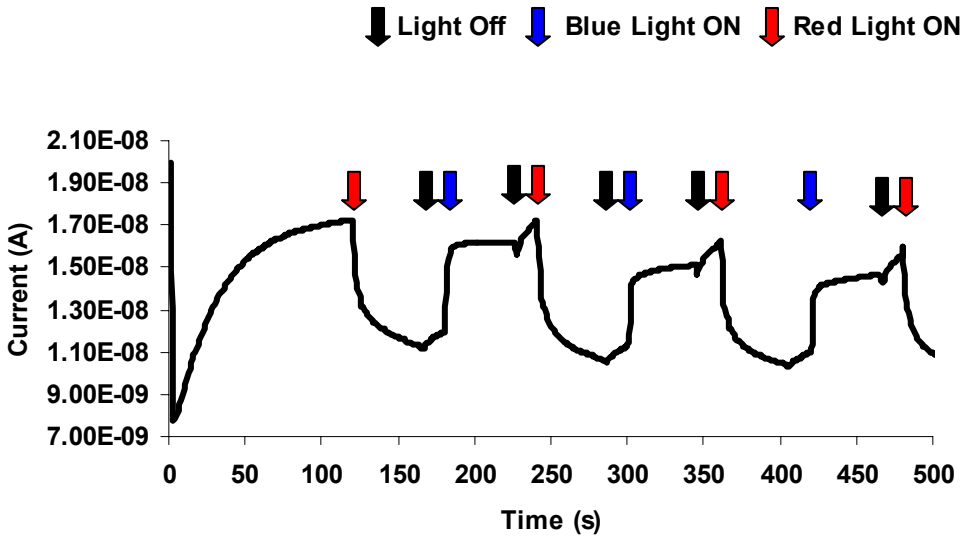

The fact that the blue light causes an increase in conductivity when applied to an open sample and a decrease in conductivity when applied to a closed sample demonstrates that the change in conductivity observed is not due to photoconductivity but instead to conductivity changes in the film between the open and the closed forms of the switch. These results show that opening and closing the switch causes a change in the conductivity of a thin film sample and that, as predicted, when the switch is open the conductivity is lower than when the switch is closed. The conductivity however in both the open and the closed form was quite low as these experiments were carried out on undoped samples.

6.2 Dual electrode voltammetry

In order to study the conductivity of a doped sample, a dual electrode voltammetry experiment was employed (Figure 6-4). In this experiment, thin films of **97** were drop coated from DCM onto an interdigitated microelectrode and assembled in an

electrochemistry cell using dry ACN as the solvent and $TMABF_4$ as the electrolyte. The cell was set up as a typical cyclic voltammetry experiment using the gold electrodes as the working electrode, a platinum wire as the counter electrode, and Ag/Ag^+ as the working electrode. A second potentiostat was used to apply a 25 mV offset potential applied across the fingers of the gold interdigitated electrodes (Figure 6-4).

Figure 6-4 Schematic diagram for dual electrode experiment

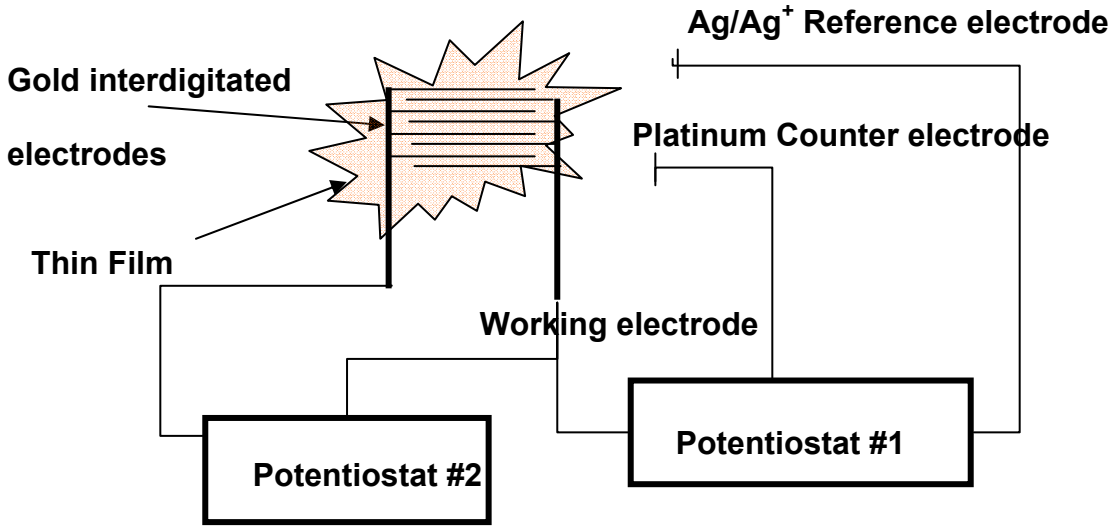

The first potentiostat measured the current due to the redox chemistry taking place in the film and the second potentiostat measured the current due to the redox chemistry and the conductivity across the fingers of the interdigitated electrodes. When examining the conductivity profile, when a fast scan rate is applied, the current due to the redox chemistry will be large, so the maximum current measured by both potentiostats was similar (Figure 6-5-A). When a slow scan rate was applied the redox component of the conductivity measured by the second potentiostat was small in comparison to the current resulting from conductivity through the film, leading to the large difference in the

maximum current measured by the two potentiostats (Figure 6-5-B). The scan rate dependence of the peak potential as noted previously is also apparent.

Figure 6-5 Dual electrode voltammetry of 97 at A) 0.02 V/s and B) 0.0005 V/s

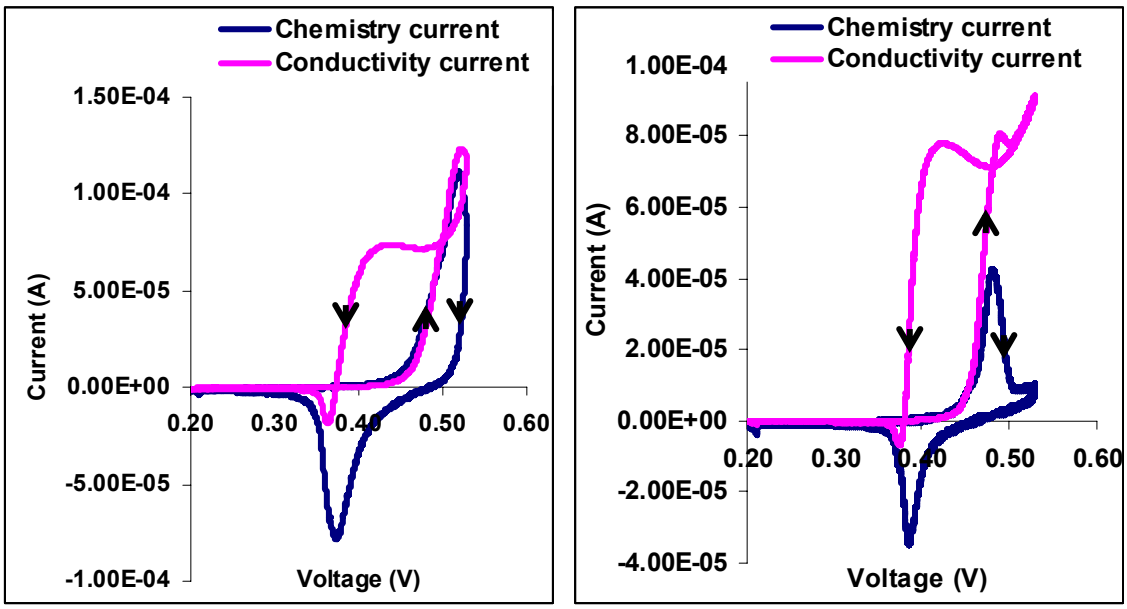

These results clearly show that as the film is doped by electrochemical oxidation, the conductivity of the sample increases and is maintained until the reduction of the oxidized film at which point the conductivity returns to its initial value.

If the film was irradiated with visible light and then cyclic voltammetry was performed on the film very little difference was observed between the open and the closed form (Figure 6-6).

Figure 6-6 Cyclic voltammetry at 0.02 V/s of A) closed and B) open (after 1 min visible light irradiation) vs Ag/Ag^{+}

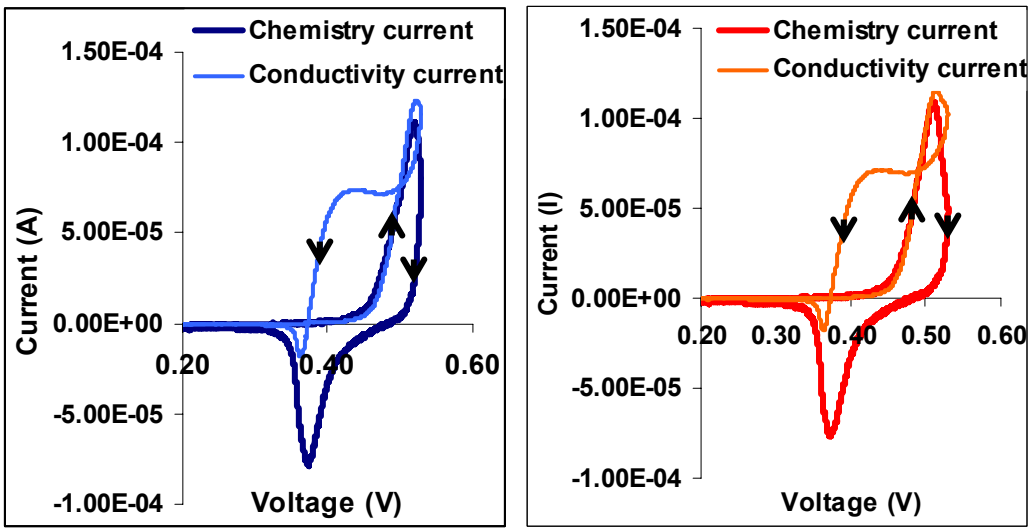

A (97 closed) **B (97 open)**

In the open form, there was a slight shift in the peak potential to a lower potential and a broadening of the oxidation curve peak. There was however no change in the conductivity current. If the sample was irradiated with visible light while the CV was run there was also a small shift of the peak potential to a lower potential but once again no change in the conductivity (Figure 6-7).

Figure 6-7 Continuous visible light irradiation of 97 at 0.02 V/s vs Ag/Ag^{+}

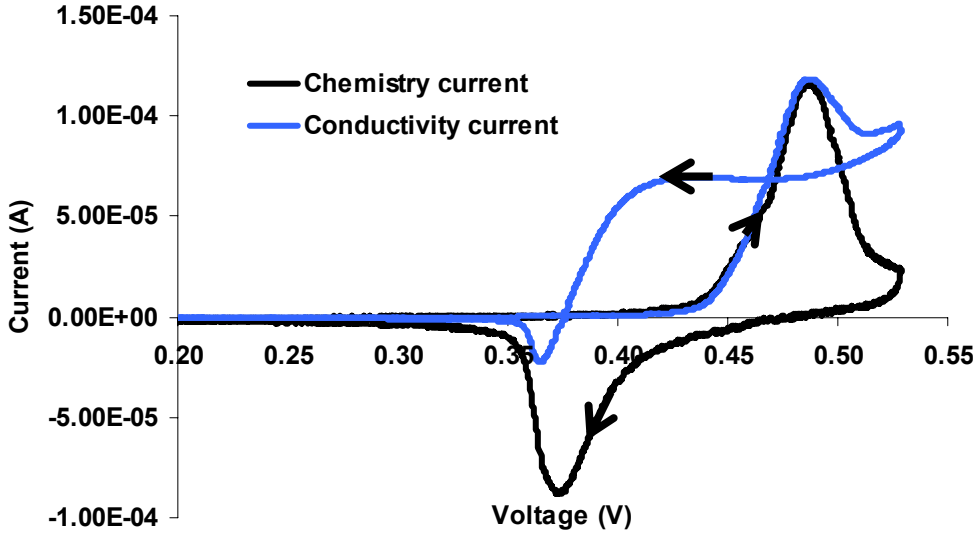

The lack of change in the conductivity after visible light irradiation indicates that either there is no conductivity change between the open and the closed form when the sample is doped or that the sample did not open or remain open during the experiment. Spectroelectrochemistry experiments indicated that electrochemical oxidation of the open form of the switch causes the switch to close. The observed lack of change in the conductivity between the "open" and the closed form can be attributed to the rapid electrochemical closing of the switch preventing a conductivity measurement of the open form from being obtained, rather than there being no difference in the conductivity between the open and the closed forms.

6.3 Conclusion

Conductivity changes were observed for **97** when it was opened and closed in the undoped form. However because the sample was undoped the conductivity measured

was quite low. In the doped form the conductivity was much higher but rapid electrochemical closure of the switch prevented a measurement of the switch in the open form from being obtained.

Chapter Seven: Conclusions

7.1 Synthesis

Thiophene oligomers of varying lengths were attached to the BDHP photoswitch on the same side of the switch (**27**, **28**), and on opposite sides of the switch (**75**, **76**, **77**, **78**). Thiophene oligomers of varying lengths were also added to DHP switches (**96**, **97**, **98**) which had improved photo-opening properties due to the replacement of one of the *t*-butyls in the 2 position with a naphthoyl functional group. These DHP switches were chemically polymerized with hexyl functionalized quinquethiophene oligomers **99**. When dihexyl quinquethiophene oligomers **102** were used the switches were soluble in dichloromethane but insoluble in acetonitrile. These solubility properties allowed the compounds to be easily studied in a solid film by standard electrochemistry techniques. All of these compounds appear to be quite stable as they could be left exposed to air for months at room temperature with no visible change observed.

7.2 Photochromism

The switching properties of the BDHP based switches functionalized with terthiophene and dihexyl quinquethiophene oligomers attached on the same side **27**, **28** and opposite sides with one side attached via a carbonyl spacer **76**, **77** were studied. It was found that the addition of the thiophene oligomers increased the rate of visible light photo-opening (490 nm cut off filter) over that of simple BDHP **12**. Longer oligothiophenes gave faster opening suggesting that the oligothiophenes were channelling the light energy into the switch causing it to open faster. The thermal closing was also faster than that of BDHP, however the half lives were still quite long at over 1 hour at

50°C and over 2 days at 20°C. UV closing rates were studied for the quinquethiophene functionalized BDHP switches **28**, **77** and they showed little change when compared to the BDHP switch.

The switching properties for the naphthoyl functionalized DHP switches containing terthiophene **96**, dihexylquinquethiophene **97** oligomers and phenyls **100** on either side of the switch were studied. These molecules showed dramatically faster photo-opening rates when irradiated with visible light (490 nm cut off filter) compared to BDHP. As in the BDHP case, longer thiophene oligomers gave faster photo-opening rates. However the rate of thermal closing for these compounds was also dramatically faster, with thermal half lives at 50°C of less than 3 minutes and at 20°C they were less than 2 hours.

Using 254 nm UV light to close thiophene functionalized switches was found to be problematic. Long irradiations with 254 nm UV light caused a decrease in the region of the long wavelength thiophene absorption and the development of an insoluble film suggesting polymerization was occurring. It was also found that UV light could induce an acceleration in the thermal return. This acceleration in the thermal return was attributed to the formation of radicals which led to radical catalyzed thermal closing.

7.3 Electrochemistry

The electrochemistry of the thiophene functionalized switches was studied in solution and in a thin film. Multiple oxidation peaks were observed for these compounds and when in solution it was found that scanning past the first or the second oxidation peak led to polymerization on the electrode. Very little or no change was observed between the CVs of the open and the closed forms. Spectroelectrochemistry indicated

this was because the electrochemistry was causing rapid electrochemically induced thermal closing.

7.4 Conductivity

From the variety of oligothiophene functionalized switches synthesized, **97** was selected for conductivity testing as it showed the most potential to give a conductivity change between the open and the closed form. Conductivity measurements were performed on thin film samples of the oligomer using an interdigitated microelectrode array. When in an undoped film, a small change in the conductivity between the open and the closed form was observed. This was shown to be due to the opening and the closing of the switch rather than to photoconductivity. Unfortunately the overall conductivity of the open and the closed form was quite low. In the doped form no change was observed between the conductivity in the film before and after irradiation with visible light. This lack of change in conductivity was attributed to rapid electrochemically induced thermal closing preventing a conductivity measurement of the switch in the open form.

7.5 Conclusions and future work

This project has demonstrated that DHP based photoswitches can be used to control conductivity when inserted into an oligothiophene molecular wire. However, because the electrochemistry leads to accelerated closing of the switch especially when in the more highly conducting doped form, the use of these switches for this purpose is not very practical.

The undoped conductivity measurements conducted during this project showed that the conductivity through the film was related to whether the switch was open or closed. Performing spectroelectrochemistry experiments during the conductivity measurements would be helpful in confirming these results. They would also be helpful in correlating the extent of opening and closing with the conductivity observed.

A more extensive study of the electrochemical properties of the DHP based switches would be useful to determine whether this electrochemical closing can be controlled or if a dual photo-electrochemical switch can be effectively controlled. Branda *et al.*[102] has shown that with the dithienylethene switches, the functional groups on the switch can be used to control whether the switch electrochemically opens or closes under oxidative or reductive conditions. A similar result might be possible with the DHP switches.

All of the conductivity testing performed in this project was performed on electrodes coated with a bulk film. The advantage of using this approach is that sample preparation is relatively simple and can be easily scaled up. The disadvantage of this approach is that there is little control over the contact between the metal electrode and the film and also the orientation of the molecules in the film. If there is a large barrier to charge injection from the metal into the film then the conductivity measured would be significantly lower than the total conductivity possible through the film. Using a four point probe conductivity test would help determine what impact the metal to film charge injection barrier has on the conductivities measured. Single molecule studies where the oligomers are attached directly to the electrodes would be ideal for minimizing effects due to charge injection barriers. Single molecule studies would also be ideal as they

would negate the effects due to the various orientations of oligomers in the film. Using the approach of Nuckolls *et.*[51] where carbon nanotubes are used as the electrodes show particular promise. They found that when looking at the single molecule conductivity through dithienylethene photoswitches only single direction switching was possible. The switches could be closed with UV light but could not be opened with visible light. This was thought to be the result of extended conjugation from the carbon nanotube into the switch dissipating the photo-opening energy. The DHP photoswitches have been shown in this project to be easier to photo-open when there is extended conjugation into the switch and therefore using carbon nanotubes as electrodes would be ideal.

The development of molecular scale components that can be used in molecular devices has much potential but in order to reach this potential there is much that needs to be learned. This project has been one small step in the development of the tools and knowledge base that is required for unlocking this potential.

Chapter Eight: Experimental

8.1 General experimental conditions and instrumentation

^{1}H and ^{13}C NMR spectra were recorded on a Bruker Avance 500 MHz spectrometer (500.1 MHz for ^{1}H, 125.7 MHz for ^{13}C) or a Bruker AMX 360 (360 MHz for ^{1}H, 90.6 MHz for ^{13}C). Spectra were calibrated based on the solvent residual peak (7.26 and 77.23 ppm for $CHCl_3$ and 7.16 and 128.39 ppm for C_6D_6). NMR assignments were made on the basis of 2D COSY and NOESY experiments for protons and HMQC and HMBC experiments for carbons. When peaks in the same sample were very close a third decimal place was given. Expanded data sets were used to obtain coupling constants. The numbering for the structures included in the experimental is for NMR peak identification.

Mass spectrometry was performed on a Finnigan 3300 gas chromatography-mass spectroscopy system using methane as a carrier gas for chemical ionization or electron impact (EI) at 70 eV. FAB mass spectra and exact mass measurements were obtained on a Kratos Concept-H instrument using perfluorokerosene as the standard. Elemental analyses were performed by Canadian Microanalytical services Ltd., Vancouver, B.C. Melting points were determined on a Reichert 7905 melting point apparatus integrated to an Omega Engineering Model 199 Chromel-alumel thermocouple. Infrared spectra were recorded on a Thermo Nicolet IR 200 spectrometer as KBr pellets or thin films from dichloromethane on NaCl plates. UV-vis spectra were recorded on a Cary 50 UV-vis spectrophotometer. All evaporations were carried out under reduced pressure on a rotary evaporator, or by using an oil pump and liquid nitrogen condenser. Silica gel refers to Merck silica gel, 60-200 mesh. Alumina refers to Aldrich aluminum oxide, activated,

neutral, Brockmann I, standard grade, ~150 mesh. The silica gel and alumina were deactivated with 5% H_2O. Tetrahydrofuran (THF) was dried by distillation from potassium benzophenone ketyl. DCM and DMF were dried by distillation over calcium hydride. Solution cyclic voltammetry experiments were performed using a Bioanalytical Systems (BAS) CV50W Voltammetric Analyzer interfaced to a personal computer. All measurements were conducted in oven dried glass cells cooled under a flow of argon. The working electrode was glassy carbon (BAS), the counter electrode was a platinum wire and the reference electrode was a silver wire. Ferrocene was used as the internal standard (0.46 V vs SCE). $TBAPF_6$ was recrystallized three times from 95% ethanol and dried at 80^{o}C for 24 hours prior to use. Sample concentrations of ~1 mM in 0.1M $TBAPF_6$ were used. Thin film cyclic voltammetry was performed with a Solitron 1286 using either an indium tin oxide coated glass slide or a gold interdigitated electrode with 5 μm spacing as the working electrode, a coiled platinum wire as the counter electrode and a nonaqueous Ag(s) / Ag^+ reference electrode. The reference electrode was prepared from a 3mm diameter glass tube with a Vycor frit (Bioanalytical Systems, Inc) at one end and filled with $TMABF_4$(sat) / 0.005 M $AgNO_3$ / ACN. Films were prepared by either drop coating or spin coating from DCM.

2,2':5',2"-Terthiophene **107** was synthesized using the procedure of Zimmer.[103] 3",4"-Dihexyl-2,2':5',2":5",2"':5"',2"'-quinquethiophene **102** was synthesized using the method of Barbarella *et al.*[72] with the exception that dppf was used instead of $AsPh_3$, THF was used as the solvent and the method of Leclerc *et al.*[70] was used for the purification. Tributyltin functionalized oligothiophenes **114, 104**, **106**, **108** and **109** were synthesized using the same procedure as that of Swager *et al.*[104] for **109** with the addition

that the oligomers were purified on alumina using hexanes and 1% triethylamine as eluent.

Visible light opening experiments were performed using a 500W household tungsten-halogen lamp (8500 lumens) as the light source with a 490 nm cut off filter unless otherwise stated. Samples were irradiated while in an ice cooled water bath (~5^{o}C) unless otherwise stated. For UV closing experiments samples were irradiated with a 3W low pressure Hg(Ar) pencil light (Oriel 6035, mainly 254 nm) and samples were cooled with an electric fan.

8.2 Syntheses

2,7-Di-*t*-butyl-10-carboethoxy-9,12-epoxy-*trans*-dimethyl-9,12,12c,12d-tetrahydro-benzo[e]pyrene (40)

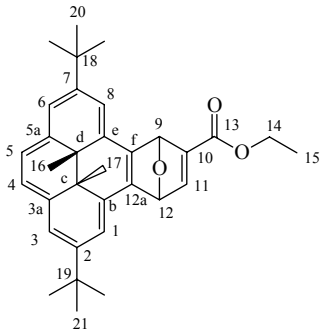

Ethyl propriolate (0.72 mL, 6.9 mmol) was added to a solution of the furan DHP **37** (273 mg, 0.710 mmol) in toluene (60 mL) and the reaction mixture was heated to 110^{o}C for 3 hours. Over this time the solution turned from a reddish purple to a light green. The reaction mixture was then cooled to room temperature and the solvent evaporated. The product mainly consists of two isomers of the product, one of which B is much more soluble in hexane than isomer A. The latter could be obtained reasonably pure by trituration with hexane, and collecting the insoluble green powder, which is

predominately isomer A (128 mg, 36%). The hexane extract was purified by chromatography on silica gel (deactivated with 5% water) using hexanes:ethyl acetate (20:1) as eluent, which gave a mixture of isomers A and B (120 mg, 35%) as a brownish powder. These could be combined with the previously obtained A for direct use in the preparation of **52**. For characterization purposes, recrystalization of the mixture from hexanes several times, yielded the less soluble isomer A, as a green powder, mp - color change at 109-112^{o}C, then melts at 185-188^{o}C. The more soluble B isomer was isolated by recrystalization from hexanes of the collected mother liquors from the previous recrystalizations, as green crystals, mp 185-186^{o}C.

Isomer A

^{1}H NMR (500 MHz, C_6D_6) δ 8.53 (d, *J* = 1.2 Hz, 1H, H-8), 8.18 (brs, 2H, H-6,3), 8.07 (d, *J* = 0.8 Hz, 2H, H-4,5), 8.05 (d, *J* = 1.3Hz, 1H, H-1), 7.39 (d, *J* = 1.9 Hz, 1H, H-11), 6.95 (d, *J* = 0.8 Hz, 1H, H-9), 6.33 (dd, *J* = 1.9, 0.8 Hz,1H, H-12), 3.97 (dq, *J* = 10.9, 7.1 Hz, 1H, H-14a or 14b), 3.83 (dq, *J* = 10.9, 7.1 Hz, 1H, H-14b or 14a), 1.58 (s, 9H, H-21), 1.56 (s, 9H, H-20), 0.84 (t, *J* = 7.1 Hz, 3H, H-15), -2.72 (s, 2H, H-17), -3.04 (s, 2H, H-16). ^{13}C NMR (125.8 MHz, C_6D_6) δ 163.78 (C-13), 149.68 (C-11), 148.20 (C-10), 146.44 (C-2), 146.06 (C-7), 138.57 (C- 3a), 138.11 (C-5a), 135.79 (C-12f), 134.47 (C-12a), 129.76 (C-12e), 128.96 (C-12b), 125.74 (C-4 or 5), 125.48 (C-5 or 4), 122.48 (C-6), 122.19 (C-3), 116.87(C-8), 115.01 (C-1), 82.61 (C-12), 82.00 (C-9), 60.74 (C-14), 36.22 (C-18,19), 34.19 (12d), 33.49 (12c), 31.87 (C-20,21), 17.53 (C-17), 14.98 (C-16), 14.56 (C-15).

Isomer B

^{1}H NMR (500 MHz, C_6D_6) δ 8.53 (d, *J* = 1.3 Hz, 1H, H-8), 8.22 (d, *J* = 1.3 Hz, 1H, H-6), 8.19 (d, *J* = 1.2 Hz, 1H, H-3), 8.09 (s, 2H, H-4,5), 8.07 (d, *J* = 1.2 Hz, 1H, H-1), 7.60 (d, *J* = 2.0 Hz, 1H, H-11), 7.0 (dd, *J* = 0.9, 0.4 Hz, 1H, H-9), 6.30 (ddd, *J* = 2.0, 0.9, 0.4 Hz, 1H, H-12), 3.91 (dqd, *J* = 10.9, 7.1, 0.4 Hz, 1H, H-14a or 14b), 3.78 (dqd, *J* = 10.9, 7.1, 0.4 Hz, 1H, H-14a or 14b), 1.58 (s, 9H, H-20), 1.57 (s, 9H, H-21), 0.83 (t, *J* = 7.1 Hz, 3H, H-15), -2.79 (s, 3H, H-16), -3.16 (s, 3H, H-17). ^{13}C NMR (125.8 MHz, C_6D_6) δ 163.76 (C-11), 149.80 (C-11), 147.70 (C-10), 146.37 (C-2), 146.16 (C-7), 138.33 (C-5a), 138.28 (C-3a), 135.55 (C-12f), 134.62 (C-12a), 129.61 (C-123), 129.56 (C-12b) 125.74 (C-5), 125.32 (C-4), 122.51 (C-6), 122.15 (C-3), 116.32 (C-8), 115.36 (C-1), 83.05 (C-9), 81.77 (C-12), 60.74 (C-14), 36.25 (C-18,19), 34.46 (C-12c), 32.98 (C-12d), 31.92 (C-20 or 21), 31.89 (C-21 or 20), 17.56 (C-16), 15.52 (C-17), 14.51 (C-15). UV-vis (cyclohexane) λ_{max} (ε_{max}, L mol^{-1}cm^{-1}) nm, 238 (12400), 352 (41900), 361 (41300), 383 (35800), 464 (11400), 575 (285), 643 (605). IR (KBr) ν 2924, 1714, 1603, 1460, 1367, 1231, 1095, 1028, 876, 676, 652 cm^{-1}. EI MS, *m/z* 482 (M^+), 467 (M^+-CH_3), 452 (M^+-2 CH_3), 395 (M^+-2 CH_3,-t-butyl),365 (M^+- CH_3,-t-butyl,- OEt), 337 (M^+-2 CH_3,- 2 t-butyl). HRMS calc'd for $C_{33}H_{38}O_3$ 482.2821, found 482.2807. Anal. Calc'd for $C_{33}H_{38}O_3$: C,82.12; H,7.93. Found: C,82.57; H,7.91.

2,7-Di-*tert*-butyl-4,5-diformyl-*trans*-10b,10c-dimethyl-10b,10c-dihydropyrene (43)

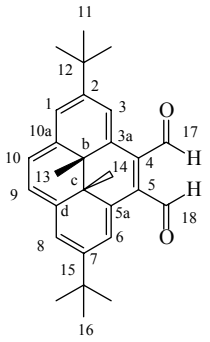

The dialdehyde **43** was almost always obtained as a minor impurity from reactions of **37**, with the amount of dialdehyde **43** varying from ~5-20%. The larger amounts of dialdehyde were obtained from longer running sluggish reactions. In the purification of **40** the dialdehyde **43** was eluted late from the chromatography column using 3:1 hexanes EtOAc. The dialdehyde **43** could be further purified by recrystalization from cyclohexane as green crystals, mp 205-207°C. ^{1}H NMR (500 MHz, C_6D_6) δ 11.31 (s, 2H, H-17,18), 9.56 (s, 2H, H-3,6), 8.351 (s, 1H, H-1 or 8), 8.349 (s, 1H, H-8 or 1), 8.17 (s, 2H, H-9,10), 1.51 (s, 18H, H-11,16), -3.43 (s, 6H, H-13,14). ^{13}C NMR (125.8 MHz, C_6D_6) δ 190.83 (C-17 or 18), 190.80 (C-18 or 17), 152.18 (C-2,7), 140.84 (C-10a,10d), 139.66 (C-3a,5a), 127.47 (C-4,5), 126.99 (C-9,10), 124.07 (C-1,8), 118.58 (C-3,6), 36.92 (C-12,15), 32.13 (C-10b,10c), 31.77 (C-11,16), 16.13 (C-13,14). IR (NaCl, thin film) ν 2964, 2921, 2901, 2866, 1677, 1649, 1265, 886, 737 cm^{-1}. EI MS, *m/z*, 400 (M^+), 485 (M^+-CH_3), 329. HRMS calc'd for $C_{28}H_{32}O_2$ 400.2402, found 400.2391.

2,7-Di-*tert*-butyl-10,11-dicarboethoxy-9,12-epoxy-*trans*-dimethyl-9,12,12c,12d-tetrahydrobenzo[e]pyrene (41)

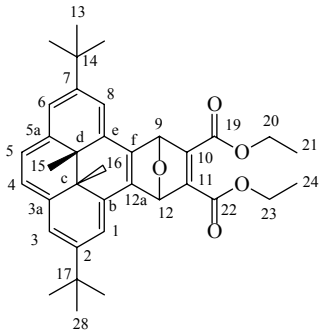

Diethyl 2-butynedioate (1mL, 6.3 mmol) was added to a red solution of the furan DHP **37** (459mg, 1.19mmol) in toluene (150mL) and the solution was refluxed for 4 hours turning a green brown. The reaction mixture was then cooled and the solvent evaporated. The product was washed with hexanes (6 x 5mL) to give the solid green product (230 mg, 0.41 mmol, 35%). The hexane washings were combined and purified by chromatography on silica gel (5% H_2O) using 20:1 hexanes:ethyl acetate, followed by 10:1 hexanes:ethyl acetate to elute the product (260mg, 0.47 mmol, 39%) as a green powder, mp 166-168^{o}C. ^{1}H NMR (500 MHz, C_6D_6) δ 8.46 (d, *J* = 1.3 Hz, 1H, H-8), 8.40 (d, *J* = 1.3 Hz, 1H, H-1), 8.21 (d, *J* = 1.3 Hz, 1H, H-3), 8.20 (d, *J* = 1.3 Hz, 1H, H-6), 8.08 (s, 2H, H-4,5), 6.91 (d, *J* = 1.2 Hz, 1H, H-9 or 12), 6.90 (d, *J* = 1.2 Hz, 1H, H-12 or 9), 3.98 (dq, *J* = 10.7, 7.1 Hz, 1H, H-20 or 23), 3.91 (dq, *J* = 10.7, 7.1 Hz, 1H, H-20 or 23), 3.89 (dq, *J* = 10.8, 7.1 Hz, 1H, H-20 or 23), 3.83 (dq, *J* = 10.7, 7.1 Hz, 1H, H-20 or 23), 1.58 (s, 9H, H-13 or 28), 1.57 (s, 9H, H-28 or 13), 0.84 (t, *J* = 7.1 Hz, 3H, H-21 or 24), 0.80 (t, *J* = 7.1 Hz, 3H, H-24 or 21), -2.77 (s, 3H, H-16), -3.07 (s, 3H, H-15). ^{13}C NMR (125.8 MHz, C_6D_6) δ 163.39 (C-19 or 22), 163.33 (C-22 or 19), 149.80 (C-10 or 11), 149.36 (C-11 or 10), 146.76 (C-2 or 7), 146.46 (C-7 or 2), 138.64 (C-3a), 138.40 (C-

5a), 133.90 (C-12a or 12f), 133.83 (C-12f or 12a), 130.49 (C-12b), 130.05 (C-12e), 125.67 (C-4 or 5), 125.57 (C-5 or 4), 122.44 (C-3 or 6), 122.39 (C-6 or 3), 116.79 (C-8), 116.05 (C-1), 84.87 (C-9 or 12), 84.52 (C-12 or 9), 61.33 (C-20 or 23), 61.26 (C-23 or 20), 36.26 (C-14,17), 34.61 (C-12d), 33.18 (C-12c), 31.90 (C-13 or 28), 31.88 (C-28 or 13), 17.54 (C-16), 15.29 (C-15), 14.42 (C-21 or 24), 14.39 (C-24 or 21). IR (KBr) ν 2964, 2925, 2901, 2867, 1739, 1625, 1464, 1369, 1318, 1263, 1243, 1204, 1108, 870 cm^{-1}. UV-vis (cyclohexane) λ_{max} (ε_{max}, L $mol^{-1}cm^{-1}$) nm, 203 (28800), 239 (14000), 339 (34100), 358 (30800), 377 (33200), 448 (9200), 531 (453), 581 (493), 646 (898). EI MS, *m/z*, 554 (M^+), 539 (M^+-CH_3), 524 (M^+-$2CH_3$). HRMS calc'd for $C_{36}H_{42}O_5$ 554.3032, found 554.3032.

2,7-Di-*tert*-butyl-10-carboethoxy-*trans*-12c,12d-dimethyl-12c,12d-dihydrobenzo[e]pyrene (52)

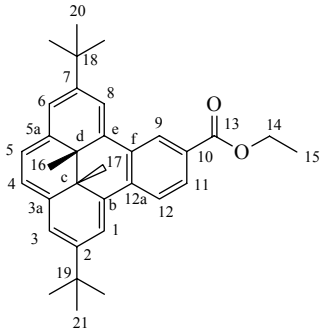

$Fe_2(CO)_9$ (106 mg, 0.292 mmol) was added to a solution of the furan adduct **40** (132 mg, 0.266 mmol) in degassed benzene (50 mL) and the solution was heated to reflux for 4 h during which time it turned from green to red. The solution was then filtered through a small (5cm) silica gel column using benzene as eluent and then the solvent was evaporated. The product was purified by chromatography on silica gel (60-200 mesh,

deactivated with 5% water) using hexanes:ethyl acetate (2:1) as eluent to give the product **52** as a red solid (89mg, 0.191 mmol, 72%) followed by a small amount of a green iron adduct. On larger scales, an additional short alumina column using hexanes as eluent was needed to separate the product from the green iron adduct. Recrystallization from acetonitrile gave a red crystals, mp 140-141°C. ^{1}H NMR (500 MHz, C_6D_6) δ 10.00 (s, 1H, H-9), 8.86 (d, *J* = 8.7 Hz, 1H, H-12), 8.67 (s, 1H, H-8), 8.53 (d, *J* = 1.1 Hz, 1H, H-11), 8.51 (s, 1H, H-1), 7.54 (s, 1H, H-3), 7.51 (s, 1H, H-6), 7.24 (AB, *J* = 6.5 Hz, 1H, H-4), 7.21 (AB, *J* = 6.5 Hz, 1H, H-5), 4.31 (q, *J* = 7.1 Hz, 2H, H-14), 1.43 (s, 9H, H-21), 1.37 (s, 9H, H-20), 1.16 (t, *J* = 7.1Hz, 3H, H-15), -1.40 (s, 6H, H-16,17) ^{13}C NMR (125.8 MHz, C_6D_6) δ 167.16 (C-13), 145.55 (C-7), 144.84 (C-2), 139.52 (C-3a), 138.73 (C-5a), 135.57 (C-12b), 134.87 (C-12e), 133.15 (C-12a), 129.59 (C-12f), 128.68 (C-10), 127.81 (C-9), 126.41 (C-11), 125.50 (C-12), 122.96 (C-4), 122.31 (C-5), 121.99 (C-3), 121.26 (C-6), 119.80 (C-1), 118.51 (C-8), 61.40 (C-14), 36.02 (C-12d), 35.90 (C-12c), 35.85 (C-18), 35.83 (C-19), 31.16 (C-20), 31.03 (C-21), 17.98 (C-16 or 17), 17.96 (C-17 or 16), 14.84 (C-15). IR (KBr) ν 2964, 1719, 1639, 1366, 1253, 767 cm^{-1}. UV-vis (cyclohexane) λ_{max} (ε_{max}, L mol^{-1}cm^{-1}) nm, 264 (14800), 318 (21000), 377 (19200), 395 (24900), 513 (4060), 630 (650). EI MS, *m/z* 466 (M^+), 451(M^+-CH_3), 436 (M^+-2 CH_3), 395 (M^+-2 CH_3,-*t*-butyl, +1H), 366 (M^+-*t*-butyl,- OEt, +1H). HRMS calc'd for $C_{33}H_{38}O_2$ 466.2867, found 466.2875. Anal. Calc'd for $C_{33}H_{38}O_2$: C, 84.94; H, 8.21. Found C, 84.97; H, 7.97.

General procedure A for opening NMR samples:

For NMR samples 5-20 mg of the sample was dissolved in the NMR solvent. Argon was bubbled through the sample for 1 minute and the NMR tube capped and wrapped with paraffin film. The NMR tube was placed in a ~5^{o}C water bath and irradiated with light using a 500W household tungsten-halogen lamp (8500 lumens) as the light source and a 490 nm cut off filter until the color had faded (usually 5-10 minutes).

General procedure B for opening UV-vis samples:

For UV-vis samples, approximately 1 mg of the compound was dissolved in an appropriate solvent and 5 fold and 10 fold dilutions were made. The solutions were placed in quartz UV-vis cells and argon was bubbled through for 2 minutes. The samples while being cooled in a ~5^{o}C water bath were irradiated with light using a 500W household tungsten-halogen lamp (8500 lumens) as the light source and a 490 nm cut off filter until the color faded (usually 1-5 minutes).

Open CPD form. ^{1}H NMR (500 MHz, C_6D_6) δ 8.75 (d, *J* = 1.9 Hz, 1H), 8.21 (dd, *J* = 8.1, 1.9 Hz, 1H), 7.65 (d, *J* = 8.1 Hz, 1H), 7.06 (d, *J* = 2.2 Hz, 1H), 6.94 (d, *J* = 2.2 Hz, 1H), 6.86 (d, *J* = 2.2, 1H), 6.85 (d, *J* = 2.1 Hz, 1H), 6.35 (s, 2H), 4.22 (dq, *J* = 10.8, 7.1 Hz), 4.14 (dq, *J* = 10.8, 7.1 Hz), 1.47 (s, 3H), 1.44 (s, 3H), 1.24 (s, 9H), 1.17 (s, 9H), 1.05 (t, *J* = 7.1 Hz, 3H). ^{13}C NMR (125.8 MHz, C_6D_6) δ 166.53, 151.65, 151.27, 149.27, 145.12, 140.81, 140.41, 140.03, 137.93, 137.79, 133.10, 132.86, 131.57, 130.63, 130.33, 129.57, 128.96, 123.92, 123.63, 61.26, 35.37, 35.31, 34.53, 34.48, 31.75, 31.68, 19.69, 19.49, 14.71. UV-vis (cyclohexane) λ_{max} (ε_{max}, L mol^{-1}cm^{-1}) nm, 213 (29200), 226 (29200), 251 (30600).

2,7-Di-*tert*-butyl-10,11-dicarboethoxy-*trans*-12c,12d-dimethyl-12c,12d-dihydrobenzo[e]pyrene (53)

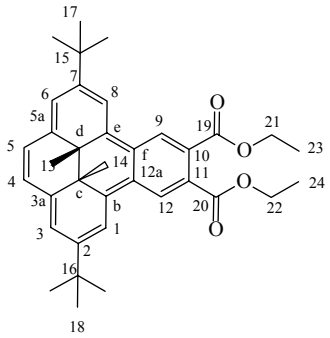

$Fe_2(CO)_9$ was added to a solution of the furan adduct **41** (450mg, 0.81mmol) in benzene (150mL) and the reaction mixture was heated to reflux for 4 hours. It was then cooled to room temperature and passed through a small silica gel filter column using 10:1 benzene:ethyl acetate as eluent. The red product was collected and the solvent evaporated. The product was purified by chromatography on silica gel using 10:1 hexanes:ethyl acetate giving **53** as a red powder (350 mg, 0.65mmol, 80%), mp 171-172°C. ^{1}H NMR (500 MHz, C_6D_6) δ 9.61 (s, 2H, H-9,12), 8.64 (d, *J* = 1.3 Hz, 2H, H-1,8), 7.59 (d, *J* = 1.3 Hz, 2H, H-3,6), 7.28 (s, 2H, H-4,5), 4.34 (q, *J* = 7.2 Hz, 4H, H-21,22), 1.34 (s, 18H, H-17,18), 1.17 (t, *J* = 7.2 Hz, 6H, H-23,24), -1.59 (s, 9H, H-13,14). ^{13}C NMR (125.8 MHz, C_6D_6) δ 168.51 (C-19,20), 145.44 (C-2,7), 139.08 (C-3a,5a), 134.53 (C-12b,12e), 130.89 (12a,12f), 129.85 (10,11), 127.13 (C-9,12), 122.95 (C-4,5), 122.11 (C-3,6), 119.92 (C-1,8), 61.95 (C-21,22), 35.84 (C-15,16), 35.54 (C-12c,d), 31.09 (C-17,18), 17.73 (C-13,14), 14.65 (C-23,24). IR (NaCl, Thin film) ν 2963, 2922, 2900, 2857, 1722, 1619, 1525, 1464, 1366, 1344, 1268, 1137, 1055, 877, 781 cm^{-1}. UV-vis (cyclohexane) λ_{max} (ε_{max}, L mol^{-1}cm^{-1}) nm, 274 (15400), 332 (26900), 350 (26300), 380 (27400), 398 (34900), 5310 (6310), 635 (1350). EIMS, *m/z*, 538 (M^+), 523 (M^+-CH_3),

508 (M^+-2CH_3), 493 (M^+-OEt). HRMS calc'd for $C_{36}H_{42}O_4$ 538.3083, found 538.3086. Anal. Calc'd for $C_{36}H_{42}O_4$: C, 80.26; H, 7.85. Found: C, 79.71; H, 7.44.

Open CPD Form. Procedure: see (B), p 165. UV-vis (cyclohexane) λ_{max} (ε_{max}, L mol^{-1}cm^{-1}) nm, 215 (36800), 255 (40200).

2,7-Di-*tert*-butyl-10-carboxy-*trans*-12c,12d-dimethyl-12c,12d-dihydrobenzo[e]pyrene (57)

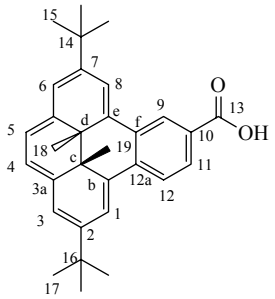

NaOH (2M, 10 mL) was added to a solution of the ester **52** (44.5 mg, 0.095 mmol) in EtOH (95%, 30 mL) and the solution was heated at reflux for 3 hours. After cooling, the mixture was poured into hexanes and H_2O. Dilute HCl was then added, and the resulting dark red organic layer was washed with aq.NaCl and then H_2O. The organic layer was dried with $MgSO_4$ and concentrated to give the crude product **57** (40 mg, 95%) as a dark red solid. The product was pure enough to be used in subsequent steps but could be further purified by recrystallization from hexanes, mp 197-199 ^oC (dec); ^1H NMR (500 MHz, C_6D_6) δ 10.03 (s, 1H, H-9), 8.79 (d, *J* = 8.7 Hz, 1H, H-11), 9.69 (s, 1H, H-8), 8.52 (s, 1H, H-1), 8.51 (d, *J* = 8.8 Hz, 1H, H-12), 7.57 (s, 1H, H-3), 7.54 (s, 1H, H-6), 7.24 (AB, *J* = 6.5 Hz, 2H, H-4,5), 1.45 (s, 9H, H-15), 1.41 (s, 9H, H-17), -1.43 (s, 6H, H-18,19). ^{13}C NMR (125.8 MHz, C_6D_6) δ 172.44 (C-13), 145.72 (C-7), 144.87 (C-2),

139.62 (C-5a), 138.70 (C-3a), 135.45 (C-12e), 134.72 (C-12b), 133.80 (C-12a), 129.46 (12f), 128.7 (C-9), 126.79, 126.63 (C-11), 125.65 (C-12), 123.15 (C-5), 122.36 (C-4), 122.26 (C-3), 121.35 (C-6), 120.24 (C-1), 118.64 (C-8), 35.94 (C-12c or 12d), 35.88 (C-16 or 14), 35.87 (C-14 or 16), 35.81 (C-12d or 12c), 31.15 (C-15), 31.05 (C-17), 17.94 (C-18 or 19), 17.91 (C-19 or 18). IR (NaCl, thin film) ν 3411, 2965, 2933, 2867, 1716, 1685, 1605, 1379, 1363, 1261, 1230, 1104, 1201, 876, 802, 738 cm^{-1}. UV-vis (cyclohexane) λ_{max} (ε_{max}, L $mol^{-1}cm^{-1}$) nm, 264 (9180), 322 (19000), 380 (19300), 398 (26500), 518 (5020), 636 (1810). EI MS, *m/z*, 438 (M^+), 423 (M^+-CH_3), 408 (M^+-2 CH_3), 367 (M^+- CH_3,-*t*-butyl). HRMS calc'd for $C_{31}H_{34}O_2$, 438.2559, found 438.2564.

PEG Ester (60)

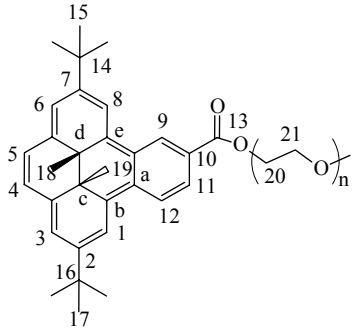

n = 6-11

1,3-Diisopropylcarbodiimide (0.04 mL, 0.25 mmol) was added to a solution of the acid **57** (62mg, 0.14 mmol), methoxypolyethyleneglycol 350 (75 mg, 0.21 mmol) and 4-dimethylaminopyridine (25 mg, 0.20 mmol) in dichloromethane (30 ml) and the reaction stirred for 18 h at 22°C. The solution was filtered through Celite while washing with dichloromethane and the solvent was evaporated. The product was purified by

chromatography on silica gel using 3:1 hexanes:EtOAc to removed firstly the N-O acyl transfer product followed by 1:3 hexanes: EtOAc and then 1:3:1 hexanes:EtOAc:MeOH to obtain the desired product (53 mg, 0.067 mmol, 48%) as a red solid. ^{1}H NMR (500 MHz, C_6D_6) δ 10.01 (d, *J* = 1.7 Hz, 1H, H-9), 8.84 (br d, *J* = 8.6 Hz, H-12), 8.67 (d, *J* = 1.2 Hz, 1H, H-8), 8.53 (dd, *J* = 8.6, 1.7 Hz, 1H, H-11), 8.51 (s, 1H, H-1), 7.54 (s, 1H, H-3), 7.52 (s, 1H, H-6), 7.24 (AB, *J* = 6.4 Hz, 1H, H-4), 7.21 (AB, *J* = 6.4 Hz, 1H, H-5), 4.50-4.48 (m, 2H, H-20), 3.62-3.59 (m, 2H, H-21), 3.55-3.51 (m, 4H), 3.50-3.44 (m, 24H), 3.36-3.32 (m, 4H), 3.13-3.10 (m, 4H), 1.43 (s, 9H, H-17), 1.39 (s, 9H, H-15), -1.39 (s, 6H, H-18,19); ^{13}C NMR (125.8 MHz, C_6D_6) δ 167.22 (C-13), 145.61 (C-7), 144.88 (C-2), 139.56 (C-5a), 138.76 (C-3a), 135.67 (C-12e), 134.88 (C-12b), 133.21 (C-12a), 129.56 (C-12f), 128.15 (C-10), 127.96 (C-9), 126.51 (C-11), 125.51 (C-12), 122.94 (C-4), 122.29 (C-5), 121.99 (C-3), 121.25 (C-6), 119.84 (C-1), 118.54 (C-8), 72.72, 71.46, 71.38, 71.36, 71.24, 71.16, 71.13, 70.76, 69.94 (C-21), 64.92 (C-20), 59.03, 36.02 (C-12c or 12d), 35.90 (C-14), 35.86 (C-16 and C-12d or 12c), 31.15 (C-17), 31.05 (C-15), 17.98 (C-18 or 19), 17.95 (C-19 or 18); IR (NaCl, thin film) ν 3501, 2961, 2869, 1716, 1621, 1605, 1463, 1363, 1273, 1253, 1110, 1043, 876, 767 cm^{-1}. UV-vis (cyclohexane) λ_{max} (ε_{max}, L $mol^{-1}cm^{-1}$) nm, 630 (1000), 516 (5100), 396 (30000), 378 (23000), 340 (20000), 327 (22000), 319 (23000), 253 (15000). LSIMS (n=ethylene glycol repeat unit), *m/z*, 959.5 (M+Na (n=11)), 929.5 (M+Na (n=11) – $2CH_3$), 915.5 (M+Na (n=10), 885.4 (M+Na (n=10) – $2CH_3$), 871.5 (M+Na (n=9)), 841.4 (M+Na (n=9) – $2CH_3$), 827.4 (M+Na (n=8)), 797.4 (M+Na (n=8) – $2CH_3$), 783.4 (M+Na (n=7)), 753.4 (M+Na (n=7) – $2CH_3$), 739.4 (M+Na (n=6)), 709.4 (M+Na (n=6) – $2CH_3$).

Open CPD Form. Procedure: see (B), p 165. UV-vis (cyclohexane) λ_{max} (ε_{max}, L $mol^{-1}cm^{-1}$) nm, 273 (26000), 246 (35000).

5-Bromo-2,7-di-*tert*-butyl-10-carboethoxy-*trans*-12c,12d-dimethyl-12c,12d-dihydrobenzo[e]pyrene (61) and the 4-bromo isomer

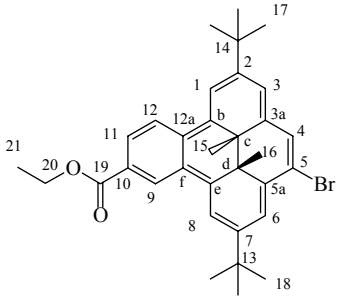

NBS (42.4 mg, 0.238 mmol) was added to a refluxing solution of the ester **52** (111 mg, 0.238 mmol) in dry dichloromethane (30 mL). The reaction mixture was refluxed for 30 minutes after which it was cooled to 22^{o}C and stirred for a further 3 hours. Hexanes (60 mL) was added and the solution was washed repeatedly with water (5 x 30 mL). The organic layer was then dried over $MgSO_4$ and the solvent evaporated to give a red solid. The product was purified by chromatography on silica gel (deactivated with 5% H_2O) using 20:1 hexane:ethyl acetate to give the product as a red powder (127 mg, 0.234 mmol, 98%) along with a small amount of the dibromide **63**. The product could be further purified by recrystallization from ACN to give red crystals, mp 105-107 ^{o}C. Unfortunately the product was obtained as a 3:1 mixture of the two monobromide isomers (Br in the 4 or 5 position) which could not be separated from each other. The major 5-bromo isomer is assigned. *Indicates that the major and minor isomer peaks were indistinguishable. ^{1}H NMR (500 MHz, C_6D_6) δ 9.90 (d, J = 1.7 Hz, 1H, H-9), 8.71 (d, J = 8.7 Hz, 1H, H-12), 8.58 (d, J = 1.1 Hz, 1H, H-8), 8.48 (dd, J = 8.7 Hz, 1.7 Hz, 1H,

H-11), 8.37 (d, *J* = 1.2 Hz, 1H, H-1), 8.10 (d, *J* = 1.2 Hz, 1H, H-6), 7.38 (d, *J* = 0.9 Hz, 1H, H-4), 7.26 (brs, 1H, H-3), 4.28 (q, *J* = 7 Hz, 2H, H-20), 1.36 (s, 1H, H-17), 1.35 (s, 1H, H-18), 1.142 (t, *J* = 7 Hz, 3H, H-21), -1.35 (brs, 6H, H-15,16)*. Minor 4-bromo Isomer: ^{1}H NMR (500 MHz, C_6D_6) δ 9.88 (d, *J* = 1.7 Hz), 8.73 (d, *J* = 8.7 Hz), 8.54 (d, *J* = 1.2 Hz), 8.47 (dd, *J* = 8.6, 1.7 Hz), 8.42 (d, *J* =1.1 Hz), 8.13 (d, *J* = 1.2 Hz), 7.35 (d, *J* = 0.9 Hz), 7.23 (brs), 4.29 (q, *J* = 7 Hz), 1.41 (s), 1.30 (s), 1.140 (t, *J* = 7 Hz). Major isomer peaks are assigned when possible. ^{13}C NMR (125.7 MHz, C_6D_6), δ 166.97, 166.95 (C-19), 148.04 (C-7), 147.34, 147.32, 146.62 (C-2), 140.59, 139.83 (C-3a), 136.19 (C-12e), 136.03, 135.54, 135.40 (C-12b), 134.46 (C-5a), 133.72, 133.06, 133.01 (C-12a), 129.56, 129.52 (C-12f), 128.95 (C-10), 128.92, 127.91 (C-9), 127.64, 126.88 (C-11), 126.75 (C-4), 126.19, 125.67, 125.41 (C-12), 120.94 (C-3), 120.85, 120.26, 120.18 (C-6), 120.03, 119.78 (C-1), 118.80 (C-8), 118.56, 116.15, 115.45 (C-5), 61.50 (C-20), 39.48 (C-12d), 39.36, 36.36, 36.27, 36.25 (C-12c and 1 of C-13,14), 35.88 (C-14 or 13), 35.86, 30.95, 30.91 (C-17), 30.82, 30.78 (C-18), 18.25 (C-15), 18.21, 17.56, 17.52 (C- 16), 14.80 (C-21), 14.69. IR (KBr) ν 2963, 1711, 1618, 1459, 1364, 1253, 1124, 1024, 869, 767 cm^{-1}. UV-vis (cyclohexane) λ_{max} (ε_{max}, L mol^{-1}cm^{-1}) nm, 254 (12900), 330 (2380), 345 (23300), 381 (2910), 400 (39800), 516 (5670), 627 (785). EIMS, *m/z* 546 (M^+), 531 (M^+-CH_3), 516 (M^+-2CH_3), 501 (M^+-OEt), 473 (M^+-*t*-butyl, - CH_3). HRMS calc'd for $C_{33}H_{37}BrO_2$ 544.1977, found 544.1974. Anal. Calc'd for $C_{33}H_{37}BrO_2$: C, 72.65; H, 6.83. Found: C, 72.11; H, 6.17.

Open CPD Form. Procedure: see (B), p 165. UV-vis (cyclohexane) λ_{max} (ε_{max}, L mol^{-1}cm^{-1}) nm, 211 (32800), 236 (43900).

4,5-Dibromo-2,7-di-*tert*-butyl-10-carboethoxy-*trans*-12c,12d-dimethyl-12c,12d-dihydrobenzo[e]pyrene (63)

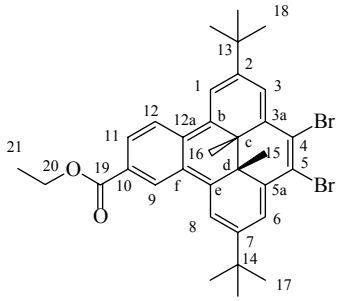

If impure **52** was used or if there was an excess of NBS then higher percentages of the dibromide **63** was obtained. Isolation of the dibromide was generally not performed as it was difficult to separate from the mono-bromide and because separation of the di-addition products due to the presence of the dibromide was much easier in the subsequent step. The dibromide could be isolated from the mono-bromide by careful chromatography on silica gel using 20:1 hexanes:ethyl acetate as eluent, giving the dibromide as a red solid eluting slightly before the mono-bromide. It could be further purified by recrystallization from acetonitrile, mp 166-167^{o}C.

^{1}H NMR (500 MHz, C_6D_6) δ 9.77 (d, *J* = 1.7Hz, 1H, H-9), 8.62 (d, *J* = 8.6Hz, 1H, H-12), 8.47 (dd, *J* = 1.3, 0.6 Hz, 1H, H-8), 8.43 (ddd, *J* = 8.6, 1.6, 0.5 Hz, 1H, H-11), 8.32 (dd, *J* = 1.3, 0.6 Hz, 1H, H-1), 8.13 (dd, *J* = 1.3, 0.6 Hz, 1H, H-3), 8.10 (dd, *J* = 1.3, 0.6 Hz, 1H, H-6), 4.28 (qd, *J* = 7.2, 1.5 Hz, 2H, H-20), 1.37 (s, 9H, H-18), 1.36 (s, 9H, H-17), 1.14 (t, *J* = 7.2 Hz, 3H, H-21), -1.28 (s, 6H, H-15,16). ^{13}C NMR (125.8 MHz, C_6D_6) δ 166.78 (C-19), 149.76 (C-7), 149.05 (C-2), 136.87 (C-5a or 12e), 136.84 (C-12e or 5a), 136.26 (C-3a or 12b), 136.17 (C-12b or 3a), 132.91 (C-12a), 129.47 (C-12f), 129.38 (C-10), 127.77 (C-9), 127.32 (C-11), 125.61 (C-12), 122.39 (C-3), 121.75 (C-6), 120.17 (C-1), 119.31 (C-4), 118.98 (C-8), 118.69 (C-5), 61.58 (C-20), 39.83 (C-12c), 39.72 (C-12d),

36.28 (C-13 or 14), 36.26 (C-14 or 13), 30.75 (C-18), 30.63 (C-17), 17.59 (C-15 or 16), 17.75 (C-16 or 15), 14.79 (C-21). IR (NaCl, thin film) ν 2964, 2868, 1717, 1620, 1463, 1364, 1319, 1299, 1256, 1200, 1127, 1027, 961, 911, 869, 767, 741 cm^{-1}. UV-vis (cyclohexane) λ_{max} (ε_{max}, L $mol^{-1}cm^{-1}$) nm, 255 (13800), 334 (22600), 349 (23700), 365 (19700), 385 (33300), 405 (46200), 520 (5680), 629 (760). EI MS, *m/z* 624 (M^+), 609 (M^+-CH_3), 594 (M^+-2 CH_3), 579 (M^+-OEt), 553 (-CH_3,-*t*-butyl). HRMS calc'd for $C_{33}H_{36}Br_2O_2$(^{79}Br,^{81}Br) 624.1062, found 624.1061. Anal. Calc'd for $C_{33}H_{36}Br_2O_2$: C,63.47; H,5.81. Found C,63.73; H,6.09.

Open CPD form. Procedure: see (B), p 165. UV-vis (cyclohexane) λ_{max} (ε_{max}, L $mol^{-1}cm^{-1}$) nm, 242 (55400), 307 (11400).

2,7-Di-*t*-butyl-10-carboethoxy-*trans*-12c,12d-dimethyl-5-(2-3",4"-dihexyl-5,2':5',2":5",2"':5"',2""-quinquethienyl)-12c,12d-dihydrobenzo[e]pyrene (66) and the 4-quinquethienyl isomer.

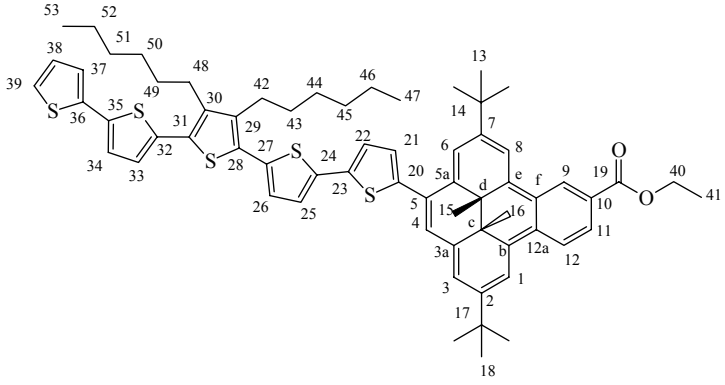

Major Isomer

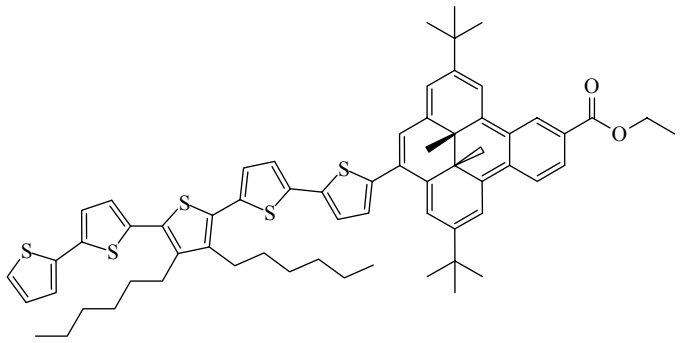

Minor Isomer

Bis(dibenzylideneacetone)palladium(0) ($Pd_2(dba)_3$) (21 mg, 0.02 mmol) and 1,1'-bis(diphenylphosphino)ferrocene (dppf) (25 mg, 0.04 mmol) were added to a solution of the bromide **61** (273 mg, 0.456 mmol) and 2-tributylstannyl-3",4"-dihexyl-5,2':5',2":5",2"':5"',2"'':quinquethiophene **103** (405 mg, 0.465 mmol) in tetrahydrofuran (15mL). The solution was heated to reflux and stirred for 72 hours. The solution was then cooled to room temperature, aq.KF (10 mL) was added and the solution was stirred vigorously for 10 minutes and then filtered through Celite washing with THF. The solution was extracted between hexanes and water (3x) and the organic layer was dried ($MgSO_4$), filtered through Celite and the solvent evaporated to give a red solid. The product was purified by chromatography on silica gel (deactivated with 5% H_2O) using first 10:1 hexanes:dichloromethane to remove the excess quinquethiophene and then 10:1 hexanes:ethyl acetate to elute first a small amount of un-reacted bromide **61** followed by the desired product **66** (270 mg, 0.258 mmol, 56%) as a reddish brown solid. The product could be further purified by recrystallization from pentane/methanol, mp 79-82^{o}C. The product was obtained as a mixture of 2 isomers with a ratio of ~3:1. The major isomer is assigned. * Indicates when the major isomer is indistinguishable from

the minor isomer. ^{1}H NMR (500 MHz, C_6D_6) δ 9.99 (d, *J* = 1.5 Hz, 1H, H-9), 8.83 (d, *J* = 8.7 Hz, 1H, H-12), 8.70 (s, 1H, H-8), 8.54-8.51 (m, 1H, H-11)*, 8.49 (d, *J* = 1.1Hz, 1H, H-1), 8.48 (d, *J* = 1.1 Hz, 1H, H-6), 7.57 (d, *J* = 0.7 Hz, 1H, H-4), 7.51 (s, 1H, H-3), 7.26 (d, *J* = 3.7 Hz, 1H, H-21), 7.20 (d, *J* = 3.6 Hz, 1H, H-22), 7.11 (d, *J* = 3.7 Hz, 1H, H-25), 7.08 (d, *J* = 3.7 Hz, 1H, H-26), 7.029 (d, *J* = 3.7 Hz, 1H, H-33), 7.01 (dd, *J* = 3.5, 0.9 Hz, 1H, H-37 or 39)*, 6.95 (d, *J* = 3.7 Hz, 1H, H-34)*, 6.73 (dd, *J* = 5.5,1.1 Hz, 1H, H-39 or 37)*, 6.65 (dd, *J* = 5.5, 3.5 Hz, 1H, H-38)*, 4.32 (dq, *J* = 7.2, 1.2 Hz, 2H, H-40)*, 2.88-2.81 (m, 4H, H-42,48)*, 1.72-1.66 (m, 4H, H-43,49),* 1.47-1.41 (m, 4H, H-44,50),* 1.44 (s, 9H, H-18), 1.37 (s, 9H, H-13), 1.13- 1.25 (m, 8H, H-45,46,51,52)*, 1.16 (t, *J* = 7.2 Hz, 3H, H-41)*, 0.91-0.85 (m, 9H, H-47,53)*, -1.24 (s,3H, H-15 or 16), -1.263 (s, 3H, H-16 or 15). Minor isomer peaks where distinguishable. ^{1}H NMR (500 MHz, C_6D_6) δ 9.98 (d, *J* = 1.7 Hz), 8.85 (d, *J* = 8.7 Hz), 8.66 (d, *J* = 1.1 Hz)*, 7.54 (d = 0.7 Hz), 7.49 (s), 7.27 (d, *J* = 3.7 Hz), 7.21 (d, *J* = 3.5 Hz), 7.12 (d, *J* = 3.7 Hz), 7.09 (d, *J* = 3.7 Hz), 7.031 (d, *J* = 3.7 Hz), 1.43 (s), 1.38 (s), -1.23 (s), -1.26 (s). Identified Major isomer peaks are assigned. ^{13}C NMR (125.8 MHz, C_6D_6) δ 167.09 (C-19), 147.29 (C-7), 146.54, 146.47, 145.76 (C-2), 143.71 (C-20), 141.18 (C-29 or 30), 141.14 (C-30 or 29), 139.28, 138.49 (C-3a), 138.33 (C-24), 138.30, 138.13 (C-32), 137.78 (C-35 or 36), 137.76, 137.67 (C-23), 136.50 (C-12e), 136.09 (C-5a), 135.90, 135.87, 135.82, 135.77, 135.31, 135.13 (C-12b), 133.31, 133.06 (C-12a), 131.03 (C-28), 130.96 (C-31), 129.77 (C-12f), 129.55, 128.90 (C-10), 128.56[a] (C-21), 128.48[a] (C-38), 128.00 (C-9), 127.67, 127.63 (C-26), 127.47 (C-33), 126.70 (C-11), 126.63, 126.00, 125.97 (C-4), 125.69, 125.39 (C-12), 125.35, 125.09 (C-37 or 39), 124.90 (C-34), 124.78 (C-22), 124.69, 124.66 (C-25), 124.50 (C-39 or 37), 121.97 (C-3), 121.25, 119.98, 119.81 (C-1), 119.09

(C-6), 118.72 (C-8), 61.47 (C-40), 37.33 (C-12d), 37.24, 36.33, 36.31 (C-14), 36.04, 35.92 (C-12c or 17), 35.89 (C-17 or 12c), 35.87, 34.78, 32.23 (C-45 or 46 or 51 or 52), 32.20 (C-45 or 46 or 51 or 52), 31.49 (C-43 or 49), 31.47 (C-49 or 43), 31.12, 31.09 (C-13 or 18), 30.99 (C-18 or 13), 30.96, 30.37 (C-44 or 50), 30.33 (C-40 or 44), 29.06 (C-42 or 48), 29.03 (C-48 or 42), 27.58 (C-45 or 46 or 51 or 52), 23.38 (C-45 or 46 or 51 or 52), 23.36, 23.06, 18.53 (C-15 or 16), 18.42, 18.39 (C-16 or 15), 14.83 (C-41), 14.67 (C-47 or 53), 14.64 (C-53 or 47), 14.61. [a] obtained from DEPT. IR (KBr) ν 3065, 2960, 2926, 2867, 1714, 1604, 1463, 1365, 1252, 1112, 793, 741 cm^{-1}. UV-vis (cyclohexane) λ_{max} (ε_{max}, L $mol^{-1}cm^{-1}$) nm, 251 (30900), 320 sh (31000), 353 sh (35000), 426 (68100), 526 (10200), 646 (1250). LSIMS, *m/z* 1045 (M+1), 1029, 1015, 973. HRMS calc'd for $^{12}C_{64}{}^{13}CH_{72}O_2S_5$ 1045.4136, found 1045.416. Anal. Calc'd for $C_{65}H_{72}O_2S_5$: C,74.67; H,6.94. Found: C,74.94; H,6.93.

Open CPD Form. Procedure: see (A, B), p 165. * indicates when the major isomer is indistinguishable from the minor isomer. ^{1}H NMR (500 MHz, C_6D_6) δ 8.78 (d, *J* = 1.8 Hz, 1H), 8.24 (dd, *J* = 8.0 Hz, 1.9 Hz), 7.68 (d, *J* = 8.1 Hz, 1H), 7.32 (d, *J* = 2.1 Hz, 1H), 7.17-7.14 (m)*, 7.06 (AB, *J* = 3.7 Hz)*, 7.05 (AB, *J* = 3.7 Hz)*, 7.02-7.0 (m, 3H)*, 6.98 (d, *J* = 2.0 Hz, 1H), 7.0-6.96 (m, 2H)*, 6.94 (d, *J* = 3.7 Hz, 1H)*, 7.2 (dd, *J* = 5.1, 1.0 Hz, 1H)*, 6.65 (dd, *J* = 5.1, 3.6 Hz, 1H)*, 4.26-4.14 (m, 2H)*, 2.85-2.80 (m, 4H)*, 1.72-1.64 (m, 4H)*, 1.50 (s, 3H), 1.46-1.38 (m, 4H)*, 1.40 (s, 3H), 1.31-1.26 (m, 8H),* 1.26 (s, 9H), 1.13 (s, 9H), 1.068 (t, *J* = 1.1 Hz, 3H), 0.91-0.88 (m, 6H)*. Minor isomer peaks where distinguishable ^{1}H NMR (500 MHz, C_6D_6) δ 8.79 (d, *J* = 1.7 Hz), 8.25-8.23 (m), 7.65 (d, *J* = 7.9 Hz), 7.35 (d, *J* = 2.1 Hz), 7.08 (d, *J* = 2.0 Hz), 1.48 (s), 1.42 (s), 1.20 (s),

1.19 (s), 1.07 (t, J = 1.1 Hz). UV-vis (cyclohexane) λ_{max} (ε_{max}, L $mol^{-1}cm^{-1}$) nm, 247 (45200), 427 (55700).

2,7-Di-*tert*-butyl-10-carboethoxy-*trans*-12c,12d-dimethyl-5-(2-5,2':5',2"-terthienyl)-12c,12d-dihydrobenzo[e]pyrene (65) and 4-terthienyl isomer

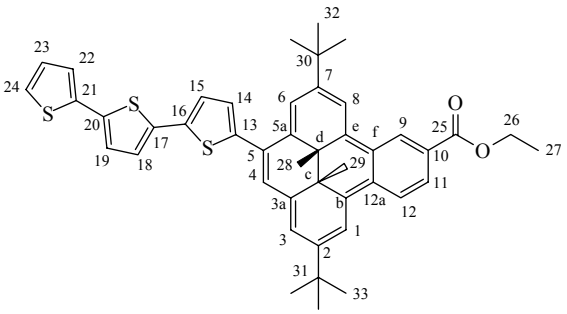

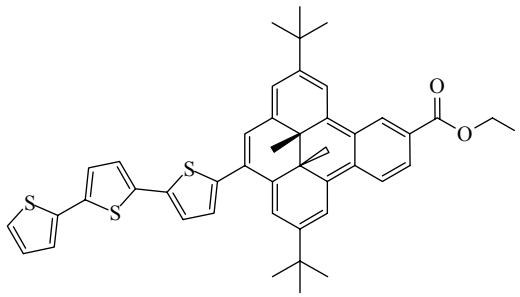

Major Isomer Minor Isomer

From **61** (438 mg, 0.73 mmol), $Pd_2(dba)_3$ (33 mg, 0.036 mmol), dppf (32mg, 0.058 mmol) and an excess of 2-tributylstannyl-5,2':5',2"-terthiophene **108** the same reaction conditions were used as above for **66**. The product was purified by chromatography on silica gel (deactivated with 5% H_2O) using 20:1 hexanes:dichloromethane to elute the excess terthiophene followed by 20:1 hexanes:ethyl acetate and finally 10:1 hexanes:ethyl acetate to elute the product (400mg, 0.56 mmol, 77%) as a reddish brown solid which was a ~3:1 mixture of isomers. The product could be further purified by recrystallization from ACN to give red crystals, mp 149-150^{o}C. The major isomer is assigned. * Indicates when the major isomer peaks are indistinguishable from the minor isomer. ^{1}H NMR (500 MHz, C_6D_6) δ 10.00 (d, J = 1.6 Hz, 1H, H-9), 8.82 (d, J = 8.7 Hz, 1H, H-12), 8.70 (d, J = 1.1 Hz, 1H, H-8), 8.54 (dd, J = 8.7, 1.6 Hz, 1H, H-11), 8.49 (d, J = 1.2 Hz, 1H, H-1), 8.47 (d, J = 1.2 Hz, 1H, H-6), 7.56

(d, J = 0.9 Hz, 1H, H-4), 7.52 (s, 1H, H-3), 7.24 (d, J = 3.7 Hz, 1H, H-14), 7.13 (d, J = 3.6 Hz, 1H, H-15), 7.01-6.98 (m, 2H, H-24,18)*, 6.88 (d, J = 6.7 Hz, 1H, H-19), 6.72 (dd, J = 5.1, 1.1 Hz, 1H, H-22), 6.658 (dd, J = 5.1, 3.5 Hz, 1H, H-23), 4.35-4.26 (m, 2H, H-26)*, 1.44 (s, 9H, H-33), 1.35 (s, 9H, H-32), 1.16 (t, J = 7.2 Hz, 3H, H-27)*, -1.23 (s, 3H, H-28), -1.26 (s, 3H, H-29). Distinguishable Minor Isomer Peaks. ^{1}H NMR (500 MHz, C_6D_6), δ 9.99 (d, J = 1.7 Hz), 8.84 (d, J = 8.7 Hz), 8.66 (d, J = 1.1 Hz), 8.52-8.51 (m), 7.54 (d, J = 0.9 Hz), 7.50 (t, J = 1.0 Hz), 7.25 (d, J = 3.7 Hz), 7.14 (d, J = 3.5 Hz), 6.89 (d, J = 3.7 Hz), 6.73 (dd, J = 5.1, 1.1 Hz), 6.660 (dd, J = 5.2, 3.6 Hz), 1.42 (s), 1.38 (s), -1.225 (s), -1.25 (s). Major isomer peaks are assigned where identifiable. ^{13}C NMR (125.7 MHz, C_6D_6) δ 167.10 (C-25), 147.30 (C-2), 146.54, 146.48, 145.76 (C-7), 143.63 (C-13), 139.28, 138.49 (C-3a), 137.88 (C-21), 137.78, 137.69 (C-16), 137.20 (C-17), 137.18, 136.98, 136.94 (C-20), 136.48 (C-12e), 136.07 (C-5a), 135.81, 135.76, 135.29, 135.13 (C-12b), 133.31, 133.06 (C-12a), 129.78 (C-12f), 128.50-128.30 (C-23, C-14), 128.00 (C-9), 127.88, 127.67, 126.70 (C-11), 126.62, 125.99 (C-5), 125.97 (C-4), 125.70, 125.40, 125.34 (C-12), 125.02 (C-22), 124.94, 124.91 (C-24 or 18), 124.74 (C-15), 124.47 (C-18 or 24), 121.94 (C-3), 121.23, 119.98 (C-1), 119.79, 119.07 (C-6), 118.74 (C-8), 61.48 (C-26), 37.33 (C-12d), 37.23, 36.31, 36.30 (C-30), 36.05, 35.92 (C-31), 35.88 (C-12c), 35.87, 35.32, 31.09, 31.07 (C-33), 30.96 (C-32), 30.93, 18.52 (C-28 or 29), 18.49, 18.41, 18.39 (C-29 or 28), 14.82 (C-27), 14.68. IR (NaCl, Thin film) ν 3066, 2963, 2921, 2897, 2867, 1715, 1604, 1463, 1445, 1365, 1251, 113, 1026, 874, 836, 795, 767, 740, 694 cm^{-1}. UV-vis (cyclohexane) λ_{max} (ε_{max}, L mol^{-1}cm^{-1}) nm, 251 (2100), 319 sh (22600), 420 (49300), 524 (7800), 645 (1000). EI MS, *m/z* 712 (M^+), 697 (M^+-CH_3), 682 (M^+-2 CH_3), 667 (M^+-OEt), 641 (M^+-CH_3,-*t*-butyl). HRMS calc'd for

$C_{45}H_{44}O_2S_3$ 712.2503, found 712.2527. Anal. Calc'd for $C_{45}H_{44}O_2S_3$: C, 75.80; H, 6.33. Found: C, 75.51; H, 6.54.

Open CPD form. Procedure: see (B), p 165. UV-vis (cyclohexane) λ_{max} (ε_{max}, L mol^{-1}cm^{-1}) nm, 258 (41700), 365 (20700), 419 (29300).

2,7-Di-*tert*-butyl-10-carboethoxy-*trans*-12c,12d-dimethyl-4,5-di-(2-5,2':5',2"-terthienyl)-12c,12d-dihydrobenzo[e]pyrene (67)

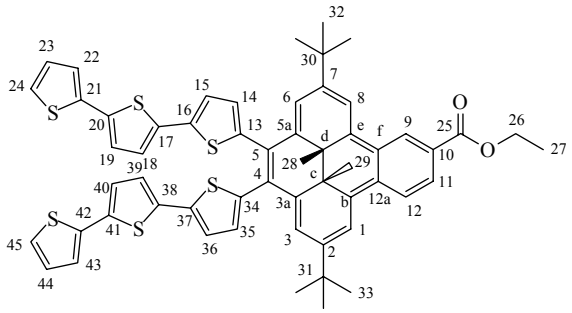

2-Tributylstannyl-5,2':5',2"-terthiophene **108** (615 mg, 1.14 mmol) was added to a solution of the dibromide **63** (263 mg, 0.388 mmol), $Pd_2(dba)_3$ (17 mg, 0.018 mmol) and dppf (0.03 mmol) in 6 mL dry THF and the reaction mixture was heated to reflux for 56 hours. It was cooled and an additional portion of $Pd_2(dba)_3$ (10 mg, 0.011mmol) was added and the reaction mixture was heated to reflux for a further 24 hours. It was then cooled and aq.KF (10 mL) was added and the reaction mixture stirred for 30 minutes. The product was filtered through Celite washing with THF and then extracted between hexanes and H_2O (3x). The organic layer was dried with $MgSO_4$, filtered through Celite and the solvent was evaporated to give a reddish brown solid. The product was purified by chromatography on silica gel (deactivated with 5% H_2O) using 20:1 hexanes:dichloromethane to remove the excess terthiophene, and then 20:1 hexanes:ethyl

acetate to elute the product as a red brown solid (250 mg, 0.261 mmol, 67%). The product could be purified further by recrystallization from acetonitrile, mp 167-169 ^{o}C. ^{1}H NMR (500 MHz, C_6D_6) δ 9.99 (d, *J* = 1.6Hz, 1H, H-9), 8.82 (d, *J* = 8.9 Hz, 1H, H-12), 8.69 (d, *J* = 1.2 Hz, 1H, H-8), 8.55 (dd, *J* = 8.6,1.7 Hz), 8.52 (d, *J* = 1.3 Hz, 1H, H-1), 8.10 (d, *J* = 1.3 Hz, 1H, H-3), 8.07 (d, *J* = 1.2 Hz, 1H, H-6), 6.98 (dd, *J* = 3.6,2.4 Hz, 2H, H-15, 36), 6.90-6.88 (m, 4H, H-14, 22, 35, 43), 6.80 (dd, *J* = 3.7, 1.8 Hz, 2H, H-18, 39), 6.73 (dd, *J* = 3.7, 1.7 Hz, 2H, H-19, 40), 6.67-6.66 (m, 2H, H-24, 45), 6.61-6.60 (m, 2H, H-23, 44), 4.35-4.20 (m, 2H, H-26), 1.36 (s, 9H, H-33), 1.29 (s, 9H, H-32), 1.16 (t, *J* = 7.2 Hz, 3H, H-27), -0.987 (s, 6H, H-28, 29). ^{13}C NMR (125.7 MHz, C_6D_6) δ 167.03 (C-25), 147.74 (C-2), 147.01 (C-7), 140.90 (C-13 or C-34), 140.88 (C-34 or C-13), 139.00 (C-5a), 138.75 (C-16 or 37), 138.72 (C-37 or 16), 138.20 (C-3a), 137.90 (C-21,42), 137.11 (C-17 or 38), 137.08 (C-38 or 17), 136.72 (C-20 or 41), 136.70 (C-41 or 20), 136.49 (C-12e), 135.81 (C-12b), 133.18 (C-12a), 130.74 (C-14 or 35), 130.71 (C-35 or 14), 129.68 (12f), 128.38 (23, 44), 127.78 (C-4), 127.15 (C-5), 127.01 (C-11), 125.61 (C-12), 125.16 (C-9), 124.83 (C-24,18 or C-39,45), 124.81 (C-39,45 or 24,18), 124.31 (C-22,43), 123.99 (C-15, 36), 120.61 (C-3), 120.21 (C-1), 119.92 (C-6), 118.97 (C-8), 61.53 (C-26), 36.90 (C-12c or 12d), 36.81 (C-12d or 12c), 36.20 (C-30 or 31), 36.18 (C-31 or 30), 30.86 (C-33), 30.76 (C-32), 18.83 (C-28, 29), 14.82 (C-27). IR (NaCl, Thin film) ν 3065, 2963, 2921, 2091, 2806, 1713, 1654, 1620, 1448, 1365, 1338, 1261, 1187, 1097, 1026, 874, 793 cm^{-1}. UV-vis (cyclohexane) λ_{max} (ε_{max}, L $mol^{-1}cm^{-1}$) nm, 253 (29800), 363 sh (49200), 392 sh (60500), 411 (66800), 519 (6660), 644 (1000). LSIMS, *m/z* 959.2 (M^+), 943.2 (M^+- CH_3), 929.1 (M^+-$2CH_3$). HRMS calc'd for $C_{57}H_{50}O_2S_6$

958.2135, found 958.2124. Anal. Calc'd for $C_{57}H_{50}O_2S_6$: C,71.36; H,5.25. Found C,71.07; H,5.17.

Open CPD form. Procedure: see (A,B), p 165. ^{1}H NMR (500 MHz, C_6D_6) δ 8.82 (d, *J* = 1.9 Hz, 1H, H-9), 8.27 (dd, *J* = 8.0, 1.9 Hz, 1H, H-11), 7.68 (d, *J* = 8.0 Hz, 1H, H-12), 7.32 (d, *J* = 2.1 Hz, 1H, H-3), 7.29 (d, *J* = 2.1 Hz, 1H, H-6), 7.12 (d, *J* = 2.0 Hz, 1H, H-8), 7.00 (d, *J* = 2.1 Hz, 1H, H-1), 6.96 (dd, *J* = 3.7, 1.7 Hz, 2H), 6.90-6.88 (m, 4H), 6.78 (dd, *J* = 3.8, 2.6 Hz, 2H), 6.72 (dd, *J* = 3.7, 0.7 Hz, 2H), 6.67 (dt, *J* = 5.2, 1.0 Hz, 2H), 6.60 (ddd, *J* = 5.1, 3.6, 1.0 Hz, 2H, H-23,44), 4.30-4.12 (m, 2H, H-26), 1.65 (s, 3H, H-28), 1.63 (s, 3H, H-29), 1.17 (s, 9H, H-33), 1.11 (s, 9H, H-32), 1.07 (t, *J* = 7.1 Hz, 3H, H-27). ^{13}C NMR (125.7 MHz, C_6D_6) δ 166.51, 151.32, 150.91, 149.48, 145.36,144.85, 144.82, 141.08, 140.96, 140.44, 140.12, 139.88, 138.89, 138.87, 137.77, 137.02, 136.85, 136.61, 136.32, 131.77, 131.46, 131.44, 130.69, 130.52, 130.29, 129.28, 128.42*, 127.87, 127.01, 126.75, 125.22, 125.15, 124.98, 124.43, 124.02, 61.36, 34.64, 34.59, 31.61, 31.54, 19.88, 19.69, 14.73. *From DEPT. UV-vis (cyclohexane) λ_{max} (ε_{max}, L mol^{-1}cm^{-1}) nm, 254 (49000), 373 (54800), 425 (28600).

2,7-Di-*tert*-butyl-10-carboxy-*trans*-12c,12d-dimethyl-5-(2-3",4"-dihexyl-5,2':5',2":5",2"':5"',2""-quinquethienyl)-12c,12d-dihydrobenzo[e]pyrene (70) and the 4-quinquethienyl isomer

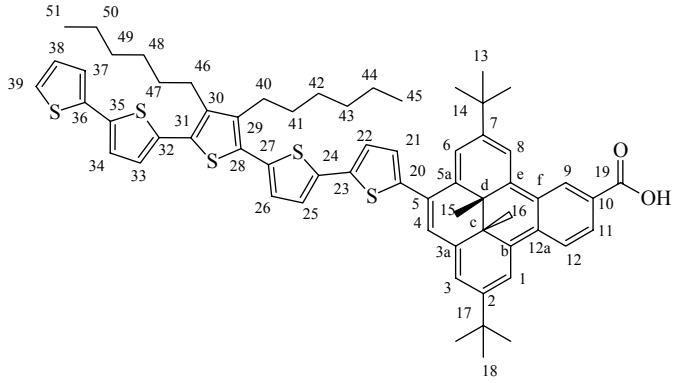

Aq. NaOH (2M, 20 mL) was added to a solution of the ester **66** (386 mg, 0.369 mmol) in hexanes (20mL) and EtOH (100mL), and the solution was heated to reflux for 12 hours. It was cooled to room temperature and then poured into diethyl ether and water and neutralized with HCl. The resulting red organic layer was washed with NaCl(aq) and then water. The organic layer was dried with $MgSO_4$ and the solvent evaporated to give the crude product (370 mg, 0.364 mmol, 98%) as a red solid. The product was pure enough to be used in subsequent steps but could be further recrystallized from hexanes, mp 129-131^{o}C. The NMR is solved for the major isomer where possible. * Indicates where major and minor isomers are indistinguishable from each other. ^{1}H NMR (500 MHz, C_6D_6) δ 10.03 (br s, 1H, H-9)*, 8.81-8.77 (m, 1H, H-12)*, 8.73 (s, 1H, H-8), 8.57-8.52 (m, 3H, H-1,6,11)*, 7.60 (s, 1H, H-4), 7.55 (s, 1H, H-3), 7.28 (dd, *J* = 3.6, 1.3 Hz, 1H, H-21)*, 7.22 (dd, *J* = 3.6, 1.3 Hz, 1H, H-22)*, 7.13 (dd, *J* = 3.7, 1.1 Hz, 1H)*, 7.10 (dd, *J* = 3.7, 1.0 Hz, 1H)*, 7.03 (dd, *J* = 3.7, 0.7 Hz, 1H)*, 7.02 (dd, *J* = 3.5, 1.0 Hz, 1H)*, 6.96 (d, *J* = 3.7 Hz, 1H)*, 6.73 (dd, *J* = 5.1, 1.1 Hz, 1H, H-37 or 39)*, 6.66 (dd, *J* = 5.1, 3.5 Hz, 1H, H-38)*, 2.88-2.82 (m, 4H, H-40,46)*, 1.73-1.65 (m, 4H, H-41,47)*,

1.51-1.39 (m, 4H, H-42,48)*, 1.47 (s, 9H, H-18), 1.41 (s, 9H, H-13), 1.31-1.27 (m, 8H, H-43,44,49,50)*, 0.94-0.88 (m, 6H, H-45,51)*, -1.27 (s, 3H, H-15), -1.29 (s, 3H, H-16)*. Minor Isomer ^{1}H NMR (500 MHz, C_6D_6) δ 8.69 (s), 7.57 (s), 7.53 (s), 1.46 (s), 1.44 (s), -1.26 (s). Distinguishable ^{13}C peaks from the major isomer are assigned. ^{13}C NMR (125.8 MHz, C_6D_6) δ 173.57 (C-19), 147.43 (C-7), 146.62, 146.54, 145.78 (C-2), 143.63 (C-20), 141.17, 139.35, 138.43 (C-3a), 138.29, 138.25, 138.12, 137.86, 137.78, 137.75, 136.35 (C-12e), 136.14 (C-5a), 135.96, 135.91, 135.89, 135.69, 135.59, 135.24, 134.97 (C-12b), 134.02, 133.77, 131.00, 130.99, 130.98, 129.63 (C-12f), 129.40, 128.98 (C-9), 128.90, 128.61 (C-21), 128.49 (C-38), 127.62, 127.46, 127.32, 127.18, 126.95 (C-11), 126.86, 126.17, 126.08 (C-4), 125.85, 125.56 (C-12), 125.42, 125.32, 125.23, 125.10, 124.90, 124.80, 124.72, 124.69, 124.49, 122.27 (C-3), 121.34, 120.46 (C-1), 120.12, 119.20 (C-6), 118.86, 37.24, 37.13 (C-12d), 36.39, 36.36, 35.96, 35.93, 35.82 (C-12c), 32.23 (C-43 or 44 or 49 or 50), 32.20 (C-43 or 44 or 49 or 50), 31.49 (C-41 or 47), 31.46 (C-47 or 41), 31.15, 31.11 (C-13 or 18), 31.06 (C-18 or 13), 31.03, 30.38 (C-42 or 48), 30.33 (C-48 or 42), 29.07 (C-40 or 46), 29.03 (C-46 or 40), 23.39 (C-43 or 44 or 49 or 50), 23.37 (C-43 or 44 or 49 or 50), 18.51 (C-15 or 16), 18.48, 18.40, 18.37 (C-16 or 15), 14.69 (C-45 or 51), 14.66 (C-51 or 45). IR (NaCl, thin film) ν 3064, 2959, 2925, 2867, 1686, 1604, 1462, 1256, 793 cm^{-1}. UV-vis (cyclohexane) λ_{max} (ε_{max}, L mol^{-1}cm^{-1}) nm, 250 (30100), 322 sh (26100), 355 sh (32600), 425 (55200), 531 (77300), 647 (1250). LSIMS, *m/z*, 1017.4 (M^+), 1001.3, 987.3, 945.3. HRMS calc'd for $^{12}C_{63}{}^{13}CH_{68}O_2S_5$ 1017.3822, found 1017.3850. Anal. Calc'd for $C_{63}H_{68}O_2S_5$: C, 74.36; H, 6.74. Found: C, 74.09; H, 6.76.

Open CPD form. Procedure: see (B), p 165. UV-vis (cyclohexane) λ_{max} (ε_{max}, L $mol^{-1}cm^{-1}$) nm, 247 (41700), 426 (43500).

2,7-Di-*tert*-butyl-10-carboxy-trans-12c,12d-dimethyl-5-(2-5,2':5',2"-terthienyl)-12c,12d-dihydrobenzo[e]pyrene (69) and the 4-terthienyl isomer

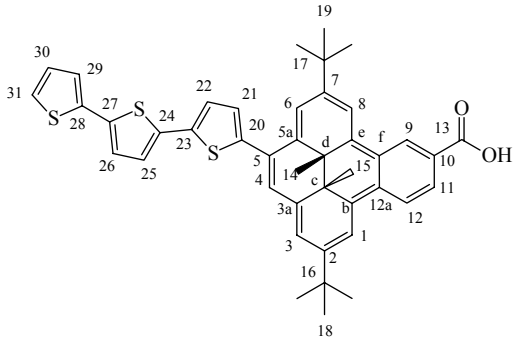

From **65** (400 mg, 0.56 mmol) and aq.NaOH (2M, 20mL) the same conditions were used as for **70**. The desired product **69** (300mg, 0.44mmol, 78%) was obtained as a red solid. The product was pure enough to be used in subsequent steps but could be further purified by recrystallization from ethanol to give a red brown powder, mp 184-187°C. The major isomer peaks were assigned where possible and the minor isomer peaks were noted when distinguishable from the major isomer peaks. ^{1}H NMR (500 MHz, CD_2Cl_2) δ 9.67 (brs), 9.65 (brs, 1H, H-9), 8.95 (d, *J* = 9 Hz, 1H, H-12), 8.57 (brs, 1H, H-1), 8.54 (brs, 1H, H-8), 8.32 (brd, *J* = 7 Hz, 1H, H-11), 8.25, 8.23 (s, 1H, H-6), 7.58 (brs, 1H, H-4), 7.50 (brs, 1H, H-3), 7.32 (brd, *J* = 3 Hz, 2H, H-25,26), 7.28 (dd, *J* = 5,1 Hz, 1H, H-29), 7.20 (brd, *J* = 3Hz, 1H, H-21 or 22), 7.16 (d, *J* = 3 Hz, 1H, H-22 or 21), 7.07 (dd, *J* = 5,3 Hz, 1H, H-30), 1.9 (brs, 1H, H-O**H**), 1.57 (s), 1.56 (s, 9H, H-18 or 19), 1.55 (s, 9H, H-19 or 18), 1.54 (s), -1.53 (s, 3H, H-14 or 15), -1.548 (s, 3H, H-15 or 14), -1.552 (s). ^{13}C NMR (125.8 MHz, C_6D_6) δ 171.65, 137.63, 136.98, 136.61, 133.52,

129.11, 128.56, 128.34, 128.26, 128.15, 126.46, 126.26, 125.52, 125.35, 125.18, 125.05, 124.64, 124.58, 124.33, 36.00, 32.22, 32.19, 32.16, 30.96, 29.40, 18.09. Due to poor solubility not all the ^{13}C peaks were observed. IR (NaCl, thin film) ν 3066, 2963, 2917, 2897, 2867, 1685, 1604, 1415, 1363, 1255, 1058, 793, 691 cm^{-1}. UV-vis (cyclohexane) λ_{max} (ε_{max}, L $mol^{-1}cm^{-1}$) nm, 249 (19900), 328 (21800), 421 (41600), 531 (5790), 645 (1020). LSIMS, *m/z* 684 (M^+), 669 (M^+-CH_3), 654 (M^+-$2CH_3$), 639 (M^+-COOH), 613 (M^+-CH_3, - *t*-butyl), 599 (M^+-$2CH_3$ - *t*-butyl), 557 (M^+-$2CH_3$ - 2 *t*-butyl). HRMS calc'd for (M^+) $C_{43}H_{40}O_2S_3$ 684.2190, found 684.2175.

2,7-Di-*tert*-butyl-10-(N-methoxy-N-methylcarbamoyl)-*trans*-12c,12d-dimethyl-5-(2-3",4"-dihexyl-5,2':5',2":5",2"':5"',2"":-quinquethienyl)-12c,12d-dihydrobenzo[e]pyrene (74) and the 4-quinquethienyl isomer

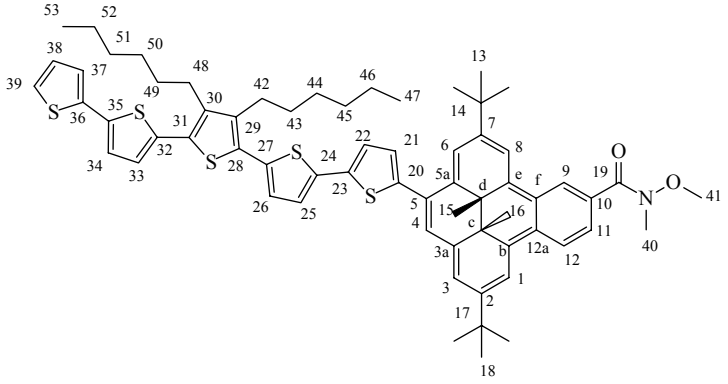

N,N'-Diisopropylcarbodiimide was added to a stirred solution of the acid **70** (412 mg, 0.39 mmol), N,O-dimethylhyrdoxylamine hydrochloride (139 mg, 1.42 mmol), pyridine (0.13 mL, 1.6 mmol), 4-dimethylaminopyridine (10 mg, 0.08 mmol), and NaOH (2M, 5 drops) in dichloromethane (60 mL) at 0°C. The mixture then stirred for 4 hours warming to room temperature. The solution was filtered through Celite, washing with dichloromethane. The solvent was evaporated and the product purified by

chromatography on silica gel (deactivated with 5% H_2O) using 6:1 hexanes:ethyl acetate until the early red spot (anhydride) had eluted, then 4:1 hexanes:ethyl acetate to elute the desired product (0.316g, 0.30 mmol, 77%) as a red solid. The product was pure enough to be used in the subsequent step, but could be further purified by recrystallization from pentane to give the product **74** as a dark red powder, mp 84-85 ^{o}C. The major isomer is assigned. * Indicates when major isomer peaks are indistinguishable from the minor isomer. ^{1}H NMR (500 MHz, C_6D_6) δ 9.72 (d, *J* = 1.6 Hz, 1H, H-9), 8.78 (d, *J* = 8.7 Hz, 1H, H-12), 8.66 (s, 1H, H-8), 8.49 (d, *J* = 1.1 Hz, 1H, H-1), 8.460 (s, 1H, H-6), 8.20 (dd, *J* = 8.6, 1.6 Hz, 1H, H-11), 7.55 (d, *J* = 0.8 Hz, 1H, H-4), 7.49 (s, 1H, H-3), 7.25 (d, *J* = 3.7 Hz, 1H, H-21), 7.19 (d, *J* = 3.7 Hz, 1H), 7.11 (d, *J* = 3.8 Hz, 1H), 7.08 (d, *J* = 3.8 Hz, 1H), 7.03-7.01 (m, 2H)*, 6.94 (d, *J* = 3.8 Hz, 1H), 6.72 (dd, *J* = 5.1, 1.2 Hz, 1H, H-37 or 39)*, 6.65 (dd, *J* = 5.1, 3.6 Hz, 1H, H-38)*, 3.178 (s, 1H, H-40), 3.130 (s, 1H, H-41), 2.88-2.81 (m, 4H, H-42,48)*, 1.72-1.66 (m, 4H, H-43,49)*, 1.47-1.39 (m, 4H, H-44,50)*, 1.46 (s, 9H, H-18), 1.35 (s, 9H, H-13), 1.30-1.24 (m, 8H, H-45,46,51,52)*, 0.92-0.88 (m, 6H, H-47,53)*, -1.18 (s, 3H, H-15), -1.21 (s, 3H, H-16)*. Minor isomer. ^{1}H NMR (500 MHz, C_6D_6) δ 9.71 (d, *J* = 1.6 Hz), 8.79 (d, *J* = 8.7 Hz), 8.61 (d, *J* = 1.0 Hz), 8.50 (s), 8.462 (s), 8.19 (dd, *J* = 8.6, 1.6 Hz), 7.52 (d, *J* = 0.8 Hz), 7.46 (s), 7.26 (d, *J* = 3.7 Hz), 7.20 (d, *J* = 3.7 Hz), 7.12 (d, *J* = 3.8 Hz), 7.09 (d, *J* = 3.8 Hz), 6.95 (d, *J* = 3.7 Hz), 3.18 (s), 3.133 (s), 1.44 (s), 1.37 (s), -1.19 (s). Major isomer peaks are assigned where possible. ^{13}C NMR (125.8 MHz, C_6D_6) δ 170.56, 170.54 (C-19), 147.12 (C-7), 146.55, 146.28, 145.74 (C-2), 143.81 (C-20), 141.18 (C-29 or 30), 141.12 (C-30 or 29), 139.17, 138.62 (C-3a), 138.38, 138.11, 137.78, 137.64, 137.57, 136.62 (C-12e), 136.04, 136.01, 135.90, 135.84, 135.81, 135.45, 135.37 (C-12b), 132.74

(C-10), 131.75, 131.53 (C-12a), 131.05, 130.93, 129.72 (C-12f), 129.49, 128.52, 128.48 (C-38), 127.88, 127.63, 127.47, 126.81 (C-9), 126.56, 126.53, 126.47 (C-11), 126.32, 125.90, 125.70 (C-4), 125.30, 125.09, 124.91, 124.78 (C-12), 124.65, 124.63, 124.50, 121.53 (C-3), 121.11, 119.34, 119.24 (C-1), 118.93 (C-6), 118.51 (C-8), 60.94 (C-41), 37.46 (C-12d), 37.37, 36.33, 36.29 (C-14), 36.15, 36.06 (C-12c), 35.89 (C-17), 35.85, 33.69 (C-40), 32.22 (C-45 or 46 or 51 or 52), 32.19 (C-45 or 46 or 51 or 52), 31.49 (C-43 or 49), 31.46 (C-49 or 43), 31.09, 31.05 (C-18), 31.00 (C-13), 30.97, 30.36 (C-44 or 50), 30.32 (C-50 or 44), 29.06 (C-42 or 48), 29.02 (C-48 or 42), 23.37 (C-45 or 46 or 51 or 52), 23.35 (C-45 or 46 or 51 or 52), 18.60 (C-15 or 16), 18.49 (C-16 or 15), 14.66 (C-47 or 53), 14.64 (C-53 or 47). IR (NaCl thin film) ν 3065, 2959, 2927, 2867, 1642, 1463, 1363, 1262, 794, 737 cm^{-1}. UV-vis (cyclohexane) λ_{max} (ε_{max}, L $mol^{-1}cm^{-1}$) nm, 251 (30800), 323 sh (28800), 359 sh (36000), 423 (64100), 524 (9210), 647 sh (897). LSIMS, *m/z*, 1060 (M^+), 1044, 1030, 988, 957. HRMS calc'd for (M+H) $C_{65}H_{74}NO_2S_5$ 1060.4323, found 1060.4312. Anal. Calc'd for $C_{65}H_{73}NO_2S_5$: C,73.61; H, 6.94; N,1.32. Found: C, 73.57; H, 7.13; N, 1.37.

Open CPD form. Procedure: see (B), p 165. UV-vis (cyclohexane) λ_{max} (ε_{max}, L $mol^{-1}cm^{-1}$) nm, 251 (43900), 351 sh (27500), 425 (51800).

2,7-Di-*tert*-butyl-10-(N-methoxy-N-methylcarbamoyl)-*trans*-12c,12d-dimethyl-5-(2-5,2':5',2"-terthienyl)-12c,12d-dihydrobenzo[e]pyrene (73) and the 4-terthienyl isomer

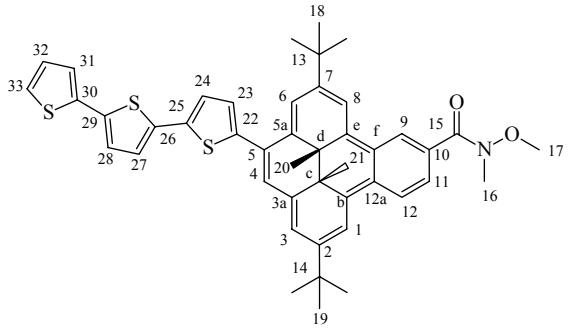

From **69** (370mg, 0.54 mmol), 1,3-diisopropylcarbodiimide (0.335 mL, 2.7 mmol), N,O-Dimethylhydroxylamine hydrochloride (105.4mg, 1.1 mmol), pyridine (0.131 mL, 1.6 mmol), 4-dimethylaminopyridine (5mg, 0.04 mmol) and 2M NaOH (5 drops) the same conditions were used as for **74**. The product was purified by chromatography on silica gel (deactivated with 5% H_2O) using 3:2 hexanes:ethyl acetate as eluent to give the product as a dark red solid (349 mg, 0.48 mmol, 89%), mp171-172^{o}C. The product was a ~ 3:1 mixture of isomers. The major isomer was assigned. *Indicates where major isomer peaks are indistinguishable from the minor isomer peaks. ^{1}H NMR (500 MHz, C_6D_6) δ 9.72 (d, *J* = 1.7 Hz, 1H, H-9), 8.78 (d, *J* = 8.7 Hz, 1H, H-12), 8.65 (d, *J* = 1.1 Hz, 1H, H-8), 8.46 (d, *J* = 1.3 Hz, 1H, H-1), 8.45 (d, *J* = 1.2 Hz, 1H, H-6), 8.19 (dd, *J* = 8.6, 1.6 Hz, 1H, H-11), 7.54 (d, *J* = 0.9 Hz, 1H, H-4), 7.49 (s, 1H, H-3), 7.23 (d, *J* = 3.7 Hz, 1H, H-23), 7.12 (d, *J* = 3.7, 1H, H-24), 6.99 (m, 1H, H-33)*, 6.98 (d, *J* = 3.7 Hz, 1H, H-27), 6.88 (d, *J* = 3.7 Hz, 1H, H-28), 6.73 (dd, *J* = 1.2 Hz, 5.1 Hz, 1H, H-31), 6.66 (dd, *J* = 3.6, 5.1 Hz, 1H, H-32), 3.177 (s, 3H, H-17), 3.129 (s, 3H, H-16), 1.45 (s, 9H, H-18), 1.34 (s, 9H, H-19), -1.18 (s, 3H, H-21), -1.21 (s, 3H, H- 20)*. Minor isomer peaks. ^{1}H NMR (500 MHz, C_6D_6) δ 9.71 (d, *J* = 1.8 Hz), 8.79 (d, *J* = 8.6 Hz),

8.61 (d, J = 1.3 Hz), 8.50 (d, J = 1.0 Hz), 8.48 (d, J = 1.1 Hz), 8.18 (dd, J = 8.6,1,6 Hz), 7.52 (d, J = 0.9 Hz), 7.47 (s), 7.25 (d, J = 3.7 Hz), 7.14 (d, J = 3.7 Hz), 6.89 (d, J = 3.7 Hz), 6.72 (d, J = 5.1 Hz), 6.67 (dd, J = 3.6, 5.1 Hz), 3.18 (s), 3.13 (s), 1.43 (s), 1.37 (s), -1.183 (s). Where possible the major isomer ^{13}C peaks are assigned. ^{13}C NMR (125.8 MHz, C_6D_6) δ 170.55 (C-15), 147.13 (C-7), 146.54, 146.29, 145.75 (C-2), 143.73 (C-22), 139.17, 138.62 (C-3a), 137.90 (C-30), 137.66, 137.59 (C-25), 137.25 (C-26), 136.92, 136.89 (C-29), 136.61 (C-12e), 136.03, 135.99 (C-5a), 135.91, 135.43, 135.37 (C-12b), 132.74 (C-10), 131.75, 131.52 (C-12a), 129.72 (C-12f), 129.49, 128.90, 128.6-128.4 (C-32,23), 127.88, 126.81 (C-9), 126.56 (C-11), 126.48, 126.32, 125.90 (C-5), 125.70 (C-4), 125.33 (C-28), 125.29, 125.10, 125.00 (C-31 or 33), 124.90, 124.88 (C-27 and/or 28), 124.79 (C-12 or 24), 124.73 (C-24 or 12), 124.45 (C-33 or 31), 121.51 (C-3), 121.09, 119.32, 119.25 (C-1), 118.91 (C-6), 118.53 (C-8), 60.94 (C-17), 37.46 (C-12d), 37.36, 36.32, 36.28 (C-14), 36.16, 36.06 (C-12c), 35.89 (C-13), 35.84, 33.69 (C-16), 31.07 (C-18), 31.05, 30.98, 30.97 (C-19), 18.60 (C-21 or 20), 18.49 (C-20 or 21). IR (NaCl, Thin film) ν 3064, 2962, 2924, 2866, 1641, 1462, 1364, 1260, 1213, 873, 795, 737, 694 cm^{-1}. UV-vis (cyclohexane) λ_{max} (ε_{max}, L $mol^{-1}cm^{-1}$) nm, 252 (20400), 352 (24000), 420 (47600), 521 (7600). EIMS, *m/z* 727 (M^+), 712 (M^+-CH_3), 697 (M^+-$2CH_3$), 682 (M^+-$3CH_3$), 667 (M^+-N(OMe)CH_3), 656 (M^+ - *t*-butyl, -CH_3), 626, 596, 569. HRMS calc'd for $C_{45}H_{45}NO_2S_3$ 727.2612, found 727.2609. Anal. Calc'd for: $C_{45}H_{45}NO_2S_3$: C, 74.24; H, 6.23. Found C, 73.66; H, 6.21.

Open CPD form. Procedure: see (B), p 165. UV-vis (cyclohexane) λ_{max} (ε_{max}, L $mol^{-1}cm^{-1}$) nm, 255 (39000), 372 (21000), 419 (31000).

2,7-Di-*t*-butyl-10-[2-(3",4"-dihexyl-5,2':5',2":5",2"':5"',2""-quinquethienyl)carbonyl]-*trans*-12c,12d-dimethyl-5-(2-3",4"-dihexyl-5,2':5',2":5",2"':5"',2""-quinquethienyl)-12c,12d-dihydrobenzo[e]pyrene (77) and the 4-quinquethienyl isomer

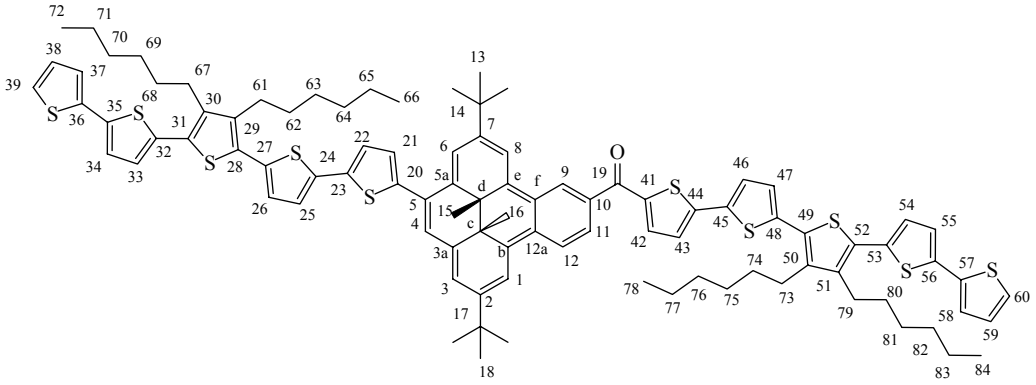

Major Isomer

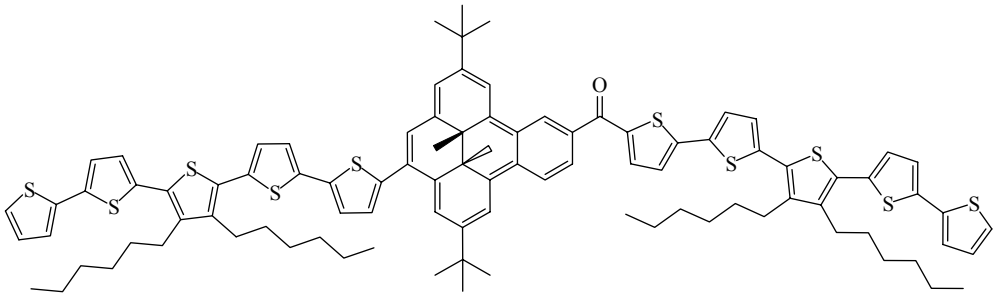

Minor Isomer

n-Butyl lithium (1.0 mL, 2.5M) was added to a bright yellow solution of the quinquethiophene **102** (1.484 g, 2.55 mmol) in dry THF (60mL) at -78^{o}C. The solution changed from yellow to a reddish orange. After the solution had warmed to -30^{o}C over 30 minutes it was re-cooled to -78^{o}C and the Weinreb amide **74** (337mg, 0.318 mmol) was added in dry THF (5mL) giving a dark red solution. The solution warmed to ~22^{o}C while stirring for 2 hours. It was quenched with dilute HCl and extracted between hexanes and water (3x). It was dried with $MgSO_4$ and the solvent evaporated to give a dark red brown solid. The product was purified by chromatography on silica gel

(deactivated with 5% H_2O) using 10:1 hexanes:dichloromethane to elute the excess quinquethiophene **102**, and then 10:1 hexanes:ethyl acetate to elute the product as a dark red black powder (301 mg, 0.190 mmol, 60%). 3:1 Hexanes:ethyl acetate could then be used to recover any un-reacted Weinreb amide starting material **74**. The product could be further purified by recrystallization by adding methanol to a diethyl ether solution to give a dark red black powder, mp 91-94^oC. The product was a ~3:1 mixture of isomers. The major isomer was assigned. * Indicates when major and minor isomer peaks were indistinguishable. ^1H NMR (500 MHz, C_6D_6) δ 9.77 (d, *J* = 1.9 Hz, 1H, H-9)*, 8.81 (d, *J* = 8.9 Hz, 1H, H-12), 8.69 (s, 1H, H-8), 8.54 (s, 1H, H-1), 8.51 (s, 1H, H-6), 8.23-8.20 (m, 1H, H-11)*, 7.59-7.51 (m, 3H, H-3,4,42)*, 7.27 (d, *J* = 3.7Hz, 1H), 7.21 (d, *J* = 3.7 Hz, 1H), 7.13 (d, *J* = 3.7 Hz, 1H), 7.09 (d, *J* = 3.7 Hz, 1H), 7.04-6.98 (m, 6H)*, 6.97-6.94 (m, 3H)*, 6.72 (d, *J* = 5.1 Hz, 2H)*, 6.65 (dd, *J* = 5.1, 3.6 Hz, 2H, H-59,38), 2.88-2.80 (m, 8H, H-61,67,73,79)*, 1.76-1.63 (m, 8H, H-62,68,74,80)*, 1.48 (s, 9H, H-18), 1.44-1.40 (m, 8H, H-63,69,75,81)*, 1.38 (s, 9H, H-13), 1.32-1.26 (m, 16H, H-64,65,70,71,76,77,82,83)*, 0.92-0.88 (m, 12H, H-66,72,78,84)*, -1.19 (s, 3H, H-15)*, -1.21 (s, 3H, H-16). Minor ^1H isomer peaks where distinguishable from the major isomer peaks. ^1H NMR (500 MHz, C_6D_6) δ 8.82 (m), 8.64 (s), 8.59 (s), 8.55 (s), 7.29 (d, *J* = 3.7 Hz), 7.22 (d, *J* = 3.6 Hz), 7.14 (d, *J* = 3.8 Hz), 7.10 (d, *J* = 3.3 Hz), 6.652 (dd, *J* = 5.1, 3.5 Hz), 1.47 (s), 1.40 (s), 1.39 (s), -1.22 (s). The major ^{13}C isomer peaks are assigned where possible. ^{13}C NMR (125.8 MHz, C_6D_6) δ 187.04 (C-19), 147.29 (C-7), 146.61, 146.48 (C-2), 146.09, 145.95, 145.85, 143.66, 143.38, 143.23, 141.77, 141.62, 141.26, 141.18, 141.15, 139.30, 138.55, 138.34, 138.30, 138.12, 138.11, 137.82, 137.78, 137.72, 137.67, 137.00, 136.73, 136.51, 136.19, 136.16, 136.10, 135.93, 135.89, 135.83, 135.63, 135.35,

135.19, 132.82, 132.57, 131.51, 131.01, 130.97, 130.46, 129.85, 129.63, 128.90, 128.68, 128.58, 128.50, 128.49, 128.39, 128.30, 128.20, 127.87, 127.76, 127.62, 127.60, 127.57, 127.47, 127.36 (C-9), 127.01, 126.94 (C-11), 126.72, 126.58, 126.13, 126.05 (C-12), 125.69, 125.46, 125.40, 125.32, 125.20, 125.10, 124.91, 124.80, 124.71, 124.69, 124.62, 124.57, 124.50, 122.04, 121.38, 120.00 (C-1), 119.89, 119.24 (C-6), 118.89 (C-8), 37.38 (C-12d), 37.27, 36.38, 36.36 (C-14), 36.09, 35.97 (C-12c), 35.94 (C-17), 35.92, 32.23 (C-64 or 65 or 70 or 71 or 76 or 77 or 82 or 83), 32.19 (C-64 or 65 or 70 or 71 or 76 or 77 or 82 or 83), 31.49 (C-62 or 68 or 74 or 81), 31.46 (C-62 or 68 or 74 or 81), 31.44 (C-62 or 68 or 74 or 81), 31.37 (C-62 or 68 or 74 or 81), 31.14, 31.11 (C-18), 31.05 (C-13), 31.02, 30.37 (C-63 or 69 or 75 or 81), 30.32 (C-63 or 69 or 75 or 81), 29.06 (C-61 or 67 or 73 or 79), 28.99 (C-61 or 67 or 73 or 79), 23.38 (C-64 or 65 or 70 or 71 or 76 or 77 or 82 or 83), 23.36 C-64 or 65 or 70 or 71 or 76 or 77 or 82 or 83), 18.63 (C-16), 18.60, 18.52, 18.48 (C-15), 14.67 (C-66 or 72 or 28 or 84), 14.64 (C-66 or 72 or 28 or 84). IR (NaCl, Thin film) ν 3066, 2954, 2926, 2857, 1622, 1436, 1273, 1054, 792 cm^{-1}. UV-vis (cyclohexane) λ_{max} (ε_{max}, L $mol^{-1}cm^{-1}$) nm, 248 (43900), 337 sh (44200), 433 (99500), 655 (1850). LSIMS, *m/z*, 1580 (M^+), 1565 (M^+-CH_3), 1550 (M^+-$2CH_3$). Anal. Calc'd for $C_{95}H_{102}OS_{10}$: C, 72.19; H, 6.50. Found: C, 71.80; H, 6.71.

Open CPD form. Procedure: see (A,B), p 165. * Indicates when major and minor isomer peaks were indistinguishable. ^{1}H NMR (500 MHz, C_6D_6) δ 8.53 (brs, 1H)*, 7.91-7.89 (m, 1H)*, 7.72 (d, J = 7.9 Hz, 1H), 7.43 (d, J = 3.9 Hz, 1H)*, 7.35 (s, 1H), 7.21-7.19 (m, 1H)*, 7.18-7.17 (m, 1H)*, 7.11-7.10 (m, 1H)*, 7.06-6.94 (m, 13H)*, 6.87 (d, J = 4.0 Hz, 1H), 6.72 (d, J = 5.0 Hz, 2H)*, 6.66-6.64 (m, 2H)*, 2.86-2.80 (m, 8H)*, 1.76-1.61 (m, 8H)*, 1.56 (s, 3H)*, 1.46 (s, 3H), 1.45-1.38 (m, 8H)*, 1.30 (s, 9H), 1.29-1.26 (m,

16H)*, 1.16 (s, 9H), 0.94-0.86 (s, 12H)*. Minor Isomer where distinguishable from the major isomer. ^{1}H NMR (500 MHz, C_6D_6) δ 7.69 (d, J = 7.8 Hz, 1H), 7.39 (s, 1H), 6.88 (d, J = 4.0 Hz, 1H),1.47 (s, 3H), 1.24 (s, 9H), 1.22 (s, 9H). UV-vis (cyclohexane) λ_{max} (ε_{max}, L mol^{-1}cm^{-1}) nm, 245 (56700), 431 (89200).

2,7-Di-*tert*-butyl-*trans*-12c,12d-dimethyl-5-(2-5,2':5',2"-terthienyl)-10-[(2-5,2':5',2"-terthienyl)carbonyl]-12c,12d-dihydrobenzo[e]pyrene (76) and the 4-terthienyl isomer

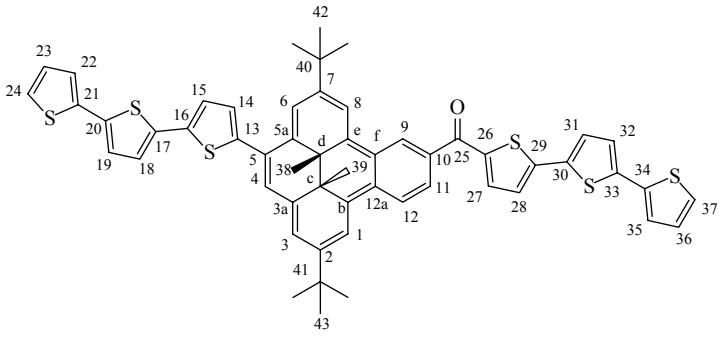

From *n*-BuLi (0.34 *u*L, 2.5 M), terthiophene (21.2 mg, 0.085 mmol), and the Weinreb amide **73** (42.5 mg, 0.058mmol), the same procedure was used as for **77**. The product was purified by chromatography on silica gel (deactivated with 5% H_2O) using 10:1 hexanes:dichloromethane to remove the excess terthiophene followed by 3:1 hexanes:dichloromethane and finally 2:1 hexanes:dichloromethane to elute the product **76**, a reddish brown powder (55 mg, 0.034 mmol, 59%) as a ~7:3 mixture of 2 isomers. A small amount of the dianion product **79** was also isolated after the product had eluted. The product **76** could be further purified by recrystallization from acetonitrile, to give the product **76** as a dark red powder, mp 164-166^{o}C. The major isomer was assigned. * Indicates when major and minor isomers are indistinguishable ^{1}H NMR (500 MHz, C_6D_6) δ 9.77 (d, *J* = 1.9Hz, 1H, H-9)*, 8.81 (d, *J* = 8.8Hz, 1H, H-12), 8.68 (d, *J* = 1.0Hz,

1H, H-8), 8.54 (d, *J* = 1.1 Hz, 1H, H-1), 8.50 (d, *J* = 1.1 Hz, 1H, H-6), 8.22 (dd, *J* = 8.5, 1.8 Hz, 1H, H-11), 7.59 (d, *J* = 0.9 Hz, 1H, H-4), 7.57 (d, *J* = 3.8 Hz, 1H, H-27), 7.56 (d, *J* = 1.1 Hz, 1H, H-3)*, 7.26 (d, *J* = 3.7 Hz, 1H, H-14), 7.15 (d, *J* = 3.7 Hz, 1H, H-15), 7.01-6.98 (m, 3H, H-22,35 and one of 19,18, 31,32)*, 6.90-6.87 (m, 3H, H-28, and two of 19,18,31,31)*, 6.80 (d, *J* = 3.7 Hz, 1H, one of H- 19,18,31,32), 6.74-6.72 (m, 2H, H-24,37)*, 6.68-6.64 (m, 2H, H-36,23)*, 1.48 (s, 9H, H-43), 1.37 (s, 9H, H-42), -1.19 (s, 3H, H-38 or 39), -1.21 (s, 3H, H-39 or 38). Minor isomer peaks. ^{1}H NMR (500 MHz, C_6D_6) δ 8.82 (d, *J* = 8.8 Hz), 8.63 (d, *J* = 1.2 Hz), 8.59 (s), 8.545 (d, *J* = 1.2 Hz), 8.21 (dd, *J* = 8.5,1.8 Hz), 7.58 (s), 7.52 (s), 7.27 (d, *J* = 3.7 Hz), 6.78 (d, *J* = 3.8 Hz), 1.46 (s), 1.39 (s), -1.189 (s), -1.22 (s). Major isomer peaks are assigned where possible. ^{13}C NMR (125.7 MHz, C_6D_6) δ 187.01 (C-25), 147.29 (C-7), 146.62, 146.49, 146.08, 145.86 (C-2), 143.59 (C-13), 143.12, 143.11, 139.31, 139.05, 138.56, 137.88, 137.85, 137.76, 137.37, 137.19, 137.17, 137.03, 136.99, 136.51, 136.20 (C-3a), 136.17, 136.09 (C-5a), 135.88 (C-27), 135.83, 135.71, 135.35, 135.19 (C-12b), 132.83, 132.58 (C-12a), 129.85 (C-12f), 129.62, 128.59, 128.56, 128.51, 127.35 (C-9), 127.15, 127.01, 126.73, 126.59 (C-11), 126.14 (C-5), 126.05 (C-4), 125.71, 125.65 (C-24 or 37), 125.47, 125.43, 125.38 (C-12), 125.34, 125.04 (C-37 or 24), 124.97, 124.94 (C-22 or 35), 124.76 (C-15), 124.59, 124.48 (C-35 or 22), 122.03 (C-3), 121.37, 120.01 (C-1), 119.88, 119.23 (C-6), 118.89 (C-8), 37.38 (C-12d), 37.28, 36.37, 36.35 (C-40), 36.10, 35.98 (C-12c or 41), 35.94 (C-41 or 12c), 35.91, 31.12, 31.10 (C-42 or 43), 31.02 (C-43 or 42), 31.00, 18.62 (C-38 or 39), 18.59, 18.52, 18.48 (C-39 or 38). IR (NaCl, Thin film) ν 3066, 2962, 2922, 2866, 1621, 1052, 1456, 1435, 1362, 1341, 1271, 1258, 1224, 1055, 873, 836, 793, 736, 692 cm^{-1}. UV-vis (cyclohexane) λ_{max} (ε_{max}, L mol^{-1}cm^{-1}) nm, 246 (30700), 321 (27500),

426 (69300), 526 (8400), 647 (1700). EIMS, *m/z* 914 (M^+), 900 (M^+-CH_3), 886 (M^+-$2CH_3$). HRMS calc'd for $C_{55}H_{46}OS_6$ 914.1872, found 914.1828. Anal. Calc'd for $C_{55}H_{46}OS_6$: C,72.17; H, 5.06. Found: C, 71.56; H, 5.72.

Open CPD form. Procedure: see (A,B), p 165. The NMR spectrum of the open CPD form was done in $CDCl_3$ due to the low solubility of the open CPD form in C_6D_6. * Indicates when major and minor isomers are indistinguishable. ^1H NMR (500 MHz, $CDCl_3$) δ 8.18 (d, *J* = 2.1 Hz, 1H), 7.92 (dd, *J* = 7.9, 1.8 Hz, 1H)*, 7.81 (d, *J* = 7.9 Hz, 1H), 7.75 (d, *J* = 4.0 Hz, 1H), 7.30 (d, *J* = 3.9 Hz, 1H)*, 7.28-7.27 (m, 1H)*, 7.25-7.23 (m, 3H)*, 7.20 (dd, *J* = 3.6, 0.5 Hz, 1H)*, 3.17 (d, *J* = 3.8 Hz, 1H), 7.15 (d, *J* = 3.8 Hz, 1H)*, 7.14-7.11 (m, 6H)*, 7.06-7.03 (m, 2H)*, 6.98-6.96 (m, 2H), 6.88 (d, *J* = 2.1 Hz, 1H), 6.85 (brs, 1H), 1.31 (s, 3H), 1.30 (s, 9H)*, 1.29 (s, 9H)*, 1.27 (s, 3H). Minor isomer ^1H NMR (500 MHz, $CDCl_3$) δ 8.19 (*J* = 2.3 Hz, 1H), 8.79 (d, *J* = 7.9 Hz, 1H), 7.76 (d, *J* = 4.0 Hz, 1H), 3.16 (d, *J* = 3.8 Hz, 1H), 6.89 (d, *J* = 2.1 Hz, 1H), 1.32 (s, 3H), 1.267 (s, 3H). UV-vis (cyclohexane) λ_{max} (ε_{max}, L $mol^{-1}cm^{-1}$) nm, 247 (47200), 407 (57100).

2,7-Di-*tert*-butyl-10-[2-(3",4"-dihexyl-5,2':5',2":5",2"':5"',2""-quinquethienyl)carbonyl]-*trans*-12c,12d-dimethyl-5-(2-5,2':5',2"-terthienyl)-12c,12d-dihydrobenzo[e]pyrene (78) and the 4-terthienyl isomer

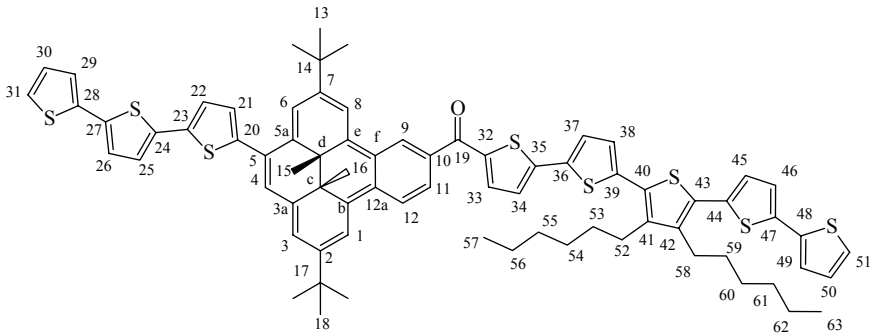

Major Isomer

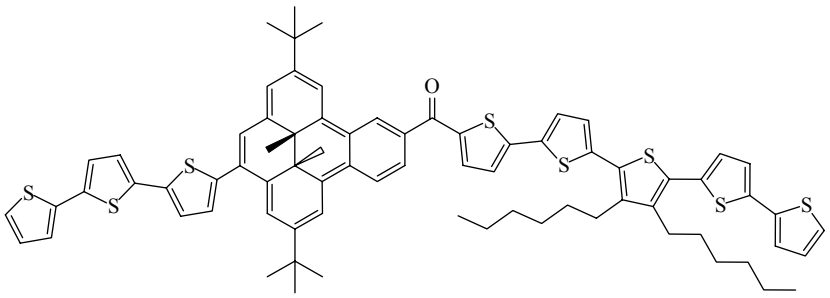

Minor Isomer

From *n*-BuLi (0.09 mL, 2.5 M), quinquethiophene (110mg, 0.19 mmol), and the Weinreb amide (92mg, 0.13 mmol) the same procedure was used as for **77**. The product **78** was purified by chromatography on silica gel (5% H_2O deactivation) using first 10:1 hexanes:dichloromethane to elute the excess quinquethiophene **102** followed by 10:1 hexanes:ethyl acetate to elute the product **78** as a red brown solid (118 mg, 0.094 mmol, 72 %). The product **78** could be further purified by recrystallization from 1:1 diethyl ether: hexane to give a dark red brown powder, mp 121-125^{o}C. The major isomer was assigned where possible. * Indicates where major and minor isomer peaks were indistinguishable. ^{1}H NMR (500 MHz, C_6D_6) δ 9.77-9.76 (m, H-9)*, 8.81 (d, *J* = 8.8 Hz, 1H, H-12), 8.68 (d, *J* = 1.1 Hz, 1H, H-8), 8.546-8.545 (m, 1H, H-1)*, 8.50 (d, *J* = 1.2 Hz, 1H, H-6), 8.22 (dd, *J* = 1.7, 8.5 Hz, 1H, H-11), 7.60-7.55 (m, 3H, H-4, 33, 3)*, 7.26 (d, *J* = 3.7 Hz, 1H, H-21), 7.15 (d, *J* = 3.7 Hz,1H, H-22)*, 7.03 (d, *J* = 3.8, Hz, 1H, H-38 or 45), 7.02-6.98 (m, 5H)*, 6.96 (d, *J* = 3.9 Hz, 1H, H-34), 6.94 (d, *J* = 3.7 Hz, 1H), 6.89 (d, *J* = 3.7 Hz, 1H), 6.74-6.71 (m, 2H)*, 6.67-6.64 (m, 2H)*, 2.84-2.80 (m, 4H, H-52,58)*, 1.70-1.64 (m, 4H, H-53,59), 1.49-1.36 (m, 4H, H-54,60)*, 1.48 (s, 9H, H-18), 1.37 (s, 9H, H-13), 1.31-1.25 (m, 8H, H-55,56,61,62)*, 0.92-0.86 (m, 6H, H-57,63), -1.19 (s, 3H, H-15)*, -1.21 (s, 3H, H-16). Minor ^{1}H isomer peaks where distinguishable from the

major isomer. ^{1}H NMR (500 MHz, C_6D_6) δ 8.82 (d, *J* = 8.8 Hz, 1H, H-12), 8.64 (d, *J* = 1.1 Hz, 1H), 8.58 (s, 1H), 8.22 (dd, *J* = 1.7, 8.5, 1H, H-11), 7.52 (s, 1H), 7.27 (d, *J* = 3.7 Hz, 1H), 7.04 (d, *J* = 3.8 Hz, 1H), 6.97 (d, *J* = 3.9 Hz, 1H), 6.95 (d, *J* = 3.7 Hz, 1H), 6.90 (d, *J* = 3.7 Hz, 1H), 1.47 (s, 9H), 1.40 (s, 9H), -1.22 (s, 3H). The major isomer ^{13}C peaks are assigned where possible. ^{13}C NMR (125.8 MHz, C_6D_6) δ 187.04 (C-19), 147.29 (C-2), 146.61, 146.49, 146.08 (C-35), 145.85 (C-7), 143.59 (C-20), 143.24, 143.23 (C-32), 141.63 (C-41 or 42), 141.27 (C-42 or 41), 139.31, 138.55, 138.36, 138.10, 137.87, 137.84, 137.75, 137.66, 137.17, 137.02, 136.98, 136.75, 136.50 (C-12e), 136.21, 136.18, 136.09, 135.92, 135.83 (C-33), 135.63, 135.34, 135.20 (C-12b), 132.82, 132.57 (C-12a), 131.51 (C-40 or 43), 130.46 (C-43 or 40), 129.86 (C-12f), 129.63, 128.59, 128.55, 128.50, 127.62, 127.59, 127.35 (C-9), 127.01, 126.94, 126.72, 126.58 (C-11), 126.12 (C-5), 126.05 (C-4), 125.68, 125.45, 125.40, 125.34 (C-12), 125.21, 125.04, 124.97, 124.92, 124.76 (C-22), 124.62, 124.58, 124.48, 122.02 (C-3), 121.36, 120.00 (C-1), 119.87, 119.22 (C-6), 118.89 (C-8), 37.38, 37.28 (C-12d), 36.36, 36.34 (C-14), 36.09, 35.98 (C-12c), 35.94 (C-17), 35.91, 32.18 (C-55 or 56 or 61 or 62), 31.44 (C-b), 31.37 (C-b), 31.12, 31.10 (C-18), 31.03 (C-13), 31.00, 30.30 (C-c), 29.05 (C-52 or 58), 28.99 (C-58 or 52), 23.36 (C-55 or 56 or 61 or 62), 23.35 (C-55 or 56 or 61 or 62), 18.62 (C-16), 18.59, 18.51, 18.48 (C-15), 14.65 (C-57 or 63), 14.63 (C-63 or 57). IR (NaCl, thin film) ν 3066, 2958, 2924, 2867, 1624, 1596, 1436, 1362, 1328, 1271, 1253, 1053, 791, 736, 690 cm^{-1}. UV-vis (cyclohexane) λ_{max} (ε_{max}, L mol^{-1}cm^{-1}) nm, 250 (27700), 326 sh (25900), 432 (60800), 540 sh (7540), 581 sh (5210), 652 (2550), 742 (2090). LSIMS, *m/z*, 1247 (M^+), 1231 (M^+-CH_3), 1217 (M^+-2CH_3), 1175 (M^+-CH_3, -*t*-butyl). HRMS calc'd for $C_{75}H_{75}OS_8$ (M+H) 1247.3584, found 1247.3584.

Open CPD form. Procedure: see (A,B), p 165. ^{1}H NMR (500 MHz, C_6D_6) δ 8.53-8.52 (m, 1H)*, 7.91 (dd, *J* = 7.8, 1.9 Hz, 1H), 7.72 (d, *J* = 7.9 Hz, 1H), 7.421 (d, *J* = 4.0 Hz, 1H), 7.34 (d, *J* = 2.1 Hz, 1H), 7.18 (d, *J* = 3.7 Hz, 1H), 7.11-7.10 (m, 1H)*, 7.05-6.93 (m, 11H)*, 6.857 (d, *J* = 3.8 Hz, 2H), 6.73-6.71 (m, 2H)*, 6.66-6.64 (m, 2H)*, 2.83-2.80 (m, 4H)*, 1.70-1.64 (m, 4H)*, 1.556 (s, 3H), 1.465 (s, 3H), 1.45-1.38 (m, 4H)*, 1.30 (s, 9H), 1.32-1.25 (m, 4H)*, 1.15 (s, 9H), 0.92-0.86 (m, 6H)*. Minor ^{1}H isomer peaks where distinguishable from the major isomer peaks. ^{1}H NMR (500 MHz, C_6D_6) δ 7.89 (dd, *J* = 8.0, 2.0 Hz, 1H), 7.68 (d, *J* = 7.9 Hz, 1H), 7.423 (d, *J* = 4.0 Hz, 1H), 7.38 (d, *J* = 2.1 Hz, 1H), 7.19 (d, *J* = 3.8 Hz, 1H), 6.860 (d, *J* = 3.8 Hz, 2H), 1.552 (s, 3H), 1.47 (s, 3H), 1.23 (s, 9H), 1.21 (s, 9H). ^{13}C NMR (125.8 MHz, C_6D_6) δ 186.65, 152.23, 151.87, 151.07, 150.72, 148.78, 146.50, 146.43, 146.04, 145.33, 145.17, 142.76, 141.62, 141.25, 140.77, 140.66, 140.40, 140.25, 139.24, 139.18, 139.04, 138.35, 138.22, 138.09, 137.96, 137.78, 137.66, 137.21, 137.03, 136.72, 136.69, 135.81, 135.62, 131.51, 130.43, 130.32, 130.16, 130.04, 129.93, 129.62, 129.46, 129.32, 128.90, 127.88, 127.76, 127.59, 126.91, 126.49, 126.24, 125.32, 125.20, 125.12, 124.92, 124.82, 124.61, 124.57, 124.53, 34.72, 34.67, 34.60, 34.55, 32.18, 31.82, 31.75, 31.70, 31.64, 31.44, 31.37, 31.12, 30.30, 29.04, 28.98, 23.35, 20.19, 20.03, 19.35, 19.22, 14.65. UV-vis (cyclohexane) λ_{max} (ε_{max}, L mol^{-1}cm^{-1}) nm, 247 (38300), 426 (53200), 742 (2060).

2,7-Di-*tert*-butyl-10-[(2-5,2'-bithienyl)carbonyl]-*trans*-12c,12d-dimethyl-5-(2-5,2'-dithienyl)-12c,12d-dihydrobenzo[e]pyrene (75) and the 4-bithienyl isomer

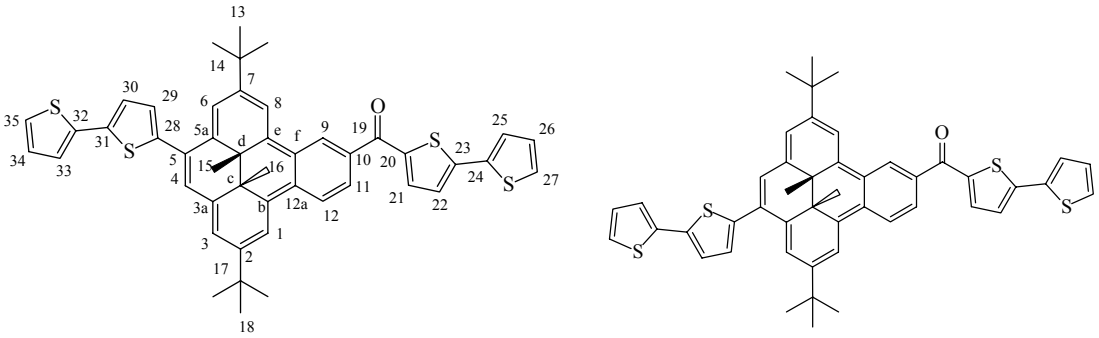

From *n*-BuLi (0.5 mL, 1.26 mmol), bithiophene (210 mg, 1.26 mmol) and the Weinreb amide **72** (25mg, 0.038 mmol), the same procedure was used as for **77**. The product **75** was purified by chromatography on silica gel (deactivated with 5% H_2O) using hexanes to remove the excess bithiophene and then 20:1 hexanes:ethyl acetate to elute the product **75** as a red brown solid (20mg, 0.027 mmol, 71%), mp, 122-123°C. The major isomer was assigned where possible. ^{1}H NMR (500 MHz, CD_2Cl_2) δ 9.37 (d, *J* = 1.8 Hz, 1H, H-9), 8.96 (d, *J* = 8.6 Hz, 1H, H-12), 8.52 (d, *J* = 1.2 Hz, 1H, H-1), 8.49 (d, *J* = 1.2 Hz, 1H, H-8), 8.20 (d, *J* = 1.2, 1H, H-6), 8.11 (dd, *J* = 8.6, 1.7 Hz, 1H, H-11), 7.77 (d, *J* = 3.9 Hz, 1H, H-21), 7.57 (br t, *J* = 1.0 Hz, 1H, H-3), 7.49 (d, *J* = 0.9 Hz, 1H, H-4), 7.45 (dd, *J* = 3.6, 1.1 Hz, 1H, H-25), 7.41 (dd, *J* = 5.2, 1.2 Hz, 1H, H-27), 7.34 (d, *J* = 3.9 Hz, 1H, H-22), 7.309 (brs, 2H, H-29,30), 7.30-7.27 (m, 2H, H-33,35), 7.13 (dd, *J* = 5.1, 3.6 Hz, 1H, H-26), 7.08 (dd, *J* = 4.8, 3.9 Hz, 1H, H-34), 1.55 (s, 9H, H-18), 1.51 (s, 9H, H-13), -1.51 (s, 3H, H-15), -1.52 (s, 3H, H-16). Minor isomer peaks where distinguishable from the major isomer. ^{1}H NMR (500 MHz, CD_2Cl_2) δ 9.36 (d, *J* = 1.8 Hz), 8.97 (s), 8.56 (d, *J* = 1.0 Hz), 8.46 (d, *J* = 1.2 Hz), 8.23 (d, *J* = 1.2 Hz), 7.76 (d, *J* = 3.9 Hz), 7.54 (br t, *J* = 1.0 Hz), 7.47 (d, *J* = 0.9 Hz), 7.313 (brs), 7.09 (dd, *J* = 4.8,3.9

Hz), 1.534 (s), 1.533 (s), -1.523 (s). Major isomer ^{13}C peaks are assigned where possible. ^{13}C NMR (125.8 MHz, CD_2Cl_2) δ 187.91 (C-19), 147.08 (C-7), 146.77, 146.48 (C-23), 146.45, 146.16 (C-2), 143.26 (C-28), 142.71, 142.70 (C-20), 139.09, 138.51 (C-3a), 138.16 (C-32), 137.53, 137.45 (C-31), 136.95 (C-24), 136.36 (C-21), 135.94 (C-12e), 135.58 (C-5a), 135.41 (C-10), 135.36, 135.31, 135.20, 135.00, 134.61 (C-12b), 132.70, 132.46 (C-12a), 129.44 (C-12f), 129.21, 128.95 (C-26), 128.54 (C-34), 128.18, 128.13 (C-29 or 30), 127.29 (C-27), 127.01 (C-9), 126.73, 126.40 (C-25), 126.13, 125.94 (C-11), 125.62, 125.45, 125.31 (C-4), 125.19 (C-12), 124.93 (C-22), 124.91 (C-33), 124.82, 124.54 (C-30 or 29), 124.07, 124.05 (C-35), 121.66 (C-3), 120.94, 120.16 (C-1), 120.09, 119.50, 118.78 (C-6), 118.70, 118.66 (C-8), 36.86 (12c), 36.72, 36.44 (C-14), 36.40, 36.04, 36.00 (C-17), 35.62, 35.47 (C-12d), 31.05, 31.01 (C-13), 30.98 (C-18), 30.93, 30.27, 18.20 (C-16), 18.16, 17.97, 17.93 (C-15). IR (NaCl, thin film) ν 3064, 2961, 2918, 2860, 1624, 1444, 1270, 1255, 839, 802, 693 cm^{-1}. UV-vis (cyclohexane) λ_{max} (ε_{max}, L $mol^{-1}cm^{-1}$) nm, 643 (2210), 532 (10300), 414 (70200), 369 (55700), 309 (36000), 273 (32200), 34900 (240). LSIMS, *m/z* 751 (M^+),735 (M^+-CH_3), 721 (M^+-$2CH_3$), 679 (M^+-CH_3, -*t*-butyl). HRMS calc'd for $C_{47}H_{42}OS_4$ 750.2118, found 750.2111. Anal. Calc'd for: $C_{47}H_{42}OS_4$: C,75.16; H,5.64, Found: C,74.91; H,6.02.

Open CPD form. Procedure: see (B), p 165. UV-vis (cyclohexane) λ_{max} (ε_{max}, L $mol^{-1}cm^{-1}$) nm, 358 (56700), 251 (58700), 235 (63100).

2,7-Di-*tert*-butyl-*trans*-12c,12d-dimethyl-4,5-di-(2-3”,4”-dihexyl-5,2’:5’,2”:5”,2”’:5”’,2””-quinquethienyl)-12c,12d-dihydrobenzo[e]pyrene (28)

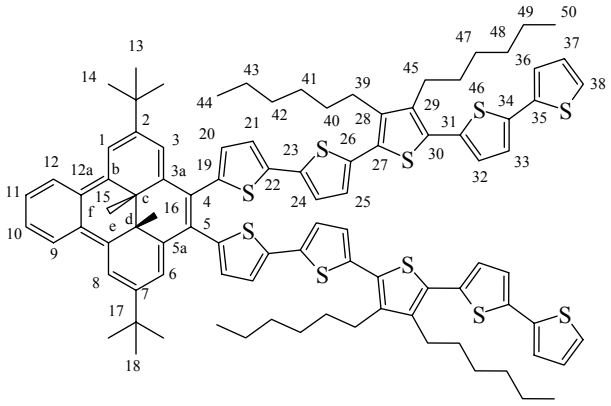

$Pd_2(dba)_3$ (35mg, 0.038 mmol), and dppf (40mg, 0.077 mmol) were added to a solution of the dibromide **24** (210mg, 0.38 mmol) and 2-tributylstannyl-3”,4”-dihexyl-5,2’:5’,2”:5”,2”’:5”’,2””’-quinquethiophene **103** (750mg, 0.86 mmol) in dry THF (8mL) and then refluxed for 4 days. The solution was cooled, aq.KF (10mL) was added and the reaction mixture stirred a further 15 minutes. After filtering through Celite and washing with dichloromethane it was extracted between dichloromethane and H_2O (3x). The organic layer was dried with $MgSO_4$, filtered through Celite and the solvent evaporated. The product was purified by chromatography on silica gel using hexanes as eluent followed by 20:1 hexanes:dichloromethane to elute the excess quinquethiophene **102** followed by 10:1 hexanes:dichloromethane to elute the desired product as a red solid (120mg, 0.08mmol, 20%), mp 98-100^{o}C. 10:1 Hexanes:ethyl acetate followed by 1:1 hexanes: ethyl acetate was used to elute slower moving oligomeric products. ^{1}H NMR (500 MHz, C_6D_6) δ 8.80-8.78 (AA’XX’, 2H, H-9,12), 8.45 (s, 2H, H-1,8), 8.01 (m, 2H, H-3,6), 7.54-7.52 (AA’XX’, 2H, H-10,11), 7.05-7.03 (m, 2H), 7.00-6.98 (m, 4H), 6.94-6.90 (m, 7H), 6.80-6.78 (dd, J = 4.7, 3.8, 1H), 6.74-6.70 (m, 2H), 6.64-6.62 (m, 2H),

2.80-2.75 (m, 8H,H-39,45), 1.64-1.61 (m, 8H, H-40,46), 1.41-1.34 (m, 8H, H-41,47) 1.37 (s, 18H, H-13), 1.30-1.20 (m, 16H, H-42,43,48,49), 0.95-0.85 (m, 12H, H-44,50), -0.87 (s, 6H, H-15,16). ^{13}C NMR (125.8 MHz, C_6D_6) δ 147.13 (C-2 or 7), 147.10 (C-7 or 2), 141.34, 141.26, 141.23, 141.06, 140.94, 138.67, 138.56, 138.51, 138.38, 138.36, 137.97, 137.86, 137.83, 137.75, 137.36, 136.82, 136.26, 135.99, 135.47, 135.44, 131.11, 131.09, 130.86, 130.75, 130.67, 130.29, 128.92, 128.90, 128.44, 127.88, 127.47, 127.35, 127.17 (C-10,11), 126.89, 125.53 (C-12,19), 125.28, 125.23, 125.17, 125.13, 125.01, 124.95, 124.92, 124.91, 124.87, 124.81, 124.50, 124.43, 124.37, 124.05, 119.42 (C-3,6), 118.12 (C-1,8), 37.17 (C-12c,12d), 36.20 (C-14,17), 32.17 (C-d or e), 32.15 (C-d or e), 31.40 (C-b), 30.87 (C-13,18), 30.31 (C-c), 30.24 (C-c), 28.99 (C-a), 28.91 (C-a), 23.35 (C-e or d), 18.96 (C-15,16), 14.68 (C-f), 14.63 (C-f). IR (NaCl, thin film) ν 3065, 2954, 2925, 2856, 1464, 1367, 789 cm^{-1}. UV-vis (cyclohexane) λ_{max} (ε_{max}, L $mol^{-1}cm^{-1}$) nm, 251 (67000), 346 (50800), 412 (103000), 554 (5380). LSIMS, *m/z*,1552 (M^+), 1536, 1522, 1479.

Open CPD form. Procedure: see (A,B), p 165. ^{1}H NMR (360 MHz, C_6D_6) δ 7.7-6.6 (m, 2H), 7.23 (d, *J* = 2.1 Hz, 2H), 7.22-7.19 (m, 2H), 6.99 (d, *J* = 2.1 Hz, 2H), 6.96-6.91 (m, 8H), 6.88-6.86 (m, 6H), 6.69 (dd, *J* = 5.1, 1.1 Hz, 2H), 6.60 (dd, *J* = 5.1, 3.5 Hz, 2H), 2.76-2.70 (m, 8H), 1.61 (s, 6H), 1.62-1.56 (m, 8H), 1.38-1.29 (m, 8H), 1.24-1.17 (m, 16H), 1.12 (s, 18H), 0.85-0.79 (m, 12H). UV-vis (cyclohexane) λ_{max} (ε_{max}, L $mol^{-1}cm^{-1}$) nm, 249 (83900), 408 (83800).

2,7-Di-*tert*-butyl-*trans*-12c,12d-dimethyl-4,5-di-(2-5,2':5',2"-terthienyl)-12c,12d-dihydrobenzo[e]pyrene (27)

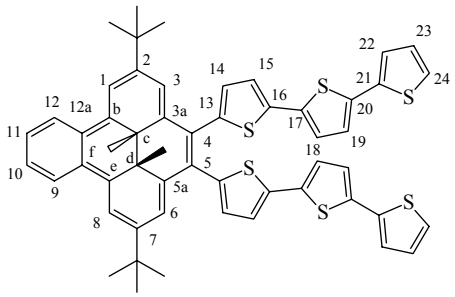

$Pd_2(dba)_3$ (10mg, 0.011 mmol) and dppf (14mg, 0.025 mmol) was added to a solution of 2-tributylstannyl-5,2':5',2" terthiophene **108** (855 mg, 1.59 mmol) and the dibromide **24** (226 mg, 0.409 mmol) in dry THF (10mL) and the solution was heated to reflux for 63 hours. The reaction mixture was then cooled and aq.KF (5 mL) was added and the reaction mixture stirred a further 15 minutes. It was filtered through Celite washing with hexanes. The solution was then washed with water (3x100 mL), dried over $MgSO_4$, filtered through Celite and the solvent evaporated. The product was purified by chromatography on silica gel (deactivated with 5% H_2O) using hexanes until all the excess terthiophene had been eluted and then 10:1 hexane:dichloromethane to obtain the product **27** as a rusty brown powder (218 mg, 0.245 mmol, 60%). The product **27** could be purified further by recrystallization from acetonitrile as a rusty brown powder, mp 167-169^{o}C. ^{1}H NMR (500 MHz, C_6D_6) δ 8.79 (AB, *J* = 3.4Hz, 1H, H-9 or 12), 8.78 (AB, *J* = 3.4 Hz, 1H, H-12 or 9), 8.45 (d, *J* = 1.2 Hz, 2H, H-1,8), 8.01 (d, *J* = 1.2 Hz, 2H, H-3,6), 7.54 (AB, *J* = 3.3 Hz, 1H, H 10 or 11), 7.53 (AB, *J* = 3.3 Hz, 1H, H-11 or 10), 6.98 (d, *J* = 3.5 Hz, 2H, H-15), 6.89 (d, *J* = 3.5 Hz, 2H, H-14), 6.88 (d, *J* = 3.6 Hz, 2H, H-24), 6.79 (d, *J* = 3.7 Hz, 2H, H-18), 6.73 (d, *J* = 3.7 Hz, 2H, H-19), 6.66 (dd, *J* = 1.2 Hz, 5.1 Hz, 2H**,** H-22), 6.60 (dd, *J* = 3.6, 5.1 Hz, 2H, H-23), 1.36 (s, 18H, C(C**H**$_3$)$_3$),

-0.87 (s, 6H, C**H**$_3$). ^{13}C NMR (125.7 MHz, C_6D_6) δ 147.09 (C-2,7), 141.19 (C-13), 138.64 (C-12b,12e), 138.54 (C-16), 137.95 (C-21), 137.22 (C-17), 136.80 (C-3a,5a),136.59 (C-20), 130.62 (C-14),130.28 (C-12a,12f), 128.37 (C-23), 127.16 (C-10,11), 126.89 (C-4,5), 125.52 (C-9,12), 125.15 (C-19), 124.78 (C-22), 124.73 (C-18), 124.27 (C-24), 123.99 (C-15), 119.41 (C-3,6), 118.12 (C-1,8), 37.16 (C-12c,12d), 36.18 (**C**$(CH_3)_3$), 30.85 (C(**C**$H_3)_3$) 18.95 (**C**H_3). IR (NaCl, thin film) ν 3065, 2962, 2923, 2865, 1618, 1475, 1446, 1368, 1258, 872, 789 cm^{-1}. UV-vis (cyclohexane) λ_{max} (ε_{max}, L mol^{-1}cm^{-1}) nm, 250 (28000), 355 (47300), 507 (69800), 510 (6630). LSIMS, *m/z* 886.1 (M^+), 871.1 (M^+ - CH_3), 857.1 (M^+ - 2CH_3), 815.0 (M^+ - CH_3,-C$(CH_3)_3$), 800.0 (M^+ - 2CH_3,-2C$(CH_3)_3$), 759.0 (M^+ - 2CH_3, -2C$(CH_3)_3$). HRMS calc'd for $C_{54}H_{46}S_6$ 886.1924, found 886.1924. Anal. Calc'd for $C_{54}H_{46}S_6$: C, 73.09; H, 5.23. Found: C,72.27; H, 5.45.

Open CPD form. Procedure: see (A,B), p 165. ^{1}H NMR (500 MHz, C_6D_6) δ 7.73-7.71 (AA'XX',1H), 7.29 (d, *J* = 2.1 Hz, 2H), 7.26-7.24 (AA'XX', 2H), 7.04 (d, *J* = 2.1 Hz, 2H), 6.97 (d, *J* = 3.8 Hz, 2H), 6.90 (d, *J* = 3.8 Hz, 2H), 6.88 (dd, *J* = 3.6,1.1 Hz, 2H), 6.78 (d, *J* = 3.8 Hz, 2H), 6.72 (d, *J* = 3.8Hz, 2H), 6.67 (dd, *J* = 5.0, 1.0 Hz, 2H), 6.60 (dd, *J* = 5.0, 3.6 Hz, 2H), 1.68 (s, 6H), 1.15 (s, 18H). ^{13}C NMR (125.7 MHz, C_6D_6) δ 150.74, 145.20, 145.11, 140.97, 140.79, 140.26, 138.73, 137.81, 136.94, 136.93, 136.48, 131.37, 130.68, 129.19, 129.08, 128.90, 126.49, 125.22, 125.08, 124.93, 124.40, 124.02, 34.60, 31.63, 30.55, 19.81. UV-vis (cyclohexane) λ_{max} (ε_{max}, L mol^{-1}cm^{-1}) nm, 250 (49800), 380 (53900).

2,7-Di-*t*-butyl-*trans*-12c,12d-dimethyl-4,5-di-(2-5”-tributylstanyl-5,2’:5’,2”-terthienyl)]-12c,12d-dihydrobenzo[e]pyrene (34)

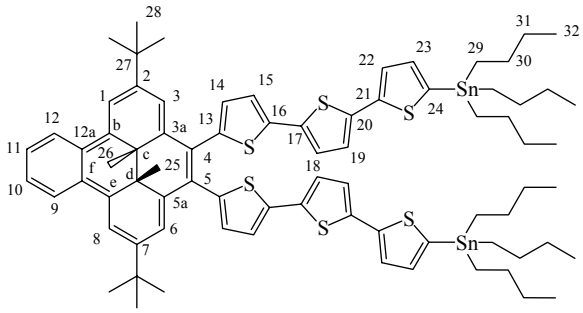

n-BuLi (0.61mL, 0.976mmol) was added to a solution of **27** (217 mg, 0.244 mmol), in dry THF (75mL) at -78^{o}C. The solution was warmed to 22^{o}C over 2 hours whereupon it was cooled to -78^{o}C and $SnBu_3Cl$ (0.265mL, 0.976mmol) was added. After warming to 22^{o}C over 3 hours the solution was poured into water and extracted with hexanes. The organic layer was washed with H_2O (3x), dried with $MgSO_4$ and concentrated. The product was purified by chromatography on alumina (deactivated with 5% H_2O), using 10:1 hexanes: dichloromethane and 1% triethylamine as eluent, giving the product **34** as a red oil (209 mg, 0.143 mmol, 59%). ^{1}H NMR (500 MHz, C_6D_6) δ 8.79-8.77 (AA’XX’, 2H, H-9,12), 8.45 (s, 2H, H-1,8), 8.01 (s, 2H, H-3,6), 7.54-7.52 (AA’XX’, 2H, H-10,11), 7.22 (d, *J* = 3.4 Hz , 2H, H-23), 7.04 (d, *J* = 3.4 Hz, 2H, H-22), 6.98 (d, *J* = 3.6 Hz , 2H, H-15), 6.88 (d, *J* = 3.6 Hz, 2H, H-14), 6.84 (AB, *J* = 3.8 Hz, 2H, H-19), 6.82 (AB, *J* = 3.8 Hz, 2H, H-18), 1.67-1.59 (m, 12H, H-29), 1.40-1.15 (m, 12H, H-30), 1.36 (s, 18H, H-28), 1.12-1.09 (m, 12 H, H-31), 0.92 (t, *J* = 7.3 Hz, 18H, H-32), -0.88 (s, 6H, H- 25, 26). ^{13}C NMR (125.7 MHz, C_6D_6) δ 147.00 (C-2,7), 143.72 (C-21), 140.99 (C-13), 138.68 (C-16), 138.61 (C-3a,5a), 137.05 (C-23), 136.98 (C-17), 136.87 (C-20), 136.77 (C-12b,12e), 136.66 (C-24), 130.59 (C-14), 130.28 (C-12a,12f), 127.13 (C-10,11), 126.99 (C-4,5), 124.72 (C-22), 125.52 (C-9,12), 125.05 (C-18 or 19), 124.84

(C-19 or 18), 123.90 (C-15), 119.48 (C-1,8), 118.12 (C-3,6), 37.15 (C-12c,12d), 36.18 (C-27), 30.87 (C-28), 29.72 (C-29), 27.99 (C-30), 18.95 (C-25,26), 14.24 (C-32), 11.46 (C-31). IR (NaCl, Thin film) ν 3065, 2957, 2917, 2869, 2844, 1618, 1463, 1416, 1368 1342, 1257, 1195, 1072, 1046, 1001, 940, 871, 790, 755, 693, 662, cm^{-1}. LSIMS, *m/z* 1465.2 (M^+), 1449.2 (M^+- CH_3), 1435.2 (M^+- 2 CH_3).

2,7-Di-*tert*-butyl-*trans*-12c,12d-dimethyl-5-(5,2':5',2"-2-terthienyl)-4-(5"-tributylstannyl-5,2':5',2"-2-terthienyl)-12c,12d-dihydrobenzo[e]pyrene (33)

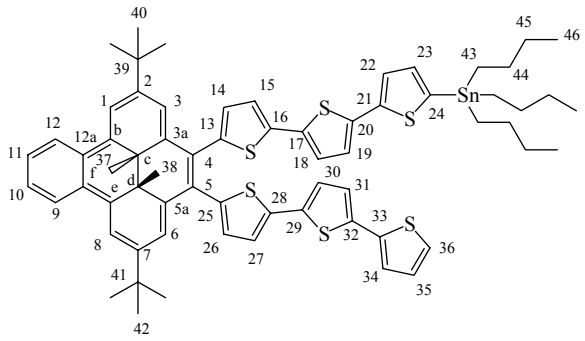

Using the same procedure as for **34** except with a smaller excess of *n*-BuLi (0.33 mL, 2.5M) added to **27** (0.29mg, 0.327 mmol) followed by $SnBu_3Cl$ (0.290 mL, 0.98 mmol), gave a mixture of **34** and **33**. These could be separated by chromatography on alumina (deactivated with 5% H_2O) using 20:1 hexanes:dichloromethane and 1% triethylamine followed by 10:1 hexanes:dichloromethane and 1% triethylamine, eluting first **34** (150mg, 0.10 mmol, 31%) followed by the desired product **33** as red brown crystals (215mg, 0.182 mmol, 56%), mp 79-80°C**.**

^{1}H NMR (500 MHz, C_6D_6) δ 8.79-8.77 (AA'XX', 2H, H-9,12), 8.44 (s, 2H, H-1,8), 8.01 (d, *J* = 1.1 Hz, 1H, H-3 or 6), 8.00 (d, *J* = 1.0 Hz, 1H, H-6 or 3), 7.54-7.52 (AA'XX', 2H, H-10,11), 7.23 (d, *J* = 3.5 Hz, 1H, H-23), 7.04 (d, *J* = 3.4 Hz, 1H, H-22), 6.99 (d, *J* = 3.7

Hz, 1H, H-19), 6.80 (d, *J* = 3.7 Hz, 1H, H-18), 6.89 (dd, *J* = 3.6, 1.15 Hz, 1H, H-36), 6.88 (dd, *J* = 0.4, 2.6, 1H, H-14 or 15), 6.88 (dd, *J* = 0.4, 2.6 Hz, 1H, H-14 or 15), 6.85 (d, *J* = 3.9 Hz, 1H, H-26), 6.82 (d, *J* = 3.9 Hz, 1H, H-27), 6.80 (d, *J* = 3.8 Hz, 1H, H-30), 6.73 (d, *J* = 3.8 Hz, 1H, H-31), 6.68 (ddd, *J* = 5.2, 1.2, 0.4 Hz, 1H, H-34), 6.60 (ddd, *J* = 5.2, 3.6, 0.4 Hz, 1H, H-35), 1.65-1.58 (m, 6H, H-44), 1.39-1.32 (m, 6H, H-45), 1.36 (s, 18H, H-40,42), 1.15-1.09 (m, 6H, H-43), 0.91 (t, *J* = 7.3 Hz, 9H, H-46), -0.88 (s, 6H, H-37,38). ^{13}C NMR (125.8 MHz, $CDCl_3$) δ 147.04 (C-2,7), 143.69 (C-20), 141.19 (C-17), 141.00 (C-16), 138.72, 138.62 (C-3a or 5a), 138.60 (C-5a or 3a), 138.51, 137.96 (C-33), 137.24, 137.06 (C-22), 136.94 (C-21), 136.91, 136.77 (C-12b,12e), 136.71 (C-24), 136.57 (C-32), 130.61 (C-14,15), 130.27 (C-12a, 12f), 127.87 (C-35), 127.15 (C-10,11), 126.94 (C-4 or 5), 126.93 (C-5 or 4), 125.74 (C-23), 125.52 (C-9,12), 125.14 (C-31), 125.04 (C-26), 124.84 (C-27), 124.76 (C-34), 124.73 (C-30), 124.26 (C-36), 124.00 (C-18), 123.88 (C-19), 119.46 (C-3 or 6), 119.42 (C-6 or 3), 118.12 (C-1 or 8), 118.11 (C-8 or 1), 37.14 (C-12c, 12d), 36.19 (C-39,41), 30.87 (C-40,42), 29.72 (C-44), 29.63 (C-45), 27.99 (C-46), 18.95 (C-37,38), 14.25 (C-43). IR (NaCl, thin film) ν 3065, 2960, 2913, 2868, 1618, 1463, 1368, 1257, 871, 790, 755 cm^{-1}. LSIMS, *m/z*, 1176 (M^+), 1161 (M^+-CH_3). HRMS calc'd for $C_{66}H_{72}S_6Sn$ 1176.2980, found 1176.2950.

2,7-Di-*tert*-butyl-*trans*-12c,12d-dimethyl-4,5-bis-(2-5"'-bromo-3"',4"'-dihexyl-5,2':5',2":5",2"'-2-quaterthienyl)-12c,12d-dihydrobenzo[e]pyrene (36)

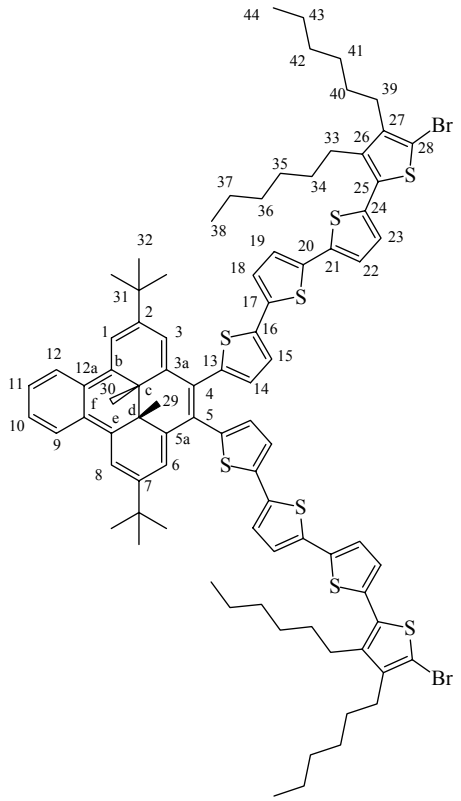

$Pd_2(dba_3)$ (5mg, 0.005mmol) and dppf (6mg, 0.01 mmol) was added to a solution of **34** (73mg, 0.05mmol) and 2,5-dibromo-3,4-dihexylthiophene **35** (230mg, 0.56mmol) in dry THF (3mL) and the reaction mixture was heated to reflux for 4 days. The reaction mixture was cooled and aq.KF (10mL) was added and the reaction mixture stirred for 15 minutes. The reaction mixture was poured into hexanes while rinsing with dichloromethane. It was washed with H_2O (3x), dried with $MgSO_4$ filtered through Celite and the solvent evaporated. The product **36** was purified by chromatography on alumina (deactivated with 5% H_2O) using 20:1 hexanes:dichloromethane to remove the excess thiophene followed by 10:1 hexanes:dichloromethane to elute the product **36** as a

red powder (45mg, 0.029mmol, 58%), mp 148-149°C. ^{1}H NMR (500 MHz, C_6D_6) δ 8.79-8.77 (AA'XX', 2H, H-9,12), 8.449 (s, 1H, H-1 or 8), 8.448 (s, 1H, H-8 or 1), 8.016 (s, 1H, H-3 or 6), 8.014 (s, 1H, H-6 or 3), 7.54-7.52 (AA'XX', 2H, H-10,11), 6.99 (d, *J* = 3.6 Hz, 2H, H-15), 6.90 (d, *J* = 3.6 Hz, 2H, H-14), 6.80 (d, *J* = 3.7 Hz, 2H, H-18),6.79 (AB, *J* = 3.7 Hz, 1H, H-22 or 23), 6.78 (AB, *J* = 3.7 Hz, 1H, H-23 or 22), 6.72 (d, *J* = 3.7 Hz, 2H, H-19), 2.70 (t, *J* = 8 Hz, 4H, H-33), 2.55 (t, *J* = 8 Hz, 4H, H-39), 1.57-1.52 (m, 8H, H-34,40), 1.37 (s, 18H, H-32), 1.36-1.29 (m, 8H, H-35,41), 1.29-1.26 (m, 8H, H-36,42) 1.26-1.21 (m, 8H, H-37,43), 0.91-0.88 (m, 12H, H-38,44), -0.86 (s, 6H, H-29,30). ^{13}C NMR (125.7 MHz, C_6D_6) δ 147.19 (C-2,7), 143.37 (C-26 or 27), 141.43 (C-13), 139.72 (C-26 or 27), 138.69 (C-3a,5a), 138.18 (C-20 or 21), 137.46 (C-16), 137.56 (C-17), 136.85 (C-12b,12e), 136.01 (C-20 or 21), 134.99 (C-24), 131.99 (C-25), 130.69 (C-14), 130.28 (C-12a,12f), 127.77 (C-22 or 23), 127.20 (C-10,11), 126.80 (C-4,5), 125.53 (C-9,12), 125.27 (C-19), 124.82 (C-18), 124.58 (C-22 or 23), 124.11 (C-15), 119.37 (C-1,8), 118.14 (C-3,6), 109.68 (C-28), 37.18 (C-12c or 12d), 36.20 (C-31), 32.27 (C-34 or 40), 32.14 (C-40 or 34), 31.40 (C-35 or 41), 30.86 (C-32), 30.36 (C-41 or 35), 30.11 (C-36,42), 29.46 (C-39), 29.19 (C-33), 23.34 (C-37 or 43), 23.31 (C-43 or 37), 18.96 (C-29,30), 14.64 (C-38 or 44), 14.62 (C-44 or 38). IR (NaCl, thin film) ν 2955, 2925, 2856, 1463, 788 cm^{-1}. UV-vis (cyclohexane) λ_{max} (ε_{max}, L $mol^{-1}cm^{-1}$) nm, 250 (40100), 414 (100000), 562 sh (4960). LSIMS, *m/z*, 1546 (M^+), 1529, 1514.

2,7-Di-*tert*-butyl-*trans*-12c,12d-dimethyl-4-(2-5,2':5',2"-terthienyl)-12c,12d-dihydrobenzo[e]pyrene (29)

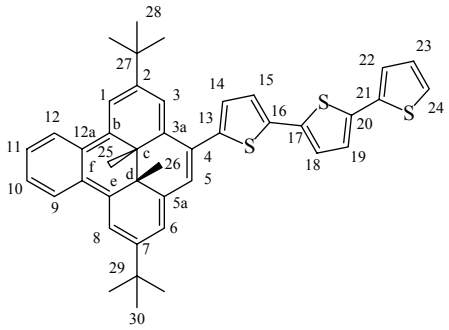

$Pd_2(dba_3)$ (26 mg, 0.028 mmol) and dppf (28 mg, 0.05 mmol) were added to a solution of the bromide **30** (463 mg, 0.98 mmol) and excess 2-tributylstannyl-5,2':5',2"-terthiophene **108** in dry THF (15 mL) and the reaction mixture was heated to reflux for 3 days. The reaction mixture was then cooled and aq.KF(10 mL) was added and the reaction mixture stirred a further 10 minutes. It was extracted between hexanes and H_2O (3x), dried with $MgSO_4$, filtered through Celite and then concentrated. The product was purified by chromatography on silica gel (deactivated with 5% H_2O) using first 15:1 hexanes:dichloromethane and 1% triethylamine to elute un-reacted starting material (89 mg, 0.19 mmol) and the excess terthiophene, followed by 10:1 hexanes:dichloromethane and then 5:1 hexanes:dichloromethane to elute the product as a red solid (300 mg, 0.47 mmol, 48%) mp. 178-179^{o}C, followed by some of the di-terthiophene addition product (81 mg, 0.09 mmol). ^{1}H NMR (500 MHz, C_6D_6) δ 8.81-8.78 (m, 2H, H-9,12), 8.46 (d, *J* = 1.0 Hz, 1H, H-1), 8.42 (d, *J* = 1.2 Hz ,1H, H-3), 8.41 (d, *J* = 1.2 Hz, 1H, H-8), 7.52-7.51 (m, 2H, H-10,11), 7.49 (d, *J* = 0.8 Hz, 1H, H-5), 7.44 (t, *J* = 1.0 Hz, 1H, H-6), 7.25 (d, *J* = 3.7 Hz, 1H, H-14), 7.14 (d, *J* = 3.7 Hz, 1H, H-15), 6.99 (dd, *J* = 3.5, 1.1 Hz, 1H, H-22), 6.98 (d, *J* = 3.8 Hz, 1H, H-18), 6.88 (d, *J* = 3.8 Hz, 1H, H-19), 6.72 (dd, *J* = 5.1,

1.1 Hz, 1H, H-24), 6.60 (dd, *J* = 5.1, 3.5 Hz, 1H, H-23), 1.45 (s, 9H, H-30), 1.43 (s, 9H, H-28), -1.09 (s, 3H, H-25), -1.11 (s, 3H, H-26). ^{13}C NMR (125.7 MHz, C_6D_6) δ 146.65 (C-2), 145.79 (C-7), 143.94 (C-13), 138.91 (C-5a), 137.95 (C-21), 137.46 (C-16), 137.34 (C-17), 136.83 (C-20, C-12b), 136.11 (C-12e), 135.76 (C-3a), 130.41 (C-12a), 130.19 (C-12f), 128.47 (C-23), 128.35 (C-14), 126.87 (C-10, C-11), 125.75 (C-4), 125.62 (C-9 or 12), 125.32 (C-9 or 12, C-19), 125.20 (C-5), 124.96 (C-24), 124.71 (C-15), 124.42 (C-22), 120.80 (C-6), 118.58 (C-3), 117.89 (C-1,8), 37.64 (C-12c), 36.32 (C-12d or 27), 36.30 (C-27 or 12d), 35.85 (C-29), 31.05 (C-28 or 30), 31.03 (C-30 or 28), 18.66 (C-26), 18.54 (C-25). IR (NaCl, Thin film) ν 3065, 2962, 2921, 2893, 2865, 1618, 1504, 1474, 1445, 1366, 1343, 1259, 1238, 872, 793, 755, 739 cm^{-1}. UV-vis (cyclohexane) λ_{max} (ε_{max}, L $mol^{-1}cm^{-1}$) nm, 242 (21900), 308 (20500), 345 (25500), 413 (49900), 516 (8200). EI MS, *m/z* 640 (M^+), 625 (M^+- CH_3), 610 (M^+- 2 CH_3), 569 (M^+ -CH3, - *t*-butyl, + 1H), 513 (M^+ -CH3, - 2 *t*-butyl). HRMS calc'd for $C_{42}H_{40}S_3$ 640.2292, found 640.2285. Anal. Calc'd for $C_{42}H_{40}S_3$: C,78.70; H,6.29. Found C,78.37; H,5.73.

Open CPD Form. Procedure: see (A,B), p 165. ^1H NMR (500 MHz, C_6D_6) δ 7.75-7.72 (m, 1H, H-9), 7.71-7.68 (m, 1H, H-12), 7.32 (d, *J* = 2.2 Hz, 1H, H-3),7.24-7.23 (m, 2H, H-10,11), 7.18 (d, *J* = 3.8 Hz, 1H, H-14), 7.08 (d, *J* = 2.2 Hz, 1H, H-1), 7.02 (d, *J* = 2.2 Hz, 1H, H-8), 6.98-6.70 (m, 3H, H-6,5,22), 6.94 (d, *J* = 3.8 Hz, 1H, H-15), 6.92 (d, *J* = 3.7 Hz, 1H, H-18), 6.85 (d, *J* = 3.7 Hz, 1H, H-19), 6.71 (dd, *J* = 5.1, 1.2 Hz, 1H, H-24), 6.65 (dd, *J* = 5.1, 3.6 Hz, 1H, H-23), 1.53 (s, 3H, H-26), 1.45 (s, 3H, H-25), 1.25 (s, 9H, H-30), 1.19 (s, 9H, H-28). ^{13}C NMR (125.7 MHz, C_6D_6) δ 151.60 (C-2), 145.79 (C-7), 146.77 (C-13), 145.09 (C-12a), 144.93 (C-12f), 142.24 (C-12b), 140.54 (C-12d), 140.34 (C-12c), 140.13 (C-12e), 139.04 (C-4), 138.12 (C-5a), 137.92 (C-3a), 137.83 (C-21),

137.15 (C-17 or 20), 137.07 (C-20 or 17), 136.49 (C-16), 130.27 (C-1), 129.70 (C-6), 129.55 (C-8) 129.40 (C-9,12), 129.08 (C-10 or 11), 129.03 (C-11 or 10), 128.48 (C-23), 127.53 (C-14), 125.86 (C-3), 125.31 (C-19), 125.09 (C-18), 125.05 (C-24), 124.80 (C-15), 124.57 (C-22 or 5) 124.48 (C-5 or 22), 34.63 (C-27 or 29), 34.51 (C-29 or 27), 31.80 (C-30), 31.69 (C-28), 20.01 (C-26), 19.20 (C-25). UV-vis (cyclohexane) λ_{max} (ε_{max}, L $mol^{-1}cm^{-1}$) nm, 249 (45700), 363 (21700), 415 (33000).

10-Bromo-2,7-di-*tert*-butyl-*trans*-10b,10c-dimethyl-4-naphthoyl-10b,10c-dihydropyrene (81)

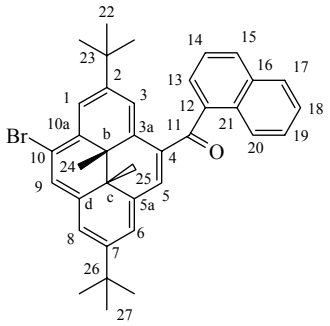

NBS (80mg, 0.45mmol) in DMF (5mL) was added to a solution of **14** (225mg, 0.45mmol) in DCM (100mL) at -78°C. After warming to room temperature over 5 hours the solution was poured into hexanes and washed with water (6 x 30 mL). The organic layer was dried ($MgSO_4$) and the solvent evaporated. The product was purified by chromatography on silica gel (deactivated with 5% H_2O) using toluene as eluent to obtain the pure product as a dark greenish black solid (195mg, 0.34 mmol, 75%), mp 196-198°C. ^{1}H NMR ($CDCl_3$, 500 MHz) δ 9.38 (s, 1H, H-3), 8.92 (s, 1H, H-1), 8.79 (s, 1H, H-9), 8.68 (s, 1H, H-5), 8.56 (s, 1H, H-8), 8.54 (s, 1H, H-6), 8.54-8.51 (m, 1H, H-20), 8.09 (d, *J* = 8.15 Hz, 1H, H-15), 8.01 (d, *J* = 7.85 Hz, 1H, H-17), 7.65 (dd, *J* = 7.0, 1.1

Hz, 1H, H-13), 7.60-7.57 (m, 1H, H-18), 7.54-7.48 (m, 2H, H-14, 19), 1.66 (s, 9H, H-27), 1.60 (s, 9H, H-22), -3.64 (s, 6H, H-24,25). ^{13}C NMR ($CDCl_3$, 125.8 MHz) δ 200.77 (C-11), 151.06 (C-2), 147.60 (C-7), 139.81 (C-12), 136.83 (C-5a or 10d), 136.48 (C-3a), 135.18 (C-10d or 5a), 134.47 (C-10a), 134.11 (C-16), 131.82 (C-15), 131.44 (C-21), 131.16 (C-4), 129.24 (C-13), 128.67 (C-17), 128.51 (C-9), 127.70 (C-14 or 19), 126.80 (C-5), 126.69 (C-18), 126.12 (C-20), 124.78 (C-19 or 14), 124.63 (C-6), 123.01 (C-8), 122.10 (C-1), 121.40 (C-3), 116.71 (C-10), 36.90 (C-23), 36.18 (C-26), 33.53 (C-10b), 31.95 (C-27), 31.87 (C-22), 29.57 (C-10c), 15.18 (C-24 or 25), 14.56 (C-25 or 24). IR (NaCl, Thin film) ν 3045, 2963, 2924, 2867, 2867, 1647, 1590, 1508, 1462, 1446, 1382, 1362, 1344, 1274, 1256, 1240, 1196, 952, 891, 782 cm^{-1}. UV-vis (cyclohexane) λ_{max} (ε_{max}, L mol^{-1}cm^{-1}) nm, 215 (53800), 291 (8940), 349 (47500), 402 (41600), 491 (7650), 612 (520), 667 (2410). EI MS, *m/z*, 578 (M+,^{81}Br), 576 (M+,^{79}Br), 507 (M-CH_3, *t*-butyl), 505 (M-CH_3, *t*-butyl). HRMS calc'd for $C_{37}H_{37}BrO$ 576.2027, found 576.2018.

Naphthoylation of dibromide (85) to give 4,9-Dibromo-7-*tert*-butyl-*trans*-10b,10c-dimethyl-2-naphthoyl-10b,10c-dihydropyrene (84), 4-naphthoyl derivative (82) and the monobromide (86)

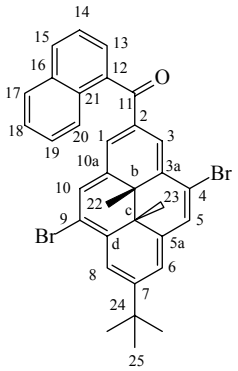

Aluminum chloride (200 mg, 1.5mmol) was added to a solution of the dibromide **85** (545mg, 1.08mmol) and naphthoyl chloride (490mg, 2.6mmol) in dichloromethane (35mL), and the green solution was stirred for 24 hours at 22°C. H_2O (2 mL) was then added turning the solution purple from aquamarine. The solution was poured into hexanes and washed with NaOH (2M), and H_2O (2x). The organic layer was dried ($MgSO_4$) and the solvent evaporated. The product was purified by chromatography on alumina (deactivated with 5% H_2O) using 2:1 hexanes:dichloromethane as eluent. Eluted first was green un-reacted starting material **85** (180mg, 0.36mmol), eluted second the 4-naphthoyldibromide **82** (68 mg, 0.10mmol, mp 202-204), eluted third the brown monobromide-4-naphthoyl **86** (131mg, 0.23 mmol, mp 202-203) and fourthly the desired purple 2-naphthoyl product **84** (195mg, 0.32 mmol, 30%). 3:1 Dichloromethane:hexanes was used to elute a small amount of a late running purple compound. A small portion of the product **84** was further purified by recrystallization from ACN giving purple crystals, mp. dec 211-212°C. ^{1}H NMR (500 MHz, $CDCl_3$) δ 9.38 (s, 1H, H-3), 8.87 (s, 1H, H-1), 8.86 (s, 1H, H-8), 8.79 (s, 1H, H-10), 8.71 (s, 1H, H-5), 8.53 (s, 1H, H-6), 8.19 (d, *J* = 8.6 Hz, H-20), 8.10 (d, *J* = 8.3 Hz, H-15), 7.99 (d, *J* = 7.8 Hz, H-17), 7.79 (dd, *J* = 7.0, 0.9 Hz, 1H, H-13), 7.63-7.61 (m, 1H, H-14), 7.57-7.54 (m, 1H, H-18), 7.50-7.47 (m, 1H, H-19), 1.69 (s, 9 H, H-25), -3.57 (s, 3H, H-23), -3.62 (s, 3H, H-22). ^{13}C NMR (125.8 MHz, $CDCl_3$) δ 198.49 (C-11), 153.26 (C-7), 141.88 (C-5a), 137.55 (C-12), 137.30 (C-10d), 135.45 (C-10a), 134.11 (C-16), 132.58 (C-10), 131.69 (C-2), 131.56 (C-21), 131.51 (C-3a), 131.37 (C-15), 128.74 (C-17), 128.12 (C-13), 127.98 (C-5), 127.43 (C-19), 126.95 (C-1), 126.73 (C-18), 126.57 (C-3), 126.15 (C-20), 124.71 (C-14), 123.04 (C-8), 122.94 (C-4), 122.55 (C-6), 116.95 (C-9), 37.03 (C-24), 33.51 (C-10c), 33.23 (C-10b), 31.90 (C-

25), 16.07 (C-22), 14.82 (C-23). IR (KBr) ν 3052, 2965, 2926, 2901, 2860, 1643, 1548, 1507, 1461, 1335, 1276, 1189, 1132, 1108, 901, 783, 738 cm^{-1}. UV-vis (cyclohexane) λ_{max} (ε_{max}, L $mol^{-1}cm^{-1}$) nm, 220 sh (68200), 360 (76800), 388 (23800), 412 (39600), 527 (13300), 604 (1440), 670 (325). EI MS, *m/z*, 600 (M^+), 570 (M^+-$2CH_3$), 529 (M^+-CH_3,-*t*-butyl). HRMS calc'd for $C_{33}H_{28}Br_2O$ 598.0507, found 598.0501.

Open CPD form. Procedure: see (A,B), p 165. ^{1}H NMR (500 MHz, $CDCl_3$) δ 8.11 (d, *J* = 7.2Hz, 1H), 8.02 (d, *J* = 7.4Hz, 1H), 7.95-7.93 (m, 1H), 7.87 (s, 1H), 7.58-7.50 (m, 4H), 7.24 (s, 1H), 7.21 (s, 1H), 6.87 (s, 1H), 6.80 (s, 1H), 6.75 (s, 1H), 1.58 (s, 3H), 1.56 (s, 3H), 1.28 (s, 9H). ^{13}C NMR (125.8 MHz, CDCl3) δ 196.14,153.12, 150.21, 138.37, 138.13, 137.78, 137.53, 137.49, 135.99, 135.44, 133.99, 133.87, 131.69, 130.97, 129.95, 128.91, 128.66, 127.79, 127.56, 126.94, 126.73, 125.68, 125.23, 124.53, 124.10, 124.06, 34.65, 31.29, 20.47, 19.78. UV-vis ($CHCl_3$) λ_{max} (ε_{max}, L $mol^{-1}cm^{-1}$) nm, 261 sh (30200), 303 (20100).

5,10-Dibromo-2,7-di-*tert*-butyl-*trans*-10b,10c-dimethyl-4-naphthoyl-10b,10c-dihydropyrene (82)

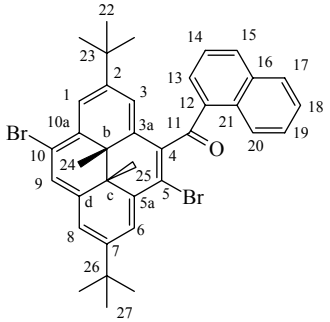

^{1}H NMR (500 MHz, $CDCl_3$) δ 9.43 (d, *J* = 8.6 Hz, 1H, H-20), 8.98 (s, 1H, H-6), 8.89 (s, 1H, H-1), 8.76 (s, 1H, H-9), 8.55 (s, 1H, H-8), 8.49 (brs, 1H, H-3), 8.03 (d, *J* =

8.2 Hz, 1H, H-15), 7.99 (d, *J* = 8.2 Hz, 1H, H-17), 7.85 (dd, *J* = 8.6, 1.4 Hz, 1H, H-19), 7.69 (dd, *J* = 8.2, 0.9 Hz, 1H, H-18), 7.52 (brs, 1H, H-13), 7.26-7.23 (m, 1H, H-14), 1.59 (s, 9H, H-27), 1.50 (s, 9H, H-22), -3.50 (s, 3H, H-25), -3.53 (s, 3H, H-24). ^{13}C NMR (125.8 MHz, $CDCl_3$) δ 199.83 (C-11), 149.61 (C-2), 149.40 (C-7), 137.85 (C-5a), 136.08 (C-12), 135.62 (C-4), 134.77 (C-3a), 134.41 (C-16), 134.09 (C-15), 133.09 (C-10a), 132.29 (C-10d), 132.07 (C-13), 131.20 (C-21), 129.00 (C-19), 128.85 (C-17), 127.99 (C-9), 126.97 (C-18), 126.69 (C-20), 124.57 (C-14), 122.97 (C-6), 122.68 (C-1), 122.61 (C-8), 120.86 (C-3), 117.40 (C-10), 114.41 (C-5), 36.66 (C-23), 36.63 (C-26), 32.69 (C-10b), 32.45 (C-10c), 32.01 (C-27), 31.82 (C-22), 15.13 (C-25), 14.43 (C-24). IR (NaCl, Thin film) ν 3054, 2964, 2926, 2905, 2867, 1662, 1591, 1508, 1464, 1335, 1264, 1253, 1220, 1178, 1125, 1088, 1072, 956, 899, 780, 739 cm^{-1}. UV-vis (cyclohexane) λ_{max} (ε_{max}, L $mol^{-1}cm^{-1}$) nm, 211 (61800), 242 (27300), 353 (70900), 394 (50800), 445 (5880), 471 (7640), 491 (8550), 660 (2150). EI MS, *m/z*, 656 (M^+),641 (M^+-CH_3), 626 (M^+-$2CH_3$), 585 (M^+-CH_3, - *t*-butyl), 506 (M^+-CH_3, - *t*-butyl, -Br). HRMS calc'd for ($C_{37}H_{36}{}^{79}Br^{81}BrO$) 656.1112, found 656.1123.

9-Bromo-2,7-di-*tert*-butyl-*trans*-10b,10c-dimethyl-4-naphthoyl-10b,10c-dihydropyrene (86)

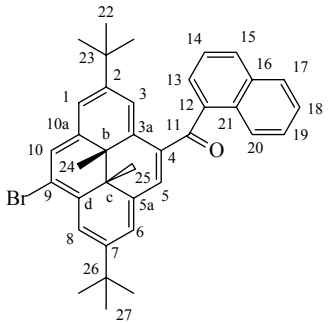

^{1}H NMR (500 MHz, $CDCl_3$) δ 9.37 (s, 1H, H-3), 8.89 (s, 1H, H-8), 8.71 (s, 1H, H-10), 8.64 (s, 1H, H-5), 8.53 (s, 1H, H-1), 8.51 (s, 1H, H-6), 8.47 (d, *J* = 8.4 Hz, 1H, H-20), 8.08 (d, *J* = 8.2 Hz, 1H, H-15), 8.00 (d, *J* = 8.4 Hz, 1H, H-17) 7.63 (dd, *J* = 7.1, 1.1 Hz, 1H, H-13), 7.59-7.56 (m, 1H, H-18), 7.53-7.49 (m, 2H, H-14,19), 1.66 (s, 9H, H-27), 1.55 (s, 9H, H-22), -3.66 (s, 3H, H-24), -3.68 (s, 3H, H-25). ^{13}C NMR (125.7 MHz, $CDCl_3$) δ 200.70 (C-11), 151.33 (C-2), 147.52 (C-7), 139.89 (C-12), 139.75 (C-10a), 136.93 (C-3a), 135.00 (C-5a), 134.14 (C-16), 131.99 (C-10d), 131.75 (C-15), 131.47 (C-21), 130.82 (C-4), 129.14 (C-13), 128.68 (C-17), 127.69 (C-14 or 19), 127.13 (C-10), 127.02 (C-5), 126.71 (C-18), 126.15 (C-20), 125.14 (C-6), 124.82 (C-19 or 14), 123.99 (C-8), 121.31 (C-1), 121.14 (C-3) 118.43 (C-9), 36.69 (C-23), 36.44 (C-26), 32.05 (C-27), 31.88 (C-10c), 31.81 (C-22), 31.29 (C-10b), 15.35 (C-24), 14.53 (C-25). IR (NaCl, Thin film) ν 3043, 2964, 2926, 2905, 2867, 1645, 1508, 1462, 1363, 1242, 1197, 892, 781 cm^{-1}. UV-vis (cyclohexane) λ_{max} (ε_{max}, L $mol^{-1}cm^{-1}$) nm, 213 (64000), 293(9170), 350 (46500), 403 (53100), 496 (7780), 612(565), 668 (2520). EI MS, *m/z*, 578 (M+, ^{81}Br), 576 (M+, ^{79}Br), 548 (M-CH_3), 546(M-CH_3), 507 (M-CH_3, *t*-butyl), 505 (M-CH_3, *t*-butyl).

2,7-Di-*tert*-butyl-*trans*-10b,10c-dimethyl-4-naphthoyl-5,10-di-(2-5,2':5',2"-terthienyl)-10b,10c-dihydropyrene (83)

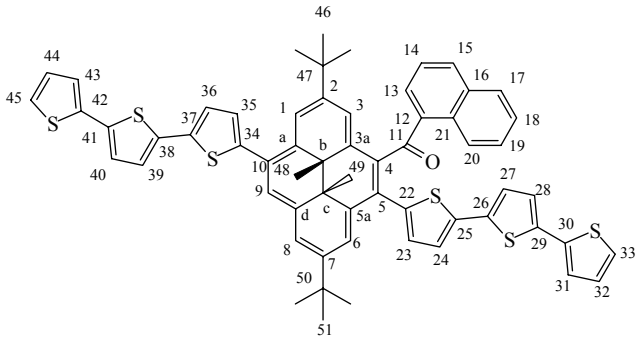

$Pd_2(dba)_3$ (6 mg, 0.006mmol) and dppf (8 mg, 0.014 mmol) was added to a solution of the dibromide **82** (120mg, 0.183 mmol) and 2-tributylstannyl-5,2':5',2"-terthiophene **108** (excess) in dry THF (15 mL) and the solution was heated to reflux stirring for 18 h under N_2. Over the course of the reaction the solution turned from green to red. The reaction mixture was cooled, aq.KF(15 ml) was added and the reaction mixture stirred a further 20 minutes. The solution was then poured into hexanes and washed with H_2O (3x). The organic layer was dried with $MgSO_4$, filtered through Celite and then concentrated. The residue was purified by chromatography on alumina (deactivated with 5% H_2O) using 1:1 hexane:dichloromethane as eluent to give the product **83** (125.2 mg, 0.126 mmol, 69%). The product **83** could be further purified by recrystallizing from acetonitrile, giving a red powder, mp 220-221°C. ^{1}H NMR (500 MHz, $CDCl_3$) δ 9.23 (d, *J* = 0.7 Hz, 1H, H-1), 8.90 (br s, 1H, H-3), 8.81 (d, *J* = 8.4 Hz, 1H, H-20), 8.76 (s, 1H, H-6), 8.72 (s, 1H, H-9), 8.60 (s, 1H, H-8), 7.85 (d, *J* = 8.2 Hz, 1H, H-15), 7.75 (d, *J* = 8.0 Hz, 1H, H-17), 7.57 (d, *J* = 3.7 Hz, 1H, H-35), 7.54 (ddd, *J* = 8.5, 7.0, 1.5 Hz, 1H, H-19), 7.46 (ddd, *J* = 8.2, 7.0, 1.0 Hz, 1H, H-18), 7.42 (d, *J* = 3.7 Hz, 1H, H-36), 7.26 – 7.21 (m, 4H, H-39,45,43,31), 7.18-7.16 (m, 3H, H-40,33,13), 7.14-7.11 (m, 1H, H-14), 7.06 (dd, *J* = 5.0, 3.7 Hz, 1H, H-44), 7.032 (dd, *J* = 7.0, 3.7 Hz 1H,

H-32), 7.027 (dd, *J* = 3.7, 1.8 Hz, 1H, H-28), 6.90 (br d, *J* = 3.5 Hz, 1H, H-23), 6.79 (d, *J* = 3.7 Hz, 1H, H-27), 6.71 (d, *J* = 3.7 Hz, 1H, H-24), 1.585 (s, 9H, H-46 or 51), 1.582 (s, 9H, H- 51 or 46), -3.30 (s, 3H, H-49), -3.42 (s, 3H, H-48). ^{13}C NMR (125.8 MHz, $CDCl_3$) δ 201.56 (C-11), 149.49 (C-7), 148.16 (C-2), 143.77 (C-34), 140.40 (C-22), 138.95 (C-25), 138.74 (C-12), 137.99 (C-37), 137.49 (C-30), 137.31 (C-42), 137.33 (C-5a), 136.66 (C-38), 136.48 (C-41), 136.18 (C-26 or 29), 136.17 (C-29 or 26), 135.90 (C-4), 135.41 (C-10d), 135.17 (C-3a), 134.96 (C-10a), 133.90 (C-16), 132.70 (H-15), 131.51 (C-23), 130.38 (C-21), 129.48 (C-13), 128.36 (C-35), 128.30 (C-17), 128.16 (C-44), 128.10 (C-32), 127.70 (C-18), 127.52 (C-10), 126.51 (C-19), 126.40 (C-9), 126.09 (C-20), 125.10 (C-5), 124.78 (C-45 or 43), 124.74 (C-40), 124.59 (C-31), 124.50 (C-36), 124.39 (C-43 or 45), 124.36 (C-28), 124.11 (C-39 and 27), 123.99 (C-24 and 14), 123.78 (C-33), 123.25 (C-8), 121.67 (C-6), 121.47 (C-1), 120.71 (C-3), 36.80 (C-47), 36.40 (C-50), 31.87 (C-46 or 51), 31.82 (C-51 or 46), 31.37 (C-10b), 30.51 (C-10c), 15.97 (C-49), 15.44 (C-48). IR (NaCl Thin film) ν 3066, 2963, 2866, 1654, 1590, 1507, 1462, 1260, 1230, 1176, 1124, 1105, 1066, 886, 836, 792, 738, 693 cm^{-1}. UV-vis (cyclohexane) λ_{max} (ε_{max}, L $mol^{-1}cm^{-1}$) nm, 211 (132000), 245sh (60800), 333sh (39000), 371 (86400), 429 (136000), 500sh (17300), 676 (3470). LSIMS, *m/z* 991 (M^+), 975 (M^+-CH_3), 961 (M^+-2 CH_3). HRMS calc'd for $C_{61}H_{51}OS_6$ (M+H) 991.2264, found 991.2220. Anal. Calc'd for $C_{61}H_{50}OS_6$: C,73.90; H,5.08. Found C,73.50; H,5.16.

7-*tert*-Butyl-*trans*-10b,10c-dimethyl-2-naphthoyl-4,9-di-(2-5,2':5',2"-terthienyl)-10b,10c-dihydropyrene (96)

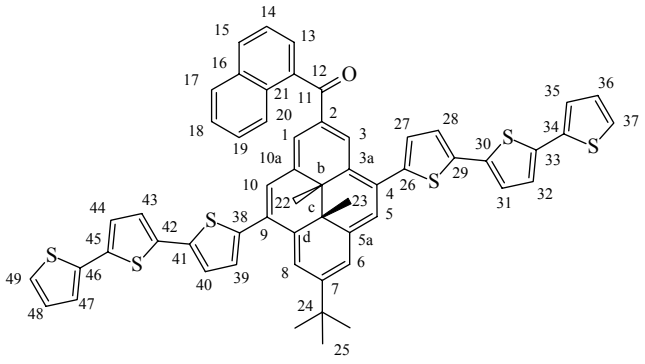

$Pd_2(dba)_3$ (5 mg, 0.005 mmol) and dppf (10 mg, 0.018 mmol) were added to a solution of the dibromide **84** (28 mg, 0.047 mmol) and 2-tributylstannyl-5,2':5',2"-terthiophene **108** (0.126 mg, 0.234 mmol) in dry THF (10 mL) and the reaction mixture was heated to reflux for 18 hours. After cooling to 21°C aq.KF (10 mL) was added and the reaction mixture stirred for a further 20 minutes. The solution was then extracted between 1:1 hexane:diethyl ether and H_2O (3x), dried with $MgSO_4$, filtered through Celite and concentrated. The product **96** was purified by chromatography on silica gel (5% H_2O) using 20:1 hexanes:ethyl acetate to remove the excess terthiophene then 10:1 hexanes:ethyl acetate to elute the product (40 mg, 43 mmol, 91%) as a green brown powder. The product **96** could be further purified by recrystallization from acetonitrile to give a dark green brown powder, mp 218-220°C. ^{1}H NMR (500 MHz, $CDCl_3$) δ 9.53 (d, *J* = 0.8 Hz, 1H, H-3), 9.15 (d, *J* = 1.1 Hz, 1H, H-8), 9.05 (s, 1H, H-1), 8.78 (s, 1H, H-10), 8.62 (s, 1H, H-5), 8.57 (s, 1H, H-6), 8.16 (dd, *J* = 8.6, 0.8 Hz, 1H, H-20), 8.10 (d, *J* = 8.3 Hz, 1H, H-15), 8.01 (d, *J* = 8.4 Hz, 1H, H-17), 7.87 (dd, *J* = 7.0, 1.2 Hz, 1H, H-13), 7.66 (dd, *J* = 8.3, 7.0, 1H, H-14), 7.56 (m, 1H, H-18), 7.49 (d, *J* = 3.8 Hz, 1H, H-39), 7.47 (m, H, H-19), 7.39 (d, *J* = 3.8 Hz, 1H, H-40), 7.36 (d, *J* = 3.8 Hz, 1H, H-27), 7.27-7.21 (m,

6H), 7.16-7.15 (m, 3H), 7.08-7.05 (m, 2H), 1.68 (s, 9H, H-25), -3.30 (s, 3H, H-22), -3.37 (s, 3H, H-23). ^{13}C NMR (125.8 MHz, $CDCl_3$) δ 198.71 (C-11), 152.17 (C-7), 142.97 (C-38), 142.75 (C-26), 142.32 (C-5a), 138.71 (C-29), 138.59 (C-10d), 138.32 (C-12), 138.25 (C-41), 137.40, 137.37, 136.71, 136.61, 136.47 (C-42), 136.36, 135.05 (C-10a), 134.06 (C-16), 132.81 (C-4), 131.54 (C-21), 131.49 (C-3a), 131.12 (C-10), 130.94 (C-15), 130.62 (C-2), 139.11 (C-27), 128.71 (C-17), 128.47 (C-39), 128.18, 128.16, 127.67 (C-13), 127.41 (C-1), 127.29 (C-9), 127.17 (C-19), 126.5 (C-18), 126.35 (C-20), 125.93 (C-3), 125.54 (C-5), 124.97 (C-14), 124.82, 124.74, 124.68, 124.65, 124.60, 124.51 (C-40), 124.03, 124.01, 122.82 (C-6), 121.52 (C-8), 36.88 (C-24), 32.23 (C-10c), 32.05 (C-10b), 31.08 (C-25), 17.06 (C-23), 15.90 (C-22). IR (NaCl, Thin film) ν 3065, 2962, 2917, 2849, 1636, 1548, 1506, 1462, 1441, 1282, 1236, 1183, 1134, 1074, 792, 692 cm^{-1}. UV-vis (cyclohexane/DCM) λ_{max} (ε_{max}, L $mol^{-1}cm^{-1}$) nm, 248 sh (59800), 371 (47200), 456 (78200), 568 (16200), 703 (1600). LSIMS, *m/z* 935.1 (M^+), 919.1 (M^+- CH_3), 904.1 (M^+-$2CH_3$). HRMS calc'd for $C_{57}H_{43}OS_6$ (M+H) 935.1638, found 935.1636.

Open CPD form. Procedure: see (A,B), p 165. ^{1}H NMR (500 MHz, $CDCl_3$) δ 8.06 (dd, *J* = 7.0, 2.1 Hz, 1H), 7.97 (d, *J* = 8.0, 1H), 7.91-7.89 (m, 1H), 7.63 (d, *J* = 1.6 Hz, 1H), 7.56 (dd, *J* = 7.0, 1.1 Hz, 1H), 7.54-7.49 (m, 3H), 7.37 (d, *J* = 1.6 Hz, 1H), 7.24-7.22 (m, 2H), 7.20-7.18 (m, 2H), 7.14-7.07 (m, 5H), 7.07 (d, *J* = 2.0 Hz, 1H), 7.06 (d, *J* = 2.0 Hz, 1H), 7.05-7.01 (m, 2H), 7.00 (d, *J* = 3.7 Hz, 1H), 6.98 (d, *J* = 2.0 Hz, 1H), 6.91 (d, *J* = 2.0 Hz, 1H), 6.75 (s, 1H), 6.65 (s, 1H), 1.64 (s, 3H), 1.60 (s, 3H), 1.26 (s, 9H). UV-vis (1:1 cyclohexane:DCM) λ_{max} (ε_{max}, L $mol^{-1}cm^{-1}$) nm, 252 (41000), 310 (23100), 388 (56800), 446 (43100).

7-*tert*-Butyl-*trans*-10b,10c-dimethyl-2-naphthoyl-4,9-di-(2-3",4"-dihexyl-5,2':5',2":5",2"':5"',2""-quinquethienyl)-10b,10c-dihydropyrene (97)

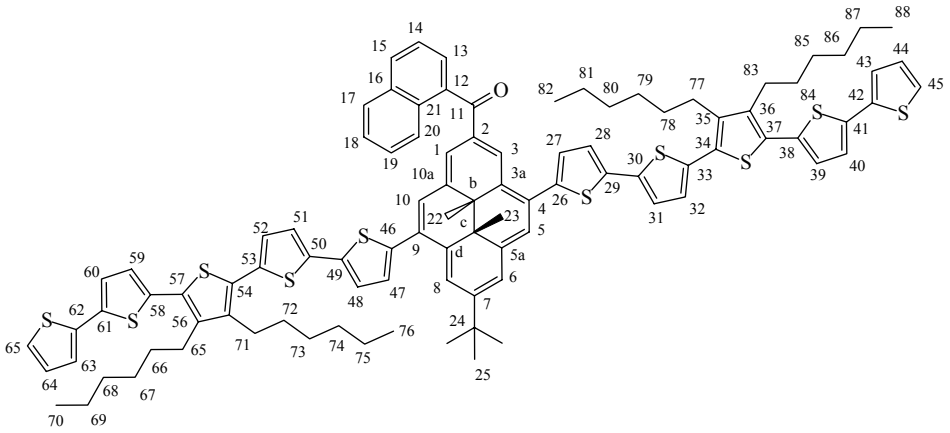

$Pd_2(dba)_3$ (9mg, 0.01 mmol) and dppf (10mg, 0.02 mmol) were added to a solution of the dibromide **84** (115 mg, 0.19 mmol) and the quinquethiophene **103** (384 mg, 0.44 mmol) in dry THF (5 mL) and the solution was heated to reflux for 18 hours. Additional $Pd_2(dba)_3$ (9 mg, 0.01 mmol) was added and the reaction mixture was heated at reflux for an additional 12 hours. The reaction mixture was then cooled and aq.KF (10 mL) was added and the reaction mixture stirred for 15 minutes. It was extracted between diethyl ether:H_2O (3x), dried with $MgSO_4$, filtered through Celite and the solvent evaporated to give a dark brown black solid. The product **97** was purified by chromatography on silica gel (deactivated with 5% H_2O) using 20:1 hexanes:ethyl acetate, eluting first the excess quinquethiophene **102**, second a mixture of mono addition product (28 mg), third the desired product **97** (171mg, 0.11mmol, 56%) and fourth some later oligomeric products (47 mg). A portion of the product **97** could be further purified by recrystallization from cyclohexane giving a dark brown black powder, mp 98-100°C. ^{1}H NMR (500 MHz, $CDCl_3$) δ 9.54 (s, 1H, H-3), 9.16 (s, 1H, H-8), 9.05 (s, 1H, H-1), 8.79 (s, 1H, H-10), 8.63 (s, 1H, H-5), 8.58 (s, 1H, H-6), 8.17 (d, *J* = 8.3 Hz, 1H, H-20),

8.09 (d, *J* = 8.3 Hz, 1H, H-15), 8.01 (d, *J* = 8.5 Hz, 1H, H-17), 7.86 (dd, *J* = 7.0, 1.0 Hz, 1H, H-13), 7.67 (dd, *J* = 8.2,7.0 Hz, 1H, H-14), 7.59-7.55 (m, 1H, H-18), 7.50 (d, *J* = 3.7 Hz, 1H, H-47), 7.48 (m, 1H, H-19), 7.40 (d, *J* = 3.7 Hz , 1H, H-48), 7.37 (d, *J* = 3.7 Hz , 1H, H-27), 7.27 (d, *J* = 3.7 Hz ,1H), 7.24 (d, *J* = 3.7 Hz, 1H, H-28) 7.24-7.23 (m, 1H), 7.23-7.19 (m, 4H), 7.15 (t, *J* = 3.6 Hz, 2H), 7.12 (dd, *J* = 3.7,3.1 Hz , 2H), 7.07 (dd, *J* = 5.5,3.7 Hz , 2H), 7.06-7.03 (m, 2H), 2.81-2.73 (m, 8H, H-65,71,77,83), 1.68 (s, 9H, H-25), 1.66-1.59 (m, 8H, H-66,72,78,84), 1.51-1.47 (m, 8H, H-67,73,79,85), 1.41-1.34 (m, 16H, H-68,69,74,75,80,81,86,87), 0.96-0.91 (m, 12H, H-70,76,82,88), -3.29 (s, 3H, H-22), -3.36 (s, 3H, H-23). ^{13}C NMR (125.8 MHz, $CDCl_3$) δ 198.66 (C-11), 152.12 (C-7), 142.89 (C-46), 142.73 (C-26), 142.28 (C-5a), 140.64, 138.73, 138.56, 138.29 (C-10d), 137.36, 137.32, 137.27, 137.15, 135.62, 135.48, 135.29, 135.27, 135.01 (10a), 134.03, 132.84 (C-4), 131.52, 131.49 (C-3a), 131.09 (C-10), 130.92 (C-15), 130.58, 130.06, 130.01, 129.99, 129.14 (C-27), 128.69 (C-17), 128.47 (C-47), 128.09, 127.67 (C-13), 127.45 (C-1), 127.29 (C-9), 127.16 (C-19), 126.71, 126.64, 126.59, 126.55 (C-18), 126.33 (C-20), 125.88 (C-3), 125.53 (C-5), 124.94 (C-14), 124.68, 124.54, 124.42 (C-48), 124.34, 124.22, 124.15, 123.85, 122.80 (C-6), 121.49 (C-8), 36.86 (C-24), 32.22 (C-10b), 32.03 (C-10c), 31.79 (C-25), 31.75 (C-two of 68 or 69 or 74 or 75 or 80 or 81 or 86 or 87), 31.71 (C- two of 68 or 69 or 74 or 75 or 80 or 81 or 86 or 87), 30.88 (C-66), 29.85 (C-two of 67 or 73 or 79 or 85), 29.81 (C- two of 67 or 73 or 79 or 85), 28.51 (C-two of 65 or 71 or 77 or 83), 28.47 (C-two of 65 or 71 or 77 or 83), 22.89 (C-two of 68 or 69 or 74 or 75 or 80 or 81 or 86 or 87), 22.88 (C-two of 68 or 69 or 74 or 75 or 80 or 81 or 86 or 87), 22.85 (C-68,69), 17.06 (C-23), 15.89 (C-22), 14.36 (C-two of 70 or 76 or 82 or 88), 14.33(C-70 or 76 or 82 or 88), 14.32 (C-70 or 76 or 82 or 88). IR (NaCl, Thin film)

ν 3065, 2953, 2925, 2855, 1640, 1548, 1449, 1462, 1282, 1236, 1183, 1134, 1073, 791, 690 cm^{-1}. UV-vis (cyclohexane) λ_{max} (ε_{max}, L $mol^{-1}cm^{-1}$) nm, 221 (82100), 249 sh (35600), 382 (57800), 459 (81800), 566 (18900), 703 (1600). LSIMS, *m/z*, 1600 (M^+), 1584 (M^+-CH_3), 1569 (M^+-$2CH_3$). HRMS calc'd for $C_{97}H_{99}OS_{10}$ (M+H) 1599.4903, found 1599.4935. Anal. Calc'd for $C_{97}H_{98}OS_{10}$: C,72.79; H,6.17. Found C,72.82; H,6.25.

Open CPD form. Procedure: see (A,B), p 165. ^{1}H NMR (500 MHz, $CDCl_3$) δ 8.10-8.09 (m, 1H), 7.98 (d, *J* = 8.3 Hz, 1H), 7.92-7.90 (m, 1H), 7.66 (d, *J* = 1.5 Hz, 1H), 7.58 (d, *J* = 7 Hz, 1H), 7.55-7.50 (m, 3H), 7.41 (d, *J* = 1.2 Hz, 1H), 7.24 (d, *J* = 4.9 Hz, 2H), 7.21-7.20 (m, 2H), 7.15-7.14 (m, 5H), 7.10-7.0 (m, 10H), 6.94 (d, *J* = 1.9 Hz, 1H), 6.78 (s, 1H), 6.68 (s, 1H), 2.77-2.73 (m, 8H), 1.67 (s, 3H), 1.64 (s, 3H), 1.62-1.59 (m, 8H), 1.48-1.41 (m, 8H), 1.39-1.36 (m, 16H), 1.29 (s, 9H), 1.0-0.92 (m, 12H). ^{13}C NMR (125.8 MHz, $CDCl_3$) δ 196.50 (C-11), 152.54, 152.19, 144.73, 144.53, 40.64, 140.61, 139.76, 139.51, 139.17, 139.02, 138.59, 137.57, 137.34, 137.32, 137.25, 137.09, 136.84, 136.55, 136.15, 135.65, 135.62, 135.26, 135.23, 133.92, 131.34, 131.14, 130.25, 130.08, 130.06, 129.94, 129.91, 129.19, 128.61, 128.09, 127.66, 127.53, 127.32, 127.20, 126.64, 126.58, 125.97, 125.81, 125.06, 124.69, 124.58, 124.35, 124.31, 124.20, 124.00, 123.85, 34.54, 31.79, 31.72 (CH_2), 31.46 (C-25), 30.86 (CH_2), 29.82 (CH_2), 28.46 (CH_2), 27.13 (CH_2), 22.85 (CH_2), 20.69(C23 or 22), 20.00 (C22 or 23), 14.34 (C-70), 14.32 (C-70). UV-vis (cyclohexane) λ_{max} (ε_{max}, L $mol^{-1}cm^{-1}$) nm, 218 (86900), 398 (60700), 434 (63300).

7-*tert*-Butyl-4,9-di-(2-3”’,4”’-dihexyl-5,2’:5’,2”:5”,2”’:5”’,2””:5””,2”””:5”””,2””””-septithienyl)-*trans*-10b,10c-dimethyl-2-naphthoyl-10b,10c-dihydropyrene (98)

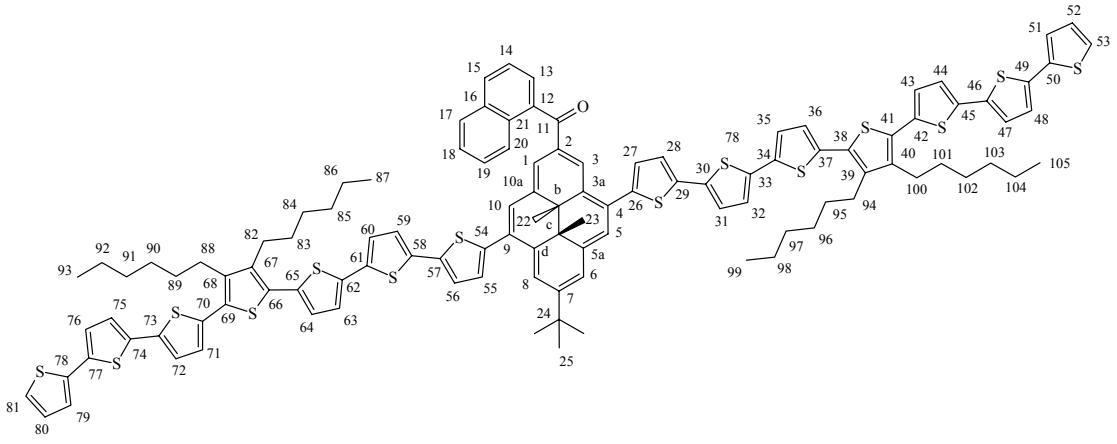

$Pd_2(dba)_3$ (6 mg, 0.006mmol) and dppf (8 mg, 0.014 mmol) were added to a solution of the dibromide 84 (82mg, 0.137 mmol) and 3”’,4”’-dihexyl-2-tributylstannyl-5,2’:5’,2”,5”,2”’:5”’,2””:5””’,2”””’-septithiophene **106** (283mg, 0.27 mmol) in dry THF (10 mL) and the solution was heated to a reflux stirring for 36 h under N_2. More $Pd_2(dba)_3$ (6mg, 0.006 mmol) was added and the reaction stirred a further 36 hours. The reaction was then cooled and KF_{aq}(15 ml) was added and the reaction stirred a further 20 minutes. It was then extracted between 1:1 hexanes:dichloromethane and H_2O (3x), dried with $MgSO_4$, filtered through Celite and then concentrated. It was purified by chromatography on silica gel column (deactivated with 5%H_2O) using 10:1 hexanes:dichloromethane to elute any remaining septithiophene **105** followed by 10:1, and then 5:1 hexanes:ethyl acetate to elute the product **98** (90 mg, 0.05 mmol, 34%). Dichloromethane was used to elute a later mixture of oligomeric products. The product **98** could be further purified by recrystalization from cyclohexane:dichloromethane to

give dark black crystals, mp, 115-116°C. ^{1}H NMR (500 MHz, $CDCl_3$) δ 9.54 (s, 1H, H-3), 9.16 (s, 1H, H-8), 9.06 (s, 1H, H-1), 8.79 (s, 1H, H-10), 8.63 (s, 1H, H-5), 8.58 (s, 1H, H-6), 8.18 (d, *J* = 8.5 Hz, 1H, H-20), 8.10 (d, *J* = 8.3 Hz, 1H, H-15), 8.02 (d, *J* = 8.3 Hz, 1H, H-17), 7.87 (d, *J* = 7.0 Hz, 1H, H-13), 7.67 (dd, *J* = 8.3, 7.0 Hz, 1H, H-14), 7.57 (dd, *J* = 8, 7 Hz, 1H, H-18), 7.50-7.46 (m, 2H, H-19, H-thienyl), 7.40 (d, *J* = 3.6 Hz, 1H, H-55), 7.37 (d, *J* = 3.7 Hz, 1H, H-27), 7.25-7.22 (m, 4H), 7.20-7.16 (m, 7H), 7.135 (d, *J* = 3.7 Hz, 1H), 7.132 (d, *J* = 3.7 Hz, 1H), 7.12-7.10 (m, 4H), 7.09-7.08 (m, 2H), 7.07 (d, *J* = 3.7 Hz, 1H), 7.06 (d, *J* = 3.7 Hz, 1H), 7.03 (dd, *J* = 5.1, 3.6 Hz, H- 52, 80), 2.80-2.70 (m, 8H, H-82,88,94,100), 1.69 (s, 9H, H-25), 1.65-1.58 (m, 8H, H-83,89, 95,101), 1.52-1.45 (m, 8H, H-84,90,96,102), 1.40-1.33 (m, 16H, H-85,86,91,92,97,98, 103,104), 0.97-0.90 (m, 12H, H-87,93,99,105), -3.29 (s, 3H, H-22), -3.36 (s, 3H, H-23). ^{13}C NMR (125.8 MHz, $CDCl_3$) δ 198.69 (C-11), 152.18 (C-7), 143.05, 142.83, 142.32 (C-5a), 140.73 (C-39,40,68,67), 138.69, 138.59 (C-10d), 138.33 (C-12), 138.23, 137.33, 137.00, 136.57, 136.47, 136.42, 136.31, 136.15, 135.58, 135.44, 135.07 (C-10a), 134.07 (C-16), 132.80 (C-4), 131.56 (C-21), 131.51 (C-3a), 131.11 (C-10), 130.95 (C-15), 130.65, 130.08 (2 of 38,41,66,69), 130.04 (1 of 38,41,66,69), 130.02 (1 of 38,41,66,69), 129.16 (C-27), 128.72 (C-17), 128.51, 128.13, 127.68 (C-13), 127.45, 127.29 (C-1), 127.24, 127.18 (C-19), 126.72, 126.67, 126.63, 126.58 (C-18), 126.37 (C-20), 125.93 (C-3), 125.55 (C-5), 124.98 (C-14), 124.77, 124.63, 124.57, 124.43, 124.28, 124.18, 123.97, 122.84 (C-6), 121.53 (C-8), 36.89 (C-24), 33.82, 32.25, 32.07 (C-10c), 31.91 (C-10b), 31.81 (C-25), 31.76 (C- 2 C's of 91, 92, 85,86, 97,98, 103, 104), 31.74 (C- 2 C's of 91, 92, 85,86, 97,98, 103, 104), 30.87 (C-89,83,95,101), 29.84 (C-90,84,96,102), 28.51 (C-82,88,94,100), 22.88 (C- 4 C's of 91, 92, 85,86, 97,98, 103, 104), 17.07 (C-23), 15.92 (C-

22), 14.35 (C-2 C's of 87,93,99,105), 14.33 (C-2 C's of 87,93,99,105). IR (NaCl, Thin film) ν 3064, 2952, 2925, 2855, 1641, 1548, 1462, 1281, 1237, 788 cm^{-1}. UV-vis (cyclohexane) λ_{max} (ε_{max}, L $mol^{-1}cm^{-1}$) nm, 255 (58800), 401 (87900), 470 (132000), 567 (26300), 704 (3750).

Open CPD Form. Procedure: see (B), p 165. UV-vis (cyclohexane) λ_{max} (ε_{max}, L $mol^{-1}cm^{-1}$) nm, 254 (64400), 458 (119000).

4,9-Dibromo-7-*tert*-butyl-*trans*-10b,10c-dimethyl-2-pyrenoyl-10b,10c-dihydropyrene (88)

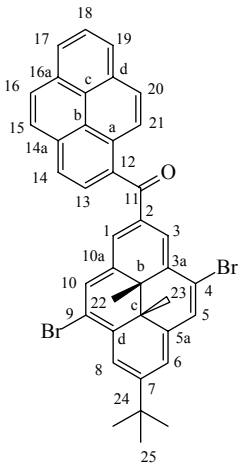

$AlCl_3$ (143 mg, 1.07mmol) was added to a solution of freshly prepared pyrenoyl chloride (275 mg, 1.04 mmol) and the dibromide **85** (302 mg, 0.537 mmol) in dry DCM (30 mL). The solution instantly changed from a dark green to a dark red. The reaction mixture then stirred for 16 hours at 21°C turning a reddish purple. The reaction was quenched with H_2O and extracted between diethylether:10%NaOH (3x) and then H_2O (3x). It was dried with $MgSO_4$ and the solvent evaporated. It was purified by chromatography on alumina (deactivated with 5% H_2O) using 9:1

hexanes:dichloromethane to elute the green starting material **85** (173 mg) and then 3:2 hexanes:dichloromethane to elute closely running green and brown bands of **92** and **93** (148 mg, internal methyl peaks in the ^{1}H NMR at δ -3.50, -3.59, -3.64, -3.69) followed by the desired purple product **88** (123 mg, 0.182 mmol, 34%). The product could be further purified by recrystallization from hexanes as purple crystals, mp 154-156^{o}C dec. ^{1}H NMR (500 MHz, $CDCl_3$) δ 9.46 (s, 1H, H-3), 8.91 (s, 1H, H-1), 8.89 (d, *J* = 1.1 Hz, 1H, H-8), 8.79 (s, 1H, H-10), 8.74 (s, 1H, H-5), 8.56 (s, 1H, H-6), 8.47 (d, *J* = 9.2 Hz, 1H, H-21), 8.32 (m, 3H, H-13), 8.24 (m, 3H), 8.10 (d, *J* = 9.4 Hz, 1H, H-20), 8.09 (t, *J* = 7.6Hz, 1H, H-18), 1.71 (s, 9H, H-25), -3.51 (s, 3H, H-23), -3.58 (s, 3H, H-24). ^{13}C NMR (125.8 MHz, $CDCl_3$) δ 198.88 (C-11), 153.26 (C-7), 141.90 (C-5a), 137.31 (C-10d), 135.49 (C-10a), 134.44, 133.29, 132.58 (C-10), 132.20 (C-2), 131.44 (C-3a), 131.04, 130.27, 129.34, 129.04 (C-20), 128.00 (C-5), 127.62, 127.48, 127.20 (C-1), 126.80 (C-3), 126.66 (C-18), 126.30, 126.16, 125.23 (C-21), 124.84, 124.16, 123.07 (C-8), 122.98 (C-4), 122.57 (C-6), 117.00 (C-9), 37.04 (C-24), 33.54 (C-10b), 33.29 (C-10c), 31.91 (C-25), 16.09 (C-22), 14.89 (C-23). IR (NaCl, Thin film) ν 3042, 2965, 2926, 2900, 2859, 1644, 1548, 1447, 1328, 1269, 1243, 1224, 1145, 1128, 1090, 899, 847, 754 cm^{-1}. UV-vis (cyclohexane) λ_{max} (ε_{max}, L mol^{-1}cm^{-1}) nm, 242 (44700), 266 (24100), 276 (27300), 360 (62400), 388 (26900), 411 (36900), 527 (12100), 604 (1050), 669(363). EI MS, *m/z*, 674 (M^+), 659, 644, 603. HRMS calc'd for $C_{39}H_{30}Br_2O$ 672.0663, found 672.0673.

2-Anthranoyl-4,9-dibromo-7-*tert*-butyl-*trans*-10b,10c-dimethyl-10b,10c-dihydropyrene (90)

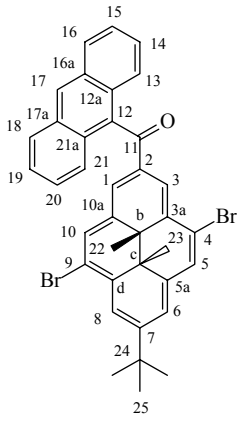

$AlCl_3$ (300 mg, 2.25 mmol) was added to a green solution of the dibromide **85** (0.525 mg, 0.935 mmol) and anthranoyl chloride (0.541g, 2.25 mmol) in dichloromethane (30 mL). The solution stirred for 24 hours at room temperature turning a reddish brown color. It was then poured into hexanes and H_2O and extracted with 10% NaOH, brine and then H_2O. It was dried with $MgSO_4$ and concentrated. The product was purified by chromatography on alumina (deactivated with 5% H_2O) using 20:1 hexanes:ethyl acetate as eluent. Eluting first was the green dibromide starting material **85** (245 mg, 0.435 mmol), eluting second close running green and brown bands of **94** and **95** (157 mg, internal methyl peaks in the ^{1}H NMR δ -3.63, -3.70 and -3.78), eluting third was the product **90** (81 mg, 0.125 mmol, 13%) as a purple powder, mp 227-229^{o}C. ^{1}H NMR (500 MHz, $CDCl_3$) δ 9.56 (br s, 1H, H-3), 8.83 (s, 1H, H-8), 8.73 (s, 1H, H-5), 8.68 (s, 1H, H-17), 8.61 (br s, 1H, H-10), 8.57 (br s, 1H, H-1), 8.53 (s, 1H, H-6), 8.15 (d, *J* = 8.6 Hz, 2H, H-16,18), 7.90 (d, *J* = 8.8, 2H, H-13,21), 7.50 (ddd, *J* = 8.6, 6.6, 1.2 Hz, 2H, H-15,19), 7.37 (ddd, *J* = 8.8, 6.6, 1.3 Hz, 2H, H-14,20), 1.69 (s, 9H, H-25), -3.58 (s, 3H, H-22), -3.60 (s, 3H, H-23). ^{13}C NMR (125.8 MHz, $CDCl_3$) δ 200.47 (C-11), 153.62 (C-

7), 142.15 (C-10a), 137.74 (C-10d), 135.52 (C-5a), 135.14 (C-12), 133.00 (C-10), 131.84 (C-2), 131.77 (C-3a), 131.47 (C-17a,16a), 129.35 (C-21a,12a), 128.99 (C-16,18), 128.76 (C-17), 128.18 (C-5), 127.34 (C-1 br), 126.77 (C-14,20), 125.86 (C-21,13), 125.75 (C-15,19), 125.33 (C-3 br) 123.55 (C-4), 122.92 (C-8), 122.65 (C-6), 116.71 (C-9), 37.05 (C-24), 33.61 (C-10c), 33.29 (C-10b), 31.86 (C-25), 16.24 (C-22), 14.94 (C-23). IR (NaCl, Thin film) ν 3054, 2965, 2926, 2856, 1653, 1646, 1636, 1559, 1540, 1165, 1149, 897, 731 cm^{-1}. EI MS, *m/z*, 650 (M^+), 635 (M^+-CH_3), 620 (M^+-$2CH_3$). UV-vis (cyclohexane) λ_{max} (ε_{max}, L $mol^{-1}cm^{-1}$) nm, 255 (169000), 355 (69200), 365 sh (59000), 386 (43400), 413 (50500), 532 (16100). HRMS calc'd for: $C_{37}H_{30}Br_2O$ ($Br^{79}Br^{81}$), 650.0643; Found, 650.0641. Anal. Calc'd for: $C_{37}H_{30}Br_2O$: C,68.32; H,4.65. Found: C,67.77; H,4.90.

2-Benzoyl-4,9-dibromo-7-*tert*-butyl-*trans*-10b,10c-dimethyl-10b,10c-dihydropyrene (89)

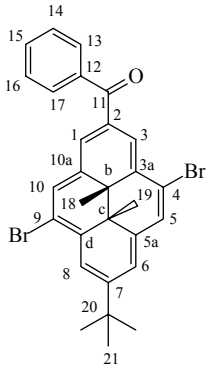

$AlCl_3$ (294 mg, 2.2 mmol) was added to a solution of the dibromide **85** (1.03g, 1.8 mmol) and benzoyl chloride (0.42 mL, 3.6 mmol) in dry dichloromethane (60 mL) and the reaction mixture stirred at 22°C for 36 hours. The reaction was then quenched with H_2O and extracted between hexanes and H_2O (3x), dried with $MgSO_4$ and concentrated.

The dark brown solid was purified by chromatography on alumina (deactivated with 5% H_2O) using 20:1 hexanes:ethyl acetate as eluent. Eluting first was green un-reacted starting material **85**, eluting second was green **91** (227 mg, 0.37 mmol, internal methyl peak in the ^{1}H NMR δ -3.56 br), and eluting third was the desired product **89** as a purple solid (50 mg, 0.09 mmol, 5%), mp 82-84 ^{o}C. ^{1}H NMR (500 MHz, $CDCl_3$) δ 9.30 (s, 1H, H-3), 8.95 (s, 1H, H-1), 8.92 (d, *J* = 1.0 Hz, 1H, H-8), 8.90 (s, 1H, H-10), 8.74 (s, 1H, H-5), 8.57 (s, 1H, H-6), 8.02-8.00 (m, 2H, H-17), 7.68 (*tt*, *J* = 7.4, 1.4 Hz, 1H, H-15), 7.62-7.59 (m, 2H, H-14, 16), 1.71 (s, 9H, H-21), -3.58 (s, 3H, H-19), -3.64 (s, 3H, H-18). ^{13}C NMR (125.8 MHz, $CDCl_3$) δ 197.27 (C-11), 152.79 (C-7), 141.43 (C-5a), 138.93 (C-12), 136.77 (C-10d), 135.41 (C-10a), 132.43 (C-15), 132.01 (C-10), 131.31 (C-3a), 130.56 (C-17,13), 128.59 (C-14,16), 127.84 (C-5), 126.82 (C-3), 126.40 (C-1), 123.09 (C-8), 122.51 (C-6), 122.19 (C-4), 117.06 (C-9), 36.98 (C-20), 33.30 (C-10c), 33.12 (C-10b), 31.92 (C-21), 15.86 (C-18), 14.68 (C-19). IR (NaCl, Thin film) ν 3053, 2965, 2926, 2906, 2867, 1645, 1597, 1550, 1447, 1333, 1273, 1241, 1177, 1102, 901, 738, 721 cm^{-1}. UV-vis (cyclohexane) λ_{max} (ε_{max}, L $mol^{-1}cm^{-1}$) nm, 248 (16600), 339 sh (33200), 357 (71700), 383 sh (21800), 408 (32100), 517 (9770), 603 (701), 670 (562). EI MS, *m/z*, 550 (M^+), 535 (M^+-CH_3), 520 (M^+-$2CH_3$), 479 (M^+-CH_3, - *t*-butyl). HRMS calc'd for $C_{29}H_{26}Br_2O$ 550.0330, found 550.0329.

2,7-Di-*tert*-butyl-*trans*-10b,10c-dimethyl-4-(2-thienylcarbonyloxy)-10b,10c-dihydropyrene (113)

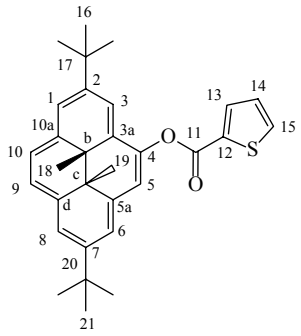

n-BuLi (0.124 mL, 1.93M), was added to a solution of the bromide **31** (102 mg, 0.24 mmol) at -78°C in dry THF (25 mL). The solution was allowed to warm to 22°C over 1 hour whereupon it was cooled to -78°C and 2-thiophenecarbonyl chloride (0.1 mL, 0.94 mmol) was added. The reaction mixture was warmed slowly to 22°C and stirred for 30 hours. It was extracted between hexanes:H_2O (3x) and the green organic layer was dried with $MgSO_4$ and the solvent evaporated to give a green solid. The product was purified by chromatography on silica gel (5% H_2O) using first 6:1 hexanes:dichloromethane to elute a mixture of bromide starting material **31** and DHP **11** and then 2:1 hexanes:dichloromethane to elute next the green ester **113** (37.5 mg, 0.08 mmol). ^{1}H NMR (500 MHz, C_6D_6) δ 8.64 (d, *J* = 0.8 Hz, 1H, H-3), 8.537 (s, 1H, H-1 or 6 or 8), 8.535 (s, 1H, H- 6 or 1 or 8), 8.531 (s, 1H, H-8 or 1 or 6), 8.48 (AB, *J* = 7.8Hz, 1H, H-9 or 10), 8.46 (AB, *J* = 7.8 Hz, 1H, H-10 or 9), 8.35 (s, 1H, H-5), 8.22 (dd, *J* = 3.7, 1.3 Hz, 1H, H-13), 7.76 (dd, *J* = 5.1, 1.3 Hz, 1H, H-15), 7.29 (dd, *J* = 5.1, 3.7 Hz, 1H, H-14), 1.66 (s, 9H, H-21), 1.62 (9H, H-16), -3.76 (s, 3H, H-19), -3.81 (s, 3H, H-18). ^{13}C NMR (125.8 MHz, C_6D_6) δ 162.00 (C-11), 146.94 (C-7), 145.71 (C-2), 141.67 (C-4), 137.59 (C-10d), 136.49 (C-5a), 135.96 (C-10a), 134.85 (C-13), 133.62 (C-15,C-12),

128.46 (C-14), 125.41 (C-3a), 123.80 (C-9 or 10), 123.40 (C-10 or 9), 121.54 (C-6), 121.32 (C-8), 121.21 (C-1), 116.88 (C-5), 114.85 (C-3), 36.30 (C-17 or 20), 36.24 (C-20 or 17), 32.13 (C-16 or 21), 32.09 (C-21 or 16), 30.15 (C-10c), 29.97 (C-10b), 14.87 (C-19), 14.39 (C-18). IR (KBr) ν 2962, 1719, 1416, 1356, 1250, 1063, 883, 726 cm^{-1}. UV-vis (cyclohexane) λ_{max} (ε_{max}, L $mol^{-1}cm^{-1}$) nm, 245 (13900), 345 (73800), 383 (34800), 457 (6340), 479 (8420), 649 (1230). EI MS, *m/z*, 470 (M^+), 455 (M^+-CH_3), 440 (M^+-$2CH_3$). HRMS calc'd for $C_{31}H_{34}O_2S$ 470.2279, found 470.2290.

2,7-Di-*tert*-butyl-10-(N-methylcarbamoyl)-*trans*-12c,12d-dimethyl-12c,12d-dihydrobenzo[e]pyrene (55)

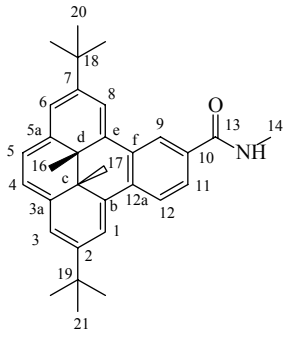

$Fe_2(CO)_9$ (266mg, 0.73mmol) was added to a solution of **51** (252 mg, 0.51 mmol) in degassed benzene (100mL) and the reaction mixture was heated at reflux for 3 hours turning from green to red. The product was filtered through a short silica gel column (5% H_2O deactivated) using benzene followed by 1:1 benzene:ethyl acetate as eluent. Numerous products were observed. The product was purified by chromatography on silica gel using hexanes:ethyl acetate (3:1 followed by 2:1 followed by 1:1) as eluent. The major product was found to be the amide **55** (77mg, 0.17mmol), mp 198-200 dec. A small amount of the intact Weinreb amide **54** (28mg, 0.06 mmol) and the alcohol **56**

(20mg, 0.05 mmol, EIMS *m/z* 467) were also isolated. ^{1}H NMR (500 MHz, C_6D_6) δ 9.30 (s, 1H, H-9), 8.83 (d, *J* = 8.6 Hz, 1H, H-12), 8.44 (s, 1H, H-8), 8.39 (s, 1H, H-1), 7.90 (d, *J* = 8.4 Hz, 1H, H-11), 7.46 (s, 1H, H-3 or 6), 7.45 (s, 1H, H-6 or 3), 7.23 (brs, 2H, H-4,5), 6.48 (brs, 1H, N-H), 3.15 (d, *J* = 4.3 Hz, 3H, H-14), 1.52 (s, 18H, H-20,21), -1.69 (s, 6H, H-16,17). ^{13}C NMR (125.8 MHz, C_6D_6) δ 169.06 (C-13), 145.00 (C-2 or 7), 144.58 (C-7 or 2), 138.81 (C-3a or 5a),138.31 (C-5a or 3a), 134.61 (C-12e), 134.05 (C-12b), 131.49 (C-12a), 131.37 (C-10), 129.15 (C-12f), 125.00 (C-12), 124.44 (C-9), 122.86 (C-11), 121.93 (C-4 or 5), 121.55 (C-5 or 4), 120.95 (C-3 or 6), 120.50 (C-6 or 3), 118.79 (C-1), 118.08 (C-8), 35.73 (C-18 or 19), 35.65 (C-19 or 18), 35.21 (C-12c or 12d), 35.10 (C-12d or 12c), 30.96 (C-20 or 21), 30.92 (C-21 or 20), 27.26 (C-14), 17.47 (C-16,17). IR (NaCl, Thin film) ν 3283, 2963, 2921, 2901, 2864, 1635, 1540, 1477, 1362, 875 cm^{-1}. UV-vis (cyclohexane) λ_{max} (ε_{max}, L $mol^{-1}cm^{-1}$) nm, 258 (12900), 325 (25600), 342 (23700), 377 (25600), 396 (34300), 516 (5930), 626 (844). EI MS, *m/z*, 451 (M^+), 436 (M-CH_3), 421 (M-2CH_3), 380 (M-CH_3, *t*-butyl). HRMS calc'd for $C_{32}H_{37}NO$ 451.2875, found 451.2866.

2,7-Di-*tert*-butyl-*trans*-10b,10c-dimethyl-4-(2-thienylethynyl)-10b,10c-dihydropyrene (112)

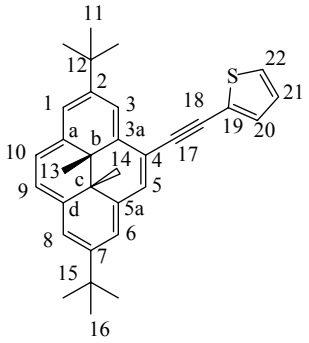

LDA (1.14 mL, 2.3 mmol) was added to a solution of the acetylene **110** (630 mg, 1.71 mmol) in dry THF (30 mL) at -78^{o}C and then the solution warmed to -10^{o}C over 30 minutes. It was then cooled to -78^{o}C and $SnBu_3Cl$ (0.696 mL, 2.5 mmol) was added. The solution was then warmed to 22^{o}C over 30 minutes and then the solvent was evaporated. It was purified by chromatography on alumina (deactivated with 5% H_2O) using hexanes and 1% triethylamine. The product from this reaction **111**, 2-bromothiophene (0.32 mL, 3.33 mmol), $Pd_2(dba)_3$ (16 mg, 0.017 mmol) and dppf (19 mg, 0.034) were dissolved in dry THF (10 mL) and heated to reflux for 48 hours. The reaction mixture was then cooled to 22^{o}C and aq.KF (10 mL) was added and stirred for 10 minutes. The reaction mixture was extracted between hexanes:H_2O using a minimal amount of DCM to aid solubility, dried with $MgSO_4$, filtered through Celite and then concentrated. The solid was purified first using 10:1 hexanes:dichloromethane to give first the product **112** as an impure mixture followed by a black polymeric product. The product **112** was then further purified by chromatography on alumina (deactivated with 5% H_2O) using hexanes as eluent to give **112** as a green solid (206.5 mg, 0.459 mmol, 27%). A small portion of the product **112** was further purified by recrystallization from

cyclohexanes as dark green crystals, mp 168-170°C. ^{1}H NMR (500 MHz, $CDCl_3$) δ 9.12 (d, *J* = 1.3 Hz, 1H, H-3), 8.68 (s, 1H, H-5), 8.59 (d, *J* = 1.1 Hz, 1H, H-1), 8.56 (s, 2H, H-8,6), 8.50 (d, *J* = 1.3 Hz, 2H, H-9,10), 7.52 (dd, *J* = 3.6, 1.1 Hz, 1H, H-20), 7.39 (dd, *J* = 5.2,1.1 Hz, 1H, H-22), 7.14 (dd, *J* = 5.2, 3.6 Hz, 1H, H-21), 1.78 (s, 9H, H-11), 1.72 (s, 9H, H-16), -3.78 (s, 6H, H-13,14). ^{13}C NMR (125.8 MHz, $CDCl_3$) δ 147.56 (C-2), 146.51 (C-7), 138.59 (C-10a or d), 137.74 (C-3a), 137.19 (C-10d or 10a), 136.01 (C-5a), 131.43 (C-20), 127.49 (C-21), 127.10 (C-22), 125.16 (C-5), 124.68 (C-19), 124.24 (C-9), 123.67 (C-10), 122.10 (C-6), 121.64 (C-1), 121.29 (C-8), 119.76 (C-3), 113.88 (C-4), 94.59 (C-17), 88.07 (C-18), 36.49 (C-12), 36.15 (C-15), 32.15 (C-11), 32.09 (C-16), 30.67 (C-10b), 29.75 (C-10c), 15.22 (C-13 or 14), 14.87 (C-14 or 13). IR (NaCl, Thin film) ν 3039, 2963, 2917, 2901, 2886, 2187, 1594, 1477, 1461, 1383, 1361, 1344, 1256, 1231, 887, 698 cm^{-1}. UV-vis (cyclohexane) λ_{max} (ε_{max}, L $mol^{-1}cm^{-1}$) nm, 250 (14900), 289 (9640), 359 (61500), 400 (59800), 475 (9930), 497 (10300), 666 (2040). EI MS, *m/z*, 450 (M^+), 420, 379, 323. HRMS calc'd for $C_{32}H_{34}S$ 450.2328, found 450.2370.

2,7-Di-*tert*-butyl-*trans*-10b,10c-dimethyl-4-tributylstannyl-10b,10c-dihydropyrene (32)

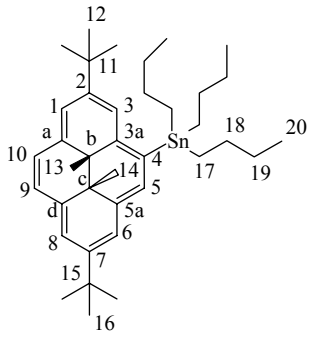

n-BuLi was added to a solution of the bromide **31** (168 mg, 0.40mmol) in dry THF at -78°C which turned the solution from green to red. The solution was stirred for 30 minutes at -78°C and then $SnBu_3Cl$ was added (0.129 mL, 0.48 mmol) which turned the solution a dark green. The solution stirred for 1 hour warming to 22°C. It was then poured into hexanes and washed with water (3x), dried with $MgSO_4$ and the solvent evaporated to give a green oil. The product was purified by chromatography on alumina (5% H_2O deactivated) using hexanes and 1% triethylamine as eluent to obtain the product as a green solid (200mg, 0.32 mmol, 80%). The product could be further purified by recrystallization from acetonitrile to give a green powder, mp 84-87°C. ^1H NMR (500 MHz, C_6D_6) δ 9.02 (s, 1H, H-5), 8.81 (s, 1H, H-3), 8.72 (s, 1H, H-6), 8.67 (s, 1H, H-1), 8.66 (s, 1H, H-8), 8.51 (s, 2H, H-9,10), 1.89-1.76 (m, 6H, H-18), 1.75 (s, 9H, H-12), 1.63 (s, 9H, H-16), 1.63-1.58 (m, 6H, H-17), 1.44 (sextet, J = 7.4, 6H, H-19), 0.86 (t, J = 7.4, 9H, H-20) -3.607 (s, 3H, H-13), -3.613 (s, 3H, H-14). ^{13}C NMR (125.7 MHz, C_6D_6) δ 146.18 (C-7), 145.86 (C-2), 143.97 (C-3a), 139.00 (C-10a), 138.41 (C-4), 137.33 (C-10d), 137.00 (C-5a), 132.70 (C-5), 124.05 (C-3), 123.66 (C-9 or 10), 123.64 (C-10 or 9), 121.63 (C-8), 121.43 (C-1), 121.26 (C-6), 36.56 (C-11), 36.41 (C-15), 32.51 (C-12), 32.41 (C-16), 32.09 (C-10b), 30.55 (C-10c), 30.28 (C-18), 28.15 (C-19), 15.55 (C-13), 15.23 (C-14), 14.28 (C-20), 11.77 (C-17). UV-vis (cyclohexane) λ_{max} (ε_{max}, L $mol^{-1}cm^{-1}$) nm, 242sh (11400), 330sh (41600), 347 (125000), 361 (41400), 387 (69500), 438sh (7360), 464sh (11700), 485 (14500), 648 (1590). IR (NaCl, Thin film) ν 3037, 2965, 2924, 2869, 1591, 1463, 1231, 1070, 884 cm^{-1}. EIMS, *m/z* 634 (M^+), 391. HRMS calc'd for $C_{38}H_{58}Sn$ 634.3560, found 634.3568. Anal. Calc'd for $C_{38}H_{58}Sn$: C,72.04; H, 9.23. Found: C, 71.70; H, 8.81.

7-*tert*-Butyl-*trans*-10b,10c-dimethyl-2-naphthoyl-4,9-diphenyl-10b,10c-dihydropyrene (100)

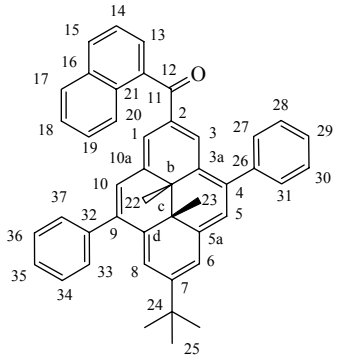

Palladium tetrakis(triphenylphosphine) (11mg, 0.01mmol) was added to a solution of the bromide **84** (111mg, 0.19 mmol) and phenylboronic acid (68mg, 0.56 mmol) in 5mL DME and 4mL sat. Na_2CO_3. The solution was heated to a reflux for 24 hours with vigorous stirring. The product was then poured into hexanes and washed with water (3x) dried with $MgSO_4$ and concentrated. It was purified by chromatography on silica gel (deactivated with 5% H_2O) using 10:1 hexanes:EtOAc to elute the product as a purple solid (115mg, 0.19mmol, 100%). The product could be further purified by recrystalization from methanol to give **84** as dark purple crystals, mp. 203-204 ^oC. ^1H NMR (500 MHz, C_6D_6) δ 9.11 (s, 1H, H-3), 9.01 (s, 1H, H-1), 8.69 (s, 1H, H-8), 8.66 (s, 1H, H-10), 8.56 (s, 1H, H-6), 8.51 (s, 1H, H-5), 8.12 (d, *J* = 8.6 Hz, 1H, H-20), 8.03 (d, *J* = 8.2 Hz, 1H, H-15), 7.98 (d, *J* = 8.2 Hz, 1H, H-17), 7.79 (brd, *J* = 7.2 Hz, 3H, H-13,33,37), 7.70 (d, *J* = 6.7 Hz, 2H, H-31,27), 7.63-7.57 (m, 3H, H-34,35,36), 7.56-7.48 (m, 2H, H-14,18), 7.48-7.40 (m, 4H, H-19,28,29,30), 1.60 (s, 9H, H-25), -3.40 (s, 3H, H-

23), -3.47 (s, 3H, H-22). ^{13}C NMR (125.8 MHz, C_6D_6) δ 198.89 (C-11), 151.38 (C-7), 142.12 (C-5a), 141.88 (C-32), 141.67 (C-26), 141.45 (C-4), 138.68 (C-10d), 138.51, 135.66 (C-9), 134.77 (C-10a), 133.98 (C-16), 131.69 (C-3a), 131.55, 131.16 (C-33,37), 131.11 (C-10), 130.99 (C-27,31), 130.71 (C-15), 129.97, 128.62 (C-17), 128.56 (C-34,36), 128.48 (C-28,30), 127.69, 127.59 (C-29), 127.46 (C-13), 126.98 (C-19), 126.70 (C-1), 126.43, 126.38 (C-20), 125.84 (C-3), 125.70 (C-5), 124.81 (C-35), 122.08 (C-6), 121.12 (C-8), 36.72 (C-24), 31.80 (C-25), 31.74 (C-10b), 31.48 (C-10c), 16.78 (C-22), 15.48 (C-23). IR (NaCl, Thin film) ν 3055, 2963, 2922, 2865, 1640, 1547, 1284, 1234, 1137, 783, 701 cm^{-1}. UV-vis (cyclohexane) λ_{max} (ε_{max}, L mol^{-1}cm^{-1}) nm, 222 (67500), 273 (16900), 363 (67400), 396 (25200), 419 (49800), 537 (13700), 676 (640).
EI MS, *m/z*, 594 (M^+), 579 (M^+-CH_3), 564 (M^+-$2CH_3$), 523 (M^+-CH_3,-*t*-butyl).
HRMS calc'd for $C_{45}H_{35}O$ 594.2922, found 594.2935.

Open CPD Form. Procedure: see (A,B), p 165. ^{1}H NMR (500 MHz, C_6D_6) δ 8.02 (d, *J* = 7.6 Hz, 1H), 7.91 (d, *J* = 8.1 Hz, 1H), 7.87-7.85 (brd, *J* = 7.3 Hz, 1H), 7.56-7.51 (m, 4H), 7.49-7.42 (m, 4H), 7.36-7.29 (m, 7H), 7.17 (d, *J* = 1.4 Hz, 1H), 6.83 (d, *J* = 2.0 Hz, 1H), 6.67 (s, 1H), 6.58 (d, *J* = 2.0 Hz, 1H), 6.52 (s, 1H), 1.76 (s, 3H), 1.73 (s, 3H), 1.17 (s, 9H). UV-vis (cyclohexane) λ_{max} (ε_{max}, L mol^{-1}cm^{-1}) nm, 222 (82800), 272 (47800), 307 (27800).

3”’,4”’-Dihexyl-2-tributylstannyl-5,2’:5’,2”,5”,2”’:5”’,2””:5””’,2”””-septithiophene (**106**)

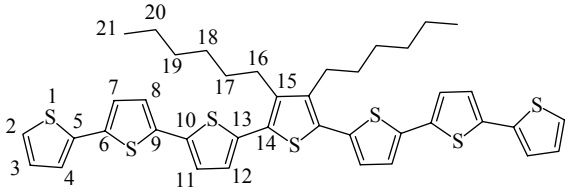

The catalyst $Pd_2(dba)_3$ (68 mg, 0.07 mmol) and dppf (82 mg, 0.14 mmol) were added to a solution of 2-tributylstannyl-5,2’:5’,2”-terthiophene **108** (2g, 3.72 mmol) and 2,5-dibromo-3,4-dihexylthiophene **35** (651 mmol, 1.6 mmol) in dry THF (10 mL). The solution was stirred at reflux for 2 days turning from yellow to a dark red. The solution was then cooled and aq. KF (10 mL) was added and the solution stirred a further 10 minutes. It was then filtered through Celite, extracted between diethyl ether and water (3x), dried with $MgSO_4$ and concentrated. The product was purified by column chromatography on silica gel using 10:1 hexanes:dichloromethane. The desired product was eluted first as an impure orange red solid followed by longer oligomers as red solids. The product was then recrystallized from DCM and EtOH to give the desired product as a red powder (400 mg, 0.536 mmol, 34%) mp, 108-111^{o}C. ^{1}H NMR (500 MHz, $CDCl_3$) δ 7.23 (dd, J = 5.1, 1.2 Hz, 2H, H-2), 7.18 (dd, J = 3.6, 1.2 Hz, 2H, H-4)), 7.12 (d, J = 3.8 Hz, 2H, H-11), 7.10 (AB, J = 3.8 Hz, 2H, H-8), 7.09 (AB, J = 3.8 Hz, 2H, H-7), 7.05 (d, J = 3.8 Hz, 2H, H-12), 7.03 (dd, J = 5.1, 3.6 Hz, 2H, H-3), 2.75-2.71 (m, 4H, H-16), 1.65-1.56 (m, 4H, H-17), 1.48-1.42 (m, 4H, H-18), 1.38-1.32 (m, 8H, H-19,20), 0.96-0.89 (m, 6H, H-21).

^{13}C NMR (125.8 MHz, $CDCl_3$) δ 140.65 (C-15), 137.32 (C-5), 136.93 (C-10), 136.52 (C-6), 136.12 (C-9), 135.42 (C-13), 130.00 (C-14), 128.12 (C-3), 126.60 (C-12), 124.74 (C-2), 124.61 (C-7 or 8), 124.39 (C-8 or 7), 124.14 (C-11), 123.94 (C-4), 31.71 (C-19 or 20), 30.83 (C-17), 29.82 (C-18), 28.47 (C-16), 22.86 (C-20 or 19), 14.32 (C-21). IR (NaCl, thin film) ν 3066, 2954, 2924, 2855, 1492, 1455, 1425, 832, 790, 685 cm^{-1}. UV-vis (cyclohexane) λ_{max} (ε_{max}, L $mol^{-1}cm^{-1}$) nm, 255 (23100), 412 (49400). EI MS, *m/z*, 744 (M^+). HRMS calc'd for $C_{40}H_{40}S_7$ 744.1175, found, 744.1144.

2,7-Di-*tert*-butyl-*trans*-10b,10c-dimethyl-9,4-di-(2-5,2':5',2"-terthienyl)-10b,10c-dihydropyrene (101)

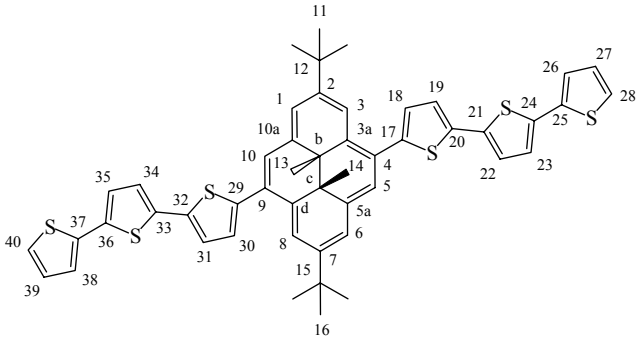

$Pd_2(dba)_3$ (45mg, 0.05 mmol) and dppf (55mg, 0.1 mmol) were added to a solution of the bromide **85** (500mg, 1mmol), and 2-tributylstannyl-5,2':5',2"-terthiophene **108** (1.6g, 3mmol) in dry THF (5mL). The solution was then heated to a reflux for 3 days turning from green to a dark red. After cooling KF (15mL, 1M) was added and the solution stirred a further 15 minutes. It was then filtered through Celite, extracted between DCM:H_2O (3x), dried with $MgSO_4$, filtered again through Celite and concentrated. The product was purified on silica gel (5% H_2O) using hexanes to elute

first the excess terthiophene and then 10:1 hexanes:dichloromethane to elute second a mixture of the mono and di terthienyl product, followed by the pure di-terthienyl product as a red powder **101** (571 mg, 0.68mmol, 68 %). The product could be further purified be recrystallization from hexanes:dichloromethane:methanol, mp 217 ^{o}C dec. ^{1}H NMR (500 MHz, $CDCl_3$) δ 9.13 (s, 2H, H-3,8), 8.61 (s, 2H, H-5,10), 8.55 (s, 2H, H-1,6), 7.53 (d, J = 3.6 Hz, 2H, H-18,30), 7.40 (d, J = 3.6 Hz, 2H, H-19,31), 7.25 (dd, J = 5.1, 1.1 Hz, 2H, H-28,40), 7.23 (dd, J = 3.6, 1.1 Hz, 2H, H-26, 38), 7.22 (d, J = 3.7 Hz, 2H, H-22,34), 7.16 (d, J = 3.8 Hz, 2H, H- 23, 35), 7.06 (dd, J = 5.1, 3.6 Hz, 2H, H-27,39), 1.68 (s, 18H, H-11,16), -3.57 (s, 6H, H-13,14). ^{13}C NMR (125.8 MHz, $CDCl_3$) δ 147.01 (C-2,7), 143.89 (C-17,29), 137.25 (C-20,32), 37.16 (C-25,37), 136.95 (C-10a,5a), 136.53 (C-21,33), 135.97 (C-24,36), 133.49 (C-3a,10d), 127.83 (C-27,39), 127.65 (C-18,30), 126.32 (C-9,4), 125.08 (C-5,10), 124.41 (C-23,35), 124.39 (C-28,40), 124.14 (C-19,31), 123.92 (C-26,38), 123.62 (C-22,34), 121.90 (C-1,6), 120.32 (C-3,8), 36.14 (C-12,15), 31.69 (C-11,16), 30.65 (C-10b,10c), 15.16 (C-13,14). IR (NaCl, Thin film) cm^{-1}: 2952, 2915, 2845, 1579, 1464, 1280, 1117. UV-vis (cyclohexane) λ_{max} (ε_{max}, L $mol^{-1}cm^{-1}$) nm, 245 (29500), 317 sh (31300), 370 (53200), 432 (104000), 528 (30300), 678 (3750). LSIMS, *m/z*, 836 (M^+), 821 (M^+-CH_3), 806 (M^+-$2CH_3$). Anal. Calc'd for $C_{50}H_{44}S_6$: C,71.73; H,5.30. Found: C, 71.16; H, 5.27.

References

(1) Fritzsche, J. *Compte. Rend. Acad. Sci.* **1867**, *69*, 1035-1037.

(2) ter Meer, E. *Ann. Chem.* **1876**, *181*, 1-22.

(3) Y.Hirshberg *Compt. Rend. Acad. Sci.* **1950**, *231*, 903-907.

(4) Bouas-Laurent, H.; Durr, H. *Pure Appl. Chem.* **2001**, *73*, 639-665.

(5) Kumar, G. S.; Neckers, D. C. *Chem.Rev.* **1989**, *89*, 1915-1925.

(6) DeLang, J. J.; Robertson, J. M.; Woodward, I. *Proc. R. Soc. London, Sect. A* **1939**, *171*, 398-410.

(7) Hugel, T.; Holland, N. B.; Cattani, A.; Moroder, L.; Seitz, M.; Gaub, H. E. *Science* **2002**, *296*, 1103-1106.

(8) Banghart, M.; Borges, K.; Isacoff, E.; Trauner, D.; Kramer, R. *Nature Neuroscience* **2004**, *7*, 1381-1386.

(9) Higgins, S. *Chem. Brit.* **2003**, *6*, 26-29.

(10) Ata, A.; Bates, K.; Benniston, A. C.; Lawrie, D. J.; Soubeyrand-Lenoir, E. *Tetrahedron Lett.* **2003**, *44*, 8245-8247.

(11) Benniston, A. C. *Chem. Soc. Rev.* **2004**, *33*, 573-578.

(12) Irie, M.; Mohri, M. *J. Org. Chem.* **1988**, *53*, 803-808.

(13) Irie, M. *Chem. Rev.* **2000**, *100*, 1685-1716.

(14) Irie, M.; Matsuda, K. *J. Photochem. Photobiol. C.* **2004**, *5*, 169-182.

(15) Matsuda, K.; Irie, M. *J. Am. Chem. Soc.* **2000**, *122*, 7195-7201.

(16) Matsuda, K.; Irie, M. *J. Am. Chem. Soc.* **2000**, *122*, 8309-8310.

(17) Matsuda, K.; Irie, M. *Polyhedron* **2005**, *24*, 2477-2483.

(18) Blattman, H. R.; Meuch, D.; Heilbronner, E.; Molyneux, R. G.; Boekelheide, V. J. *J. Am. Chem. Soc.* **1965**, *87*, 130-131.

(19) Boekelheide, V. J.; Phillips, J. *J. Am. Chem. Soc* **1967**, *89*, 1695-1704.

(20) Mitchell, R. H. In *Advances in Theoretically Interesting Molecules*; Thummel, R. P., Ed.; JAI Press: 1989; Vol. 1, p 135-199.

(21) Tashiro, M.; Yamato, T. *J. Am. Chem. Soc.* **1982**, *104*, 3701-3707.

(22) Mitchell, R. H.; Ward, T. R.; Chen, Y.; Wang, Y.; Weerawarna, S. A.; Dibble, P. W.; Marsella, M. J.; Almutairi, A.; Wang, Z. *J.Am.Chem.Soc.* **2003**, *125*, 2974-2988.

(23) Sheepwash, M. A. L.; Mitchell, R. H.; Bohne, C. J. *J. Am. Chem. Soc.* **2002**, *124*, 4693-4700.

(24) Ayub, K.; Zhang, R.; Robinson, S. G.; Twamley, B.; Williams, R. V.; Mitchell, R. H. *J. Org. Chem.* **2008**, *73*, 451-456.

(25) Mitchell, R. H.; Bohne, C. J.; Robinson, S. G.; Yang, Y. *J. Org. Chem* **2007**, *72*, 7939-7946.

(26) Shirakawa, H. L. E.; MacDiarmid, A.; Chiang, C.; Heeger, A. *Chem. Commun.* **1977**, 578-580.

(27) Dissado, L. A.; Fothergill, J. C. *Electrical Degradation and Breakdown in Polymers*; Peter Peregrinus Ltd: Wiltshire, 1992.

(28) Moliton, A.; Hiorns, R. C. *Polym. Int.* **2004**, *53*, 1397-1412.

(29) Bredas, J. L.; Street, G. B. *Acc. Chem. Res.* **1985**, *18*, 309-315.

(30) Ferraro, J. R.; Williams, J. M. *Introduction to Synthetic Electrical Conductors*; Academic Press, Inc: Toronto, 1987.

(31) Pud, A.; Ogurtsov, N.; Korzhenko, A.; Shapoval, G. *Prog. Polym. Sci.* **2003**, *28*, 1701-1753.

(32) Hoeve, W.; Wynberg, H.; Havinga, E. E.; Meijer, E. W. *J. Am. Chem. Soc.* **1991**, *113*, 5887-5889.

(33) Bumm, L. A.; Arnold, J. J.; Cygan, M. T.; Dunbar, T. D.; Burgin, T. P.; Jones, L.; Allara, D. L.; Tour, J. M.; Weiss, P. S. *Science* **1996**, *271*, 1705-1707.

(34) Blum, A. S.; Kushmerick, J. G.; Pollack, S. K.; Yang, J. C.; Moore, M.; Naciri, J.; Shashidhar, R.; Ratna, B. R. *J. Phys. Chem. B.* **2004**, *108*, 18124-18128.

(35) Jorissne, J. In *Encyclopedia of Electrochemistry:Organic Electrochemistry*; Schafer, H. J., Ed.; Wiley VCH: Weinheim, 2004; Vol. 8, p 61.

(36) Connelly, N. G.; Geiger, W. E. *Chem. Rev.* **1996**, *96*, 877-910.

(37) Ofer, D.; Crooks, R. M.; Wrighton, M. S. *J. Am. Chem. Soc.* **1990**, *112*, 7869-7879.

(38) Paul, E. W.; Ricco, A. J.; Wrighton, M. S. *J. Phys. Chem.* **1985**, *89*, 1441-1447.

(39) Kittlesen, G. P.; White, H. S.; Wrighton, M. S. *J. Am. Chem. Soc.* **1984**, *106*, 7389-7396.

(40) Gilat, S., L; Kawai, S., H; Lehn, J.-M. *Chem. Commun.* **1993**, 1439-1442.

(41) van der Veen, M. H.; Rispens, M. T.; Jonkman, H. T.; Hummelen, J. C. *Adv. Funct. Mater.* **2004**, *14*, 215-223.

(42) Irie, M.; Eriguchi, T.; Takada, T.; Uchida, K. *Tetrahedron,* **1997**, *53*, 12263-12271.

(43) Tanifuji, N.; Irie, M.; Matsuda, K. *Chem Lett.* **2005**, *34*, 1580-1581.

(44) Marsella, M. J.; Wang, Z.; Mitchell, R. H. *Org. Lett.* **2000**, *2*, 2979-2982.

(45) Kawai, T.; Kunitake, T.; Irie, M. *Chem Lett.* **1999**, 905-906.

(46) Choi, H.; Lee, H.; Kang, Y.; Kim, E.; Kang, S. O.; Ko, J. *J. Org. Chem.* **2005**, *70*, 8291-8297.

(47) Dulic, D.; van der Molen, S. J.; Kudernac, T.; Jonkman, H. T.; de Jong, J. J. D.; Bowden, T. N.; van Esch, J.; Feringa, B. L.; van Wees, B. J. *Phys. Rev. Lett.* **2003**, *91*, 207402 1-4.

(48) Katsonis, T.; Kudernac, T.; Walko, M.; van der Molen, S. J.; van Wees, B. J.; Feringa, B. L. *Adv. Mat.* **2006**, *18*, 1397-1400.

(49) Xu, B.; Tao, N. J. *Science.* **2003**, *301*, 1221-1223.

(50) He, J.; Chen, F.; Liddell, P., A; Andreasson, J.; Straight, S. D.; Gust, D.; Moore, T. A.; Moore, A. L.; Li, J.; Sankey, O. F.; Lindsay, S. M. *Nanotechnology.* **2005**, *16*, 695-702.

(51) Whalley, A.; Steigerwald, M. L.; Guo, X.; Nuckolls, C. *J. Am. Chem. Soc.* **2007**, *129*, 12590-12591.

(52) Mitchell, R. H.; Bohne, C.; Wang, Y.; Bandyopadhyay, S.; Wozniak, C. *J. Org. Chem* **2005**, *71*, 327-336.

(53) Ward, T. R. Ph.D. Thesis, University of Victoria, 2000.

(54) Geldard, J. F.; Lions, F. *J. Org. Chem.* **1965**, *30*, 318-319.

(55) Rio, G.; Scholl, M. J. *Chem. Commun.* **1975**, *12*, 474.

(56) Gollnick, K.; Griesbeck, A. *Tetrahedron.* **1985**, *41*, 2057-2068.

(57) Pu, C. In *Ph.D Thesis*; National University of Singapore: Singapore, 1992, p 140.

(58) Arnbjerg, J.; Paterson, M. J.; Nielsen, C.; Jorgensen, M.; Christiansen, O.; Ogilby, P. R. *J. Phys. Chem. A.* **2007**, *111*, 5756-5767.

(59) Cerfontain, H.; Telder, A. K.; Bakker, B. H.; Mitchell, R. H.; Tashiro, M. *Liebigs. Ann. Recueil.* **1996**, *5*, 873-878.

(60) Meunier, S.; Siaugue, J. M.; Sawicki, M.; Calbour, F.; Dezard, S.; Taran, F.; Mioskowski, C. *J. Comb. Chem.* **2003**, *5*, 201-204.

(61) Delamarche, I.; Mosset, P. *J. Org. Chem.* **1994**, *59*, 5453-5547.

(62) M, B. W.; Collins, P. A.; McCulloch, R. K.; Wege.D *Aust. J. Chem* **1982**, *35*, 843-848.

(63) Zhang, R.; Fan, W.; Twamley, B.; Berg, D. J.; Mitchell, R. H. *Organometallics* **2007**, *26*, 1888-1894.

(64) Phelan, N. F.; Orchin, M. *J. Chem. Ed.* **1968**, *45*, 633-637.

(65) Klokkenbur, M.; Lutz, M.; Spek, A. L.; van der Maas, J. H.; van Walree, C. A. *Chem. Eur. J.* **2003**, *9*, 3544-3554.

(66) Fang, Q.; Yamamoto, T. *Polymer* **2003**, *44*, 2947-2956.

(67) A, M.; Yamamoto, T. *Synth. Met.* **2006**, *156*, 1390-1395.

(68) Lee, H.-W.; Robinson, S. G.; Bandyopadhyay, S.; Mitchell, R. H.; Sen, D. *J. Mol. Biol.* **2007**, *371*, 1163-1173.

(69) Mitchell, R. H.; Chen, Y. *Tet.Lett* **1996**, *37*, 5239-5242.

(70) Donat-Bouillud, A.; Mazerolle, L.; Gagnon, P.; Goldenberg, L.; Petty, M. C.; Leclerc, M. *Chem. Mater.* **1997**, *9*, 2815-2821.

(71) Barbarella, G.; Faveretto, L.; Sotgiu, G.; Zambianchi, M.; Arbizzani, C.; Bongini, A.; Mastragostino, M. *Chem. Mater.* **1999**, *11*, 2533-2541.

(72) Barbarella, G.; Faveretto, L.; Sotgiu, G.; Zambianchi, M.; Fattori, V.; Cocchi, M.; Cacialli, F.; Gigli, G.; Cingolani, R. *Adv. Mater.* **1999**, *11*, 1375-1379.

(73) Blattmann, H. R.; Schmidt, W. *Tetrahedron* **1970**, 5885-5899.

(74) Boggio-Psqua, M.; Bearpark, M. J.; Robb, M. A. *J. Org. Chem.* **2007**, *72*, 4497-4503.

(75) Song, K. S.; Liu, L.; Guo, Q. X. *J. Org. Chem.* **2003**, *68*, 4604-4607.

(76) Herny, D. J.; Parkinson, C., J; Mayer, P. M.; Radom, L. *J. Phys. Chem. A.* **2001**, *105*, 6750-6756.

(77) Williams, R. V.; Edwards, W. D.; Mitchell, R. H.; Robinson, S. G. *J. Am. Chem. Soc* **2005**, *127*, 16207-16214.

(78) Huisman, C. L.; Huijser, A.; Donker, H.; Schoonman, J.; Goosens, A. *Macromolecules* **2004**, *37*, 5557-5564.

(79) Wochnowski, C.; Metev, S. *Applied Surface Science* **2002**, *186*, 34-39.

(80) McCullough, R. D.; Lowe, R. D.; Jayaraman, M.; Anderson, D. L. *J. Org. Chem* **1993**, *58*, 904-912.

(81) Roncali, J. *Chem. Rev.* **1992**, *92*, 711-738.

(82) Becker, R. S.; de Melo, J. S.; Macanita, A. L.; Elisei, F. *J. Phys. Chem.* **1996**, *100*, 18683-18695.

(83) Izumi, T.; Kobashi, S.; Takimiya, K.; Aso, Y.; Otsubo, T. *J. Am. Chem. Soc.* **2003**, *125*, 5286-5287.

(84) Kim, Y.; Bouffard, J.; Kooi, S. E.; Swager, T. M. *J. Am. Chem. Soc.* **2005**, *127*, 13726-13731.

(85) Cheylan, S.; Fraleoni-Morgera, A.; Puigdollers, J.; Vox, C.; Setti, L.; Alcubilla, R.; Badenes, G.; Costa-Bizzarri, P.; Lanzi, M. *Thin Sol. Films.* **2006**, *497*, 16-19.

(86) Roncali, J.; Gorgues, A.; Jubault, M. *Chem. Mater.* **1993**, *5*, 1456-1464.

(87) Bauerle, P. In *Electronic Materials: The Oligomer Approach*; Mullen, K., Wegner, G., Eds.; Wiley-VCH: Toronto, 1998, p 130-131.

(88) Asavapiriyanont, S.; Chandler, G. K.; Gunawardena, G. A.; Pletcher, D. *J. Electroanal. Chem.* **1984**, *177*, 245-251.

(89) Downard, A. J.; Pletcher, D. *J. Electroanal. Chem.* **1986**, *206*, 147-152.

(90) Asavapiriyanont, S.; Chandler, G. K.; Gunawardena, G. A.; Pletcher, D. *J. Electroanal. Chem.* **1984**, *177*, 229-244.

(91) Heinze, J.; Rasche, A.; Pagels, M.; Geschke, B. *J. Phys. Chem. B* **2007**, *111*, 989-997.

(92) Zhou, Z.; Heinze, J. *Electrochim. Acta.* **1999**, *44*, 1733-1748.

(93) Daum, P.; Lenhard, J. R.; Rolison, D.; Murray, R. W. *J. Am. Chem. Soc.* **1980**, *102*, 4649-4653.

(94) Koblhofer, K.; Braun, K.; Lange, R. *J. Electroanal. Chem.* **1986**, *206*, 93-100.

(95) Daum, P.; Murray, R. W. *J. Phys. Chem.* **1981**, *85*, 389-396.

(96) Hill, M. G.; Mann, K. R.; Miller, L. L. *J. Am. Chem. Soc.* **1992**, *114*, 2728-2730.

(97) Smie, A.; Heinze, J. *Angew. Chem. Int. Ed.* **1997**, *36*, 363-367.

(98) Mitchell, R. H.; Brkic, Z.; Sauro, V. A.; Berg, D. J. *J. Am. Chem. Soc.* **2003**, *125*, 7581-7585.

(99) Peters, A.; Branda, N. R. *Chem. Commun.* **2003**, 954-955.

(100) Heinze, J. In *Encyclopedia of Electrochemistry: Organic Electrochemistry*; Schafer, H. J., Ed.; Wiley-VCH: Weinheim, 2004; Vol. 8, p 622-623.

(101) Meerholz, K.; Heinze, J. *Electrochim. Acta.* **1996**, *41*, 1839-1854.

(102) Gorodetsky, B.; Branda, N. R. *Adv. Funct. Mater.* **2007**, *16*, 786-796.

(103) Cunningham, D. D.; Laguren-Davidson, L.; Mark, H. B.; Pham, C. V.; Zimmer, H. *Chem. Commun.* **1987**, *13*, 1021-1023.

(104) Zhu, S. S.; Swager, T. M. *J. Am. Chem. Soc* **1997**, *119*, 12568-12577.

APPENDIX A: THERMAL CLOSING DATA

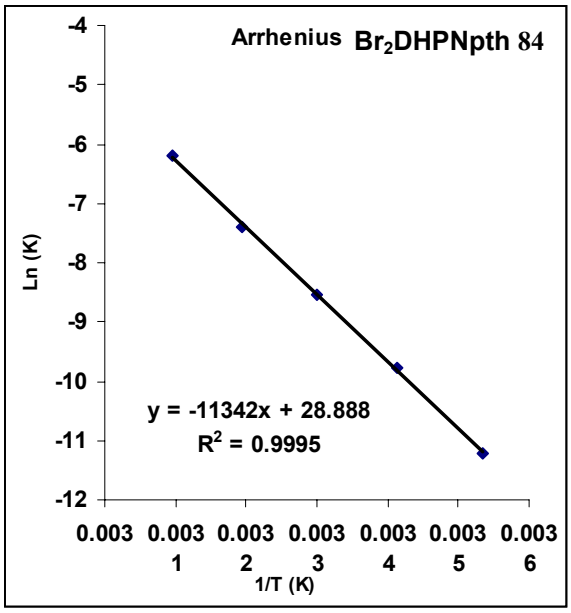

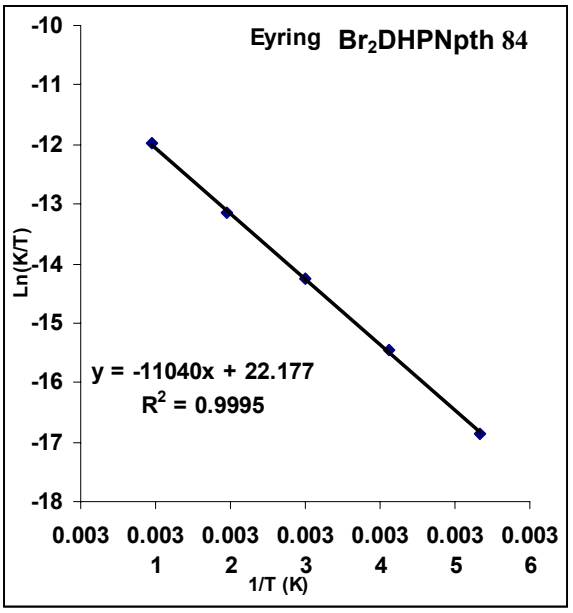

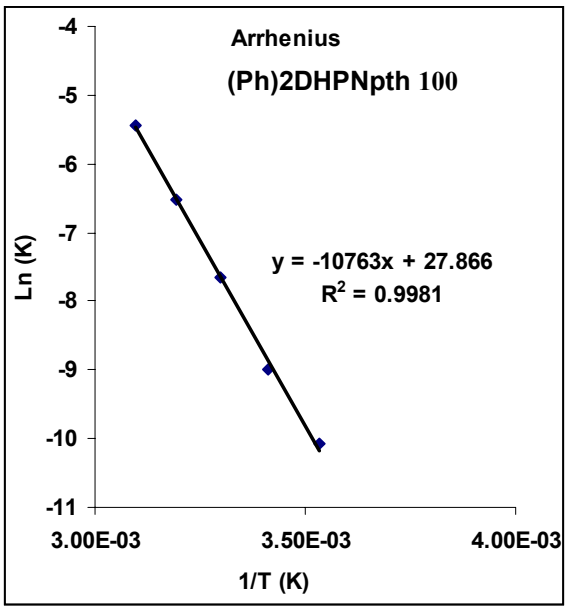

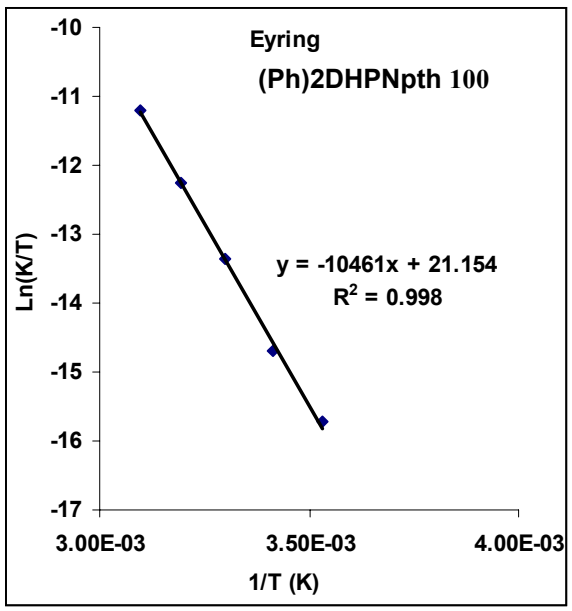

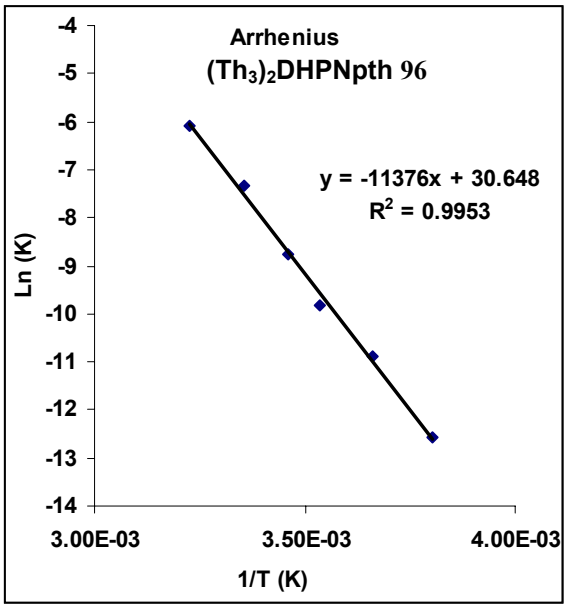
Arrhenius
(Th3)2DHPNpth 96
y = -11376x + 30.648
R2 = 0.9953
Ln (K)
1/T (K)
-4
-5
-6
-7
-8
-9
-10
-11
-12
-13
-14
3.00E-03
3.50E-03
4.00E-03

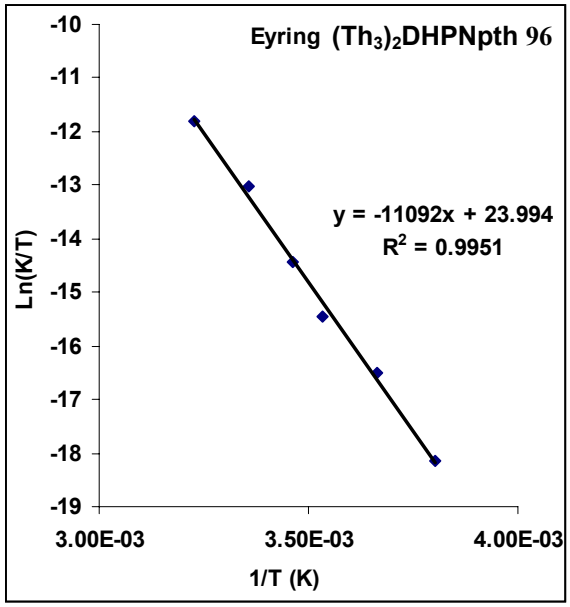
Eyring (Th3)2DHPNpth 96
y = -11092x + 23.994
R2 = 0.9951
Ln(K/T)
1/T (K)
-10
-11
-12
-13
-14
-15
-16
-17
-18
-19
3.00E-03
3.50E-03
4.00E-03

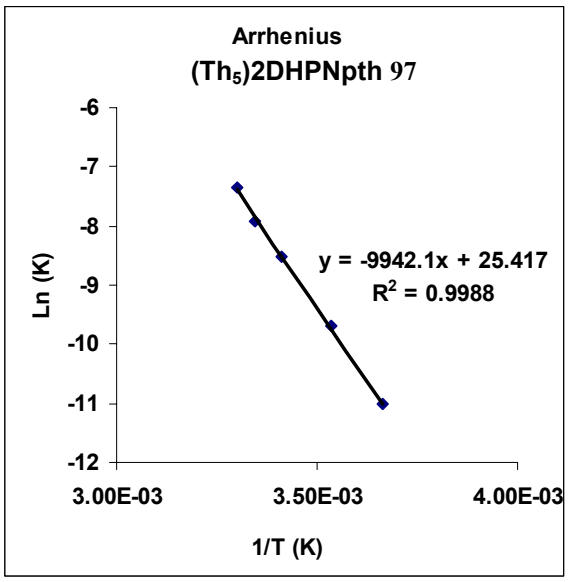
Arrhenius
(Th5)2DHPNpth 97
y = -9942.1x + 25.417
R2 = 0.9988
Ln (K)
1/T (K)
-6
-7
-8
-9
-10
-11
-12
3.00E-03
3.50E-03
4.00E-03

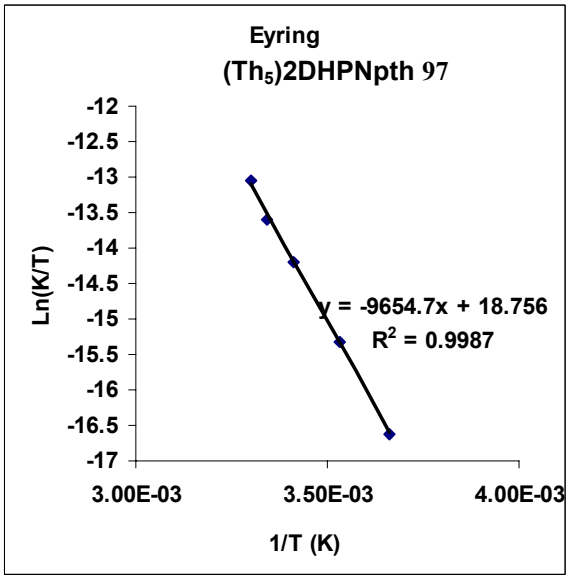
Eyring
(Th5)2DHPNpth 97
y = -9654.7x + 18.756
R2 = 0.9987
Ln(K/T)
1/T (K)
-12
-12.5
-13
-13.5
-14
-14.5
-15
-15.5
-16
-16.5
-17
3.00E-03
3.50E-03
4.00E-03

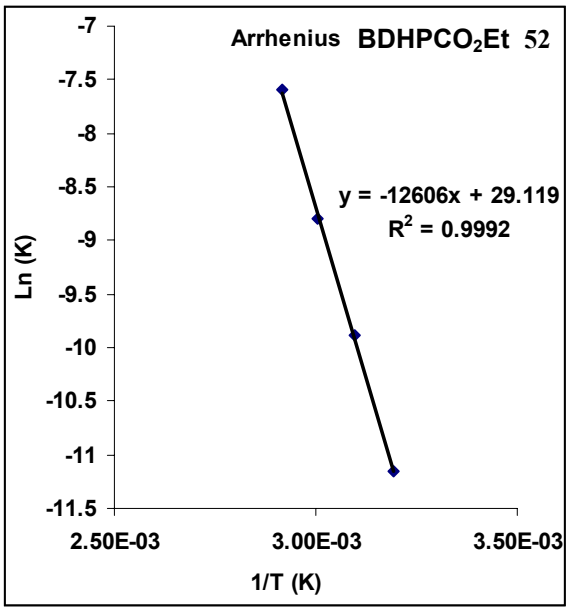
Arrhenius BDHPCO2Et 52
y = -12606x + 29.119
R2 = 0.9992
Ln (K)
1/T (K)
-7
-7.5
-8
-8.5
-9
-9.5
-10
-10.5
-11
-11.5
2.50E-03
3.00E-03
3.50E-03

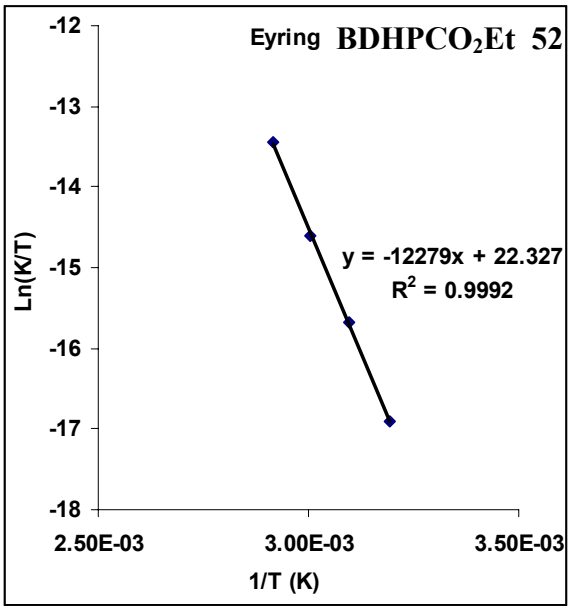
Eyring BDHPCO2Et 52
y = -12279x + 22.327
R2 = 0.9992
Ln(K/T)
1/T (K)
-12
-13
-14
-15
-16
-17
-18
2.50E-03
3.00E-03
3.50E-03

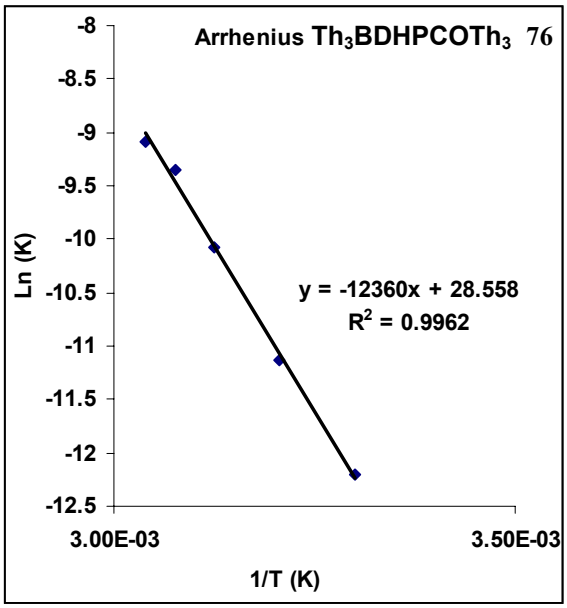
Arrhenius Th3BDHPCOTh3 76
y = -12360x + 28.558
R2 = 0.9962
Ln (K)
1/T (K)
-8
-8.5
-9
-9.5
-10
-10.5
-11
-11.5
-12
-12.5
3.00E-03
3.50E-03

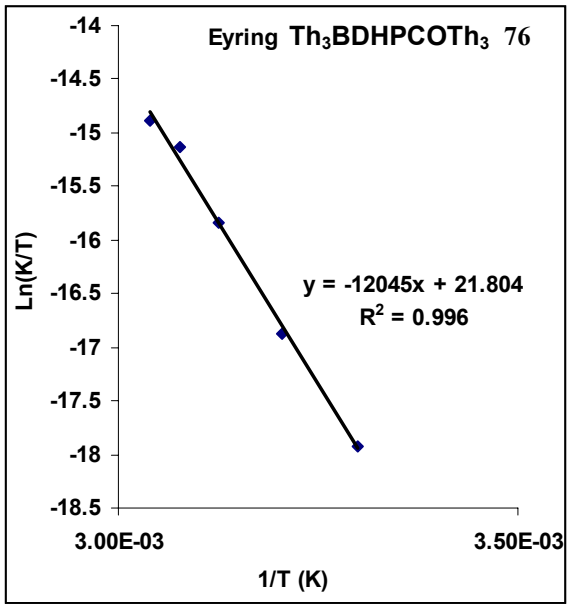
Eyring Th3BDHPCOTh3 76
y = -12045x + 21.804
R2 = 0.996
Ln(K/T)
1/T (K)
-14
-14.5
-15
-15.5
-16
-16.5
-17
-17.5
-18
-18.5
3.00E-03
3.50E-03

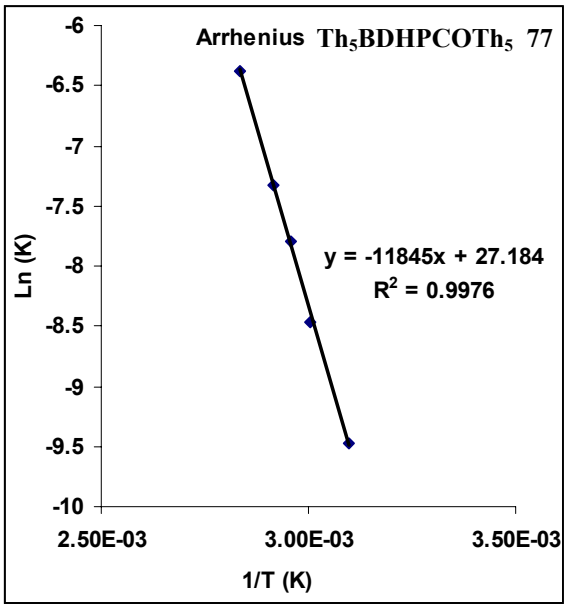
Arrhenius Th5BDHPCOTh5 77
y = -11845x + 27.184
R2 = 0.9976
Ln (K)
1/T (K)
-6
-6.5
-7
-7.5
-8
-8.5
-9
-9.5
-10
2.50E-03
3.00E-03
3.50E-03

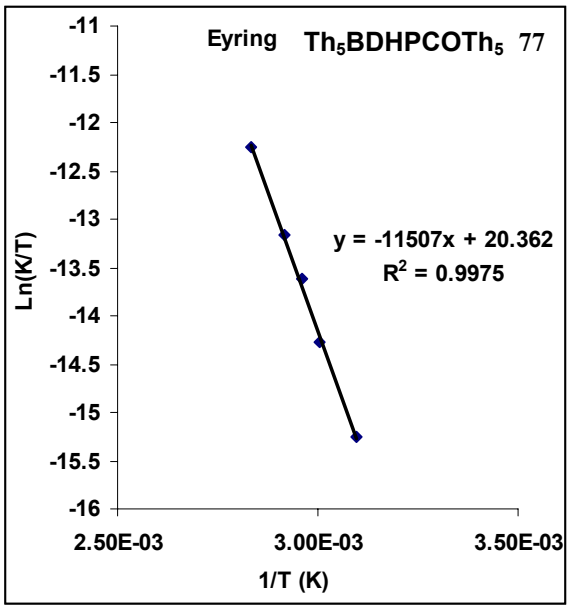
Eyring Th5BDHPCOTh5 77
y = -11507x + 20.362
R2 = 0.9975
Ln(K/T)
1/T (K)
-11
-11.5
-12
-12.5
-13
-13.5
-14
-14.5
-15
-15.5
-16
2.50E-03
3.00E-03
3.50E-03

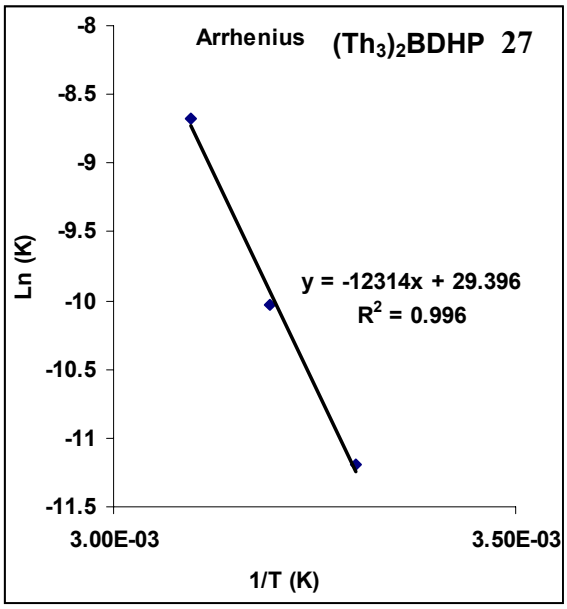
Arrhenius (Th3)2BDHP 27
y = -12314x + 29.396
R2 = 0.996
Ln (K)
1/T (K)
-8
-8.5
-9
-9.5
-10
-10.5
-11
-11.5
3.00E-03
3.50E-03

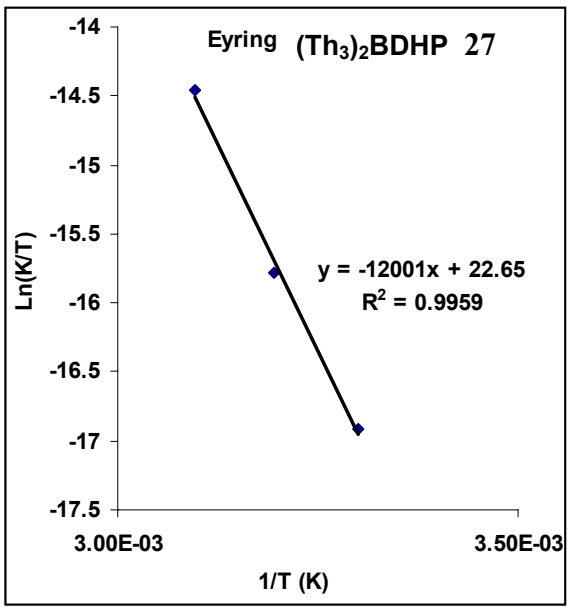
Eyring (Th3)2BDHP 27
y = -12001x + 22.65
R2 = 0.9959
Ln(K/T)
1/T (K)
-14
-14.5
-15
-15.5
-16
-16.5
-17
-17.5
3.00E-03
3.50E-03

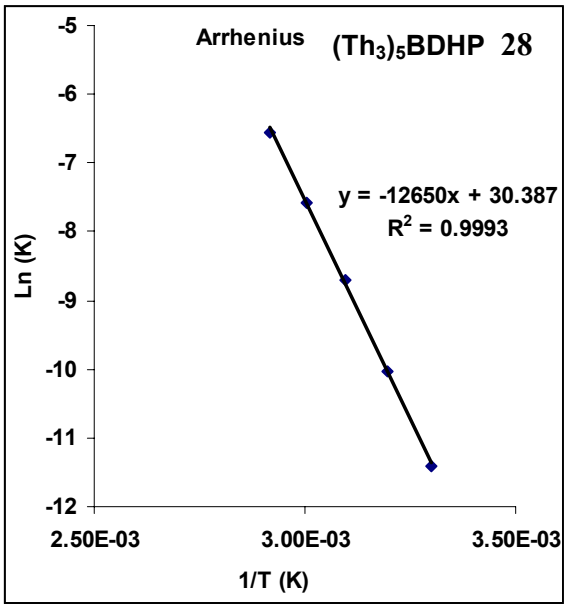
Arrhenius
(Th3)5BDHP 28
y = -12650x + 30.387
R2 = 0.9993
Ln (K)
1/T (K)
-5
-6
-7
-8
-9
-10
-11
-12
2.50E-03
3.00E-03
3.50E-03

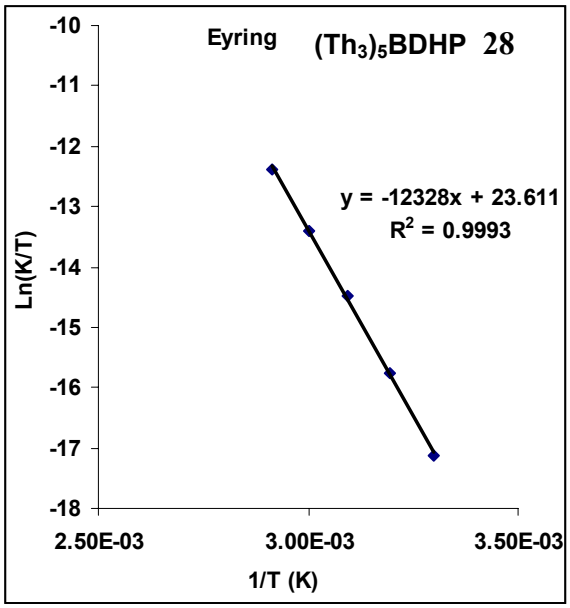
Eyring
(Th3)5BDHP 28
y = -12328x + 23.611
R2 = 0.9993
Ln(K/T)
1/T (K)
-10
-11
-12
-13
-14
-15
-16
-17
-18
2.50E-03
3.00E-03
3.50E-03

APPENDIX B: VISIBLE LIGHT OPENING DATA

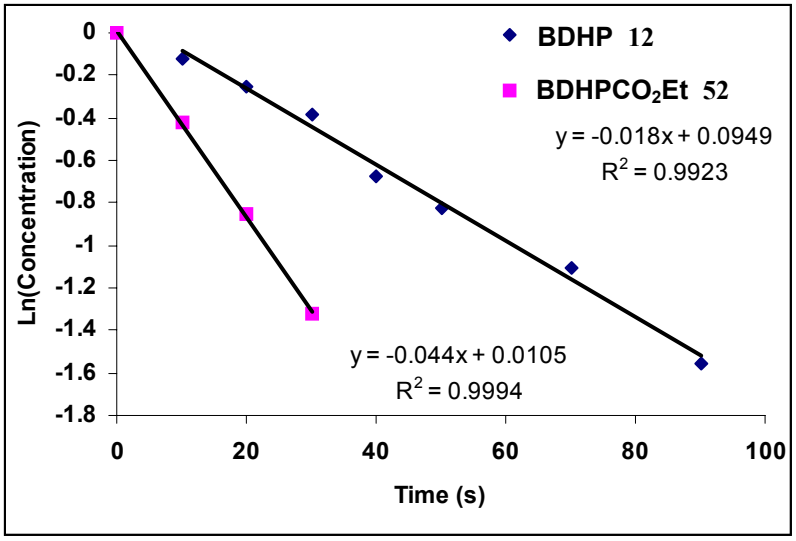

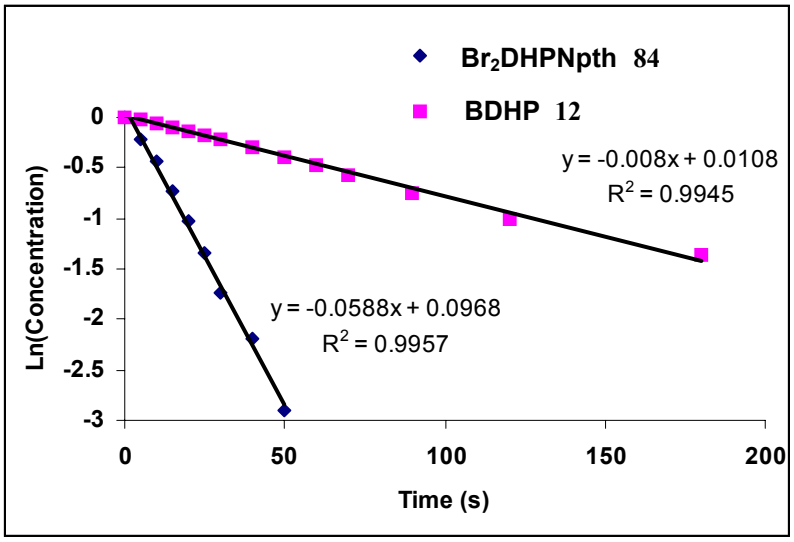

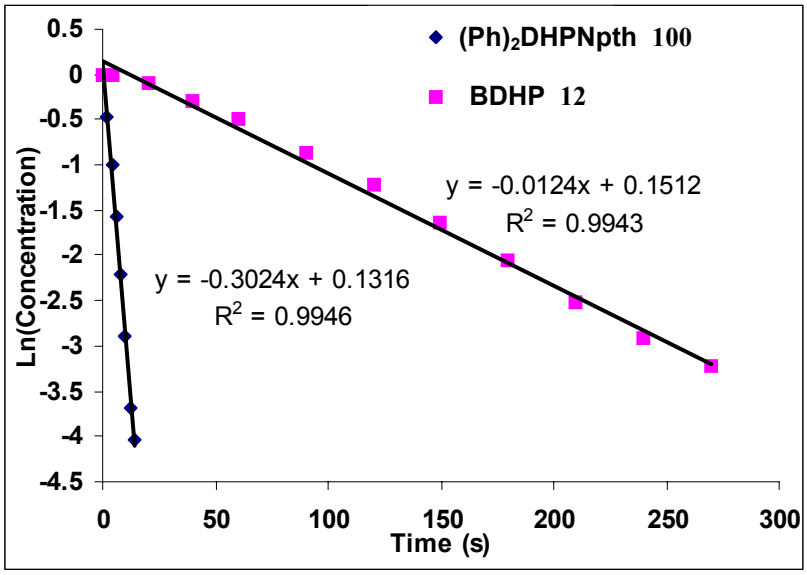
(Ph)2DHPNpth 100
BDHP 12
y = -0.0124x + 0.1512
R2 = 0.9943
y = -0.3024x + 0.1316
R2 = 0.9946
Ln(Concentration)
Time (s)
0.5
0
-0.5
-1
-1.5
-2
-2.5
-3
-3.5
-4
-4.5
0
50
100
150
200
250
300

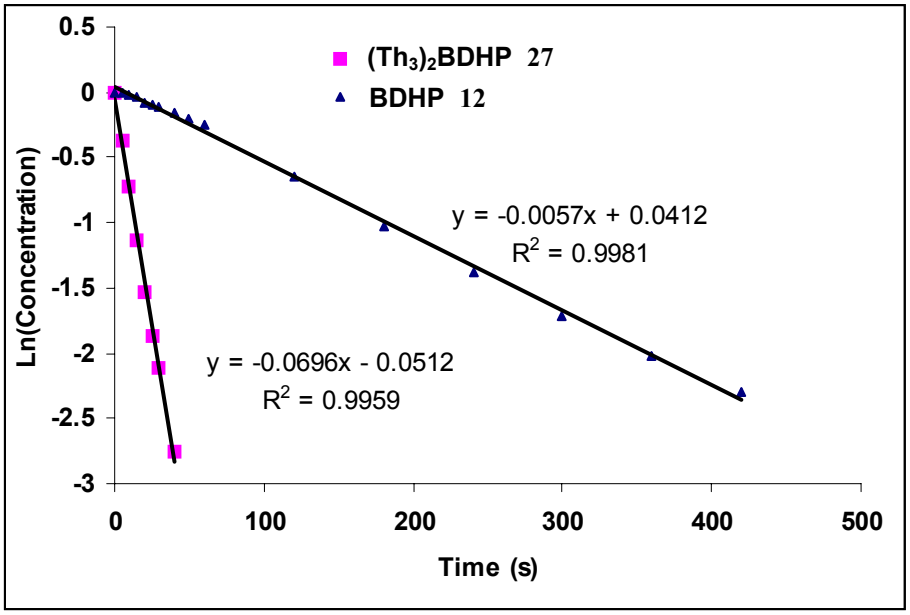
(Th3)2BDHP 27
BDHP 12
y = -0.0057x + 0.0412
R2 = 0.9981
y = -0.0696x - 0.0512
R2 = 0.9959
Ln(Concentration)
Time (s)
0.5
0
-0.5
-1
-1.5
-2
-2.5
-3
0
100
200
300
400
500

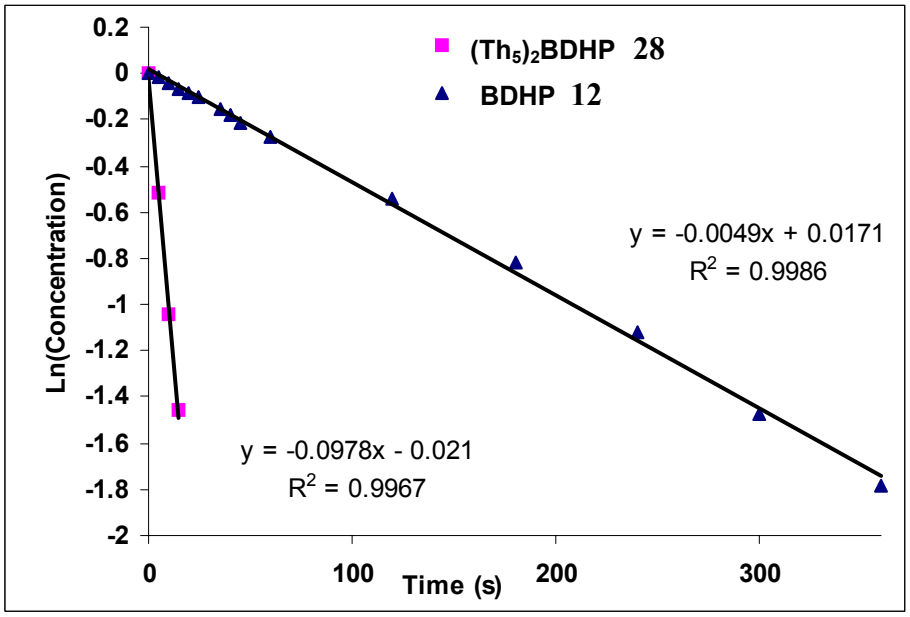
(Th5)2BDHP 28
BDHP 12
y = -0.0049x + 0.0171
R2 = 0.9986
y = -0.0978x - 0.021
R2 = 0.9967
Ln(Concentration)
Time (s)
0.2
0
-0.2
-0.4
-0.6
-0.8
-1
-1.2
-1.4
-1.6
-1.8
-2
0
100
200
300

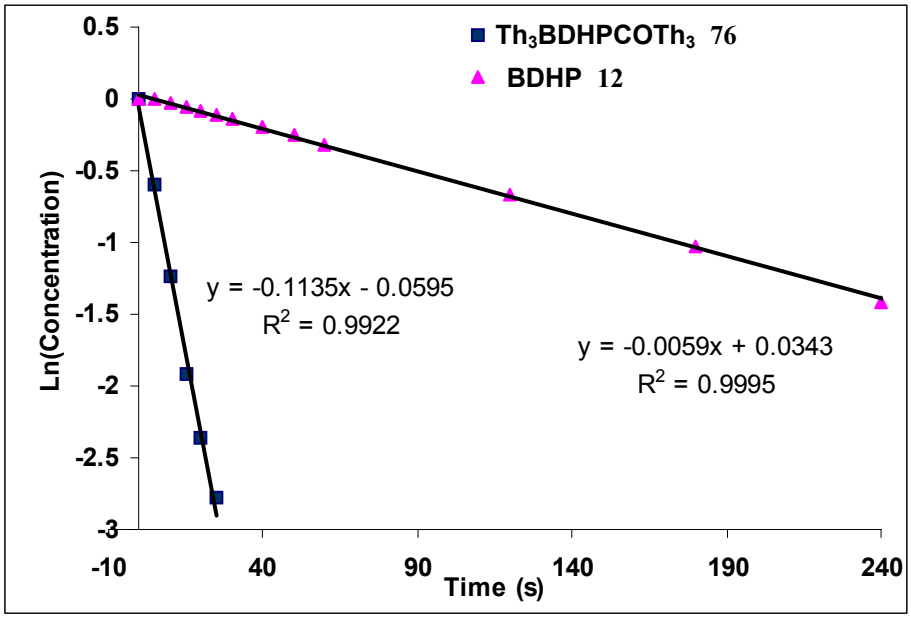
Th3BDHPCOTh3 76
BDHP 12
y = -0.1135x - 0.0595
R2 = 0.9922
y = -0.0059x + 0.0343
R2 = 0.9995
Ln(Concentration)
Time (s)
0.5
0
-0.5
-1
-1.5
-2
-2.5
-3
-10
40
90
140
190
240

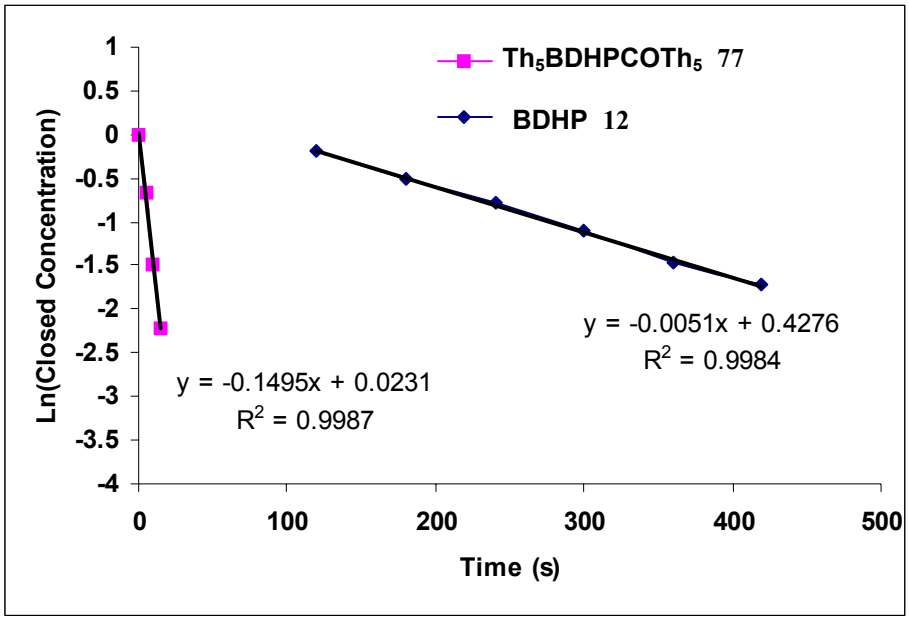
Th5BDHPCOTh5 77
BDHP 12
y = -0.0051x + 0.4276
R2 = 0.9984
y = -0.1495x + 0.0231
R2 = 0.9987
Ln(Closed Concentration)
Time (s)
1
0.5
0
-0.5
-1
-1.5
-2
-2.5
-3
-3.5
-4
0
100
200
300
400
500

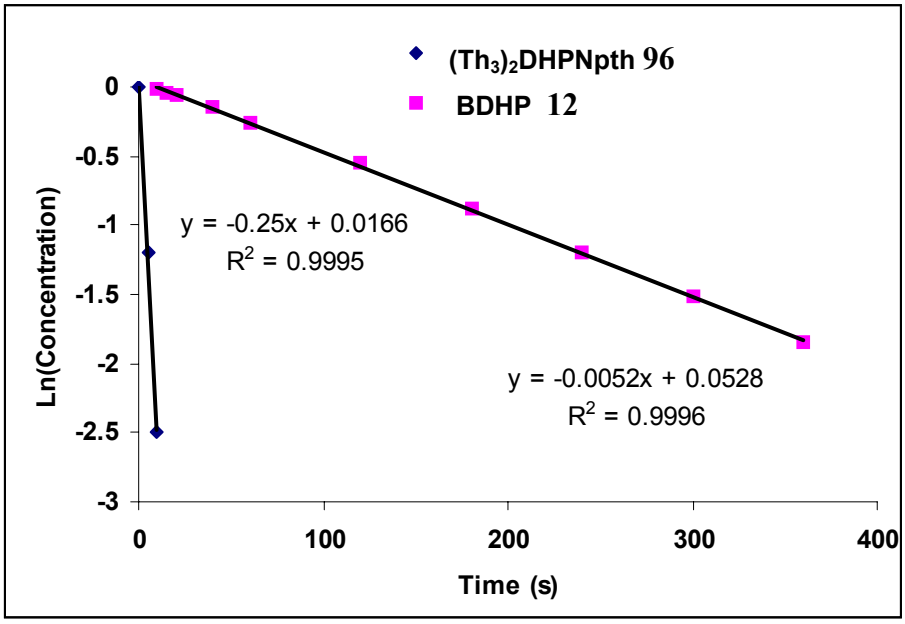
(Th3)2DHPNpth 96
BDHP 12
y = -0.25x + 0.0166
R2 = 0.9995
y = -0.0052x + 0.0528
R2 = 0.9996
Ln(Concentration)
Time (s)
0
-0.5
-1
-1.5
-2
-2.5
-3
0
100
200
300
400

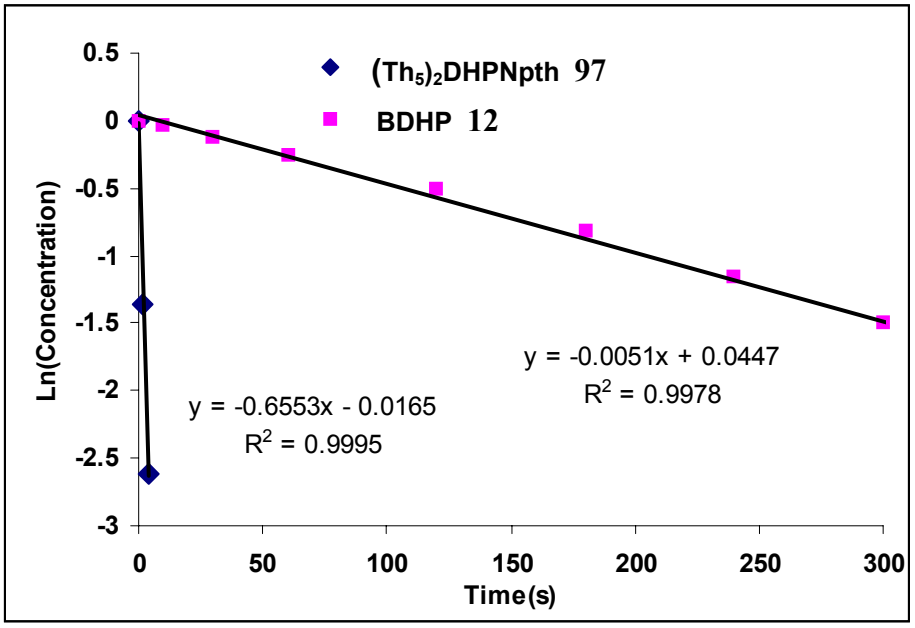
(Th5)2DHPNpth 97
BDHP 12
Ln(Concentration)
Time(s)
y = -0.6553x - 0.0165
R2 = 0.9995
y = -0.0051x + 0.0447
R2 = 0.9978
0.5
0
-0.5
-1
-1.5
-2
-2.5
-3
0
50
100
150
200
250
300

APPENDIX C: UV CLOSING VS BDHP

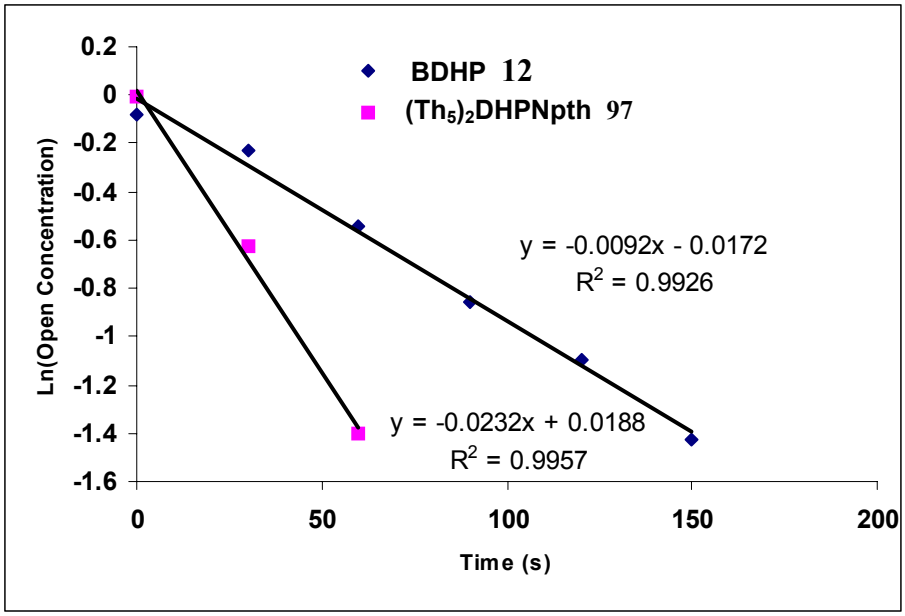

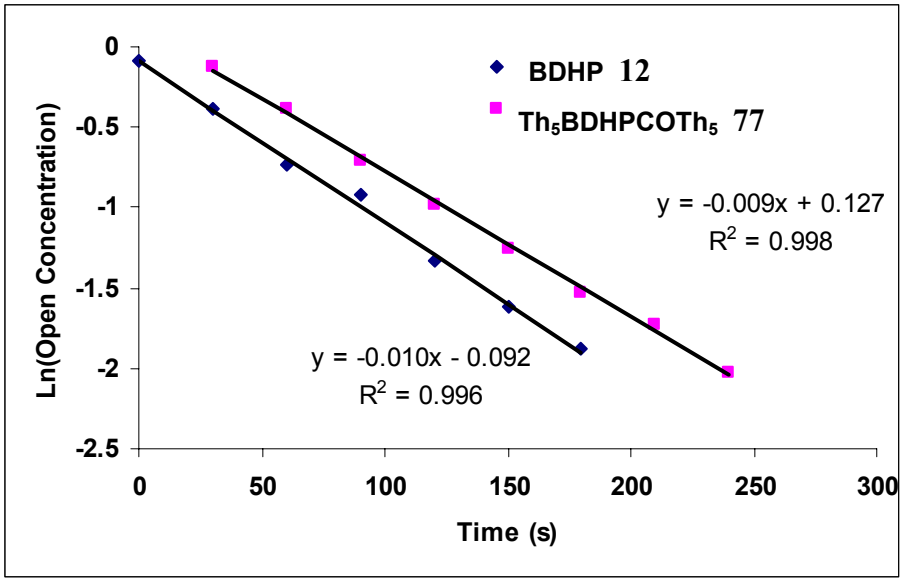

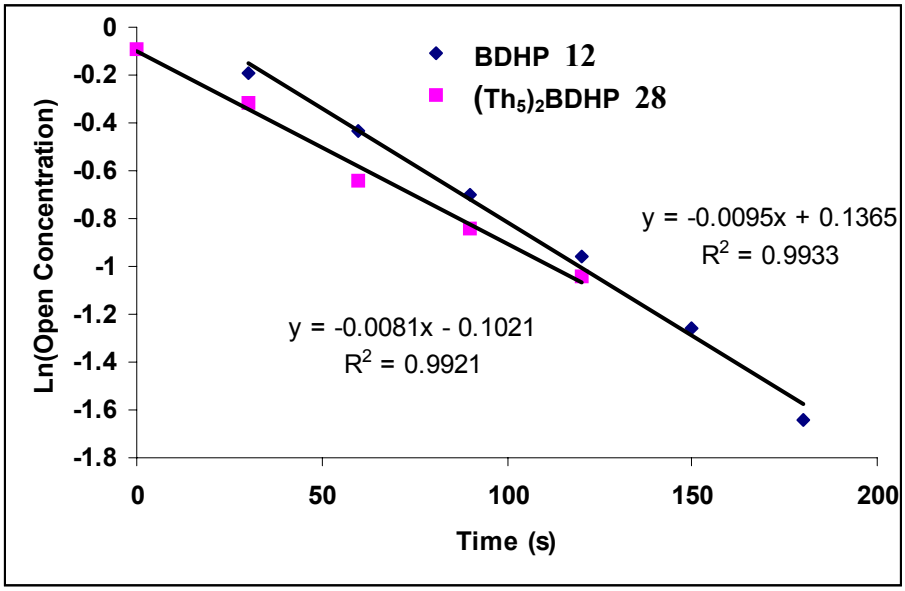
BDHP 12
(Th5)2BDHP 28
y = -0.0095x + 0.1365
R2 = 0.9933
y = -0.0081x - 0.1021
R2 = 0.9921
Ln(Open Concentration)
Time (s)
0
-0.2
-0.4
-0.6
-0.8
-1
-1.2
-1.4
-1.6
-1.8
0
50
100
150
200

APPENDIX D: CYCLIC VOLTAMMETRY DATA

Compound/Peak	$E_{p,a}$ (V) (vs SCE)	$E_{p,c}$ (V) (vs SCE)
Br_2DHPNpth **84**	1.15	1.06
	-1.06	-1.14
$(Th_5)_2$DHPNpth **97**	0.80	0.69
	1.01	0.87
	1.24	1.09
	1.58	1.27
	-1.15	-1.22
$(Th_5)_2$BDHP **28**	0.55	0.49
	0.77*	
	0.95	0.82
	1.32	1.06
Th_3BDHPCOTh_3 **76**	0.54	0.48
	0.97	0.84
	1.28	1.16
	-1.41	-1.49
Th_5BDHPCOTh_5 **97**	0.59	0.51
	0.97	0.84
	1.21	1.06
	1.51	1.43
	-1.3	-1.41

Cyclic voltammetry data was obtained in DCM with $TBAPF_6$ as the electrolyte
*Found only when the sample was opened by visible light irradiation

APPENDIX E: NMR DATA

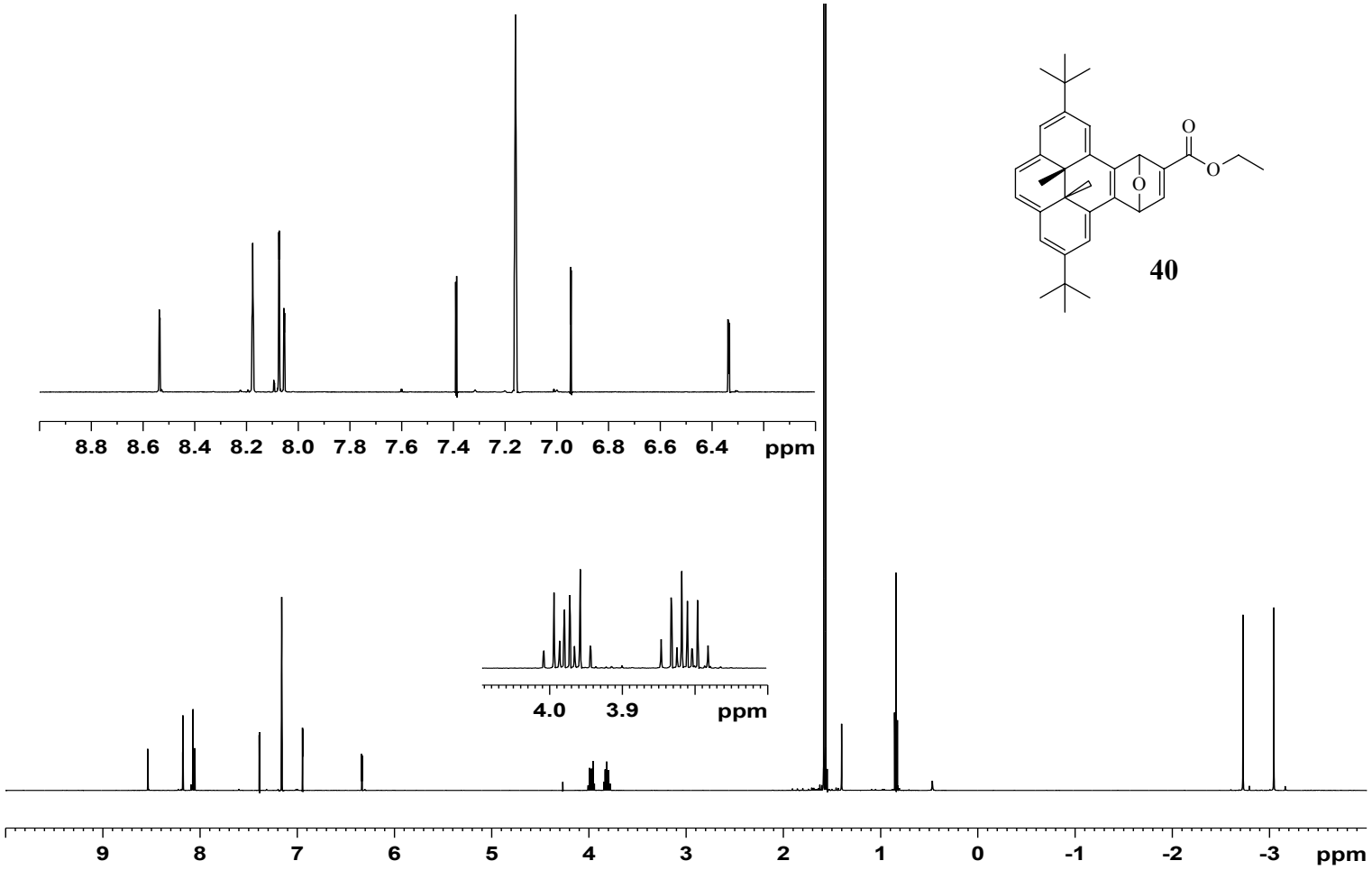

40

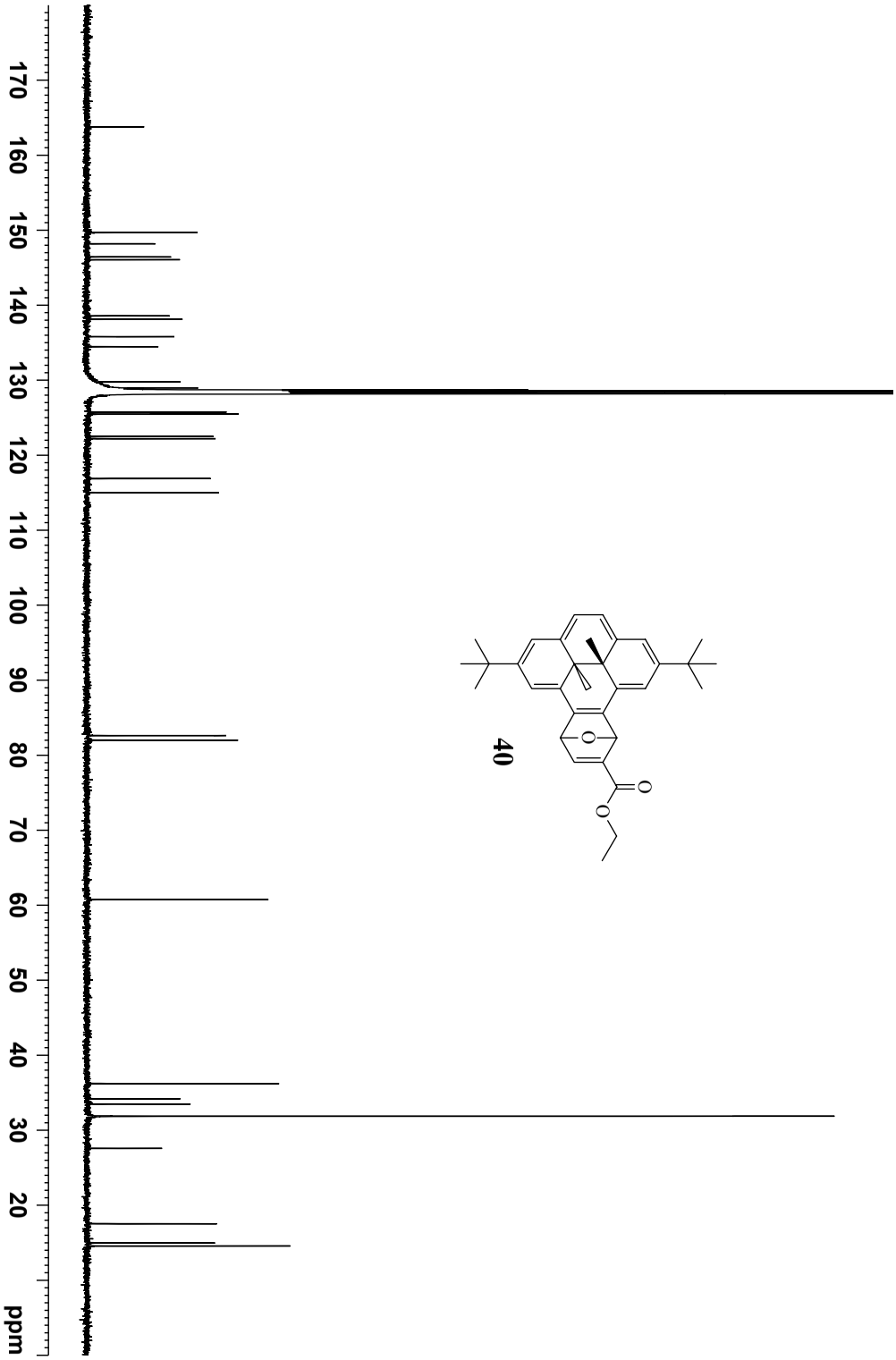
170
160
150
140
130
120
110
100
90
80
70
60
50
40
30
20
ppm
40

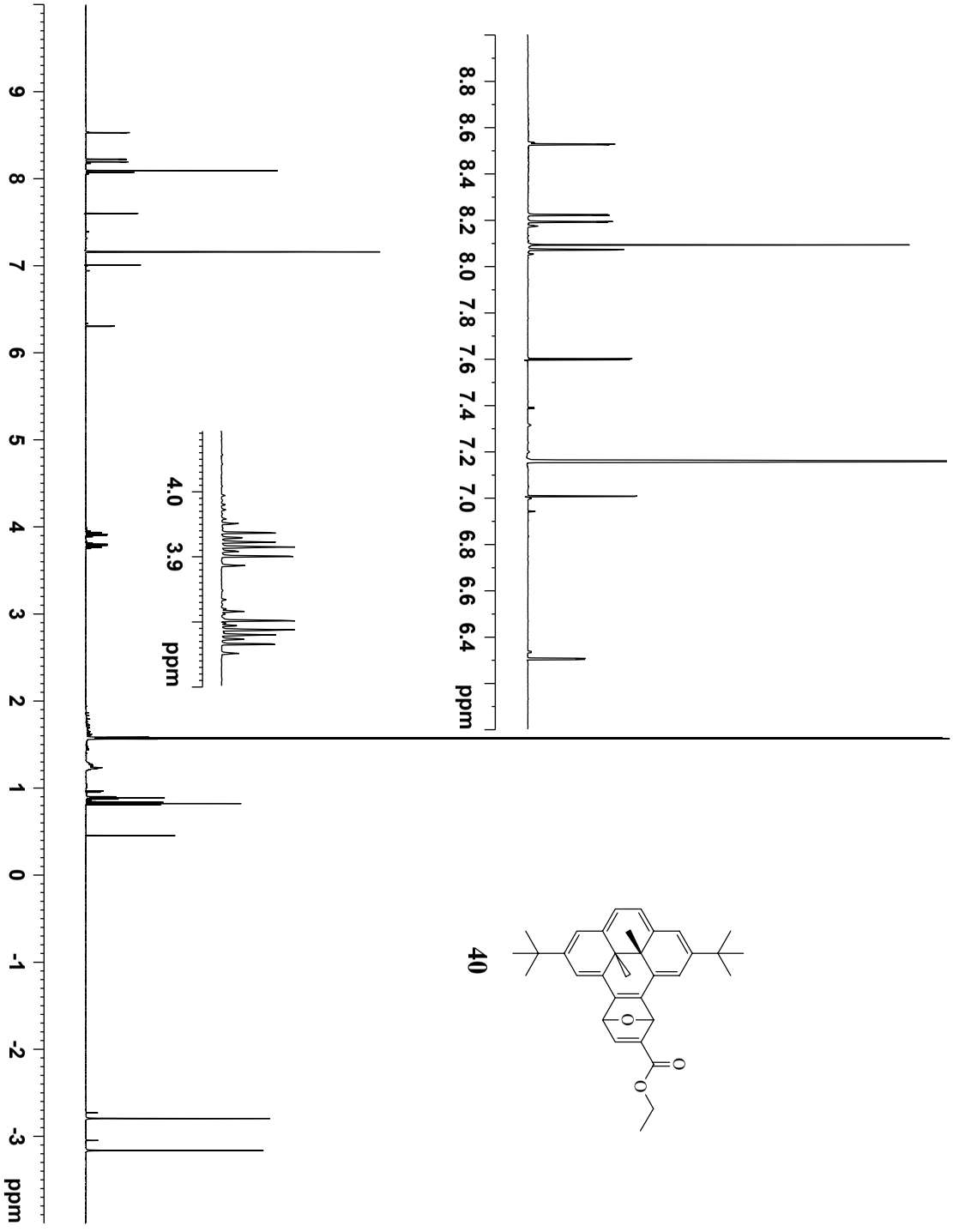
8.8 8.6 8.4 8.2 8.0 7.8 7.6 7.4 7.2 7.0 6.8 6.6 6.4 ppm
4.0 3.9 ppm
9 8 7 6 5 4 3 2 1 0 -1 -2 -3 ppm
O
O
O

40

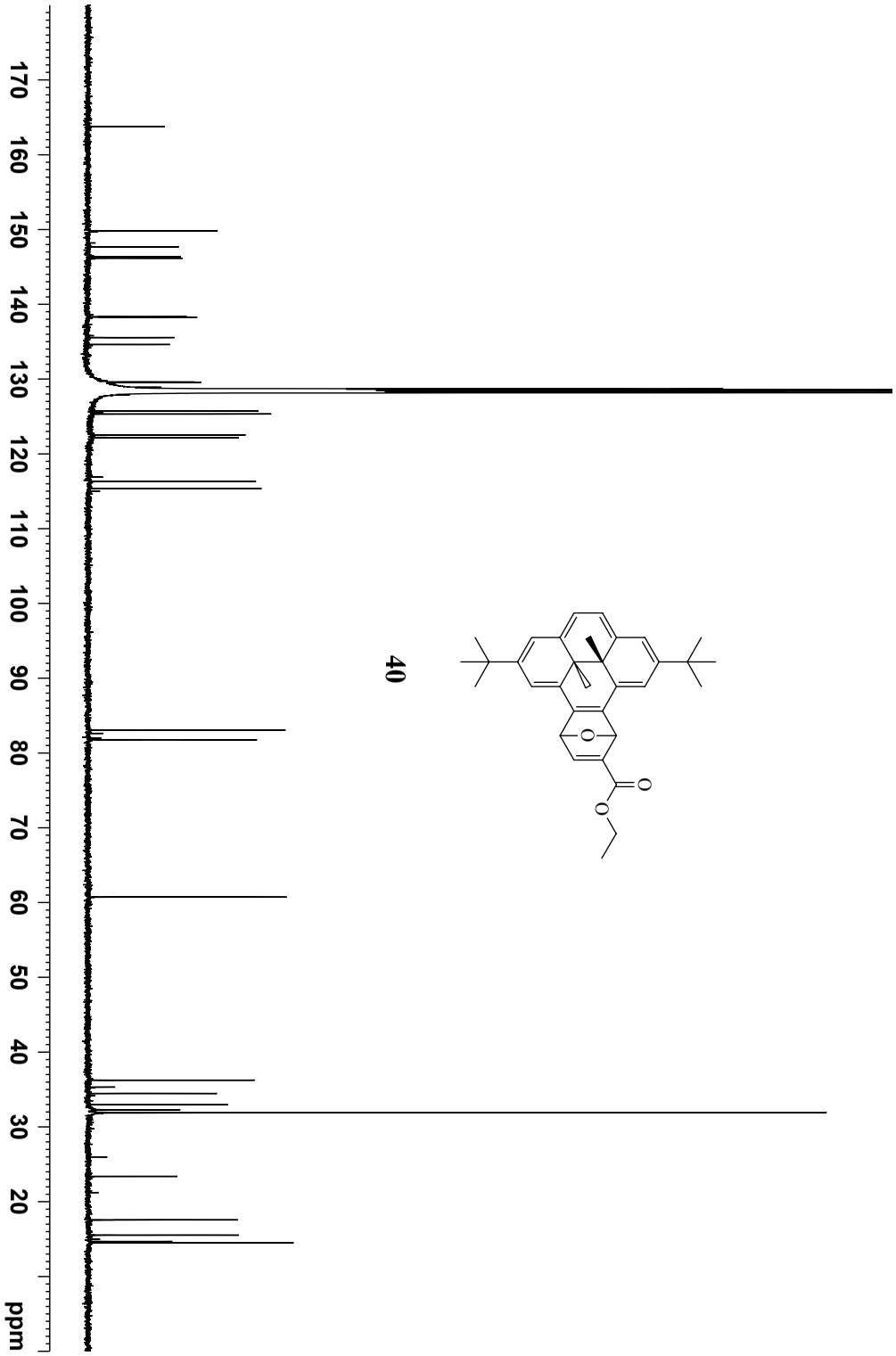
170
160
150
140
130
120
110
100
90
80
70
60
50
40
30
20
ppm
40
O
O
O

11.5
11.0
10.5
10.0
9.5
9.0
8.5
8.0
7.5
ppm
O
H
H
O
43
-3.5
ppm
11
10
9
8
7
6
5
4
3
2
1
0
-1
-2
-3
ppm

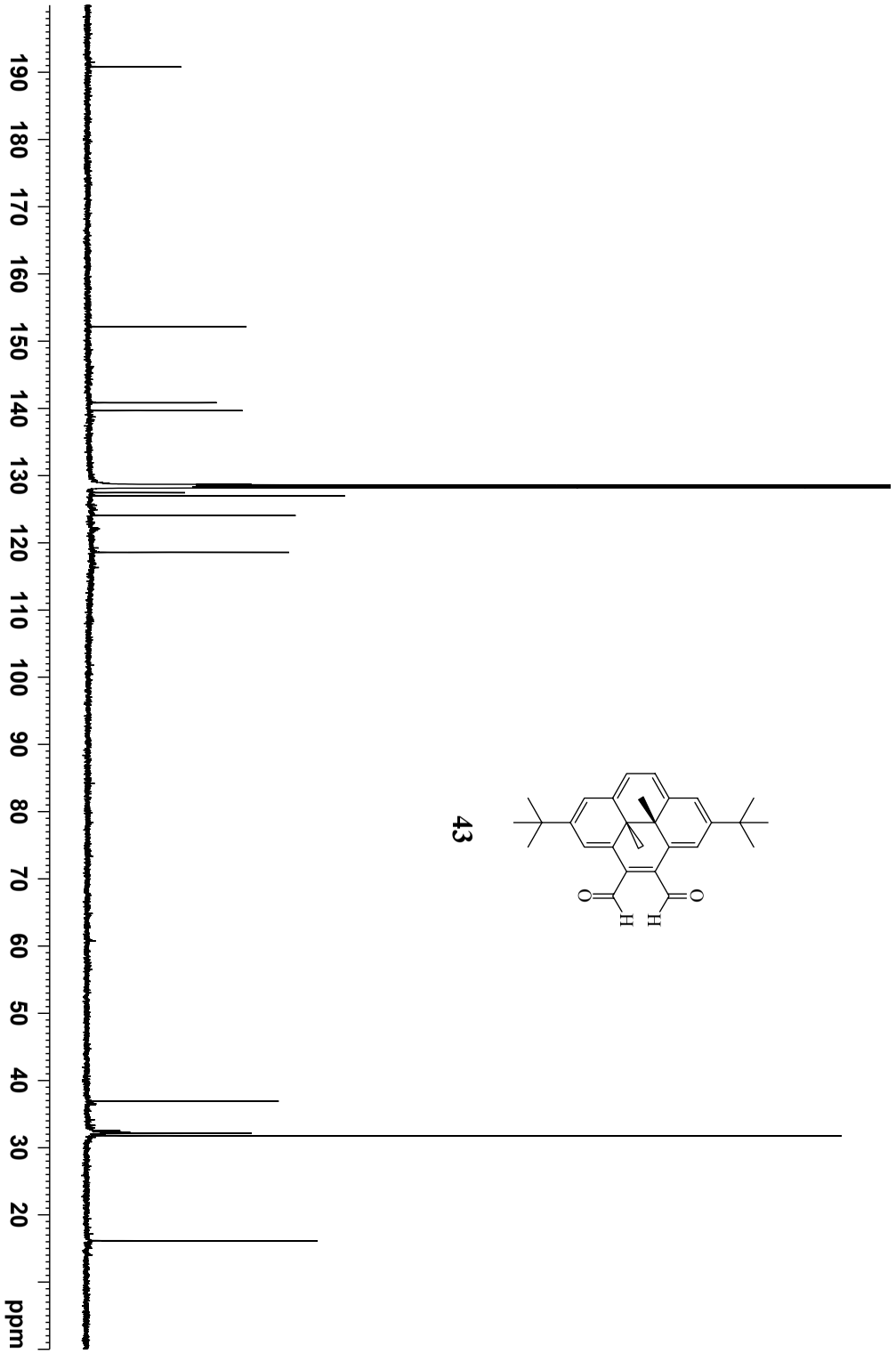
190
180
170
160
150
140
130
120
110
100
90
80
70
60
50
40
30
20
ppm
43
O
H
O
H

OEt
OEt
O
O
O
O
41
8.8 8.6 8.4 8.2 8.0 7.8 7.6 7.4 7.2 7.0 6.8 ppm
-3.0 ppm
4.4 4.2 4.0 3.8 ppm
9 8 7 6 5 4 3 2 1 0 -1 -2 -3 ppm

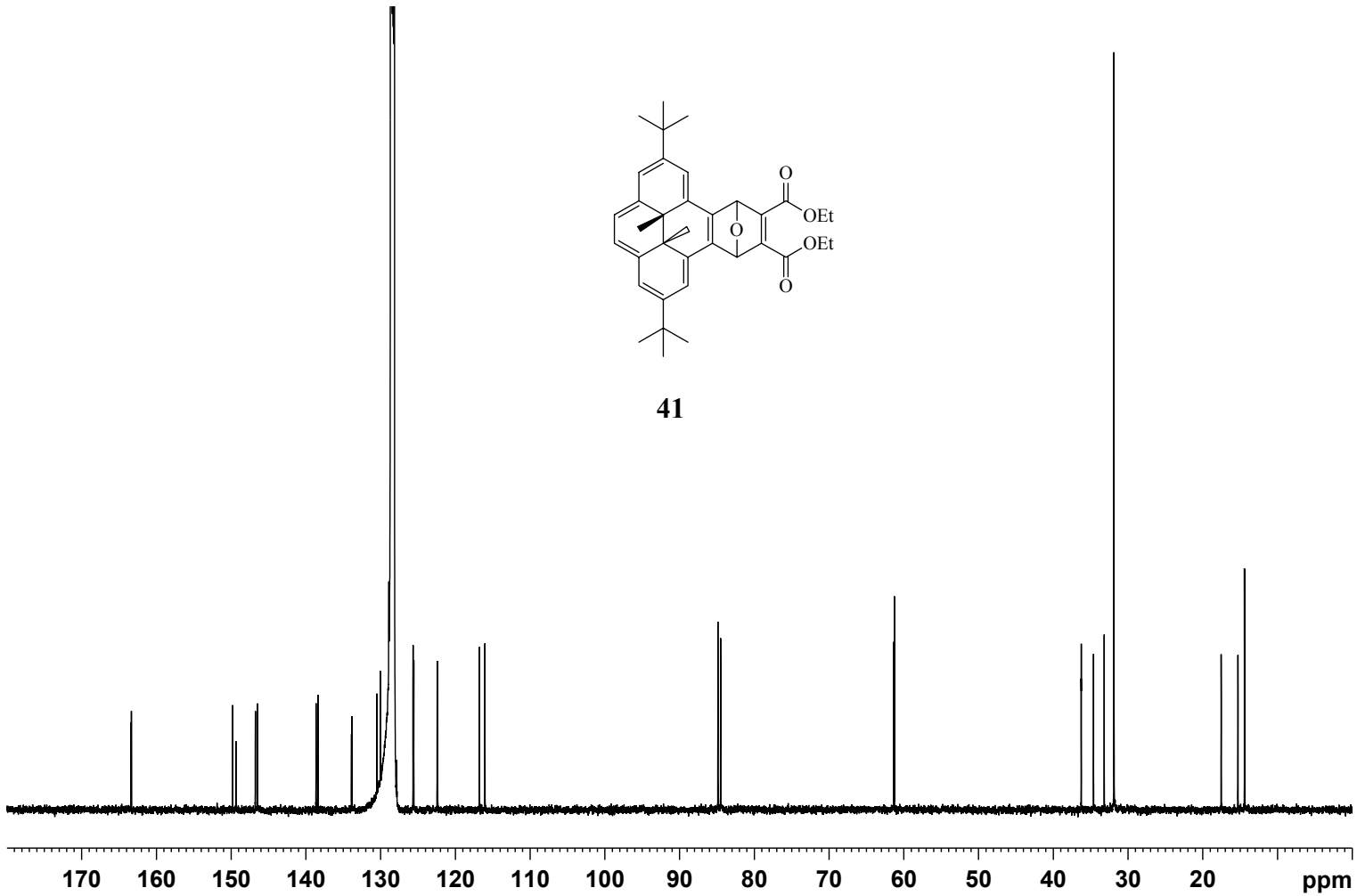
O
OEt
O
OEt
O
170
160
150
140
130
120
110
100
90
80
70
60
50
40
30
20
ppm

41

O
O
52
10.0
9.5
9.0
8.5
8.0
7.5
ppm
4.4
4.3
4.2
ppm
10
9
8
7
6
5
4
3
2
1
0
-1
-2
-3
ppm

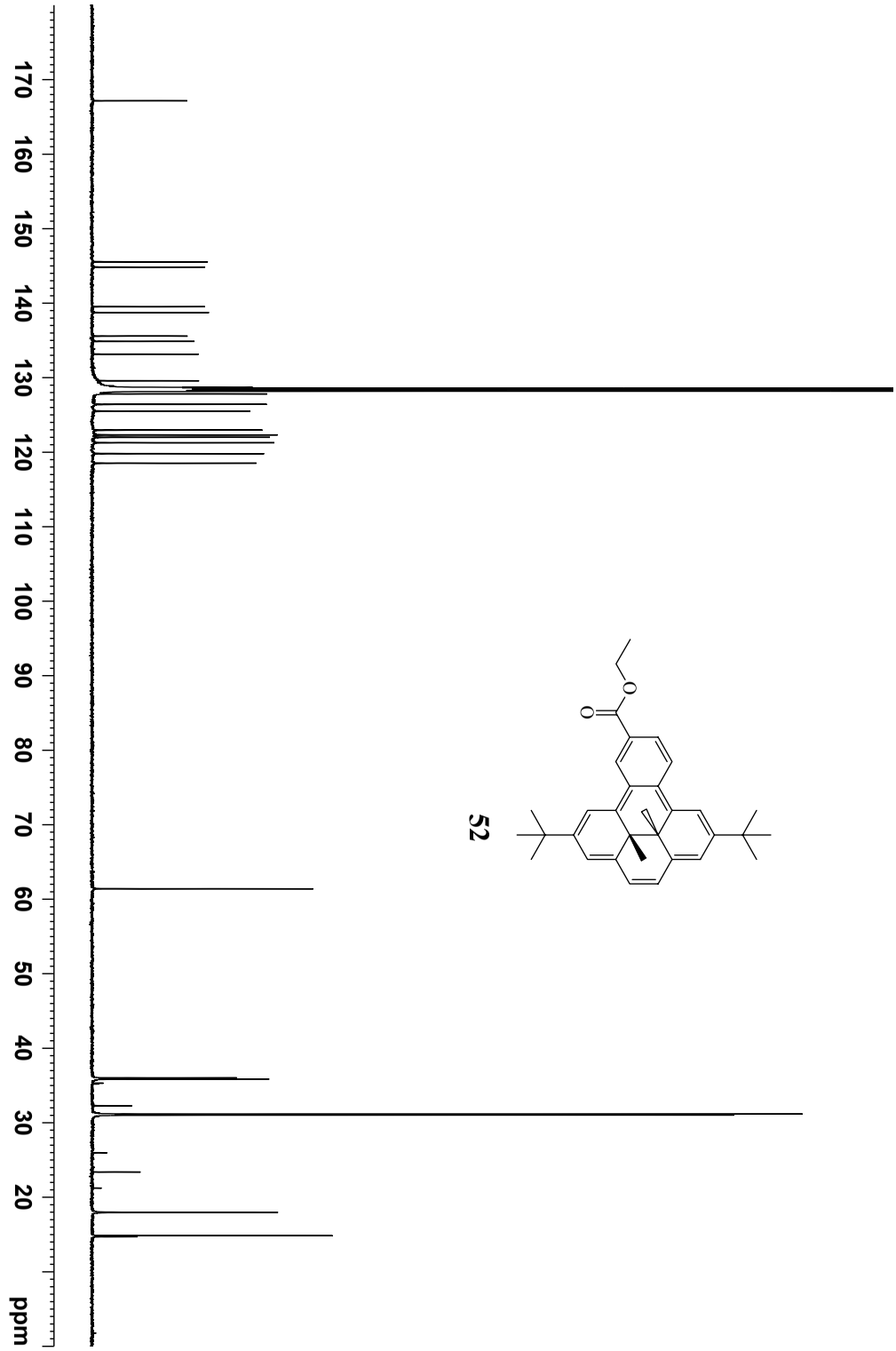
170
160
150
140
130
120
110
100
90
80
70
60
50
40
30
20
ppm
O
O
52

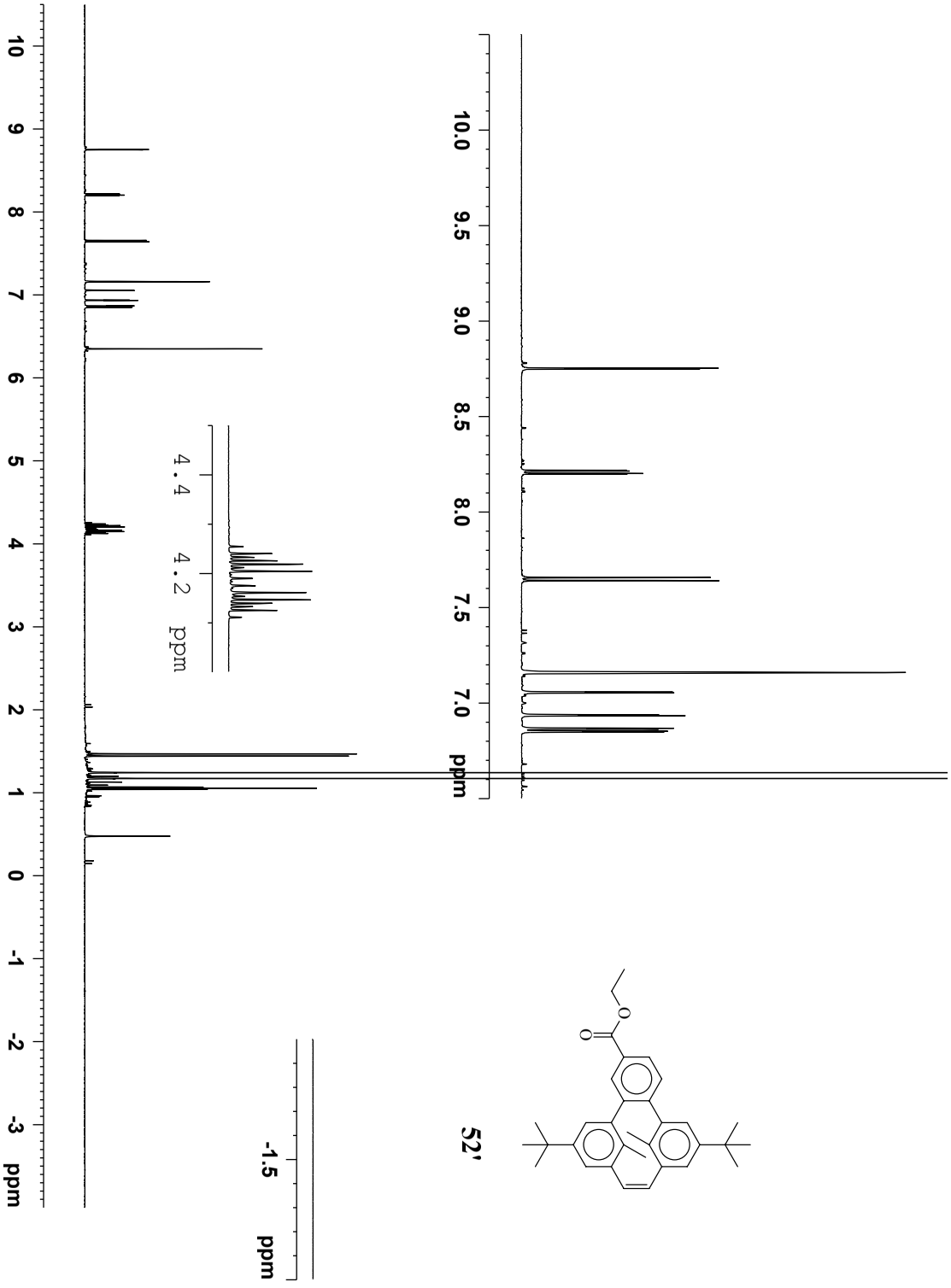
10 9 8 7 6 5 4 3 2 1 0 -1 -2 -3 ppm
4.4 4.2 ppm
-1.5 ppm
10.0 9.5 9.0 8.5 8.0 7.5 7.0 ppm
O
O

52'

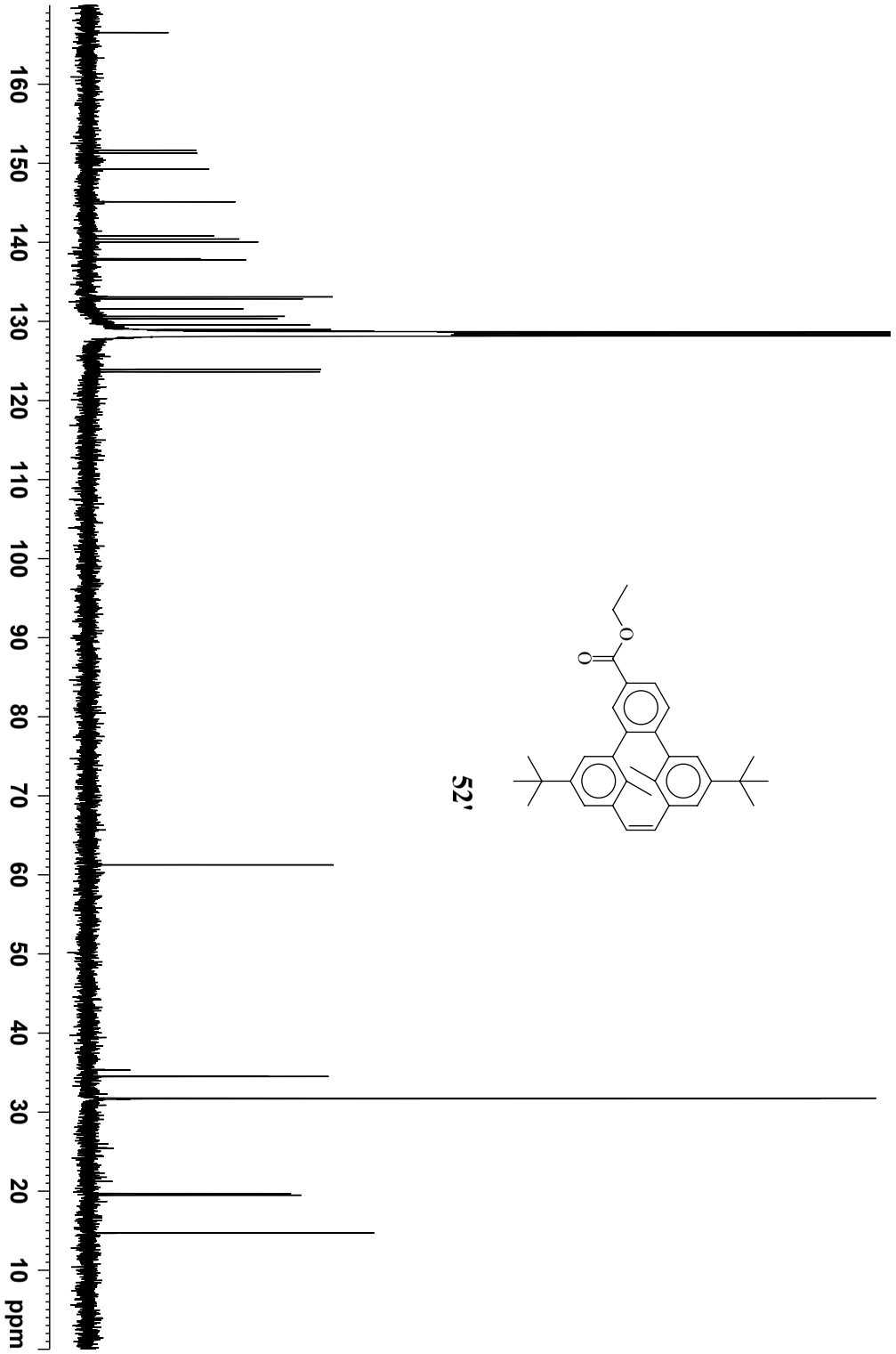

52'

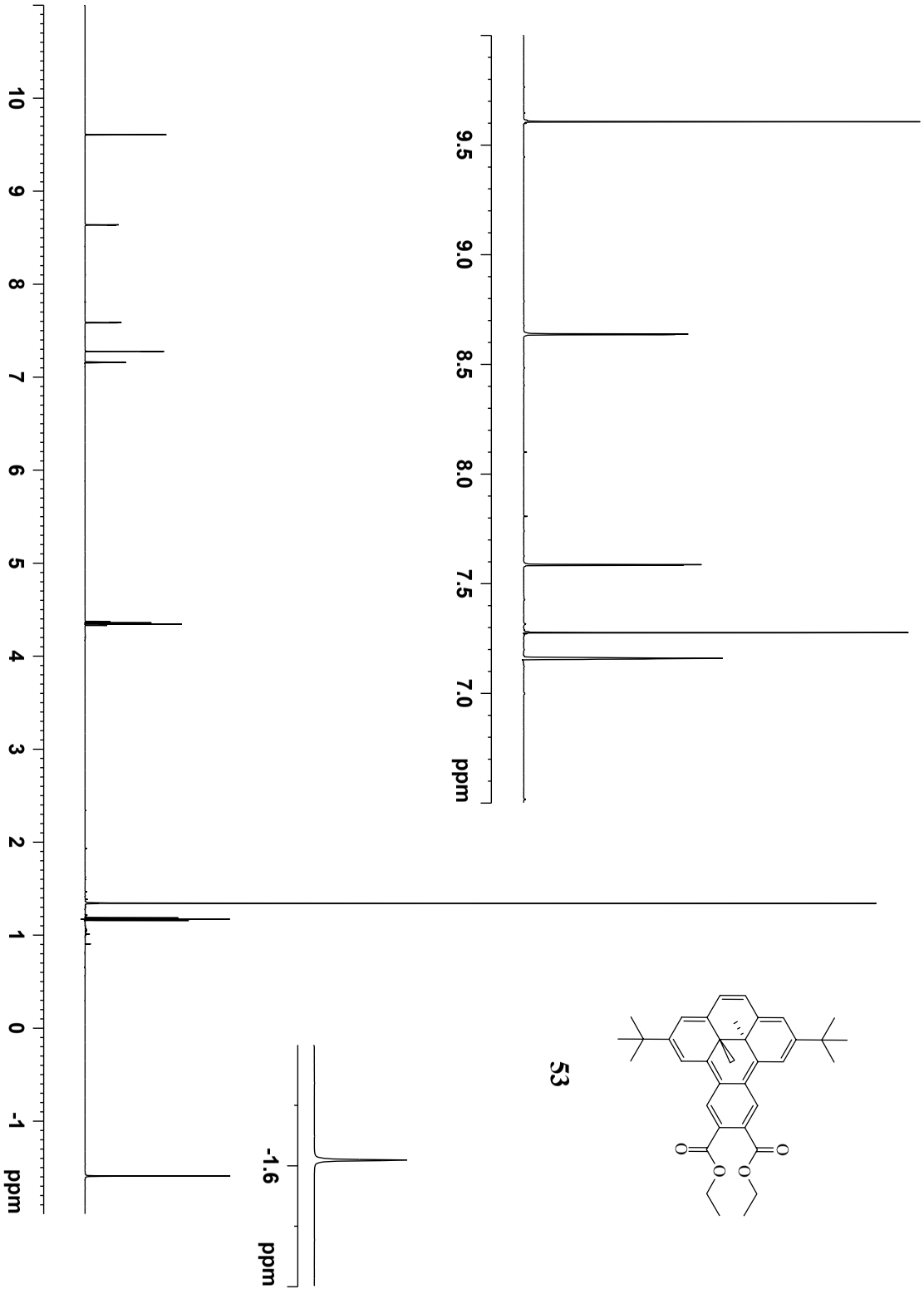

53

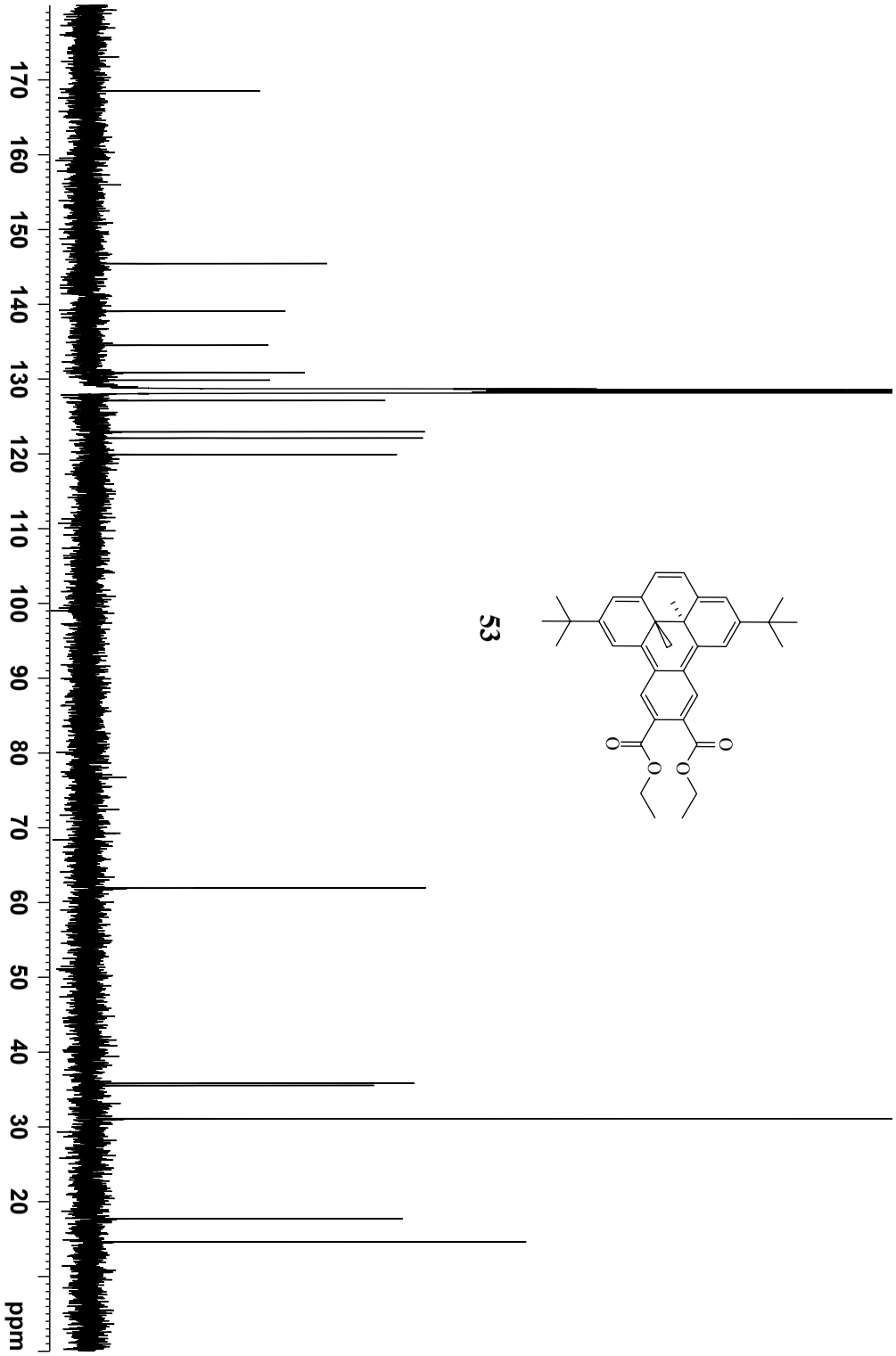
53
170
160
150
140
130
120
110
100
90
80
70
60
50
40
30
20
ppm

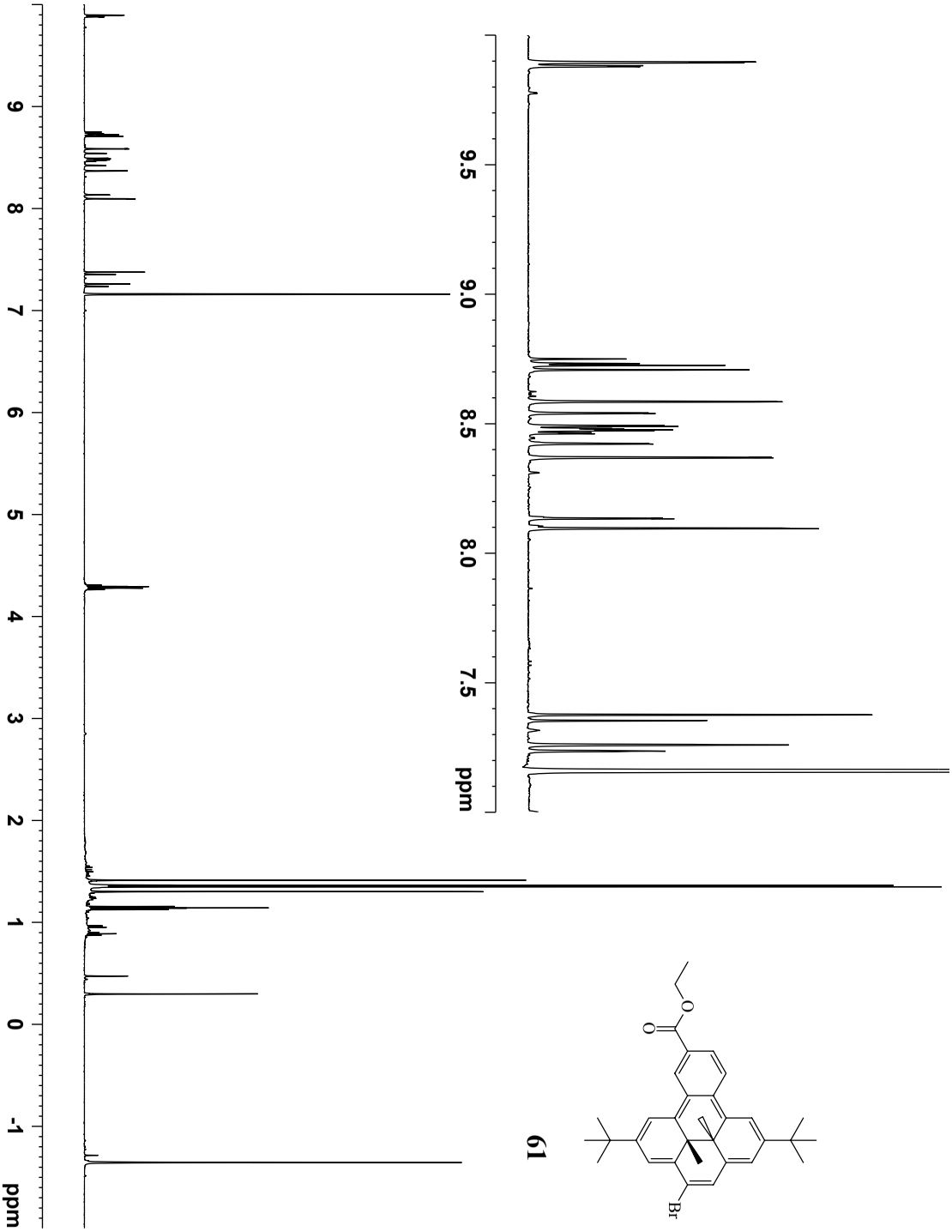

61

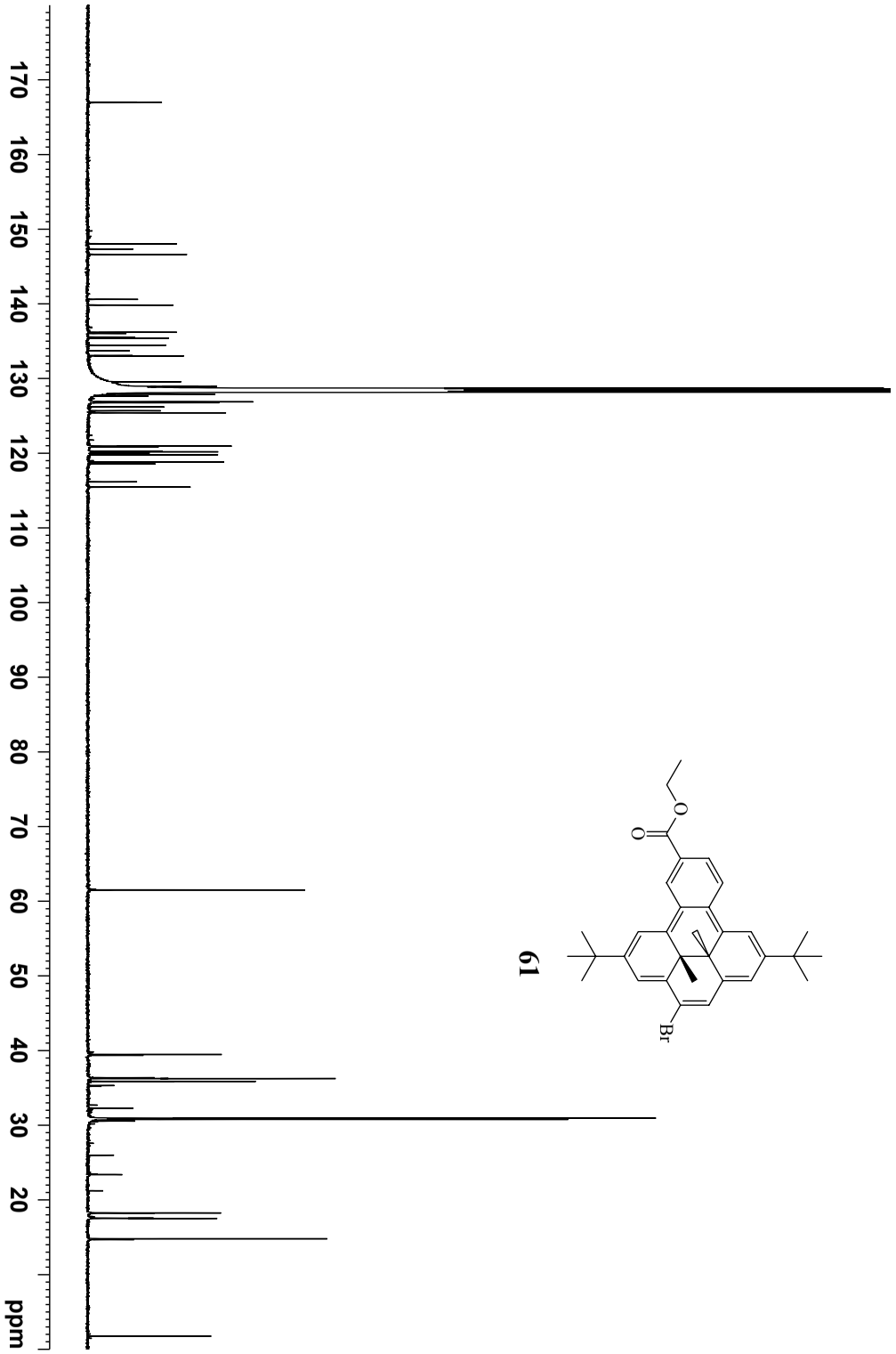

61

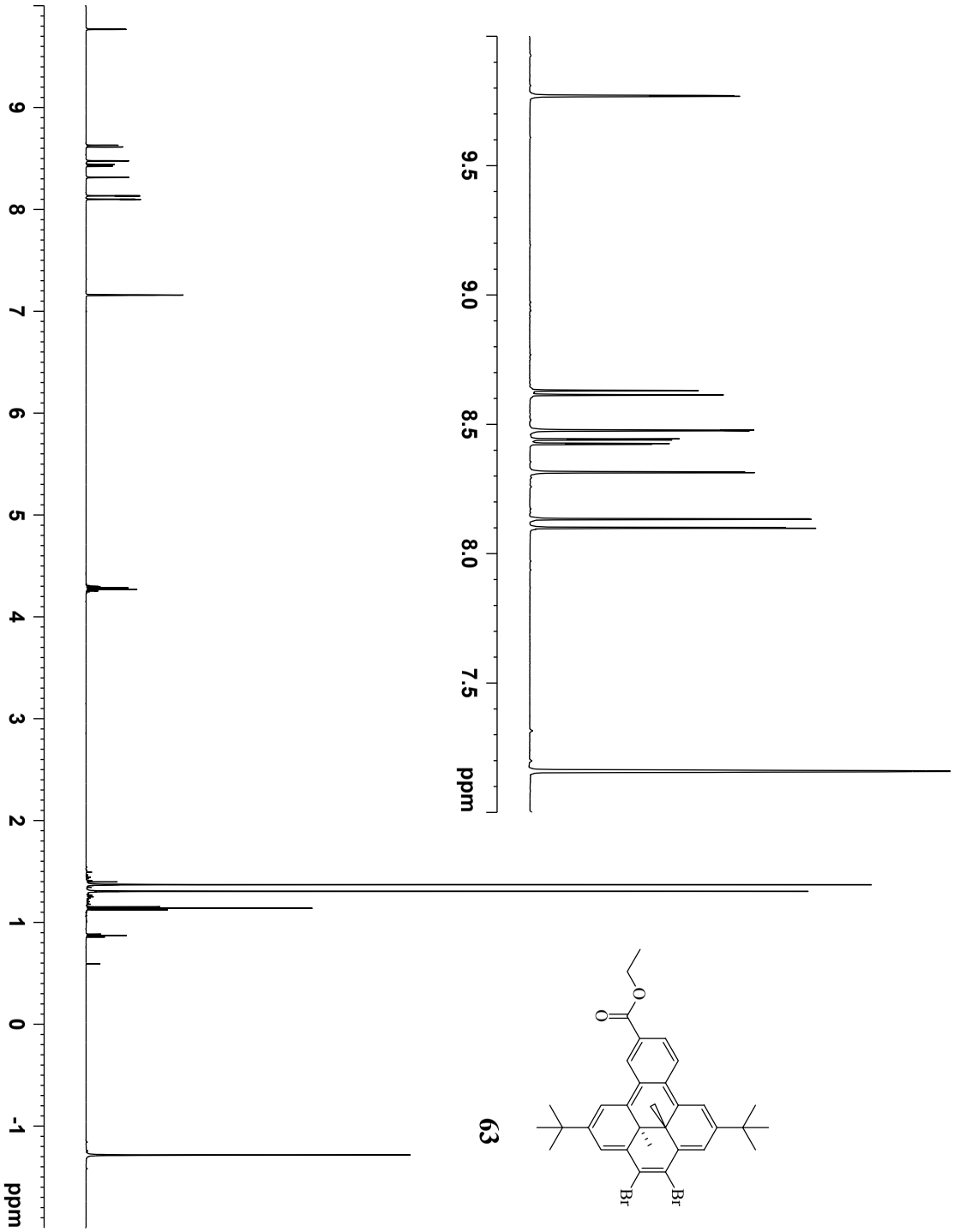

63

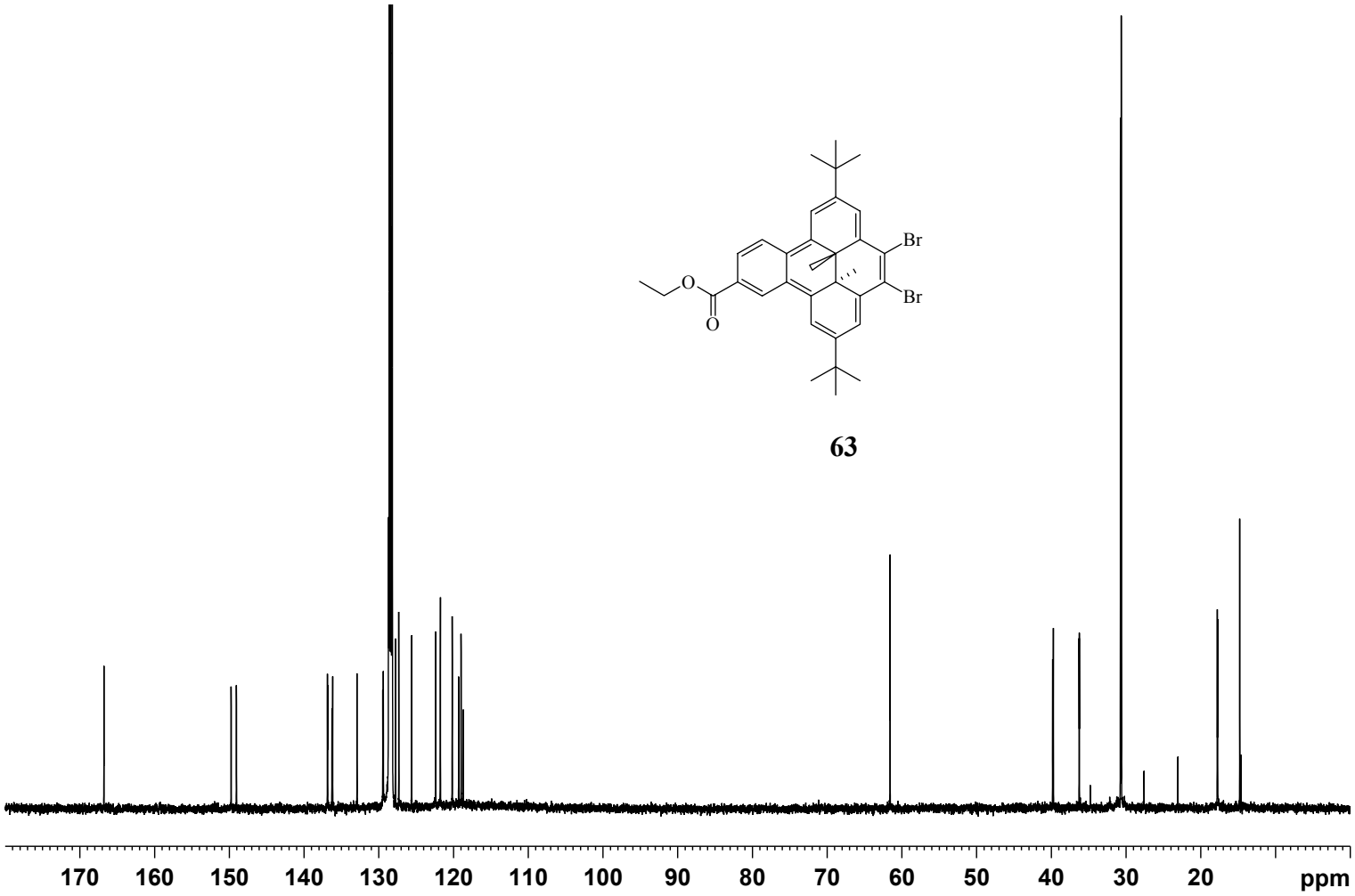

63

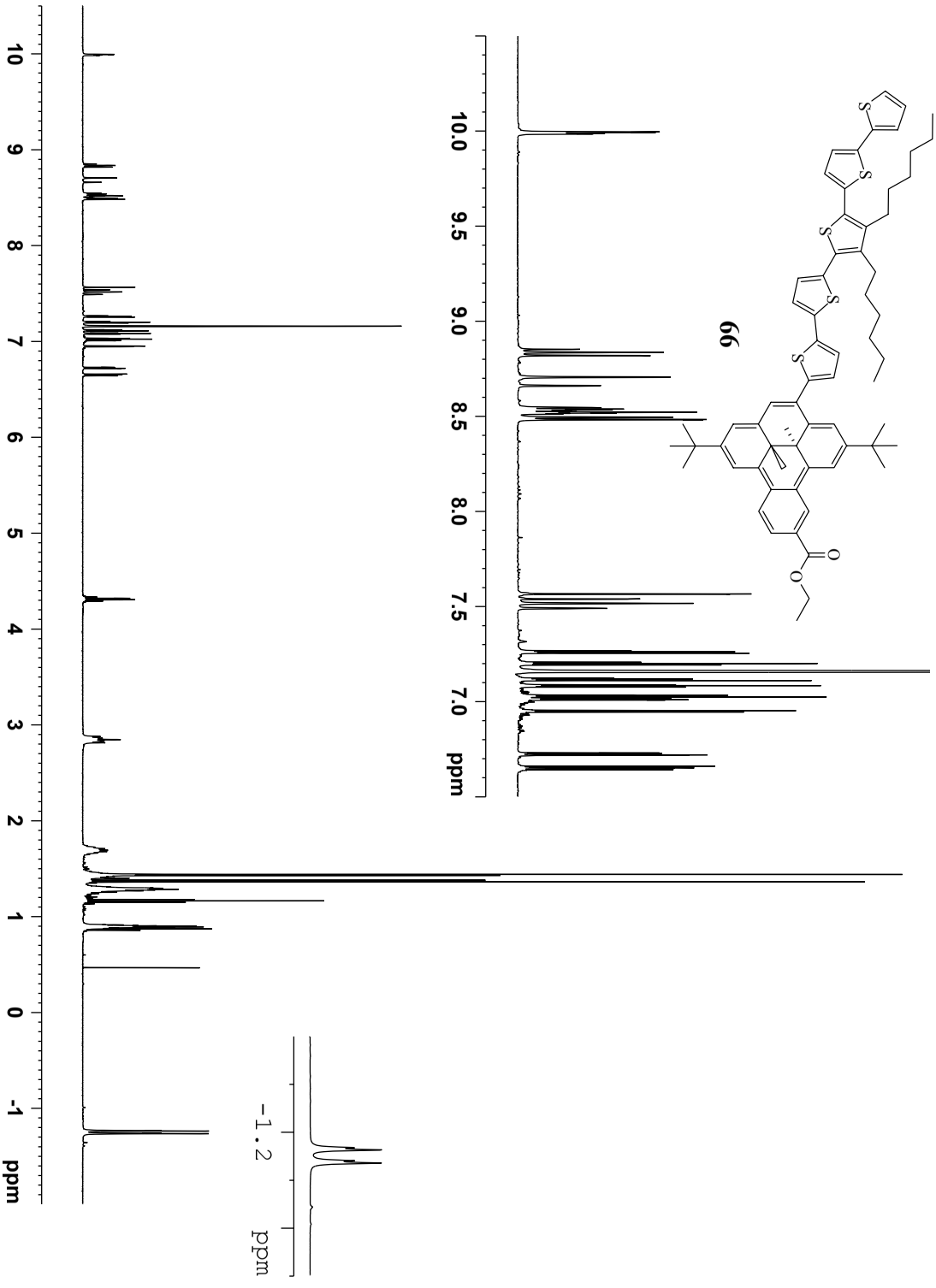

66

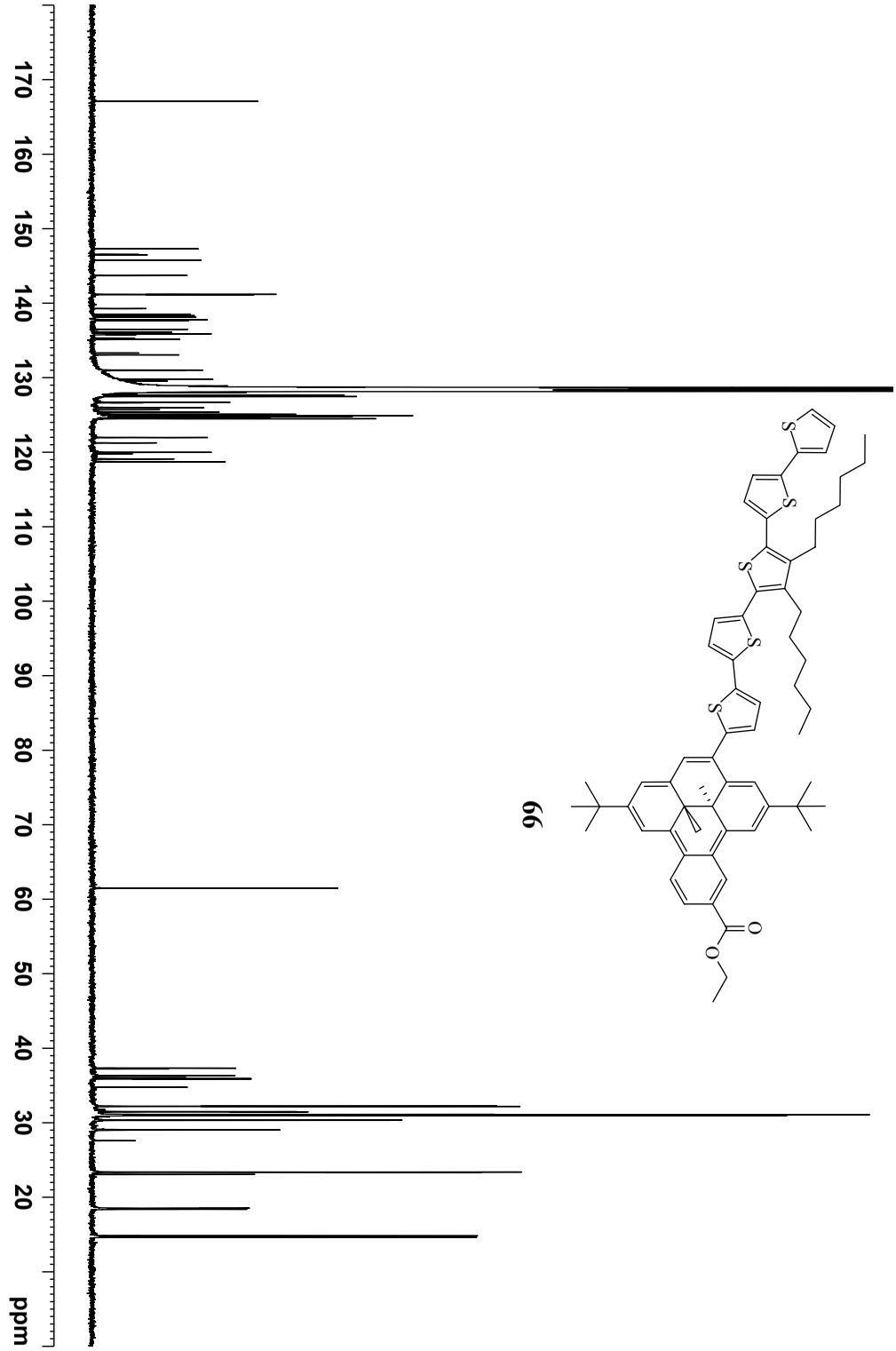
170
160
150
140
130
120
110
100
90
80
70
60
50
40
30
20
ppm
99
S
S
S
S
S
O
O

S
S
S
S
S
O
O
66'
10.0
9.5
9.0
8.5
8.0
7.5
7.0
ppm
4.4
ppm
-1.2
ppm
9
8
7
6
5
4
3
2
1
0
-1
ppm

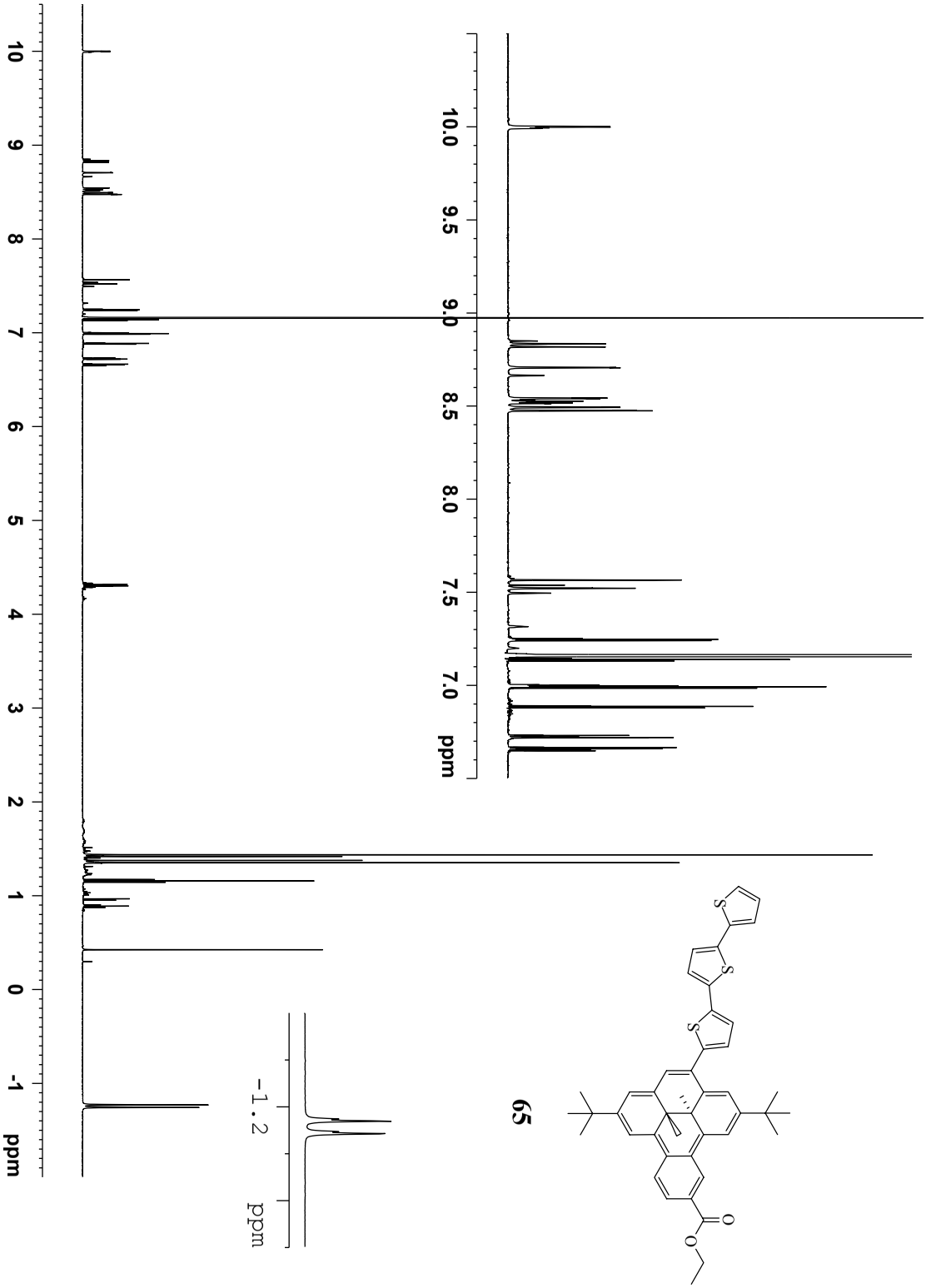

65

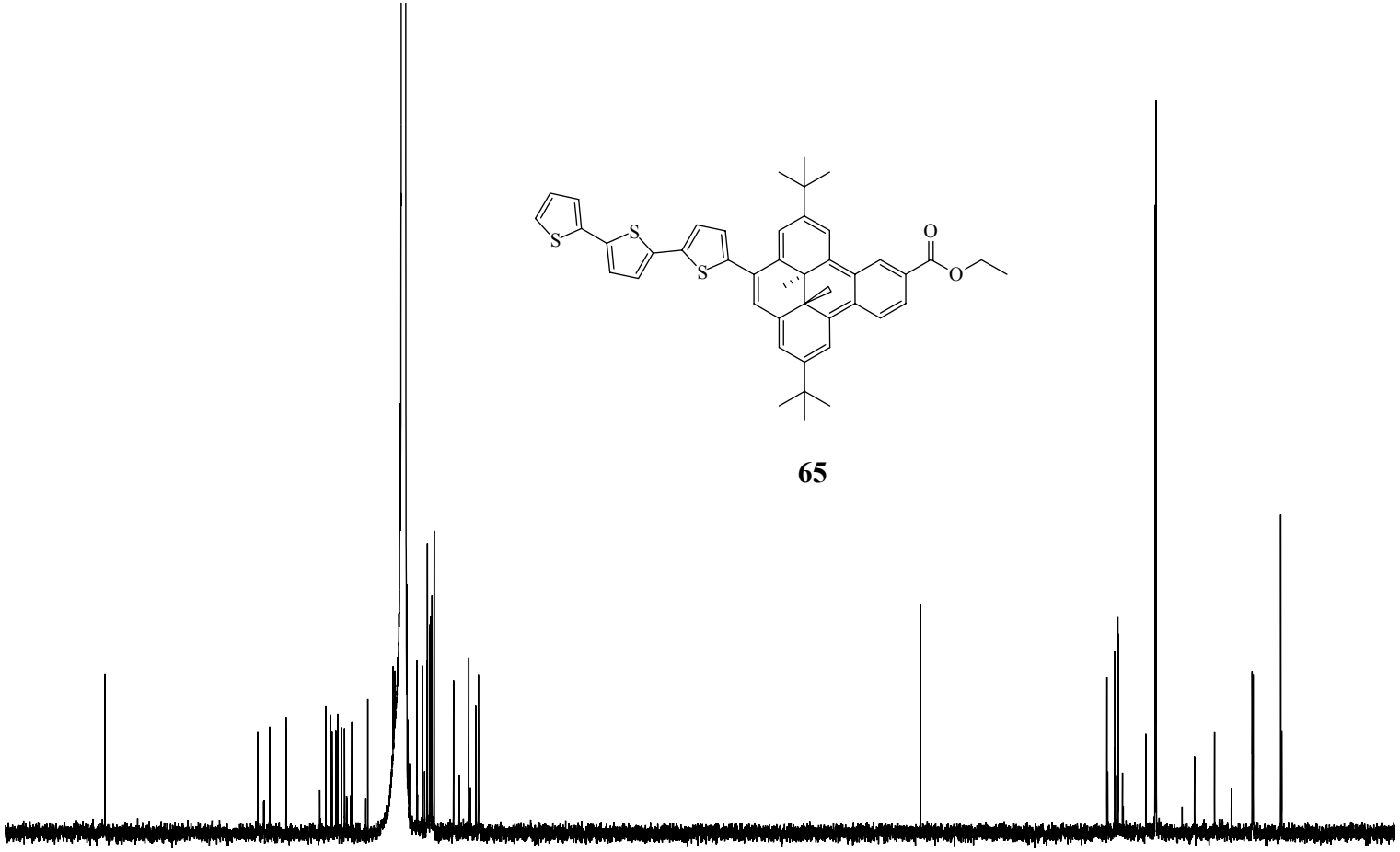

65

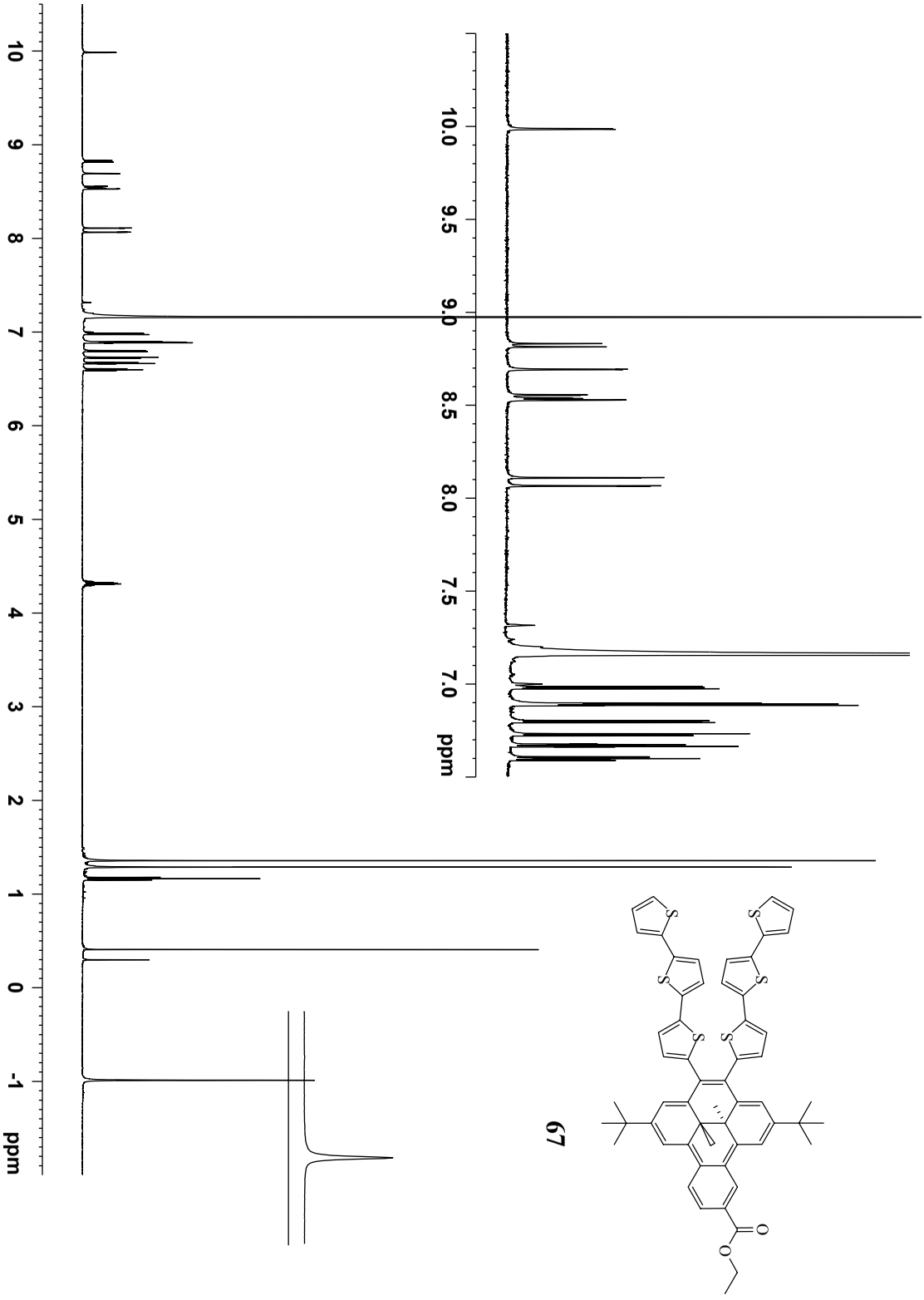

67

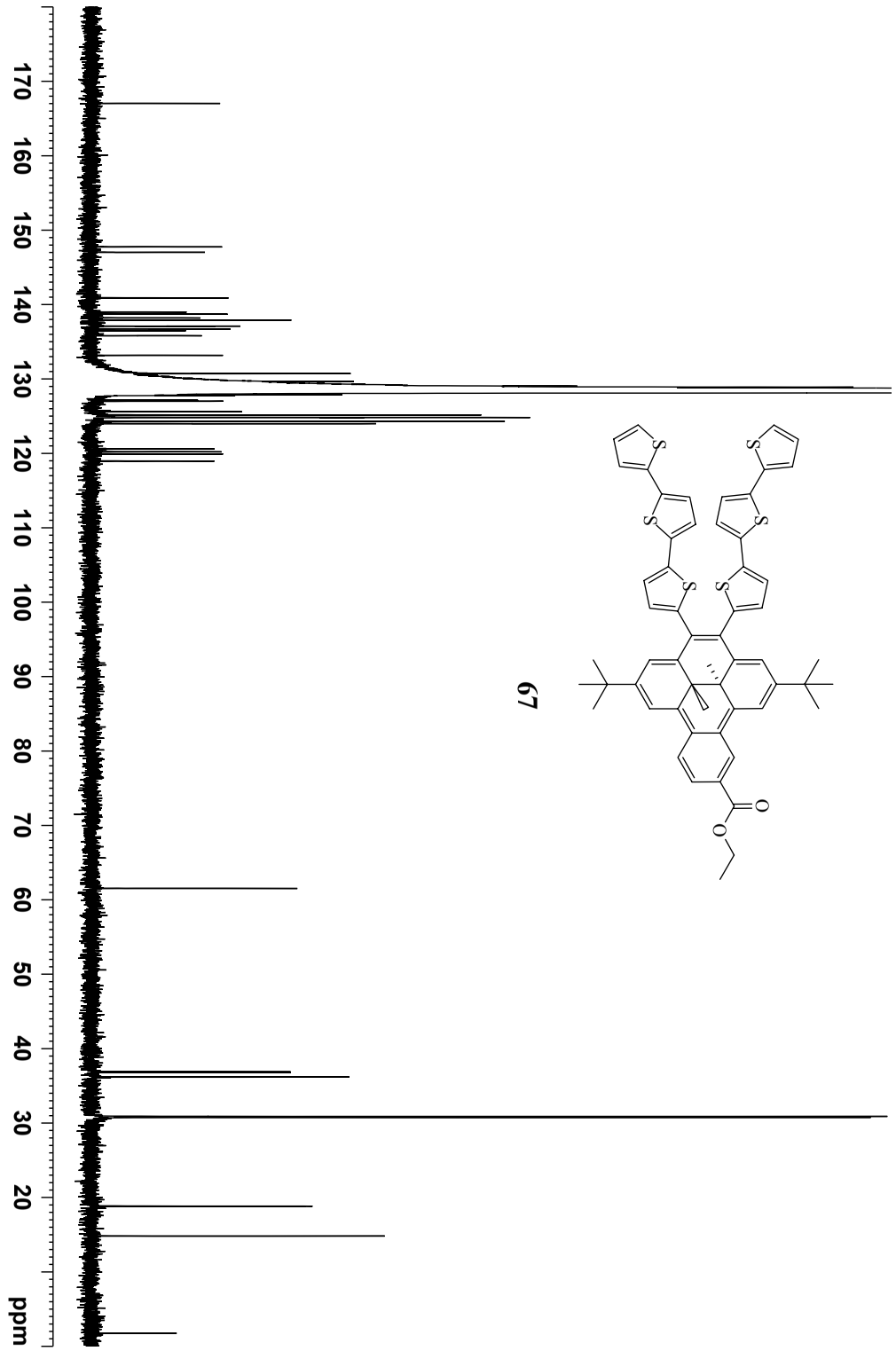
170
160
150
140
130
120
110
100
90
80
70
60
50
40
30
20
ppm
S
S
S
S
S
S
O
O

67

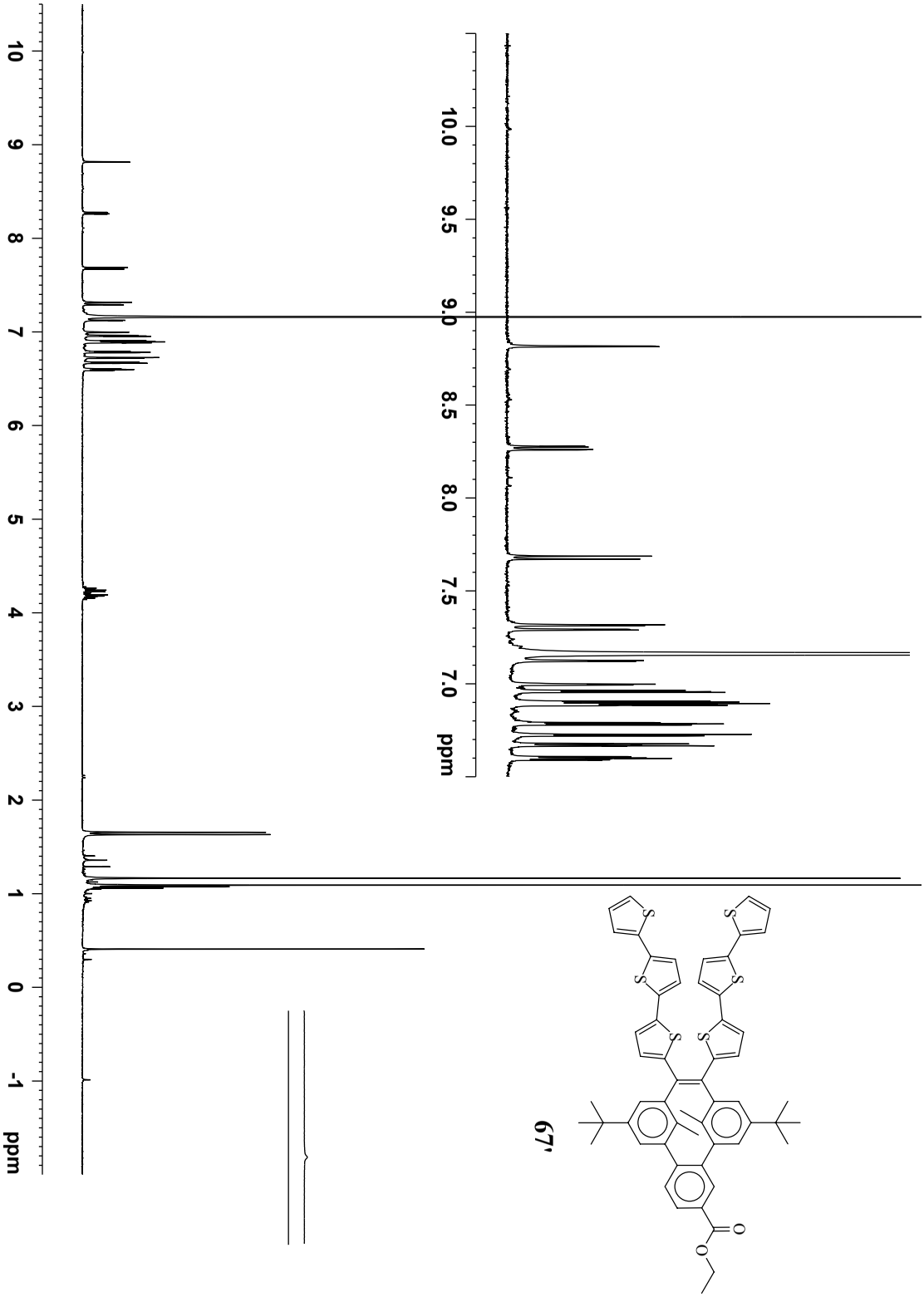

67'

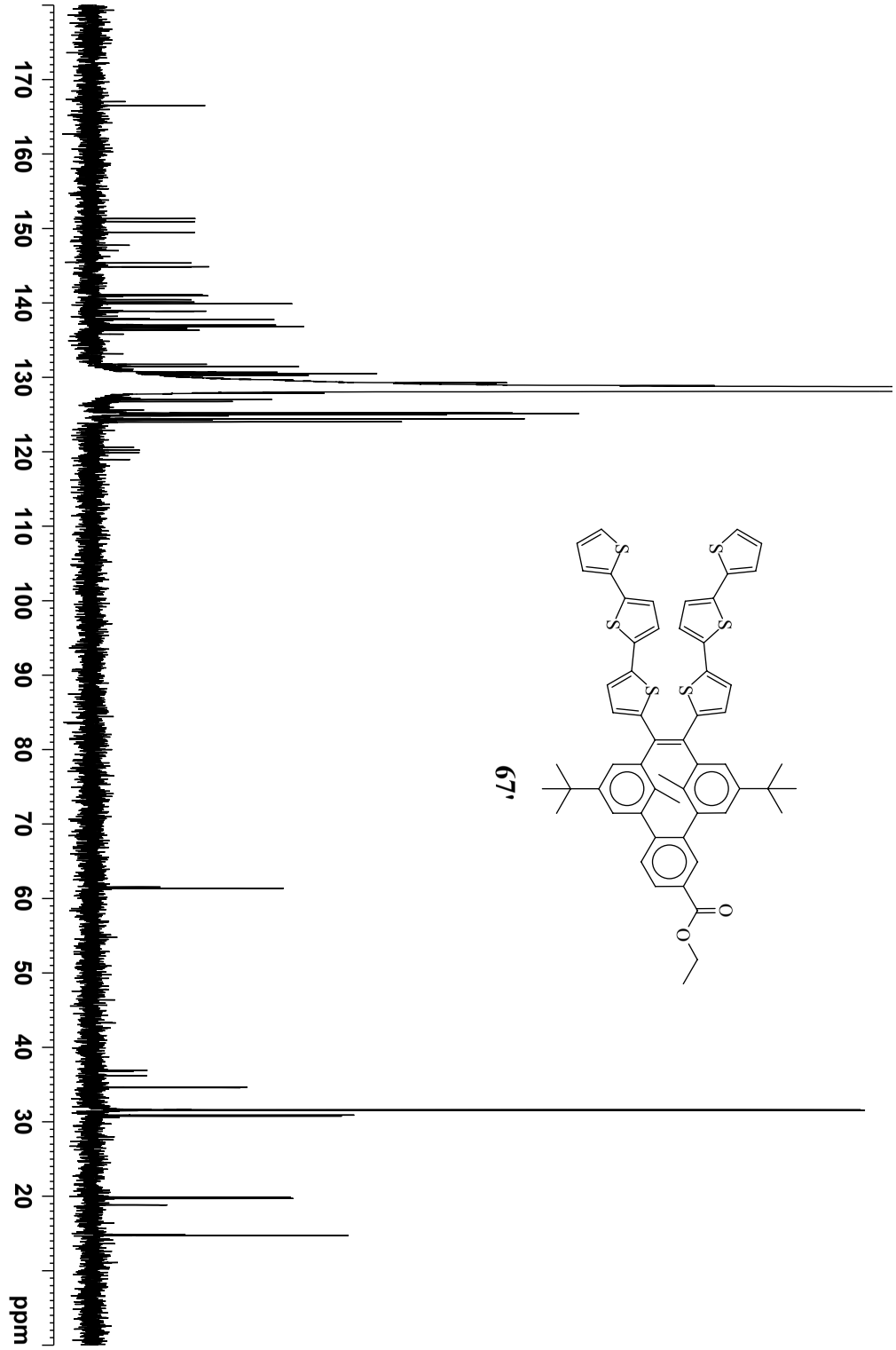
170
160
150
140
130
120
110
100
90
80
70
60
50
40
30
20
ppm
67'

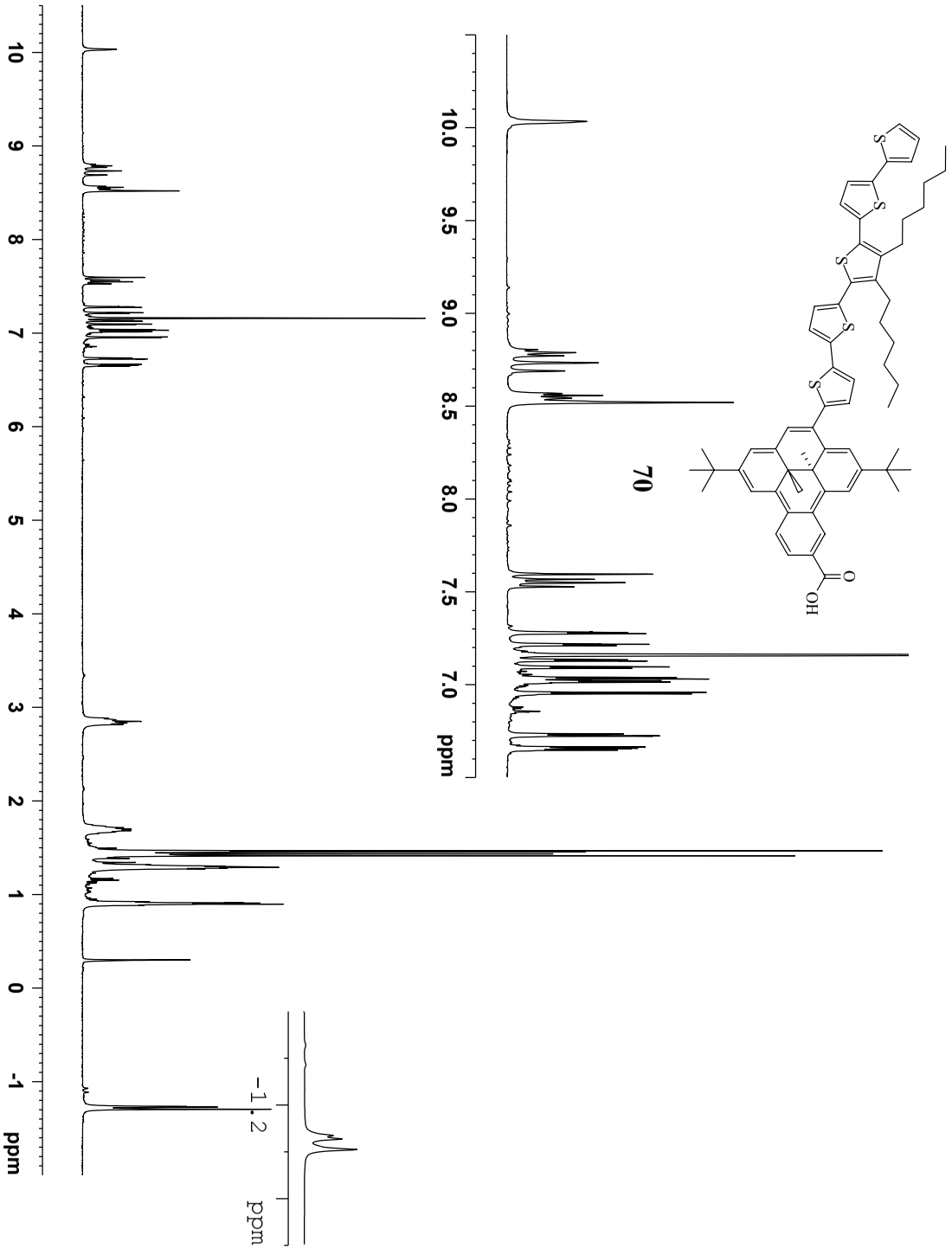
70
HO
O
S
10.0
9.5
9.0
8.5
8.0
7.5
7.0
ppm
10
9
8
7
6
5
4
3
2
1
0
-1
ppm
-1.2
ppm

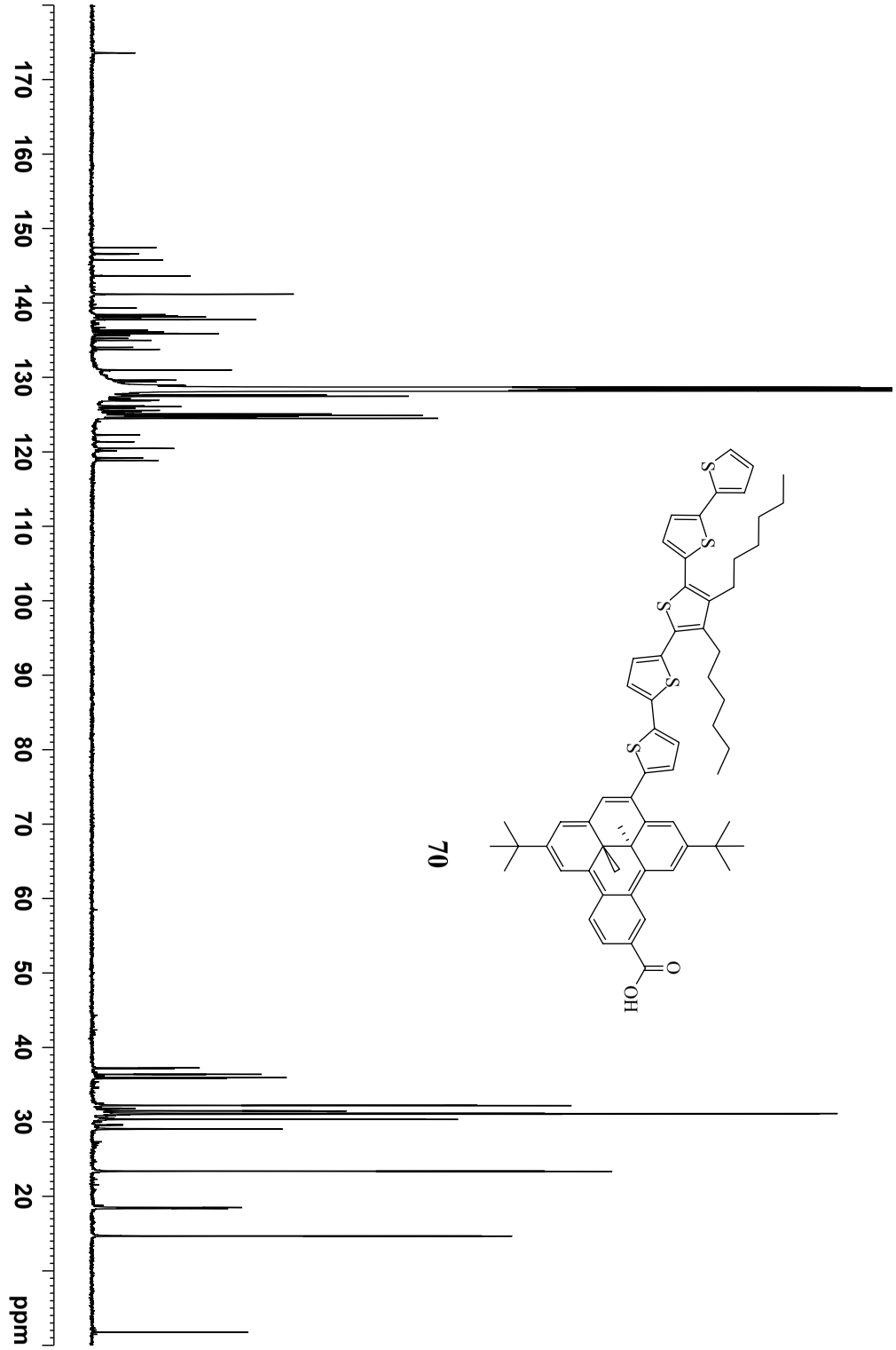
170
160
150
140
130
120
110
100
90
80
70
60
50
40
30
20
ppm
S
S
S
S
S
HO
O

70

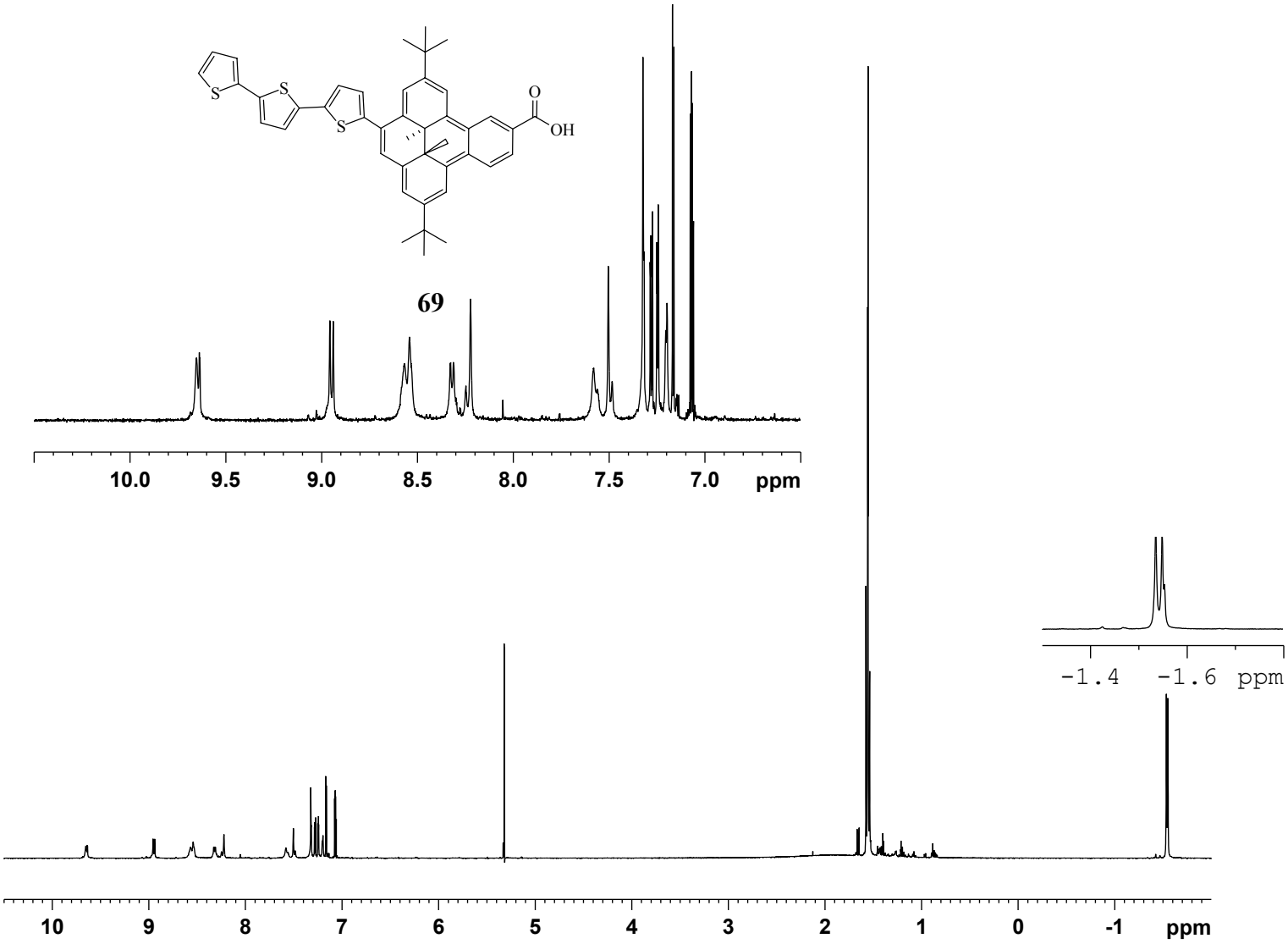
S
S
S
O
OH
69
10.0
9.5
9.0
8.5
8.0
7.5
7.0
ppm
-1.4
-1.6
ppm
10
9
8
7
6
5
4
3
2
1
0
-1
ppm

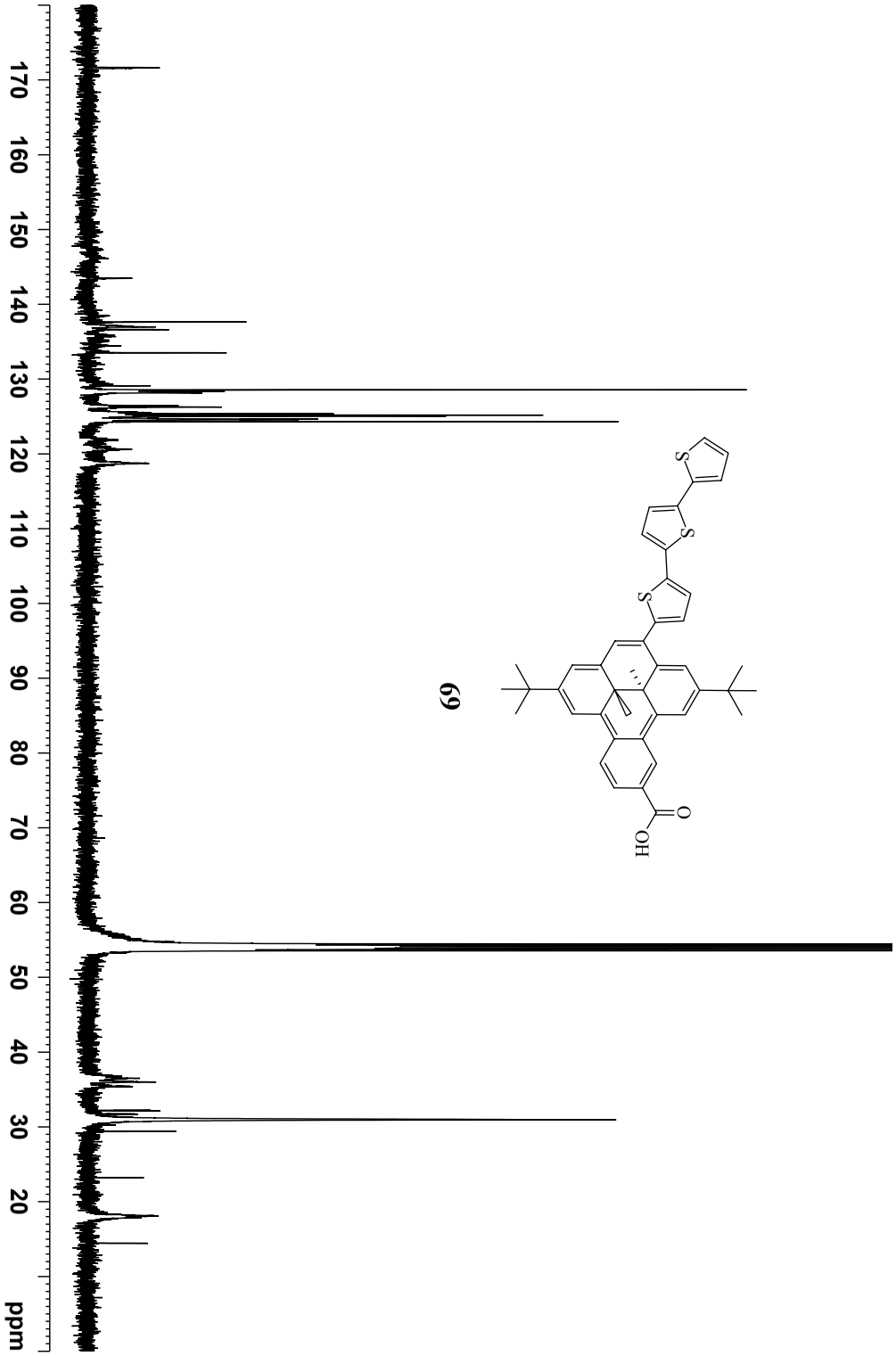

69

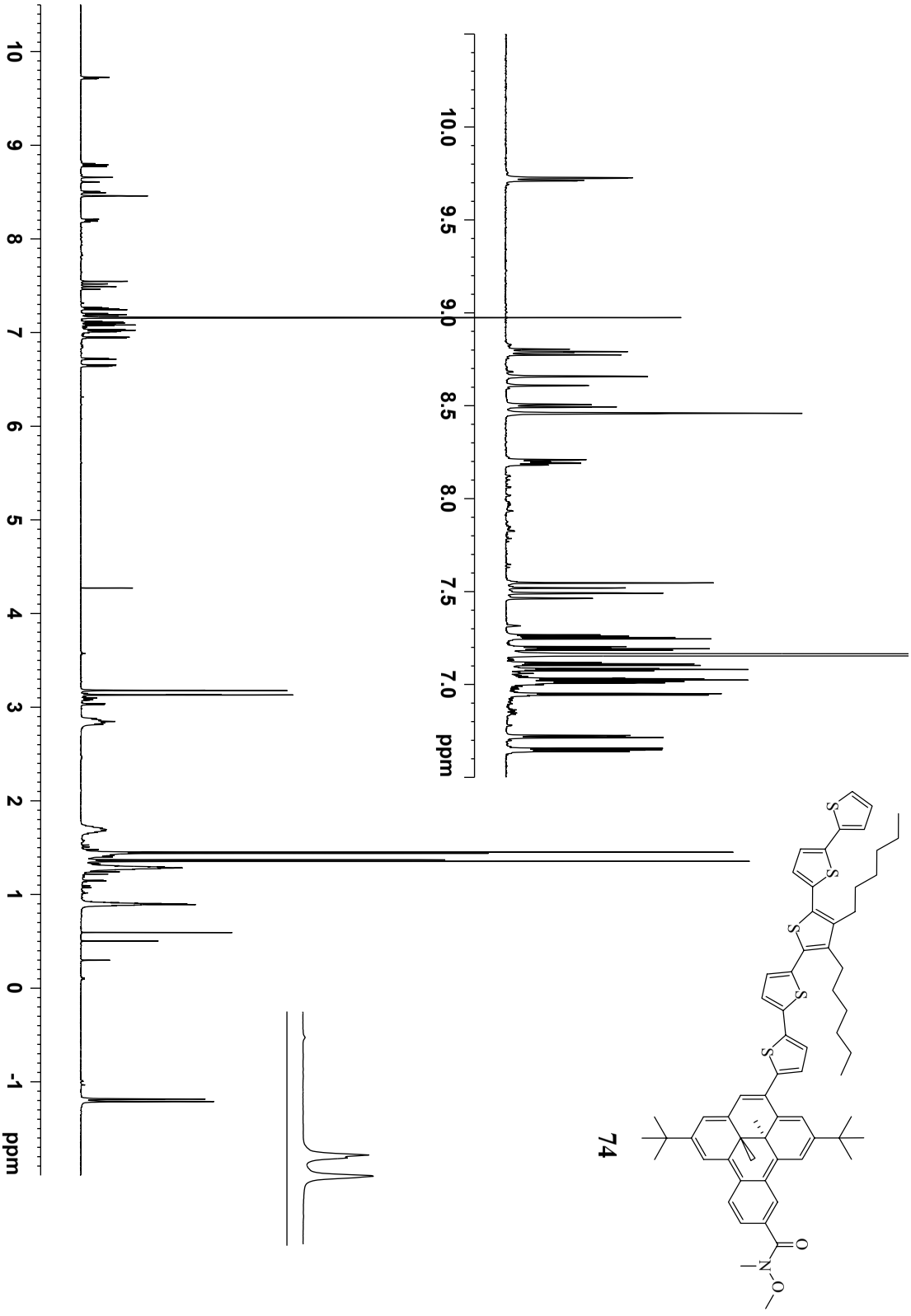
10.0
9.5
9.0
8.5
8.0
7.5
7.0
ppm
10
9
8
7
6
5
4
3
2
1
0
-1
ppm
74

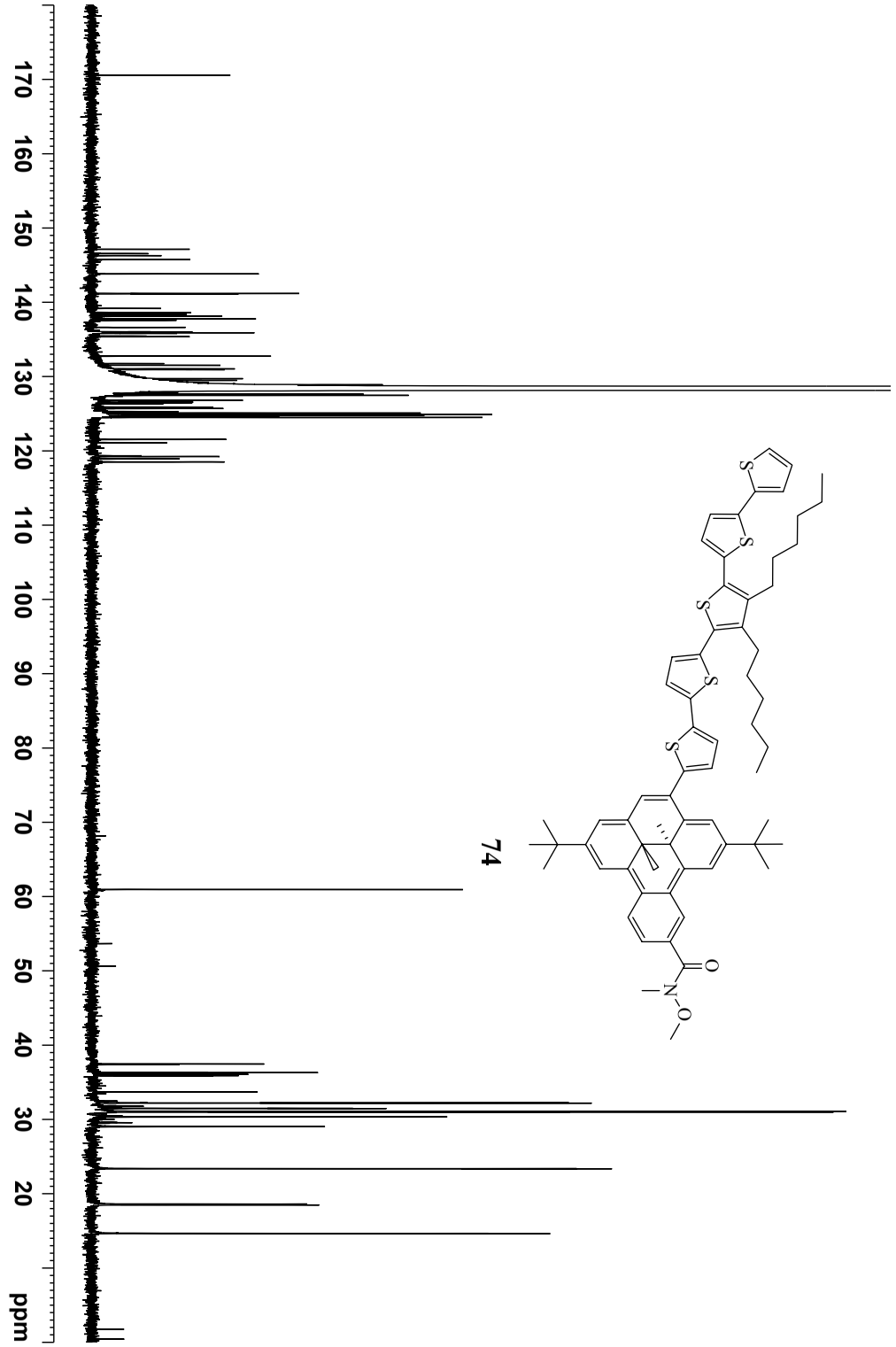
170
160
150
140
130
120
110
100
90
80
70
60
50
40
30
20
ppm
74

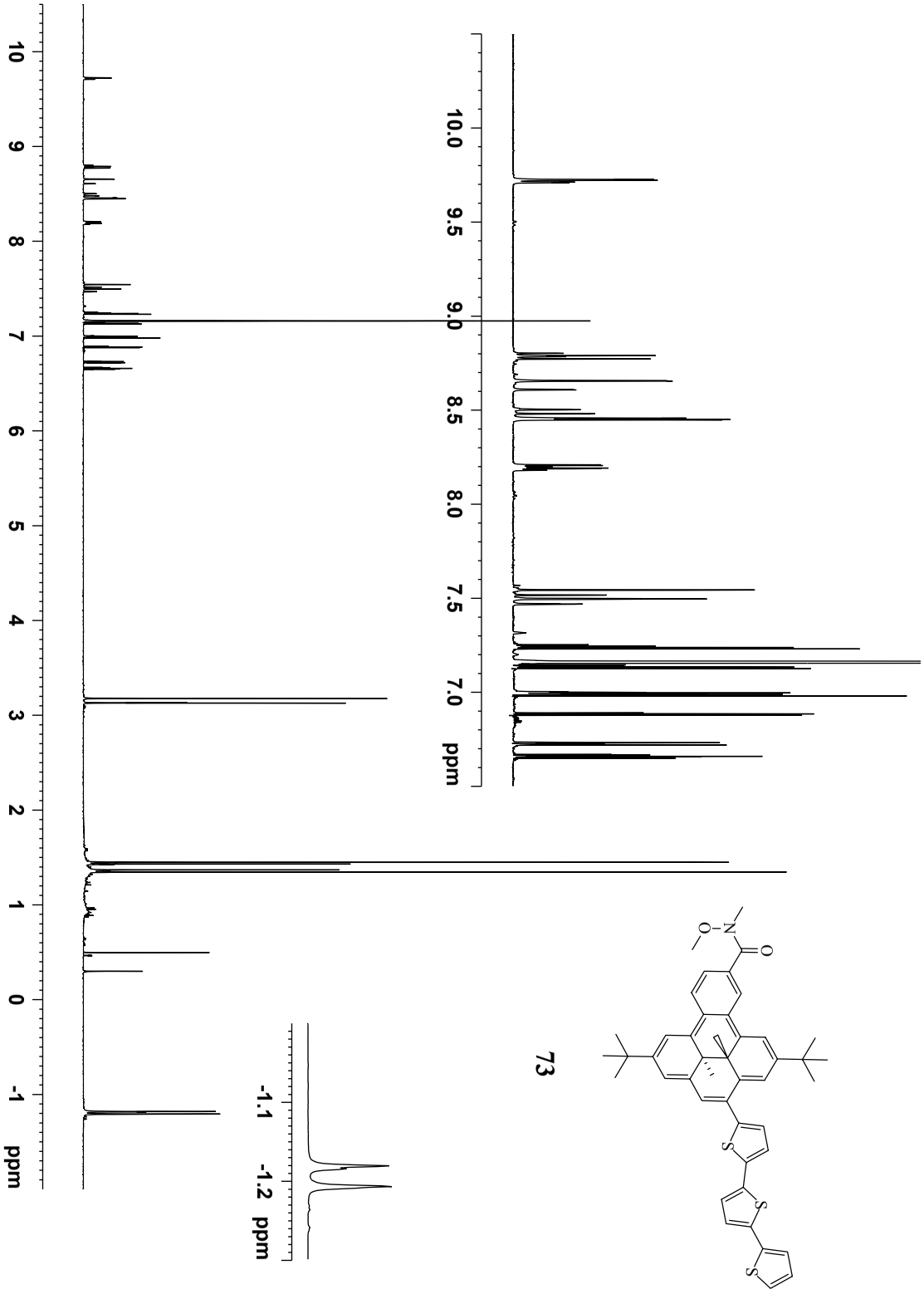

73

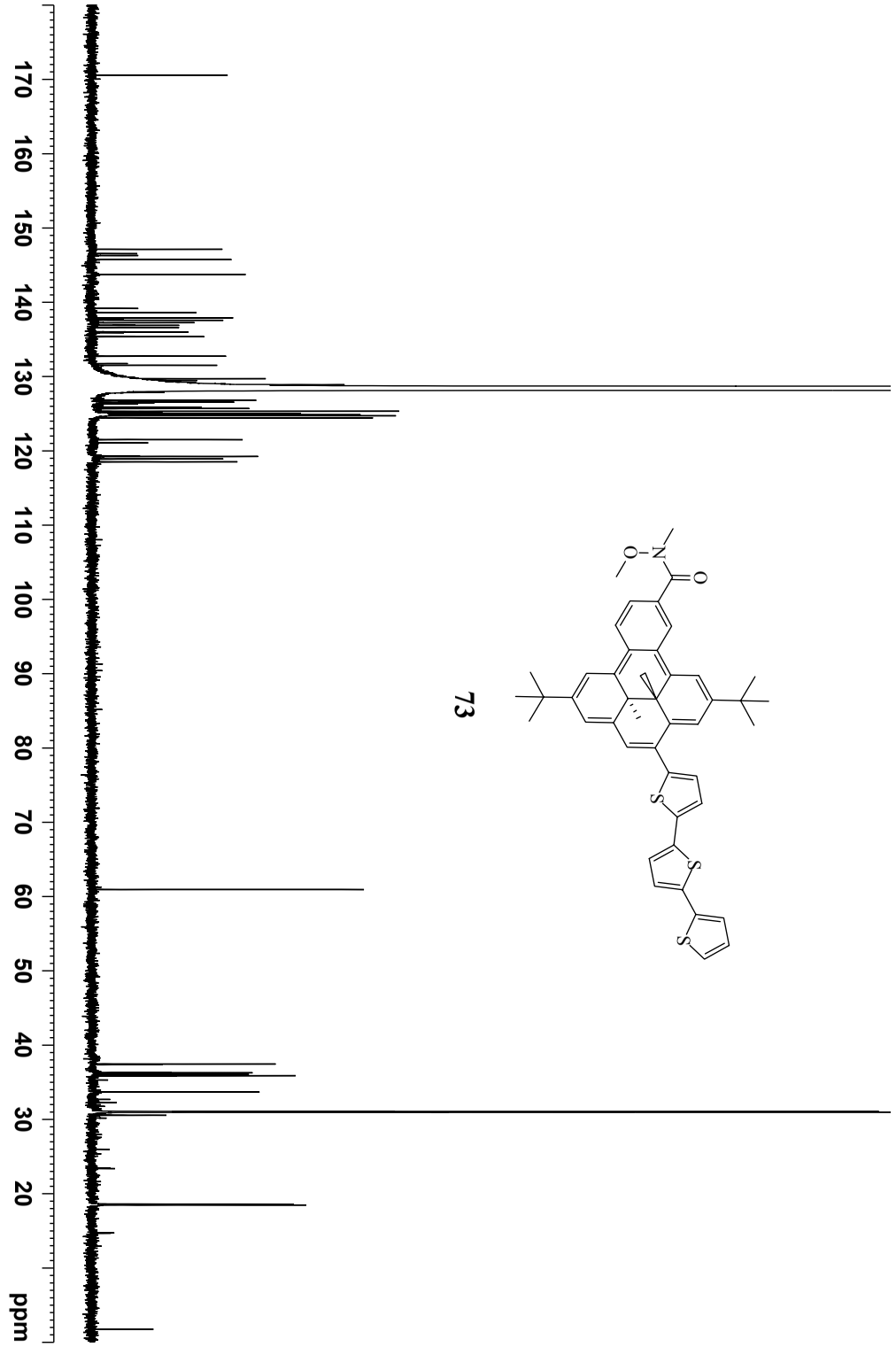

73

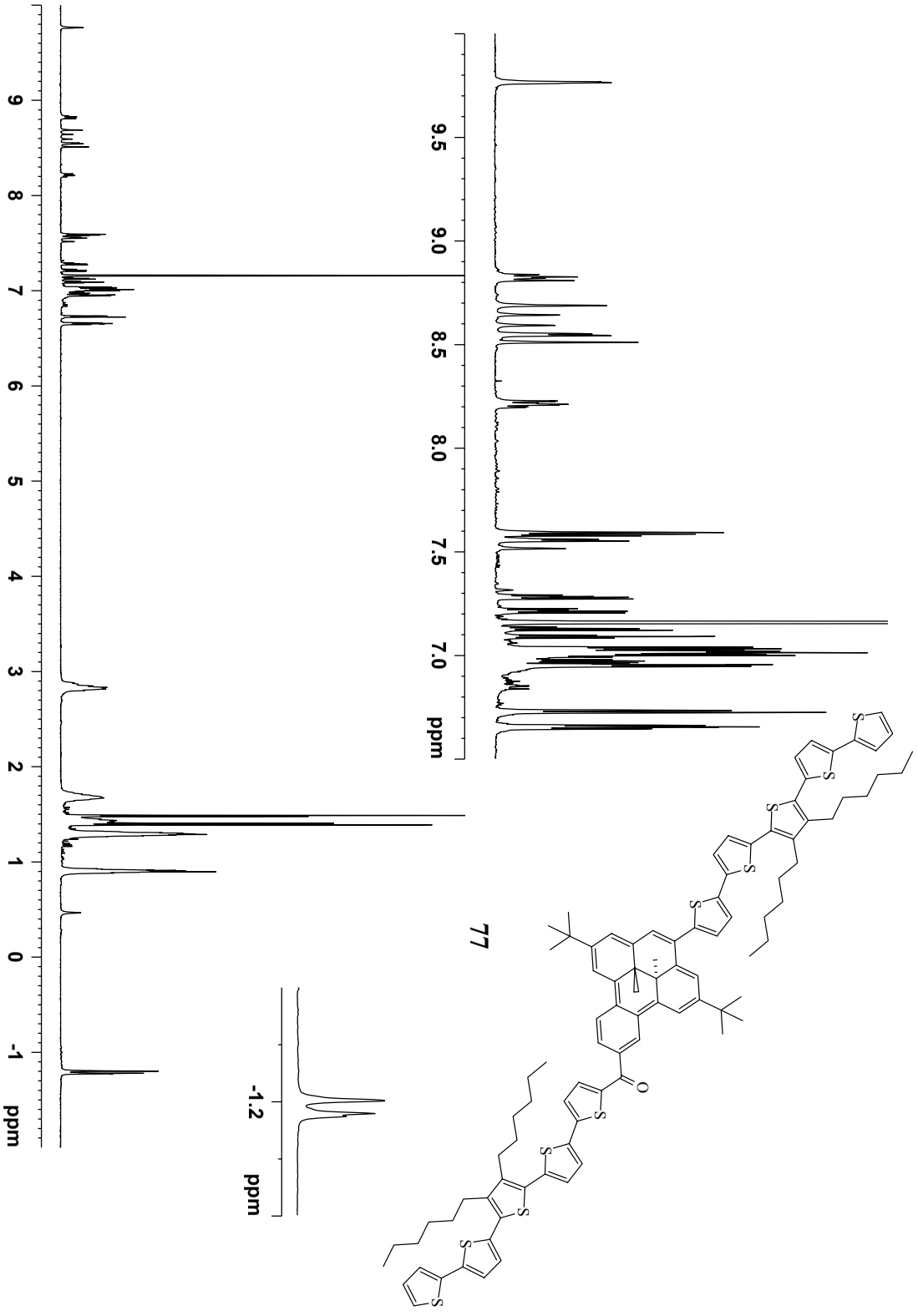
9.5
9.0
8.5
8.0
7.5
7.0
ppm
9
8
7
6
5
4
3
2
1
0
-1
ppm
-1.2
ppm
77

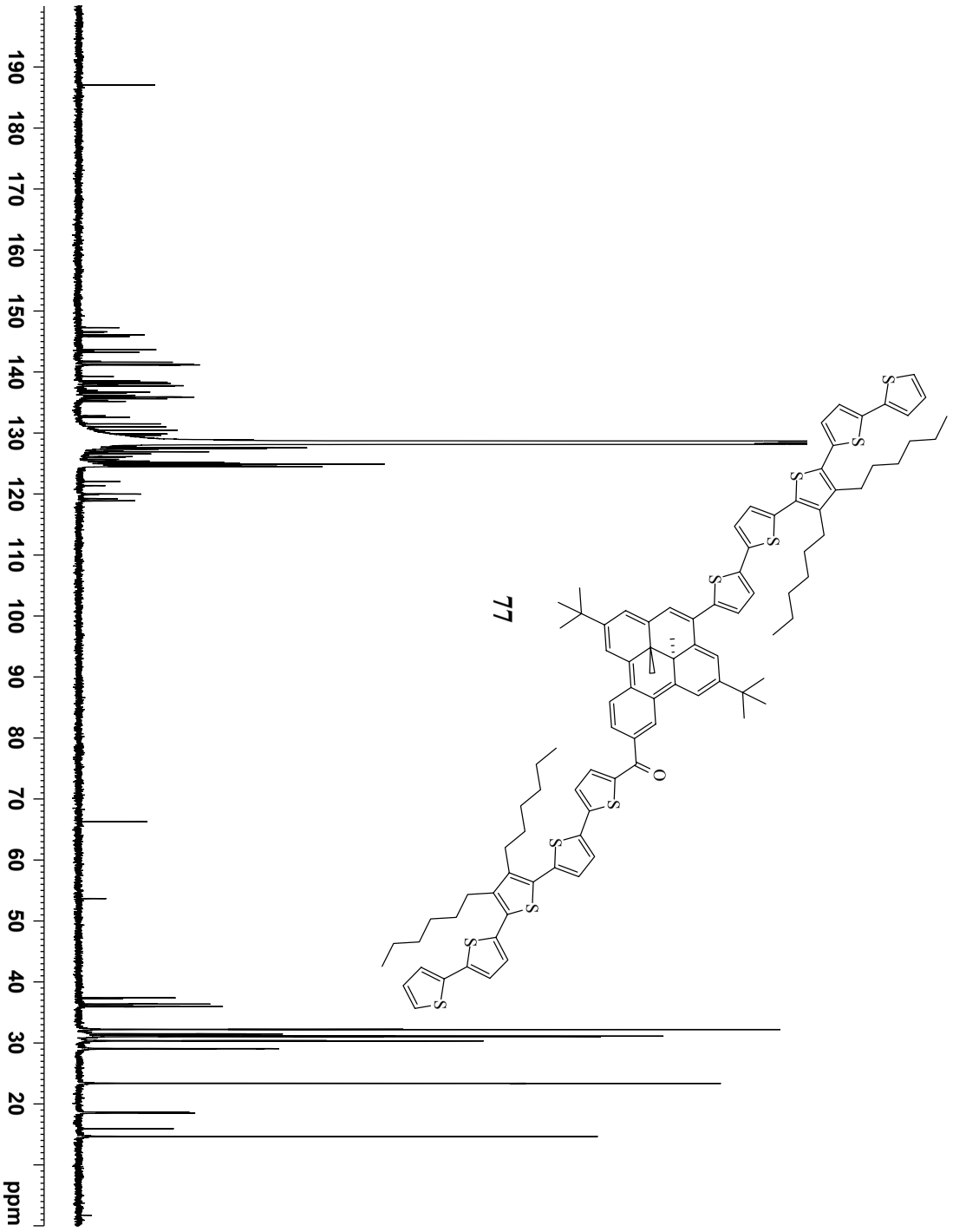
77
O
S
ppm
190
180
170
160
150
140
130
120
110
100
90
80
70
60
50
40
30
20

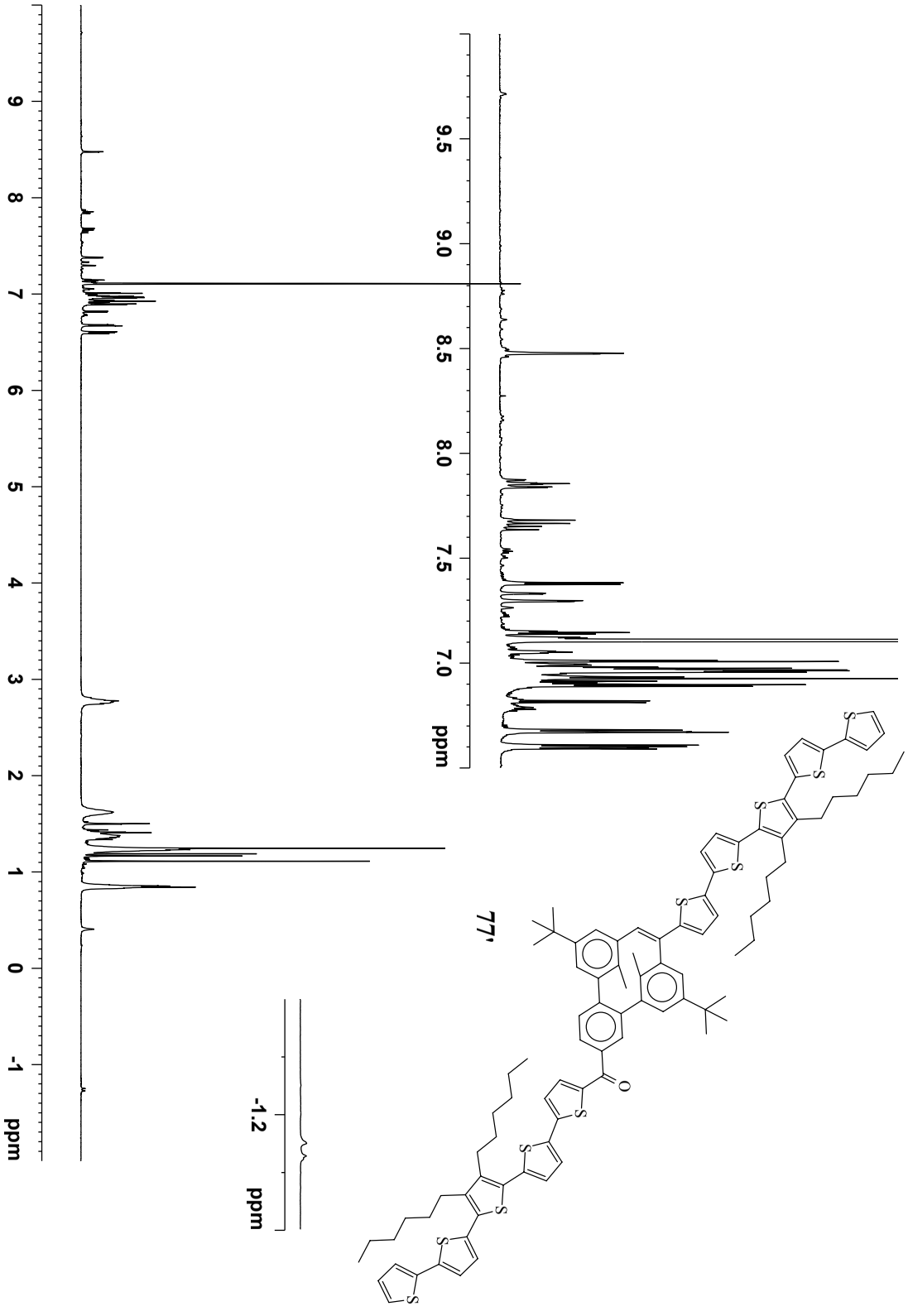
9.5
9.0
8.5
8.0
7.5
7.0
ppm
9
8
7
6
5
4
3
2
1
0
-1
ppm
-1.2
ppm
77'
S
O

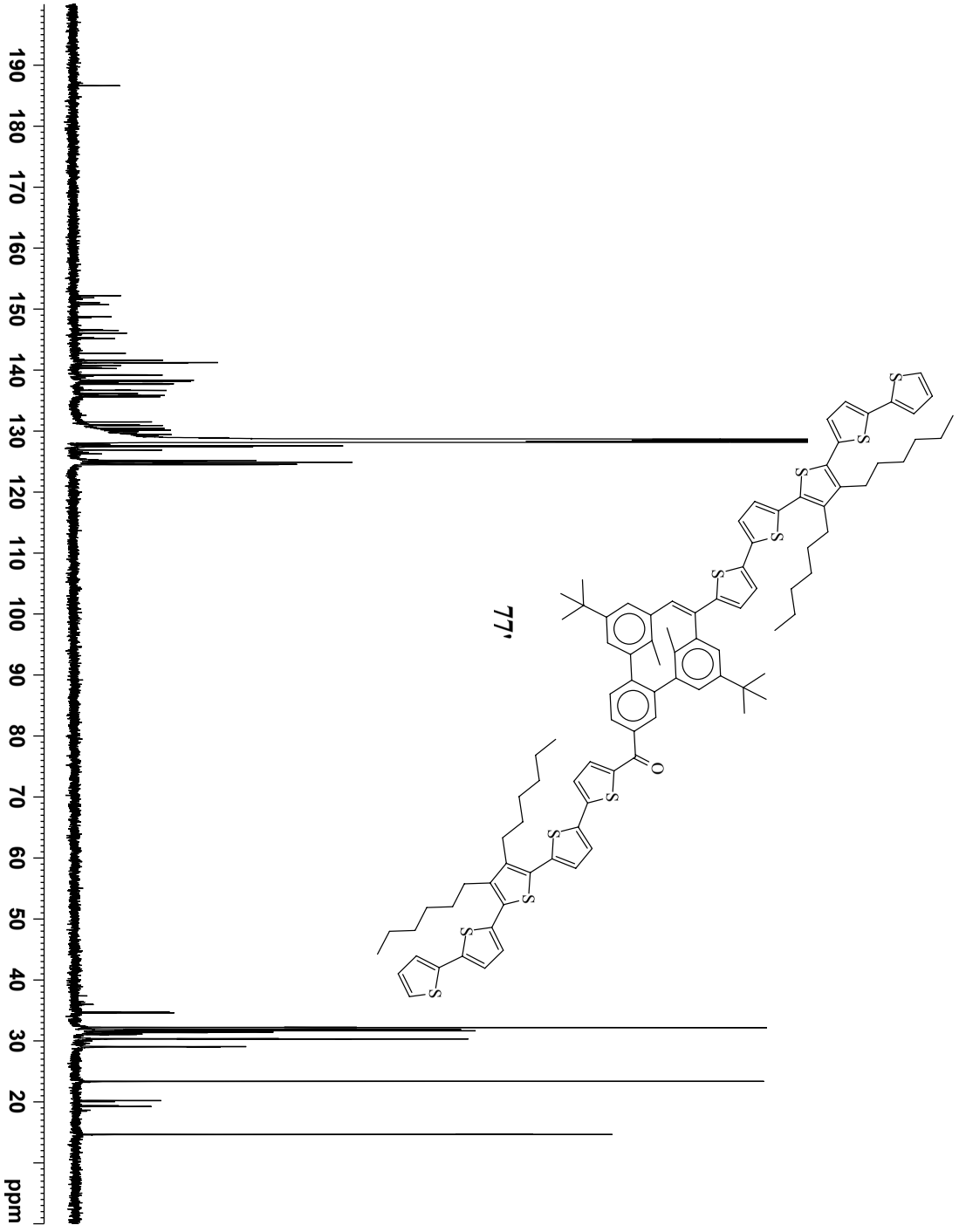
77'
O
S
190
180
170
160
150
140
130
120
110
100
90
80
70
60
50
40
30
20
ppm

76

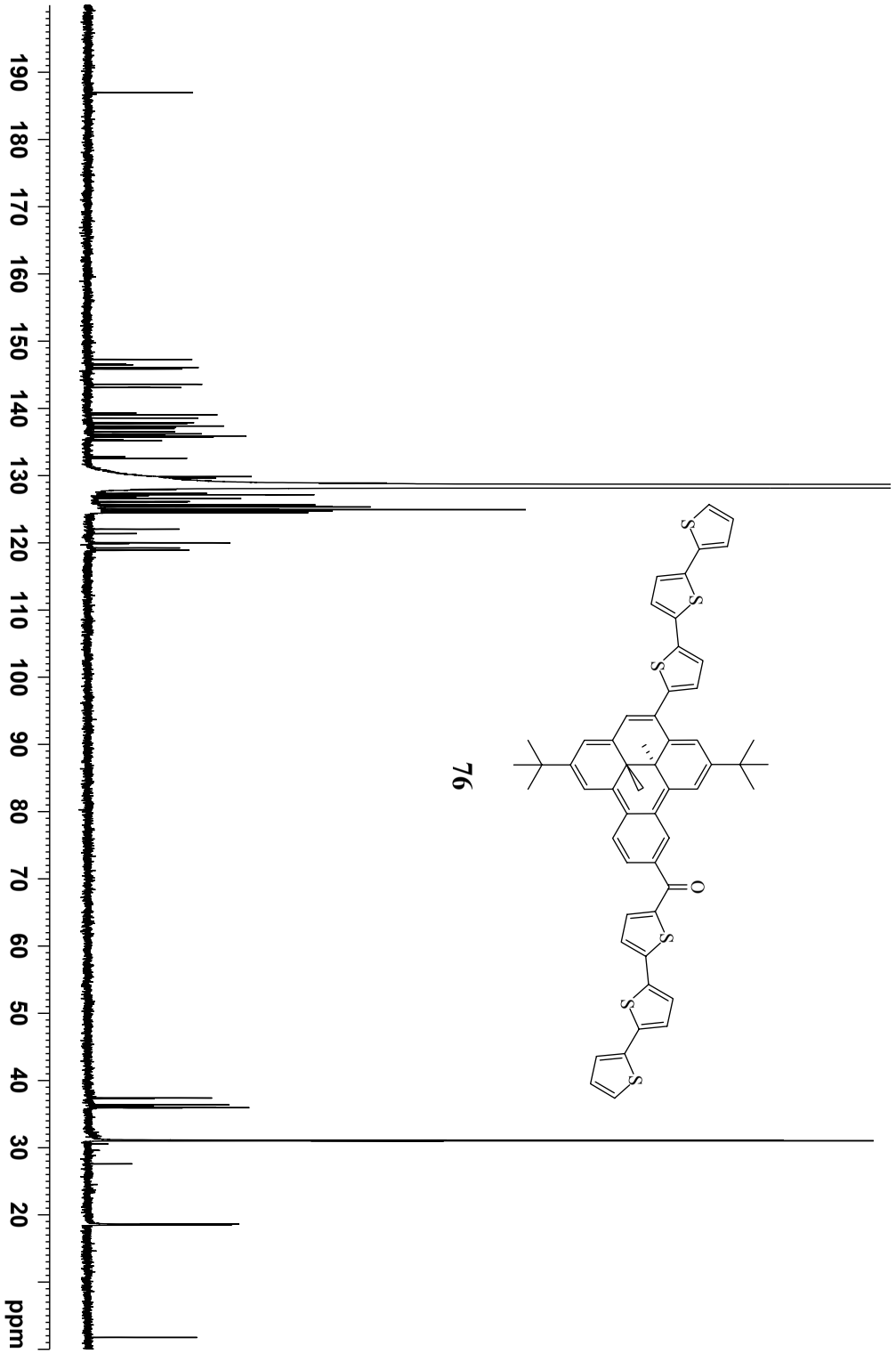
190
180
170
160
150
140
130
120
110
100
90
80
70
60
50
40
30
20
ppm
76

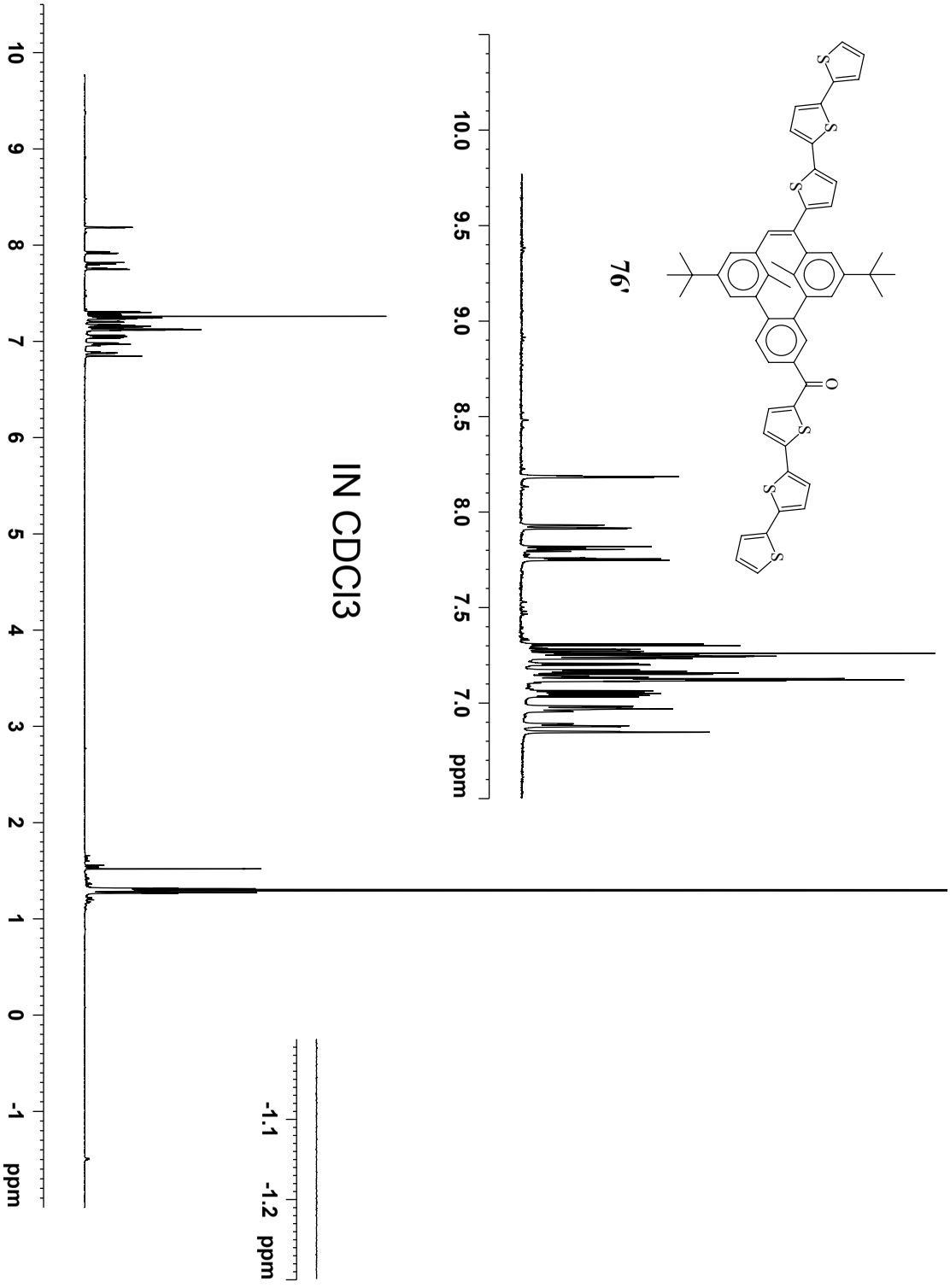
76'
IN CDCl3
10.0 9.5 9.0 8.5 8.0 7.5 7.0 ppm
10 9 8 7 6 5 4 3 2 1 0 -1 ppm
-1.1 -1.2 ppm

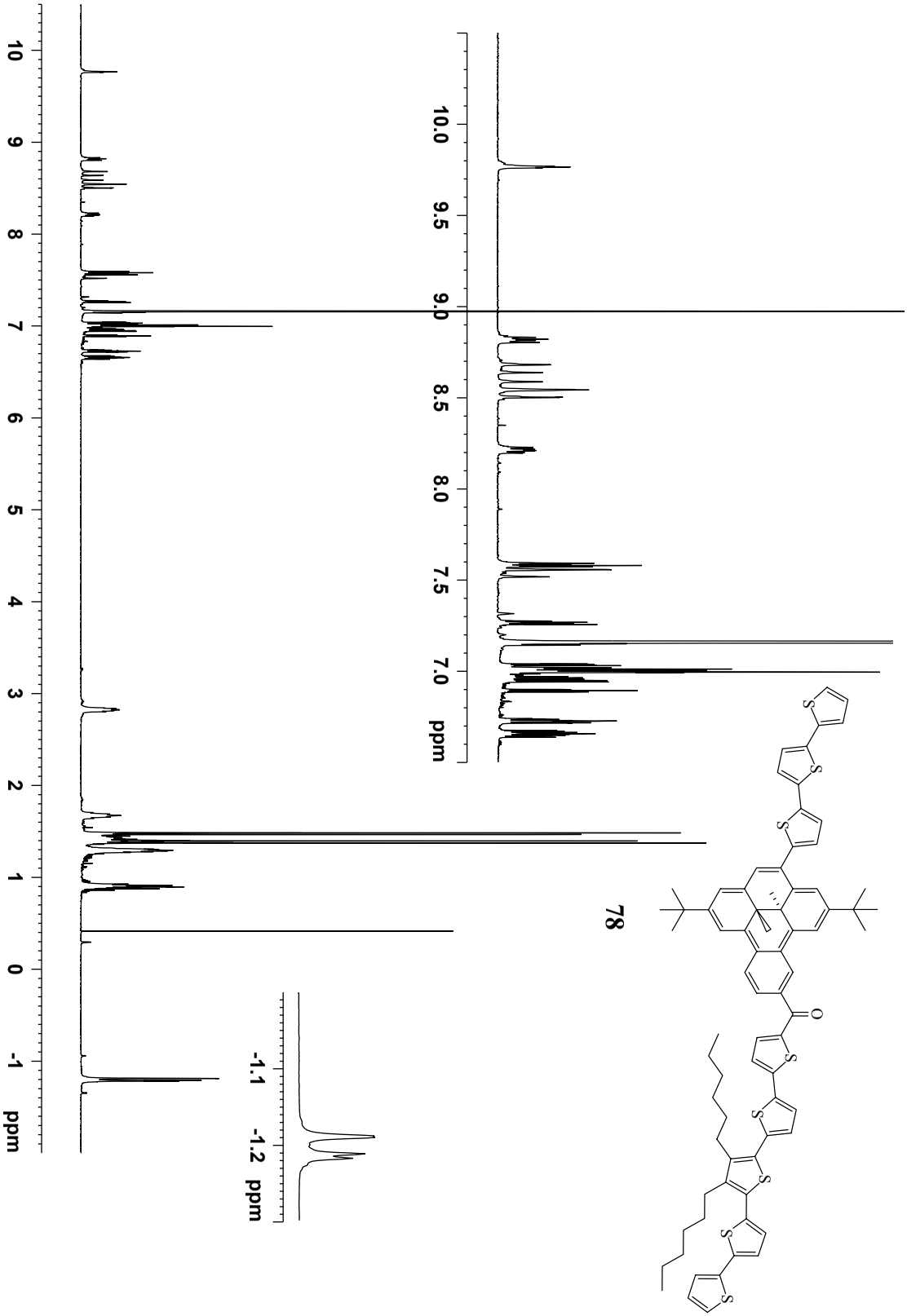

78

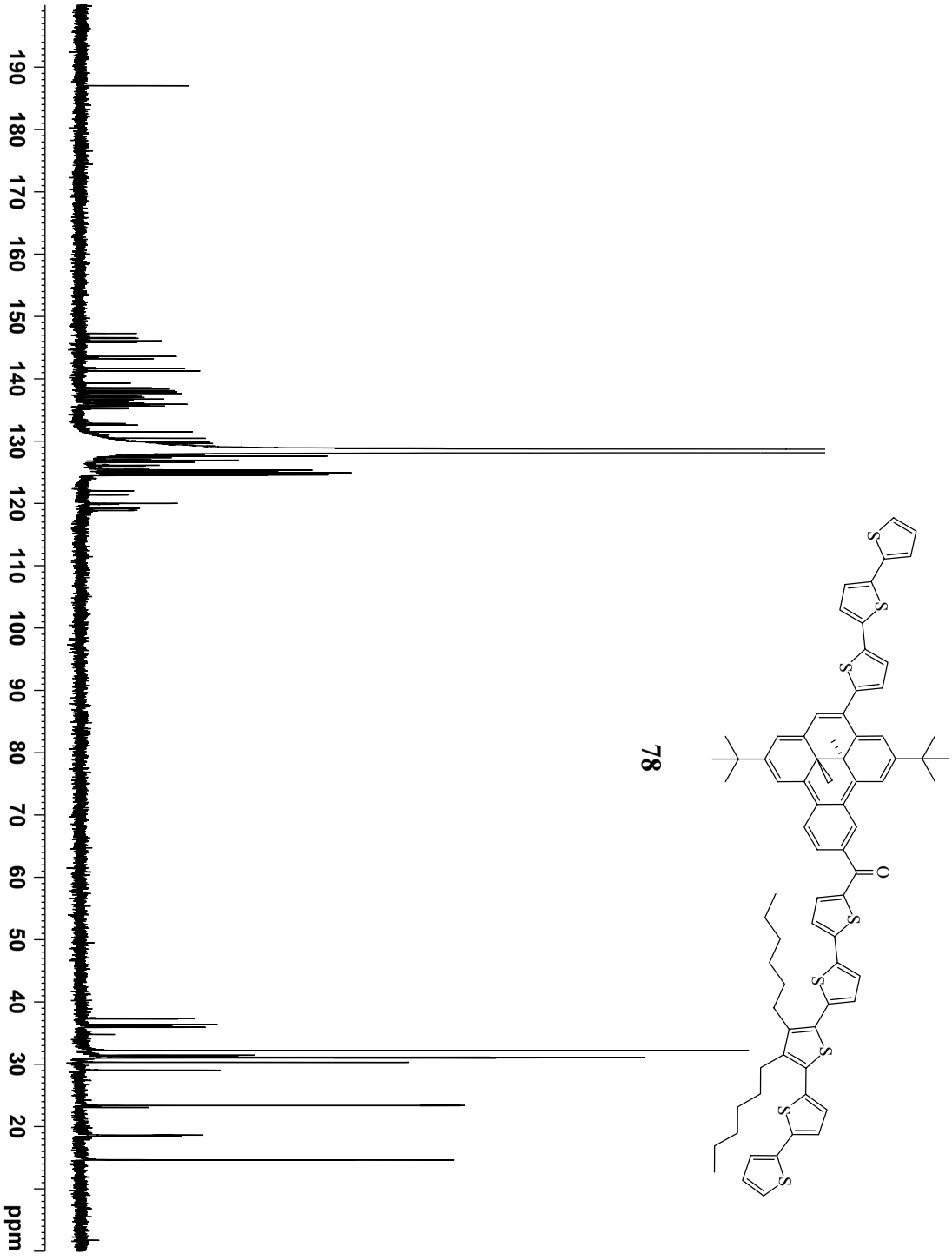
190
180
170
160
150
140
130
120
110
100
90
80
70
60
50
40
30
20
ppm
S
S
S
S
O
S
S
S
S
S
S

78

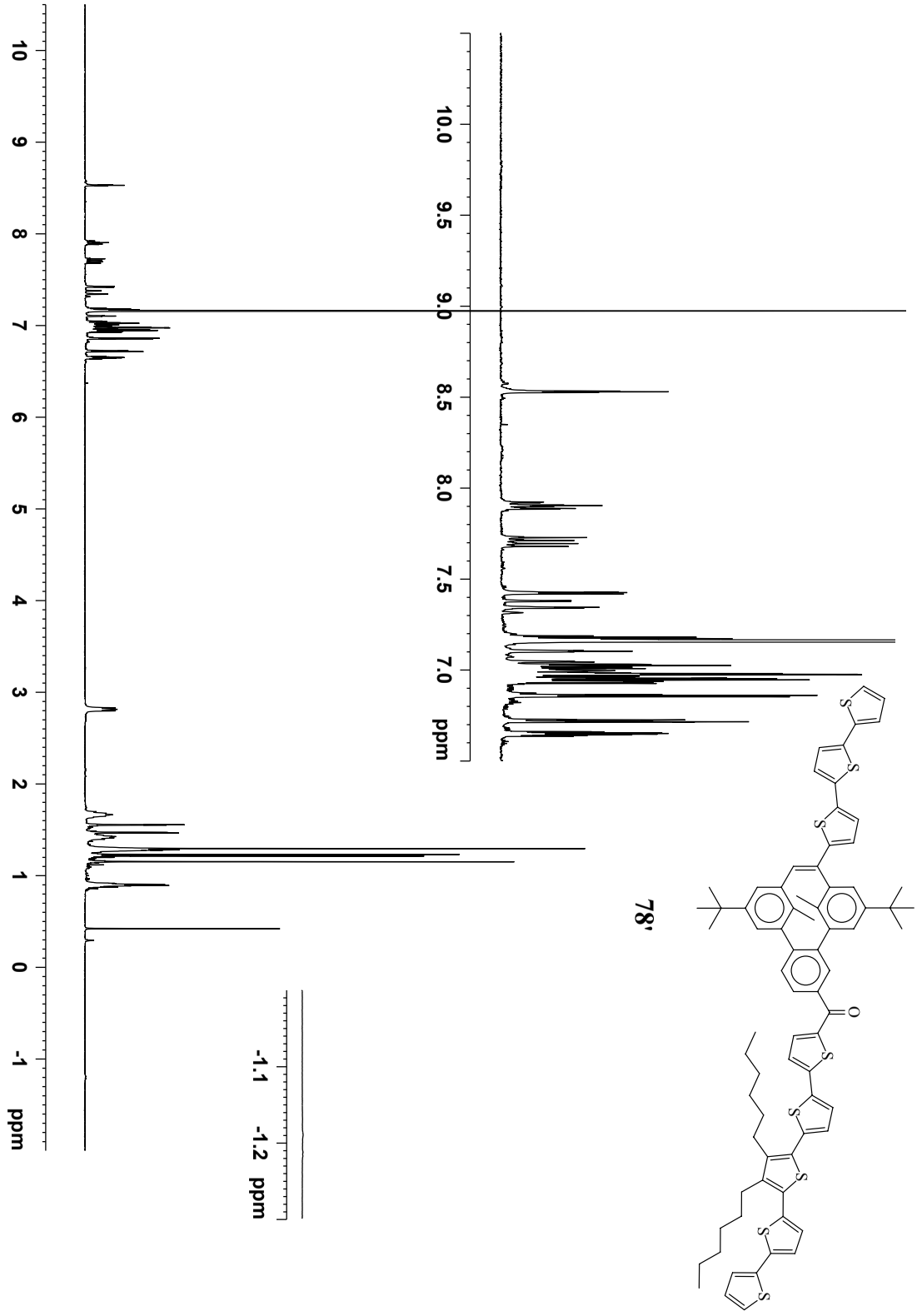

78'

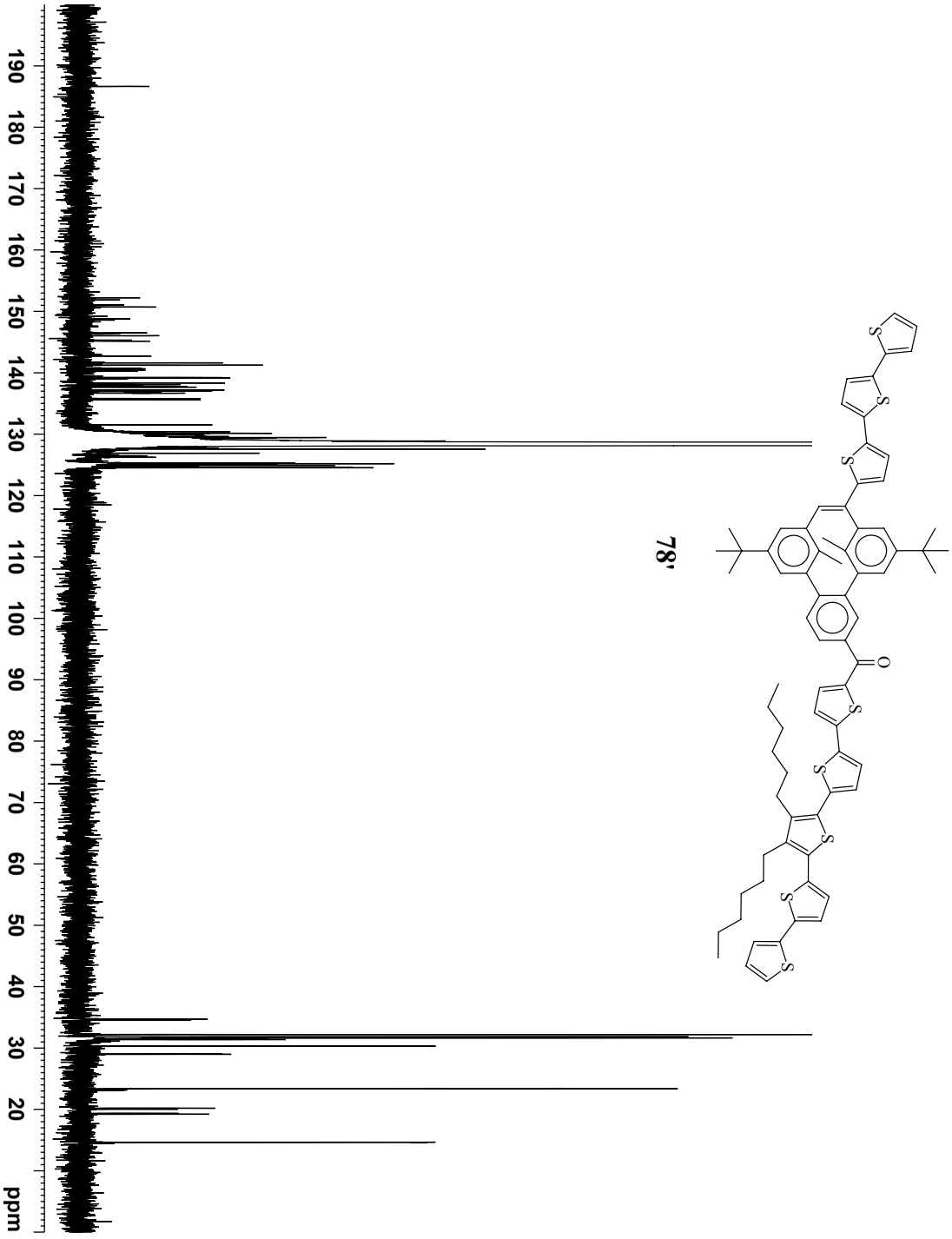
190
180
170
160
150
140
130
120
110
100
90
80
70
60
50
40
30
20
ppm
78'
S
O

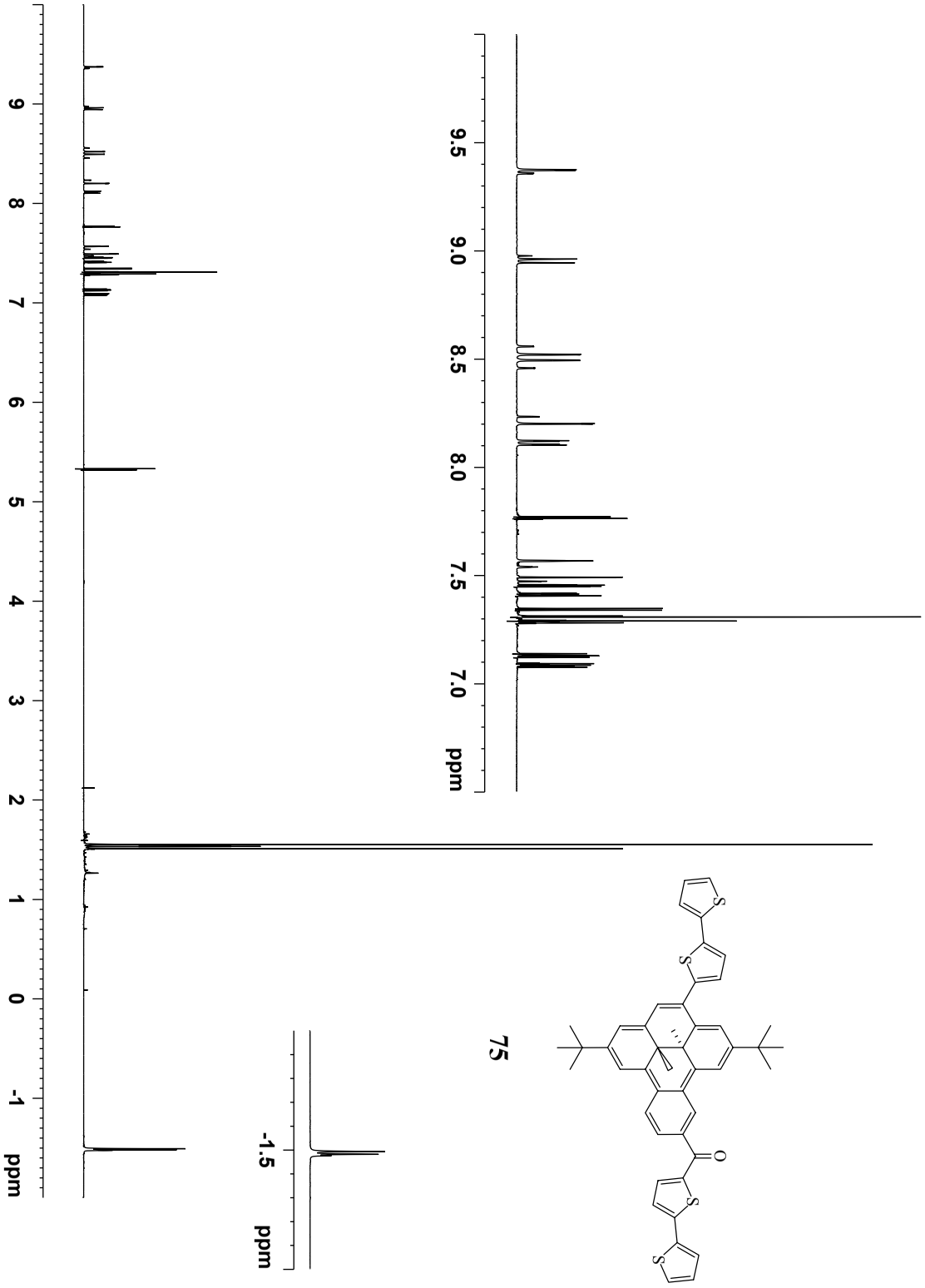
9
8
7
6
5
4
3
2
1
0
-1
ppm
9.5
9.0
8.5
8.0
7.5
7.0
ppm
-1.5
ppm
S
S
O
S
S
75

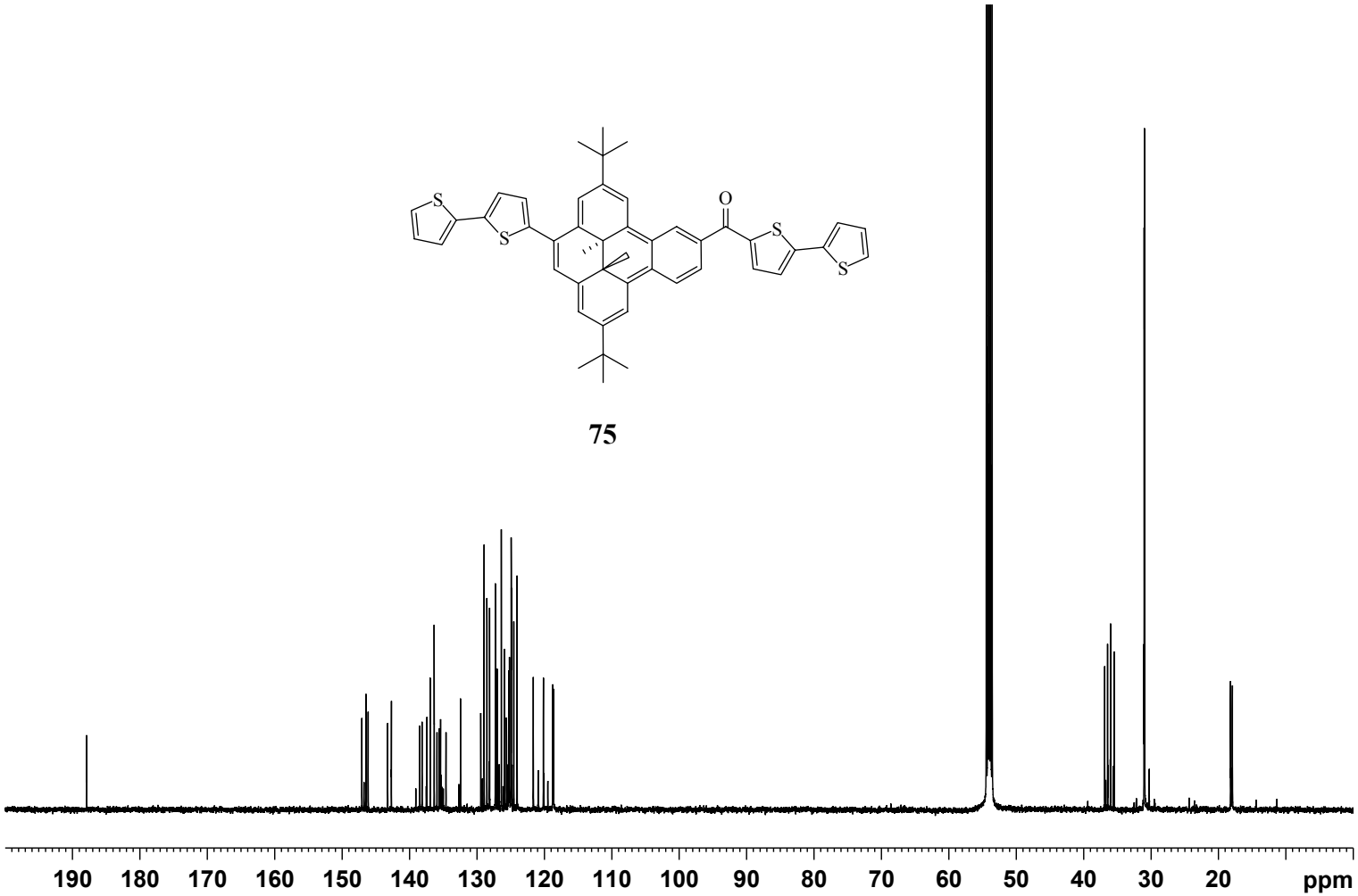
S
S
O
S
S
190
180
170
160
150
140
130
120
110
100
90
80
70
60
50
40
30
20
ppm

75

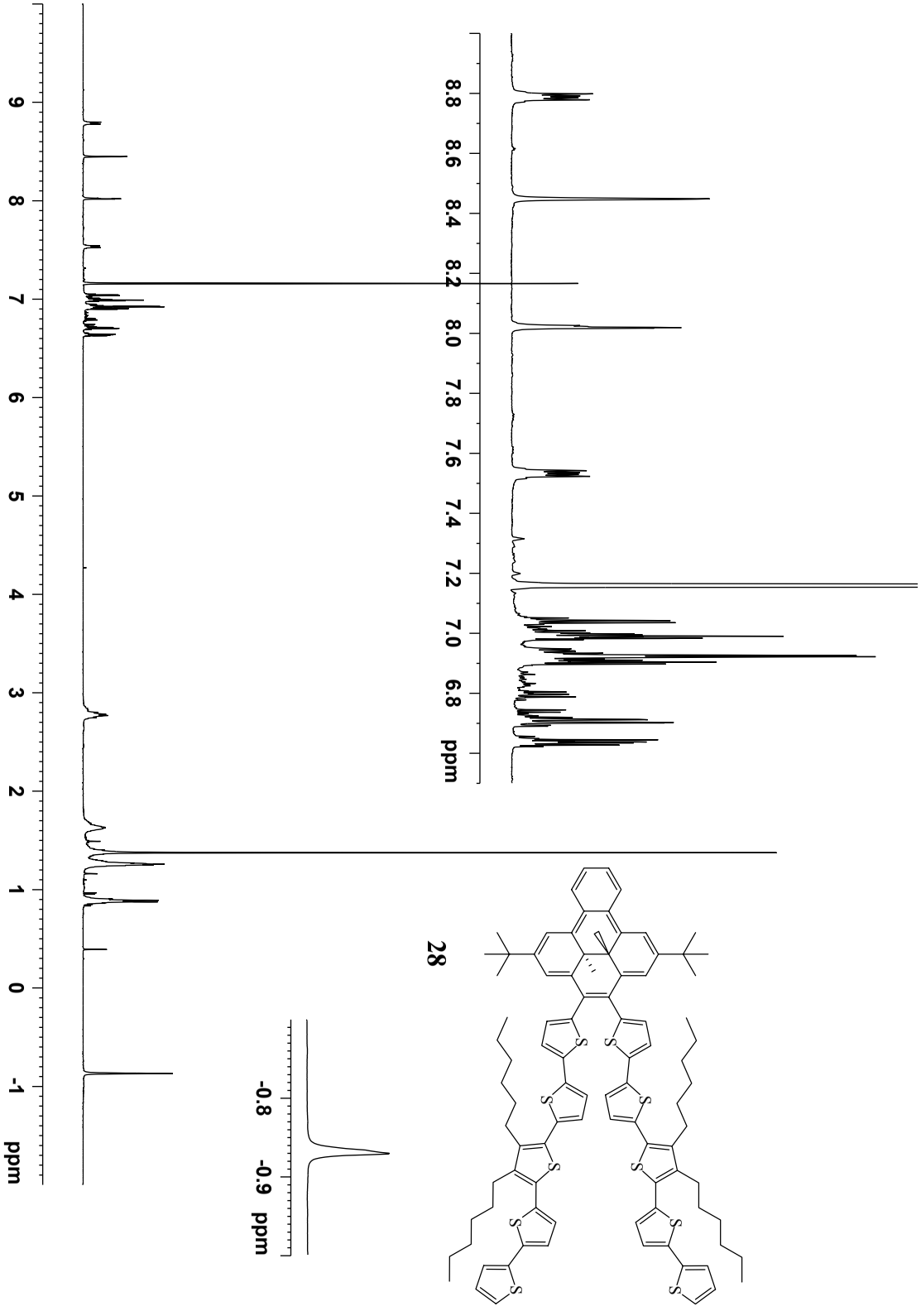

28

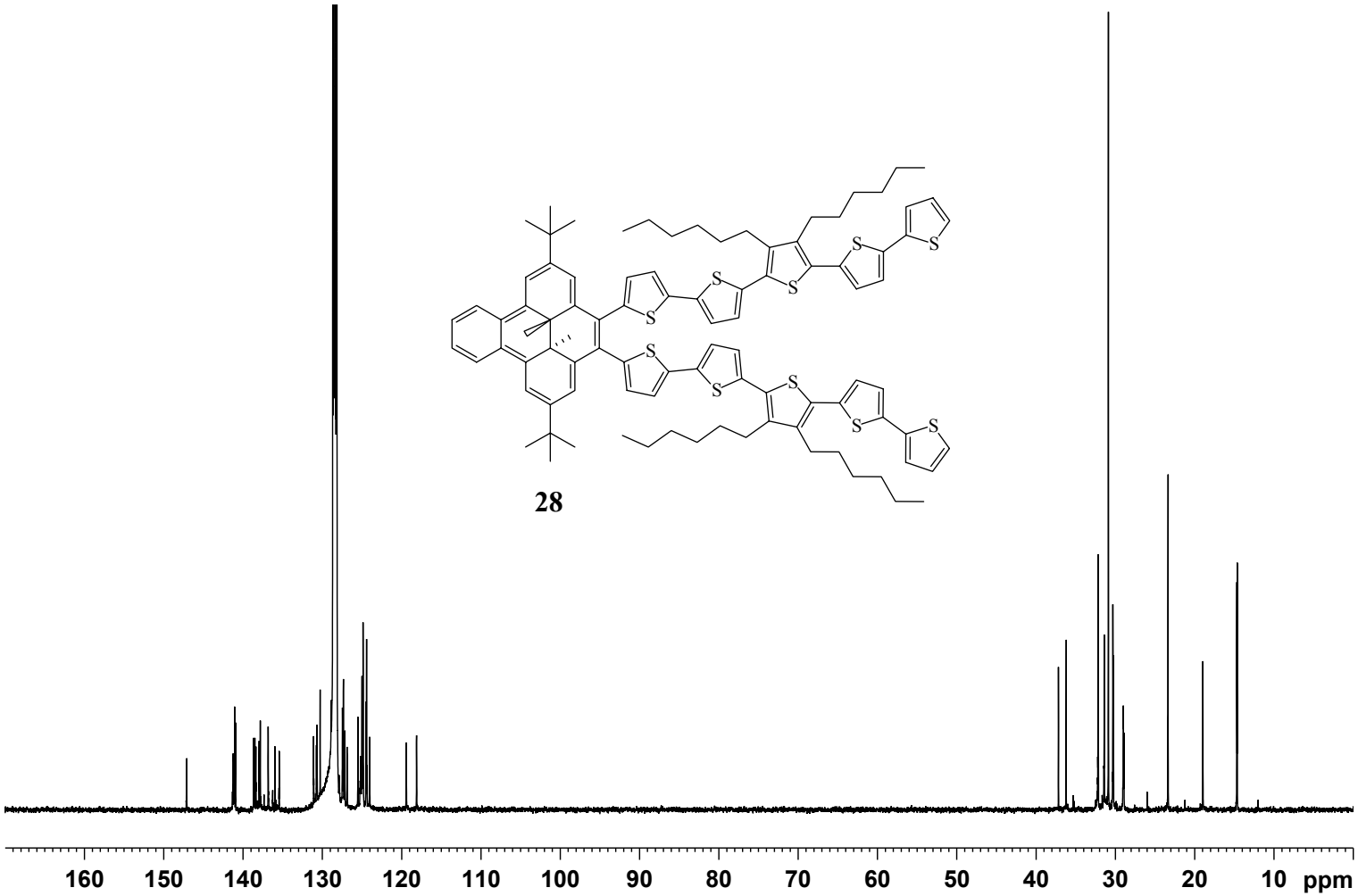

28

28'

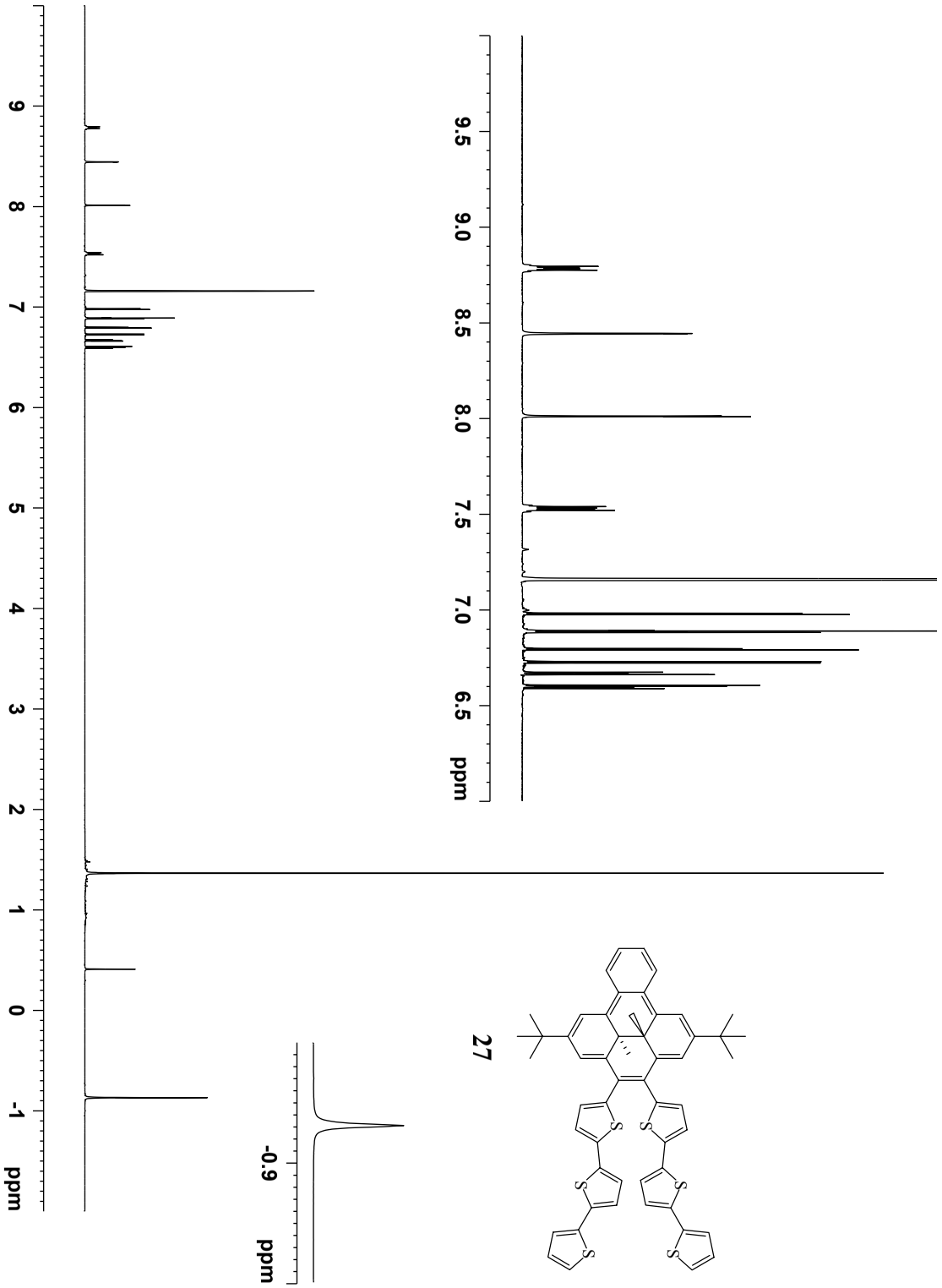
9
8
7
6
5
4
3
2
1
0
-1
ppm
9.5
9.0
8.5
8.0
7.5
7.0
6.5
ppm
-0.9
ppm
27
S
S
S
S
S
S

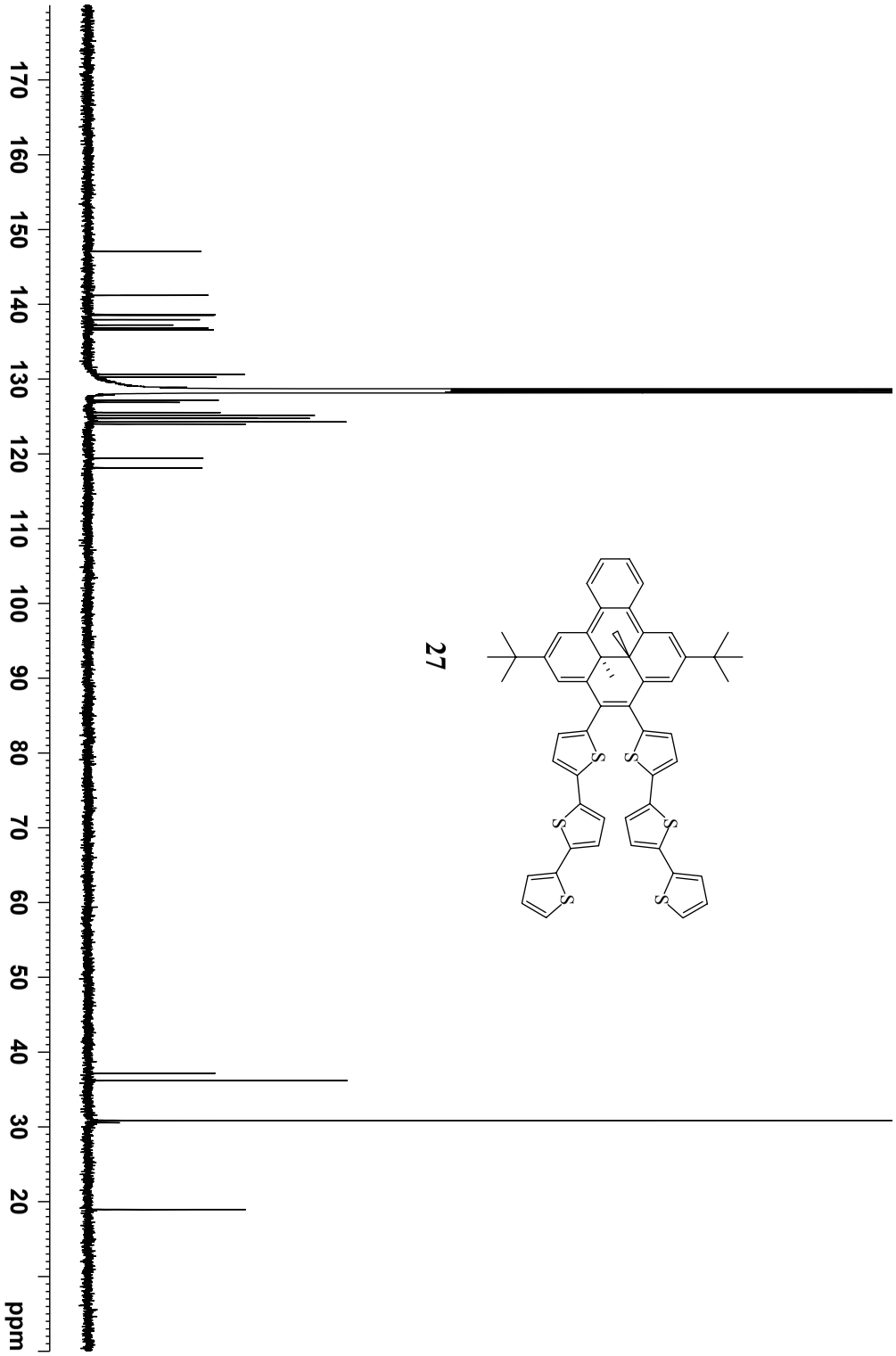
170
160
150
140
130
120
110
100
90
80
70
60
50
40
30
20
ppm
27
S
S
S
S
S
S

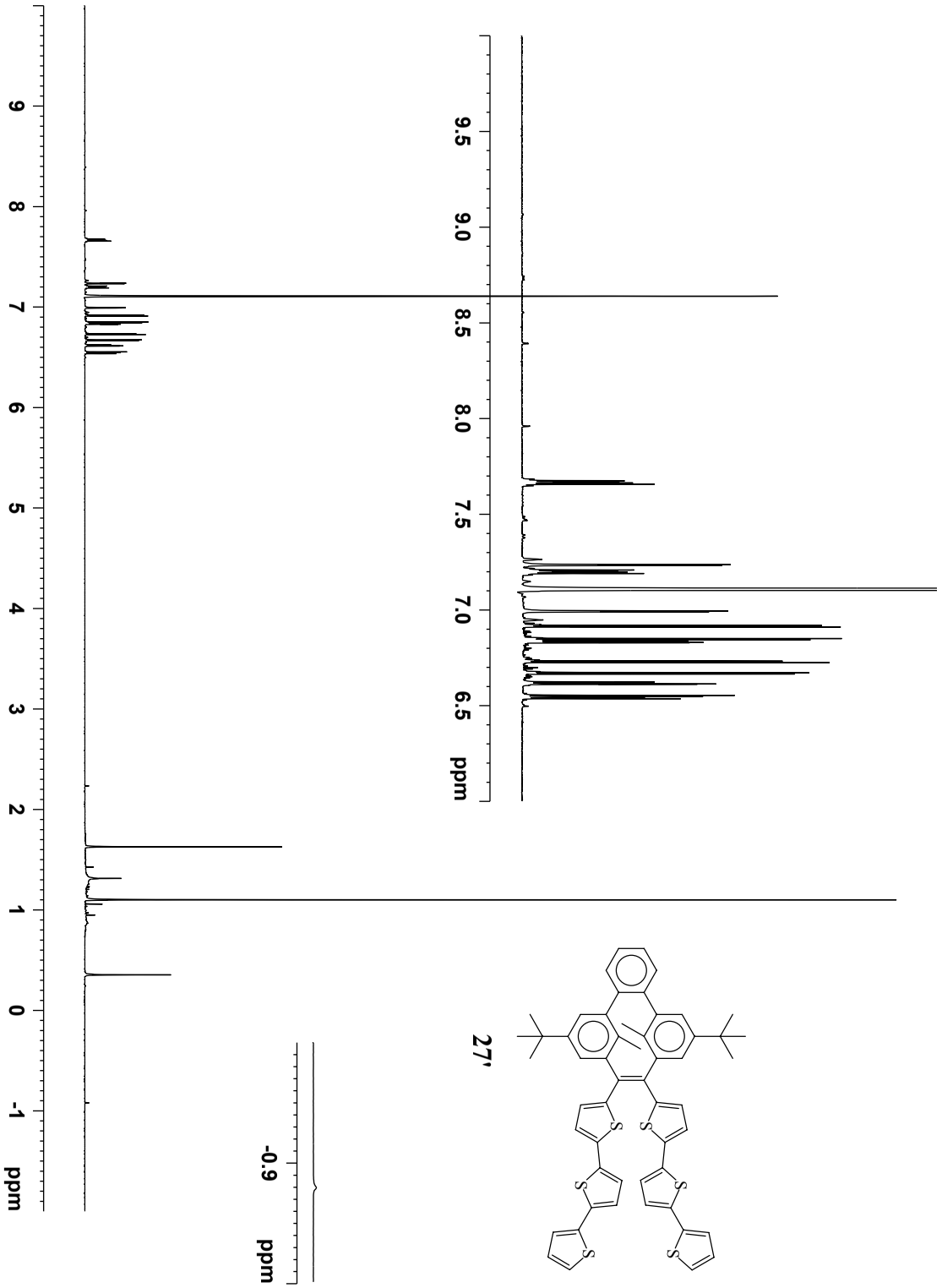
9
8
7
6
5
4
3
2
1
0
-1
ppm
9.5
9.0
8.5
8.0
7.5
7.0
6.5
ppm
-0.9
ppm
27'
S
S
S
S
S
S

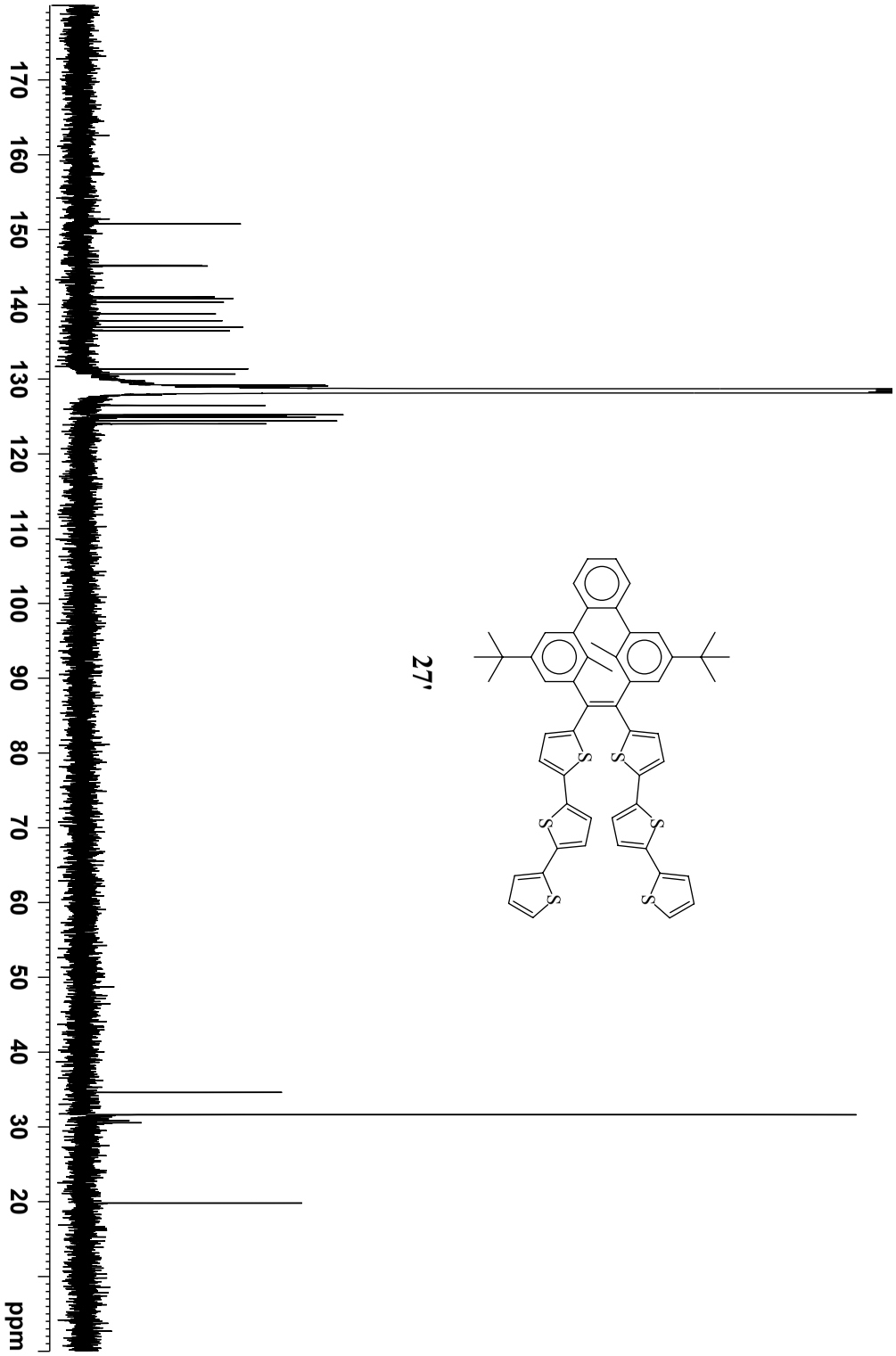
170
160
150
140
130
120
110
100
90
80
70
60
50
40
30
20
ppm
27'

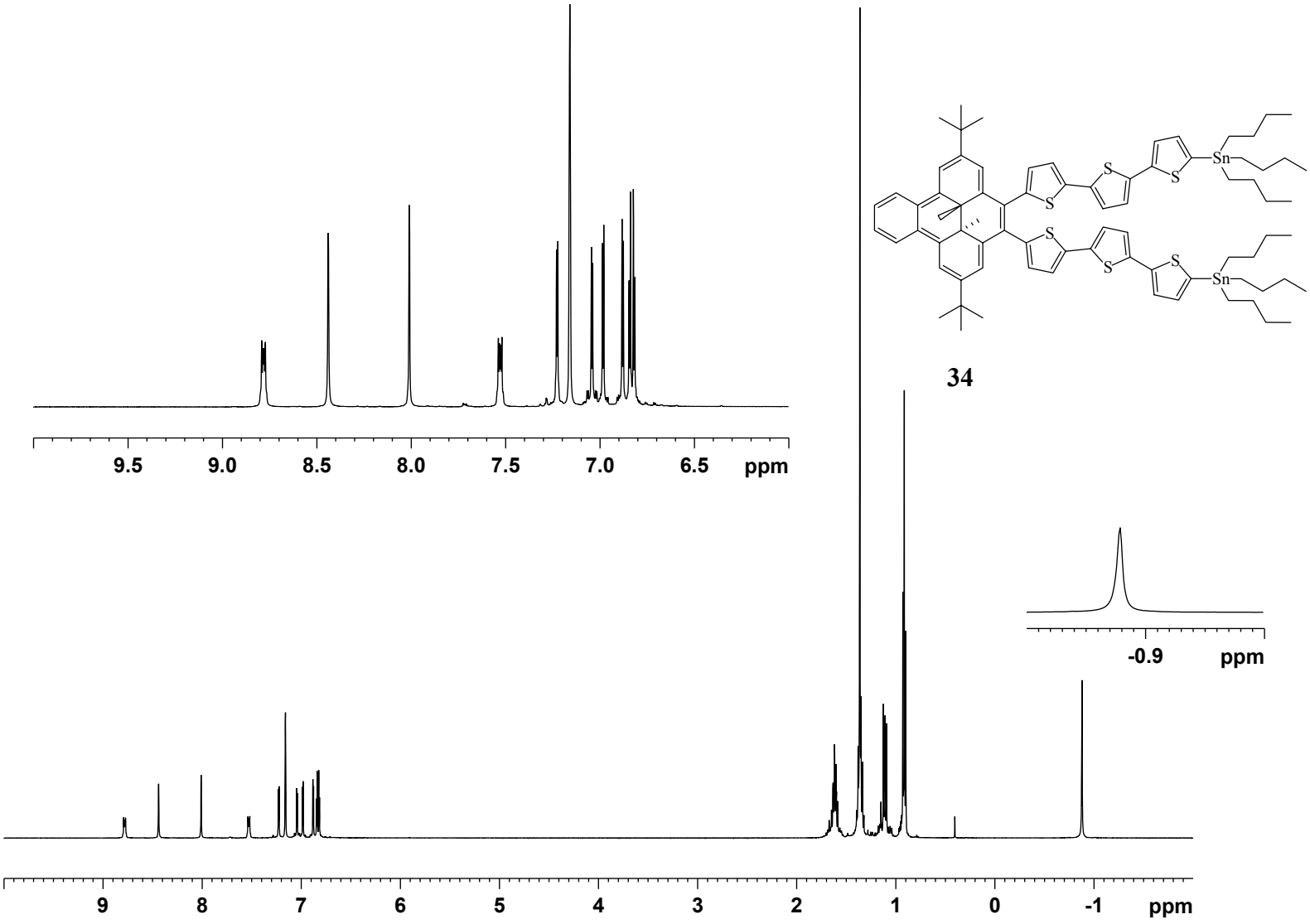

34

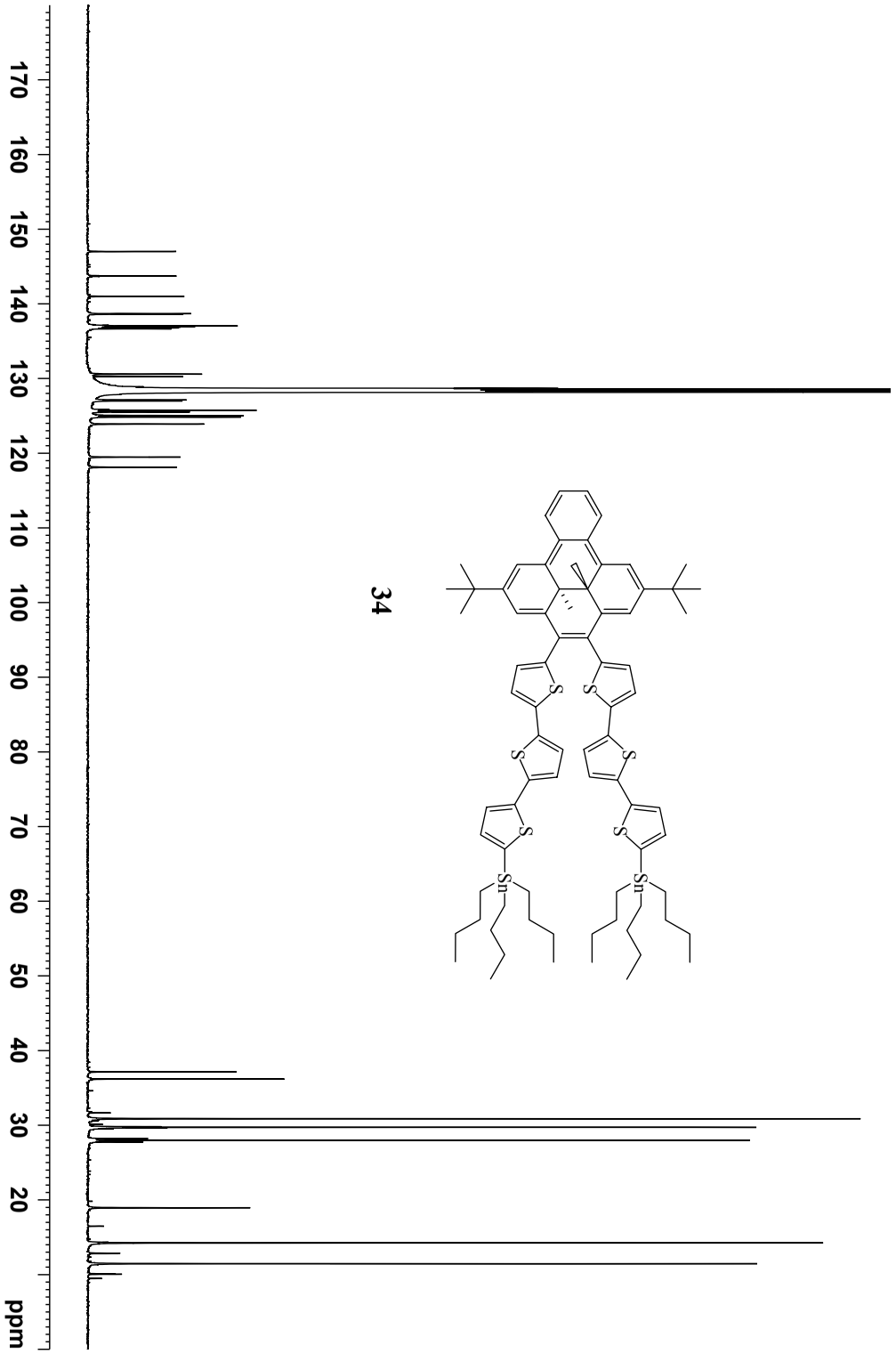
34
S
Sn
170
160
150
140
130
120
110
100
90
80
70
60
50
40
30
20
ppm

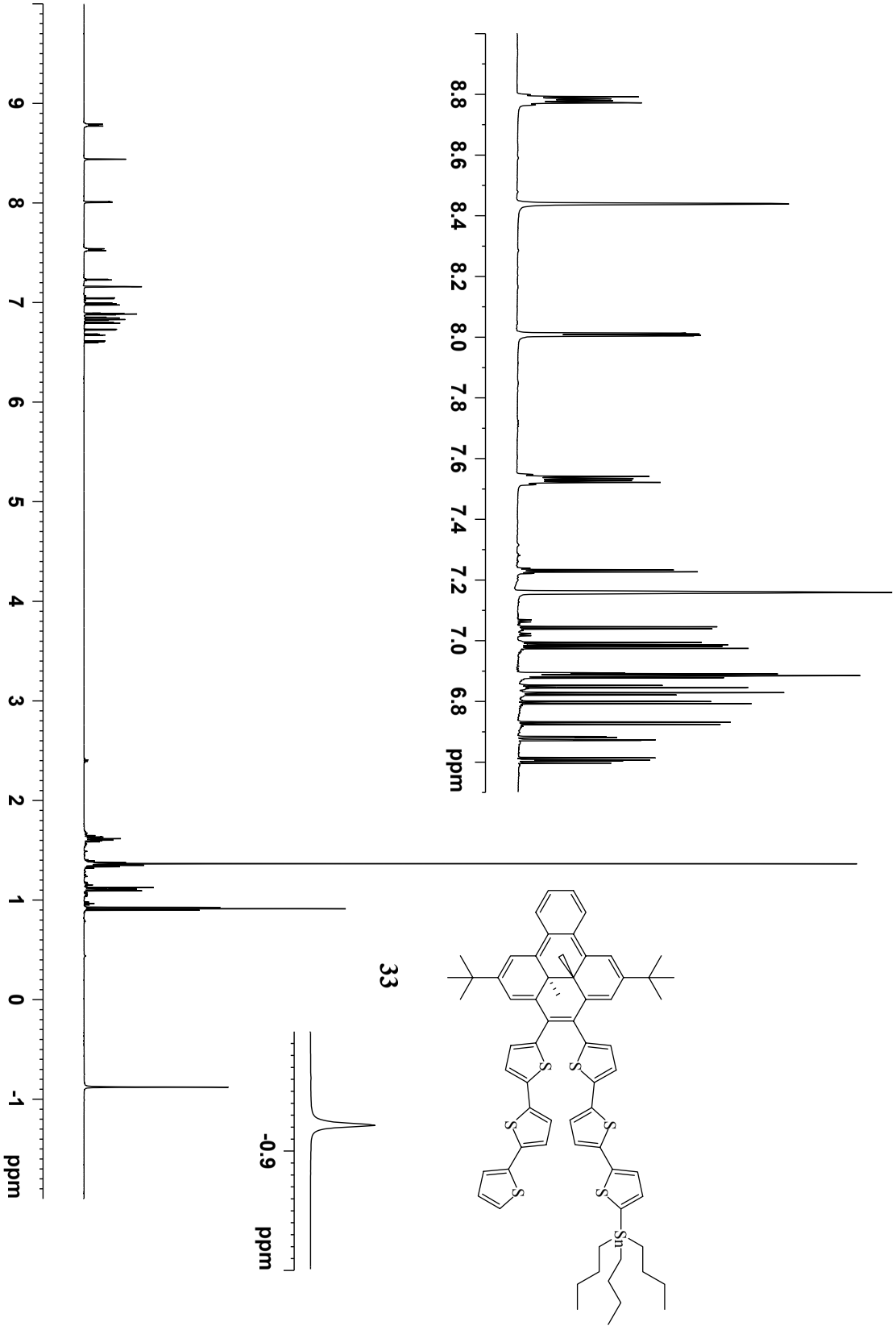
8.8
8.6
8.4
8.2
8.0
7.8
7.6
7.4
7.2
7.0
6.8
ppm
9
8
7
6
5
4
3
2
1
0
-1
ppm
-0.9
ppm
33
S
Sn

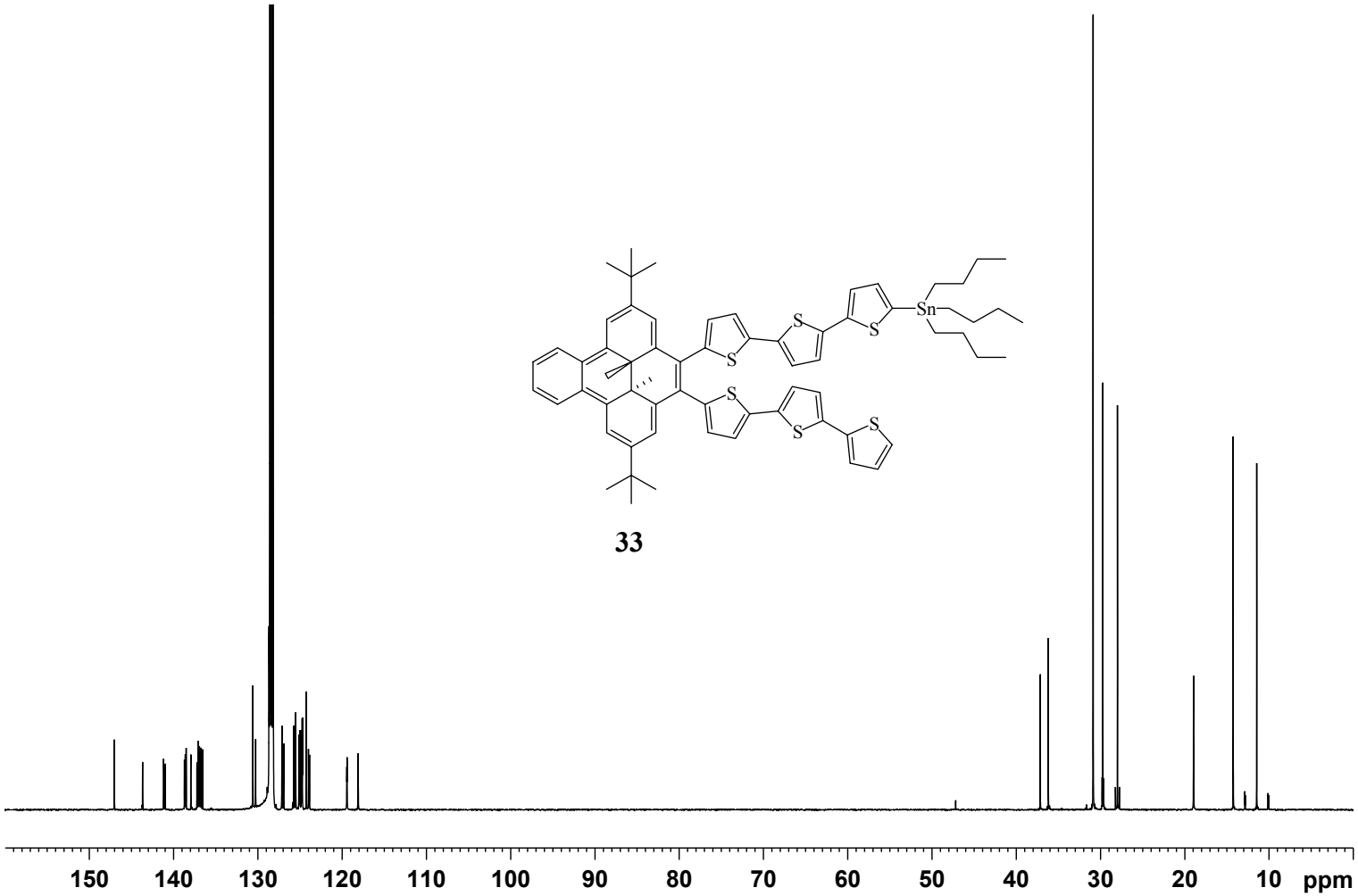

33

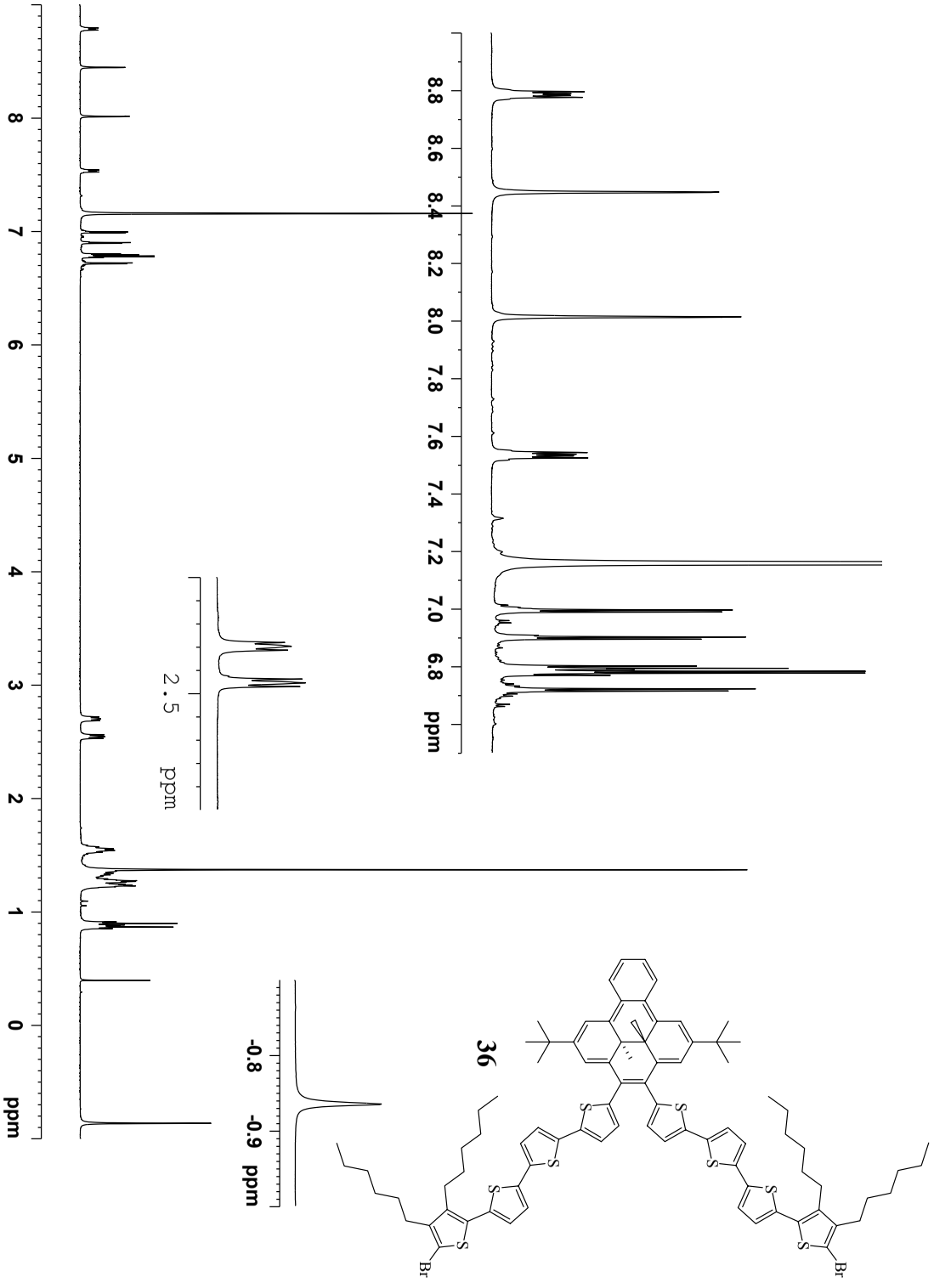
8.8 8.6 8.4 8.2 8.0 7.8 7.6 7.4 7.2 7.0 6.8 ppm
2.5 ppm
-0.8 -0.9 ppm
8 7 6 5 4 3 2 1 0 ppm
36
S
Br

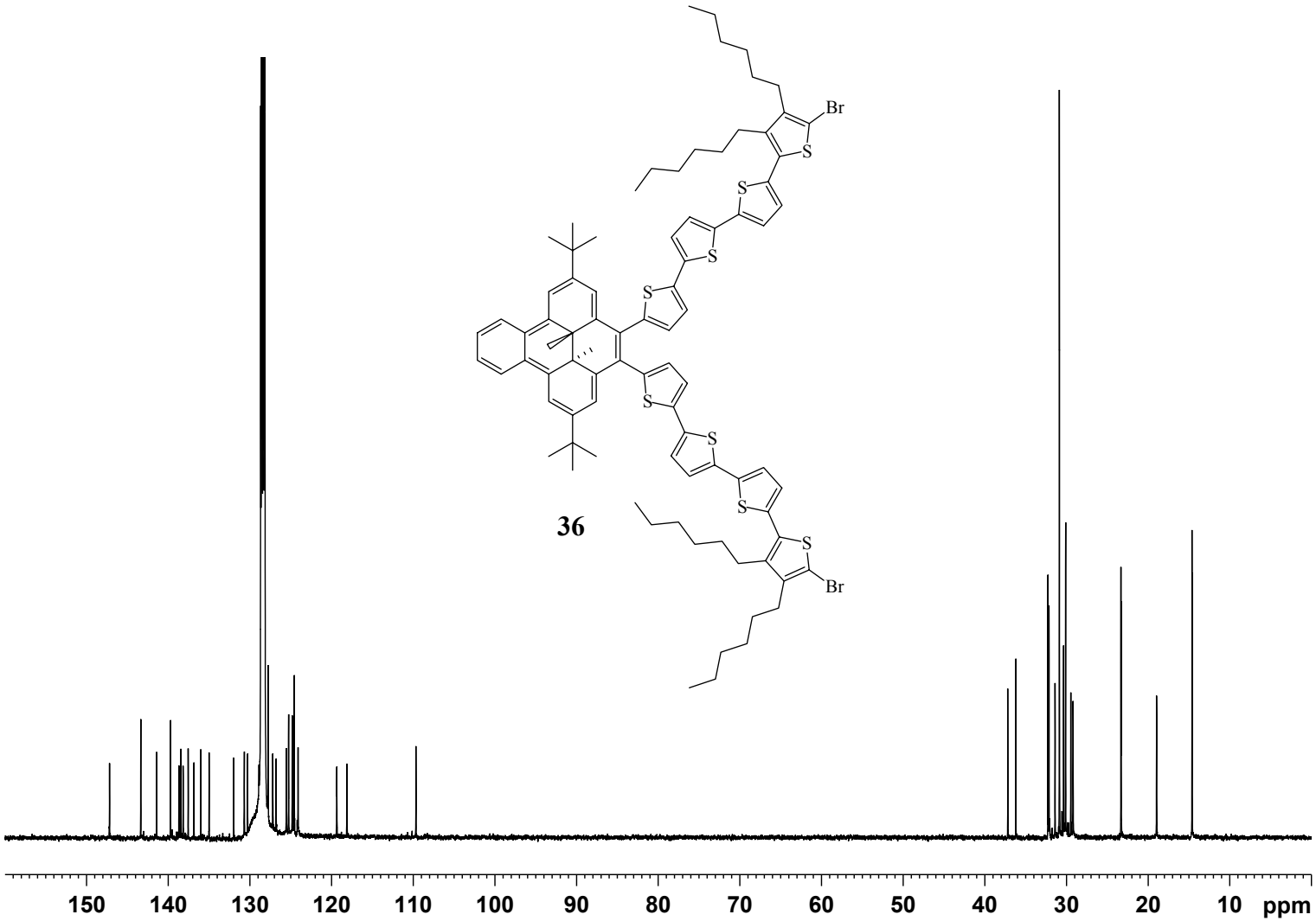
Br
S
S
S
S
S
S
S
S
S
Br
150
140
130
120
110
100
90
80
70
60
50
40
30
20
10
ppm

36

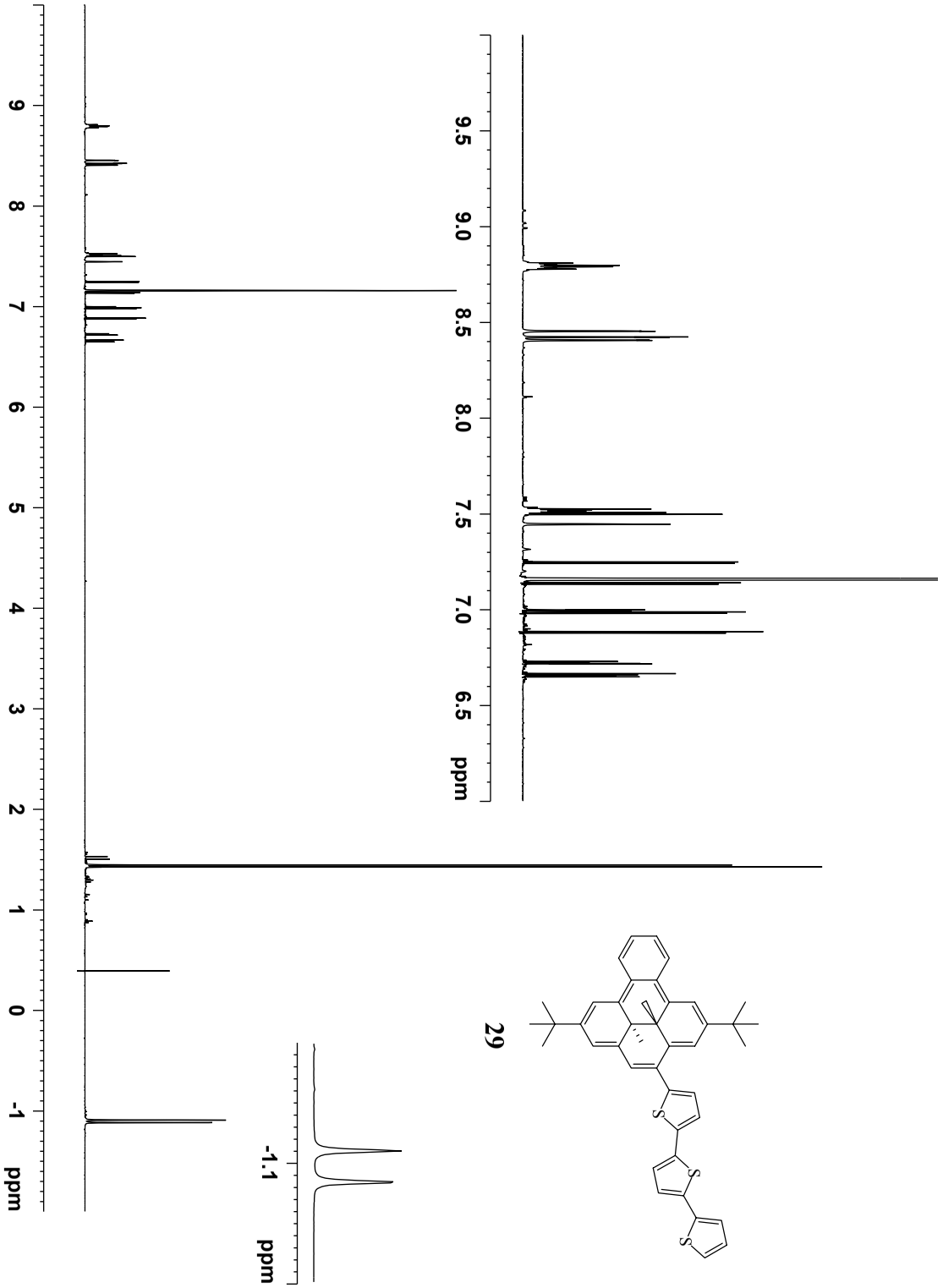

29

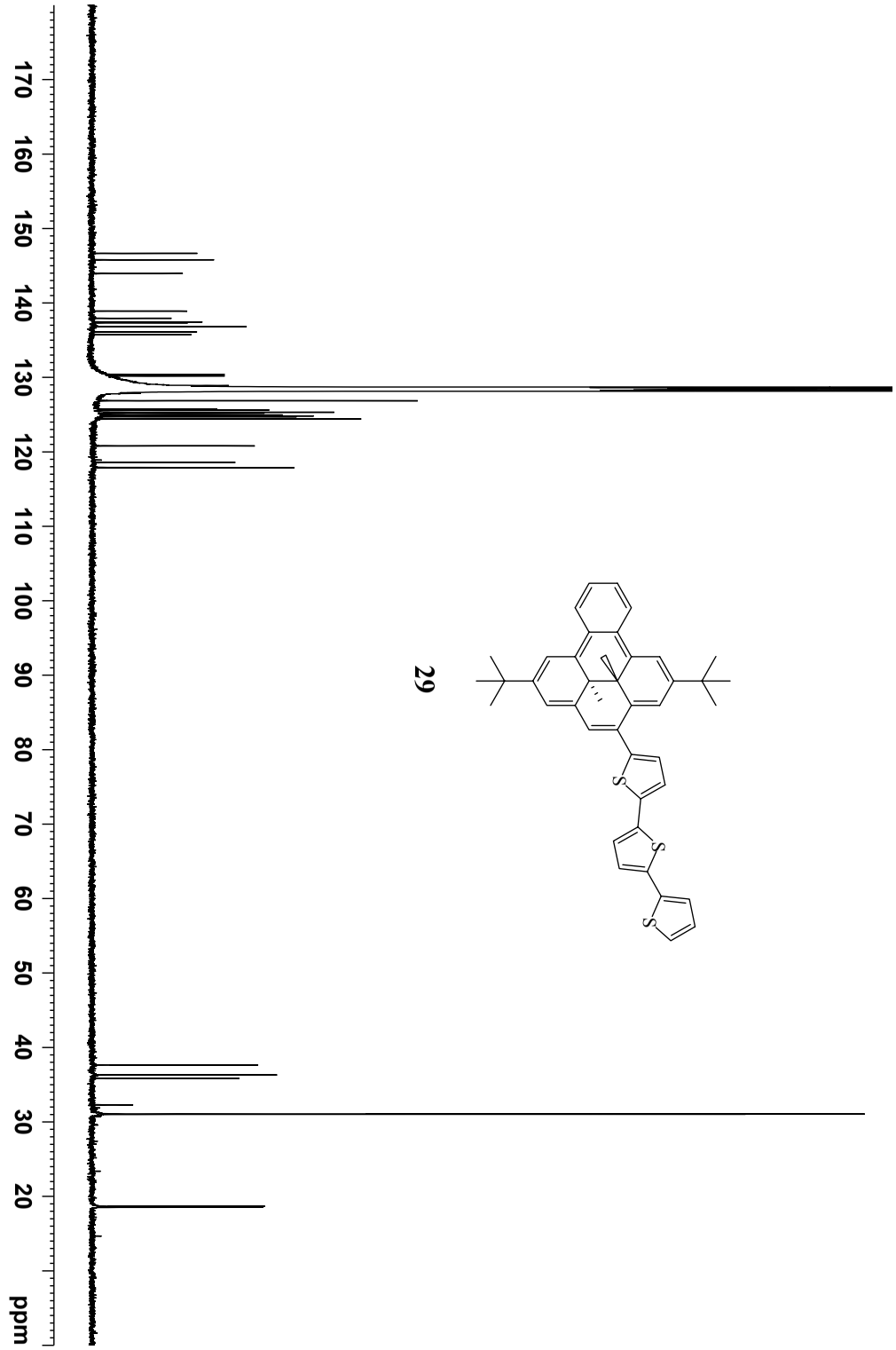
170
160
150
140
130
120
110
100
90
80
70
60
50
40
30
20
ppm
29
S
S
S

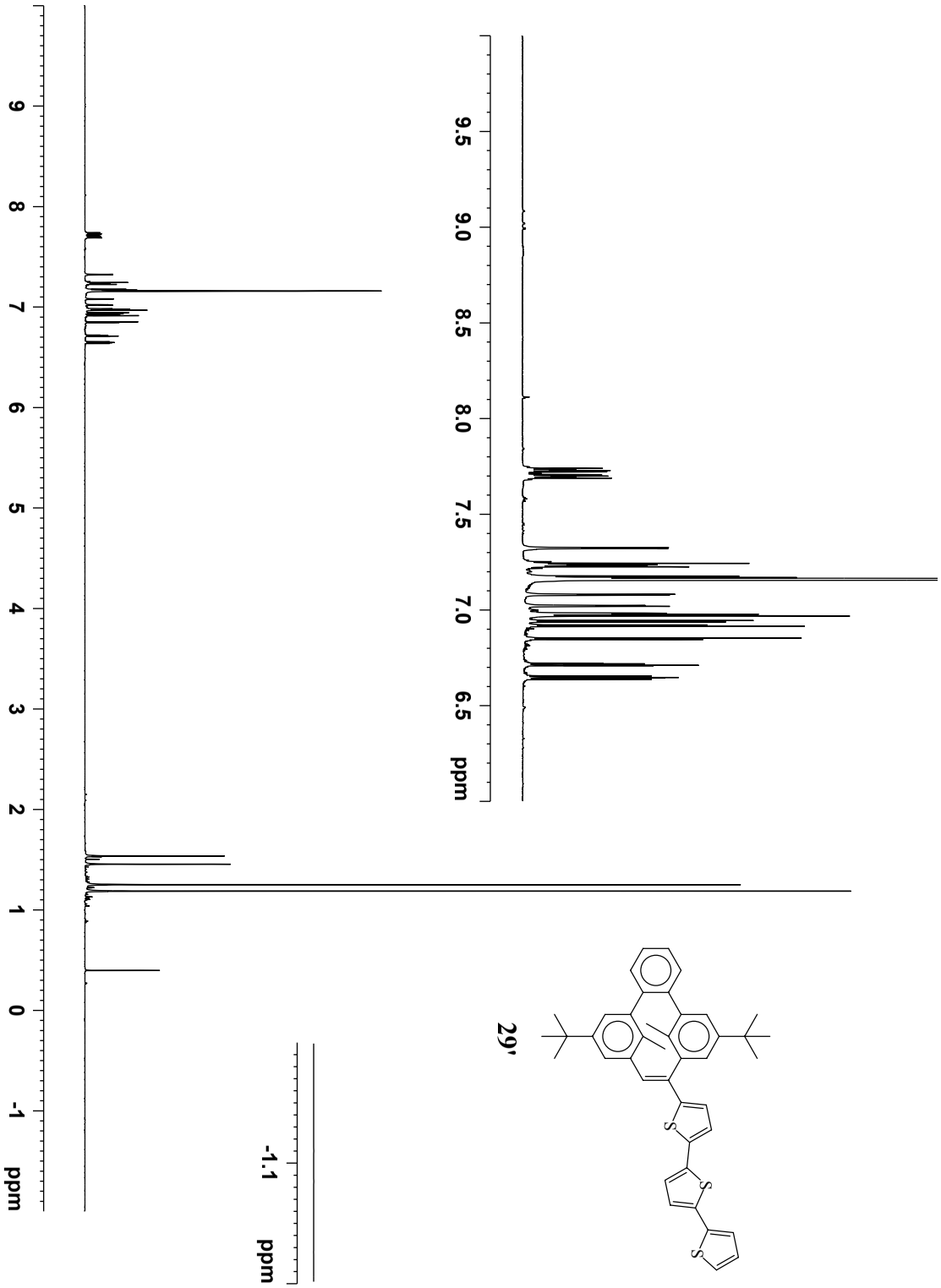

29'

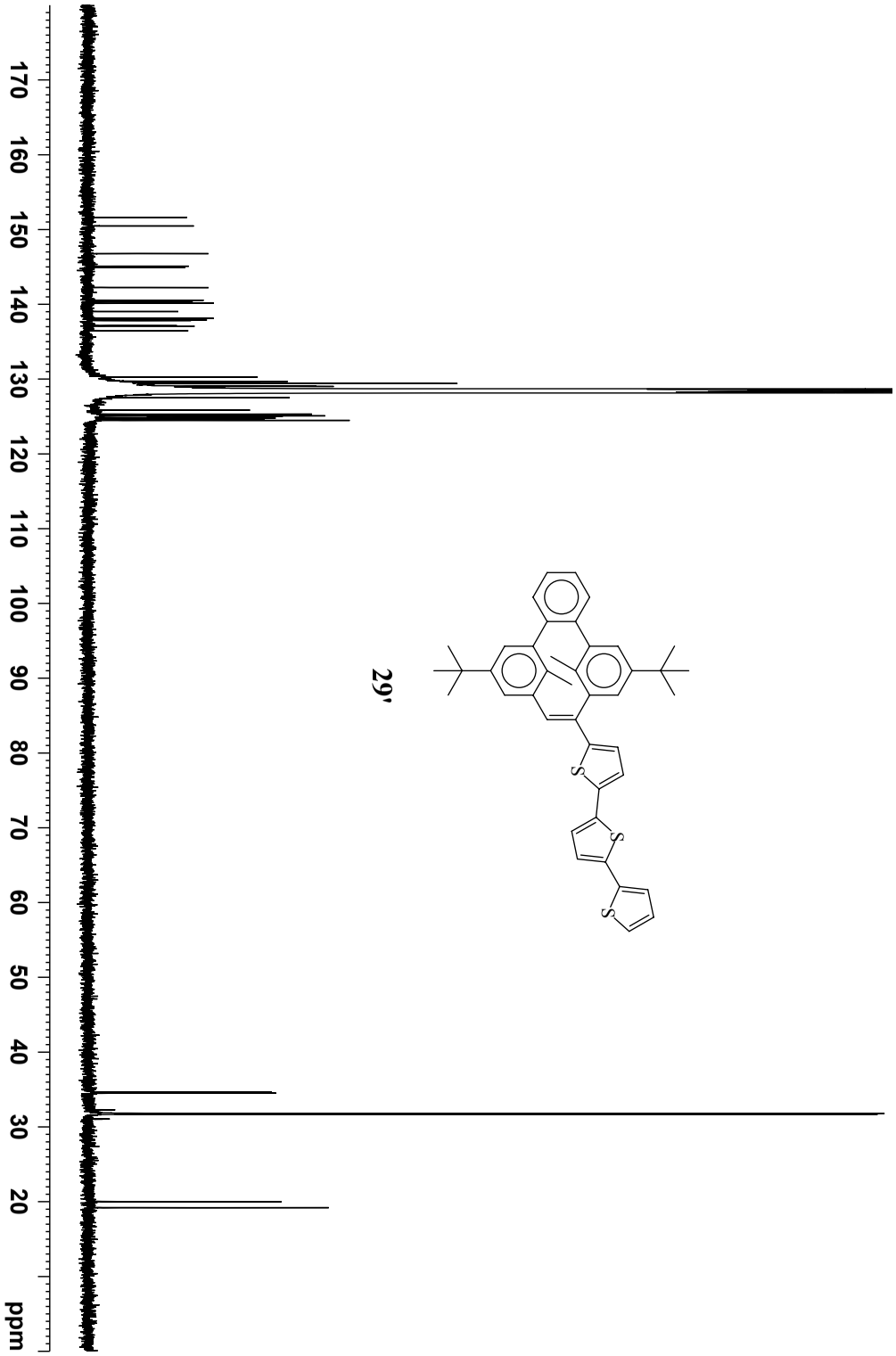

29'

101

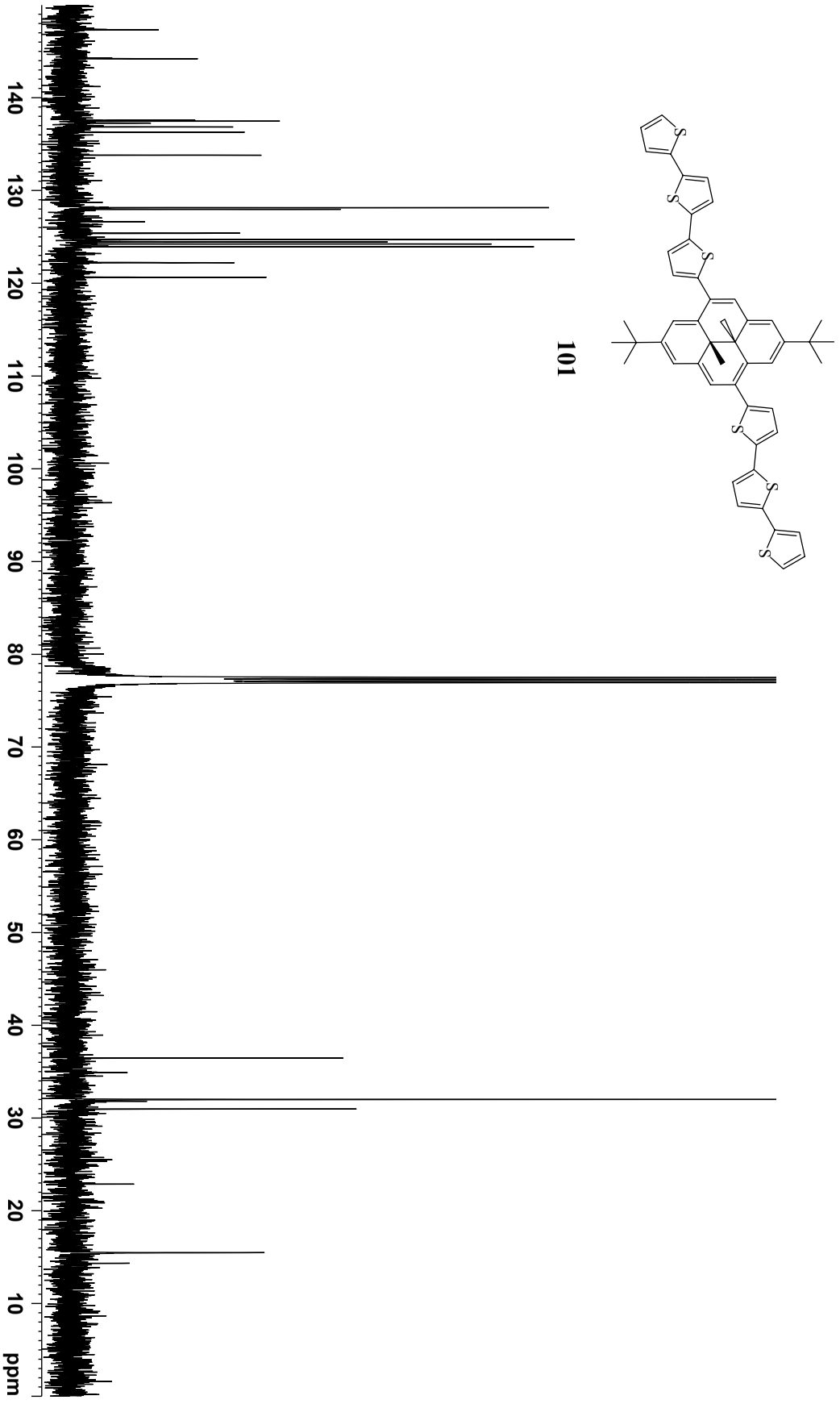
140
130
120
110
100
90
80
70
60
50
40
30
20
10
ppm
101

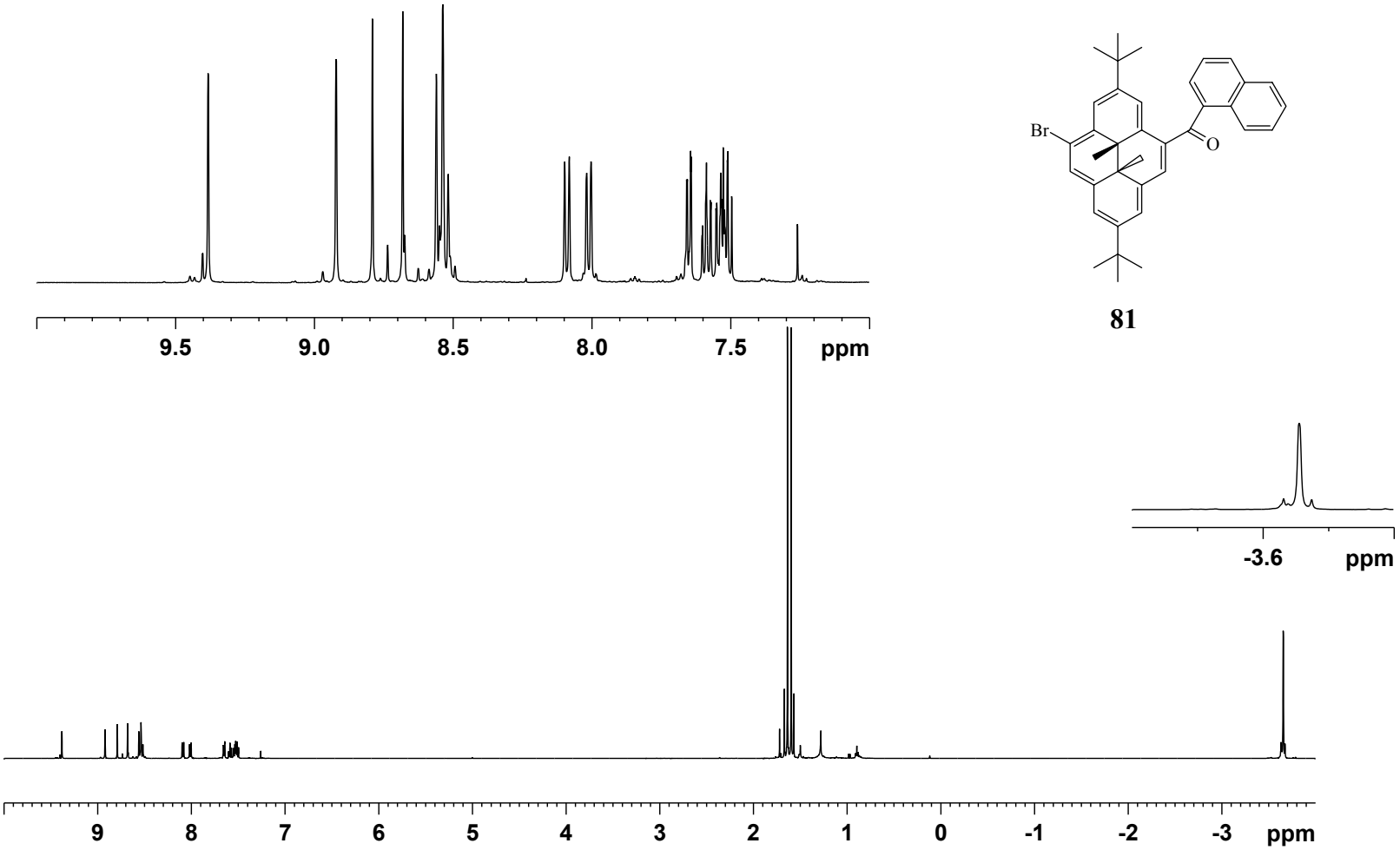

81

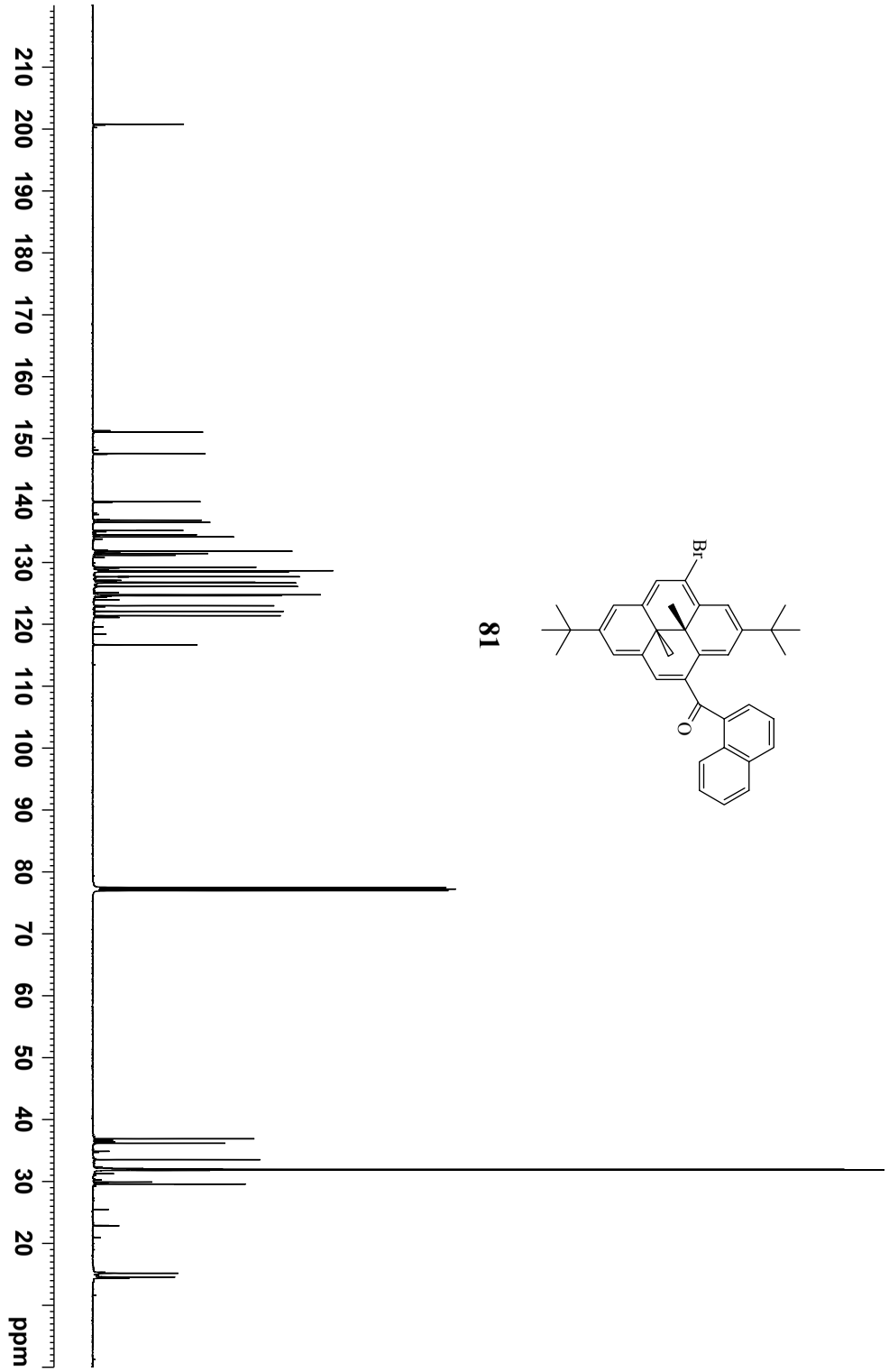
Br
O
81
210 200 190 180 170 160 150 140 130 120 110 100 90 80 70 60 50 40 30 20 ppm

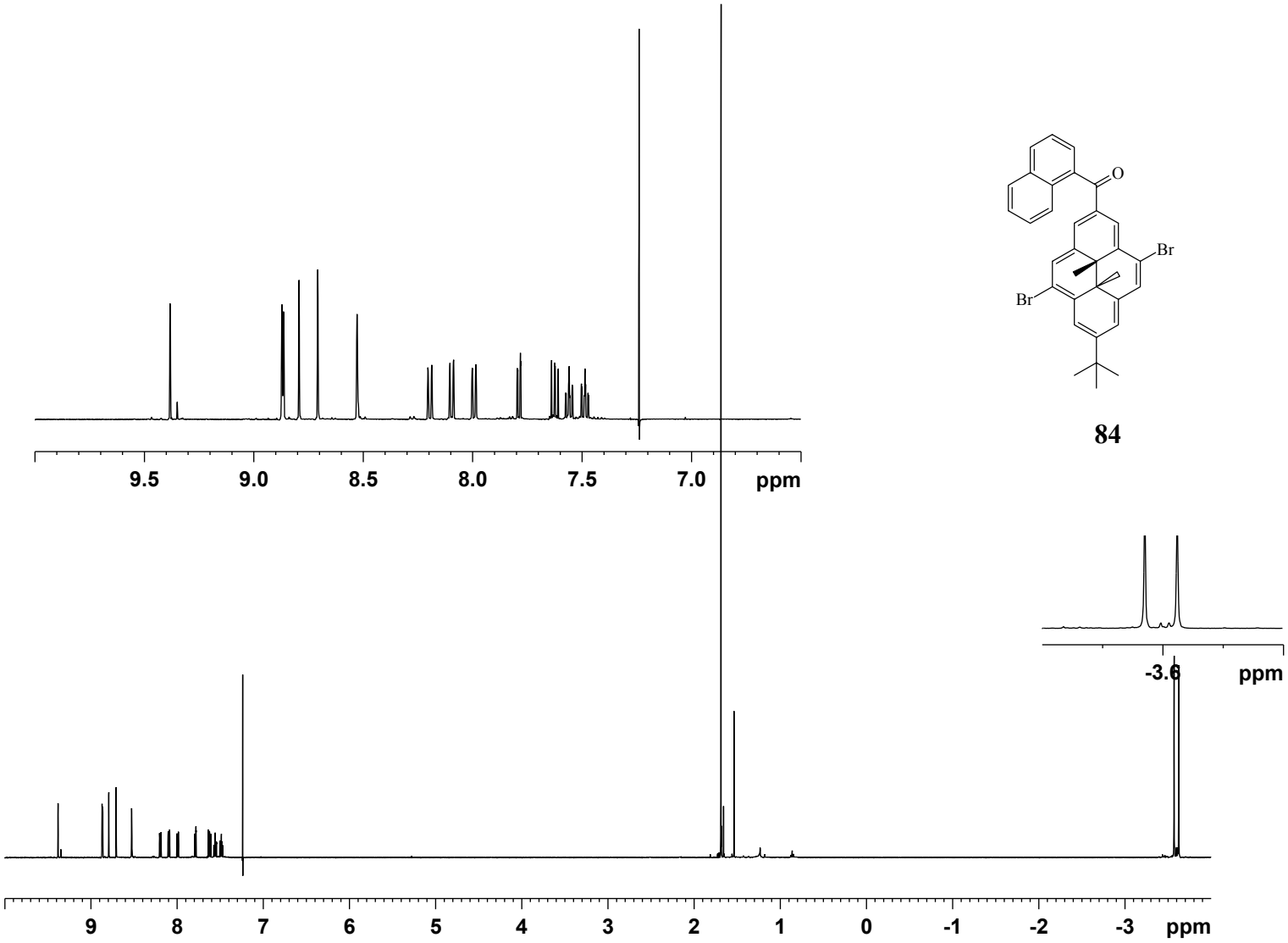

84

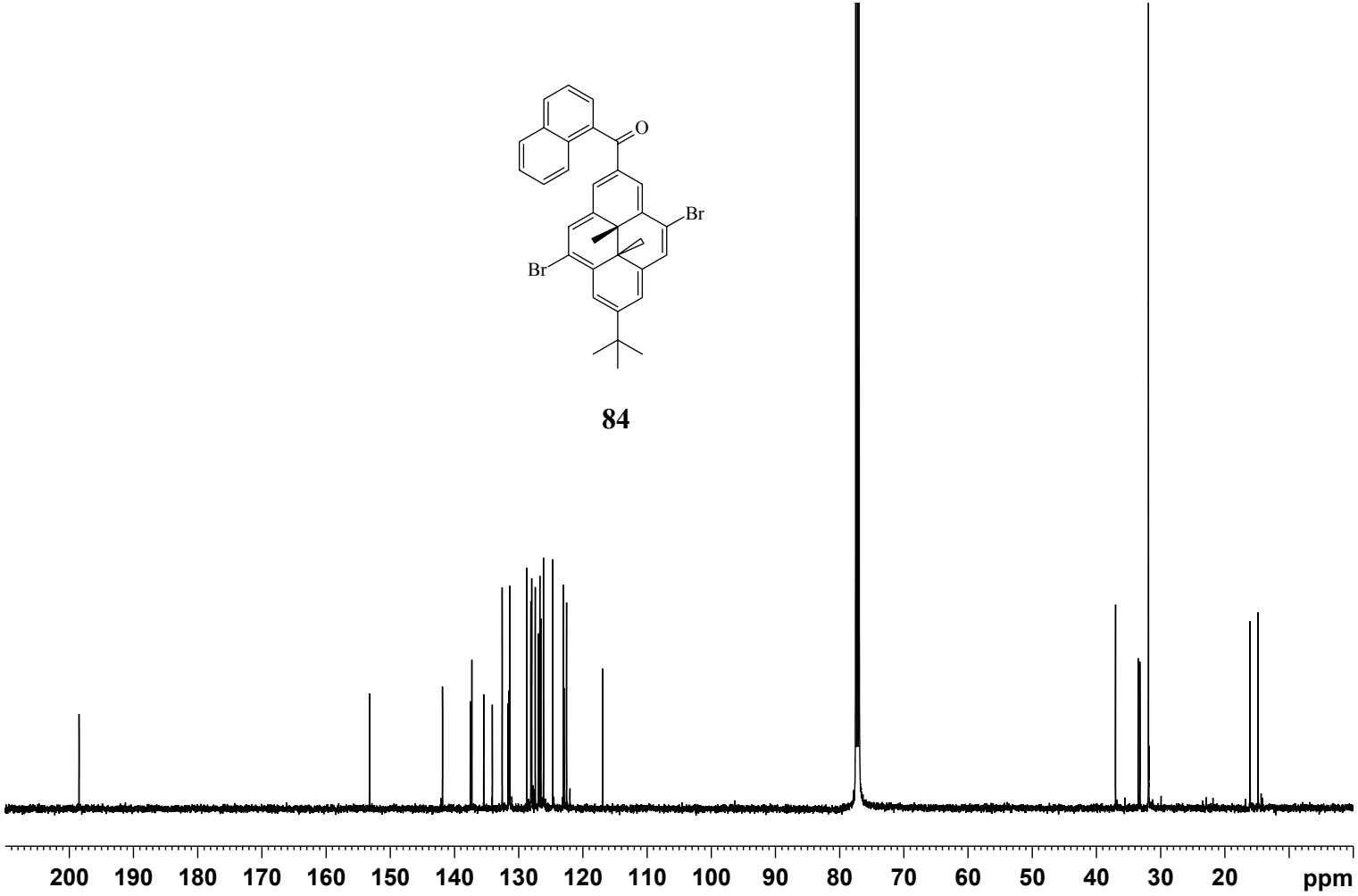
O
Br
Br
200
190
180
170
160
150
140
130
120
110
100
90
80
70
60
50
40
30
20
ppm

84

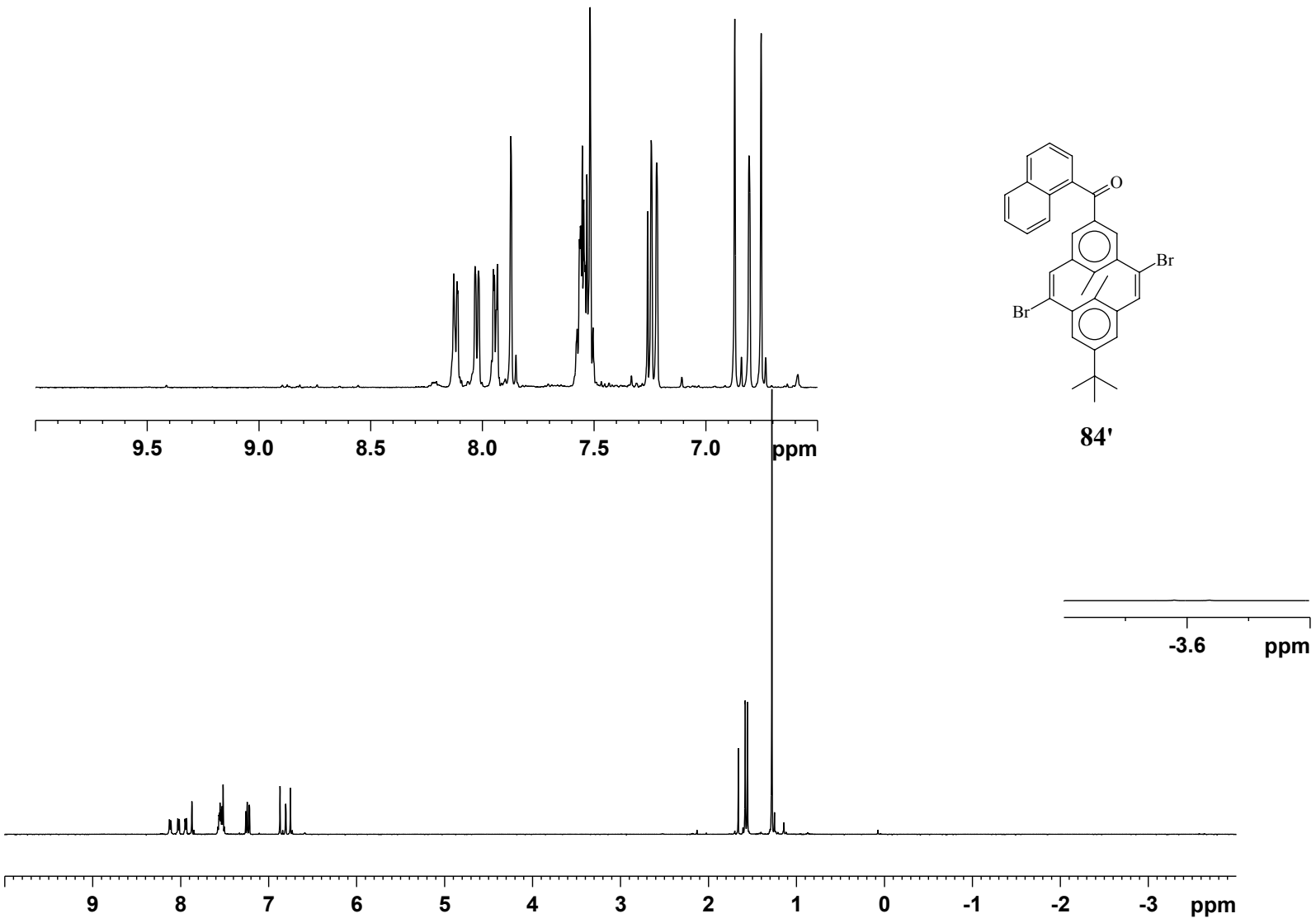

84'

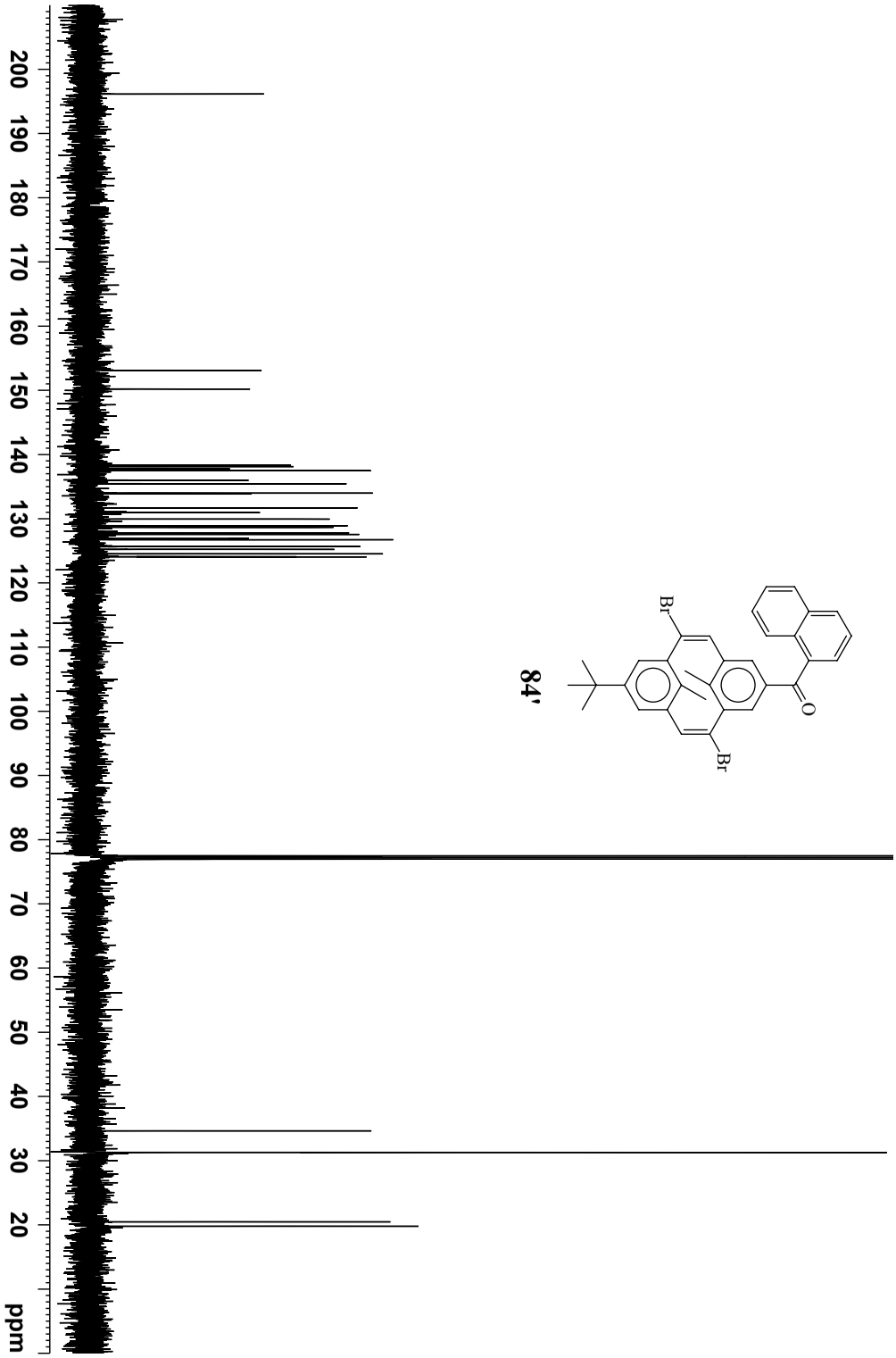
200
190
180
170
160
150
140
130
120
110
100
90
80
70
60
50
40
30
20
ppm
84'
Br
Br
O

82

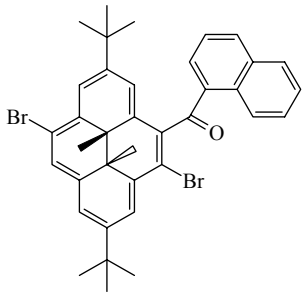
Br
O
Br

82

200
190
180
170
160
150
140
130
120
110
100
90
80
70
60
50
40
30
20
ppm

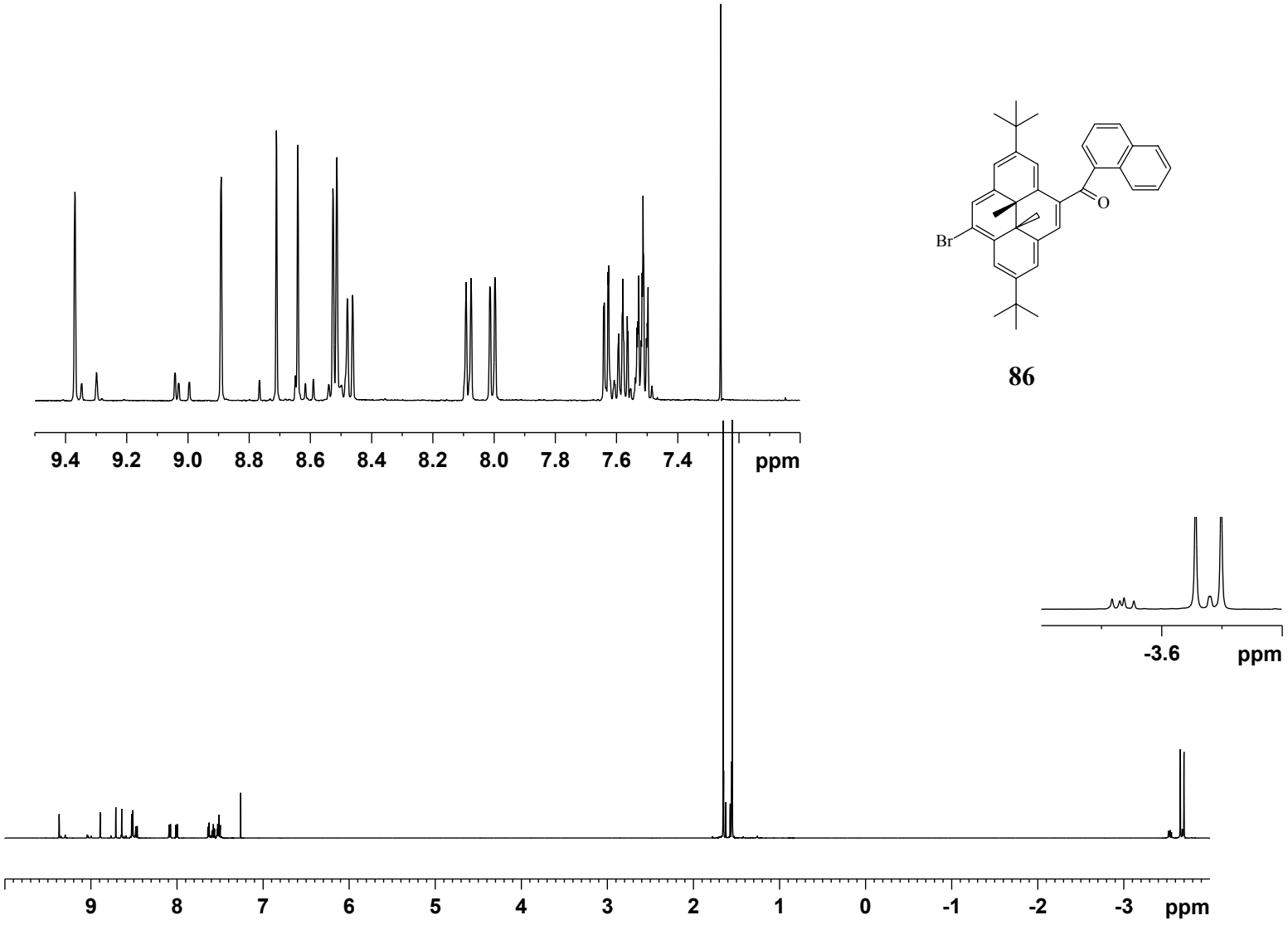

86

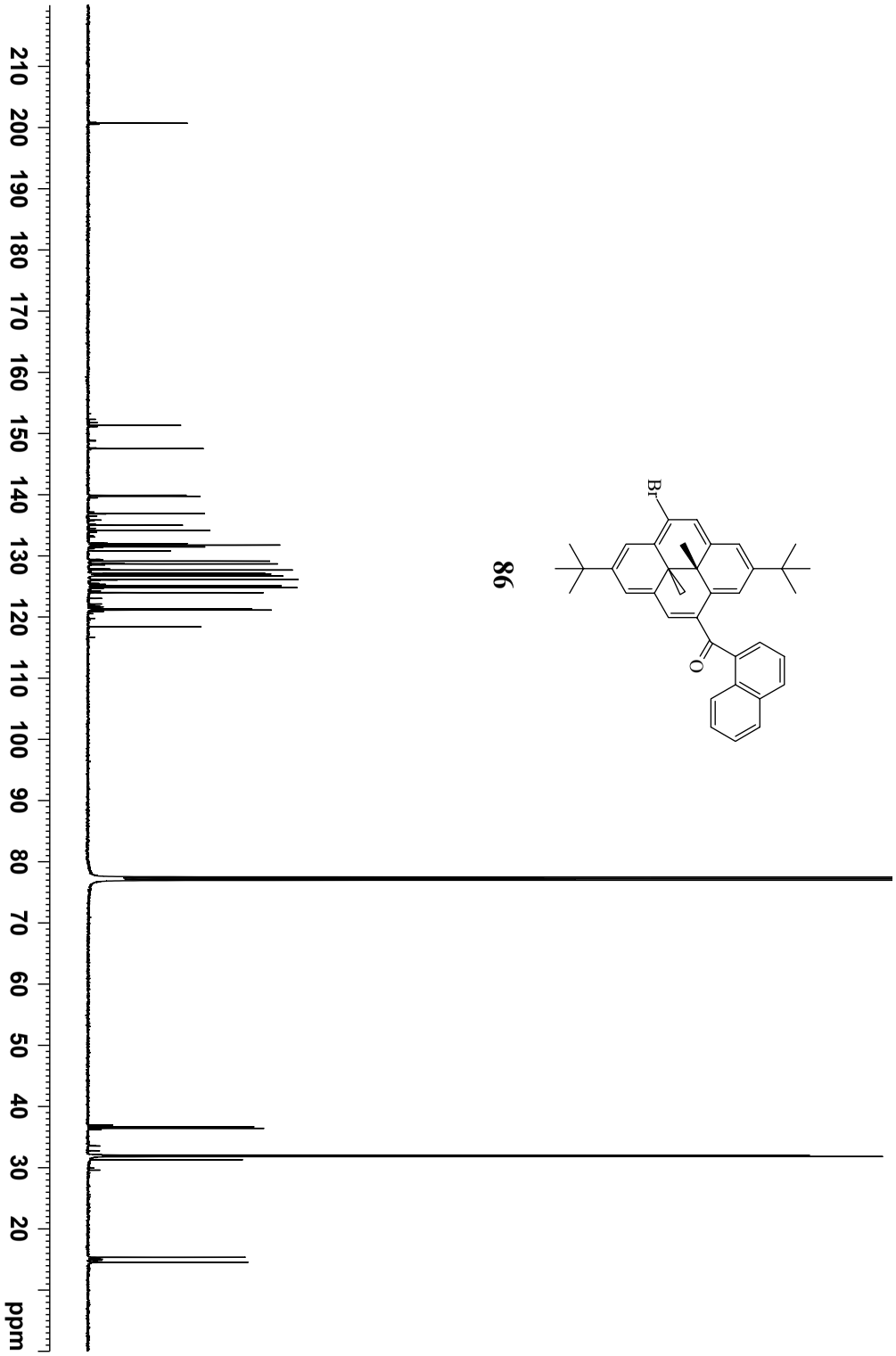
210
200
190
180
170
160
150
140
130
120
110
100
90
80
70
60
50
40
30
20
ppm
Br
O

86

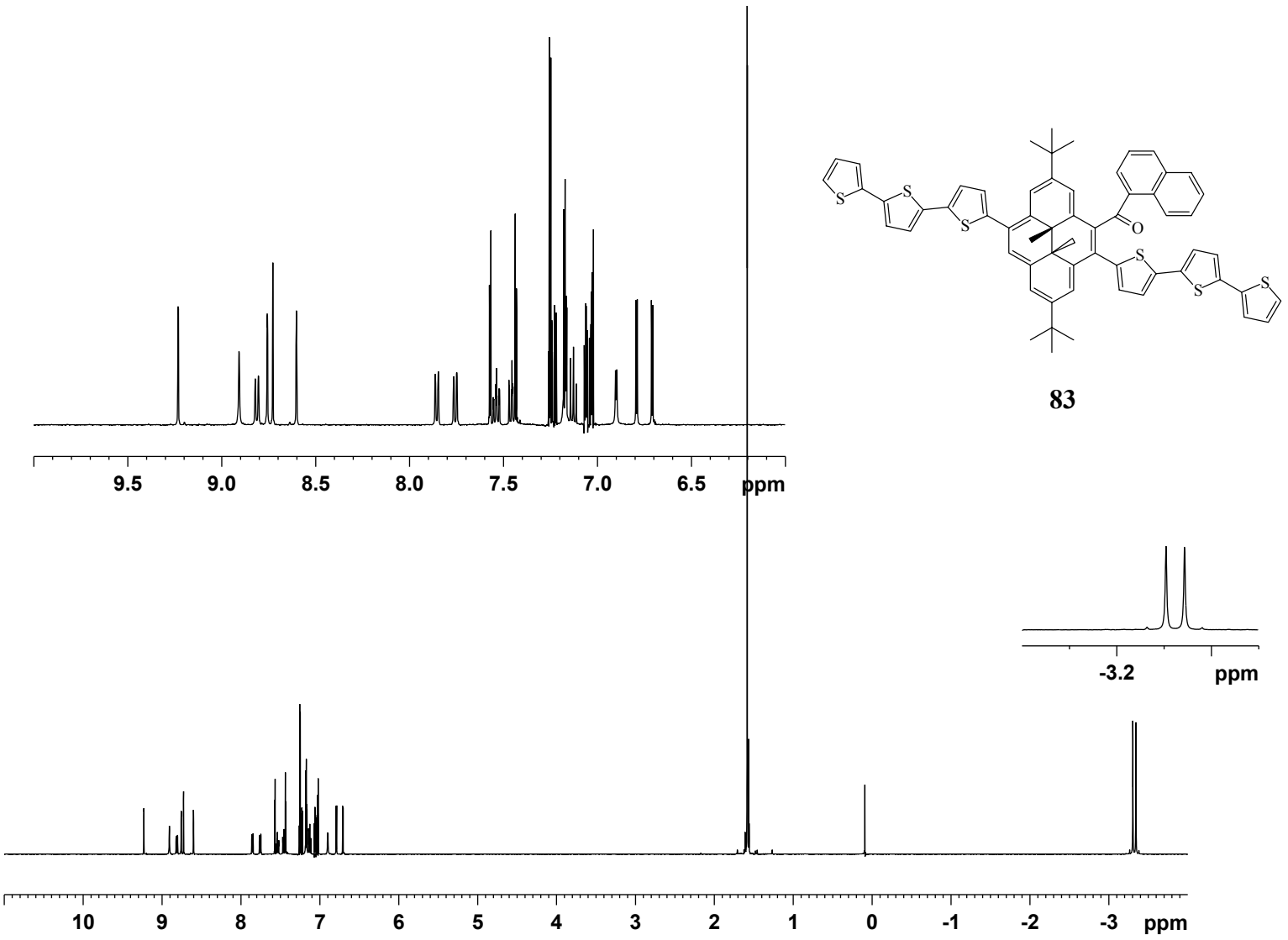

83

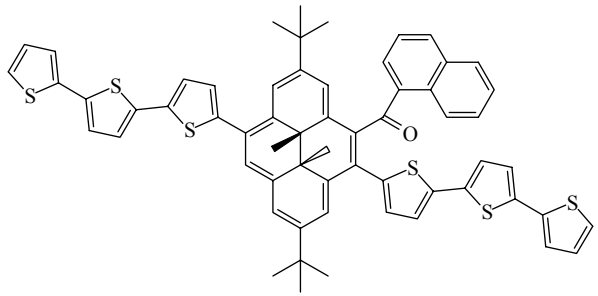
S
S
S
O
S
S
S

83

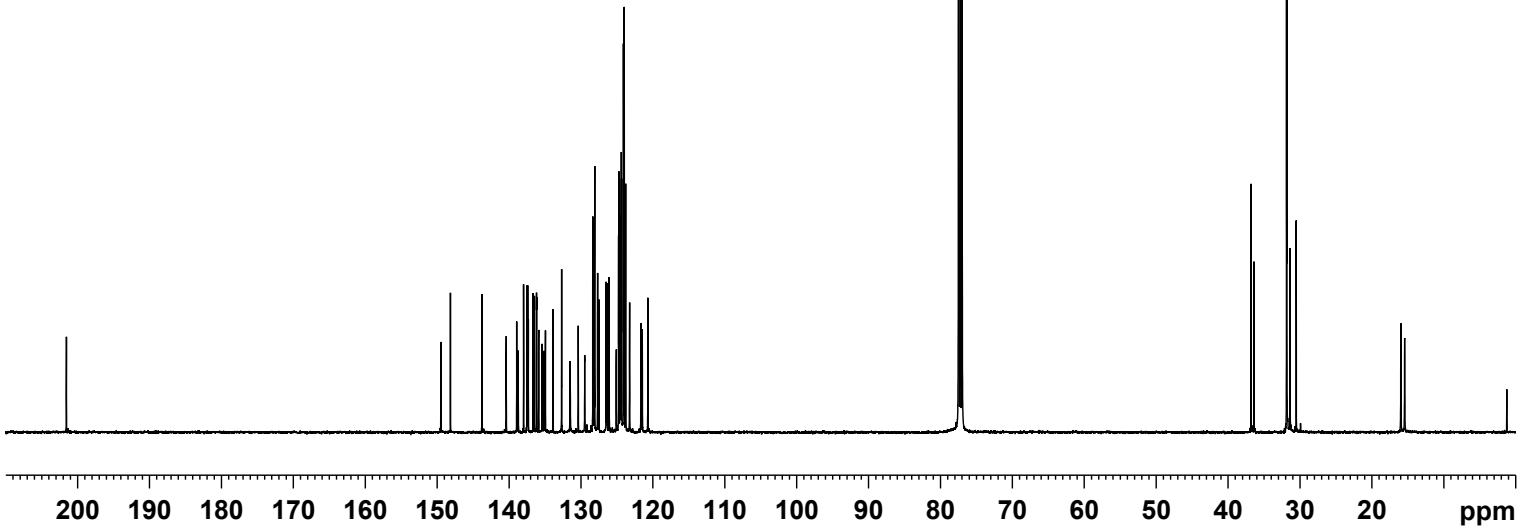
200
190
180
170
160
150
140
130
120
110
100
90
80
70
60
50
40
30
20
ppm

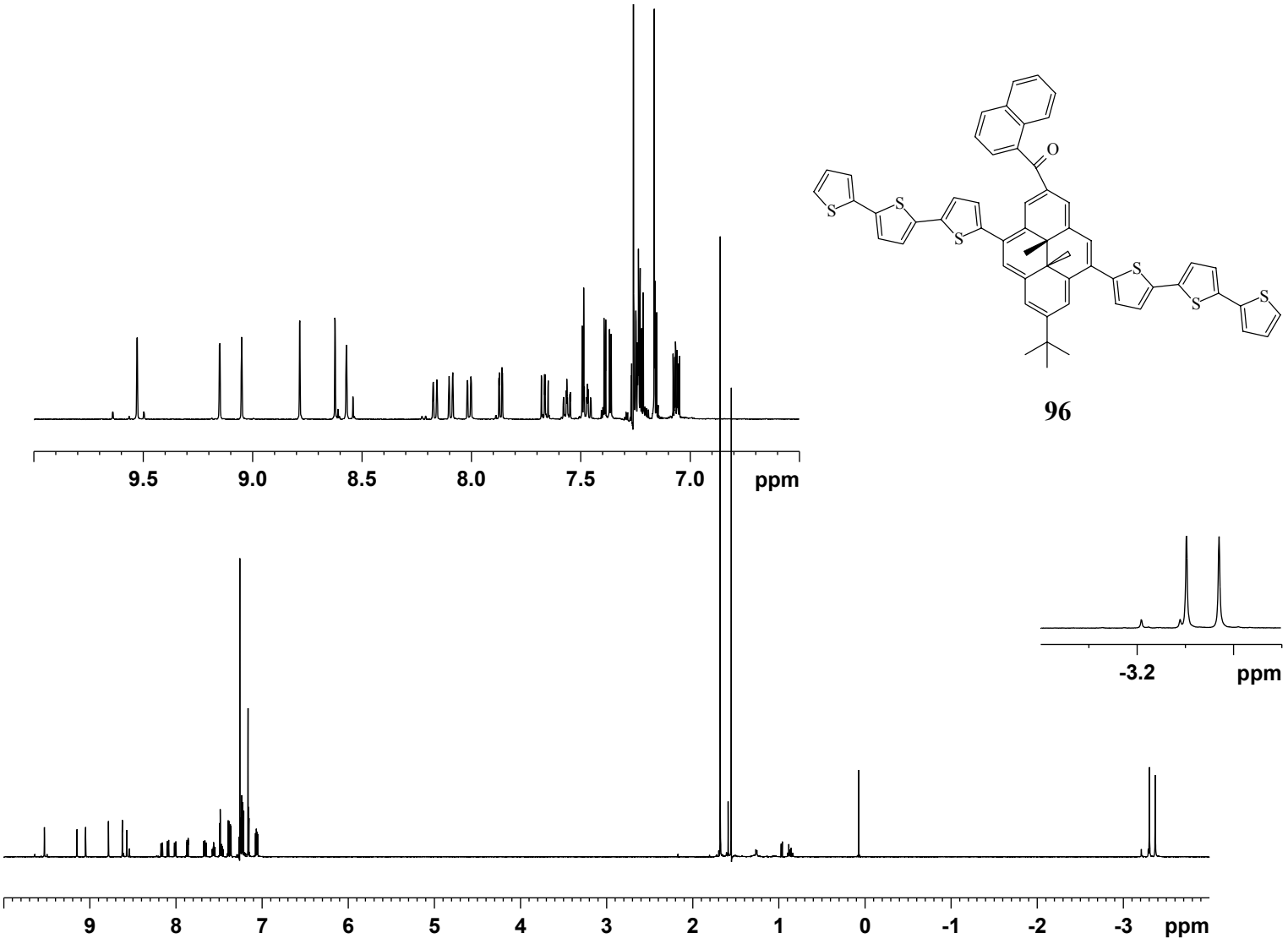

96

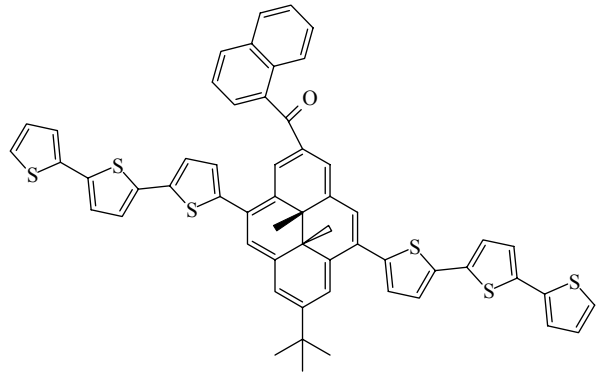
O
S
S
S
S
S
S

96

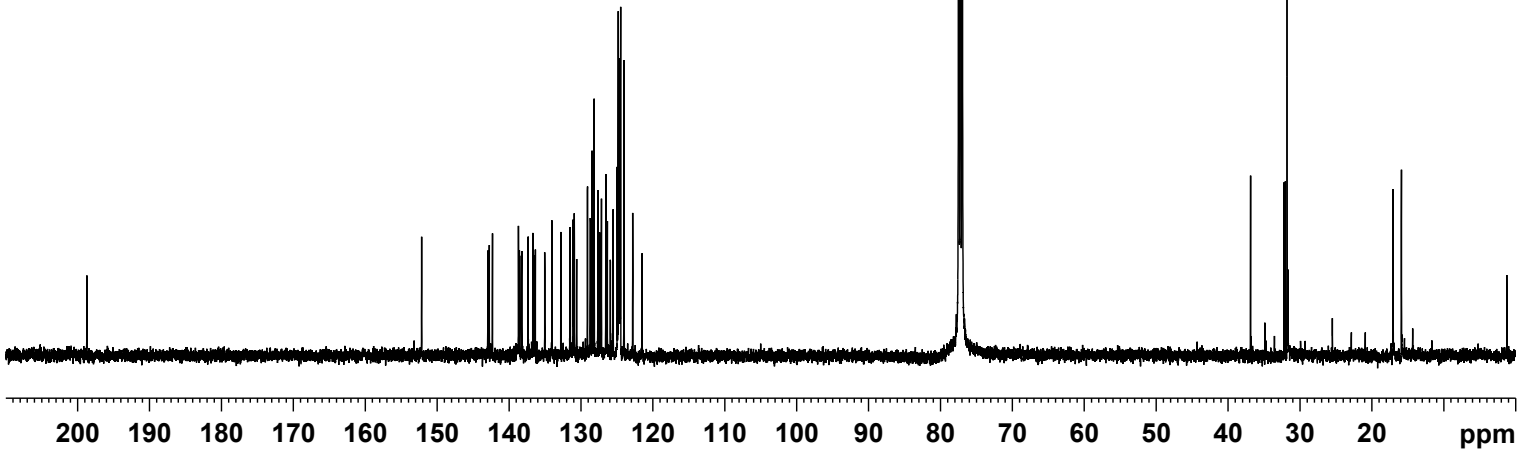
200
190
180
170
160
150
140
130
120
110
100
90
80
70
60
50
40
30
20
ppm

96'

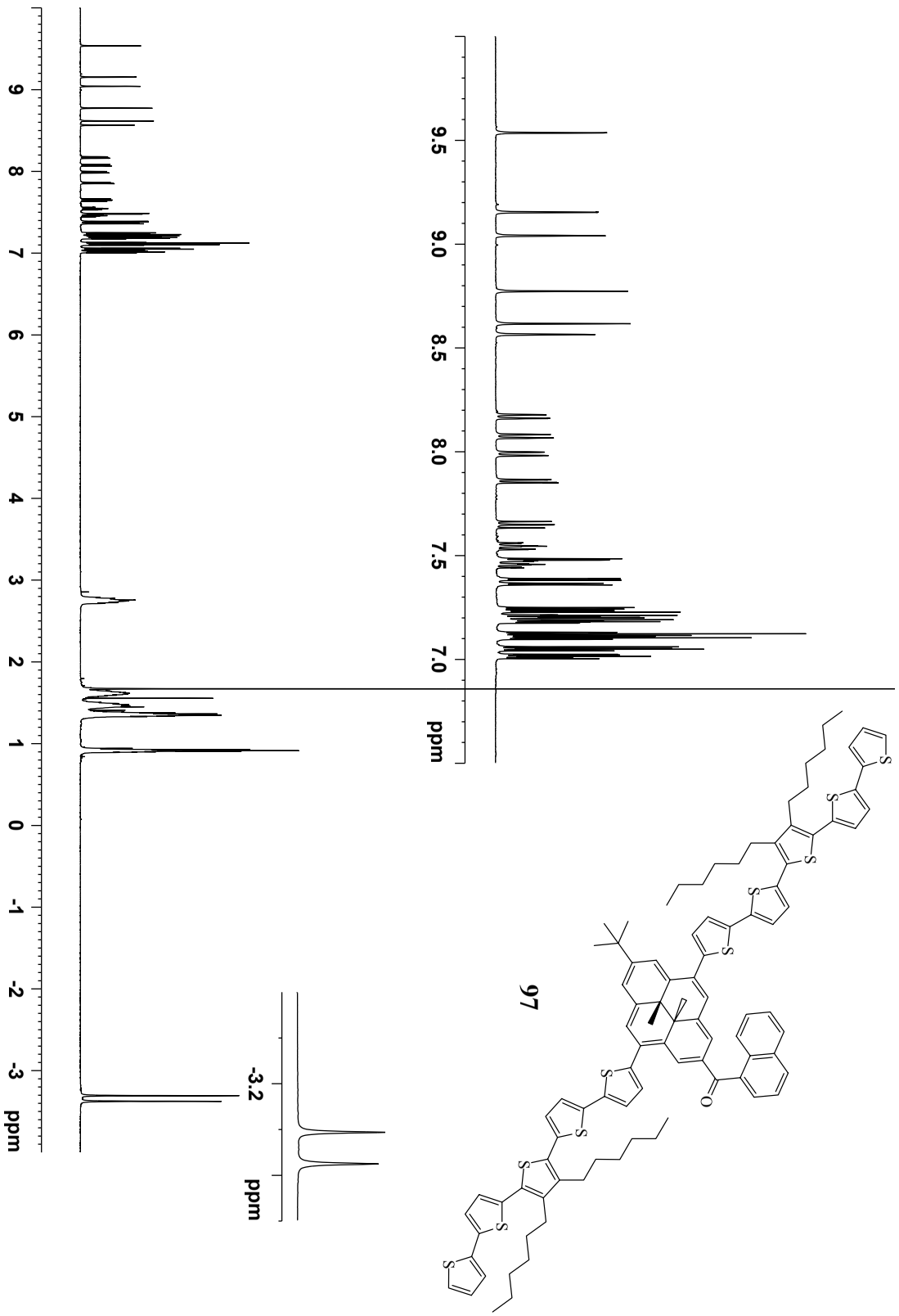

97

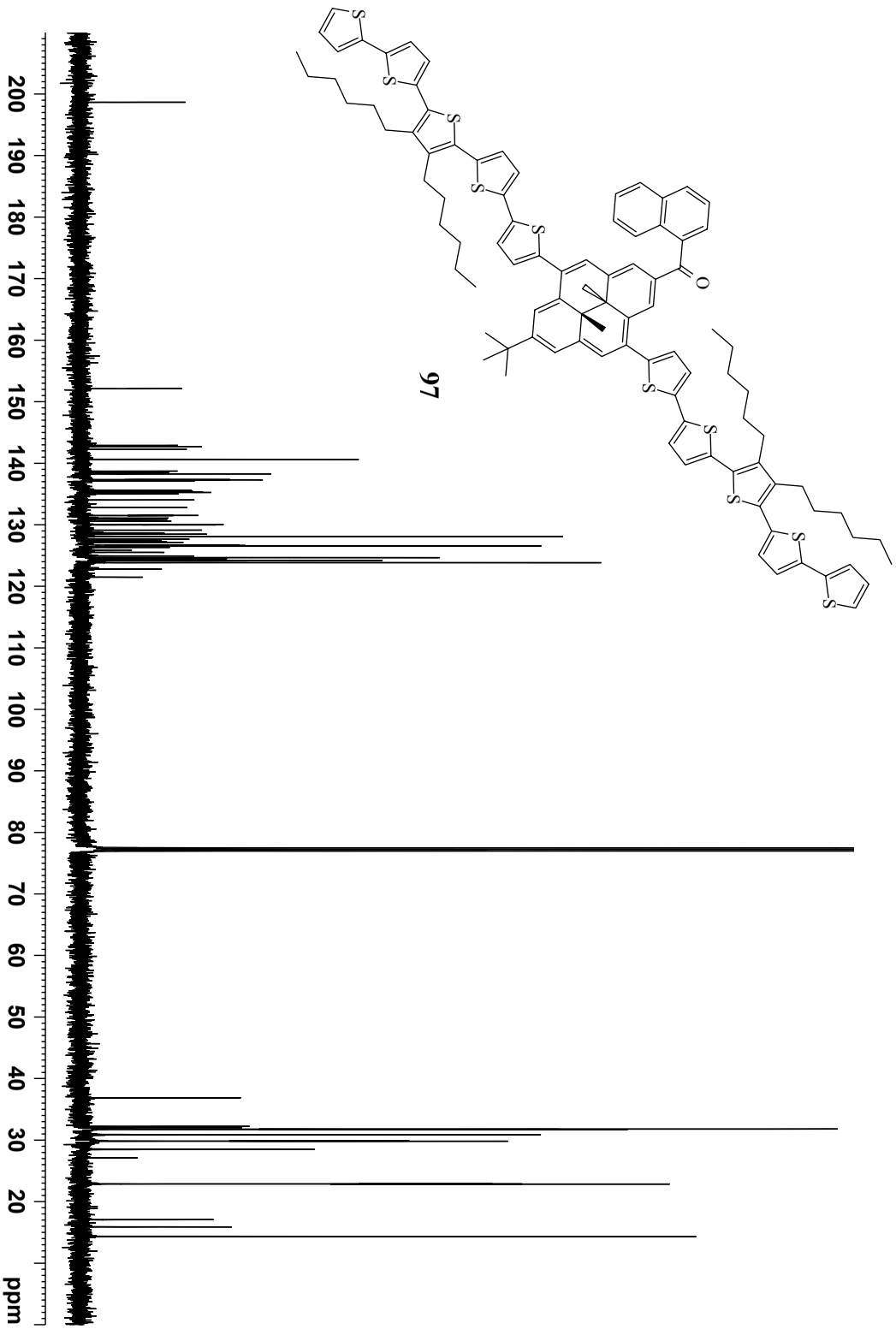
97
200
190
180
170
160
150
140
130
120
110
100
90
80
70
60
50
40
30
20
ppm

97'

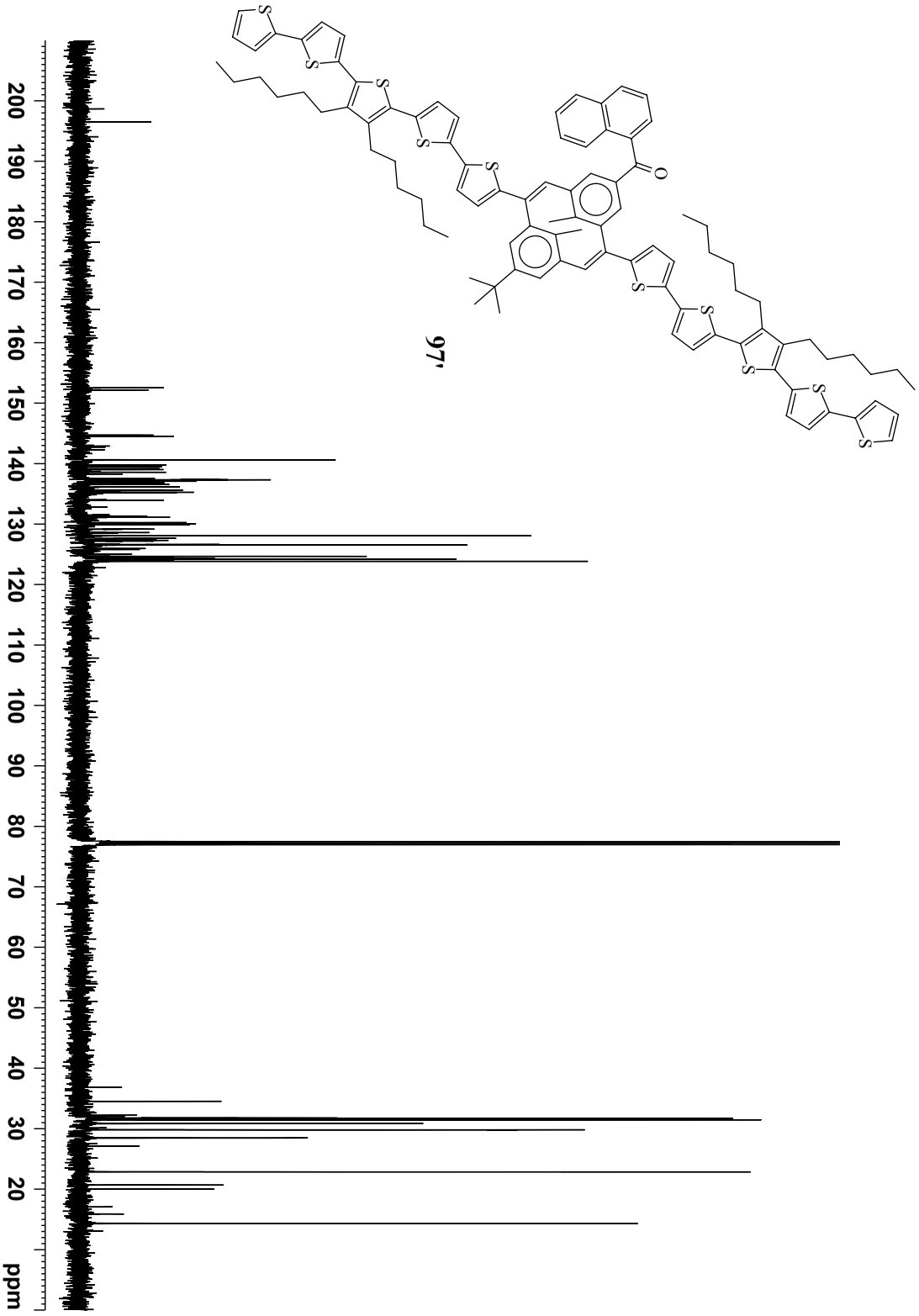
S
S
S
S
S
S
O
S
S
S
S
S
S
200 190 180 170 160 150 140 130 120 110 100 90 80 70 60 50 40 30 20
ppm

97'

9.4
9.2
9.0
8.8
8.6
8.4
8.2
8.0
7.8
7.6
7.4
ppm
O
100
-3.5
ppm
9
8
7
6
5
4
3
2
1
0
-1
-2
-3
ppm

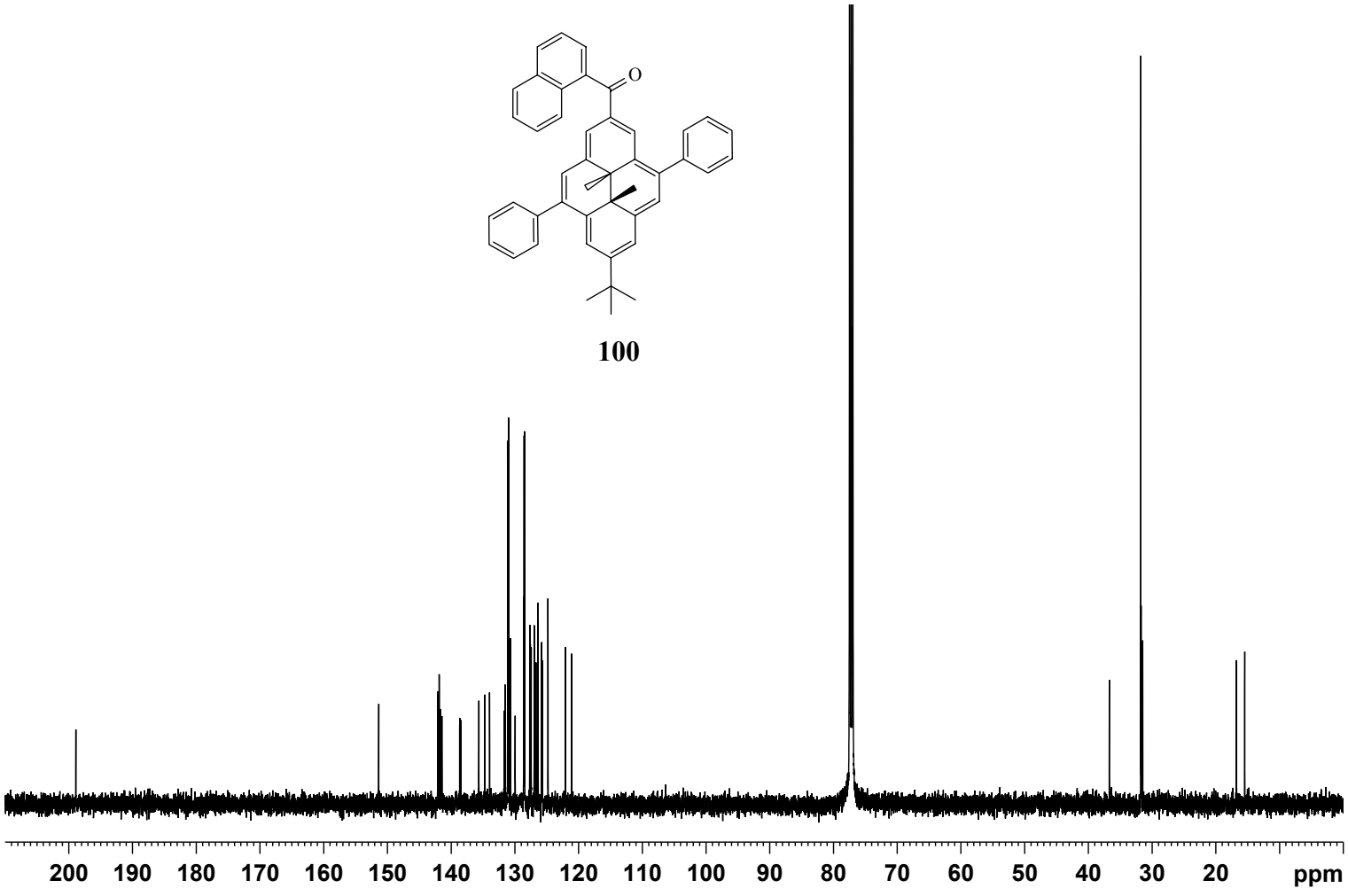
O
200
190
180
170
160
150
140
130
120
110
100
90
80
70
60
50
40
30
20
ppm

100

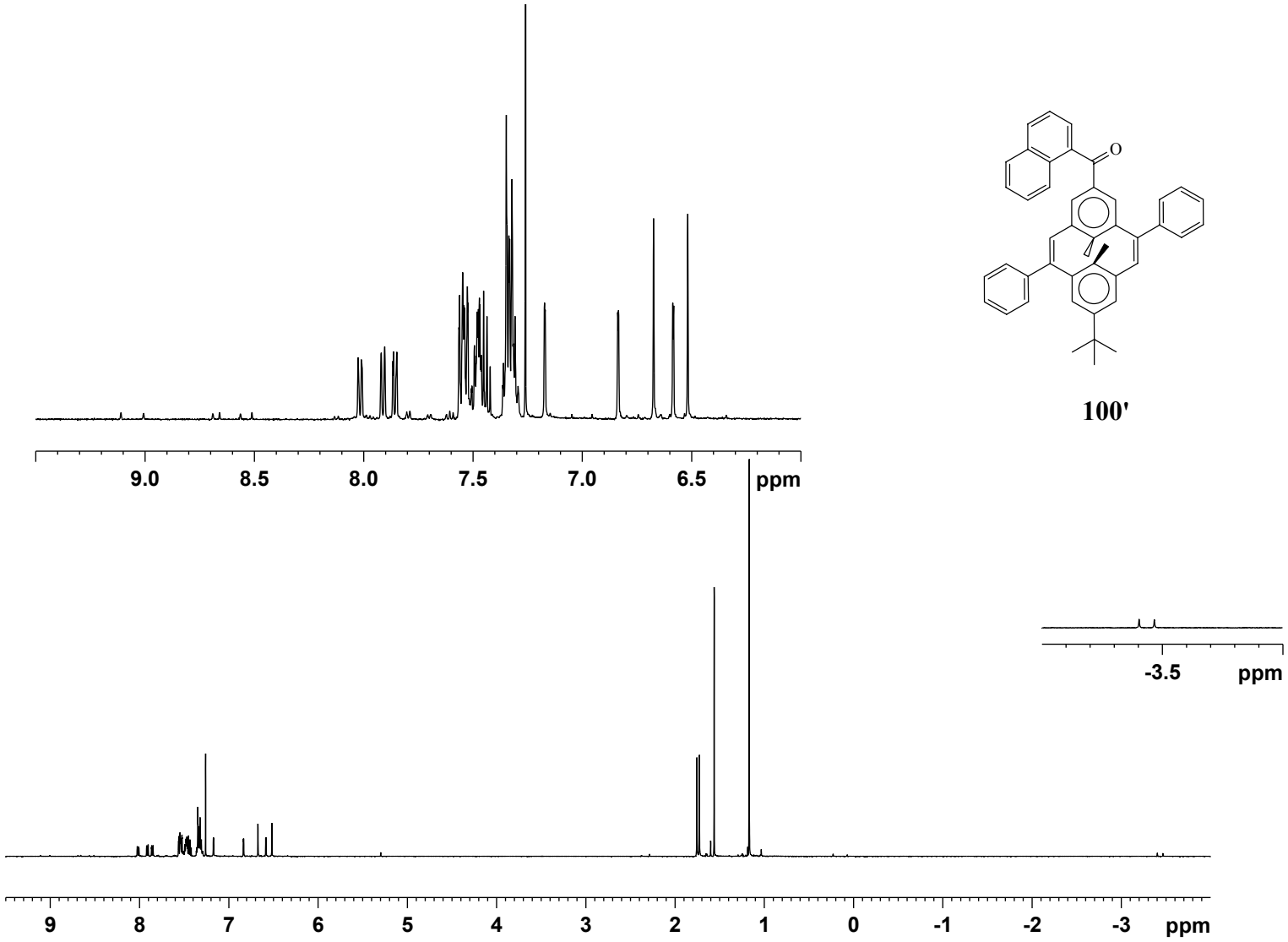

100'

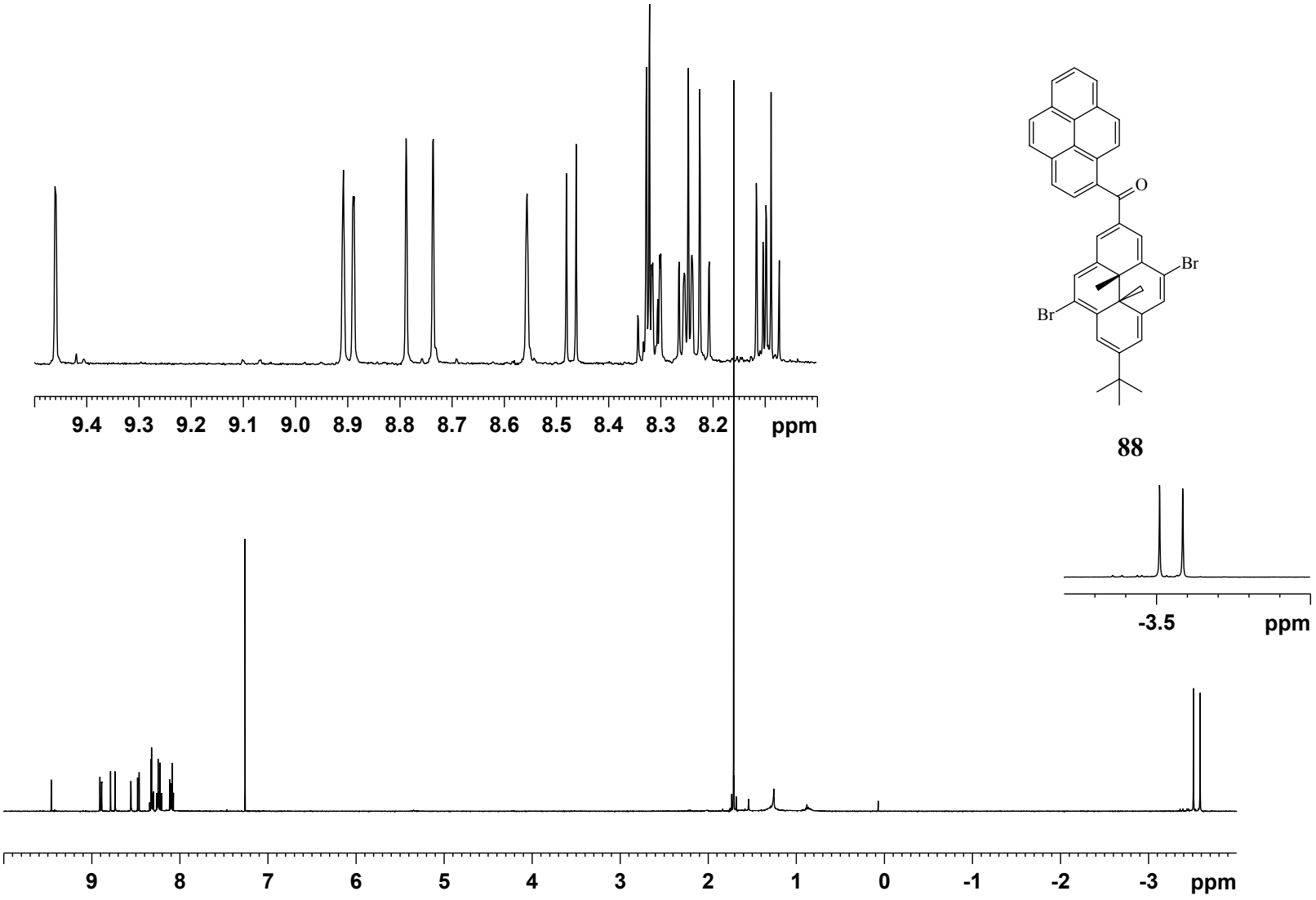
9.4 9.3 9.2 9.1 9.0 8.9 8.8 8.7 8.6 8.5 8.4 8.3 8.2 ppm
O
Br
Br
88
-3.5 ppm
9 8 7 6 5 4 3 2 1 0 -1 -2 -3 ppm

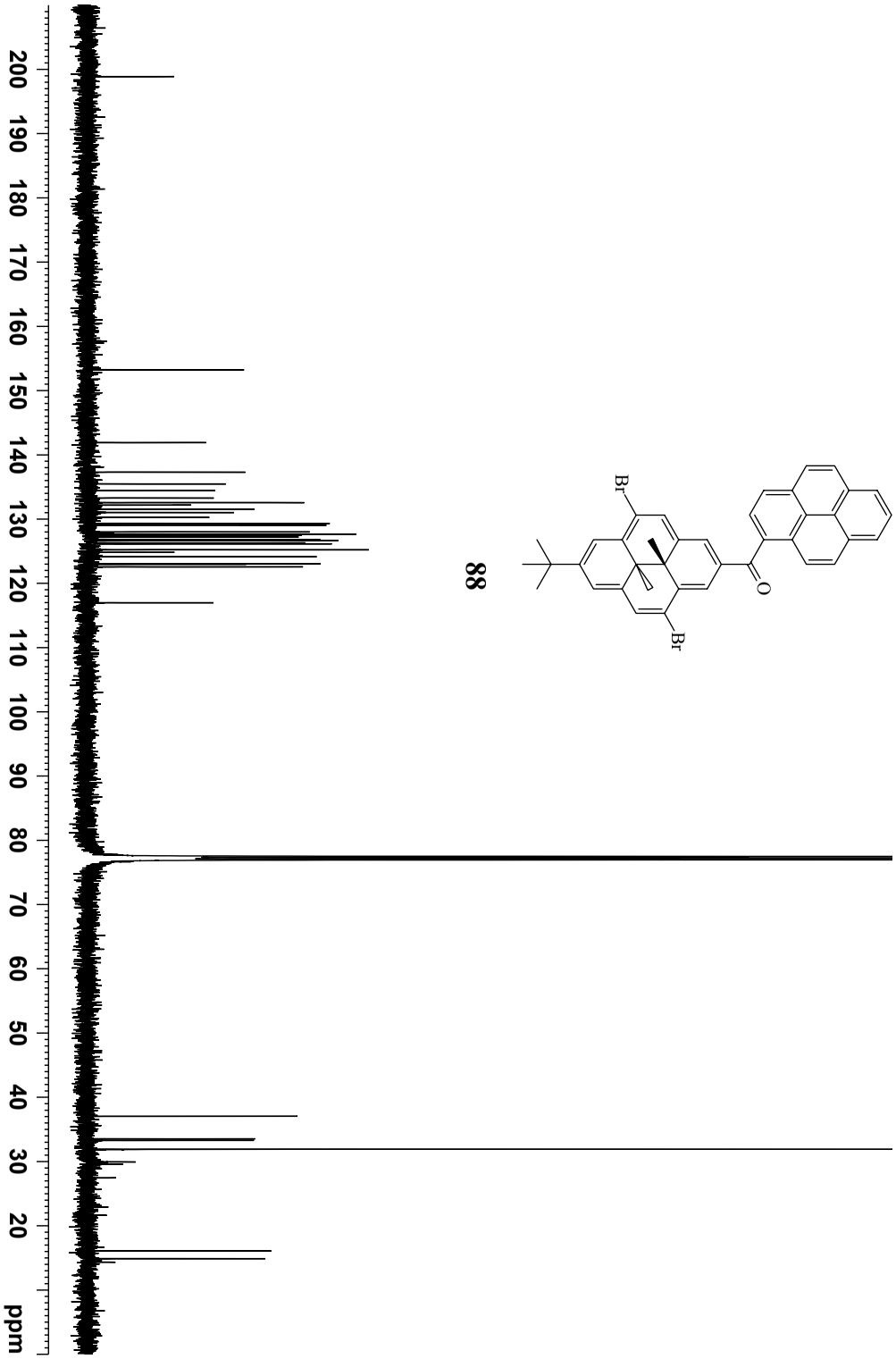
200
190
180
170
160
150
140
130
120
110
100
90
80
70
60
50
40
30
20
ppm
88
Br
Br
O

90

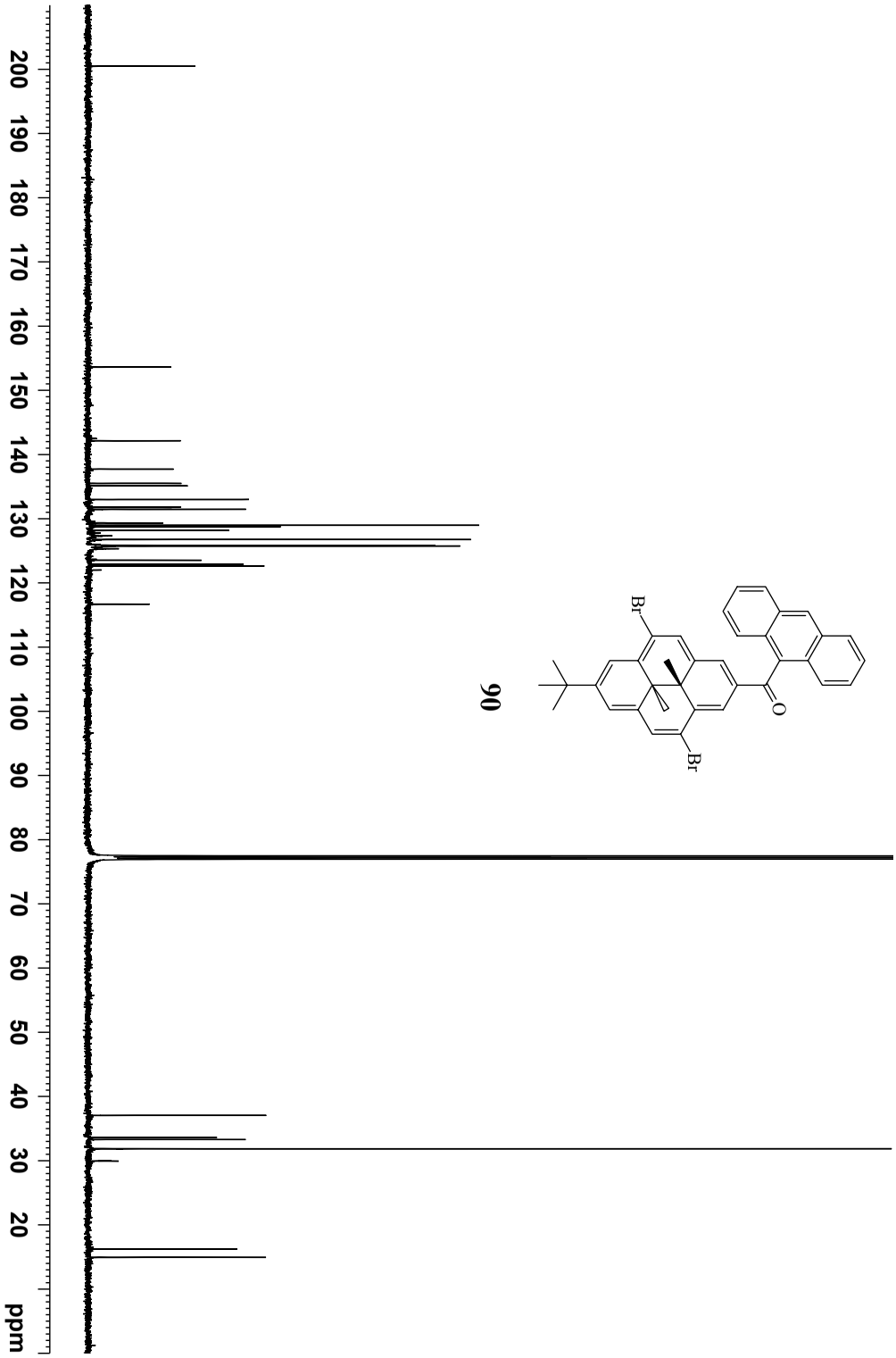
200
190
180
170
160
150
140
130
120
110
100
90
80
70
60
50
40
30
20
ppm
90
Br
Br
O

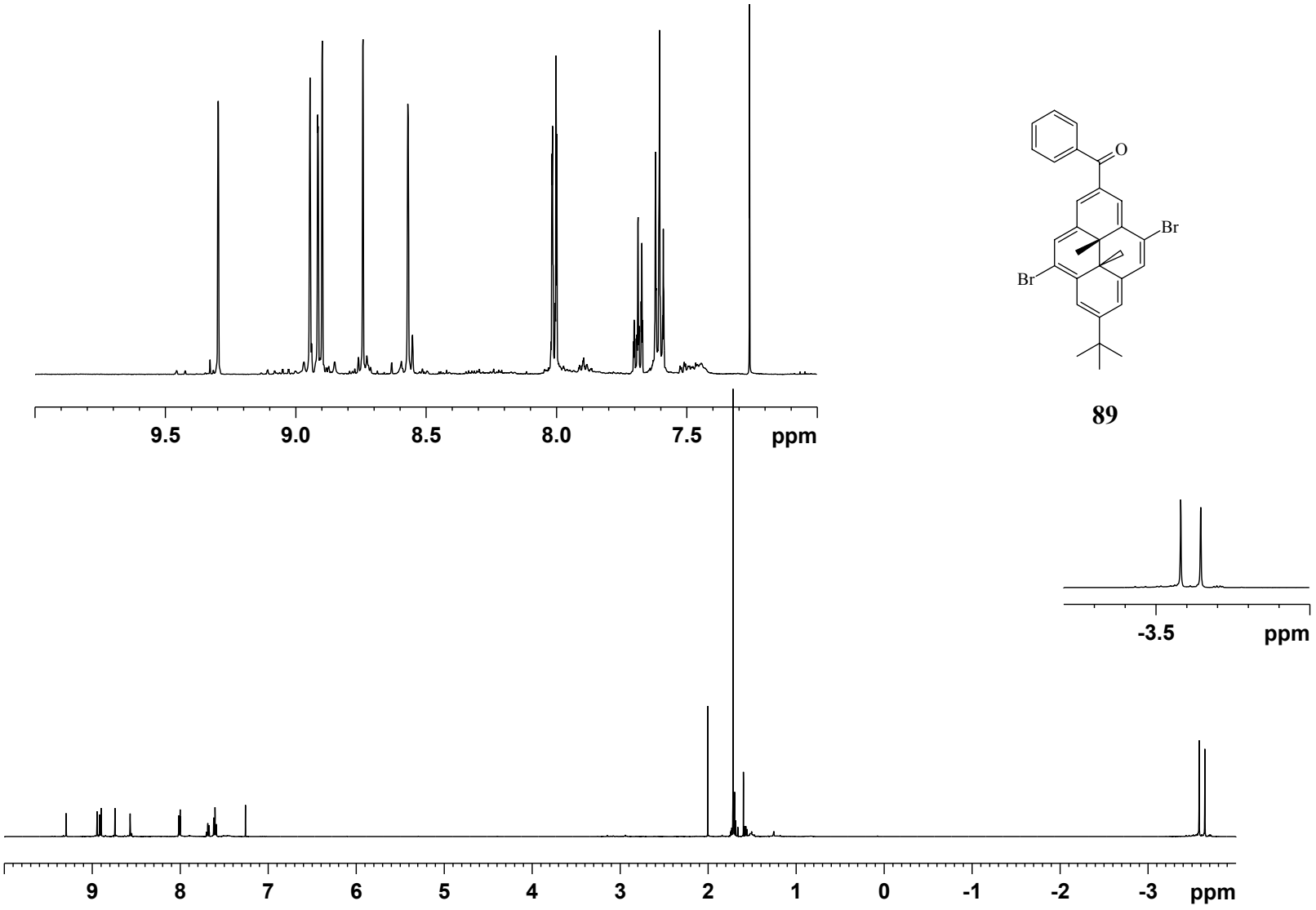

89

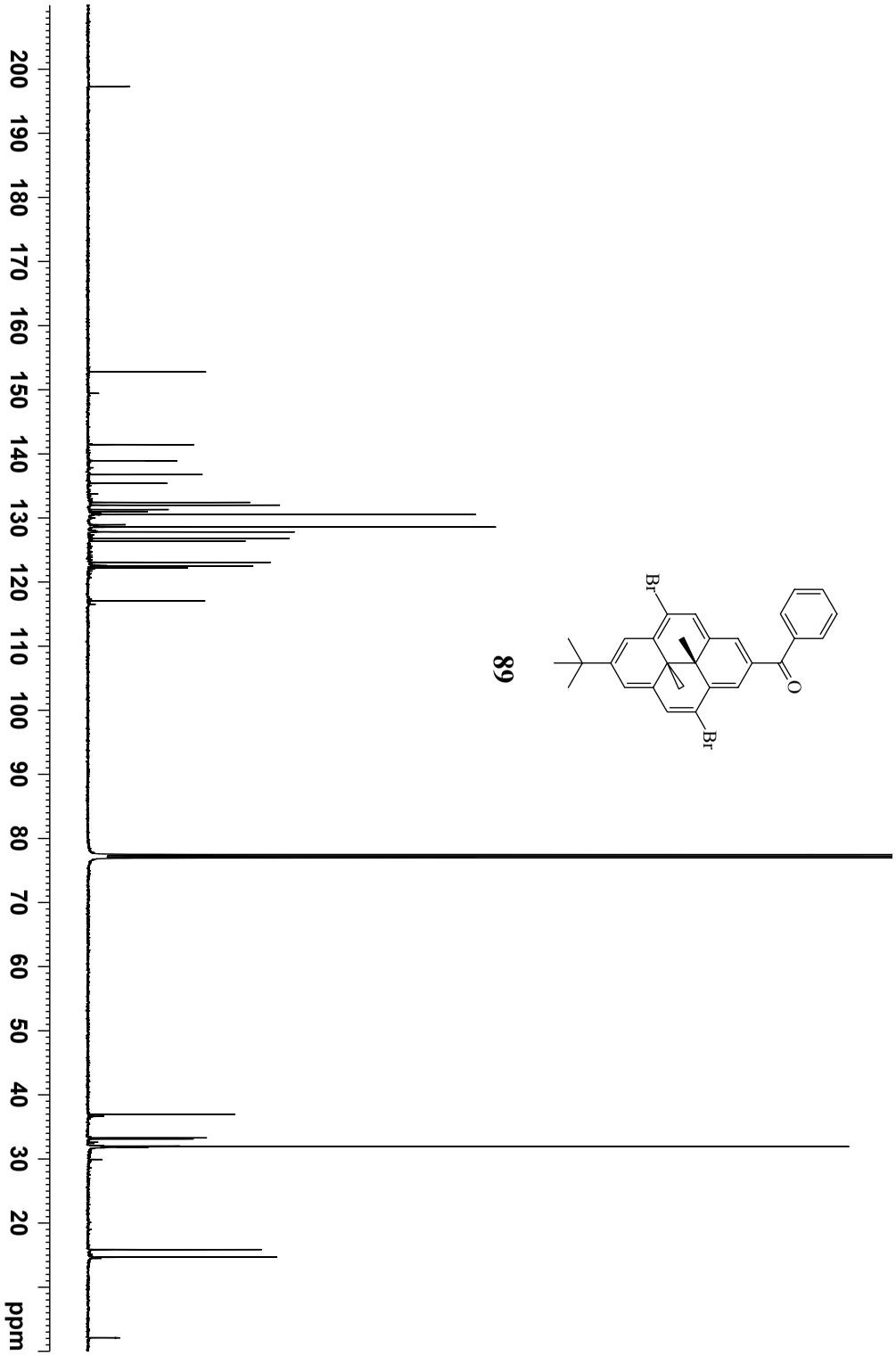
200
190
180
170
160
150
140
130
120
110
100
90
80
70
60
50
40
30
20
ppm
Br
Br
O

89

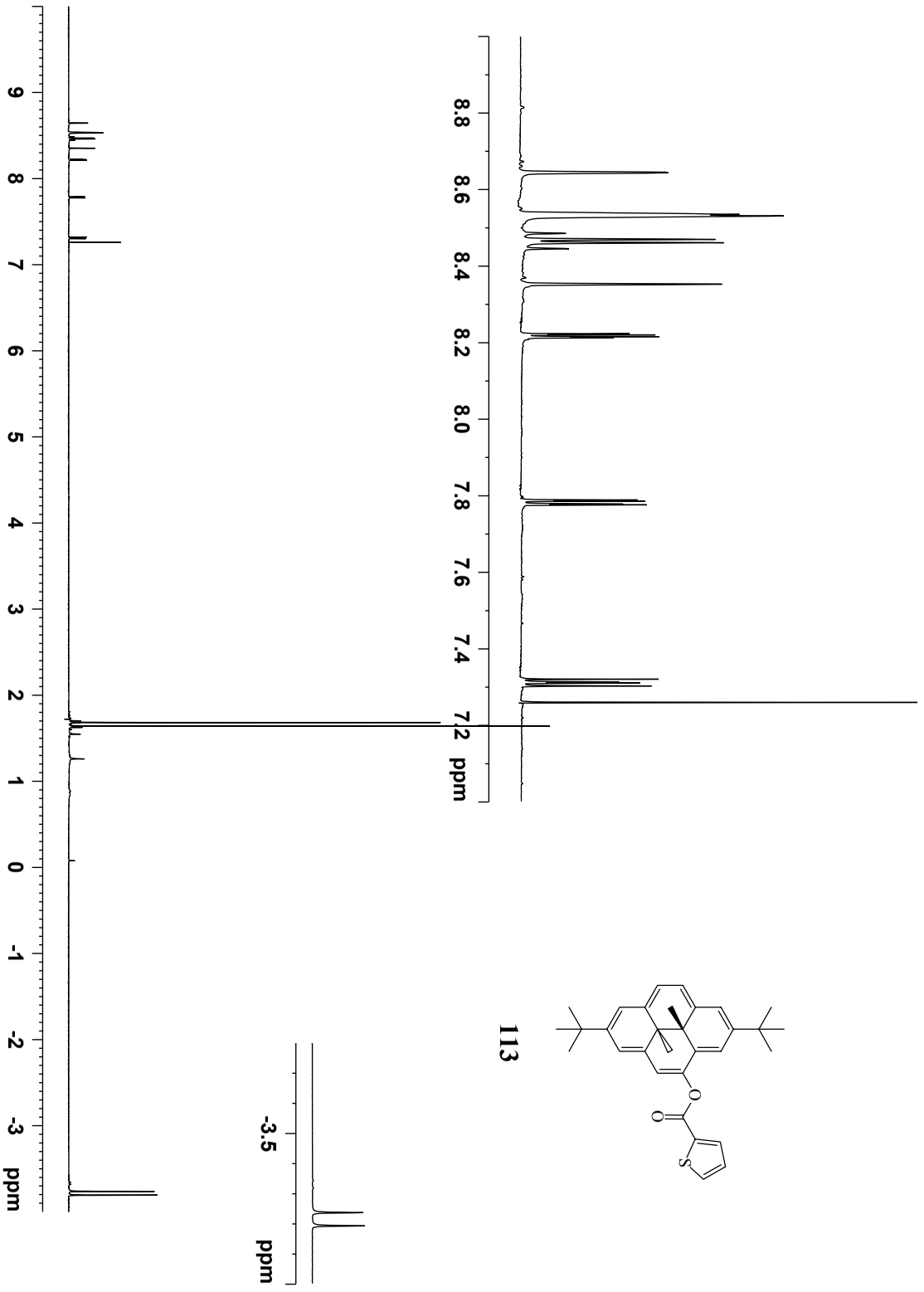

113

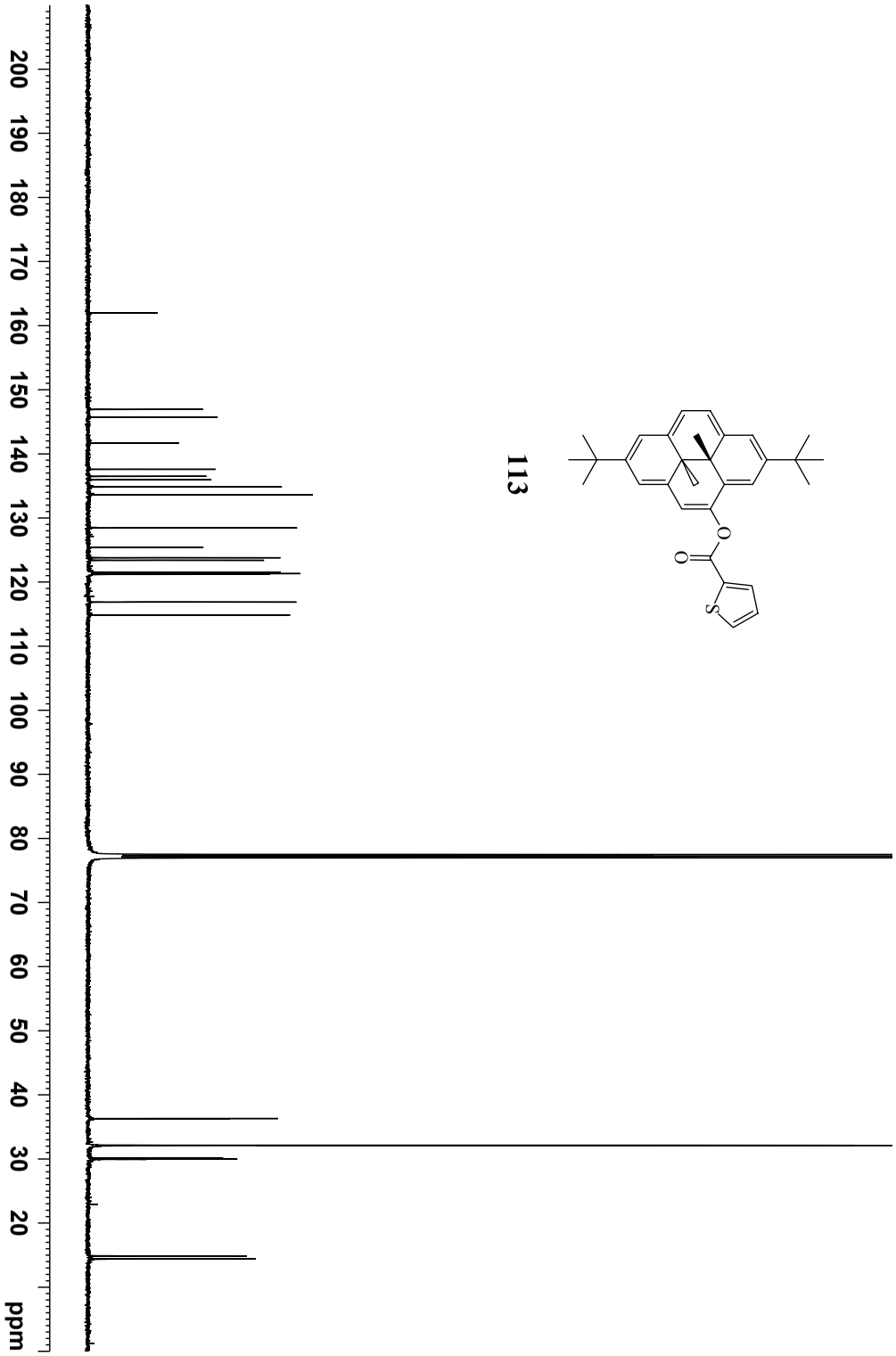
200
190
180
170
160
150
140
130
120
110
100
90
80
70
60
50
40
30
20
ppm
113
O
O
S

9.0
8.5
8.0
7.5
7.0
6.5
ppm
O
NH
55
-1.6
-1.8
ppm
9
8
7
6
5
4
3
2
1
0
-1
ppm

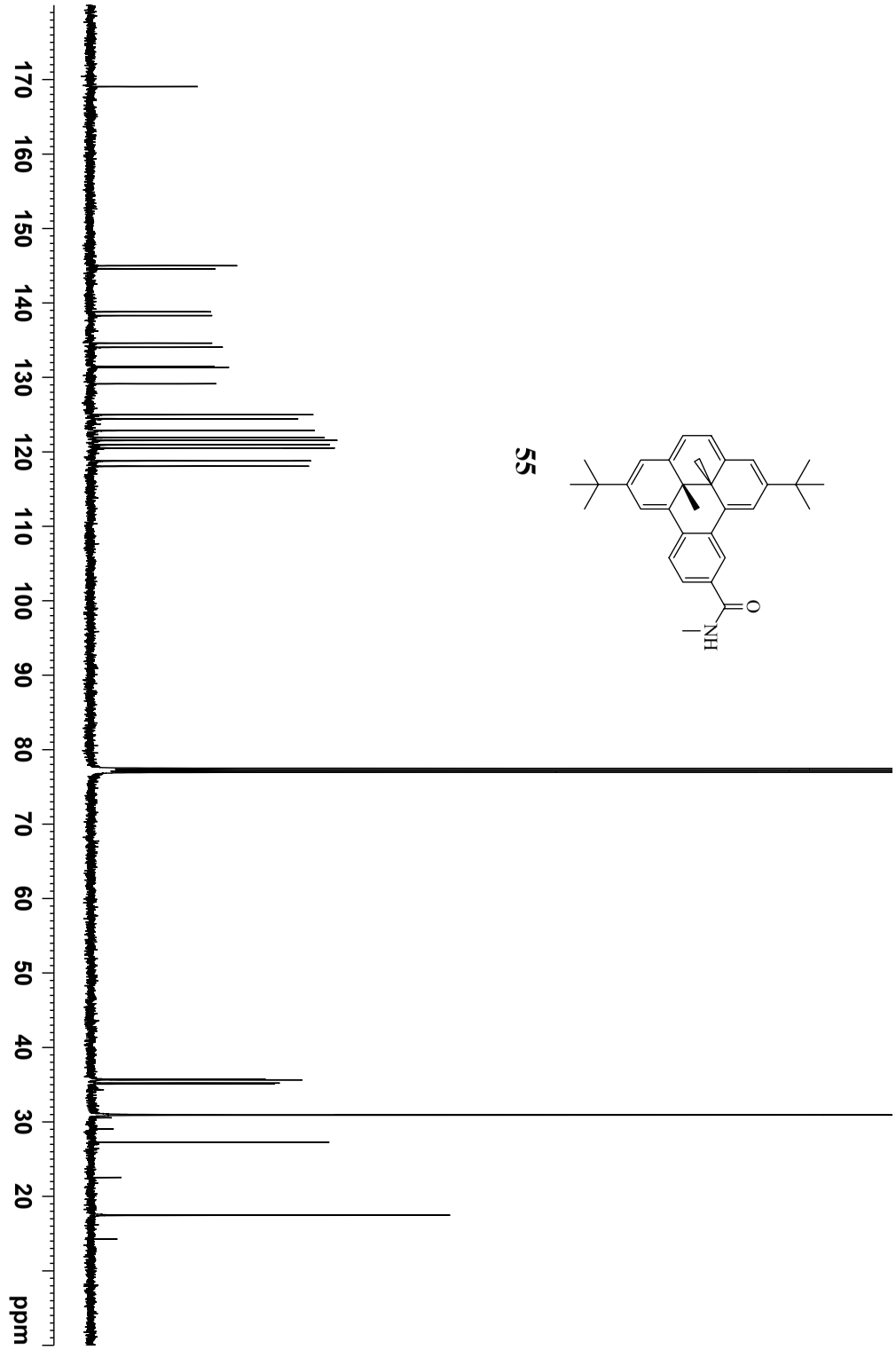
55
NH
O
170
160
150
140
130
120
110
100
90
80
70
60
50
40
30
20
ppm

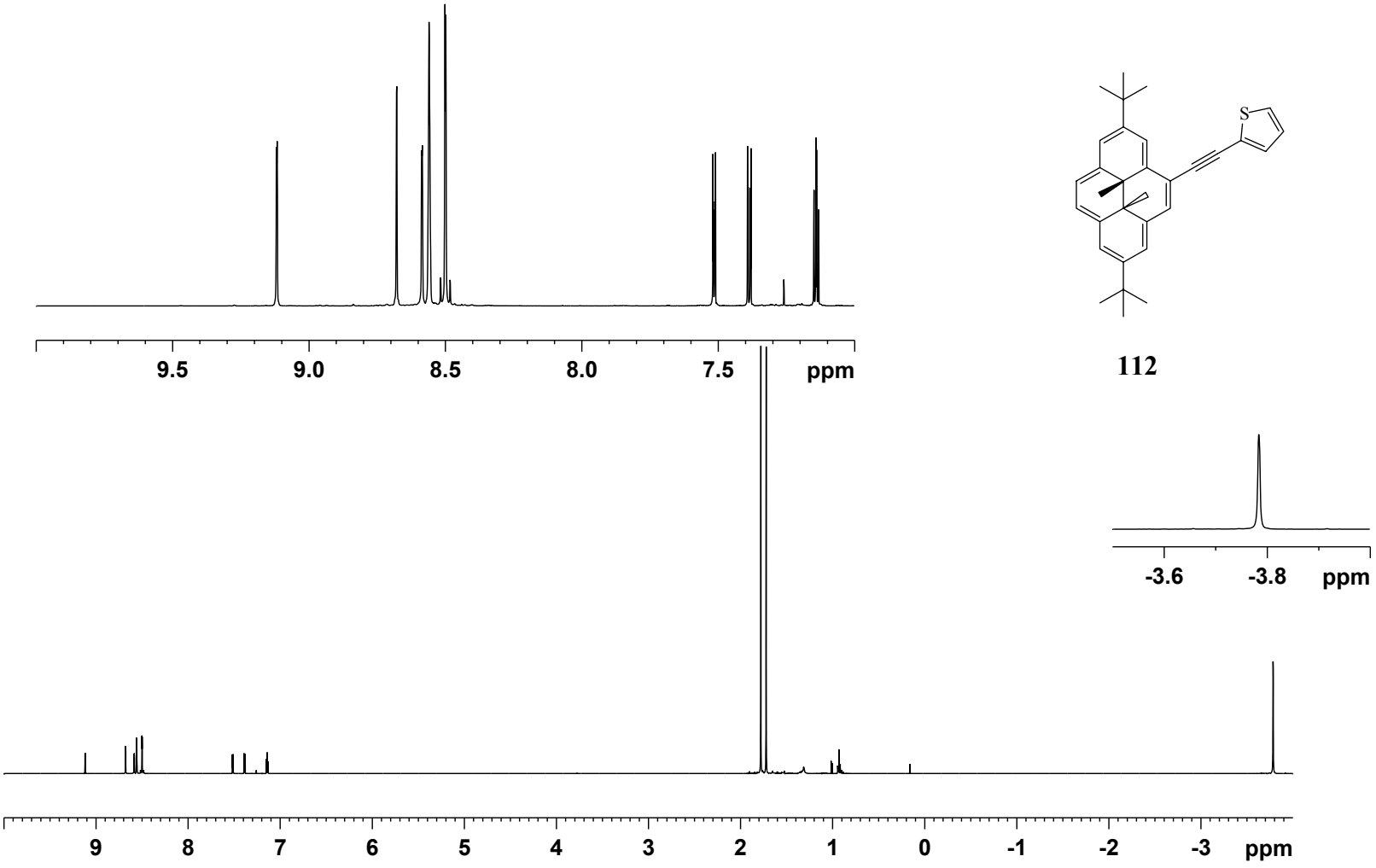
S
112
9.5
9.0
8.5
8.0
7.5
ppm
-3.6
-3.8
ppm
9
8
7
6
5
4
3
2
1
0
-1
-2
-3
ppm

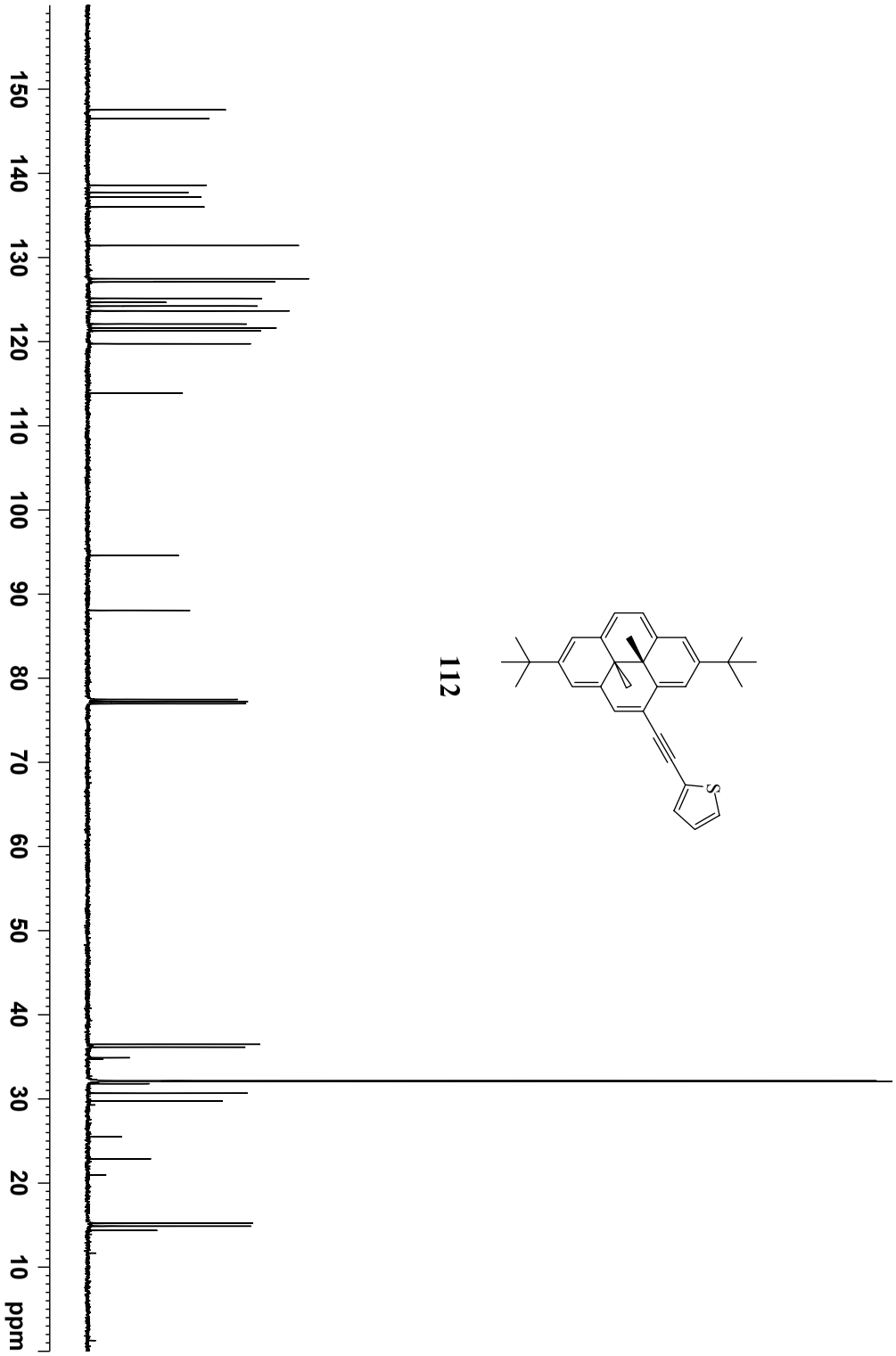
150
140
130
120
110
100
90
80
70
60
50
40
30
20
10
ppm
112
S

Sn
32
9.4 9.3 9.2 9.1 9.0 8.9 8.8 8.7 8.6 8.5 8.4 8.3 8.2 ppm
-3.6 -3.7 ppm
9 8 7 6 5 4 3 2 1 0 -1 -2 -3 ppm

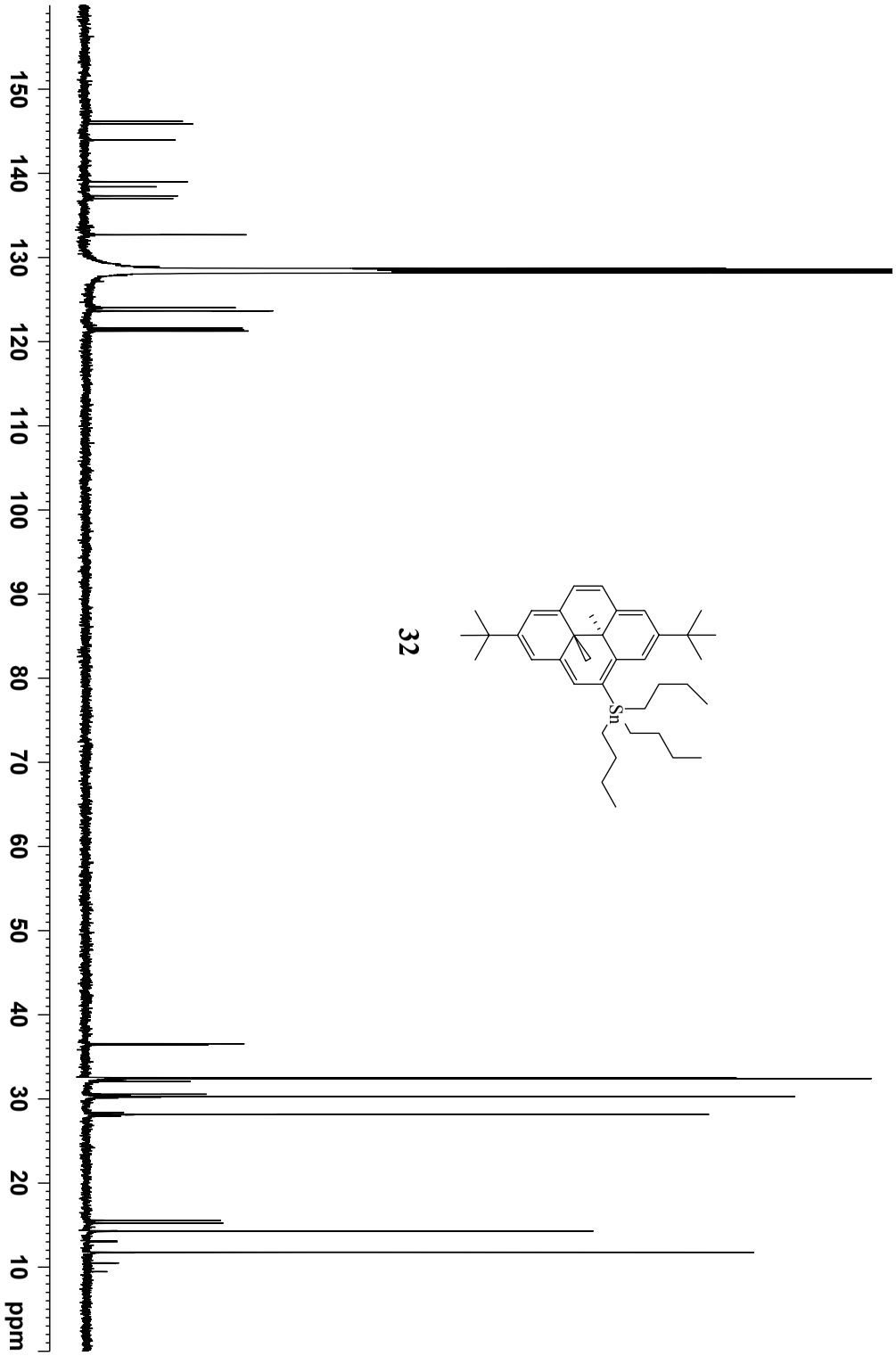
150
140
130
120
110
100
90
80
70
60
50
40
30
20
10
ppm
32
Sn

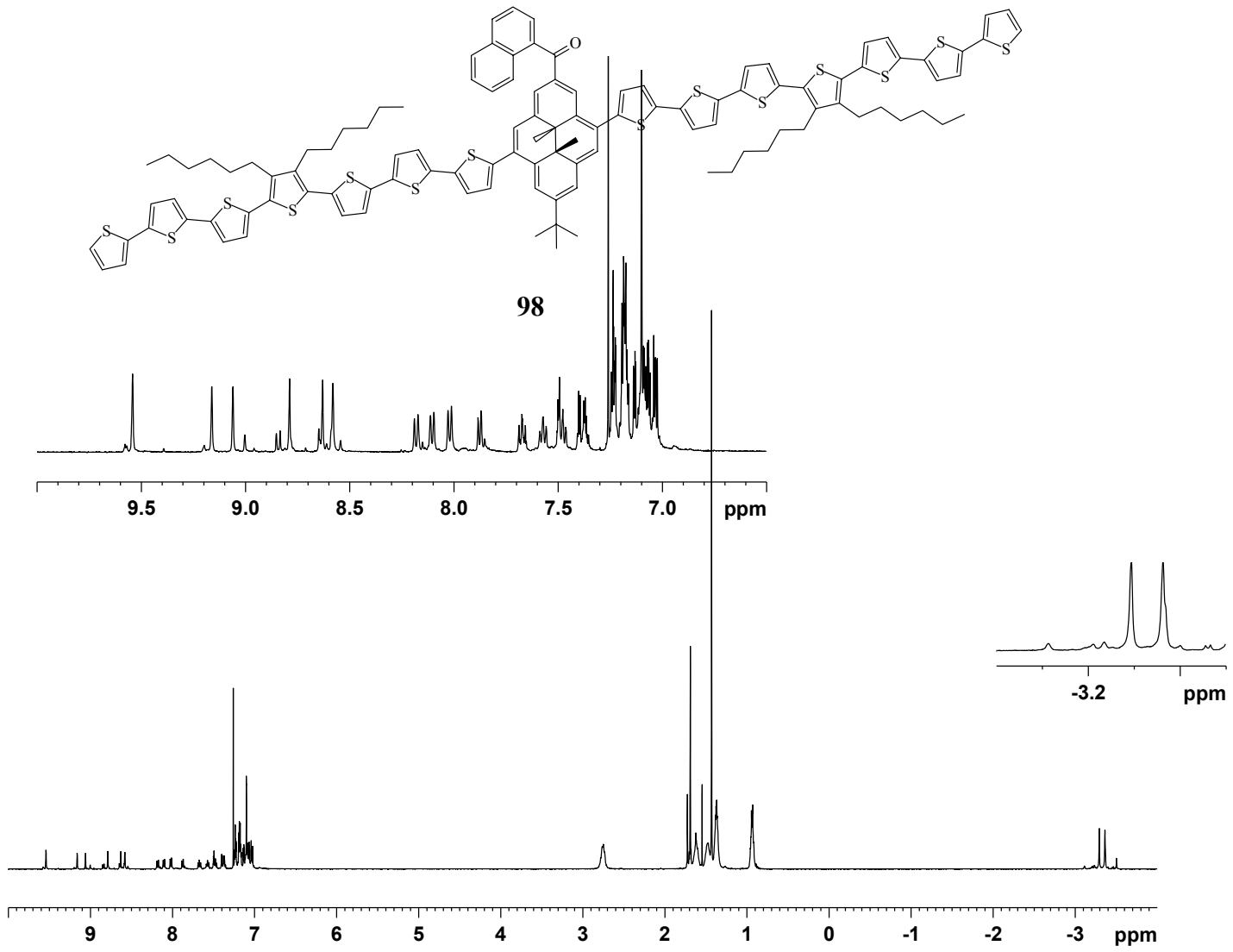
O
S
98
9.5
9.0
8.5
8.0
7.5
7.0
ppm
-3.2
ppm
9
8
7
6
5
4
3
2
1
0
-1
-2
-3
ppm

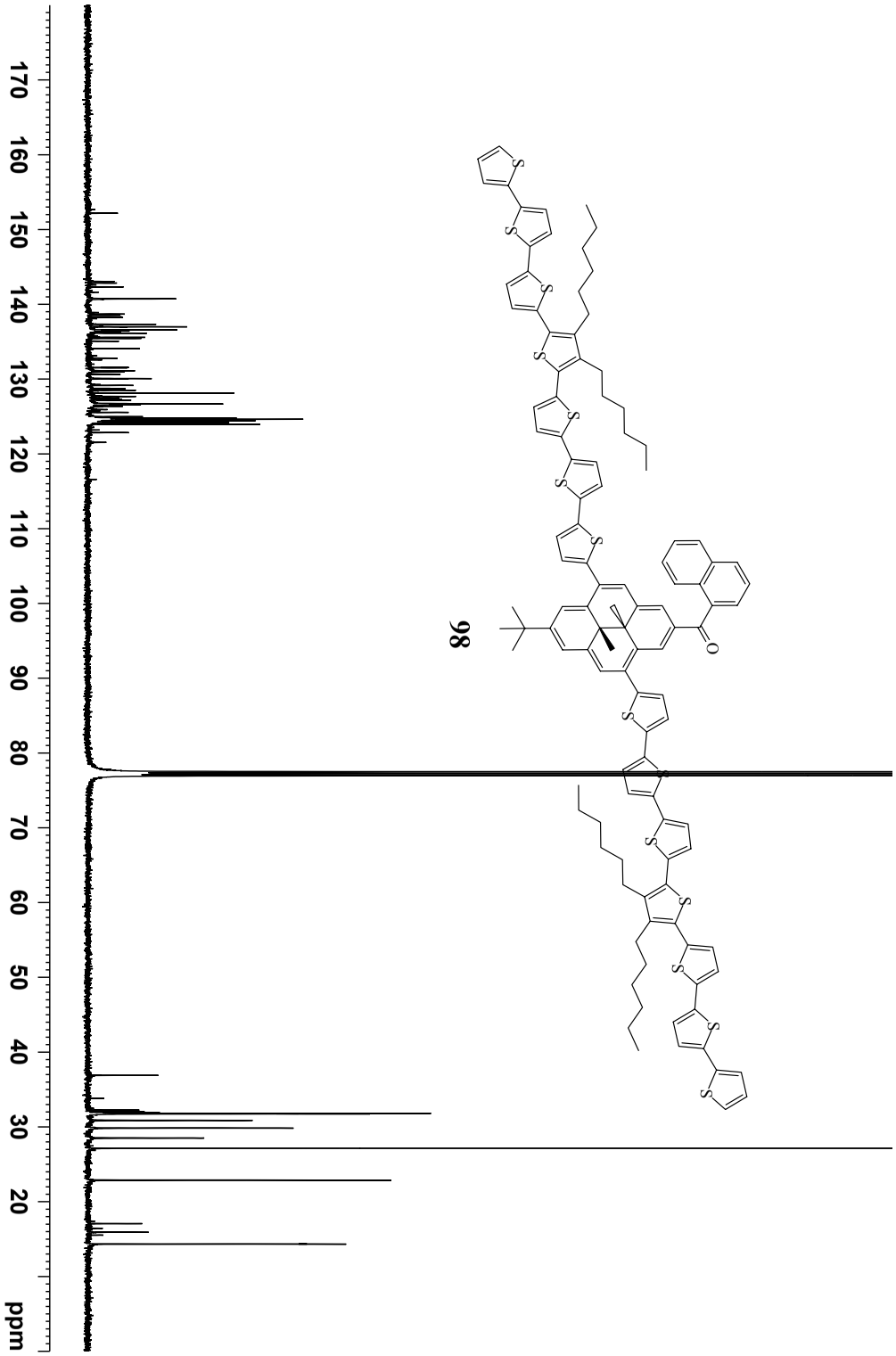
98
O
S
170
160
150
140
130
120
110
100
90
80
70
60
50
40
30
20
ppm

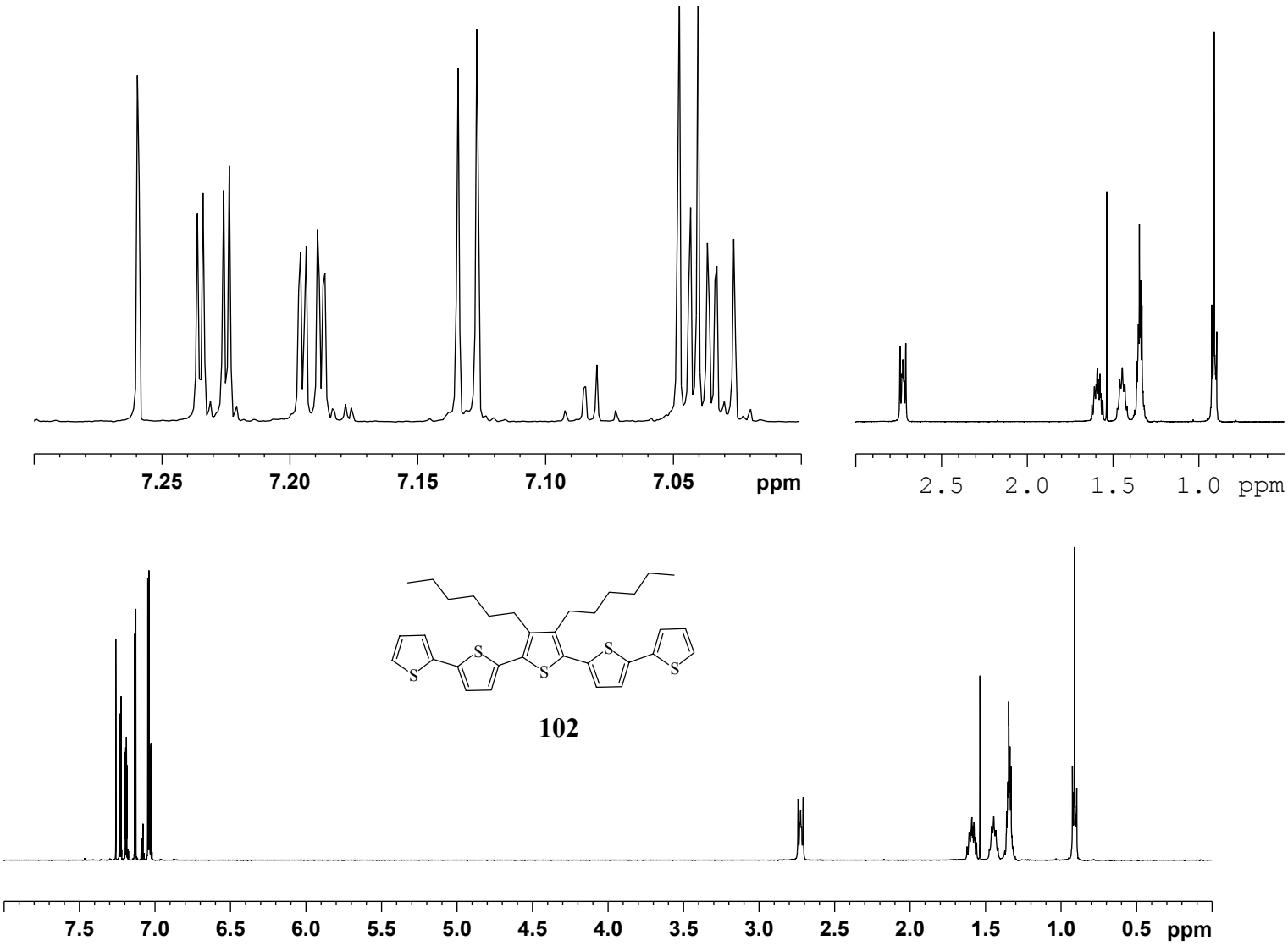
7.25
7.20
7.15
7.10
7.05
ppm
2.5
2.0
1.5
1.0
ppm
S
S
S
S
S
7.5
7.0
6.5
6.0
5.5
5.0
4.5
4.0
3.5
3.0
2.5
2.0
1.5
1.0
0.5
ppm

102

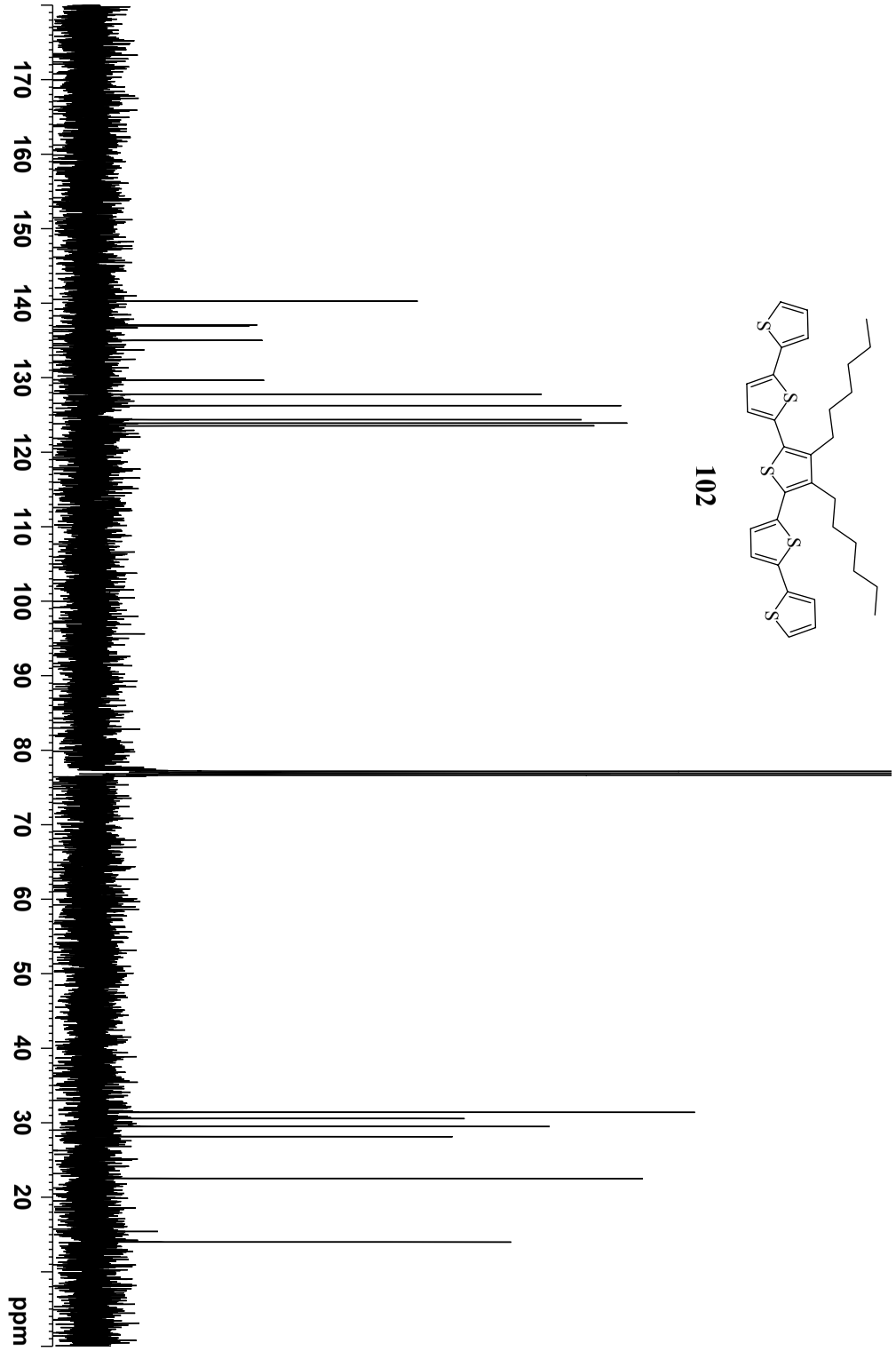

102

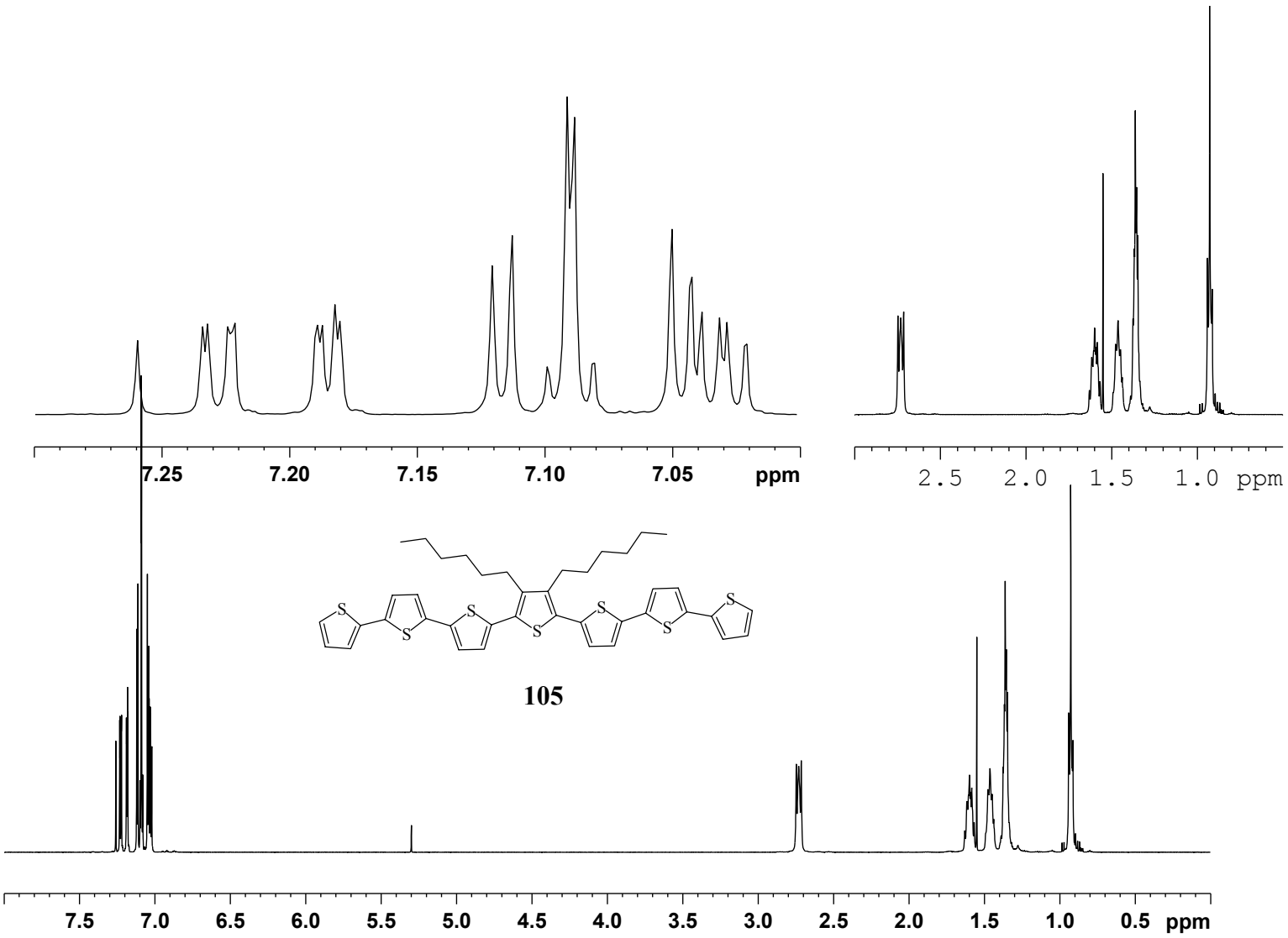
7.25
7.20
7.15
7.10
7.05
ppm
2.5
2.0
1.5
1.0
ppm
S
S
S
S
S
S
7.5
7.0
6.5
6.0
5.5
5.0
4.5
4.0
3.5
3.0
2.5
2.0
1.5
1.0
0.5
ppm

105

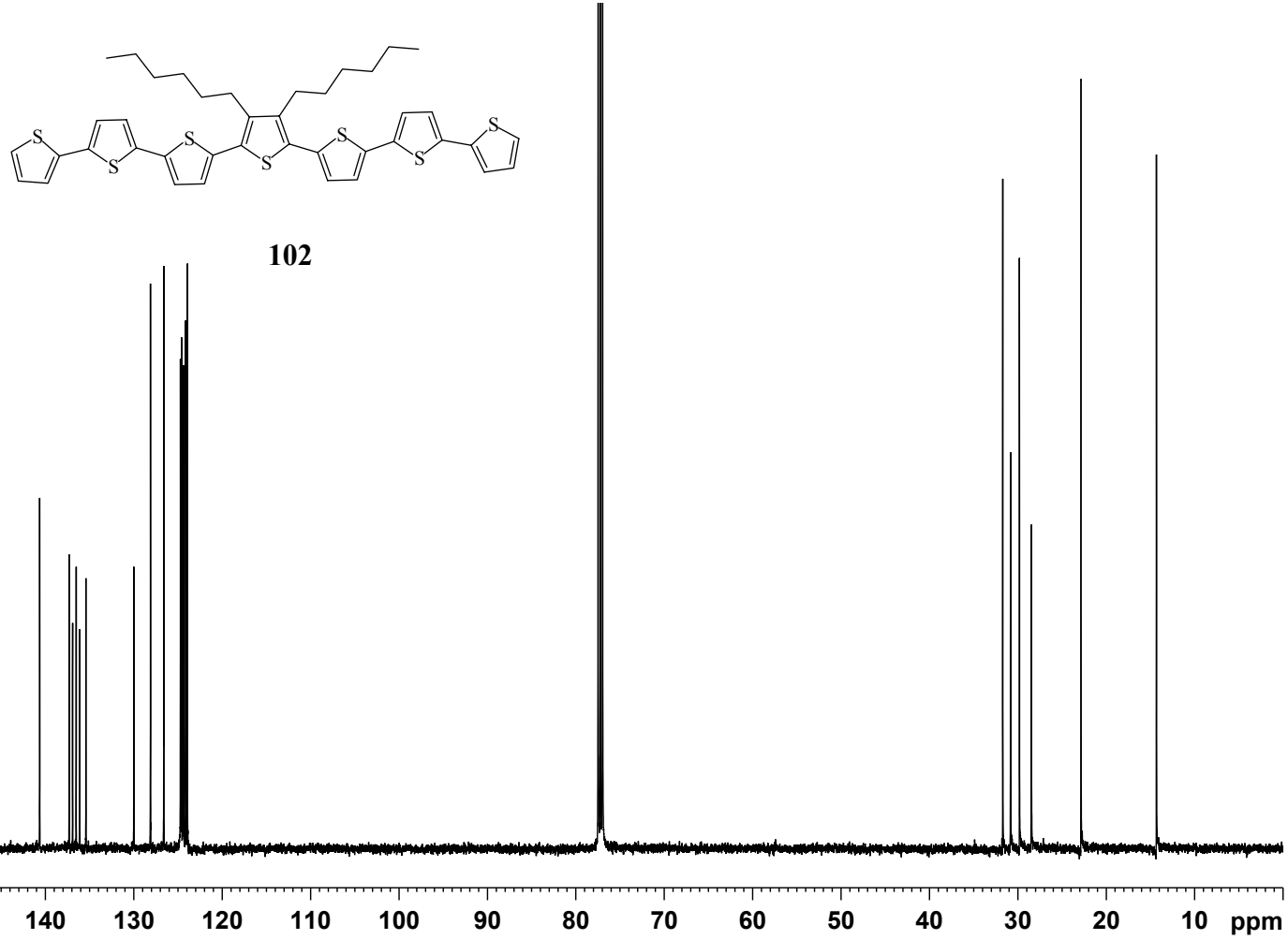

102